TECHNISCHE UNIVERSITÄT MÜNCHEN

Fakultät für Chemie

Untersuchungen zum Einfluss nicht-ionischer Co-Dispergiermittel sowie hyperverzweigter PCE- und Lignit-basierter Fließmittel auf Dispergierung und rheologische Eigenschaften zementärer Systeme

Manuel Klaus Ilg

Vollständiger Abdruck der von der Fakultät für Chemie der Technischen Universität München zur Erlangung des akademischen Grades eines

Doktors der Naturwissenschaften (Dr. rer. nat.)

genehmigten Dissertation.

Vorsitzender:	Prof. Dr. Klaus Köhler
Prüfer der Dissertation:	1. Prof. Dr. Johann Plank
	2. Prof. Dr. Thomas Brück
	3. Prof. Dr. Josef Felixberger (schriftliche Beurteilung)
	Prof. Dr. Anton Lerf (mündliche Prüfung)

Die Dissertation wurde am 20.09.2021 bei der Technischen Universität München eingereicht und durch die Fakultät für Chemie am 16.12.2021 angenommen.

„You don't have to be a fantastic hero to do certain things – to compete. You can be just an ordinary chap, sufficiently motivated to reach challenging goals."

Sir Edmund Hillary

Danksagung

Ein besonderer Dank gilt meinem verehrten akademischen Lehrer

Herrn Prof. Dr. Johann Plank

für die Aufnahme an seinen Lehrstuhl, die anspruchsvolle Themenstellung sowie für die große Unterstützung, die zum Gelingen dieser Arbeit beigetragen hat. Vielen Dank für das mir entgegengebrachte Vertrauen, die sehr gute Zusammenarbeit und den konstruktiven fachlichen Diskurs. In meiner Zeit am Lehrstuhl konnte ich Erfahrungen in unterschiedlichsten Bereichen und Aufgabenfeldern sammeln, die in vielerlei Hinsicht zu meiner fachlichen und persönlichen Weiterentwicklung beigetragen haben.

Ein großer Dank geht ebenfalls an die Deutsche Forschungsgemeinschaft (DFG), die Teile dieser Arbeit im Rahmen des Schwerpunktprogramms SPP 2005 *„Opus Fluidum Futurum – Rheologie reaktiver, multiskaliger, mehrphasiger Baustoffsysteme“* finanziell gefördert hat.

Dem Deutschen Akademischen Austauschdienst (DAAD), der Gesellschaft Deutscher Chemiker (GDCh) und der TUM Graduate School danke ich für die Finanzierung meiner Vortragsreisen. Die Eindrücke und Erlebnisse auf den Tagungen in Ottawa, Peking, Weimar und Garching werden mir in guter Erinnerung bleiben.

Dr. Thomas Hurnaus, My Linh Vo, Dr. Stefanie Gruber und Mouala Moumin danke ich für ihre Unterstützung und zusprechenden Worte. Die Zeit und Erlebnisse mit euch auch fernab des Laboralltags waren eine große Freude und haben mich immer wieder von Neuem für meine Aufgaben motiviert.

Meinen ehemaligen Laborkollegen Timon Echt und Johann Mekulanetsch danke ich für die gemeinsame Zeit, den regen Austausch zu allen möglichen Themen und die angenehme Arbeitsatmosphäre.

Danke auch an das Sekretariatsteam um Jingnu Liu und Huiqun Li für die gute Zusammenarbeit und ihre Hilfe bei organisatorischen Fragen.

Außerdem möchte ich Dagmar Lettrich für ihre tatkräftige Unterstützung bei den Mörtelversuchen danken, sowie Dr. Johannes Stecher und Dr. Claudia Chomyn für ihre Hilfe bei den GPC Messungen.

Den Firmen BASF, Clariant und Huntsman danke ich für die Bemusterung von Chemikalien und Dr. Frank Obst von HeidelbergCement für die Bereitstellung der Zemente.

Ein großer Dank gebührt ebenfalls Schwenk Zement für die Ermöglichung anwendungstechnischer Versuche in ihrem Transportbetonwerk in Ludwigsfeld. Hierbei ist insbesondere die Unterstützung von Stefan Schmid hervorzuheben. Ferner danke ich Dr. Thomas Kränkel vom Zentrum für Baustoffe und Materialprüfung der TU München für seine Hilfe bei den Betonrheologie-Versuchen.

Außerdem möchte ich mich bei meinen Forschungspraktikanten Petra Bestler, Jonas Meringdal, Olivia Rindle, Moritz Ludwig, Nicole Dietl sowie meiner studentischen Hilfskraft Johanna Plansky für ihre Mitarbeit bedanken. Die Zusammenarbeit und die fachlichen Diskussionen haben mir viel Freude bereitet und einen wichtigen Beitrag zum Erfolg dieser Arbeit geleistet.

Meinen ehemaligen Kollegen Dr. Markus Meier, Dr. Vipasri Kanchanason, Dr. Somrudee Kuhlmann, Dr. Markus Schönlein, Dr. Lei Lei, Dr. Alexander Engbert, Marlene Schmid, Dominik Staude, Christopher Schiefer, Ran Li, Kenny Chan, Haijing Yang, Matthias Theobald und Matthias Werani danke ich für die gute Zusammenarbeit.

Abschließend möchte ich mich bei meinen Eltern bedanken, die stets hinter mir gestanden sind und mir diesen Weg erst ermöglichten. Ohne eure Motivation und Unterstützung wäre diese Arbeit nicht möglich gewesen, wofür ich euch aus tiefsten Herzen dankbar bin.

Manuel, September 2021

Wissenschaftliche Veröffentlichungen

Die vorliegende Arbeit umfasst 17 Veröffentlichungen, die in wissenschaftlichen Zeitschriften sowie in Tagungsbänden mit und ohne Peer-Review Verfahren publiziert wurden. Die Publikationen 1.) – 11.) werden in der Dissertation thematisch behandelt, während die restlichen Veröffentlichungen im Anhang aufgeführt sind.

Publikationen in wissenschaftlichen Zeitschriften und Tagungsbänden mit Peer-Review Verfahren:

1.) **M. Ilg**, J. Plank

"Improvement of SCC Flow Properties Through Addition of Non-Adsorbing Small Molecule Co-Dispersants"

In: K. H. Kayat (Ed.), 8th International RILEM Symposium on Self-Compacting Concrete – SCC 2016, Washington (USA), **2016**, Proceedings, 49 – 59.

2.) **M. Ilg**, J. Plank

"Novel Admixtures to Reduce the Stickiness of Low W/C Concretes"

In: J. Liu, Z. Wang, T. C. Holland, J. Huang, J. Plank (Eds.), Superplasticizers and Other Chemical Admixtures in Concrete, Proceedings Twelfth International Conference, Beijing (China), **2018**, SP-329-07, 77 – 88.

3.) **M. Ilg**, J. Plank

"Non-adsorbing small molecules as auxiliary dispersants for polycarboxylate superplasticizers"

Colloids and Surfaces A: Physicochemical and Engineering Aspects 587 **(2020)** 124307.

4.) **M. Ilg**, J. Plank

"Effect of non-ionic auxiliary dispersants on the rheological properties of mortars and concretes of low water-to-cement ratio"

Construction and Building Materials 259 **(2020)** 119780.

5.) **M. Ilg**, J. Plank

"Synthesis and Properties of a Polycarboxylate Superplasticizer with a Jellyfish-Like Structure Comprising Hyperbranched Polyglycerols"

Industrial & Engineering Chemistry Research 58 (29) **(2019)** 12913 – 12926.

6.) **M. Ilg**, J. Plank

"A New Type of Superplasticizer Possessing Dendrimeric Structure"

In: J. Liu, Z. Wang, T. C. Holland, J. Huang, J. Plank (Eds.), Superplasticizers and Other Chemical Admixtures in Concrete, Proceedings Twelfth International Conference, Beijing (China), **2018**, SP-329-08, 89 – 102.

7.) **M. Ilg**, J. Plank

"Synthesis of a Novel Superplasticizer Prepared from Brown Coal"

In: V. M. Malhotra, P. R. Gupta, T. C. Holland (Eds.), 11th CANMET/ACI Conference on Superplasticizers and Other Chemical Admixtures in Concrete, Ottawa (Canada), **2015**, ACI SP-302-05, 63 – 76.

8.) **M. Ilg**, J. Plank

"A novel kind of concrete superplasticizer based on lignite graft copolymers"

Cement and Concrete Research 79 **(2016)** 123 – 130.

Publikationen in Tagungsbänden ohne Review Verfahren:

9.) **M. Ilg**, J. Plank

"A New Dispersing Mechanism For Cement Augmented by Non-Adsorbing Molecules"

2nd International Conference on the Chemistry of Construction Materials (ICCCM), Munich (Germany), GDCh Monographie 50 **(2016)** 63 – 66.

10.) **M. Ilg**, J. Plank

"Synthesis and Characterization of a Novel Kind of Superplasticizer with Jellyfish-Like Structure Based on Hyperbranched Polyglycerols"

20. Internationale Baustofftagung (ibausil), Weimar (Germany), **2018**, Tagungsband 1, 835 – 842.

11.) **M. Ilg**, J. Plank

"Improving the flow properties of concretes prepared at low w/c ratio by using small molecule-based co-dispersant admixtures",

2nd International RILEM Conference on Rheology and Processing of Construction Materials (RheoCon2), Dresden (Germany), **2019**, Proceedings.

Veröffentlichung aus der Mitarbeit an Projekten anderer Doktoranden:

12.) J. Plank, H. Li, **M. Ilg**, J. Pickelmann, W. Eisenreich, Y. Yao, Z. Wang

"A microstructural analysis of isoprenol ether-based polycarboxylates and the impact of structural motifs on the dispersing effectiveness"

Cement and Concrete Research 84 **(2016)** 20 – 29.

Review Beiträge:

13.) J. Plank, **M. Ilg**

"Next Generation of PCE Superplasticizers"

47th Annual ICT Convention Symposium, London (UK), **2019**, ICT Yearbook 2019/2020.

14.) J. Plank, **M. Ilg**

"Chemical Admixtures for Low Carbon Cement Systems"

1st International Conference on Innovation in Low-Carbon Cement and Concrete Technology (ILCCC), London (UK), **2019**, Proceedings.

15.) J. Plank, **M. Ilg**

"Interaction of Superplasticizers with Cement from the Point of View of Colloid Chemistry"

In: V. Mechtcherine, K. Khayat, E. Secrieru (Eds.), Rheology and Processing of Construction Materials, RheoCon 2019, SCC 2019, RILEM Bookseries 23 **(2020)** 134-141.

16.) J. Plank, **M. Ilg**

"The Role of Chemical Admixtures in the Formulation of Modern Advanced Concrete"

In: W. Boshoff, R. Combrinck, V. Mechtcherine. M. Wyrzykowski (Eds.), 3rd International Conference on the Application of Superabsorbent Polymers (SAP) and Other New Admixtures Towards Smart Concrete, SAP 2019, RILEM Bookseries 24 **(2020)** 143 – 157.

17.) **M. Ilg**, J. Plank

"Flow-enhancing PCE-based superplasticizers for concretes of low W/C ratio such as UHPC"

In: B. Middendorf, E. Fehling, A. Wetzel (Eds.), 5th International Symposium on Ultra-High Performance Concrete and High Performance Construction Materials (HiPerMat), Kassel (Germany), **2020**, Proceedings, 65 – 66.

Abkürzungsverzeichnis

AA	Acrylsäure
AFM	Atomic force microscopy (Rasterkraftmikroskopie)
APEG	Allyl-Polyethylenglykol-Ether
ATBS	2-Acrylamido-2-methylpropansulfonsäure
ATRP	Atom transfer radical polymerization
BNS	β-Naphthalinsulfonsäure-Formaldehyd-Polykondensat
bwoc	by weight of cement (bezogen auf die Zementeinwaage)
DLS	Dynamische Lichtstreuung
DLVO	*Derjaguin, Landau, Verwey, Overbeek*
DMAEMA	Dimethylaminoethylmethacrylat
FTIR	Fourier-Transformations-Infrarotspektroskopie
GPC	Gelpermeationschromatographie
HEMAP	Hydroxyethylmethacrylat-Phosphatester
HLB	Hydrophilic-lipophilic balance
HPEG	Methallyl-Polyethylenglykol-Ether
HyPG	Hyperverzweigtes Polyglycerol
IPEG	Isoprenol-Polyethylenglykol-Ether
M_w	Gewichtsmittlere Molmasse
MDS	Molecular dynamic simulations
MFS	Melamin-Formaldehyd-Sulfit-Polykondensat
MPEG	Methoxy-Polyethylenglykol-Methacrylat-Ester
NMR	Nuclear magnetic resonance spectroscopy (Kernresonanzspektroskopie)
PAAM	Polyamidoamin
PCE	Polycarboxylatether
PEG	Polyethylenglykol
PDI	Polydispersitäts-Index
RAFT	Reversible-addition-fragmentation chain-transfer polymerization
R_g	Gyrationsradius
R_h	Hydrodynamischer Radius

SN2	Nukleophile Substitutionsreaktion
SVB	Selbstverdichtender Beton (self-compacting concrete – SCC)
THF	Tetrahydrofuran
TMBS	Bromtrimethylsilan
TME	1,1,1-Trimethylolethan
TMP	1,1,1-Trimethylolpropan
TMPTA	Trimethylolpropantriacrylat
TN	Total nitrogen (Menge an Stickstoff)
TOC	Total organic carbon (Menge an organischem Kohlenstoff)
UHPC	Ultrahochfester Beton (ultra-high performance concrete)
VPEG	Vinyl-Polyethylenglykol-Ether
w/b	Wasser zu Bindemittel
wt.%	Gewichtsprozent
w/z	Wasser zu Zement
XPEG	Quervernetztes Makromonomer
XPS	X-ray photoelectron spectroscopy (Röntgenphotoelektronen-spektroskopie)

Inhaltsverzeichnis

1. Einleitung

„Panta rhei (altgriechisch πάντα ῥεῖ) – Alles fließt."

Dieser Aphorismus, der auf den griechischen Philosophen *Heraklit von Ephesos* zurückgeht, wird von der *„American Society of Rheology"* seit ihrer Gründung im Jahr 1929 als Leitspruch verwendet [1, 2]. Zu den bekanntesten Gründungsmitgliedern gehörten *Eugene Bingham* und *Markus Reiner*, die sich mit der Fluidität und Plastizität beschäftigten und hierzu pionierhafte Arbeiten leisteten [3, 4]. Diese beiden schlugen auch vor ihr Forschungsgebiet, in dem die Fließ- und Verformungseigenschaften von Stoffen in Abhängigkeit von äußeren Kräften untersucht werden, als Rheologie zu benennen. Die Bezeichnung hierfür entlehnten sie dem oben erwähnten Zitat, das auf prägnante Art verdeutlicht, dass die Materie einem ständigen Fluss bzw. Änderungen unterworfen ist, und nicht nur Fluide, sondern auch Festkörper fließen können. So zeigt beispielsweise die Lithosphäre aufgrund der tektonischen Plattenbewegungen ein Fließverhalten [5, 6] und auch für Gletscher kann ein solches infolge der Gravitationskraft gemessen werden [7-9].

Die Rheologie ist eine interdisziplinäre Wissenschaft, die in verschiedensten Bereichen angewendet wird, wie etwa in der physikalischen und technischen Chemie, den Bio- und Geowissenschaften oder in der Materialtechnik. Die starke Verflechtung der Rheologie mit diesen Disziplinen lässt sich darauf zurückführen, dass wichtige Informationen über die Stoffeigenschaften aus dem rheologischen Verhalten abgeleitet werden können, die für die Aufklärung phänomenologischer Effekte, für prozesstechnische Fragestellungen aber auch für die Entwicklung neuer Materialien von großem Nutzen sind [10-12]. Neben der Wissenschaft und Materialforschung spielt die Rheologie ebenfalls in der Industrie eine entscheidende Rolle. Hier wird sie bei der Prozessteuerung, Stabilitäts- und Qualitätskontrolle [13] oder auch bei der Produktentwicklung als wichtiges Kriterium herangezogen [14]. Die Anwendungs- und Verarbeitungseigenschaften (Pumpbarkeit, Fließfähigkeit, Extrudierbarkeit, Misch- und Schmierverhalten, Streichfähigkeit) werden von rheologischen Stoffgrößen (Fließgrenze, plastische Viskosität) maßgeblich bestimmt, die gezielt modifiziert werden können, um Produkte maßzuschneidern und sie an die entsprechende Applikation anzupassen. Daher werden rheologische Messmethoden heutzutage standardmäßig in unterschiedlichen Industriebereichen eingesetzt, wie in der Lebensmittel- [15], Kosmetik- [16], Farb- und

Lackindustrie [17], Pharmazie [18] oder bei der Kunststoffverarbeitung [19] (sh. **Abbildung 1**). In der Bauindustrie ist die Rheologie ebenfalls sehr wichtig, da sie beispielsweise bei der Verarbeitung von Baustoffen oder auch bei der Applikation von Farben und Klebstoffen entscheidend ist [20, 21]. Abhängig vom jeweiligen Einsatzgebiet ist ein bestimmtes rheologisches Verhalten erforderlich, das durch die spezifische Zusammensetzung der Formulierung bzw. den Einsatz von chemischen Zusatzmitteln eingestellt werden kann. So sind in Farben Verdickungsmittel enthalten, die dafür sorgen das die Farbe aufgrund einer hohen Viskosität gut auf der Farbrolle haftet, die Farbe jedoch leicht auf die Wand aufgetragen werden kann, da die Viskosität durch die Scherung beim Streichen erniedrigt wird (sog. strukturviskoses Verhalten) [22, 23]. Sobald keine Scherung mehr aufgewendet wird, baut sich die ursprüngliche Viskosität wieder auf und die Farbe haftet an der Wand.

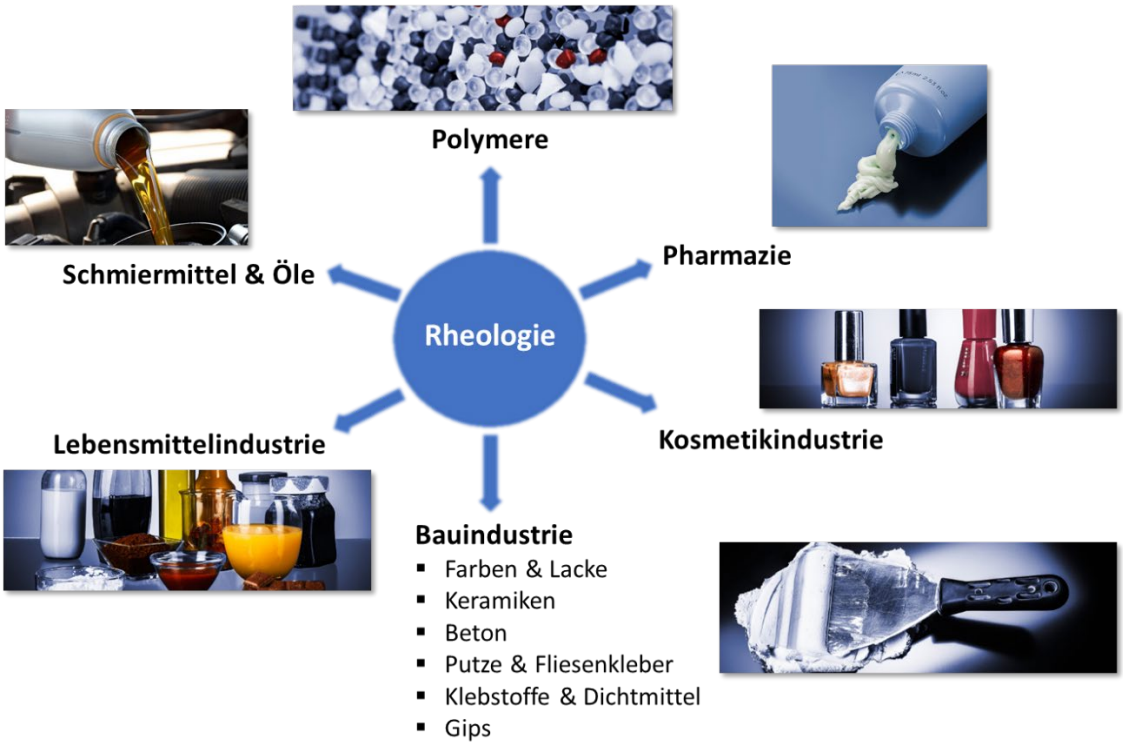

Abbildung 1: Übersicht über verschiedene Anwendungsfelder rheologischer Messmethoden (Fotos übernommen aus [24 a– e]).

Auch bei der Verarbeitung von zementären und gipsbasierten Baustoffen werden chemische Zusatzmittel eingesetzt, um das Fließverhalten bzw. die Rheologie in der Anfangsphase zu steuern und über einen gewissen Zeitraum zu kontrollieren [25, 26]. Diese Additive, die in Dosierungen zwischen 0,01 – 2,0 % verwendet werden, verbessern die Verarbeitbarkeit, gewährleisten einen schnellen und effizienten

Baufortschritt und tragen dazu bei, die Qualität sowie Materialeigenschaften zu verbessern. Heutzutage sind in Europa etwa 95 % der hergestellten Betone mit Zusatzmitteln formuliert. Es existiert eine vielfältige Produktpalette von Additiven, die gemäß ihrer Funktion in Verflüssiger, Fließmittel, Verzögerer, Beschleuniger, Stabilisierer, Verdickungsmittel, Schäumer, Entschäumer, Luftporenbildner, Schwindreduzierer etc. unterteilt werden [25, 27-29]. Diese Bandbreite ermöglicht es auf unterschiedliche Art, die Rheologie und die finalen Materialeigenschaften zu beeinflussen (sh. **Abbildung 2**). Es wird geschätzt, dass derzeit weltweit pro Jahr ein Bedarf von 8 Mio. Tonnen an Zusatzmitteln besteht, was einem Marktvolumen von etwa 6 Mrd. Euro entspricht.

Abbildung 2: Darstellung der wichtigsten Gruppen bauchemischer Zusatzmittel und Erläuterung ihrer Funktion; Fotos übernommen aus [30 a-g].

Verflüssiger und Fließmittel werden zur Desagglomeration von Bindemittelteilchen zugegeben, um die Fließfähigkeit bzw. Konsistenz zu verbessern und folglich eine leichtere Verarbeitbarkeit sicherzustellen [28, 31]. Die Dispergierwirkung von

Fließmitteln ist hierbei so effektiv, dass diese auch bei niedrigen Wasser-Bindemittel-Verhältnissen in der Lage sind, die rheologischen Eigenschaften zu verändern. Außerdem kann mit Fließmitteln der Wasseranspruch um 20 – 60 % reduziert werden, wodurch Materialien erhalten werden, die sich durch eine geringere Porosität und höhere Druckfestigkeit auszeichnen [32, 33]. Solche Baustoffe sind wesentlich dauerhafter und beständiger, da durch den verringerten Wassergehalt ein dichteres Gefüge entsteht, das weniger anfällig gegenüber Schadreaktionen ist. Da Nachhaltigkeitsaspekte und ein ressourcenschonender Umgang mit Rohstoffen auch in der Bauindustrie immer mehr von Bedeutung sind, ergab sich in den letzten Jahren eine verstärkte Nachfrage nach qualitativ sehr hochwertigen und dauerhaften Baumaterialien. Um diesen Ansprüchen gerecht zu werden, werden Hochleistungsbaustoffe, wie z.B. ultrahochfeste oder selbstverdichtende Betone, zunehmend eingesetzt. Diese Betone verfügen über eine hohe mechanische Festigkeit, sind bei niedrigen Wasser-Zement-Werten $< 0{,}4$ formuliert und enthalten oftmals Zuschlagstoffe wie Mikrosilika, um die Packungsdichte zu erhöhen [34, 35]. Damit solche Betone verarbeitet werden können, sind Fließmittel unabdingbar [26, 34, 36, 37]. Es werden vorwiegend Polycarboxylat-Fließmittel (PCEs) hierfür verwendet, die aufgrund ihrer spezifischen Polymerstruktur zu den leistungsstärkten Fließmitteln gehören. Architektonische Meisterwerke wie der Burj Khalifa in Dubai, bei dessen Bau der Beton über mehrere Stunden fließfähig sein musste, da er bis auf eine Höhe von 600 Metern gepumpt wurde, konnte nur durch den Einsatz von PCEs realisiert werden.

PCE-Fließmittel sind kammförmige Polymere, die aus einer Hauptkette mit negativ geladenen Carboxylatgruppen und mehreren ungeladenen Polyethylenglykol-basierten Seitenketten aufgebaut sind [25, 28, 38]. Seit ihrer Erfindung Anfang der 80er Jahre entwickelten sie sich aufgrund ihrer hohen Dispergiereffizienz zur wichtigsten Fließmittelgruppe, die Polykondensat-Fließmittel und Lignosulfonat-Verflüssiger in herkömmlichen Fließbetonen sukzessive ersetzte und darüber hinaus die technische Entwicklung von Hochleistungsbetonen ermöglichte. Ein großer Vorteil von PCEs ist ihre große chemische Strukturvariabilität, die es ermöglicht die Polymerstruktur gezielt zu modifizieren, um ein gewünschtes Anwendungsprofil zu erhalten [38-43]. Beispielsweise werden PCEs mit wenigen und langen Seitenketten vorwiegend im Fertigteilbeton verwendet, während PCEs mit vielen und kürzeren Seitenketten vorteilhafter im Transportbeton sind. Die starke Verflüssigungswirkung von PCEs lässt

sich dadurch erklären, dass sie im Gegensatz zu anderen Fließmitteltypen die Bindemittelteilchen sowohl über einen elektrostatischen als auch sterischen Dispergiereffekt stabilisieren [44, 45]. Um wirksam zu werden, muss eine Adsorption der PCE Polymere auf der Bindemitteloberfläche stattfinden [46-49].

Obwohl PCEs sehr potente Fließmittel sind, ergeben sich teilweise einige Probleme in der Anwendung. So wird aus der Praxis berichtet, dass PCEs bestimmte Zemente nicht ausreichend dispergieren können [50], oder sie in Gegenwart von Sulfationen [51] oder Tonmineralien nur unzureichend wirksam sind [52]. Außerdem wurde bei wasserarmen Betonen mit w/z-Werten < 0,3 häufig festgestellt, dass diese zwar mit PCEs sehr gut verflüssigt werden können, die Betone aber ein kriechendes und langsames Fließverhalten aufweisen, das die Verarbeitung erheblich erschwert [53]. Es ist daher notwendig die PCE-Technologie kontinuierlich weiterzuentwickeln und zu optimieren sowie grundlegende Untersuchungen zur Struktur-Wirkungsbeziehung durchzuführen, damit gewisse Effekte besser verstanden werden können und um PCE-Strukturen zu identifizieren, die am besten für bestimmte Anwendungen geeignet sind.

2. Aufgabenstellung

Es ist allgemein bekannt, dass PCEs über Adsorption wechselwirken, bei der sich die Polymere über die anionischen Carboxylatgruppen an den positiv geladenen Oberflächenbereichen anlagern [25, 26, 46]. Die Zementteilchen weisen danach eine negative Gesamtladung auf, die eine elektrostatische Abstoßung zur Folge hat [54]. Die Polyethylenglykol-Seitenketten sorgen hingegen für eine sterische Stabilisierung und fungieren als Abstandshalter, die eine erneute Agglomeration der Zementpartikel verhindern [44, 45, 55]. Neueste Studien deuten allerdings darauf hin, dass auch der Anteil an nicht-adsorbierten PCE-Polymeren in der Porenlösung zur Dispergierung beitragen kann [56, 57]. Dieser Effekt scheint insbesondere bei niedrigen w/z-Werten in Erscheinung zu treten. Erste Vorarbeiten zu diesem Thema am Lehrstuhl legten nahe, dass nicht-ionische Polymere, die PCE-Fließmitteln zugegeben werden, einen ähnlichen Effekt hervorrufen können [58].

Basierend auf diesen vorangegangen Ergebnissen wurde deshalb **im ersten Teil dieser Arbeit** untersucht, ob nicht-ionische Verbindungen ebenfalls dispergieren und wie sie

sich auf die Fließeigenschaften von zementären Systemen auswirken. Es wurde eine Vielzahl von ungeladenen niedermolekularen Molekülen sowie Polymeren getestet und mit strukturell unterschiedlichen PCE-Fließmitteln kombiniert. Über Untersuchungen im Zementleim sollte herausgefunden werden, bei welchen w/z-Werten die nicht-ionischen Co-Dispergiermittel besonders wirkungsvoll sind und welche PCE-Strukturen am stärksten von ihrer Zugabe profitieren. Durch das breite Screening verschiedener nicht-ionischer Verbindungen sollten diejenigen Strukturmerkmale identifiziert werden, die für die Dispergierung förderlich sind und das Fließverhalten verbessern. Mechanistische Untersuchungen zum Adsorptionsverhalten sowie zur Oberflächenspannung von Porenlösungen wurden vorgenommen, um Einblicke in den zugrundeliegenden Wirkmechanismus zu erhalten.

Der zweite Teil dieser Arbeit beschäftigte sich mit Untersuchungen zum Einfluss der nicht-adsorbierenden Co-Dispergiermittel auf die rheologischen Eigenschaften von Mörteln und Betonen mit niedrigen w/z-Werten. Wie zuvor beschrieben, sind PCE-Fließmittel in der Lage wasserarme Systeme sehr gut zu verflüssigen, sodass ein hohes Ausbreitmaß eingestellt werden kann. Allerdings benötigen solche wasserarmen Mörtel bzw. Betone eine lange Zeit, um das finale Ausbreitmaß zu erreichen. Ursache hierfür ist, dass durch die Reduzierung des Wasseranteils der Feststoffanteil stark zunimmt, wodurch eine honigartige und zähe Konsistenz resultiert, die ein langsames und kriechendes Fließverhalten zur Folge hat. Ein solches rheologisches Verhalten ist auf der Baustelle unerwünscht, da es das Verpumpen, Befüllen von Schalungen sowie das Verdichten erschwert und daher oftmals Baumängel infolge eines schlechten Formfüllungsvermögens auftreten. Bisher existieren nur wenige Lösungsansätze, wie die Fließgeschwindigkeit verbessert werden kann [59, 60]. Über eine Reduzierung der plastischen Viskosität ist es jedoch möglich, die klebrige Konsistenz zu verringern. Es müssen daher Konzepte gefunden werden, mit denen die plastische Viskosität minimiert werden kann. In diesem Zusammenhang wurden die nicht-ionischen Co-Dispergier-mittel in Mörtel und Betonen mit einer relativ klebrigen Konsistenz getestet. Ihr Einfluss auf die plastische Viskosität und Fließgrenze wurde in der Fließrinne, im V-Trichter und durch Ausbreitmaß-Versuche evaluiert. Darüber hinaus wurden anwendungstechnische Versuche in einem Transportbetonwerk durchgeführt, um festzustellen, wie sich die nicht-ionischen Verbindungen auf das Fließverhalten von selbstverdichtenden Betonen auswirken und ob die Klebrigkeit durch ihre Zugabe verringert wird. Ziel war es, mit

Hilfe der gewonnenen Erkenntnisse ein finales mechanistisches Modell aufzustellen, mit dem die Wirkungsweise der nicht-ionischen Moleküle erklärt werden konnte.

Die starke Dispergierwirkung der PCEs beruht auf dem sterischen Effekt der Polyethylenglykol-Seitenketten [25, 45]. PCEs mit längeren Seitenketten sorgen für eine bessere Stabilisierung als PCEs mit kurzkettigen PEGs [61, 62]. Mehrere Studien konnten eindeutig den Nachweis erbringen, dass sterisch anspruchsvollere PCEs mit einer höheren Schichtdicke auf der Bindemitteloberfläche adsorbieren und dadurch in der Lage sind, die Zementpartikel sterisch besser abzuschirmen [61, 63, 64]. Außerdem benötigen sie in der Regel eine niedrigere Dosierung für eine vollständige Oberflächenbelegung [65]. Bei der Entwicklung von neuen PCEs wird deshalb zunehmend versucht, ihre Wirksamkeit durch eine Erhöhung des sterischen Effekts zu verbessern. Dies kann beispielsweise durch das Einbringen von sterisch anspruchsvolleren Monomeren in das Polymer realisiert werden, aber auch verzweigte bzw. hyperverzweigte (stark verzweigte) Strukturen stellen ein interessantes Konzept hierfür dar. Bis dato gibt es allerdings nur Beispiele für verzweigte Fließmittel [66, 67], wohingegen Fließmittel mit hyperverzweigten Strukturelementen nur wenig erforscht sind. Um diese Lücke in der Literatur zu schließen, wurde **im dritten Teil der Arbeit** ein hyperverzweigtes Fließmittel synthetisiert, das ausgehend von einem linearen Polyetheramin über eine anionische Ringöffnungspolymerisation von Glycidol hergestellt wurde. Der Vorteil von hyperverzweigten Polyglycerolen ist, dass sie über einen einzelnen Syntheseschritt zugänglich sind. Im Vergleich zu kammförmigen PCEs setzt sich das neue Fließmittel aus zwei Strukturblöcken zusammen – einem linearen Polyetheramin sowie einem carboxymethylierten Polyglycerolgerüst. Das Fließmittel wurde im Zementleim getestet und dessen Robustheit in Gegenwart von Sulfationen bestimmt. Ferner wurde das Adsorptionsverhalten sowie der Einfluss auf die Zementhydratation näher beleuchtet. Das übergeordnete Ziel war es, Informationen über die Anwendungseigenschaften von PCEs mit hyperverzweigten Strukturen zu erhalten, sodass eine Einschätzung zu möglichen Einsatzfeldern vorgenommen werden konnte. Außerdem sollte durch die Synthese und das Austesten von strukturell verschiedenen Polymervorstufen untersucht werden, welcher Strukturbaustein des neuen Fließmittels jeweils am stärksten zur sterischen Stabilisierung beiträgt.

Der vierte Teil der Arbeit handelt über die Synthese und Charakterisierung eines Fließmittels, welches ausgehend von Lignit bzw. Braunkohle hergestellt wurde. Anders

als bei herkömmlichen PCEs, die meistens aus einem aliphatischen Polymerrückgrat bestehen und dadurch über eine hohe konformationelle Flexibilität verfügen, weist das neue Fließmittel eine relativ starre Hauptkette auf, die sich aus mehreren kondensierten aromatischen Strukturelementen zusammensetzt. Als Polymerhauptkette wurden Humin- und Fulvinsäuren eingesetzt, die über eine alkalische Extraktion aus Braunkohle gewonnen wurden. Auf diese löslichen Bestandteile wurden die Monomere 2-Acrylamido-2-methylpropansulfonsäure (ATBS) und Acrylsäure (AA) über eine freie radikalische Copolymerisation aufgepfropft. Dadurch wurde ein Fließmittel erhalten, welches eine Humin- bzw. Fulvinsäure als Rückgrat enthält, von der mehrere ATBS-*co*-Acrylsäure-Polymere als Seitenketten ausgehen, über die eine Wechselwirkung mit der Zementkornoberfläche erfolgen kann. Die Polymereigenschaften (Molekulargewicht, Lösungskonformation, anionische Ladung etc.) und die Dispergierwirkung des Lignit-haltigen Fließmittels wurden untersucht und Messungen zur adsorbierten Schichtdicke vorgenommen. Ziel war es herauszufinden, wie sich eine starre bzw. gestreckte Konformation auf die Verflüssigung auswirkt und welche Vorteile sich mit einer solchen Struktur gegenüber flexiblen bzw. geknäulten Polymeren ergeben.

3. Theoretischer Hintergrund

3.1. Rheologie von zementären Systemen

Zementleim, Mörtel und Beton können als eine Suspension von polydispersen Partikeln in Wasser angesehen werden [68]. Anders als im Zementleim, der nur eine Mischung aus Zement und Wasser darstellt, werden im Mörtel sowie Beton zusätzlich noch Sand und Kies verwendet. Im Mörtel beträgt die maximale Größe der Gesteinskörnungen 4 mm, während im Beton deutlich grobkörnigere Partikel (bis 32 mm) enthalten sind. Die Eigenschaften von zementbasierten Suspensionen werden im Ruhezustand und während des Fließens durch interpartikuläre Wechselwirkungen bestimmt [69]. Insbesondere die Interaktionen zwischen den Zementteilchen der Leimphase sind für das rheologische Verhalten maßgeblich entscheidend. Hierbei handelt es sich um kolloidale Oberflächenwechselwirkungen und Interaktionsarten, die durch die *Brown*'sche Molekularbewegung, hydrodynamische Effekte oder durch den direkten Kontakt zwischen den Partikeln (z.B. durch Reibung, Gleiteffekte, Kollision) zustande kommen [69, 70]. In Abhängigkeit von der Scherung, Größe, Oberflächenbeschaffenheit und Konzentration der Partikel finden eine oder mehrere dieser Wechselwirkungen bevorzugt statt [69, 71].

Die Rheologie von zementären Systemen kann in guter Näherung mit dem *Bingham* Modell beschrieben werden [68, 72]. Charakteristisch für *Bingham* Fluide ist, dass sie eine Mindestscherspanung τ_0 erfordern, die aufgewendet werden muss, damit ein Übergang von einem elastischen in einen fließfähigen Zustand stattfindet. Oberhalb von τ_0 liegt ein linearer Zusammenhang zwischen der Schergeschwindigkeit $\dot{\gamma}$ und der Viskosität μ vor (sh. **Gleichung 1**).

$$\tau = \tau_0 + \mu\,\dot{\gamma} \tag{1}$$

Abbildung 3 zeigt die charakteristische Fließkurve eines *Bingham* Fluids. Eine solche Fließkurve wird durch rheometrische Messmethoden erhalten, bei denen die Scherspannung in Abhängigkeit von der Schergeschwindigkeit gemessen wird [72-74]. Aus einem Rheogramm können wichtige rheologische Kenngrößen abgeleitet werden. So stellt der Schnittpunkt der Fließkurve mit der Ordinate die Fließgrenze dar, während die Steigung der plastischen Viskosität entspricht [75]. Die Fließgrenze ist ein Maß für die Stabilität einer Suspension und beruht auf interpartikulären Wechselwirkungen (v.a.

Van der Waals Kräften) zwischen den Zementteilchen [68, 70]. Die plastische Viskosität ist hingegen ein Maß für den Widerstand des Fluids während des Fließens. Je niedriger die plastische Viskosität, umso leichter kann ein solches System verarbeitet werden (z.B. leichter verpumpbar, streichbar etc.). Außerdem weisen Systeme mit einer niedrigen plastischen Viskosität hohe Fließgeschwindigkeiten auf [53].

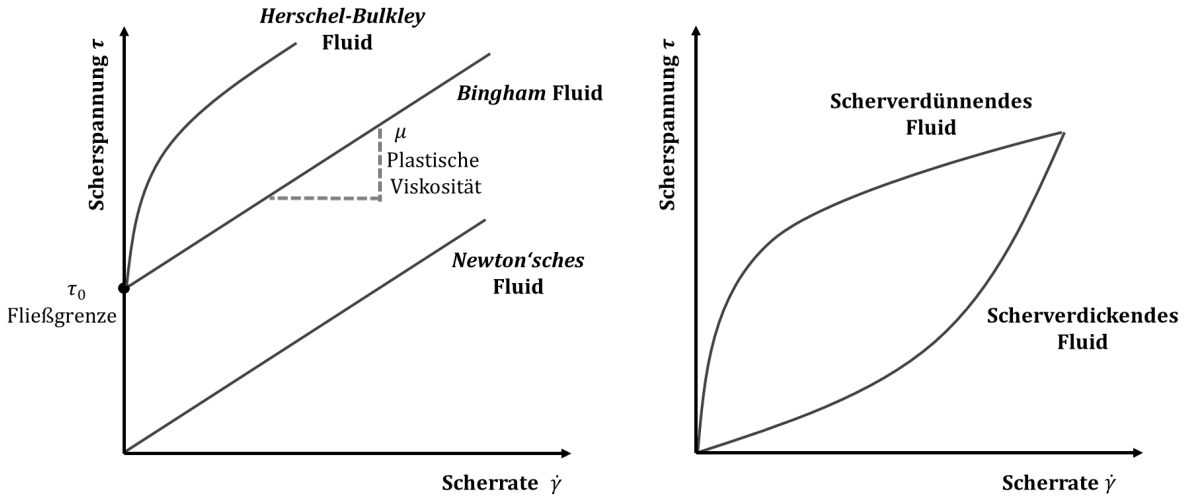

Abbildung 3: Scherspannung in Abhängigkeit von der Scherrate für unterschiedliche Arten von Fluiden.

Fluide, die keine Fließgrenze besitzen, für die aber ein linearer Zusammenhang zwischen der Scherspannung und Schergeschwindigkeit besteht, werden als *Newton'sche* Fluide bezeichnet (z.B. Wasser, niedrig siedende Kohlenwasserstoffe) [73]. Viele Fluide zeigen in der Praxis allerdings ein nicht lineares Fließverhalten in Abhängigkeit von der Scherbeanspruchung. Hierbei können zwei unterschiedliche Fälle vorliegen. Nimmt die Viskosität mit zunehmender Scherung ab, spricht man von einem sog. scherverdünnenden (strukturviskosen) Verhalten, während bei einer Viskositätszunahme das Fluid als scherverdickend (dilatant) bezeichnet wird [25, 72, 73]. Solche rheologischen Eigenschaften können durch Tone, wie beispielsweise Bentonit (strukturviskos) [76] oder hochmolekulare Polymere, wie Assoziativverdicker (dilatant) erhalten werden [77]. Um die Fließkurve von solchen Systemen zu beschreiben, wird üblicherweise das *Herschel-Bulkley* Model verwendet, bei dem zwei zusätzliche Parameter zum Einsatz kommen, der Konsistenzindex k und Fließindex n [74, 78]. Im Fall von scherverdickenden Fluiden ist $n > 1$ bzw. von scherverdünnenden Fluiden $n < 1$.

Zementbasierte Suspensionen zeigen abhängig von den eingesetzten Zusatzstoffen ein unterschiedlich starkes thixotropes Verhalten [79, 80]. Darunter versteht man die zeitliche Abnahme der Viskosität bei konstanter Scherung und den Wiederanstieg auf den Ausgangswert, sobald keine Scherbeanspruchung mehr aufgewendet wird [68]. Zurückgeführt wird dies darauf, dass ein vorhandenes Netzwerk aus frühen Hydratphasen zwischen den Zementpartikeln durch die Scherung zerstört wird, wodurch eine niedrigere Viskosität resultiert. Sobald die Scherung beendet wird, nimmt die Viskosität wieder zu, da sich das Netzwerk erneut ausbildet [81, 82].

Die Fließgrenze und Viskosität werden von unterschiedlichen Faktoren beeinflusst [75, 83, 84]. **Abbildung 4** zeigt, wie sich bestimmte Parameter auf die rheologischen Kenngrößen eines Betons auswirken. Wie ersichtlich, reduzieren Fließmittel und Verflüssiger primär die Fließgrenze, während die plastische Viskosität nahezu unverändert bleibt. Weitere Faktoren, die einen Einfluss auf die Rheologie haben, sind unter anderem die Korngrößenverteilung [84], Partikelmorphologie [85-87] und der Volumenanteil der Füllstoffe [88], die Wassermenge [89], Temperatur [90] und der Luftgehalt der Mischung [91, 92], die Anmischweise [93, 94] sowie die chemischen und physikalischen Eigenschaften des Bindemittels [95-97] und der Zusatzstoffe (z.B. Flugasche, Hüttensand, Mikrosilika etc.) [98, 99].

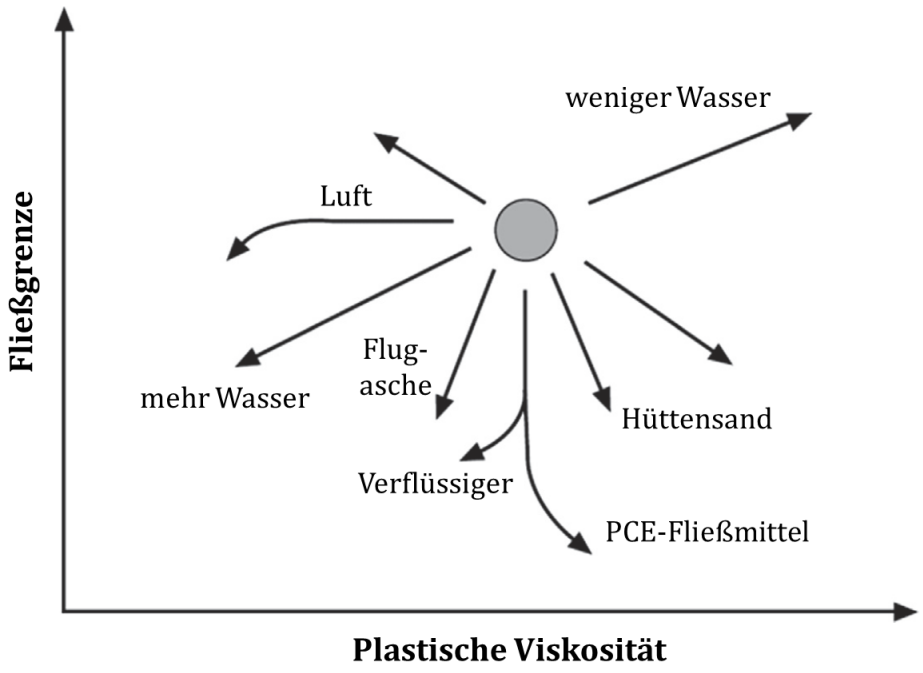

Abbildung 4: Einfluss unterschiedlicher Faktoren auf die rheologischen Kenngrößen von Beton; modifizierte Abbildung gemäß [100].

Zur Untersuchung der Rheologie haben sich neben der Rheometrie auch zahlreiche empirische Testmethoden etabliert, mit denen ebenfalls Aussagen zur Fließgrenze und plastischen Viskosität getroffen werden können. So wird zur Bestimmung der Fließgrenze häufig der Fließmaß- bzw. Ausbreitmaßtest durchgeführt [101, 102]. Hierbei wird das zementäre Gemisch in einen Konus gefüllt, der anschließend hochgehoben wird. Die Masse breitet sich danach solange unter dem Einfluss der eigenen Gewichtskraft aus, bis die Schubspannung unterhalb der Fließgrenze liegt [103]. Basierend auf dem Durchmesser des resultierenden „Kuchens" kann auf die Fließgrenze zurückgeschlossen werden [104]. Hierbei gilt, dass eine umso niedrigere Fließgrenze vorliegt, je größer der Durchmesser ist. Die plastische Viskosität wird hingegen über eine Messung der Fließgeschwindigkeit bestimmt. Ein Test, der häufig zum Einsatz kommt, ist der sog. V-Trichter Versuch. Ein Mörtel bzw. Beton wird hier in einen Trichter gefüllt und anschließend wird die Zeit gemessen, die dieser benötigt, um aus dem Trichter vollständig entleert zu werden [105, 106]. Je schneller die Auslaufzeit, umso niedriger ist die vorherrschende plastische Viskosität. Eine weitere Testmethode ist die Fließrinne. Hierbei wird der Mörtel in einen trichterförmigen Behälter überführt und von dort aus in eine horizontale Rinne entleert [53]. Dabei wird die Zeit ermittelt, die der Mörtel benötigt, um eine bestimmte Strecke zurückzulegen.

3.2. Wirkmechanismus von PCE-Fließmitteln

Zement setzt sich aus vier verschiedenen Klinkerphasen zusammen – Tricalcium-oxysilikat ($Ca_3O(SiO_4)$; C_3S) [107], Dicalciumsilikat (Ca_2SiO_4; C_2S), Tricalciumaluminat ($Ca_9(Al_6O_{18})$; C_3A) sowie Tetracalciumaluminatferrat ($Ca_4(Al,Fe)_4O_{10}$; C_4AF) [108, 109]. Ebenfalls sind in geringen Mengen Calciumsulfat Halbhydrat ($CaSO_4 \cdot ½\ H_2O$) oder Gips ($CaSO_4 \cdot 2\ H_2O$) enthalten, die bei der Aufmahlung des Zementklinkers zur Abbinderegelung zugegeben werden. Ohne jegliches Sulfat würde das C_3A gleich zu Beginn der Hydratation zu Calciumaluminathydrat-Phasen reagieren, die den Porenraum durch ein kartenhausähnliches Gefüge überbrücken und zu einem raschen Erstarren führen, wodurch das System nicht verarbeitbar wäre (sog. „Löffelbinder") [109, 110]. Beim Vorhandensein einer ausreichenden Menge an Sulfat (C_3A/Gips Verhältnis ≥ 3) wird hingegen Ettringit (Calciumaluminattrisulfat; Aft) gebildet, das eine kurzstielige und gedrungene Kristallmorphologie aufweist und den Porenraum nicht verbrückt [111]. Die Ettringitkristalle bedecken die Oberfläche des Zements bzw. von

C_3A und verlangsamen durch eine Passivierung die C_3A-Hydratation, weshalb das System zu Beginn länger verarbeitbar bleibt [112].

Wird Wasser zum Zement gegeben, finden Lösungsvorgänge statt, bei denen Ca^{2+}, Al^{3+}, Mg^{2+}, OH^-, SO_4^{2-} und eine Reihe anderer Ionen in Lösung gehen [110]. Sobald eine Sättigung erreicht ist, kristallisieren erste Hydratationsprodukte wie Ettringit und Portlandit aus der Porenlösung aus. Während des Auflösevorgangs entwickeln die silikatischen Klinkerphasen eine negative Oberflächenladung durch die Deprotonierung ihrer Silanolgruppen infolge des stark alkalischen pH-Werts der Porenlösung, während die Aluminatphasen sowie Ettringit eine positive aufweisen [46, 111, 113]. Durch die heterogene Oberflächenladung treten anziehende *Van der Waals*-Wechselwirkungskräfte zwischen den entgegengesetzt geladenen Bereichen auf, das zu einer Agglomeration der Zementpartikel führt [114, 115]. Bei der Zusammenlagerung der Zementteilchen wird ein Teil des Anmachwassers eingeschlossen (sog. Flockenbildung), das danach nicht mehr für die Fließfähigkeit zur Verfügung steht und daher eine schlechte Verarbeitbarkeit bedingt [116]. Anionische Polymere wie Polycarboxylat-Fließmittel können jedoch eingesetzt werden, um diese Agglomerate aufzulösen. Durch die Desagglomeration wird das eingeschlossene Wasser freigesetzt und das Fließverhalten dadurch verbessert [116]. PCE-Fließmittel erzielen die Dispergierung über eine elektrostatische und sterische Stabilisierung, die im Folgenden erläutert werden sollen [25, 28]:

PCEs weisen anionische Carboxylat-Gruppen auf, über die das Polymer auf der Bindemitteloberfläche adsorbiert [117, 118]. Die Adsorption ist ein mehrstufiger Prozess, bei dem das Polymer zunächst an die fest-flüssig Grenzfläche diffundiert, über Physisorption an die Oberfläche bindet und sich anschließend dort so lange neu umorientiert, bis die maximale Anzahl an Bindungspunkten erreicht ist [119]. Das PCE-Polymer adsorbiert hierbei nicht auf dem gesamten Zementkorn, sondern vorwiegend auf den positiv geladenen Oberflächen der aluminatischen Phasen sowie den ersten Hydratationsprodukten Ettringit und Monosulfat [46, 113]. Nach der Adsorption der PCEs weisen die Zementpartikel eine negative Oberflächenladung auf, die zu einer elektrostatischen Abstoßung führt. Die elektrostatische Stabilisierung wird durch die DLVO Theorie beschrieben, die nach ihren Endeckern *Derjaguin, Landau*, *Verwey* und *Overbeek* benannt wurde [120, 121]. Die Stärke des elektrostatischen Effekts hängt von der elektrischen Ladung sowie der *Debye*-Länge ab, die die Dicke der Ionenschicht um

die Zementpartikel darstellt [69, 122]. Allerdings beruht die starke Dispergierwirkung der PCEs hauptsächlich auf dem sterischen Effekt der PEG Seitenketten [44, 45, 123]. Diese ragen nach der Adsorption des Polymers in die Porenlösung und verhindern durch osmotische und entropische Effekte eine Agglomeration der Zementpartikel (sh. **Abbildung 5**) [48]. Da der sterische Effekt im Vergleich zum elektrostatischen viel weitreichender ist, können PCEs eine stärkere Dispergierung als Polykondensat-Fließmittel (z.B. MFS, BNS) erzielen, die nur über einen elektrostatischen Mechanismus wirken [124]. Die sterische Stabilisierung wird durch die *Ottewill-Walker*-Gleichung beschrieben (sh. **Gleichung 2**) [125].

$$V_{sterisch}(a) = \frac{4\,\pi\,k\,T\,C_v^2}{3\,v_1^2\,\rho_2^2}\,(\psi_1 - \kappa_1)(\delta - a)^2\left(3R + 2\delta + \frac{a}{2}\right) \qquad (2)$$

Darin ist C_v die Konzentration des adsorbierten Polymers, v_1 das molare Volumen der Lösungsmittelmoleküle, δ die adsorbierte Schichtdicke, ρ_2 die Dichte des Adsorbats, ψ_1 die Entropie, κ_1 die Enthalpie, R der Radius des Adsorbats und a der Abstand zwischen zwei Adsorbat-Teilchen. Aus dieser Gleichung geht hervor, dass die Größe des sterischen Effekts unter anderem davon abhängt, mit welcher Schichtdicke δ das Polymer auf der Oberfläche adsorbiert. Das bedeutet, dass insbesondere Polymere, die eine hohe adsorbierte Schichtdicke erzeugen, eine starke sterische Abstoßung bewirken.

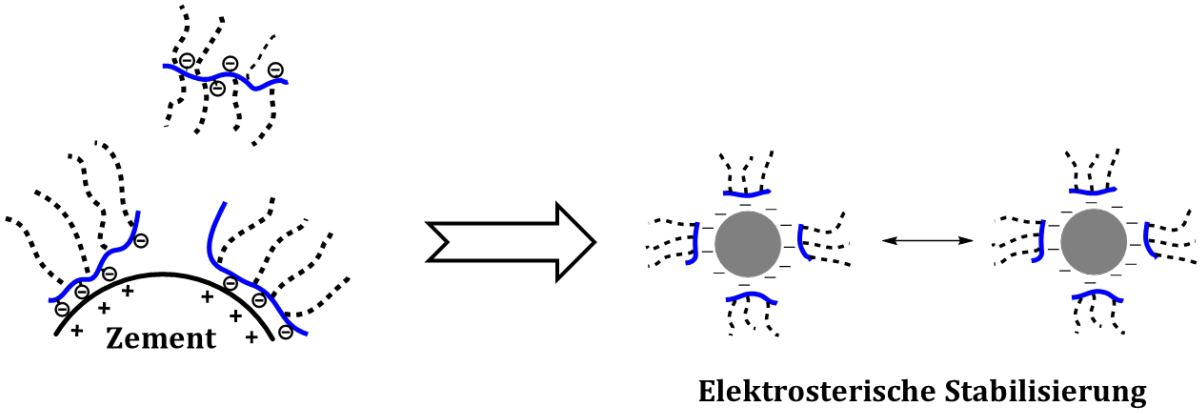

Abbildung 5: Elektrosterischer Dispergiermechanismus von PCE-Fließmitteln.

Die Bedeutung der adsorbierten Schichtdicke für die sterische Stabilisierung wurde in zahlreichen Studien gezeigt [44, 45, 64, 126, 127]. *Houst* et al. konnten über Rasterkraftmikroskopie (AFM) nachweisen, dass PCEs mit längeren Seitenketten zu einer höheren Schichtdicke führen und daher eine stärkere Dispergierung hervorrufen [63]. Neben der Seitenkettenlänge hängt die Schichtdicke aber auch davon ab, wie das

Polymer auf der Oberfläche adsorbiert [64, 126, 128-130]. Eine *„Train“*- bzw. Schleppzugkonformation, bei der sich das Polymer sehr flach auf der Oberfläche anordnet, wird zu einer niedrigeren adsorbierten Schichtdicke führen als eine *„Tail“*-Adsorption, bei der das Polymer nur über einen kleinen Teil des Rückgrats mit der Oberfläche wechselwirkt, während der Rest in die Porenlösung zeigt (sh. **Abbildung 6**). Eine *„Loop“*- bzw. Schleifenkonformation, bei der nur einzelne Abschnitte der Polymerkette adsorbieren, führt hingegen zu mittleren adsorbierten Schichtdicken. Eine Vorstellung über die Adsorptionsweise eines PCEs kann über Molekulardynamik-Simulationen (MDS) erhalten werden [131]. So legen Untersuchungen von *Sakai* et al. mit MDS nahe, dass bereits die Orientierung des PCEs vor der Adsorption entscheidend ist, wie das Polymer sich anlagern wird. Eine horizontale Ausrichtung zur Oberfläche wird eine *„Train“*- bzw. *„Loop“*-Konformation begünstigen, während bei einer vertikalen Ausrichtung eine Adsorption über den *„Tail“*-Modus wahrscheinlicher ist [132]. Mittels MDS konnten ebenfalls interessante Einblicke zum Einfluss verschiedener struktureller Paramater (z.B. Haupt- und Seitenkettenlänge, Effekt von funktionellen Gruppen) auf die Lösungs- und Adsorptionskonformation von PCEs erhalten werden [133-137].

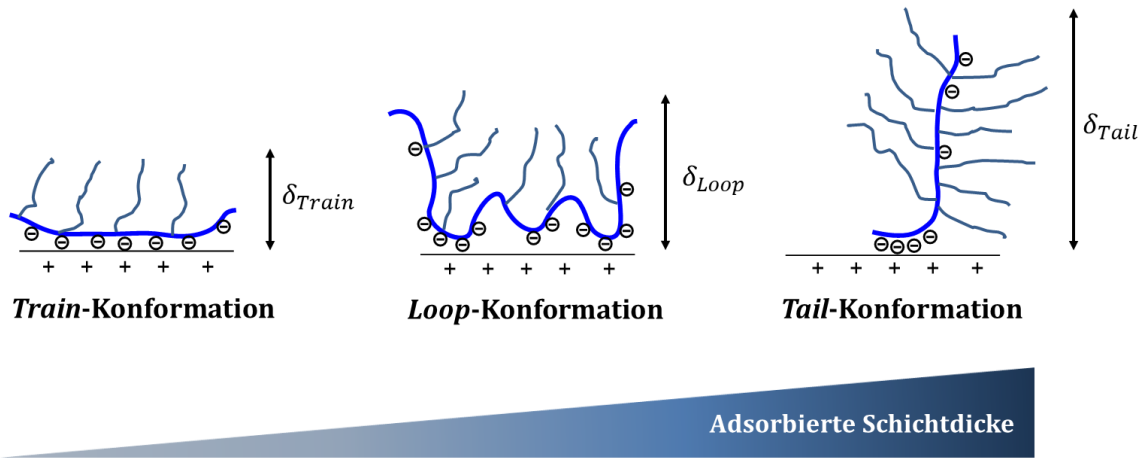

Abbildung 6: Adsorbierte Schichtdicken für verschiedene Adsorptionskonformationen.

3.3. Einfluss nicht-adsorbierter Polymere zur Dispergierung

Wie zuvor erläutert, müssen PCE-Fließmittel auf der Oberfläche adsorbieren, damit die Zementpartikel über einen elektrosterischen Effekt dispergiert werden [26, 44, 110, 138]. PCE-Polymere, die in der Porenlösung verbleiben, tragen normalerweise nicht zur Stabilisierung bei, sondern sorgen vielmehr für die zeitliche Dispergierung und den

Fließmaßerhalt [28, 139, 140]. Neue Oberflächen, die während der Zementhydratation entstehen, können durch die nicht-adsorbierten PCE-Polymere stabilisiert werden. Die Stabilisierung findet so lange statt, bis das Depot an freien PCE-Polymeren aufgebraucht ist und neu gebildete Hydratphasen nicht mehr durch Fließmittel bedeckt werden können. Untersuchungen von *Sakai* et al. deuten darauf hin, dass auch nicht-adsorbierte PCEs zur Verflüssigung beitragen [38, 56, 57]. Diese Beobachtungen wurden in einem Bindemittelsystem bestehend aus einem Portlandzement mit niedriger Hydratationswärme und Mikrosilika gemacht, das durch verschiedene MPEG-PCEs bei w/b-Werten von 0,16 – 0,32 verflüssigt wurde [56]. Die MPEG-PCEs unterschieden sich hinsichtlich ihres Molekulargewichts bzw. ihrer Größe, während ihre Seitenkettenlänge sowie molekulare Zusammensetzung identisch waren. Überraschenderweise wurde festgestellt, dass das PCE mit der kleinsten Molmasse (Polymer A mit M_w = 10.000 Da) die Viskosität am stärksten bei einem niedrigen w/b-Wert (0,16) reduzierte (sh. **Abbildung 7; (I)**). Adsorptionsmessungen ergaben jedoch, dass dieses PCE im Vergleich zu den anderen Polymeren nur in einer geringeren Menge auf der Oberfläche adsorbiert **(II)** und daher eine höhere Konzentration in der Porenlösung zurückbleibt **(III)**.

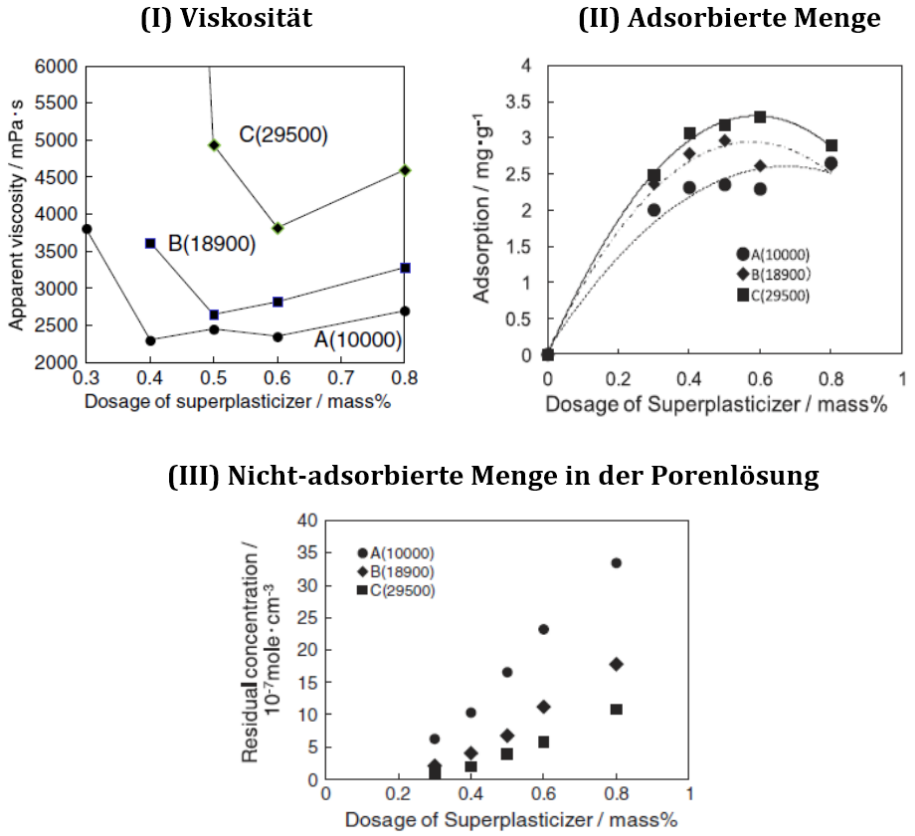

Abbildung 7: Einfluss der Polymergröße verschiedener MPEG-PCEs auf die Viskosität und das Adsorptionsverhalten bei w/b = 0,16; Abbildungen aus [38].

Diese Ergebnisse widersprechen den bisherigen Erfahrungen, dass PCEs umso wirkungsvoller sind, je mehr sie auf der Oberfläche adsorbieren und je größer das Polymer ist. Interessanterweise konnte letztere Korrelation erst ab einem höheren w/b-Wert von 0,32 für die getesteten MPEG-PCEs gefunden werden. Dies deutet darauf hin, dass bei niedrigen w/b-Werten neben der elektrosterischen Stabilisierung auch andere Dispergiermechanismen zum Tragen kommen und der Anteil an nicht-adsorbierten Polymeren hierbei eine entscheidende Rolle spielt.

Weitere Hinweise lieferte eine Folgestudie von *Sakai* et al., die zeigte, dass die Viskosität eines Zementleims auch nach dem Erreichen der Sättigungsadsorption abnahm, wenn ein PCE oberhalb der Sättigungsdosierung zugegeben wurde [57]. Dies bekräftigt die Annahme, dass nicht-adsorbierte PCEs in der Porenlösung zur Verflüssigung beitragen. Gemäß weiteren Untersuchungen von *Sun* et al. scheinen nicht nur PCE-Polymere einen solchen Effekt hervorrufen zu können, sondern auch nanoskalige Ettringit-Kristalle und andere Feinstoffanteile, die durch PCE-Polymere stabilisiert werden und gelöst zwischen den Zementpartikeln vorliegen [141].

Aufbauend auf den Ergebnissen der vorangegangenen Arbeiten wurde in Vorversuchen am Lehrstuhl getestet, wie sich nicht-ionische Polymere verhalten [58]. In diesem Zusammenhang wurde ein herkömmliches MPEG-PCE mit einigen ungeladenen Polymeren kombiniert und ihr Einfluss auf die Verflüssigung von Zementleimen bei einem w/z-Wert von 0,3 untersucht. Als nicht-ionische Polymere wurden das Homopolymer eines MPEG-Methacrylat-Esters, ein MPEG-Makromonomer sowie ein Polyethylenglykol (M_w = 2000 Da) eingesetzt. Die Untersuchungen zeigten eine Erhöhung des Fließmaßes bei Zugabe der nicht-ionischen Polymere, die offenbar ebenfalls einen stabilisierenden Beitrag leisten können. Der genaue Wirkmechanismus blieb allerdings unklar.

Wurden hingegen PEGs mit Molmassen (M_w) oberhalb von 50.000 Da mit einem MPEG-PCE kombiniert, führte dies nach Untersuchungen von *Roussel* et al. zu einer Erhöhung der Fließgrenze und zu einer Agglomeration der Zementpartikel infolge von auftretenden attraktiven Kräften [142]. Dies zeigt, dass hier Forschungsbedarf existierte, um eine Klärung der unterschiedlichen Verhaltensweisen herbeizuführen.

3.4. Synthese und Eigenschaften von PCE-Fließmitteln

Polycarboxylat-Fließmittel zählen zu den leistungsstärksten Fließmitteln. Seit ihrer Erfindung im Jahr 1981 wurden sie kontinuierlich weiterentwickelt, sodass heutzutage unterschiedliche PCE-Typen existieren (sh. **Abbildung 8**) [25, 38, 39, 143].

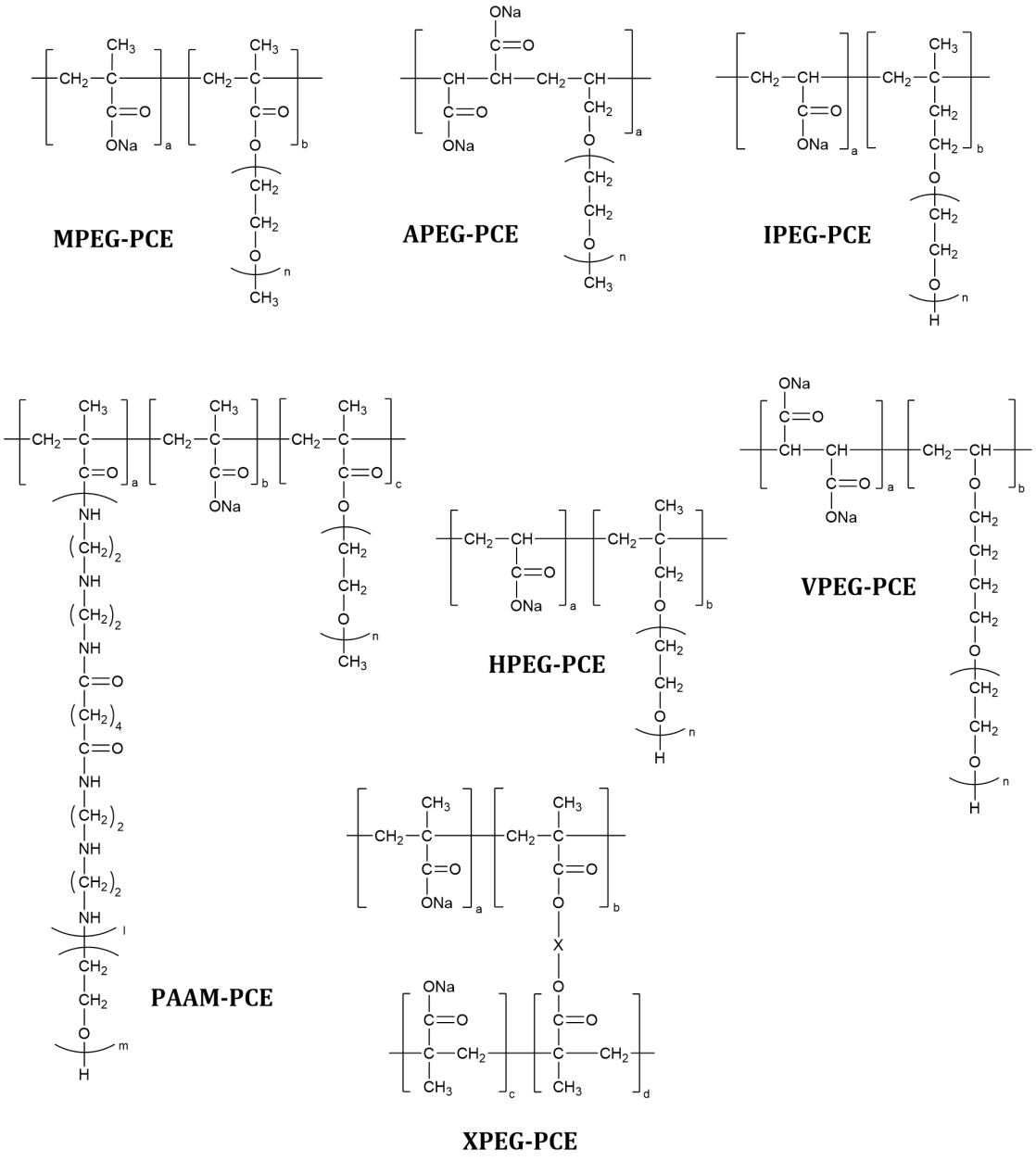

Abbildung 8: Übersicht zu den chemischen Strukturen verschiedener PCE-Fließmittel [143].

PCEs werden vorwiegend über eine freie radikalische Copolymerisation synthetisiert, bei der ungesättigte Carbonsäuren, wie Acrylsäure, Methacrylsäure, Itaconsäure, Maleinsäureanhydrid sowie verschiedene PEG-haltige Makromonomere verwendet

werden. Die PEG Ketten sind über Ester-, Ether- oder Amidbindungen mit der Monomereinheit verknüpft. Abhängig von den eingesetzten Makromonomeren wird zwischen MPEG-, [144, 145] APEG-, [37, 146] IPEG-, [147, 148] HPEG-, [149, 150] VPEG-, [151, 152] PAAM- [153] und XPEG-PCEs [154] unterschieden. Die Initiation der Polymerisation erfolgt üblicherweise durch die Zugabe von Persulfaten oder Redoxinitiatoren, wie beispielsweise H_2O_2/Eisen(II)sulfat (*Fenton*'s Reagenz) oder H_2O_2/Ascorbinsäure [155, 156]. Außerdem werden Kettenregler (z.B. Mercaptoethanole oder Methallylsulfonate) zur Kontrolle des Molekulargewichts eingesetzt. Die Polymerisation wird meistens bei einer Temperatur von 70 – 80 °C durchgeführt, einige PCEs wie VPEG-, HPEG- oder IPEG-PCEs können ebenfalls unter Raumtemperatur-bedingungen (20 – 40 °C) synthetisiert werden [155, 157-160]. Auch über eine Mikrowellen-unterstützte Synthese wurden PCEs bereits erfolgreich dargestellt [161]. Nach Beendigung der Polymerisation werden die PCE-Fließmittel mit Natronlauge neutralisiert.

Durch die Polymerisation der ungesättigten Carbonsäure mit dem PEG-haltigen Makromonomer wird die typische Kammpolymerstruktur erhalten, in der die Carboxylat-Gruppen entlang der Hauptkette angeordnet sind und die Polyethylenglykole als Seitenketten vom Polymerrückgrat ausgehen. Zur Benennung der PCEs hat sich als Nomenklatur die Abkürzung *xPCEy* etabliert, wobei *x* die Anzahl der Ethylenoxid-Einheiten der PEG Seitenkette darstellt und *y* das molare Verhältnis von ungesättigter Carbonsäure zum Makromonomer wiedergibt. Der Mittelteil bezieht sich auf die Art des verwendeten Makromonomers.

Ein entscheidender Faktor, der zum Erfolg der PCE-Fließmittel beigetragen hat, ist ihre hohe Strukturvariabilität, die es ermöglicht Polymere mit unterschiedlichen Eigenschaften zu synthetisieren. Variationsmöglichkeiten sind die Haupt- und Seitenkettenlänge des PCEs [39, 41, 43, 123], die chemische Zusammensetzung [25] oder die Abfolge der Monomere im Polymerrückgrat [162, 163]. Außerdem können Co-Monomere mit verschiedenen funktionellen Gruppen in das PCE-Polymer eingebracht werden, um die Adsorptionseigenschaften gezielt zu beeinflussen [40, 41, 164, 165]. Durch eine Variation des molaren Verhältnisses der Monomere kann die anionische Ladung und Seitenkettendichte des PCEs verändert werden und auf diese Weise ebenfalls Einfluss auf das Adsorptionsverhalten ausgeübt werden [140]. Beispielsweise werden PCEs mit einer hohen anionischen Ladung und wenigen langen Seitenketten

bevorzugt im Fertigteilbeton eingesetzt, da diese Polymerstruktur bei niedriger Dosierung (0,05 – 0,2 % bwoc) eine hohe initiale Verflüssigung ermöglicht, die nach wenigen Minuten wieder abnimmt [28]. Ursache hierfür ist die hohe anionische Ladung, die zu einer raschen und nahezu vollständigen Adsorption der PCE-Polymere führt, wodurch kein Fließmittel mehr für eine spätere Dispergierung vorhanden ist [139, 166]. PCEs mit einer geringen anionischen Ladung und vielen kurzen Seitenketten werden bevorzugt im Transportbeton verwendet. Diese Polymerstruktur erfordert eine höhere Dosierung (0,2 – 0,5 % bwoc) für die anfängliche Dispergierung, kann das Fließmaß aber länger über die Zeit konstant halten, da infolge der niedrigeren anionischen Ladung weniger Polymere zu Beginn adsorbieren und daher ein höherer Anteil an Fließmittel als Depot für eine spätere Verflüssigung zur Verfügung steht [28, 166].

Auch die mikrostrukturelle Zusammensetzung bzw. die Abfolge der Monomere innerhalb des Polymers hat einen entscheidenden Einfluss auf die Adsorptions-eigenschaften [162, 163, 167]. So zeigen Blockcopolymere ein schnelleres Adsorptionsverhalten als Polymere, bei denen die Monomere statistisch angeordnet sind [168, 169]. Blockcopolymere können über eine kontrollierte radikalische Polymerisation mittels ATRP (*„atom transfer radical polymerization“*) oder RAFT (*„reversible-addition-fragmentation chain-transfer polymerization“*) erhalten werden [167, 170]. Durch die kontrolliert stattfindende Reaktion weisen sie niedrige Polydispersitäten auf [171]. Gemäß den Untersuchungen von *Weidmann* et al. ist ein großer Vorteil dieser Polymere, dass sie kurze Anmischzeiten im Beton ergeben, da sie durch die hohe Dichte an Carboxylatgruppen in den anionischen Blöcken unmittelbar nach der Wasserzugabe auf der Bindemitteloberfläche adsorbieren und dadurch relativ schnell wirksam werden [172].

3.5. PCEs für hohe Fließgeschwindigkeiten

Im Rahmen dieser Arbeit sollte nicht nur der Wirkmechanismus der nicht-ionischen Co-Dispergiermittel aufgeklärt werden (**Publikationen #1 – #3, #5** und **#6**), sondern ebenfalls untersucht werden, wie sich nicht-adsorbierende Moleküle sowie Polymere auf die Fließgeschwindigkeit und rheologischen Eigenschaften von zementären Systemen auswirken (**Publikation #4**). Das folgende Kapitel gibt eine kurze Einführung wie mit PCEs eine hohe Fließgeschwindigkeit erzielt werden kann und von welchen

strukturellen Merkmalen sie im Wesentlichen beeinflusst wird. PCE-Fließmittel wirken hauptsächlich über eine Reduzierung der Fließgrenze, während ihr Einfluss auf die plastische Viskosität eher geringfügig ist. Dies stellt ein Problem für zementäre Systeme mit einem niedrigen w/z-Wert dar, die aufgrund ihres hohen Feststoffanteils eine hohe plastische Viskosität besitzen und deshalb ein kriechendes Fließverhalten zeigen [75]. Obwohl PCE-Fließmittel solche Mörtel bzw. Betone gut verflüssigen können, weisen sie dennoch eine langsame Fließgeschwindigkeit auf. *Lange* et al. berichteten, dass die klebrige Konsistenz für bestimmte PCE-Typen deutlich stärker ausgeprägt ist [53]. Die geringsten Fließgeschwindigkeiten wurden für MPEG-PCEs gefunden, gefolgt von IPEG- und HPEG-PCEs, während APEG-PCEs die schnellsten Geschwindigkeiten ergaben. Diese Beobachtungen wurden auf die unterschiedlichen HLB-Werte (*„hydrophilic-lipophilic balance“*) der PCEs zurückgeführt. Der HLB-Wert beschreibt das Verhältnis von hydrophilen und hydrophoben Gruppen und wurde ursprünglich von *Griffin* zur Charakterisierung von Tensiden eingeführt [173, 174]. Da PCEs makrotensidische Eigenschaften besitzen, kann das Konzept unter gewissen Annahmen auch auf PCEs übertragen werden. So werden die PEG-Seitenketten und Carboxylate als hydrophile Elemente betrachtet, während die CH_2-Einheiten und Methylgruppen als hydrophob eingestuft werden [59]. Über die Berechnung der HLB-Werte konnte gezeigt werden, dass ein niedriger Wert von 16 bis 18 zu langsameren Fließgeschwindigkeiten führt. Eine geringere Klebrigkeit und ein schnelleres Fließverhalten wurden hingegen für PCEs mit einem hohen HLB-Wert > 18,5 erhalten [53, 59].

In den letzten Jahren wurden neue PCE-Fließmittel entwickelt die es ermöglichen, sowohl die Fließgrenze als auch die plastische Viskosität zu reduzieren und hohe Fließgeschwindigkeiten einzustellen. Bei diesen Polymeren wurde als neues strukturelles Merkmal eine Phosphatgruppe eingebracht. Dies kann im Fall von herkömmlichen PCEs einfach realisiert werden, indem bei der Polymerisation zusätzlich ein phosphathaltiges Monomer, wie zum Beispiel Hydroxyethylmethacrylat-Phosphatester (HEMAP) verwendet wird [175-177]. Eine andere chemische Vorgehensweise sind Polyarylether-basierte Fließmittel, die aus Phenol, Phenolethoxylat, Phenolethoxylat-Phosphatester und Formaldehyd über eine Polykondensation hergestellt werden [178]. Dieses Polymer weist eine aromatische Hauptkette auf, an die Polyethylenglykol und Phosphatester-Gruppen gebunden sind (sh. **Abbildung 9**). Die Reduzierung der plastischen Viskosität

mit diesen Polymeren wird auf die hohe Adsorptionsaffinität und die stark hydrophilen Eigenschaften der Phosphatgruppen zurückgeführt [177].

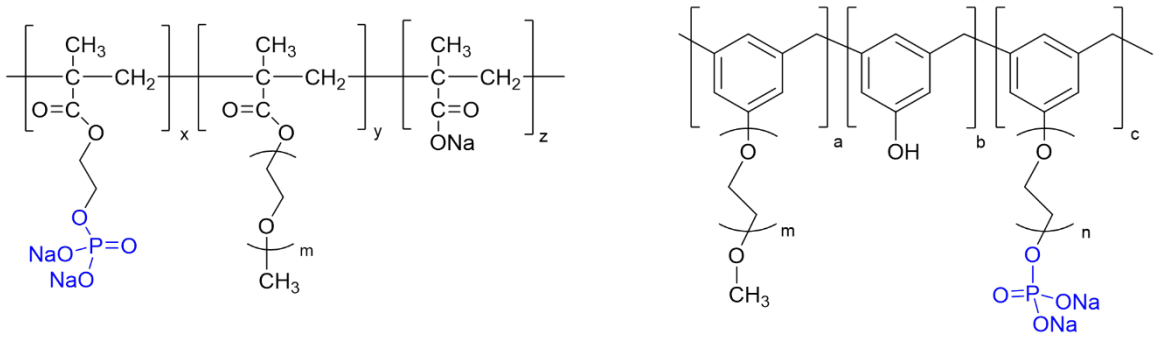

Phosphat-modifiziertes PCE **Polyarylether-basiertes PCE**

Abbildung 9: Phosphatgruppen-haltige Fließmittel zur Reduzierung der plastischen Viskosität bei niedrigen w/z-Werten.

PCE-Fließmittel mit Phosphat-Gruppen können nicht nur die rheologischen Eigenschaften von zementbasierten Systemen bei einem niedrigen w/z-Wert verbessern, sondern sind auch äußerst dosierungseffiziente Fließmittel für Gipsbindemittel und ermöglichen deutlich höhere Wassereinsparungen [179-181]. Allerdings sind phosphathaltige Monomere teurer und nicht überall verfügbar. Dies ist der Grund, warum alternative Konzepte neben diesen Fließmitteln benötigt werden, mit denen ebenfalls die Fließeigenschaften verbessert werden können.

3.6. PCEs mit erhöhtem sterischen Anspruch

Ein zweiter Schwerpunkt dieser Dissertation waren Fließmittel mit einem erhöhten sterischen Anspruch zu synthetisieren, um auf diese Weise eine Steigerung der Dispergierwirkung zu erzielen. Mit diesem Themenbereich befassen sich die **Publikationen #7 – #9**. Das folgende Kapitel stellt einige in der Literatur beschriebene Konzepte vor, mit denen der sterische Effekt von PCEs vergrößert werden soll. Die Dispergierwirkung von PCEs hängt von zwei Faktoren ab – zum einen, wie effektiv das Polymer die Oberfläche der Hydratphasen belegen kann, und zum anderen von der adsorbierten Schichtdicke. Insbesondere für die Verflüssigung bei niedrigen w/z-Werten ist es entscheidend, dass das PCE-Polymer in der Lage ist über Adsorption möglichst viele Stellen auf der Oberfläche zu besetzen und gleichzeitig über die PEG-

Seitenketten für einen starken sterischen Effekt zu sorgen. Gemäß der *Ottewill-Walker*-Gleichung ist die sterische Stabilisierung besonders stark, wenn das Polymer eine hohe Schichtdicke erzeugt. Daher werden in letzter Zeit zunehmend Ansätze verfolgt, mit denen der sterische Effekt von PCEs gesteigert werden soll. Einige Beispiele sowie aktuelle Entwicklungen werden im Folgenden vorgestellt.

Der Einbau von sperrigen bzw. sterisch anspruchsvollen Monomeren in die Kammpolymer-Struktur von PCEs stellt eine Möglichkeit dar, wie die sterische Abschirmung der Zementpartikel verbessert werden kann. *Lv* et al. verfolgten diese Strategie, indem sie ein β-Cyclodextrin-basiertes Makromonomer mit Acrylsäure, Methallylsulfonsäure und einem Polethylenglykol-Allylether (APEG) copolymerisierten [182]. Das Makromonomer synthetisierten sie aus Maleinsäureanhydrid und ß-Cyclodextrin, einem cyclischen Oligosaccharid, das aus sieben 1,4-glycosidisch verknüpften Glucosemolekülen besteht. Aufgrund des cyclischen Aufbaus ist die Struktur starrer im Vergleich zum linearen Polyethylenglykol. Die PEG-Ketten sind flexibler und liegen in Lösung vorwiegend als Polymerknäuel vor. *Lv* et al. zeigten, dass durch die Modifikation des PCEs mit ß-Cyclodextrin ein stärkerer sterischer Effekt resultierte. Außerdem konnten die Wassereinsparung und der Fließmaßerhalt verbessert werden. Wurde allerdings ein zu hoher Anteil des ß-Cyclodextrins in das Polymer eingebaut, führte dies zu einer starken Verzögerung des Abbindeverhaltens.

Aufbauend auf den Ergebnissen dieser Studie, stellten *Xu* et al. eine alternative Syntheseroute für ein weiteres β-Cyclodextrin-haltiges Monomer vor [183]. Dieses wurde über eine dreistufige Synthese hergestellt, bei der β-Cyclodextrin mit para-Toluolsulfonsäurechlorid zunächst tosyliert und anschließend mit Ethanolamin umgesetzt wurde. Das Makromonomer wurde durch eine Reaktion der aminosubstituierten Zwischenstufe mit Glycidylmethacrylat erhalten und mittels freier radikalischer Polymerisation mit anderen Monomeren copolymerisiert. Die chemische Struktur des dabei resultierenden Fließmittels ist in **Abbildung 10** dargestellt.

Wie zu erkennen ist, handelt es sich hierbei um ein Quadropolymer aus Acrylsäure, Methallylsulfonsäure, Polyethylenglykol-Methallylether (HPEG) und einem Methacrylsäureester des β-Cyclodextrins. *Xu* et al. berichteten, dass dieses PCE nicht nur eine stärkere Dispergierung, sondern auch eine verbesserte Tonrobustheit aufweist. Üblicherweise neigen PCEs aufgrund ihrer hydrophilen, linearen PEG-Seitenketten dazu,

in die Schichtstruktur von Tonmineralien (insbesondere Montmorillonit) zu interkalieren, wodurch ihre Fließwirkung drastisch reduziert wird [184-186]. Durch den hohen sterischen Anspruch des Cyclodextrin-Motivs konnte die Interkalation des PCE-Polymers in die Schichtstruktur der Tone weitestgehend unterbunden werden.

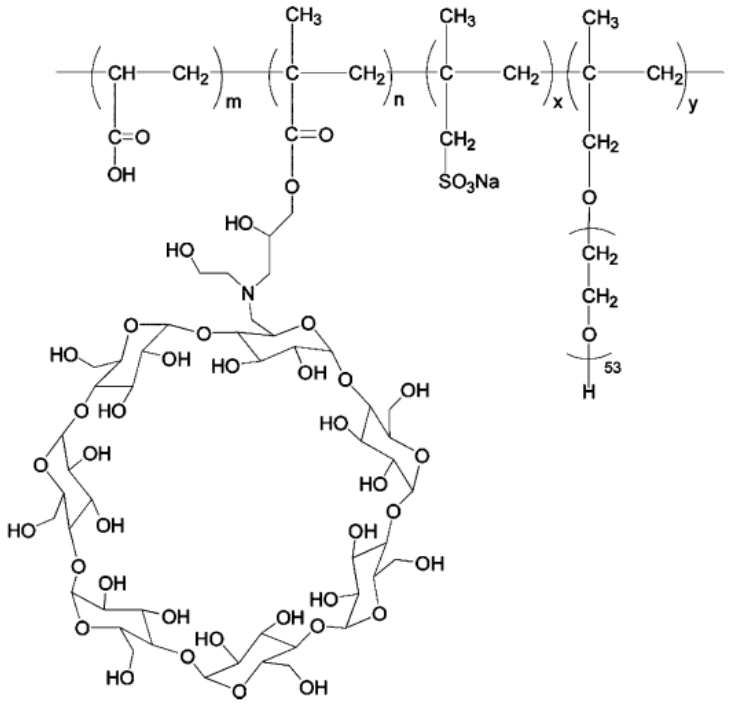

Abbildung 10: Chemische Struktur eines β-Cyclodextrin-basierten PCEs; übernommen aus [183].

Ein weiterer Ansatz zur Erhöhung des sterischen Effekts sind verzweigte Makromonomere [187]. Die Synthese dieser Monomere ist in **Abbildung 11** dargestellt. Diese werden ausgehend von Hydroxybutylvinylether oder Isoprenol über eine Ringöffnungspolymerisation hergestellt. Hierfür werden die OH-Gruppen der ungesättigten Alkohole mit Kaliummethanolat deprotoniert. Das Alkoholat wird in einen Reaktionsdruckbehälter überführt und danach abwechselnd Ethylenoxid sowie verschiedene Glycidylether ((Di/tri/hepta)ethylenglykolmethylglycidylether) bei hohem Druck (3,5 bar) und Temperatur (120 °C) zugegeben. Auf diese Weise wird das Makromonomer sequenziell aus linearen und verzweigten Blöcken aufgebaut. Die Zugabe des nächsten Monomers erfolgt erst immer dann, wenn das vorherige vollständig umgesetzt wurde, was über eine Abnahme des Drucks und der Temperatur im Reaktionsbehälter festgestellt wird. Ein Vorteil von PCEs, die diese verzweigten

Makromonomere enthalten, soll unter anderem sein, dass sie im Vergleich zu Polymeren mit linearen Seitenketten niedrigere plastische Viskositäten bewirken.

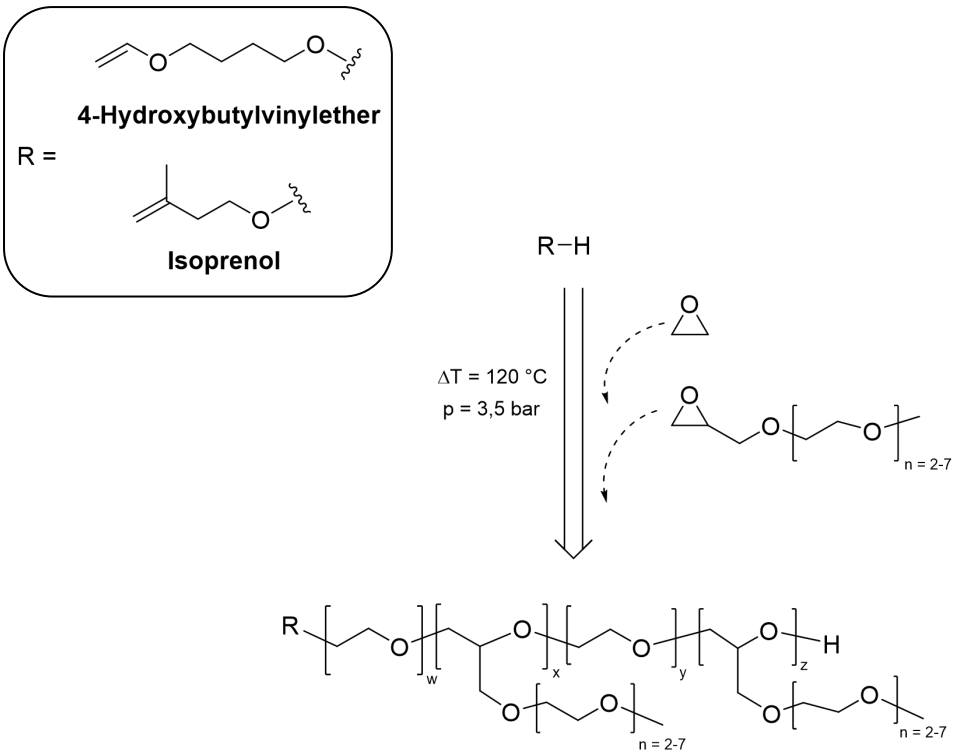

Abbildung 11: Struktur verzweigter Makromonomere auf VPEG- bzw. IPEG-Basis, gemäß [187].

Dass sperrige Makromonomere eine bessere Fließwirkung induzieren, konnte auch durch *Zhang* et al. gezeigt werden, die ein Polyamidoamin mit Acrylsäure verestertern und dieses Makromonomer mit Acrylsäure und einem Polyethylenglykolisoprenolether (IPEG) polymerisierten [188]. Untersuchungen im Beton ergaben, dass mit diesem PCE höhere Frühfestigkeiten erzielt werden konnten, was auf die Polyamidoamin-Einheiten zurückgeführt wurde.

Die bisher vorgestellten Konzepte haben alle gemeinsam, dass sie jeweils den sterischen Anspruch der Seitenkette in der Kammpolymerstruktur des PCEs vergrößerten, um auf diese Weise die sterische Abstoßung der Zementpartikel zu erhöhen. Eine andere Strategie ist es, über eine verzweigte Polymerstruktur für einen stärker ausgeprägten

sterischen Effekt zu sorgen. Bei der Suche nach geeigneten Polymerarchitekturen wurde man daher auf Sternpolymere aufmerksam, die aus einer zentralen Einheit bestehen, von der mehrere Polymerketten („Arme“) ausgehen [189]. Diese Struktur wurde als interessant empfunden, da die „Arme“ des Sternpolymers weit in die Porenlösung hineinragen könnten, um so als effektiver Abstandhalter für mehrere Zementteilchen zu fungieren. Basierend auf dieser Polymerstruktur entwickelten *Wang* et al. eine Syntheseroute für ein sternförmiges PCE-Fließmittel (sh. **Abbildung 12**) [66, 190, 191].

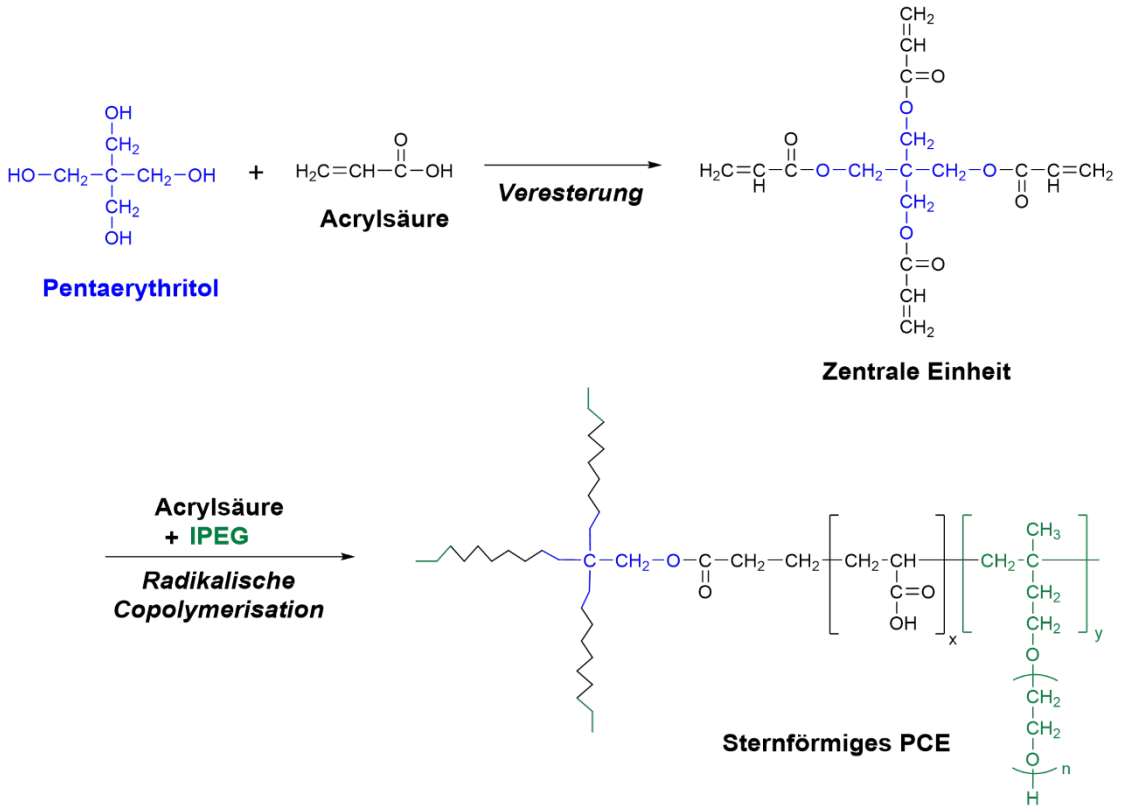

Abbildung 12: Schematische Darstellung der Synthese eines sternförmigen PCEs nach *Wang* et al. [191].

Wie aus dem Reaktionsschema zu erkennen ist, wird zunächst das Zentrum des Polymers über eine Veresterung von Acrylsäure mit Pentaerythritol hergestellt. Durch die endständigen Olefin-Gruppen der Kerneinheit ist es anschließend möglich, von dort ausgehend die Arme des Polymers über eine freie radikalische Copolymerisation von Acrylsäure und IPEG-Makromonomer anzubringen (sog. *„core-first“* Strategie). Auf diese Weise wird ein sternförmiges Fließmittel erhalten, das aus vier verknüpften IPEG-PCEs besteht, die jeweils die Arme des Polymers darstellen.

Gemäß den Untersuchungen von *Wang* et al. konnte die Dosierungseffizienz des PCEs durch die Sternpolymerarchitektur verbessert und eine um 20 % höhere Wassereinsparung realisiert werden [191]. Die höhere Dispergierwirkung wurde auf die Multi-Arm-Struktur des Polymers zurückgeführt, die eine stärkere sterische Hinderung bewirkt und gleichzeitig ermöglicht, mehrere Oberflächenbereiche der Zementpartikel zu besetzen. Adsorptionsmessungen ergaben, dass das Sternpolymer in einer höheren Menge als ein kammförmiges PCE adsorbiert. Erklärt wurde dies mit dem niedrigeren hydrodynamischen Radius des Sternpolymers infolge seiner globulären Struktur, durch die eine höhere Anzahl an Carboxylatgruppen pro Volumeneinheit vorliegt, was wiederum eine höhere Bindungsaffinität bedingt. Außerdem wurde berichtet, dass durch die sternförmige Anordnung sowohl der Fließmaßerhalt als auch die Tonrobustheit optimiert werden konnten.

Einige Studien beschäftigten sich in der Folge mit der Synthese von neuartigen multifunktionalen Zentren für Sternpolymere [192, 193]. In diesem Zusammenhang untersuchten *Zhao* et al. den Einfluss der Armanzahl auf die Dispergierwirkung von sternförmigen Fließmitteln [193]. Hierbei synthetisierten sie aus Glycerin, Xylitol und Mannitol durch die Zugabe von Acrylsäurechlorid verschiedene Zentraleinheiten, von denen ausgehend Polymere mit drei, fünf sowie sechs Armen hergestellt wurden. Interessanterweise stellten sie fest, dass eine Erhöhung der Armanzahl nicht unbedingt zu einer besseren Stabilisierung führen muss. Ihre Ergebnisse deuten darauf hin, dass eine maximale Armanzahl existiert, für die optimale Eigenschaften erzielt werden. So wurde die beste Verflüssigungswirkung für das Sternpolymer mit fünf Armen festgestellt, während für sechs Arme bereits eine reduzierte Wirksamkeit beobachtet wurde. Es wurde gefolgert, dass bei einer zu hohen Armanzahl die Wahrscheinlichkeit für Kettenverschlaufungen stark erhöht ist und die Carboxylatgruppen zunehmend abgeschirmt werden, was eine geringere Adsorptionsbereitschaft zur Folge hat.

Mittlerweile existieren in der Literatur auch Arbeiten zu sternförmigen Fließmitteln, die ausgehend von einer cyclischen Zentraleinheit synthetisiert wurden. So verwendeten *Chen* et al. einen hexafunktionalen Kern, hergestellt aus Phytinsäure – einem Hexaphosphorsäureester des myo-Inosit (Cyclohexanon), der als Nährstoffspeicher in Samen von Getreide sowie Hülsenfrüchten enthalten ist – und Ethylenglykolmonovinylether [194]. Als Arme wurden Polymerketten aus Acrylsäure, Methallylsulfonsäure und einem Polyethylenglykolallylether (APEG) aufgepfropft.

Wegen der charakteristischen Struktur und der Ähnlichkeit zu einem Eiskristall bezeichneten die Autoren das Sternpolymer als „schneeflockenartiges“ PCE. Ein Vorteil dieses Fließmittels ist die verbesserte Tonrobustheit.

Auch Lignin, ein verzweigtes Biopolymer, das in Holz enthalten ist, konnte bereits erfolgreich als Zentrum für ein sternförmiges Fließmittel verwendet werden [195, 196]. Lignin setzt sich aus Phenolgruppen und drei charakteristischen Bausteinen zusammen, die in ihrer Struktur dem Cumaryl-, Coniferyl- und Sinapylalkohol ähnlich sind. Um das Lignin mit endständigen Olefingruppen zu funktionalisieren, wurden die phenolischen OH-Gruppen im stark Alkalischen deprotoniert und mit einem Intermediat versetzt, das zuvor aus einem OH-terminierten IPEG-Makromonomer und Epichlorohydrin unter Verwendung der Lewis Säure $BF_3 \bullet Et_2O$ (Bortrifluoriddiethyletherat) dargestellt wurde [196]. Über die terminalen Doppelbindungen wurden schließlich die Monomere Acrylsäure und IPEG-Makromonomer als Arme aufpolymerisiert. Das Lignin-haltige Polymer wurde im Zementleim und Beton getestet, wobei festgestellt wurde, dass es sowohl die Fließgrenze als auch die plastische Viskosität stärker reduzierte als ein kammförmiges PCE. Zudem fand man über Röntgenphotoelektronenspektroskopie (XPS) heraus, dass das Lignin-basierte Sternpolymer wegen seiner langen Polymerarme und der bereits sterisch sehr anspruchsvollen Kerneinheit in einer höheren Schichtdicke auf der Zementkornoberfläche adsorbiert und deshalb die Zementteilchen besser stabilisieren kann [196].

Eine verzweigte Polymerstruktur wird auch erhalten, indem bei der PCE Synthese ein Co-Monomer verwendet wird, über das eine Vernetzung mit anderen Ketten erfolgt [67, 197, 198]. Ein Beispiel für ein solches Monomer ist Dimethylaminoethylmethacrylat (DMAEMA), bei dem es sich um ein sog. Inimer handelt, das sowohl die Funktion eines Initiators als auch die eines Monomers vereint. **Abbildung 13** veranschaulicht, wie ausgehend von diesem Monomer ein verzweigtes Fließmittel erhalten wird [197]. DMAEMA wird zuerst mittels Kaliumperoxodisulfat aktiviert, indem ein H-Radikal vom Kohlenstoffatom abstrahiert wird, welches benachbart zur tertiären Aminogruppe liegt. Das dadurch hervorgehende Radikal stellt eine initiierende Stelle dar, die mit der Doppelbindung eines anderen DMAEMA reagieren kann. Hierbei wird ein Dimer gebildet, das zwei Radikalstellen aufweist. Über eine Stelle erfolgt das Kettenwachstum, während die andere in der Nähe des Stickstoffatoms eine weitere Polymerisation initiieren kann und an dieser Stelle für eine Verzweigung sorgt [199, 200].

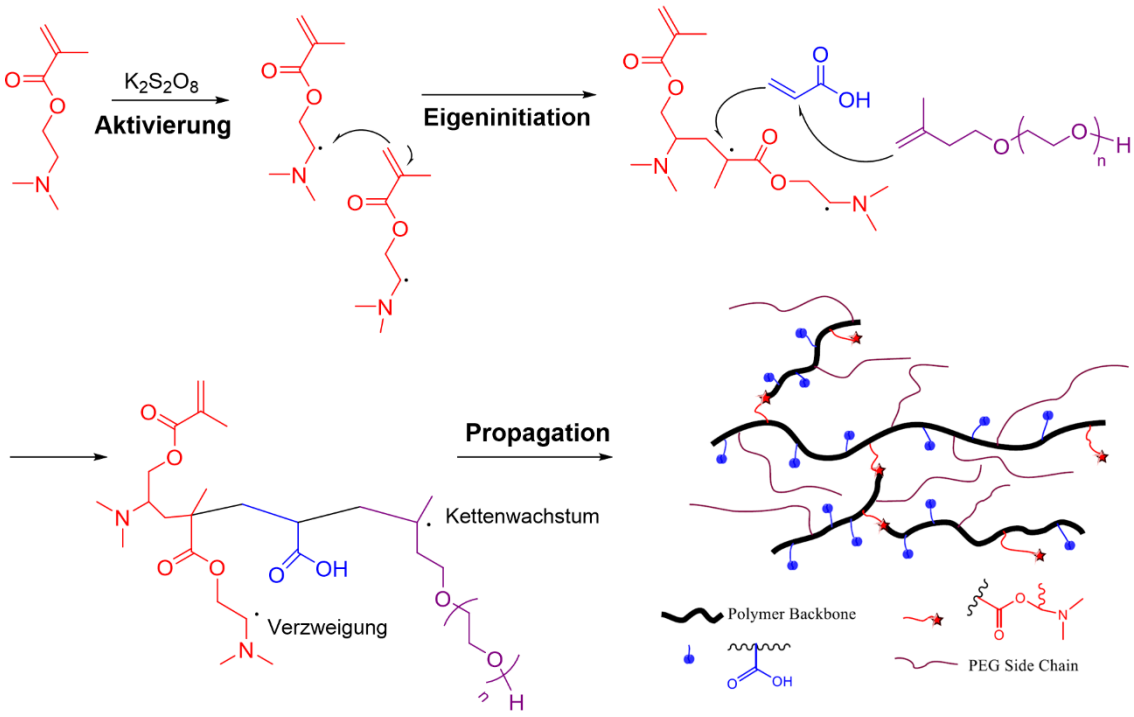

Abbildung 13: Syntheseschema eines quervernetzten PCE-Fließmittels bei Verwendung von DMAEMA; Teile der Abbildung übernommen aus [39].

Das auf diese Weise erhaltene Fließmittel zeigte trotz der verzweigten Architektur keine verbesserte Dispergierwirkung als ein kammförmiges PCE [197]. Es musste höher dosiert werden, um ein vergleichbares Fließmaß einzustellen. Als möglicher Grund wurde die starre Lösungskonformation des Fließmittels angeführt, durch die sich das Polymer bei der Adsorption nicht so gut auf der Oberfläche ausrichten kann und deshalb weniger Stellen besetzt. Das kammförmige PCE ist hingegen flexibler und kann sich aufgrund der geknäulten Konformation so auf der Oberfläche anordnen, dass möglichst viele Stellen belegt werden. Außerdem wurde festgestellt, dass der DMAEMA-Anteil im Polymer nicht zu hoch sein sollte, da ansonsten die Quervernetzung des Polymers zu stark ausgeprägt ist und daher höhere Fließmitteldosierungen benötigt werden. Positiv wurde hingegen bewertet, dass mit dem verzweigten Polymer deutlich schnellere Mörtelauslaufzeiten aus dem V-Trichter erhalten wurden und es die plastische Viskosität um bis zu 30 % reduzieren konnte.

Ein weiterer Vorteil von quervernetzen PCEs wurde von *Pang* et al. beschrieben. Sie synthetisierten ein verzweigtes Fließmittel aus Trimethylolpropantriacrylat (TMPTA) als quervernetzendes Monomer sowie Acrylsäure und Polyethylenglykolmethallylether

(HPEG) [67, 201]. Das Polymer zeigte eine verbesserte Dispergierwirkung und einen längeren Fließmaßerhalt. So konnte mit dem PCE das Ausbreitmaß über zwei Stunden nahezu konstant gehalten werden. Zurückgeführt wurde dies auf die Esterverknüpfungen im TMPTA, die in der alkalischen Porenlösung des Zements schrittweise hydrolytisch gespalten werden. Auf diese Weise werden neue Carboxylatgruppen gebildet, über die das Polymer die Oberflächen der neu gebildeten Zementhydratphasen besetzen kann. Aufgrund der fortschreitenden Hydrolyse der Quervernetzung erhalten die Seitenketten zudem mehr Platz, um sich sterisch besser entfalten zu können.

Abschließend soll ein Beispiel für eine dendrimerartige Polymerarchitektur vorgestellt werden, die in einem Patent von *Shou* et al. beschrieben wird [202]. Dieses Beispiel verdeutlicht den wesentlichen Nachteil von verzweigten Strukturen, die meistens eine mehrstufige Synthese erfordern. Grundbaustein des Fließmittels ist ein kammförmiges PCE, das an den beiden Enden der Hauptkette Polyamidoamin-Dendrimere aufweist (sh. **Abbildung 14**).

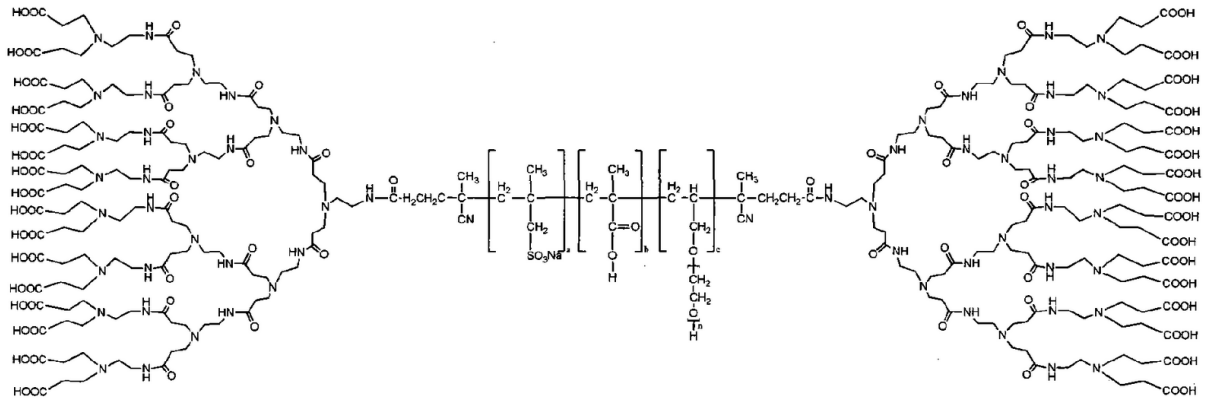

Abbildung 14: Struktur eines verzweigten Fließmittels nach *Shou* et al., übernommen aus [202].

In der Peripherie der Polyamidoamine sind zusätzlich Carboxylatgruppen vorhanden. Synthetisiert wird der Mittelteil des Polymers über eine radikalische Polymerisation von Methallylsulfonsäre, Methacrylsäure und APEG unter Verwendung von 4,4‘-Azobis(4-cyanopentansäure) als Initiator. Nach der Termination weist das PCE-Fließmittel im Idealfall den Initiator an beiden Enden auf. Über die Carbonsäure-Gruppen des eingebauten Initiators wird Ethylendiamin über eine Veresterung angebracht.

Anschließend wird über eine *Michael*-Addition Methlymethacrylat addiert und die hierbei gebildeten Carboxymethylgruppen mit Ethylendiamin wiederum amidiert. Durch abwechselnde Durchführung beider Reaktionen wird die Verzweigung sukzessive aufgebaut. Im finalen Schritt werden die terminalen Methylester hydrolytisch gespalten, um dort Carboxylatgruppen einzubringen.

Ein großer Nachteil von dendrimerartigen Polyamidoaminen ist die zeitaufwändige Mehrstufensynthese. Insgesamt sind neun Syntheseschritte notwendig, damit das in **Abbildung 14** gezeigte Fließmittel erhalten wird. Dies verdeutlicht, dass Ansätze notwendig sind, mit denen auf direktem Weg eine verzweigte Struktur erhalten wird. Nur so lässt sich der Einsatz von verzweigten Fließmitteln in der Praxis realisieren. In diesem Zusammenhang könnten hyperverzweigte Polymere wie z.B. Polyglycerole ein interessanter Baustein sein, da sie über einen einzelnen Syntheseschritt dargestellt werden. Das nächste Kapitel soll sich deshalb mit der Synthese und den Eigenschaften von hyperverzweigten Polyglycerolen befassen, die als Hauptbaustein für das in dieser Arbeit synthetisierte Fließmittel eingesetzt wurden.

3.7. Hyperverzweigte Polyglycerole

Hyperverzweigte Polymere sind statistisch stark verzweigte Makromoleküle, die zur Gruppe der dendritischen Polymere gehören [203]. Anders als bei Dendrimeren erfolgt ihre Synthese über einen einzelnen Aufbauschritt. Die Herstellung von Dendrimeren ist wesentlich zeit- und kostenintensiver, da sie sukzessive über mehrere Zwischenstufen verläuft. Das ist auch der Grund, warum Dendrimere eine perfekte Verzweigung und monodisperse Eigenschaften besitzen [204]. Hyperverzweigte Polymere sind hingegen unregelmäßiger verzweigt und weisen aufgrund der unkontrolliert stattfindenden Verzweigungsreaktion meistens eine hohe Polydispersität auf [205].

Ende der 90er Jahre berichteten *Mülhaupt* et al. über eine experimentelle Methode, die es jedoch erlaubt, die Synthese von hyperverzweigten Polymeren unter kontrollierten Bedingungen durchzuführen, sodass die Polydispersität erheblich reduziert werden konnte [206]. Diese Strategie wurde für die Synthese von hyperverzweigten Polyglycerolen (HyPGs) vorgestellt, die aufgrund ihrer außergewöhnlichen Eigenschaften zu den prominentesten Vertretern hyperverzweigter Polymere zählen und häufig als Alternative zu den klassischen dendrimerartigen Strukturen verwendet

werden. HyPGs sind Polyether-Polyole und werden durch anionische Ringöffnungspolymerisation von Glycidol erhalten [206-209]. Das Polyglycerolgerüst setzt sich aus linearen (L), dendritischen (D) und terminalen (T) Einheiten zusammen und beinhaltet eine Vielzahl von primären und sekundären Hydroxylgruppen (sh. **Abbildung 15**) [206, 207].

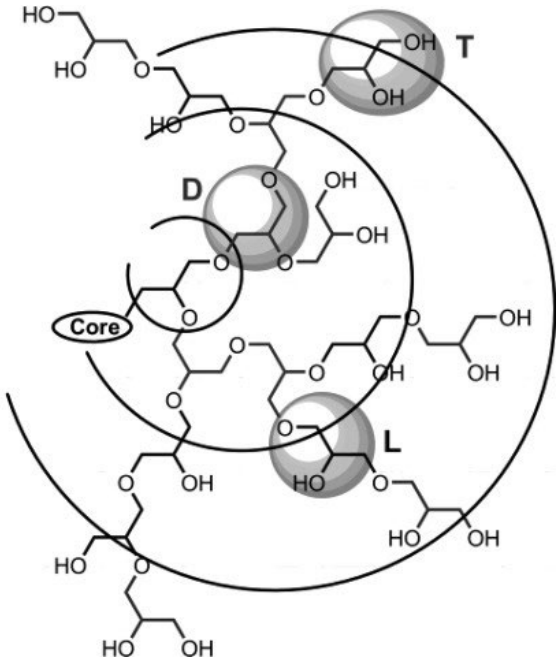

Abbildung 15: Aufbau eines hyperverzweigten Polyglycerols; Abbildung aus [207].

HyPGs sind sehr gut wasserlöslich (> 400 mg/mL), verfügen über eine hohe chemische und thermische Stabilität und sind ähnlich wie Polyethylenglykol biokompatibel [210]. Darüber hinaus kann ihr Molekulargewicht über einen großen Bereich (500 – 1 Mio. Da) variiert werden [211, 212]. HyPGs weisen eine niedrige Lösungsviskosität auf, da durch ihre globuläre Struktur die Tendenz für Kettenverschlaufungen erheblich minimiert ist [210]. Die OH-Gruppen in der Peripherie des Polyglycerolgerüsts können auf unterschiedlichste Art funktionalisiert werden, sodass sich eine Vielzahl von Anwendungsmöglichkeiten eröffnet [213-215]. So werden modifizierte HyPGs unter anderem im biomedizinischen und pharmazeutischen Bereich als Nanokapseln für die kontrollierte Freisetzung von Arzneimitteln eingesetzt, für die Beschichtung von proteinresistenten Oberflächen, beim Tissue Engineering oder als Tracer bei der Diagnostik von Tumorerkrankungen [209, 210, 216]. Außerdem konnten sie bereits erfolgreich für die Biomineralisation von Calciumcarbonat verwendet werden [217,

218], als Templat für die Herstellung von Nanopartikeln [219, 220] oder in Druckerfarben zur Verbesserung der Farbfestigkeit [221]. Bisher existieren noch keine Informationen in der Literatur über die Wirkung von HyPGs in zementbasierten Systemen.

HyPGs werden mittels einer anionischen Ringöffnungspolymerisation synthetisiert, die im Folgenden näher erläutert werden soll. Die Polymerisation wird ausgehend von einer multifunktionalen Kerneinheit gestartet, die meistens aus der Gruppe der Polyole stammt, wie z.B. 1,1,1-Trimethylolpropan (TMP), 1,1,1-Trimethylolethan (TME) oder Pentaerythritol [206, 207]. Das in dieser Arbeit hergestellte Fließmittel wurde ausgehend von einem bis-glycidolierten Polyetheramin mit vier OH-Funktionalitäten gemäß einer Vorschrift in [222] synthetisiert. Die OH-Gruppen der Kerneinheit werden zu Beginn mit Kaliummethanolat deprotoniert, um ein Alkoxid zu bilden, das als „Initiator“ fungiert (sh. **Abbildung 16**).

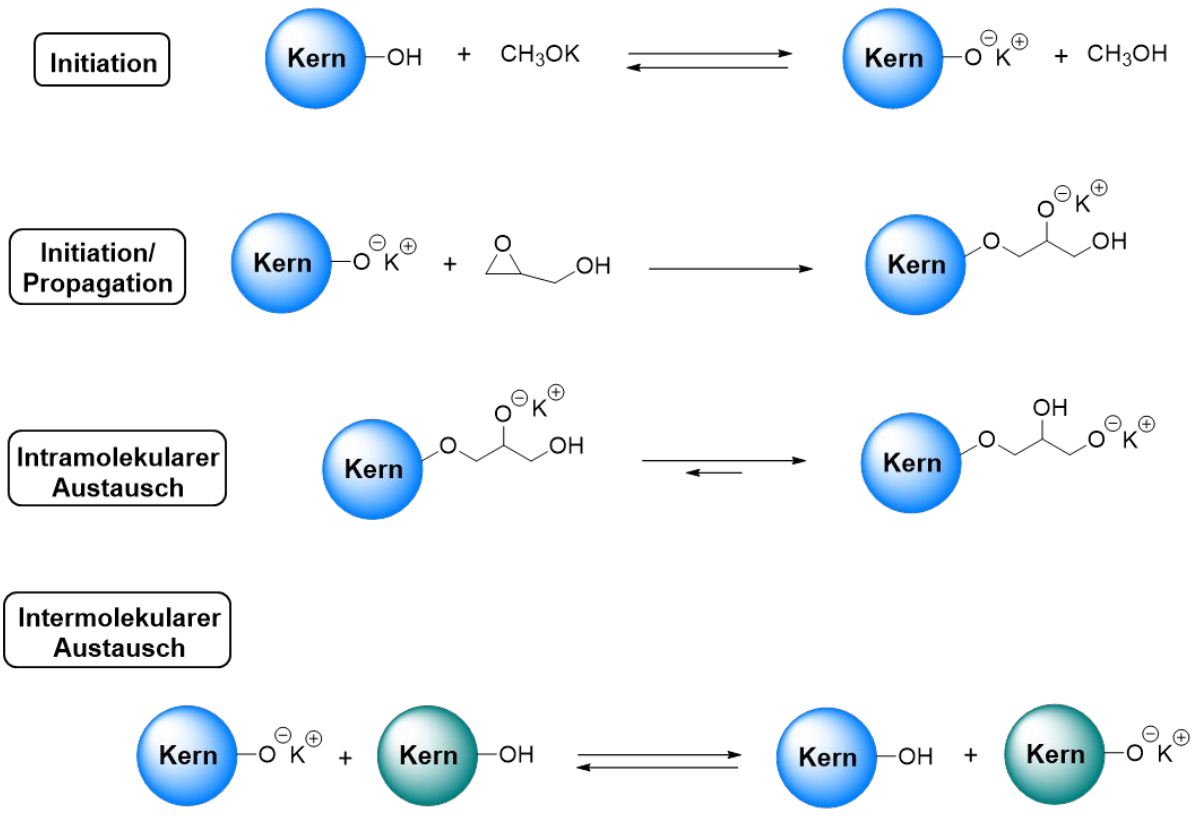

Abbildung 16: Mechanismus der anionischen Ringöffnungspolymerisation von Glycidol [206, 208].

Die Polymerisation wird gestartet, indem sich das Alkoxid in einer SN2-artigen Reaktion an das unsubstituierte Ende des Epoxids des Glycidols anlagert, wobei sich der Oxiran-

Ring unter Bildung eines sekundären Alkoxids und einer primären Alkoholgruppe öffnet. Aufgrund eines intramolekularen Protonenaustausches wurden in der Folge auch primäre Alkoholate gebildet, die stabiler und reaktiver als die Sekundären sind, wodurch das Kettenwachstum sowohl von den primären als auch den sekundären OH-Gruppen voranschreitet [206]. Der Protonenaustausch findet hierbei nicht nur intramolekular, sondern auch intermolekular statt. Wie bei einer lebenden Polymerisation kann die Propagation auch bei der Ringöffnungspolymerisation so lange fortgeführt werden, wie Monomer zugegeben wird bzw. die Kettenenden in einem aktiven Zustand vorliegen.

Ein allgemeines Problem bei der Synthese von hyperverzweigten Polymeren ist das unkontrollierte Kettenwachstum, das zu einer breiten Molmassenverteilung führt. *Mülhaupt* et. al entwickelten eine Strategie (sog. *„Slow Monomer Addition Approach"*), mit der die Synthese von HyPG kontrolliert werden kann. Hierbei wird Glycidol langsam in verdünnter Form zur aktivierten Kerneinheit zugegeben, wodurch gewährleistet wird, dass es vorwiegend mit dem Initiator-Molekül reagiert. Auf diese Weise wird die Konzentration des Glycidols im Vergleich zur Konzentration der Kerneinheit permanent niedrig gehalten und die Wahrscheinlichkeit für eine Nebenreaktion des Glycidols ohne Initiator stark reduziert. Liegt nämlich ein zu hohes Verhältnis von Glycidol zum Initiator vor, kann eine intramolekulare Ringöffnungspolymerisation stattfinden, die zu cyclischen Strukturelementen führt und dadurch die Polydispersität wesentlich erhöht (sh. **Abbildung 17**) [206].

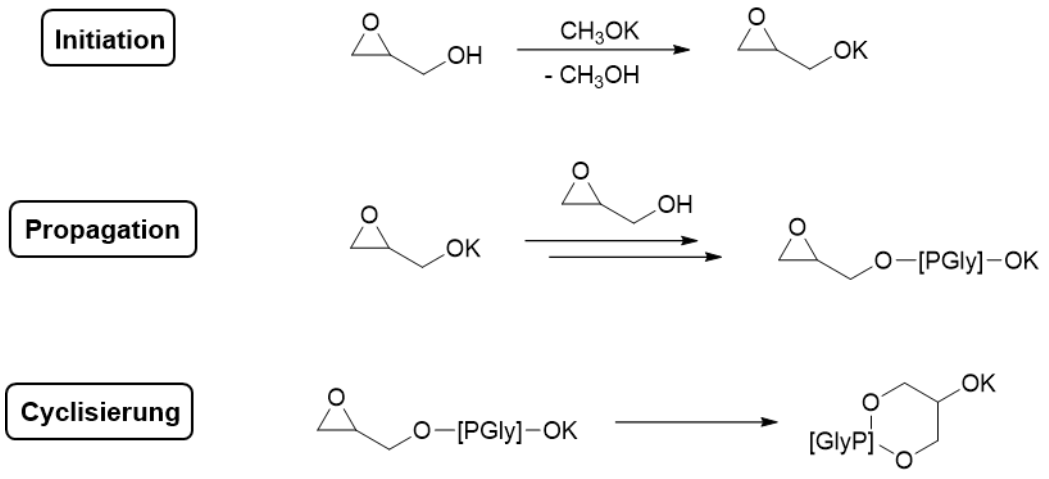

Abbildung 17: Mögliche Nebenreaktion von Glycidol bei einem zu hohen Glycidol/Initiator Verhältnis; Abbildung gemäß [206].

Diese Nebenreaktion kann durch eine langsame Glycidol-Zugabe unterdrückt werden. Außerdem werden nur 5 – 10 % der OH-Gruppen der Kerneinheit deprotoniert, um die Konzentration der aktiven Zentren möglichst gering zu halten und somit ein simultanes Anwachsen aller Kettenenden sicherzustellen. Der schnelle intra- und intermolekulare Protonenaustausch sorgt für eine gleichmäßige Verzweigung und verhindert, dass ausschließlich lineare Einheiten gebildet werden. Mit Hilfe des *„Slow Monomer Addition Approach"* können somit HyPGs erhalten werden, die eine einheitlich verzweigte Struktur sowie eine engere Molmassenverteilung mit Polydispersitäten < 1,9 aufweisen.

HyPGs stellen ein interessantes Strukturmotiv dar und wurden als Baustein für das neue Fließmittel aufgrund folgender Eigenschaften gewählt:

- Hohe Hydrophilie
- Große Strukturvariabilität
    - Größe des Polyglycerolgerüsts kann über das Glycidol/Initiator Verhältnis gesteuert werden
    - Kerneinheit variierbar
    - OH-Gruppen in der Peripherie können vielfältig modifiziert werden
- Enge Molmassenverteilung – PDI niedriger als bei PCEs
- Synthese auch im großtechnischen Maßstab möglich
- Über einen Syntheseschritt zugänglich

Neben der sehr guten Wasserlöslichkeit, die ein wichtiges Kriterium für ein Fließmittel ist, spielte insbesondere die Strukturvariabilität bei der Auswahl eine große Rolle. Ähnlich wie bei kammförmigen PCEs sollte auch für das neue Fließmittel die Möglichkeit bestehen, die Struktur verändern zu können. HyPGs bieten in dieser Hinsicht drei verschiedene Variationsmöglichkeiten. So kann sowohl die Größe des hyperverzweigten Polyglycerols als auch die multifunktionale Kerneinheit variiert werden [207, 209]. Ferner existieren mehrere Möglichkeiten, wie die OH-Funktionalitäten modifiziert werden können (sh. **Abbildung 18**).

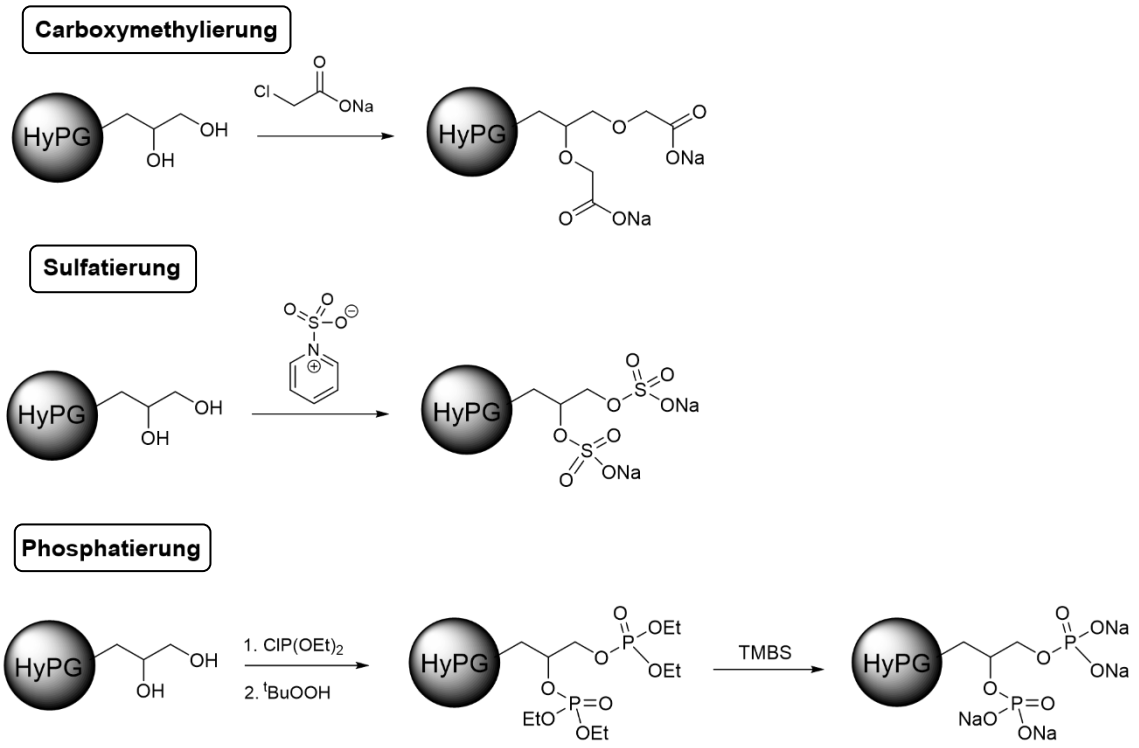

Abbildung 18: Möglichkeiten zur Derivatisierung der endständigen OH-Gruppen von hyperverzweigten Polyglycerolen.

In dieser Arbeit wurden die OH-Gruppen des HyPG carboxymethyliert, wobei sie mit Natriumchloroacetat unter stark alkalischen Bedingungen umgesetzt werden [217]. Über eine nukleophile Substitutionsreaktion (SN2) werden so Carboxymethyl-Gruppen in die Peripherie des Polyglycerolgerüsts eingebaut, über die eine Adsorption des Fließmittels stattfinden kann. Allerdings können die OH-Gruppen auch mit anderen funktionellen Gruppen, wie zum Beispiel Sulfat oder Phosphat, derivatisiert werden [215]. Die Sulfatierung erfolgt in einem Schritt mit einem Schwefeltrioxid-Pyridin-Komplex, während die Phosphatierung über eine zweistufige Synthese verläuft. Hierbei werden die OH-Gruppen zunächst mit Diethylchlorophosphit ($ClP(OEt)_2$) versetzt und anschließend mit *tert*-Butylhydroperoxid (^tBuOOH) zu einem Phosphatdiethylester oxidiert, der im finalen Schritt mittels Bromtrimethylsilan (TMBS) hydrolysiert wird. Durch das Einbringen unterschiedlicher Ankergruppen ist es möglich, die Bindungsaffinität des Polymers und somit das Adsorptionsverhalten zu verändern [40].

3.8. Titration nach *Elder*

Die Titration nach *Elder* ermöglicht es, die Anzahl der OH-Gruppen von Polyolen zu bestimmen [223]. Diese Methode wurde für die Quantifizierung der primären und sekundären OH-Gruppen des hyperverzweigten Polyglycerolgerüsts verwendet. Basierend auf der Anzahl der OH-Gruppen wurde die Menge an Natriumchloroacetat berechnet, die im finalen Syntheseschritt für die Carboxymethylierung benötigt wurde. Vor der eigentlichen Titration wurde die Probe zunächst in einer Reagenzlösung aus Phthalsäureanhydrid, Imidazol und Pyridin gelöst. Nach dem Erwärmen auf 98 °C für 15 min wurde Wasser sowie Phenolphthalein als Indikator zugegeben und eine NaOH-Lösung hinzutitriert, bis der Umschlagspunkt (Farbwechsel von farblos zu violett) erreicht wurde. Die Titrationsmethode nach *Elder* beruht auf der durch Imidazol und Pyridin katalysierten Reaktion des Phthalsäureanhydrids mit den OH-Funktionalitäten der Probe und der anschließenden titrimetrischen Erfassung der freien Carbonsäure-gruppen. In **Abbildung 19** sind die einzelnen Reaktionsschritte dargestellt:

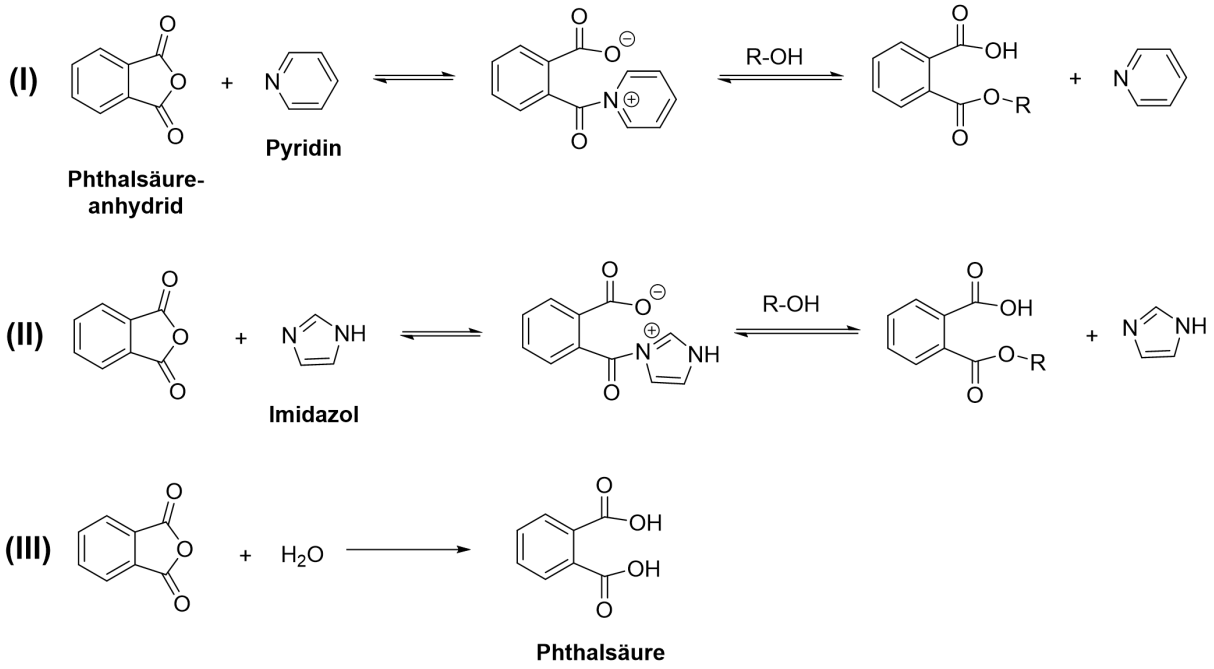

Abbildung 19: Reaktionsstufen bei der Titration nach *Elder*.

Wie aus der Abbildung ersichtlich, reagieren Imidazol und Pyridin mit Phthalsäure-anhydrid zunächst unter Bildung einer aktivierten Zwischenstufe, die am stark nukleophilen Kohlenstoffatom von der OH-Gruppe des Analyten angegriffen wird. Hierbei wird Imidazol bzw. Pyridin abgespalten und ein Säurehalbester gebildet (**I** u. **II**).

Das im Überschuss eingesetzte Phthalsäureanhydrid, das nicht benötigt wurde, wird durch die Zugabe von Wasser zu Phthalsäure hydrolysiert (**III**). Durch die Titration mit einer NaOH-Lösung werden alle Carbonsäuregruppen bestimmt, die nicht verestert wurden. Für die Neutralisation des Säurehalbesters wird nur ein Äquivalent an Natriumhydroxid benötigt, während hingegen zwei für Phthalsäure erforderlich sind. Ebenfalls wird die Titration nur für die Reagenzlösung durchgeführt (=Referenz). Die molare Menge an OH-Gruppen pro Gramm Polymer kann schließlich mit Hilfe von **Gleichung 3** berechnet werden:

$$\text{Anzahl OH-Gruppen}\left(\frac{\text{mmol}}{\text{g Polymer}}\right) = \frac{\left(V_{NaOH,Referenz} - V_{NaOH,Probe}\right)\cdot c_{NaOH}}{m_{Probe}} \qquad (3)$$

Darin ist $V_{NaOH,Referenz/Probe}$ das Volumen des NaOH-Titranten, das bis zum Erreichen des Äquivalenzpunkts benötigt wurde; c_{NaOH} die Konzentration der NaOH-Lösung und m_{Probe} die Masse der Probe.

3.9. Entstehung und Zusammensetzung von Lignit/Braunkohle

Ein weiterer Themenblock dieser Arbeit beschäftigte sich mit der Synthese eines auf Lignit-basierten Fließmittels und Untersuchungen wie sich eine gestreckte Polymerkonformation auf die Dispergiereigenschaften auswirkt (**Publikationen #10** und **#11**). Das neue Fließmittel wurde ausgehend von Humin- und Fulvinsäuren synthetisiert, die in Braunkohle enthalten sind. Nachfolgend ist der theoretische Hintergrund hierzu dargestellt.

Braunkohle ist ein organisches Sedimentgestein, welches vor 66 – 3 Mio. Jahren im Zeitalter des Tertiärs aus abgestorbenen Pflanzenresten durch bio- und geochemische Abbau- und Umwandlungsprozesse gebildet wurde [224-228]. Pflanzliches Material wurde in subtropischen Sumpfmooren zunächst durch Bakterien und Pilze abgebaut, wobei Cellulose und Lignin schrittweise zu Huminstoffen umgewandelt wurden [224-227]. Aufgrund der stark tropischen Vegetation wurden die Zersetzungsprodukte fortlaufend mit neuem Pflanzenmaterial überdeckt, dass zu einer zunehmenden Verdichtung führte und Torf aus den Huminstoffen gebildet wurde. Neben biochemischen Prozessen spielten geochemische Phänomene ebenfalls eine entscheidende Rolle [227]. Geologische Änderungen (z.B. Beckenabsenkungen) im Laufe

der erdgeschichtlichen Entwicklung führten zu einer Bedeckung der Torfschichten mit Sedimenten, wodurch der Druck und die Temperatur stetig anstiegen (sh. **Abbildung 20**) [226]. Diese Bedingungen führten zu einer Komprimierung und Entwässerung des Torfs. Bei diesem Vorgang, der auch als Inkohlung bezeichnet wird, fanden chemische sowie strukturelle Änderungen statt, wobei Torf sukzessive in Braunkohle umgewandelt wurde [228]. Kohlenstoffdioxid und Methan wurden hierbei abgespalten und der Anteil an flüchtigen Bestandteilen stark reduziert, dass einen erhöhten Kohlenstoffgehalt zur Folge hatte. Außerdem wurden durch chemische Reaktionen wie Kondensationen und Polymerisationen ein makromolekulares Gerüst aus aromatischen Strukturelementen aufgebaut [228]. Abhängig vom Inkohlungsgrad können verschiedene Kohlearten unterschieden werden: Braunkohle, Steinkohle und Anthrazit. Braunkohle stellt die erste Stufe innerhalb des Inkohlungsprozesses dar und zeichnet sich durch einen niedrigen Inkohlungsgrad (Kohlenstoffanteil 65 – 75 %) und einen hohen Wassergehalt aus (40 – 60 %) [229]. Anthrazit weist hingegen den höchsten Kohlenstoffgehalt (> 90 %) und die niedrigste Wasserrestmenge auf (< 2 %), da sie einer höheren Temperatur und einem höheren Druck über eine längere Zeit ausgesetzt war und daher die Inkohlung vollständig durchlaufen hat [226].

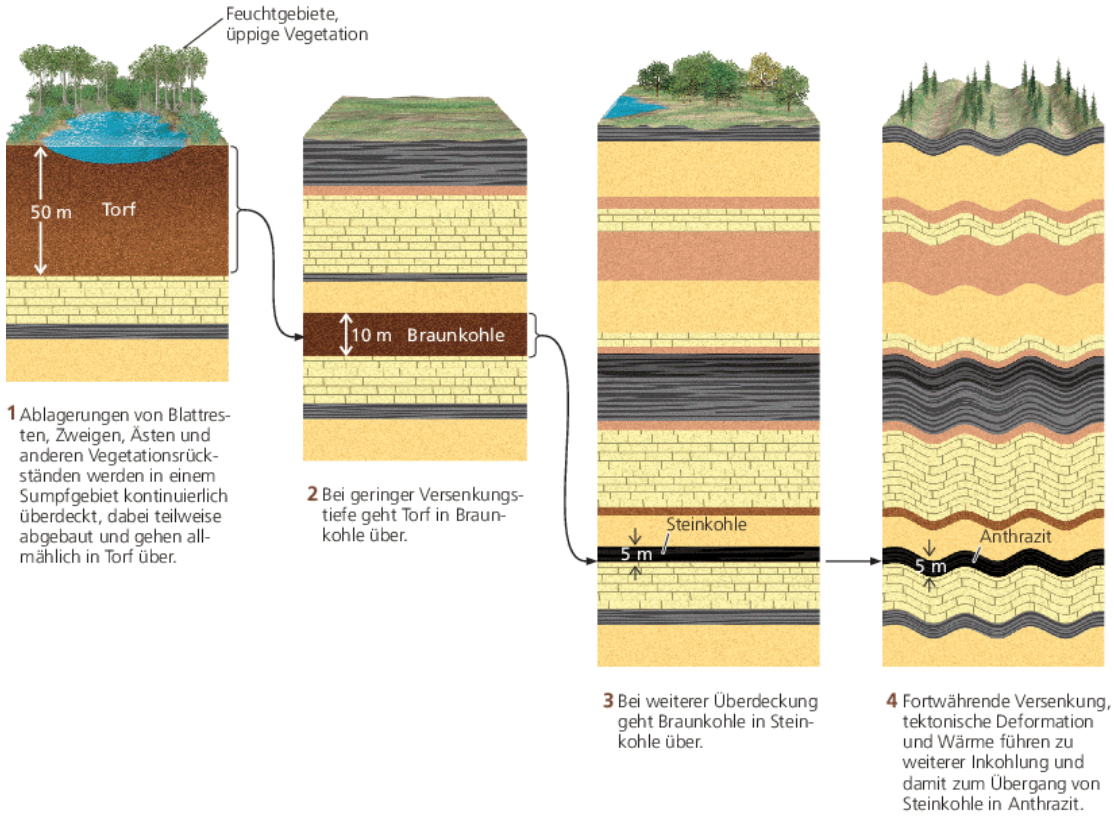

Abbildung 20: Darstellung der verschiedenen Inkohlungsstufen von Torf; Abbildung übernommen aus [226].

Der niedrige Inkohlungsgrad der Braunkohle zeigt sich dadurch, dass teilweise noch holzfaserige Komponenten (sog. „Xylit“) enthalten sind, die nicht abgebaut wurden. Aufgrund dieser Holzrückstande wird Braunkohle auch als Lignit bezeichnet [225].

Braunkohle ist ein Gemisch aus verschiedenen Stoffgruppen, die in anorganische und organische unterteilt werden [229]. Zu den anorganischen Bestandteilen gehören Asche und Mineralien (Tone, Calcit, Quarz), während Wachse, Harze, Huminstoffe, Cellulose sowie Lignin den organischen zugeordnet werden [229, 230]. Abhängig von den Inkohlungsbedingungen und dem Pflanzenmaterial aus dem Torf gebildet wurde, kann die Zusammensetzung stark variieren. Aufgrund dieser Komplexität konnte die exakte Struktur von Braunkohle bis heute noch nicht vollständig aufgeklärt werden. Es existieren ausschließlich Modelle die einzelne Strukturabschnitte beschreiben können [231]. Gemäß dem Strukturmodell von *Wolfrum* setzt sich Braunkohle aus drei Bausteinen zusammen: Lignin, Huminsäuren und aromatischen Elementen (sh. **Abbildung 21**) [232].

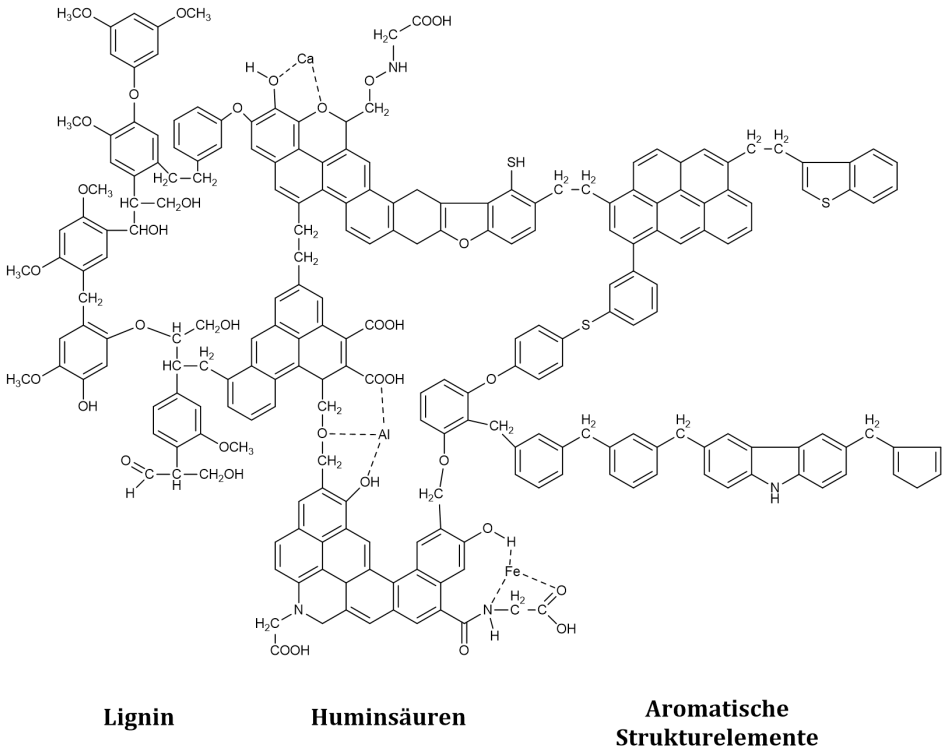

Abbildung 21: Chemische Strukturformel von Braunkohle gemäß *Wolfrum* [232].

Wie in der Abbildung zu erkennen ist, besteht die Struktur aus mehreren kondensierten Aromaten, die vorwiegend über Methylen- und Ethylenbrücken sowie Sauerstoffatome verknüpft sind. Darüber hinaus sind viele sauerstoffhaltige funktionelle Gruppen wie

Carboxylat-, Hydroxyl-, Methoxy-, Keton- und Ethergruppen enthalten [232]. Außerdem können Schwefel- und Stickstoffatome in der Struktur vorgefunden werden, die in Form von Amin-, Amid-, Hydroxylamin-, Indol-, Thiol-, Thiophen- und Thioetherbindungen vorliegen [231].

Ein wesentlicher Bestandteil von Braunkohle sind Huminsäuren, die in einem Anteil von bis zu 80 % enthalten sind [233]. Huminsäuren bilden zusammen mit den Fulvinsäuren und Huminen die Gruppe der Huminstoffe, die durch den Abbau von Pflanzenresten entstanden sind [234] und sich aus mehreren Strukturelementen wie Lignin, Polysacchariden, Proteinen, Heterocyclen, Aminosäuren und aromatischen Bausteinen zusammensetzen [235, 236]. Die einzelnen Huminstoffgruppen unterscheiden sich in ihrer Löslichkeit. Die Huminstoff-Fraktion, die oberhalb eines pH-Werts von 2 löslich ist, stellen die Huminsäuren dar, während die unlöslichen Komponenten als Humine bezeichnet werden [235, 237]. Fulvinsäuren sind alle organischen Substanzen, die über den gesamten pH-Bereich löslich sind. Die unterschiedlichen pH-Löslichkeiten können daher genutzt werden, um eine Fraktionierung vorzunehmen und die Humin- und Fulvinsäuren durch eine alkalische Extraktion von den unlöslichen Braunkohle-bestandteilen abzutrennen [237, 238]. Die chemischen Strukturen der Humin- und Fulvinsäuren sind in **Abbildung 22** dargestellt.

Huminsäure

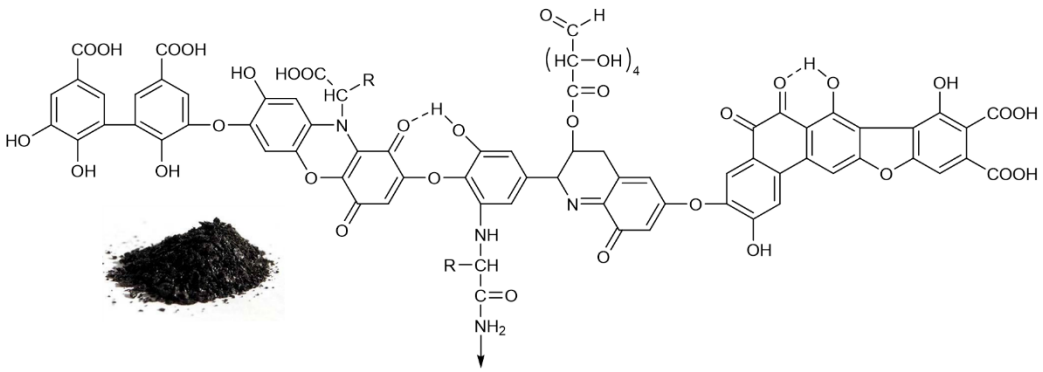

Fulvinsäure

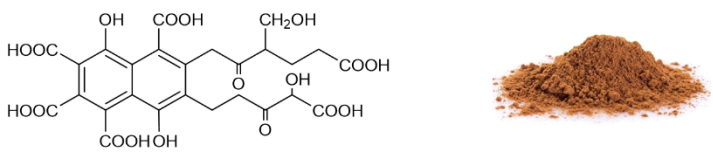

Abbildung 22: Chemische Struktur von Huminsäure gemäß *Stevenson* [239] und von Fulvinsäure gemäß *Buffle* [240]; Abbildungen aus [241 a, b].

Humin- und Fulvinsäuren enthalten als charakteristische Gruppen aliphatische und aromatische Carboxylate, Ketone, Phenole und Hydroxylfunktionalitäten [230]. Fulvinsäuren besitzen im Vergleich zu den Huminsäuren ein niedrigeres Molekulargewicht und weisen eine höhere Anzahl an sauerstoffhaltigen Gruppen auf, während sich die Huminsäuren durch einen höheren Stickstoff- und Schwefelgehalt sowie einen höheren Anteil an aromatischen Elementen auszeichnen [235]. Aufgrund der hohen Dichte an funktionellen Gruppen sind beide Verbindungen ideale Substrate für Modifizierungsreaktionen wie beispielsweise einer radikalischen Pfropfcopolymerisation, bei der ein Radikalstarter zugegeben wird, der nach dem Zerfall mehrere Radikalstellen innerhalb der Struktur bildet, an die anschließend Monomere über einen Kettenwachstumsschritt angelagert werden können.

4. Methoden und experimentelles Vorgehen

Das folgende Kapitel gibt einen kurzen Überblick zur experimentellen Vorgehensweise und erläutert, welche Messmethoden im Rahmen der Arbeit zum Einsatz kamen. Die detaillierten Versuchsbeschreibungen können den jeweiligen Veröffentlichungen entnommen werden. **Abbildung 23** zeigt die drei wesentlichen Bausteine des Versuchsprogramms. Die Untersuchungen wurden in allen Publikationen gemäß dieses Schemas durchgeführt.

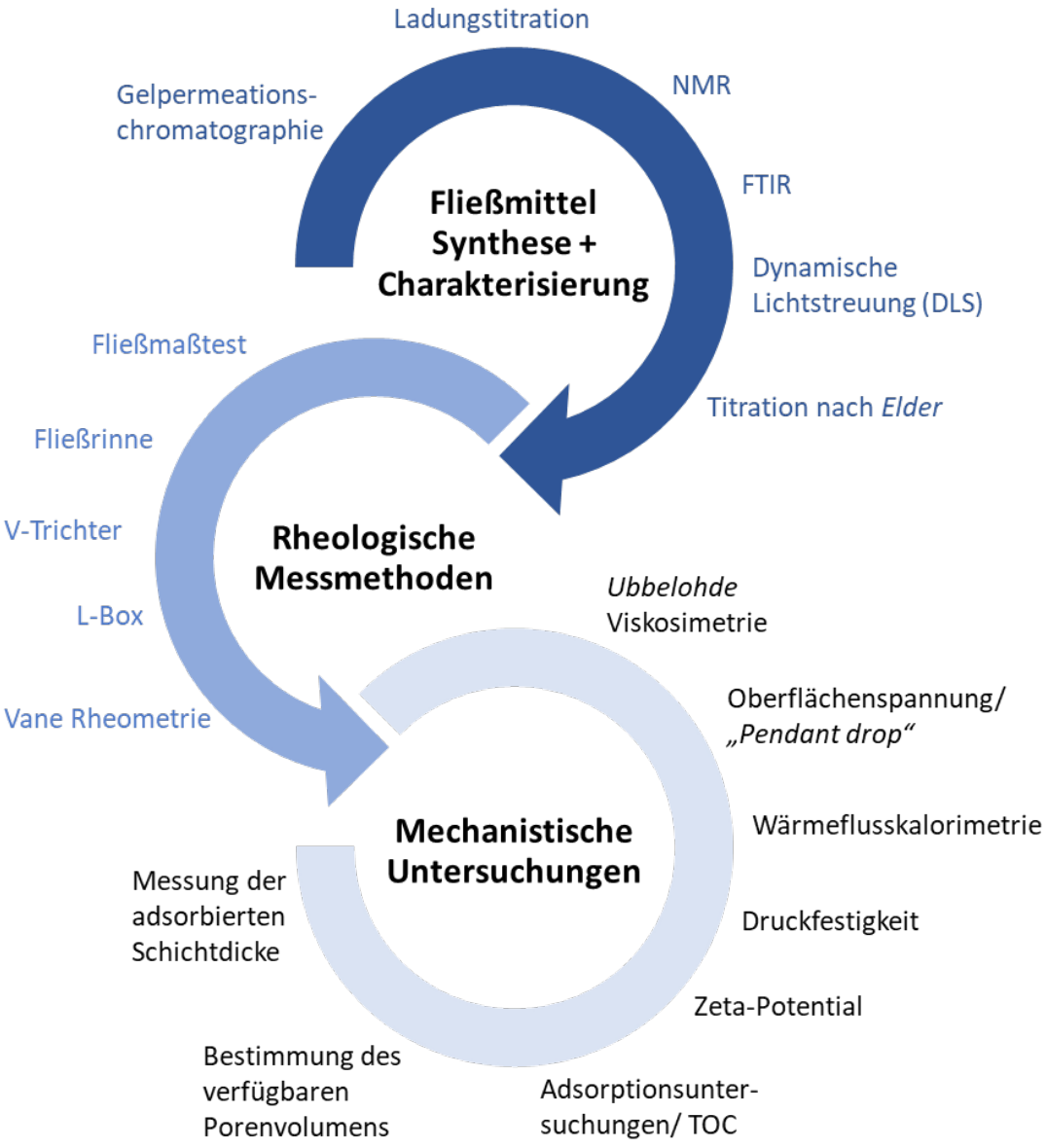

Abbildung 23: Experimentelle Abfolge und Übersicht der eingesetzten Messmethoden.

Zunächst wurden die Fließmittel synthetisiert und anschließend über verschiedene Methoden charakterisiert. Ziel war es, die Qualität der PCE-Fließmittel hinsichtlich ihrer

Polydispersität und des Makromonomer-Umsatzes zu überprüfen und Informationen zu den Polymereigenschaften zu erhalten (z.B. Molekulargewicht, anionische Ladung, hydrodynamischer Radius). Bei der Synthese des neuen hyperverzweigten Fließmittels wurden zudem NMR- und FTIR-Messungen eingesetzt, um die Bildung der Struktur zu belegen. Im zweiten Schritt wurde die Verflüssigungswirkung der Fließmittel/nicht-ionischen Co-Dispergiermittel im Zementleim, Mörtel und Beton über unterschiedliche rheologische Messmethoden bestimmt. Die hierbei gewonnenen Erkenntnisse dienten anschließend als Ausgangspunkt für die mechanistischen Studien. Zur Aufklärung der Wirkungsweise der nicht-ionischen Co-Dispergiermittel sowie zur Untersuchung der neu synthetisierten hyperverzweigten PCE- und Lignit-basierten Fließmittel wurden eine Reihe von weiteren experimentellen Messmethoden herangezogen (sh. **Abbildung 23**).

In **Kapitel 5 „Ergebnisse und Diskussion“** werden die **Publikationen #1 – #4**, **#7**, **#10** und **#11** näher ausgeführt. Die **Veröffentlichungen #1 – #6** handeln über Arbeiten zur Aufklärung des Dispergiermechanismus der nicht-ionischen Moleküle bzw. Polymere, während **Publikationen #7 – #9** die Synthese und Charakterisierung eines hyperverzweigten Fließmittels zum Gegenstand haben. Die **Veröffentlichungen #10** und **#11** beschreiben die Synthese und Eigenschaften von Lignit-ATBS-*co*-AA-Pfropfpolymeren, die als neuartige Zementfließmittel getestet wurden. Im Folgenden soll erläutert werden, wie sich die experimentelle Vorgehensweise in den einzelnen Veröffentlichungen darstellte.

Publikation #1 befasst sich mit ersten Untersuchungen zur verflüssigenden Wirkung von nicht-ionischen „kleinen“ Molekülen, die mit zwei strukturell unterschiedlichen IPEG-PCEs kombiniert wurden (sh. **Abbildung 24**). Es sollten erste Erkenntnisse erhalten werden, ob nicht-ionische Verbindungen in der Lage sind, einen Beitrag zur Dispergierung zu leisten. Dies wurde über Fließmaßbestimmungen an Zementleimen untersucht, in denen unterschiedliche Dosierungen der Co-Dispergiermittel getestet wurden. Da bei den Tests beobachtet wurde, dass Zementschlämmen mit den nicht-ionischen Molekülen eine niedrigere Viskosität aufweisen, wurden die Co-Dispergiermittel ebenfalls im Mörtel eingesetzt und die Trichterauslaufzeit bestimmt. Darüber hinaus wurden Adsorptionsuntersuchungen durchgeführt, um Einblicke in die Wirkungsweise zu bekommen und darauf aufbauend ein erstes mechanistisches Modell zu formulieren.

1. Synthese und Charakterisierung der IPEG-PCEs

- Synthese von 52IPEG2 und 52IPEG5.8 — Freie radikalische Copolymerisation
- Molmassen, PDI, Makromonomer-Umsatz — GPC
- Anionische Ladungsmenge — Ladungstitration

2. Kombination der IPEG-PCE-Fließmittel mit Diethylenglykol und Jeffamin D-230 als nicht-ionische Co-Dispergiermittel

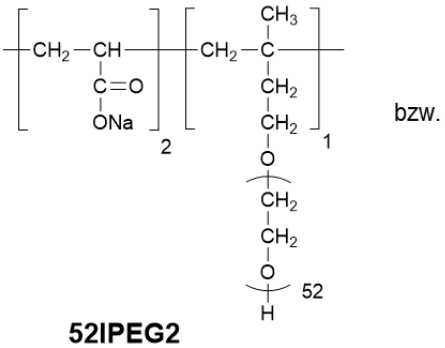

52IPEG2

bzw.

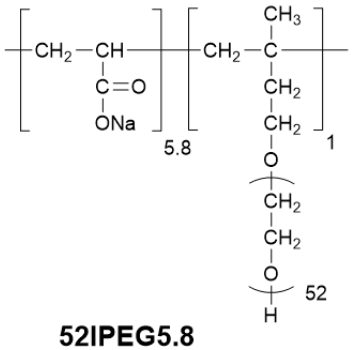

52IPEG5.8

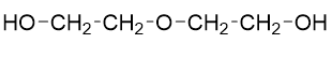

Diethylenglykol

bzw.

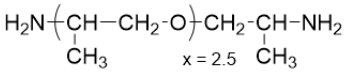

Jeffamin D-230

Einfluss von Diethylenglykol/Jeffamin D-230 auf die rheologischen Eigenschaften:

- Dispergierwirkung im Zementleim — Fließmaßtest
- Fließgeschwindigkeit von Mörtel — Trichterauslaufzeit
- Robustheit gegenüber Wasserschwankungen — Fließmaßtest

Einfluss von Jeffamin D-230 auf das Adsorptionsverhalten der PCEs:

- Adsorptionsuntersuchungen von 1:1 Mischungen der PCEs mit Jeffamin D-230 – Bestimmung der adsorbierten Jeffamin-Menge über Stickstoff-Gehalt — TOC Methode/ TN Bestimmung

Abbildung 24: Vorgehensweise und experimentelle Methoden in **Publikation #1**.

Der Hauptfokus in **Publikation #2** lag darauf, eine Struktur-Wirkungs-Beziehung für die nicht-ionischen Additive zu ermitteln, d.h. welche „kleinen“ Moleküle besonders geeignet sind, um die Fließeigenschaften zu verbessern. Hierfür wurden zu einem IPEG-PCE mit einer mittleren anionischen Ladung verschiedenste Glykolverbindungen

gegeben, die sich über die Anzahl an hydrophilen und hydrophoben Gruppen in ihrer Struktur unterschieden. Anschließend wurden rheologische Untersuchungen im Zementleim vorgenommen und einige ausgewählte nicht-ionische Moleküle im Beton getestet. Ferner wurde über Wärmeflusskalorimetrie analysiert, ob die Co-Dispergiermittel einen Einfluss auf die Zementhydratation ausüben. Die experimentelle Vorgehensweise ist in **Abbildung 25** dargestellt.

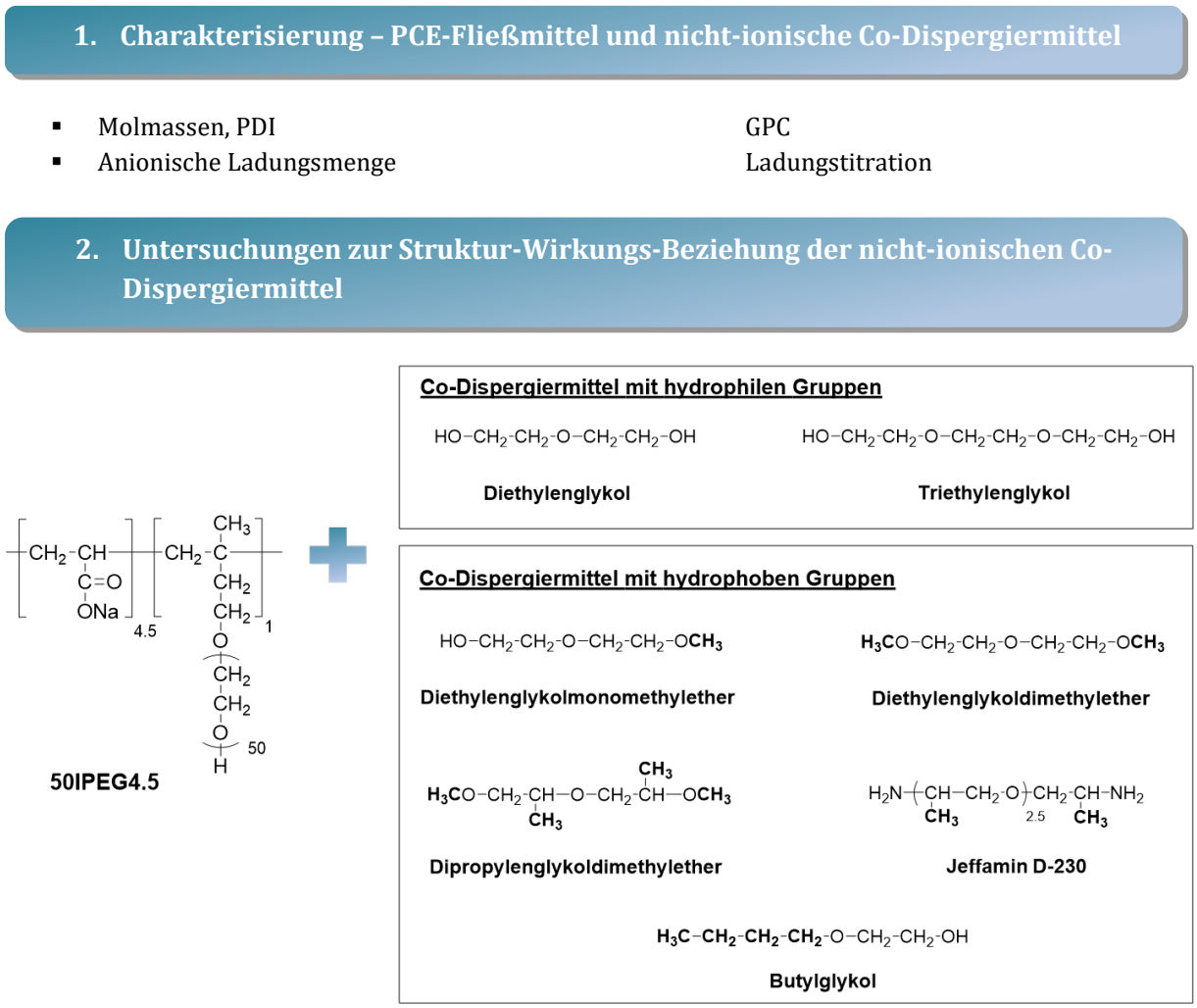

Abbildung 25: Vorgehensweise und Messmethoden in **Publikation #2**.

In **Publikation #3** wird beschrieben, welche PCE-Strukturen am stärksten von der Zugabe der Co-Dispergiermittel profitieren und welche Eigenschaften ein nicht-ionisches Molekül prinzipiell aufweisen muss, um möglichst effizient zu sein. Dazu wurden MPEG-PCEs mit unterschiedlicher anionischer Ladung und Seitenkettenlänge synthetisiert und diese mit einer Vielzahl von nicht-ionischen Molekülen im Zementleim bei verschiedenen w/z-Werten getestet (sh. **Abbildung 26**). Hierbei wurde der Kreis der Co-Dispergiermittel nochmals erweitert und neue Strukturmerkmale evaluiert. Über Adsorptionsmessungen sollte herausgefunden werden, warum die nicht-ionischen Moleküle für bestimmte PCE-Strukturen förderlicher sind. Ebenfalls wurden einige Versuche mit synthetischen Zementporenlösungen durchgeführt, wobei unter anderem der Einfluss der Co-Dispergiermittel auf die Oberflächenspannung (*„Pendant drop"* Methode) [242] sowie die Lösungsviskosität (*Ubbelohde* Viskosimetrie) ermittelt wurde. Auf Grundlage der gewonnen Erkenntnisse wurde ein erstes Modell zur Dispergierwirkung der nicht-ionischen Verbindungen konzipiert.

In **Publikation #4** wurde der Einfluss der Co-Dispergiermittel auf die rheologischen Eigenschaften von Mörtel und Beton untersucht (sh. **Abbildung 27**). Ziel war es, das Konzept der nicht-ionischen Moleküle in der Praxis zu überprüfen und anwendungstechnische Vorteile herauszuarbeiten. Ein MPEG- und IPEG-PCE mit vergleichbarer anionischer Ladung wurden in Gegenwart unterschiedlicher Co-Dispergiermittel getestet und die Auswirkungen dieser Kombinationen auf die Fließgrenze und plastische Viskosität bestimmt. Dies erfolgte im Mörtel über die Messung des Ausbreitmaßes, der Trichterauslaufzeit und der Fließgeschwindigkeit in der Fließrinne. Außerdem wurden Betonversuche in einem Transportbetonwerk durchgeführt, um in der praxisgerechten Formulierung eines selbstverdichtenden Betons, der er eine stark klebrige Konsistenz aufwies, das Potential der nicht-ionischen Moleküle auszuloten. Über die Bestimmung des frei verfügbaren Porenvolumens wurde anschließend die erste Modellvorstellung zur Wirkweise der Co-Dispergiermittel auf die Verhältnisse im Mörtel und Beton angepasst. In ergänzenden Versuchen, die nicht in der Veröffentlichung beschrieben sind (sh. Seite 120 ff.), wurden über Vane Rheometrie und L-Box-Versuche weitere Erkenntnisse zum Effekt der Co-Dispergiermittel in einem selbstverdichtenden Beton gesammelt.

1. Synthese von MPEG-PCEs mit unterschiedlicher anionischer Ladung sowie Seitenkettenlänge über freie radikalische Copolymerisation

2. Polymercharakterisierung

▪ Molmassen, PDI, Makromonomer-Umsatz	GPC
▪ Anionische Ladungsmenge	Ladungstitration
▪ Polymerradius	Dynamische Lichtstreuung (DLS)
▪ Lösungskonformation	Model nach *Gay* und *Raphaël*

3. Kombination der PCEs mit nicht-ionischen Co-Dispergiermitteln

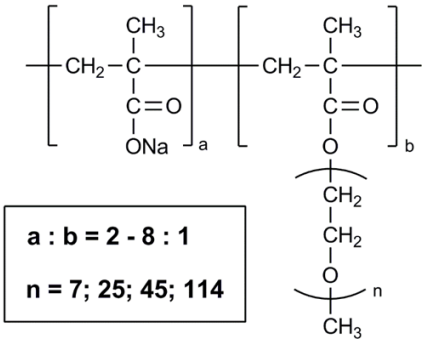

a : b = 2 - 8 : 1

n = 7; 25; 45; 114

Polyethylenglykol (M_w = 300, 1000, 3000 g/mol)
Diethylenglykol
Diethylenglykolmonomethylether
Diethylenglykoldimethylether
1,6-Hexandiol
Neopentylglykol
2-Methyl-2,4-pentandiol

Verflüssigungswirkung in Abhängigkeit von:

- w/z-Wert
- Ladungsmenge und Seitenkettenlänge des PCEs
- Molekulargewicht und chemischer Struktur des Co-Dispergiermittels

} Fließmaßtest

4. Mechanistische Untersuchungen

▪ Quantifizierung des Porenlösungsvolumens	Filterpresse
▪ Einfluss der Co-Dispergiermittel auf die kinematische Viskosität der Porenlösung	*Ubbelohde* Viskometer
▪ Adsorptionsverhalten der PCEs in Gegenwart eines nicht-ionischen Co-Dispergiermittels	TOC Methode
▪ Einfluss nicht-ionischer Co-Dispergiermittel auf die Oberflächenspannung	*„Pendant drop“* Methode

Abbildung 26: Vorgehensweise und eingesetzte Methoden in **Publikation #3**.

1. Charakterisierung der PCE-Fließmittel

- Molmassen, PDI, Makromonomer-Umsatz — GPC
- Anionische Ladungsmenge — Ladungstitration
- Dosierungskurve — Mörtelausbreitmaß

2. Kombination unterschiedlicher PCE-Fließmittel mit nicht-ionischen Co-Dispergiermitteln

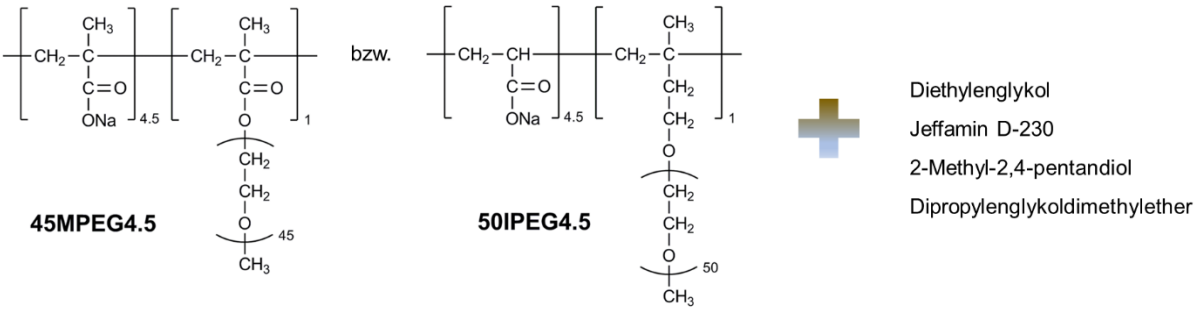

Einfluss der Co-Dispergiermittel auf:

Mörtel (w/z = 0,26)	**Selbstverdichtender Beton (w/z = 0,35)**
○ Mörtelausbreitmaß	○ Ausbreitmaß
 *Hägermann-Trichter*	 *SVB-Setztrichter*
○ Fließgeschwindigkeit	○ Fließgeschwindigkeit
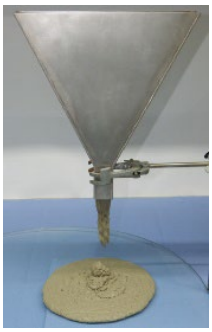 *V-Trichter*  *Fließrinne*	 *V-Trichter*
○ Festigkeitsentwicklung (1, 7 und 28 Tage)	

3. Mechanistische Untersuchungen

- Bestimmung des frei verfügbaren Porenvolumens — Zentrifugation
- Aufstellung eines abschließenden Modells zur Wirkungsweise der Co-Dispergiermittel

Abbildung 27: Vorgehensweise und experimentelle Methoden in **Publikation #4.**

In **Publikation #7** werden die Synthese und Eigenschaften eines hyperverzweigten Fließmittels beschrieben, das über eine dreistufige Syntheseroute dargestellt wurde. Ausgangspunkt war ein lineares Polyetheramin (Jeffamin) bestehend aus Ethylen- und Propylenoxid-Einheiten, welches zunächst bisglycidoliert wurde, um ein Intermediat mit vier Hydroxylgruppen zu erhalten (sh. **Abbildung 28**) [222].

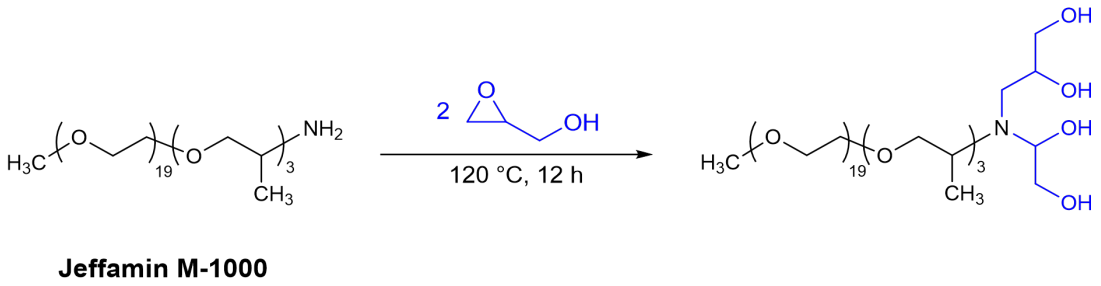

Abbildung 28: Bisglycidolierung von Jeffamin.

Diese Zwischenstufe fungierte als Makroinitiator in der anschließenden anionischen Ringöffnungspolymerisation von Glycidol, über die ein hyperverzweigtes Polyglycerolgerüst aufgebaut wurde. 10 % der Hydroxylgruppen des Initiators wurden durch Kaliummethanolat deprotoniert und eine Glycidol-THF-Lösung langsam gemäß der *„Slow Monomer Addition"*-Strategie nach *Mülhaupt* et al. über eine peristaltische Schlauchpumpe zugegeben, um die Polymerisation unter möglichst kontrollierten Bedingungen stattfinden zu lassen (sh. **Abbildung 29**).

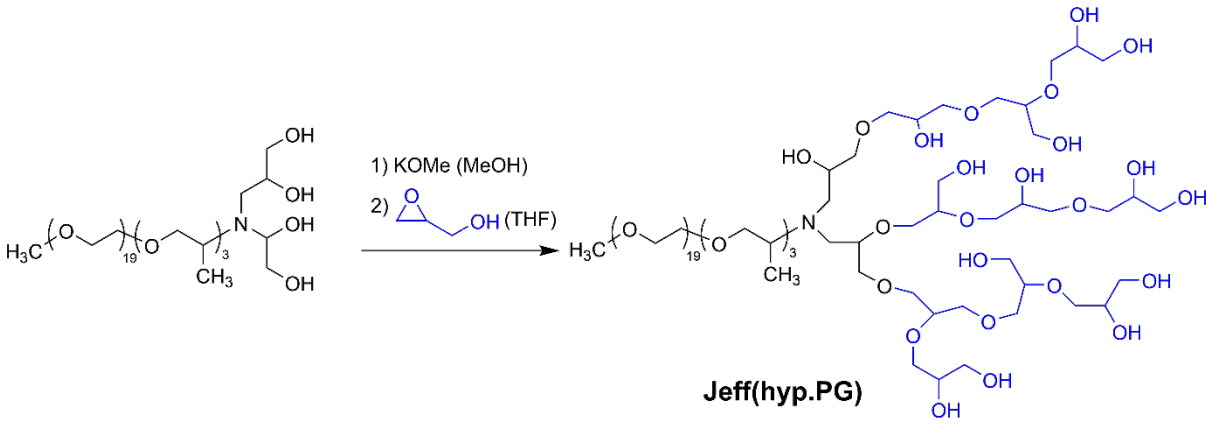

Abbildung 29: Anionische Ringöffnungspolymerisation von Glycidol.

Im finalen Schritt wurden die endständigen OH-Gruppen der Polyglycerol-Einheit durch die Zugabe von Natriumchloroacetat unter alkalischen Bedingungen carboxymethyliert (sh. **Abbildung 30**).

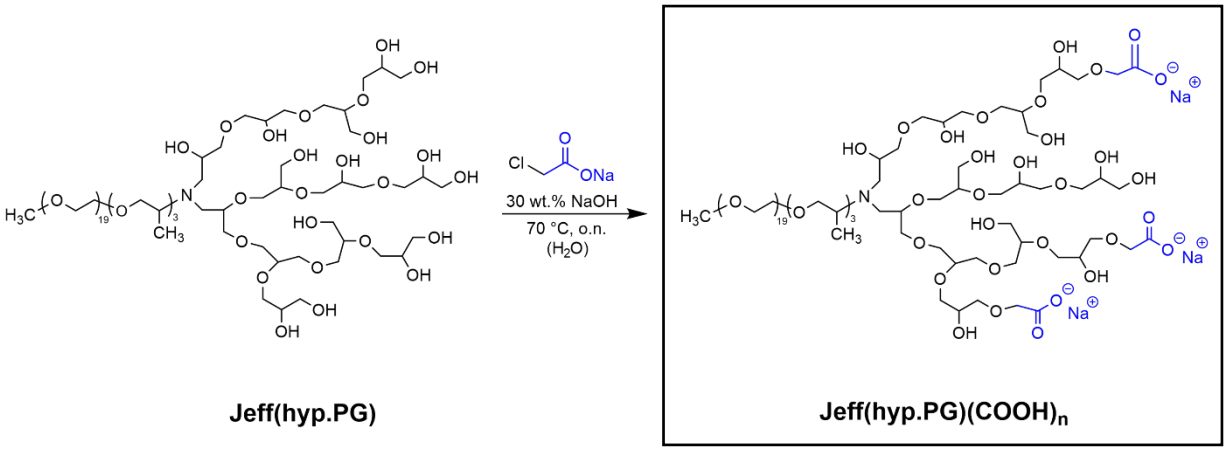

Abbildung 30: Carboxymethylierung der terminalen OH-Funktionalitäten des Polyglycerols.

Neben diesem Polymer wurde zusätzlich ein carboxymethyliertes hyperverzweigtes Polyglycerol ausgehend von TMP über eine zweistufige Synthese hergestellt, das im Gegensatz zum Fließmittel keine Seitenkette am Hauptverzweigungspunkt besitzt (sh. **Abbildung 31**).

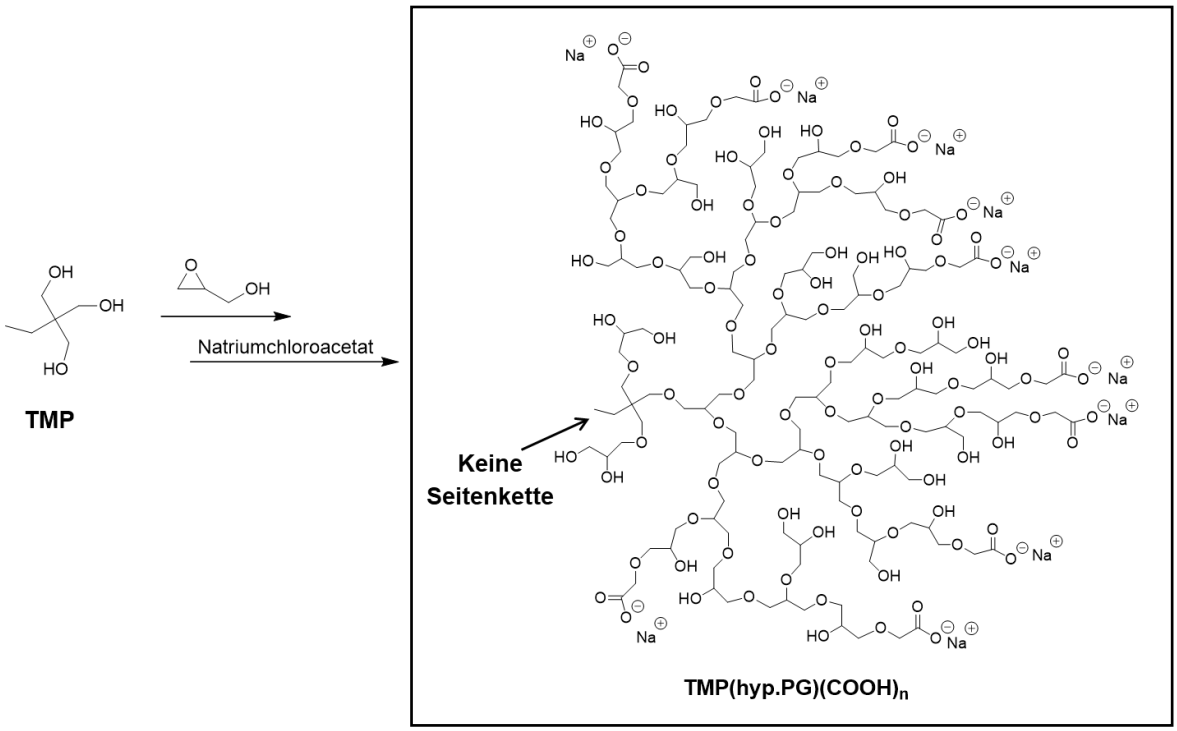

Abbildung 31: Synthese eines carboxymethylierten hyperverzweigten Polyglycerols ausgehend von TMP als Initiator.

Des Weiteren wurde ein lineares unverzweigtes Polymer mit zwei endständigen Carboxylatgruppen synthetisiert. Dieses Polymer wurde über eine *Michael*-Addition von Methylmethacrylat an Jeffamin und eine konsekutive basische Hydrolyse der Methylestergruppen dargestellt (sh. **Abbildung 32**).

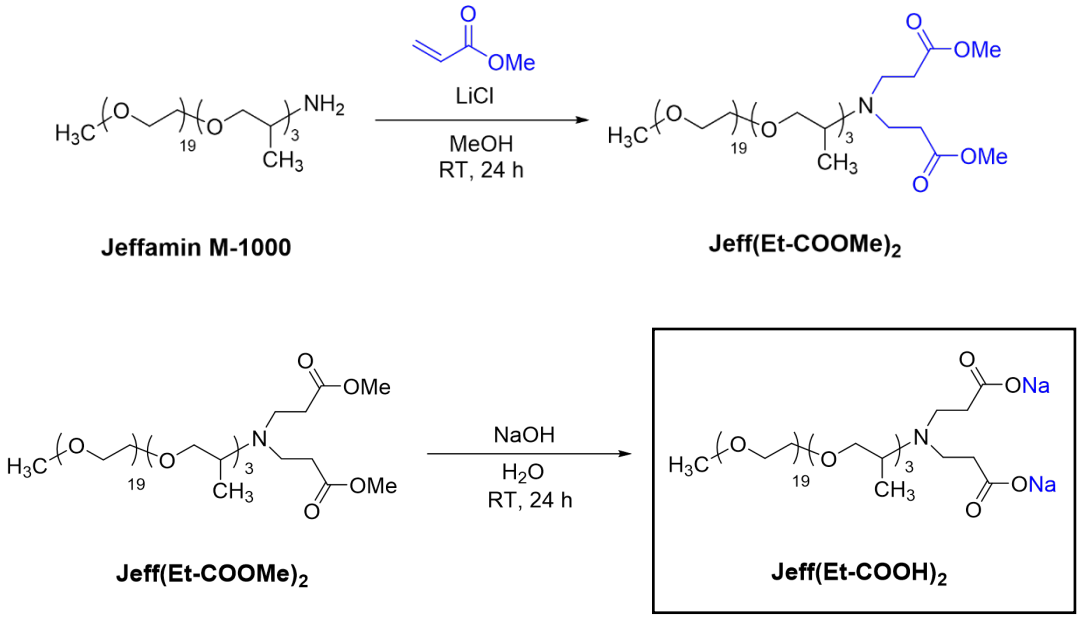

Abbildung 32: Zweistufige Synthese eines linearen, unverzweigten Polymers.

Diese Polymere wurden in der Studie eingesetzt um festzustellen, inwiefern die lineare Seitenkette des Jeffamins und das hyperverzweigte Polyglycerolgerüst zur Dispergierung beitragen und sie die Anwendungseigenschaften jeweils beeinflussen. Als Referenz wurde ein kammförmiges MPEG-PCE verwendet, das über eine radikalische Copolymerisation erhalten wurde (sh. **Abbildung 33**).

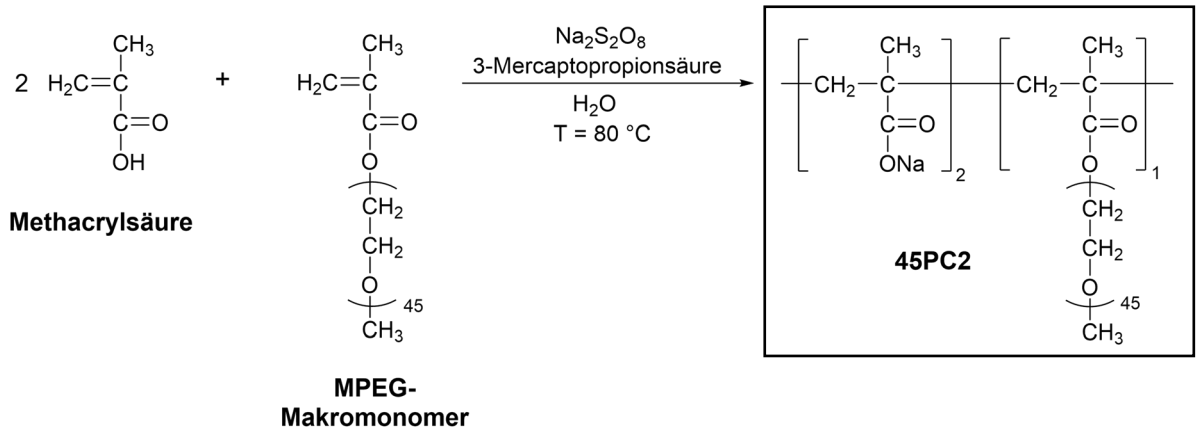

Abbildung 33: Synthese des kammförmigen Referenz-PCEs.

Alle beschriebenen Polymere wurden im Zementleim getestet und die Dispergierwirkung, zeitliche Verflüssigung sowie deren Robustheit gegenüber Sulfationen bestimmt. Über Adsorptionsmessungen (TOC Methode, Zeta-Potential) und Wärmeflusskalorimetrie sollte die Wirkungsweise des hyperverzweigten Fließmittels aufgeklärt werden (sh. **Abbildung 34**).

1. Synthese eines hyperverzweigten Fließmittels

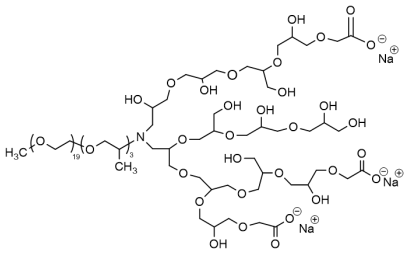

Dreistufige Synthese:

- Bisglycidolierung von Jeffamin M-1000
- Anionische Ringöffnungspolymerisation von Glycidol ausgehend vom bisglycidolierten Intermediat
- Carboxymethylierung der Polyglycerol-Einheit

2. Synthese weiterer Polymere für Untersuchungen zur Struktur-Wirkungs-Beziehung

- **Hyperverzweigtes Polymer ohne Seitenkette**

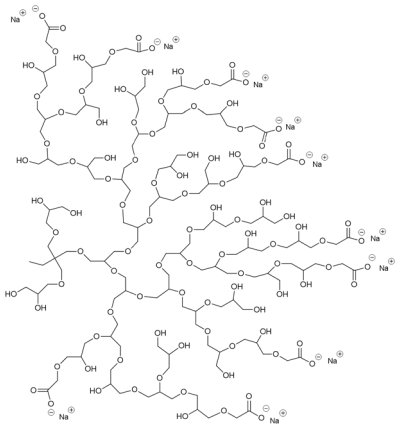

Anionische Ringöffnungspolymerisation

- **Lineares, unverzweigtes Polymer**

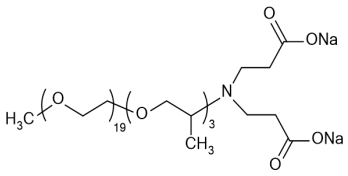

Michael-Addition

- **Kammförmiges PCE**

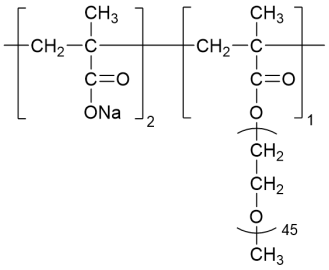

Radikalische Copolymerisation

3. Polymercharakterisierung

▪ Strukturnachweis	$^{1}H/^{13}C$ NMR; FTIR-Spektroskopie
▪ Molmassen, Polydispersität	GPC
▪ Anionische Ladungsmenge	Ladungstitration
▪ Bestimmung der OH-Anzahl	Titration nach *Elder*

4. Dispergierwirkung im Zementleim

- Dosierungsabhängige Verflüssigungswirkung
- Zeitabhängige Dispergierung
- Verflüssigung in Gegenwart von Sulfationen

} Fließmaßtest

5. Mechanistische Untersuchungen

▪ Adsorptionsuntersuchungen	TOC Methode
▪ Interaktion der Polymere mit Zement	Zeta-Potential
▪ Einfluss auf die Zementhydratation	Isothermale Wärmeflusskalorimetrie

Abbildung 34: Vorgehensweise und eingesetzte Methoden in **Publikation #7**.

Die **Publikationen #10** und **#11** handeln über die Synthese und Charakterisierung eines auf Lignit-basierten Fließmittels. In **Publikation #10** wurden zunächst aus Braunkohle-Proben (sh. **Abbildung 35**) aus dem Lausitzer Kohlerevier Humin- und Fulvinsäuren extrahiert, die als Polymerrückgrat des neuen Fließmittels verwendet wurden. Hierzu wurde die Braunkohle zerkleinert, abgesiebt und die Siebfraktion < 250 µm in einer NaOH-Lösung suspendiert und erwärmt. Die Extraktionslösung wurde zentrifugiert, um die unlöslichen Bestandteile abzutrennen und anschließend gefriergetrocknet. Auf diese Weise wurden die Na-Salze der Humin- und Fulvinsäuren als Ausgangsmaterial erhalten (*Ausbeute: 31 %*). Das Extraktionsschema ist in **Abbildung 35** dargestellt. In **Publikation #11** erfolgte die Synthese ausgehend von Superlignit, das bereits einen höheren Huminsäure-Anteil enthält (*~ 60 wt.%*), weshalb keine Extraktion für diese Probe durchgeführt wurde.

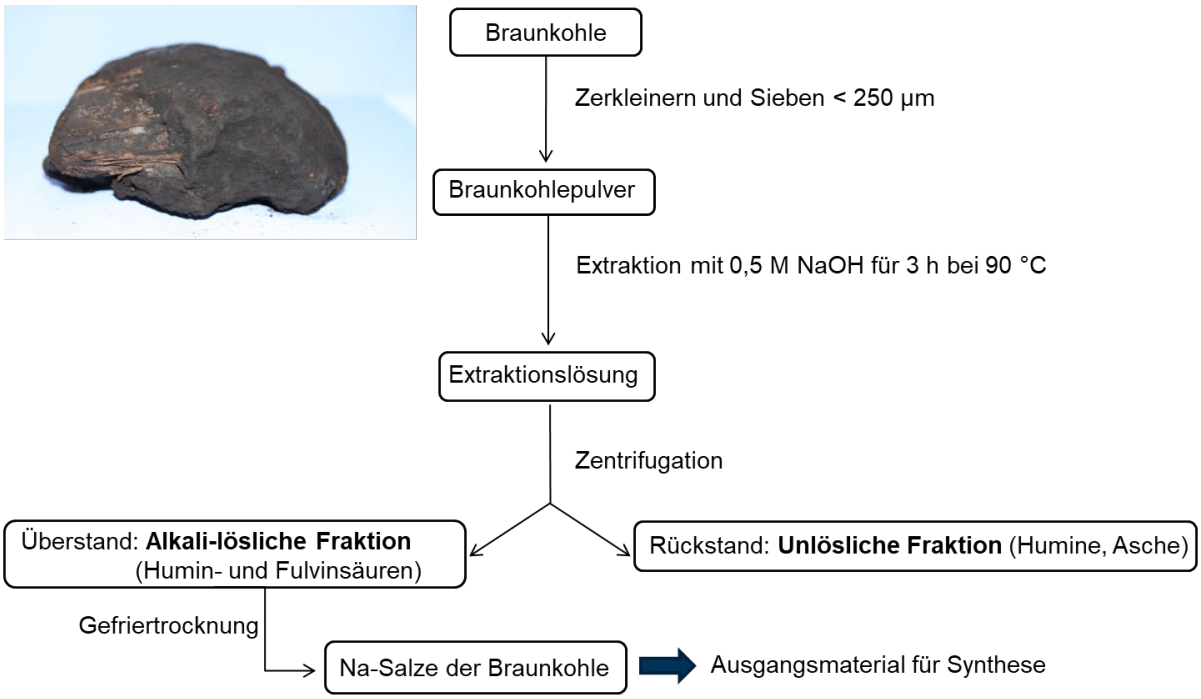

Abbildung 35: Experimentelle Vorgehensweise zur Abtrennung von Humin- und Fulvinsäuren aus Braunkohle (**Publikation #10**).

Das Fließmittel wurde über eine radikalische Propfcopolymerisation synthetisiert, bei der die extrahierten Huminsäuren aus der Braunkohle bzw. im Superlignit mit den Monomeren ATBS und Acrylsäure modifiziert wurden (sh. **Abbildung 36**). Natrium-persulfat diente als Initiator und Natriumdisulfit wurde am Ende der Polymerisation zum Quenchen der Radikale zugegeben. Ebenfalls wurde ein ATBS-*co*-AA-Polymer mittels einer freien radikalischen Copolymerisation synthetisiert, welches neben einem

Polykondensat-Fließmittel (BNS) als Referenzpolymer eingesetzt wurde (sh. **Abbildung 37**).

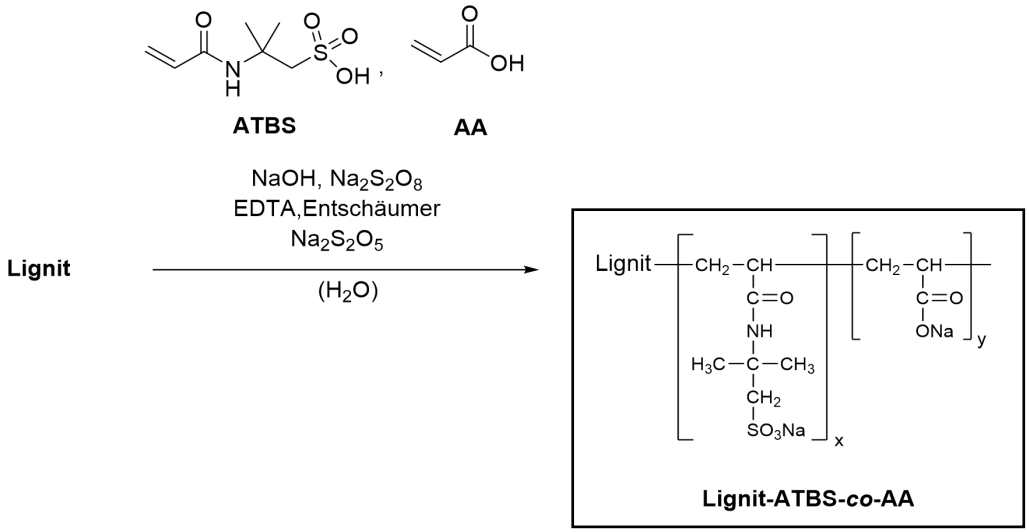

Abbildung 36: Synthese des Lignit-ATBS-*co*-AA-Pfropfpolymers.

Die Polymere wurden hinsichtlich ihrer Molmassen, Polymerradien (R_h, R_g) und anionischen Ladungsmenge charakterisiert. Außerdem wurde die Dispergierwirkung im Zementleim sowie der Fließmaßerhalt getestet und untersucht inwiefern Sulfationen die Wirksamkeit der Fließmittel beeinträchtigen. Um ein besseres Verständnis zum Dispergiermechanismus zu erhalten, wurden Zeta-Potential-Messungen durchgeführt und der Wärmefluss von Zementpasten mittels Kalorimetrie verfolgt. Darüber hinaus wurden die adsorbierten Schichtdicken der Polymere auf Modelladsorbentien gemessen. Hierzu wurden Lösungen mit verschiedenen Polymerkonzentrationen hergestellt und diese mit kationischen Polystyrolpartikeln versetzt, die mit Zinkpalmitat modifiziert waren [243]. Durch die positive Oberflächenladung sind die anionischen Fließmittel in der Lage sich durch Adsorption anzulagern. Über DLS wurde die Gesamtpartikelgröße bestimmt (Polystyrolteilchen + adsorbiertes Polymer) und mit Hilfe von **Gleichung 4** die adsorbierte Schichtdicke berechnet:

$$\text{Adsorbierte Schichtdicke (nm)} = \frac{\left(d_{\text{Gesamt}} - d_{\text{Polystyrol}}\right)}{2} \qquad (4)$$

Darin ist d_{Gesamt} die Polystyrolpartikelgröße mit adsorbierten Polymer und $d_{\text{Polystyrol}}$ die ursprüngliche Partikelgröße vor der Polymerzugabe. Die Messreihe wurde solange fortgeführt bis keine Zunahme der Schichtdicke mehr feststellbar war und die Sättigungsadsorption erreicht wurde.

1. Synthese von Lignit-ATBS-*co*-AA-Pfropfpolymeren

Publikation #10: Extraktion von Humin- und Fulvinsäuren aus Braunkohle; Verwendung der alkalilöslichen Fraktion für die Pfropfcopolymerisation

Publikation #11: Kommerzielles Superlignit mit erhöhtem Huminsäure-Anteil als Startmaterial

→ **Synthese:** Radikalische Pfropfcopolymerisation von ATBS und Acrylsäure auf Huminsäure (80/20) (wt.%/wt.%)

Variation ATBS/Acrylsäure-Verhältnis von 1 : 0,15 – 1 : 1,5 (**Publikation #11**)

2. Referenzpolymere

- **ATBS-*co*-AA-Polymer**

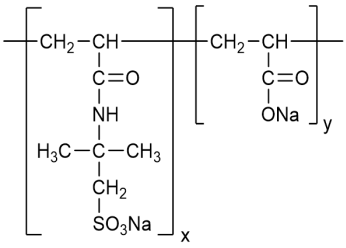

- **BNS Polykondensat**

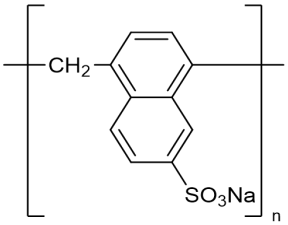

3. Polymercharakterisierung

▪ Molmassen, PDI	GPC
▪ Anionische Ladungsmenge	Ladungstitration
▪ Polymerradien R_h u. R_g	Dynamische bzw. statische Lichtstreuung
▪ Lösungsstruktur	*Burchard*-Parameter (R_g/R_h) [244]

4. Verflüssigende Wirkung

- Dosierung für Zementfließmaß von 26 ± 0,5 cm
- Zeitliche Dispergierwirkung
- Robustheit gegenüber Sulfationen

} Fließmaßtest

5. Mechanistische Untersuchungen

▪ Adsorptionsuntersuchungen	TOC Methode
▪ Interaktion der Polymere mit Zement	Zeta-Potential
▪ Einfluss auf Hydratationskinetik von Zement	Isothermale Wärmeflusskalorimetrie
▪ Messungen der adsorbierten Schichtdicke	Partikelgrößenmessung (DLS)

Abbildung 37: Vorgehensweise und experimentelle Methoden in den **Publikationen #10** und **#11**.

5. Ergebnisse und Diskussion

5.1. Einfluss nicht-ionischer Co-Dispergiermittel auf die rheologischen Eigenschaften zementärer Systeme

5.1.1. Publikation #1: Improvement of SCC Flow Properties Through Addition of Non-Adsorbing Small Molecule Co-Dispersants

Wie in **Kapitel 3.3.** erläutert, berichteten *Sakai* et al. als erste, dass nicht-adsorbierte PCE-Polymere zur Zementdispergierung beitragen können. Dies wurde insbesondere für Systeme mit einem hohen Feststoffanteil und einem niedrigen Wassergehalt beobachtet. Basierend auf dieser vorherigen Studie wurde in dieser Arbeit zunächst untersucht, ob ein ähnlicher Effekt durch die Zugabe von nicht-ionischen „kleinen" (d.h. nicht polymeren) Molekülen erzielt werden kann. Hierfür wurden Diethylenglykol sowie Jeffamin D-230 getestet, die in Dosierungen zwischen 0,1 und 0,9 % mit zwei verschiedenen IPEG-PCEs (52IPEG2.0 und 52IPEG5.8) kombiniert wurden, die sich hinsichtlich ihrer anionischen Ladungsmenge bzw. Seitenkettendichte deutlich unterschieden.

Es zeigte sich, dass die beiden nicht-ionischen Moleküle die Dispergierwirkung der PCEs verbessern konnten, was über ein höheres Zementfließmaß sichtbar wurde. Bei einem niedrigen w/z-Wert von 0,22 war der Effekt besonders stark ausgeprägt und bei w/z-Werten ≥ 0,3 kaum oder nicht mehr vorhanden. Das IPEG-PCE mit einer hohen anionischen Ladung (52IPEG5.8) profitierte mehr durch die Zugabe der nicht-ionischen Moleküle als das PCE mit der höheren Seitenkettendichte (52IPEG2.0). Beispielsweise konnte das Fließmaß für 52IPEG5.8 durch Zugabe von 0,5 % Diethylenglykol von 18 auf ~ 28 cm gesteigert werden, was einer Zunahme von 55 % entspricht. Während das Fließmaß für 52IPEG5.8 mit steigender Dosierung der niedermolekularen Verbindungen kontinuierlich größer wurde, führten höhere Dosierungen (> 0,4 %) bei 52IPEG2.0 nur zu einer minimalen Verbesserung. Dies deutet darauf hin, dass Ladung und Seitenkettendichte des PCEs entscheidend sind, wie stark der Effekt des Co-Dispergiermittels ausgeprägt ist. Ebenfalls wurde festgestellt, dass die nicht-ionischen Moleküle nur in Gegenwart von PCE wirksam sind, wohingegen sie allein (ohne PCE) keine Verflüssigungswirkung zeigten.

Bei den Fließmaßmessungen wurde zudem beobachtet, dass die klebrige Konsistenz, die vorwiegend bei einem w/z-Wert von 0,22 in Erscheinung trat, durch Zugabe der nicht-ionischen Moleküle reduziert wurde. Diethylenglykol wurde daher auch in einem viskosen Mörtel getestet und die Trichterauslaufzeit bestimmt. Für diese Versuche wurden zwei Mörtel präpariert, wobei ein Mörtel nur mit 52IPEG5.8 verflüssigt wurde, während der andere eine Kombination aus 52IPEG5.8 und Diethylenglykol enthielt. Beide Mörtel wurden auf das gleiche Ausbreitmaß (Fließgrenze) eingestellt. Über V-Trichter-Versuche wurde festgestellt, dass Diethylenglykol die Fließgeschwindigkeit erheblich erhöhte und um 50 % kürzere Trichterauslaufzeiten ermöglichte. Darüber hinaus konnte mit Hilfe der niedermolekularen Verbindungen die PCE-Dosierung für ein bestimmtes Fließmaß reduziert werden, was in einigen Formulierungen einen Kostenvorteil darstellte.

Über Adsorptionsmessungen wurde schließlich aufgedeckt, dass die nicht-ionischen Moleküle die adsorbierte Menge der PCE-Fließmittel weder erhöhen noch reduzieren und selbst frei in der Porenlösung vorliegen (sh. **Abbildung 38**).

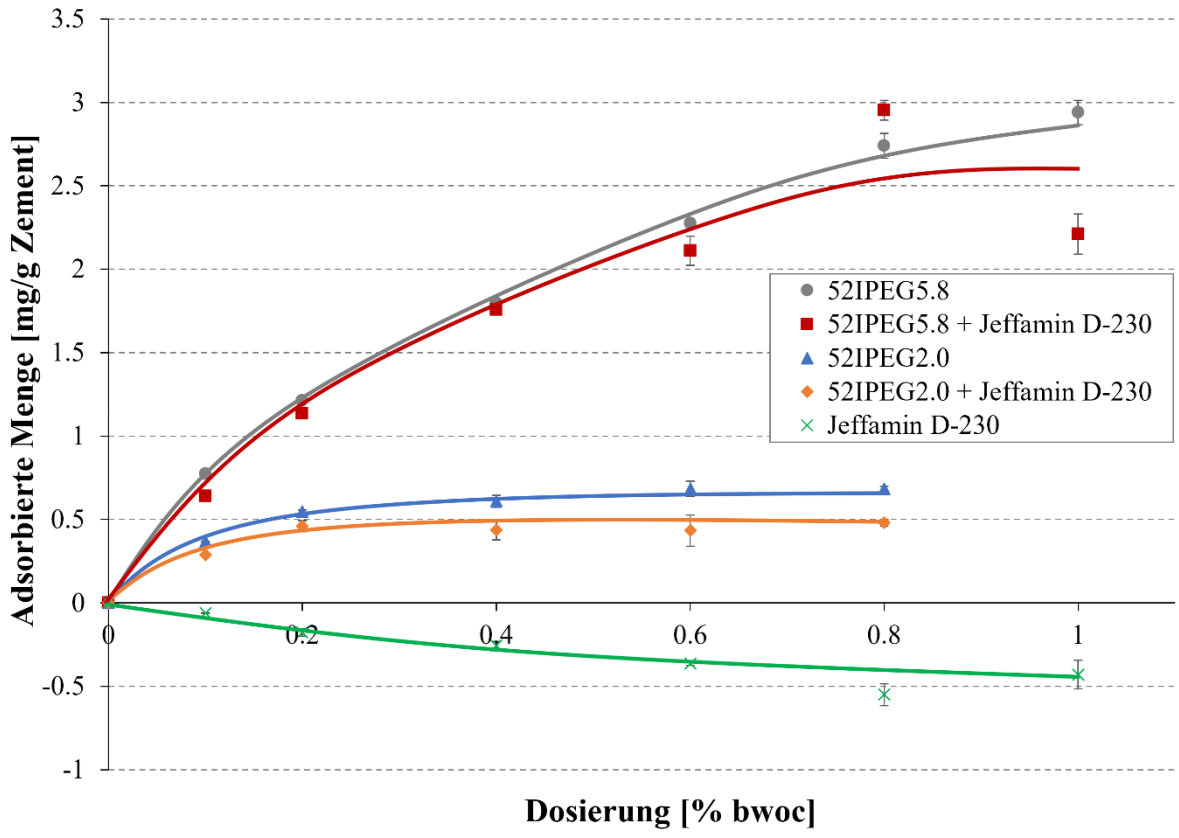

Abbildung 38: Adsorptionsisothermen der beiden IPEG-PCEs und von Jeffamin D-230 sowie für 1:1 (wt.%/wt.%)-Kombinationen.

Auf Grundlage dieser Ergebnisse wurde ein erstes mechanistisches Modell aufgestellt. Gemäß dieses Modells sind die nicht-ionischen Moleküle sog. Rheologieverbesserer, die als „Schmiermittel“ fungieren und die Reibung zwischen den Zementpartikeln während des Fließens reduzieren, weshalb eine schnellere Fließgeschwindigkeit erhalten wird.

Publikation #1

Improvement of SCC Flow Properties Through Addition of Non-Adsorbing Small Molecule Co-Dispersants

Manuel Ilg, Johann Plank

In: K. H. Kayat (Ed.), 8th International RILEM Symposium on Self-Compacting Concrete – SCC 2016, Washington (USA), 2016
Proceedings, 49 – 59

Improvement of SCC Flow Properties Through Addition of Non-Adsorbing Small Molecule Co-Dispersants

Manuel Ilg (1) and Johann Plank (1)

(1) Technische Universität München, Chair for Construction Chemistry, Lichtenbergstraße 4, 85747 Garching, Germany

Abstract: Colloidal suspensions such as e.g. cement pastes can be dispersed either through electrostatic or steric repulsive forces. These mechanisms require that the polymers applied adsorb onto the particle surface. However, it has been noticed recently that also non-adsorbing non-ionic polymers can significantly enhance the plasticizing effect of MPEG ester-based polycarboxylate (PCE) superplasticizers, especially at low w/c ratios (≤ 0.30).
In this study, the effect of non-ionic small molecules on the dispersing ability of two IPEG-based PCEs exhibiting different side chain densities was investigated. As non-adsorbing molecules, diethylene glycol and a polyether amine were probed. It was found that the non-adsorbing molecules can provoke a considerable increase of cement paste flow when combined with IPEG-PCEs. The effect is particularly strong for PCEs possessing high anionicity and at very low w/c ratios (< 0.25) in cement paste. Furthermore, V-funnel empty times of mortars revealed that the non-adsorbing molecules also improve the flow speed and reduce the stickiness of such concretes.
Our investigations suggest that non-ionic, inexpensive small molecules can act as co-dispersants for PCE superplasticizers. They can help to optimize the cost of the admixture and also provide a concrete which can be placed faster. Mechanistic considerations suggest that the non-ionic co-dispersants present spacer molecules which through an osmotic effect keep the cement particles apart.

Keywords: Dispersion, Admixture, Polycarboxylate, Flow Speed, Non-adsorbing molecules

Introduction

The high flowability of self-compacting concrete (SCC) which enables its facile placement even in restricted sections of a formwork is one pivotal attribute of this

outstanding construction material [1]. Other benefits of SCC include the high passing and filling ability as well as the property to consolidate without compaction [2, 3].
When mixed with water, cement tends to form large agglomerates (so-called flocs) [4, 5]. In these flocs the water is entrapped, thus provoking a high viscosity. The interaction between adjacent cement particles mainly originates from attractive *Van der Waals* and electrostatic forces induced by the different charge domains [6]. To break up these agglomerates, PCE superplasticizers are added which include an anionic backbone with carboxylate anchor groups and grafted side chains that predominately contain polyethylene glycol units [7]. The PCEs adsorb *via* their carboxylate groups onto the positively charged surface areas of the hydrating cement particles, whereas the non-adsorbing side chains protrude freely into the interstitial pore space. Furthermore, the dispersion mechanism of PCEs is also based on steric hindrance between the cement particles caused by the polyethylene glycol side chains. As a consequence, the cement particles are dispersed through a combination of disagglomeration and friction reduction. Thus, the principal mechanism of cement dispersion by PCE superplasticizers is well understood and was thoroughly elucidated [8, 9].
Recently it has been found that in combination with adsorbing PCEs even non-adsorbed PCE polymers which remain dissolved in the cement pore solution can contribute to cement dispersion [10, 11]. In one study a conventional MPEG-type PCE was combined with different kinds of non-adsorbing polymers (e.g. MPEG methacrylate macromonomer, polyethylene glycol etc.) and their impact on the fluidity of cement pastes was investigated [12]. It showed that such non-adsorbing polymers can act as co-dispersants and significantly enhance the plasticizing effect of MPEG-PCEs, but only at low w/c ratios of ≤ 0.30. This result was attributed to the “lubricating” effect of the non-adsorbing polymers present between the densely packed cement particles.
In the present study it was investigated whether non-adsorbing small molecules can also enhance the plasticizing effect of PCEs. For this purpose, two isoprenolether (IPEG)-based PCEs with different side chain densities were synthesized and combined with ascending dosages of non-adsorbing small molecules (diethylene glycol and a polyether amine). To consolidate our previously developed model, mortar flow tests were performed and also the flow speed of mortars was measured *via* the empty time from the V-funnel. From these results it was hoped to gain more insight into the mechanism underlying the augmented dispersion effect from non-adsorbing molecules.

Materials and methods

Chemicals

$Na_2S_2O_8$, acrylic acid (AA) and NaOH were from Merck KGaA Germany, 3-mercaptopropionic acid was received from Sigma-Aldrich, Germany. The

isoprenyl ether macromonomer (M_w = 2,400 g/mol, IPEG-2400) holding 52 ethylene oxide (EO) units was obtained from Liaoning OxiranChem Ltd., China. As non-adsorbing small molecules diethylene glycol (Merck KGaA) and a polyether amine (Jeffamine® D-230, Huntsman Corp., USA) were used (see chemical structures in *Figure 1*).

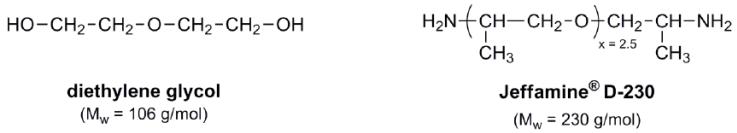

Figure 1. Chemical structures of the non-adsorbing molecules used in the study.

IPEG-PCE samples

The IPEG-PCEs were synthesized *via* aqueous free radical copolymerization and the synthetic route is presented in *Figure 2*.

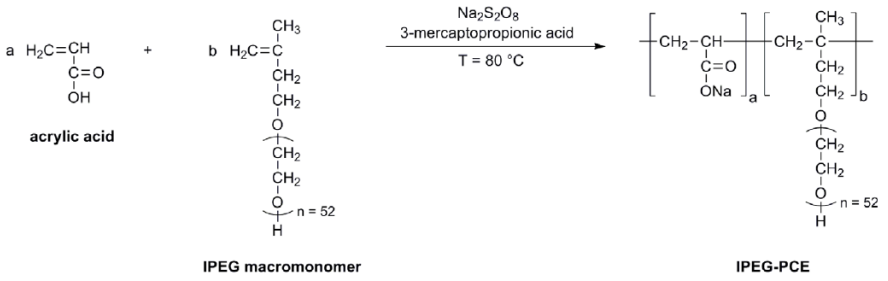

Figure 2. Reaction scheme for the synthesis of the IPEG PCE samples.

The polymers were denoted as xIPEGy, whereby x represents the number of EO units contained in the side chain while y indicates the molar ratio of acrylic acid to the macromonomer. The preparation procedure for the PCE samples followed the description in [13]. The final products were colorless, slightly viscous PCE solutions which exhibited a solid content of 40 wt.% and a pH value of 7.

Molecular properties of the polymers (M_w, M_n) were determined by size exclusion chromatography (SEC) on a Waters 2695 separation module equipped with three Ultrahydrogel™ columns (120, 250, 500) and an Ultrahydrogel™ guard column (Waters, Germany) using 0.1 N $NaNO_3$ (pH = 12) as eluent. For the calculation of M_w and M_n a *dn/dc* value of 0.135 mL/g (value for PEO) was utilized.

The specific anionic charge amount of the polymers was ascertained by means of a particle charge titrator PCD pH 03 (BTG Instruments, Germany) using cationic

polyDADMAC (0.001 M) as titrant. Based on the consumed amount of polyDADMAC measured, the specific anionic charge per gram of polymer can be calculated. A detailed description of the procedure is provided in [14].

Cement dispersion

The dispersing performance of the polymers was investigated by a modified mini slump test according to DIN 1164. The cement used was an ordinary Portland cement CEM I 52.5 N (HeidelbergCement, Germany). First, at a w/c ratio of 0.30 or 0.22 the dosages of the IPEG-PCEs required to achieve a slump flow of 18 ± 0.5 cm were determined. The non-adsorbing admixtures diethylene glycol and Jeffamine® D-230 were pre-dissolved together with the IPEG-PCEs in the mixing water. Then, mini slump tests were carried out as specified in [12] and the values for the paste flow (spread) were determined. Note that for each measurement, a new cement paste holding a higher dosage of the non-adsorbing molecule was prepared.

V-funnel empty time

To investigate the effect of the non-adsorbing admixtures on the flow speed of mortars, V-funnel empty times were determined. A mortar was prepared from 675 g cement, 1350 g standard sand and 202.5 g DI water at a constant w/c ratio of 0.30. The mixing of the mortar was performed with a ToniMIX eccentric agitator (Toni Technik, Germany) according to DIN EN 196 [15 a]. First, the dosage of IPEG-PCE to obtain a slump flow of 23 ± 0.5 cm was determined at a w/c ratio of 0.30. A defoamer (Surfynol® MD-20, Air Products, Germany) was added to avoid air entrainment. After mixing, the mortar was rested for 5 min and then used for slump flow or V-funnel testing. Furthermore, mortars were prepared holding the respective dosages of the IPEG-PCE for an initial slump flow of 18 ± 0.5 cm and additionally containing the non-adsorbing admixture (pre-dissolved in the mixing water) in such amount to finally achieve a slump flow of 23 ± 0.5 cm. The empty times from the V-funnel were determined according to DIN EN 12350-9 [15 b]. The geometric dimensions of the steel V-funnel are illustrated in *Figure 3*. "Empty time" designates the time until the steady stream of the mortar became disruptive.

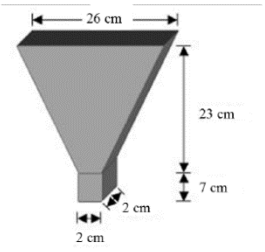

Figure 3. Dimensions of the V-funnel used in the mortar tests.

Results and discussion

Characterization of the polymers

At first, the molecular properties of the synthesized polymers were determined by SEC. The results are summarized in *Table I*.

Table I. Molecular properties of the synthesized IPEG-PCEs.

Polymer sample	M_w (g/mol)	M_n (g/mol)	PDI (M_w/M_n)
52IPEG2.0	24,700	9,256	2.7
52IPEG5.8	34,430	15,500	2.5

The specific anionic charge amounts of the IPEG polymers were captured *via* charge titration in DI water, synthetic cement pore solution (CPS) and 0.1 M NaOH. The results are listed in *Table II*.

Table II. Specific anionic charge amount of the PCEs in DI water, CPS and 0.1 M NaOH.

Polymer sample	DI water (µeq/g)	0.1 M NaOH (µeq/g)	CPS (µeq/g)
52IPEG2.0	631	884	223
52IPEG5.8	1,895	2,610	1,050

All PCE samples exhibit the highest anionicity in 0.1 M NaOH, owed to the full deprotonation of the carboxylic acid groups. A significant decrease of anionicity can be observed in synthetic cement pore solution as a result of Ca^{2+} complexation by the carboxylate groups. As expected, polymer 52IPEG5.8 always possesses a higher anionic charge than copolymer 52IPEG2.0. Therefore, adsorption of 52IPEG5.8 on cement should be more pronounced.

As non-adsorbing molecules, a large variety of small molecules including tetraethylene pentamine, triethylene glycol, propylene glycol and different kinds of Jeffamines® was tested. Among them, diethylene glycol and the polyether amine Jeffamine® D-230, a difunctional primary amine with M_w = 230 g/mol were found to provide the strongest effect and therefore were tested more extensively. Additionally, they represent two different classes of chemicals (polyol *vs.* polyether amine). Anionic charge measurements in CPS confirmed for both molecules the non-ionic character, thus no electrostatically driven adsorption onto the cement particles should occur.

Dispersing effect of non-adsorbing molecules in combination with IPEG-PCEs

At first the dispersing performance of individual diethylene glycol and Jeffamine® D-230 was determined by means of a mini-slump test using cement paste at a w/c ratio of 0.30. It was found that the individual additives do not produce any fluidity (slump flow was 8 cm which corresponds to the diameter of the *Vicat* cone). However, by the addition of the non-adsorbing admixtures a softer consistency of the cement paste was observed, albeit this had no impact on flowability.
Next, the non-adsorbing molecules were admixed to the two IPEG-PCE samples and probed *via* mini slump tests. In these experiments, at first the dosages of the IPEG-PCEs required to achieve a slump flow of 18 ± 0.5 cm were determined (w/c = 0.30), which was ascertained with 0.15 % bwoc of 52IPEG2.0 and 0.12 % bwoc of 52IPEG5.8. The cement pastes holding the IPEG-PCEs were then admixed with increasing amounts of diethylene glycol respectively Jeffamine® D-230 and mini slump tests were carried out. The results are illustrated in *Figure 4*.

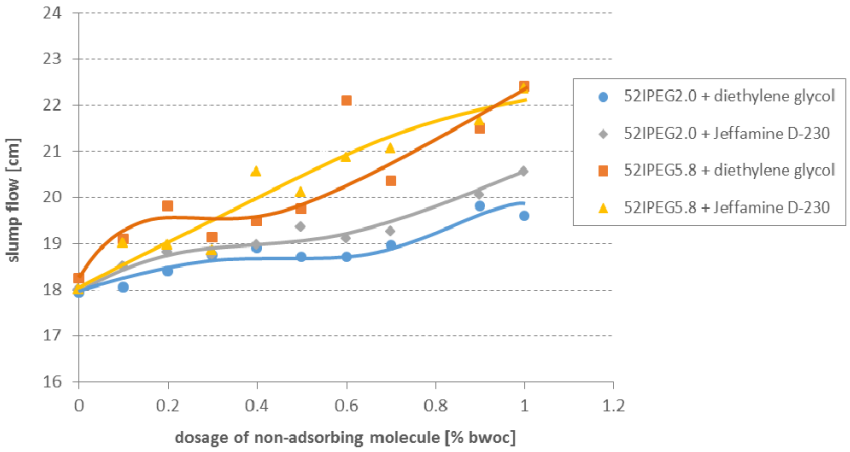

Figure 4. Slump flow of cement pastes (w/c ratio = 0.30) adjusted with respective dosages of IPEG-PCEs to a slump flow of 18 ± 0.5 cm, and admixed with increasing dosages of diethylene glycol or Jeffamine® D-230.

According to the data presented there, the enhancement in plasticizing effect provided by the small molecules is rather limited and significantly less than reported before for large molecules [12]. Diethylene glycol as well as the polyether amine only cause a moderate increase of paste fluidity. Generally, the more anionic PCE sample 52IPEG5.8 shows a stronger increase in fluidity than the less anionic PCE polymer 52IPEG2.0 which possesses a higher number of polyglycol side chains and thus can produce a stronger steric effect when adsorbed.
In the next step, additional tests were carried out at a much lower w/c ratio of 0.22. Again the dosages of the IPEG-PCEs required to achieve a slump flow of 18 ±

0.5 cm at this lower w/c ratio were determined. Here, the dosages were much higher at 0.6 % bwoc for 52IPEG2.0 and 0.23 % bwoc for 52IPEG5.8 polymer. Most remarkably, now the cement pastes prepared at this low w/c ratio exhibited a very sticky and honey-like consistency, with slow flow speed in the mini slump test. To these pastes diethylene glycol or Jeffamine® D-230 were dosed in ascending amounts and the spread values were recorded (*Figure 5*).

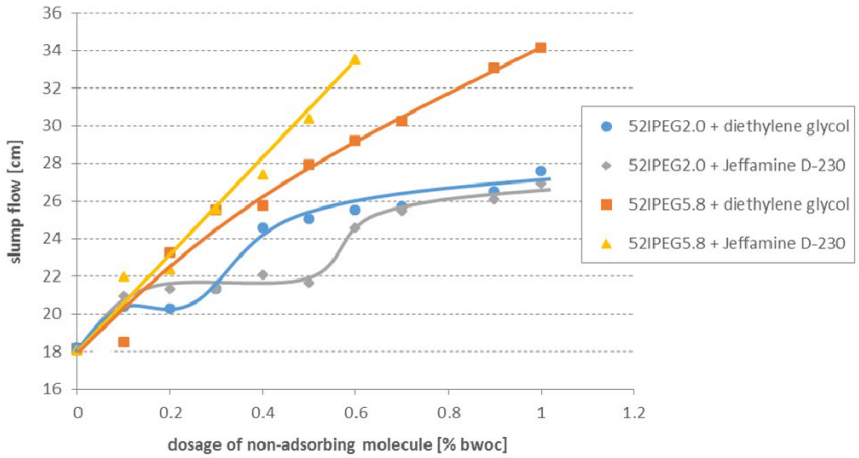

Figure 5. Slump flow of cement pastes (w/c ratio = 0.22) adjusted with respective dosages of IPEG-PCEs to a slump flow of 18 ± 0.5 cm, and admixed with increasing dosages of diethylene glycol or Jeffamine® D-230.

Compared to the previous results at w/c = 0.30, now a significant increase of the slump flow was observed for both IPEG-PCEs in combination with the non-adsorbing molecules. For instance, addition of only 0.3 % bwoc diethylene glycol or Jeffamine® D-230 to PCE polymer 52IPEG5.8 increased the fluidity of the cement paste from the initial 18 cm to ~ 26 cm. Higher additions of the non-adsorbing molecules could produce even much stronger plasticizing effects (e.g. spread values of 34 cm where massive bleeding and segregation of the cement paste occurred). PCE polymer 52IPEG2.0 requires higher dosages (0.6 – 0.7 % bwoc) of the non-adsorbing molecules for a slump flow of 26 cm. To achieve the same fluidity, the dosage of 0.87 % bwoc of polymer 52IPEG2.0 is necessary. This compares with dosages of 0.6 % bwoc 52IPEG2.0 plus 0.6 % bwoc diethylene glycol in the combination and reveals that the addition of low-cost non-adsorbing molecules like diethylene glycol can provide a substantial cost saving for the admixture.

The results from above clearly suggest that non-adsorbing small molecules can effectively augment the dispersing performance of IPEG-PCEs and that the effect is especially pronounced at low w/c ratios.

Impact of non-adsorbing molecules on SCC robustness

The robustness of SCCs is an important key factor that must be taken into account when considering its practical application. Even very minor variations in the water content can lead to bleeding and disintegration or too stiff consistency. Therefore, SCC needs to be designed with a certain degree of robustness [3]. Here, as an example the ability of diethylene glycol to enhance the robustness of SCC was tested by preparing two different cement pastes both exhibiting a slump flow of 26 ± 0.5 cm at a w/c ratio of 0.22. One cement paste was fluidized with 0.265 % bwoc of PCE polymer 52IPEG5.8, while the other paste contained 0.23 % bwoc of 52IPEG5.8 plus 0.3 % bwoc of diethylene glycol. For these pastes the w/c ratio was varied and the changes in the slump flow were captured by mini slump tests.
As is evident from *Figure 6*, diethylene glycol has no significant influence on the robustness of the cement paste, since comparable slump flow values were obtained for both systems, independent of whether diethylene glycol was admixed or not.

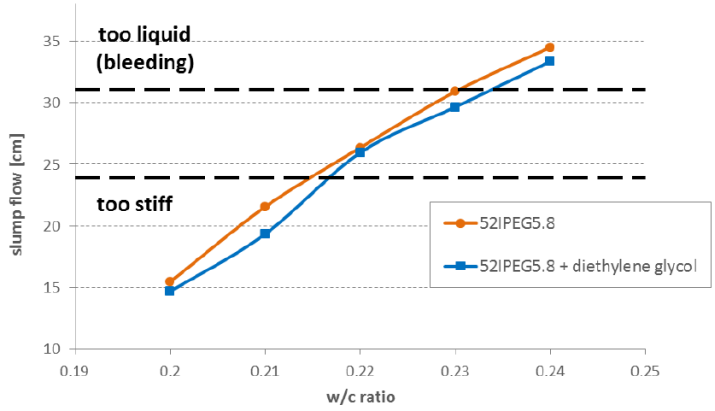

Figure 6. Effect of diethylene glycol on the robustness of a cement paste relative to variations in the water content.

Flow speed from V-funnel

As an example, the effect of diethylene glycol on the flow speed of a mortar measured *via* the empty time from the V-funnel is presented here. Usually, short empty times (corresponding to high speed of flow) are favored by applicators because a mortar with low flow rate normally delays the placement of concrete and exhibits poor compaction behavior. For the experiments, two mortars were prepared, both possessing a slump flow of 23 ± 0.5 cm at a w/c ratio of 0.30. One mortar contained 0.28 % bwoc of IPEG polymer 52IPEG5.8, whereas the other was plasticized with a combination of 0.25 % bwoc of the IPEG-PCE (this dosage corresponds to a spread flow of 18 cm) and additional 0.5 % bwoc of diethylene

glycol. Then, the time periods required for both mortars to empty from the V-funnel were determined.
For the mortar fluidized with PCE polymer 52IPEG5.8 an empty time of 2 min and 18 sec was recorded, whereas the combination of the IPEG-PCE with diethylene glycol substantially increased the flow rate and reduced V-funnel empty time by almost 50 % to 1 min and 20 sec. These results indicate that non-adsorbing small molecules such as diethylene glycol can act as friction reducer between the cement particles and thus accelerate the flow speed of mortars.

Mechanistic model

To explain the effects presented above, a first model is proposed whereby the small molecules which are dissolved in the cement pore solution act as spacer molecules between the cement particles. To support this model (*Figure 7*), adsorption measurements have been performed which proved that the polyether amine (resp. diethylene glycol) does not adsorb when combined with PCE, hence it occurs as individual dissolved molecule. Furthermore, the non-adsorbing molecules do not impact the adsorbed amounts of the IPEG-PCEs. Consequently, this model explains well why the effect of the non-adsorbing molecules is most pronounced at low w/c ratios (< 0.25) and disappears entirely at higher water contents (w/c > 0.35). At high w/c ratios the concentration of the non-adsorbed molecules is too low to provide the effect of an osmotic spacer. At low w/c ratio, however, the cement particles approach each other very closely, especially during flow of the concrete. In such case, the non-adsorbing polymers prevent the particles from coming too close, because this would result in depletion of the polymer from some parts of the pore solution. Hence, this condition is osmotically unfavorable and avoided by the system.

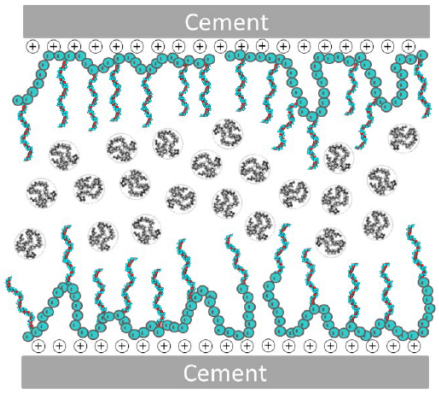

Figure 7. Illustration of the osmotic spacer effect of non-adsorbing small molecule co-dispersants dissolved in the pore solution between cement particles.

Conclusion

This paper describes the use of non-adsorbing small molecules (i.e. diethylene glycol and a polyether amine) to augment the plasticizing effect of IPEG-PCEs. It was found that the dispersing performance of IPEG PCEs is considerably improved at very low water to cement ratios (w/c < 0.25) and that the small molecules act as co-dispersant to the PCE. Their effect is more pronounced on PCE products possessing low side chain density than for those with high grafting density.
Measurement of V-funnel empty times confirmed that the non-adsorbing small molecules also greatly enhance the flow speed of mortar and reduce the stickiness of concretes prepared at low w/c ratios. A first mechanistic model suggests that these molecules act as lubricant between cement particles. They present spacer molecules which through an osmotic effect keep the cement particles at distance from each other. In future studies other non-ionic molecules like polyamines, diols, glycol ethers or polyethylene imines should be looked at.

References

[1] Okamura, H.; Ouchi, M. (2003), *J. Adv. Concr. Technol.*, vol. 1, pp. 5-15.
[2] Khayat, K. H.; Manai, K.; Trudel, A. (1997), *ACI Mater. J.*, vol. 94, n. 6, pp. 491-500.
[3] Kwan, A. K. H.; Ng, I. Y. T. (2010), *Constr. Build. Mater.*, vol. 24, pp. 2260-2266.
[4] Yoshioka, K.; Tazawa, E.; Kawai, K.; Enohata, T. (2002), *Cem. Concr. Res.*, vol. 32, pp. 1507-1513.
[5] Roussel, N.; Flatt, R. J. (2010), *Cem. Conc. Res.*, vol. 40, pp. 77-84.
[6] Yoshioka, K.; Sakai, E.; Daimon, M.; Kitahar, A. (1997), *J. Am. Ceram. Soc.*, vol. 80, pp. 2667-2671.
[7] Plank, J.; Sakai, E.; Miao, C. W.; Yu, C.; Hong, J. X. (2015), *Cem. Concr. Res.*, vol. 78, pp. 81-99.
[8] Jolicoeur, C.; Simard, M.-A. (1998), *Cem. Concr. Compos.*, vol. 20, pp. 87-101.
[9] Gelardi, G.; Flatt, R. J. (2016): "Working mechanisms of water reducers and superplasticizers", In: *Science and Technology of Concrete Admixtures*.
[10] Sakai, E.; Kakinuma, Y.; Yamamoto, K.; Daimon, M. (2009), *J. Adv. Concr. Technol.*, vol. 7, n. 1, pp. 13-20.
[11] Lange, A., Hirata, T., Plank, J. (2012), Malhotra V. M. (Ed.), CANMET/ACI Conference, Prague, SP-288.30, pp. 435-449.
[12] Lange, A., Plank, J. (2016), *Cem. Conc. Res.*, vol. 79, pp. 131-136.
[13] Lange, A.; Plank, J. (2015), *J. Appl. Polym. Sci.*, vol. 132, 42529.
[14] Plank, J.; Sachsenhauser, B. (2009), *Cem. Conc. Res.*, vol. 39, pp. 1-5.
[15] a) DIN EN 196-1:2005-05: Methods of testing cement – Part 1: Determination of strength (2005); b) DIN EN 12350-9:2010-12: Testing fresh concrete – Part 9: Self-compacting concrete – V-funnel test (2010).

5.1.2. Publikation #2: Novel Admixtures to Reduce the Stickiness of Low W/C Concretes

Aufbauend auf **Publikation #1** in der beschrieben wurde, dass die Struktur des PCE-Fließmittels einen Einfluss darauf hat, wie stark die verflüssigende Wirkung der nicht-ionischen Moleküle ist, wurde als nächstes untersucht, inwiefern sich die chemische Struktur der Co-Dispergiermittel auf ihre Dispergiereffizienz auswirkt. In dieser Arbeit wurden deshalb verschiedene niedermolekulare Glykolderivate mit einem Molekulargewicht ≤ 300 g/mol getestet (sh. **Abbildung 39**) und mit 45IPEG4.5 kombiniert, welches ein Polymer mit einer mittleren anionischen Ladungsmenge bzw. Seitenkettendichte ist.

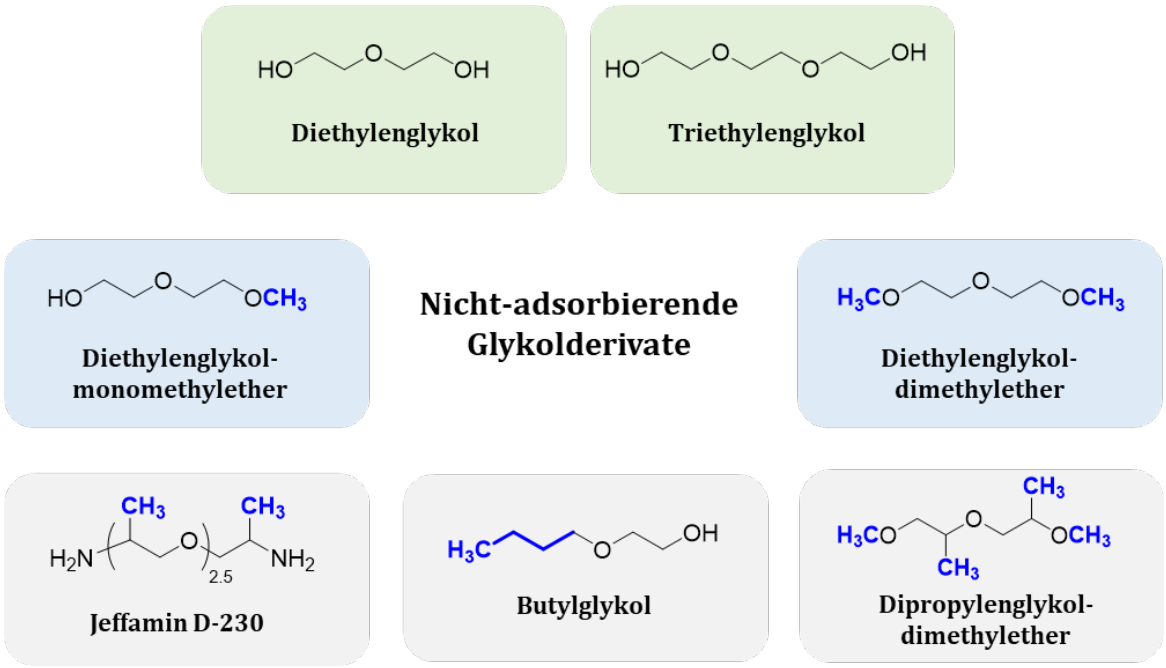

Abbildung 39: Übersicht der getesteten Glykolderivate.

Rheologische Versuche, bei denen das Fließmaß von Zementleimen gemessen wurde offenbarten, dass insbesondere diejenigen Moleküle, die mehrere hydrophobe Gruppen beinhalten, eine besonders hohe Wirksamkeit ergaben. So wurden Butylglykol und Dipropylenglykoldimethylether als äußerst potente Co-Dispergiermittel identifiziert, die bereits bei niedrigen Dosierungen zu einem hohen Zementfließmaß führten. Größere Unterschiede in der Wirksamkeit der nicht-ionischen Moleküle wurden vor allem ab

einer Dosierung > 0,3 % gefunden. Oberhalb dieses Werts war die Fließmaßzunahme umso stärker, je mehr hydrophobe Gruppen in der Struktur vorlagen.

Des Weiteren konnte gezeigt werden, dass die nicht-ionischen Moleküle ebenso in der Lage sind, die Fließgeschwindigkeit von Betonen mit niedrigem w/z-Wert zu verbessern und das klebrige Verhalten zu minimieren. Dies wurde über Messungen der Trichterauslaufzeit festgestellt. Keinen Einfluss hatten hingegen die unpolaren Glykolderivate auf die Zementhydratation.

Die Ergebnisse dieser Studie legen nahe, dass nicht nur die anionische Ladung des PCEs, sondern auch die chemische Zusammensetzung des Co-Dispergiermittels entscheidend für die Ausprägung des Dispergiereffekts sind.

Publikation #2

Novel Admixtures to Reduce the Stickiness of Low W/C Concretes

Manuel Ilg, Johann Plank

In: J. Liu, Z. Wang, T. C. Holland, J. Huang, J. Plank (Eds.),
Superplasticizers and Other Chemical Admixtures in Concrete,
Proceedings Twelfth International Conference, Beijing (China), 2018
SP-329-07, 77 – 88

NOVEL ADMIXTURES TO REDUCE THE STICKINESS OF LOW W/C CONCRETES

Manuel Ilg and Johann Plank

Technische Universität München, Chair for Construction Chemistry,

Lichtenbergstraße 4, 85747 Garching, Germany

Biography: Manuel Ilg studied chemistry and received his B.Sc. and M.Sc. degrees in chemistry from Technische Universität München. Since 2014 he is a Ph.D. student at the Chair for Construction Chemistry in Garching where he works on polycarboxylate superplasticizers with a focus on novel PCE structures and concepts, e.g. to overcome the "stickiness" of concretes prepared at low water-cement ratios.

Johann Plank is a full Professor at the Institute of Inorganic Chemistry of Technische Universität München, Germany. Since 2001, he holds the Chair for Construction Chemistry there. His research interests include cement chemistry, concrete admixtures, organic-inorganic composite and nano materials, concrete, dry-mix mortars and oil well cementing. In 2015 he received the A. Aignesberger Award of ACI for his outstanding contributions to the research and development of superplasticizers and other chemical admixtures.

ABSTRACT

Concretes formulated at low water-cement ratios exhibit good material properties. Nevertheless, such concretes exhibit a honey-like consistency with a low speed of flow ("creeping behavior") which is highly undesirable. In this paper it is shown that non-ionic

small molecules can help to improve the fluidity at low water-cement ratios significantly and eliminate the “stickiness” when combined with ordinary PCE superplasticizers. For this purpose, different non-ionic glycol derivatives were screened *via* mini-slump testing. It was found that especially less polar species behave as very powerful co-dispersants. To gain a more profound understanding of the working mechanism, heat flow calorimetry was carried out. Additionally, concrete lab tests were performed to ascertain the impact of the non-ionic molecules on the V-funnel empty time of SCCs. Based on adsorption measurements it is inferred that the co-dispersants act as osmotic spacers which keep the cement particles apart and prevent them from agglomeration.

Keywords: Concrete, Stickiness, Superplasticizer, Non-ionic co-dispersant, Polycarboxylate, Flow properties, V-funnel, Self-compacting concrete

INTRODUCTION

Superplasticizers represent the main class of chemical admixtures which are commonly applied to produce a highly flowable concrete and/or to reduce the water-to-cement ratio (w/c) [1, 2]. By decreasing the water content a building material is obtained that exhibits superior properties like high compressive strength, low porosity and enhanced durability. Based on the chemical structure, two main types of superplasticizers can be distinguished, namely polycondensates and polycarboxylates (PCEs) [3]. PCEs have become the most widely used superplasticizers, due to their superior dispersion performance even at low w/c and better slump retention capability, compared to polycondensates [4]. Special concretes like self-consolidating concrete (SCC) that consolidates with minimal compaction effort, or ultra-high performance concrete (UHPC) with compressive strength values above 150 MPa [21.8 kpsi] would not be possible without PCE-based superplasticizers. A common feature of these concretes is that they are generally prepared at low w/c.

Though such concretes can be highly fluidized with PCEs, applicators often report a honey-like consistency for them. These concretes creep rather than flow and exhibit a low speed of flow during placement at the construction site. This rheological behavior which becomes increasingly worse as w/c decreases is not desirable for placement and consolidation of the concrete into formworks or in elements containing densely packed reinforcement. The "stickiness" of these concretes can result in insufficient filling and induce voids and defects in the hardened concrete structure. Thus, academia and industry are actively researching the reasons behind these rheological properties in order to find new concepts which mitigate this creeping flow behavior. [5–7].

Previous studies suggest that the stickiness derives from a high plastic viscosity owed to the high solid volume fractions of these concretes [6]. Accordingly, a high speed of flow can be achieved by decreasing the plastic viscosity. Additionally, it was found that the hydrophilic-lipophilic balance (HLB) value of the PCE superplasticizer seems to present a key parameter which influences the plastic viscosity of concretes with w/c of 0.30 or less [6]. To obtain a high speed of flow, the PCE must be as hydrophilic as possible, whereas hydrophobic groups (e.g. methyl groups) should be avoided in the structure [7]. According to this concept, allyl ether-based (APEG) PCEs provide the highest flow speed and the least stickiness whereas the methacrylate ester-based (MPEG) PCEs induce a particularly high stickiness while HPEG and IPEG PCEs behave somewhere in the middle.

Some studies imply that for concretes exhibiting high solids contents the conventional models for dispersion like the DLVO theory (electrostatic stabilization) or the *Ottewill-Walker* equation (steric stabilization) are no longer exclusively applicable [8]. Instead, the portion of non-adsorbed PCE polymer remaining in the pore solution seems to contribute to the cement dispersion [9–11]. This concept was first described by *Sakai* et al. who investigated the fluidity of low heat Portland cement – silica blends using different PCE superplasticizers at

water-to-powder ratios ranging from 0.16 – 0.32 [9, 12]. According to their results, the high paste fluidity at low w/p ratios (i.e. 0.16) cannot be ascribed only to a steric hindrance effect of adsorbed PCE polymers, but is linked to un-adsorbed PCE polymers remaining in the interstitial pore solution.

More recent findings from our group confirm that specific non-ionic polymers (e.g. common polyethylene glycol PEG-2000) can significantly augment the dispersing performance of PCE superplasticizers at low w/c (e.g. 0.30) and enhance the paste fluidity of such systems [13]. Such combinations of the non-ionic polymers with PCEs lead to an increase in fluidity whereas the individual non-ionic polymers do not produce any fluidity at all. In a consecutive study it was found that especially non-ionic small molecules like diethylene glycol are even more effective co-dispersants than the polymers.

This work here addresses the role of different non-ionic small molecules on the fluidity of cementitious systems exhibiting low w/c (e.g. 0.22). The main goal of this study was to further investigate this new type of dispersing mechanism and to elucidate the correlation between the chemical composition and the dispersing effectiveness of the small molecule co-dispersants. Additionally, heat flow calorimetry was carried out to assess the impact of the non-ionic small molecules on cement hydration. Finally, concrete lab test were performed to verify whether the findings obtained for the co-dispersants in cement paste are also applicable in concrete.

RESEARCH SIGNIFICANCE

Concretes formulated at low w/c (≤ 0.35) have become increasingly popular during the last years due to their outstanding material properties. Typically, such concretes exhibit high plastic viscosity with a creeping flow behavior which complicates a proper processing. The aim of the present study is to offer a concept how the “stickiness” can be reduced in order to

formulate high-strength concretes with superior flow characteristics which can be placed easier at the construction site. This new strategy could help to foster an even more widespread use of high-performance concretes like SCC or UHPC.

EXPERIMENTAL PROCEDURE

Materials

Cement samples – For the screening of the non-ionic molecules an ordinary Portland cement CEM I 52.5 N was utilized. Its phase composition as determined by Q-XRD using *Rietveld* refinement is provided in **Table 1**. The cement exhibits a d_{50} value of 13.7 µm (laser granulometer) and a specific surface area of 3,523 cm^2/g (*Blaine* method). For the density a value of 3.13 g/cm^3 was found.

For the concrete lab tests a Portland/limestone cement CEM II/A-LL 42.5 R was used. The data of the mineralogical analysis as provided by the cement manufacturer can also be found in **Table 1**. The specific surface area of this Portland composite cement lies at 4,697 cm^2/g.

PCE sample – The flow-enhancing effect of the non-ionic molecules was tested in the presence of a commercial IPEG-type PCE. This PCE is composed of acrylic acid and isoprenolether polyethylene glycol (IPEG) in a molar ratio of 4.5 : 1 and comprises 50 ethylene oxide units in the side chain, thus we designated this polymer as 50IPEG4.5. The molecular properties of the IPEG PCE as determined by size exclusion chromatography were M_n = 36,000 g/mol and M_w = 82,000 g/mol which results in a polydispersity index (PDI) of 2.3. The anionic charge amount of the PCE was 1,320 µeq/g in deionized (DI) water (pH = 7) and 689 µeq/g in synthetic cement pore solution (SCPS) (pH = 12.8). The chemical structure of the polymer is provided in **Fig. 1**.

Non-ionic small molecules – A large number of different glycol derivatives was screened for their effectiveness as non-ionic co-dispersants including diethylene glycol (DEG), triethylene glycol (TEG), diethylene glycol monomethyl ether (DEGMME), diethylene glycol dimethyl ether (DEGDME), dipropylene glycol dimethyl ether (DPGDME) and butyl glycol (BG). Furthermore, a di-functional polyether amine (JA) was tested. Charge titration experiments of the small molecules in SCPS confirmed their non-ionic character, thus no electrostatically driven interaction between the small molecules and the cement surface should occur in principal. An overview of the chemical structures of the different small molecules tested is illustrated in **Fig. 2**.

Experimental methods

Cement dispersion – The dispersing efficacy of the non-ionic molecules was evaluated with a series of mini slump tests which were performed according to DIN EN 1164 [14]. At first, the dosage of the IPEG PCE was ascertained which is required to obtain a slump flow of 18 ± 0.5 cm [7.1 ± 0.2 in.] at a specific w/c (i.e. 0.22 – 0.30). This dosage was applied in the following experiments where the non-ionic small molecules were combined with the IPEG PCE in dosages ranging from 0.1 – 0.7 % bmoc. The mini slump tests were conducted as follows: 370 g [13.05 oz] cement were added within 5 sec to a solution of the PCE and the non-ionic co-dispersant and homogenized for 4 min with a spoon. The amount of water contained in the PCE solution was subtracted from the total amount of mixing water to maintain a constant w/c. After the end of stirring, the cement paste was filled into a *Vicat* cone (height 40 mm [1.57 in.], top diameter 70 mm [2.76 in.], bottom diameter 80 mm [3.15 in.]) to the rim and immediately lifted upwards. Next, the diameter of the cement paste was measured at two perpendicular axes and averaged to obtain the spread flow value. All experiments were carried out at a constant temperature of 20 °C [68 °F] and a relative humidity of 30 % to ensure the reproducibility of the results.

Heat flow calorimetry – The effect of the non-ionic co-dispersants on cement hydration was assessed *via* isothermal heat flow calorimetry. For this purpose, 4 g [0.14 oz] cement were filled into 20 mL [0.68 fl oz] glass ampoules, admixed with aqueous solutions of 0.215 % bmoc of 50IPEG4.5 and 0.3 % bmoc of the non-ionic small molecules to achieve a w/c of 0.22. The glass vials were capped, homogenized for 2 min with a vortex mixer and placed into the calorimeter. Data logging was continued until the heat evolution had subsided.

Concrete lab tests – To investigate the effect of the co-dispersants on the flow properties of a SCC, concrete lab tests were performed in a ready mix concrete plant. The mixture proportions of the SCC are provided in **Table 2**. The concrete comprises a Portland/limestone cement CEM II/A-LL 42.5 R as well as fly ash and limestone powder as supplementary cementitious materials and was prepared at a w/c ratio of 0.35.

The SCC was prepared as follows: At first, sand and the coarse aggregates were added to a bucket mixer and homogenized for one minute. Consequently, one third of the fresh water was added and the aggregates were soaked for 10 min. Fly ash, limestone powder and cement were then added to the aggregates and mixed with the remaining amount of water. The superplasticizer and the non-ionic co-dispersant were added simultaneously after 20 sec to the concrete and mixing was continued for additional 5 min. Next, the slump flow of the SCC was determined according to DIN EN 12350-8 [15]. The concrete was poured into a SCC slump cone placed on a steel plate and instantaneously lifted upwards after complete filling. The diameter of the spread concrete was measured twice and averaged to obtain the spread flow value. The PCE was dosed in such an amount to achieve a spread flow of ~ 750 mm [29.53 in.]. The concrete was then transferred back into the mixer and stirred for 2 min. Finally, the SCC was poured into a V-funnel and the empty time which corresponds to the

time the concrete needs to be fully released from the funnel was recorded. The V-funnel empty time was determined according to the specifications outlined in DIN EN 12350-9 [16].

EXPERIMENTAL RESULTS AND DISCUSSION

Effect of w/c on the spread flow enhancing effect of diethylene glycol

It has been demonstrated before that non-ionic polymers (e.g. PEG 2000) can considerably improve the paste fluidity when admixed with MPEG-type PCEs at a w/c of 0.30 [13]. Based on these findings, mini slump tests were carried out here in order to specify at which w/c the non-ionic small molecules are most effective. For this purpose, PCE polymer 50IPEG4.5 was combined with different amounts of DEG varying from 0.1 – 0.7 % bmoc at w/c ratios from 0.22 – 0.30. At first, the dosage of the IPEG PCE was ascertained which is required for a spread flow of 18 ± 0.5 cm. This was achieved with 0.1 % bmoc (w/c = 0.30), 0.145 % bmoc (w/c = 0.26) and 0.215 % bmoc (w/c = 0.22) of the PCE, respectively. When decreasing the w/c, increased stickiness of the cement paste characterized by a low speed of flow was observed which can be attributed to the increased solids content of the cement paste. The same PCE dosages were then applied in the mini slump tests where the IPEG PCE was combined with ascending amounts of DEG to ascertain its impact on the paste fluidity (see **Fig. 3**).

As can be seen from **Fig. 3**, the spread flow enhancing effect of DEG is rather minor at w/c = 0.30. Generally, high dosages of DEG have to be utilized (> 0.5 % bmoc) to provoke at least a slight increase of the fluidity. However, DEG becomes a very powerful co-dispersant at much lower w/c. For instance, at w/c = 0.22 the addition of 0.3 % bmoc DEG only provokes a significant increase of the spread flow from 18 cm [7.09 in.] to approximately 26 cm [10.24 in.] and considerably reduces the stickiness of the cement paste. This improvement

became very obvious during the mixing of the cement paste. Based on these findings, it can be concluded that DEG seems to be a very effective co-dispersant, especially for highly particle loaded systems exhibiting high plastic viscosities.

Influence of polarity of non-ionic small molecules on dispersing effectiveness

Next, 50IPEG4.5 was combined with various non-ionic glycol compounds in cement pastes at w/c = 0.22 to investigate the impact of the chemical structure of the co-dispersant on paste fluidity. A wide range of different glycol derivatives was tested whose structures are presented in **Fig. 2**. The glycol compounds were selected to exhibit different proportions of non-polar moieties in their structure in order to evaluate if any benefit can be achieved from the incorporation of hydrophobic groups into these molecules. As before, mini slump tests were conducted utilizing combinations of 0.215 % bmoc of 50IPEG4.5 and different amounts of the non-ionic small molecules. The results of the tests are illustrated in **Fig. 4**.

As shown in **Fig. 4**, the less polar glycol derivatives (e.g. DEGDME, DPGDME, BG, JA) are more effective co-dispersants than the more polar ones (e.g. DEG, TEG, DEGMME). For instance, by admixing 0.1 % bmoc DPGDME a significant improvement of the slump flow from 18 cm [7.09 in.] to 24 cm [9.45 in.] can be attained. For all less polar molecules, comparable paste fluidities can be observed at smaller dosages (0.1 – 0.3 % bmoc), whereas at higher dosages (e.g. 0.5 % bmoc) the differences become more pronounced. Here, a clear relationship between the amount of non-polar moieties in the structure and the flow enhancing effect can be identified. The less polar glycol derivatives can be arrayed according to their dispersing effectiveness in following order: BG > DPGDME > DEGDME > DEGMME. The performance of the co-dispersants declines in this sequence as fewer hydrophobic and more polar groups are incorporated. To be more specific, BG represents the most powerful small

molecule at a dosage of 0.5 % bmoc (spread flow increase: 16 cm [6.30 in.]) as it contains a strongly non-polar and hydrophobic group with butyl, while DEGMME is less effective since it exhibits only one hydrophobic methyl functionality (spread flow increase: 11 cm [4.33 in.]). These results clearly suggest that *via* the polarity of the small molecules, their spread flow enhancing effect can be manipulated specifically.

Impact of the non-ionic glycol derivatives on cement hydration

The impact of the non-ionic small molecules on cement hydration was assessed *via* isothermal heat flow calorimetry. The heat evolution from cement pastes which were fluidized with 0.215 % bmoc of 50IPEG4.5 and 0.30 % bmoc of the non-ionic glycol compounds was monitored over time and compared with that from a reference sample which only contained the IPEG PCE. The results are exhibited in **Fig. 5**.

There, it becomes evident that the less polar glycol compounds do not much affect cement hydration compared to the reference sample. Whereas, the more polar DEG accelerates cement hydration while TEG causes a slight delay (1 h 45 min). This behavior was already described in the literature [17].

Effect of the non-ionic glycol derivatives on the flow speed of SCC

Concrete lab tests were carried out in a ready mix concrete plant to investigate the performance of some selected co-dispersants in SCC with respect to the flow speed as presented by the empty time from the V-funnel. The SCC used for the experiments comprised a Portland/limestone cement and was prepared at a w/c of 0.35. A dosage of 1.3 % bmoc of 50IPEG4.5 was needed to achieve the targeted slump flow of 750 mm [29.53 in.]. Although this SCC exhibited a high final slump flow value, it showed a very sticky, honey-like

consistency combined with a creeping flow behavior. However, when admixing combinations of the non-ionic co-dispersants (e.g. DEG, DPGDME) and the PCE to the concrete, the stickiness was much reduced and a more flowable concrete was obtained. This effect became evident by much faster empty times of the SCC from the V-funnel. After addition of the co-dispersants, the empty times were reduced from 21 sec to 13 sec which corresponds to a decrease of almost 40 % (see results in **Table 3**). It is obvious that such concretes can be processed much easier and faster at the construction site. Most interestingly, it was established here that the non-ionic molecules do not affect the fluidity (= spread flow) of the SCC, but only decrease the plastic viscosity which results in faster flow. These results differ from those obtained in cement paste where the co-dispersants also increased the fluidity of the lime phase and thus induced a higher spread flow value (see **Fig. 3** & **4**).

Mechanistic model for the effect of the non-ionic small molecules

Finally, a mechanistic model was developed which can explain the working mechanism of the non-ionic co-dispersants (see **Fig. 6**). Since adsorption measurements (results will be reported elsewhere) have proven that the non-ionic small molecules do not adsorb onto the cement surface nor increase the adsorbed amount of the PCE superplasticizer, it became clear that they remain freely dissolved in the pore solution. There, they can act as osmotic spacer molecules which prevent the cement particles from approaching each other. Otherwise, this would lead to depletion of the non-ionic molecules from some parts of the pore solution which is entropically unfavorable and therefore is avoided. For this mechanism, low w/c are necessary (≤ 0.26) so that the co-dispersants can implement their osmotic spacer effect. At higher w/c, the effect of local depletion of the non-ionic co-dispersants is less significant, because there the cement particles are not so densely packed. By generating a lubricating

layer around the cement particles holding adsorbed PCE polymers, the friction during the flow is reduced which entails a much decreased stickiness of the concrete.

CONCLUSION

This study demonstrates that non-ionic glycol derivatives can be used as co-dispersants to reduce the stickiness of cementitious systems formulated at low w/c. In cement paste the small molecules reduce both the yield value and the plastic viscosity of the lime phase, whereas in concrete only the plastic viscosity is decreased. Mini slump tests revealed that less polar glycol species are more effective to enhance paste fluidity. Adsorption measurements confirmed that the co-dispersants do not influence the adsorbed amounts of the PCE, but remain dissolved in the pore solution where they act as an osmotic spacer. Additionally, they can provide lubrication between adjacent cement particles which reduces the friction and leads to much shorter V-funnel empty times. The findings signify that at such low w/c different mechanisms for cement dispersion come into play. Another paper that is currently under way will present further results which elucidate in more detail the role of non-ionic small molecules in cement dispersion.

ACKNOWLEDGMENT

The authors would like to thank Stefan Schmidt from Schwenk's ready-mix concrete plant in Munich for his support during the concrete tests. Furthermore, the authors are very grateful to Josef Kapfinger from Clariant as well as to BASF and Huntsman for providing samples of the different non-ionic small molecules.

REFERENCES

1. Ramachandran, V. S., Malhotra, V. M., Jolicoeur, C., Spiratos, N., "Superplasticizers: Properties and applications in concrete", CANMET, Ottawa, Canada, 1998.
2. Spiratos, N., Page, M., Mailvaganam, N. P., Malhotra, V. M., Jolicoeur, C., "Superplasticizers for Concrete: Fundamentals, Technology, and Practice", Supplementary Cementing Materials for Sustainable Development, Ottawa, Canada, 2003.
3. Äitcin, P.-C., Flatt, R., "Science and Technology of Concrete Admixtures (1st Edition)", Woodhead Publishing, 2016.
4. Plank, J., "Concrete admixtures – Current status and perspectives for the future", in: A. Badr, C. Fentiman, M. Grantham, R. Mangabhai, eds., "Concrete for the modern age – Developments in Materials and Process", 2017, pp. 15 – 31.
5. Liu, J., Wang, K., Zhang, Q., Han, F., Sha, J., Liu, J., "Influence of superplasticizer dosage on the viscosity of cement paste with low water-binder ratio", *Construction and Building Materials*, V. 149, 2017, p. 359-366.
6. Lange, A., Plank, P., "Optimization of comb-shaped polycarboxylate cement dispersants to achieve fast-flowing mortar and concrete", *Journal of Applied Polymer Science*, V. 132, 2015, p. 42529.
7. Lange, A., Hirata, T., Plank, J., "Influence of the HLB value of polycarboxylate superplasticizers on the flow behavior of mortar and concrete", *Cement and Concrete Research*, V. 60, 2014, pp. 45-50.
8. Schmidt, W., Brouwers, J., Kühne, H.C., Meng, B., "Effects of superplasticizer and viscosity-modifying agent on fresh concrete performance of SCC at varied ambient temperatures, design, production and placement of self-consolidating concrete", *RILEM Bookseries*, V. 1, 2010, pp. 65-77.
9. Ushiro, M., Atarashi, D., Kawakami, H., Sakai, E., "The effect of superplasticizer present in pore solution on flowability of low water-to-powder cement paste", *Cement Science and Concrete Technology*, V. 67, 2013, pp. 102-107.
10. Lange, A., Hirata, T., Plank, J., "The role of non-adsorbed PCE molecules in cement dispersion: experimental evidence for a new dispersion mechanism", in: V. M. Malhotra, ed., Proceedings of the 10th CANMET/ACI Conference on Superplasticizers and Other Chemical Admixtures in Concrete, Prague (Czech Republic), 2012, SP-288.29, pp. 423 – 434.
11. Shui, L., Sun, Z., Yang, H., Yang, X., Ji, Y., Luo, Q., "Experimental evidence for a possible dispersion mechanism of polycarboxylate-type superplasticizers", *Advances in Cement Research*, V. 28 (5), 2016, p. 287-297.

12. Sakai, E., Kakinuma, Y., Yamamoto, K., Daimon, M., "Relation between the shape of silica fume and the fluidity of cement paste at low water to powder ratio", *Journal of Advanced Concrete Technology,* V. 7 (1), 2009, pp. 13-20.
13. Lange, A., Plank, J., "Contribution of non-adsorbing polymers to cement dispersion", *Cement and Concrete Research*, V. 79, 2016, pp. 131-136.
14. DIN 1164-10:2013-03 Special cement – Part 10: Composition, requirements and conformity evaluation for cement with low effective alkali content.
15. DIN EN 12350-8:2010-12 Testing fresh concrete – Part 8: Self compacting concrete – Slump flow test.
16. DIN EN 12350-9:2010-12 Testing fresh concrete – Part 9: Self-compacting concrete – V-funnel test.
17. Jakubekova, D., Stibrany, P., Frtalova, D., "Investigation of the effects of diethylene glycol on the hydration of C_3S and C_3A pastes", *Journal of Thermal Analysis*, V. 33, 1988, pp. 651-659.

TABLES AND FIGURES

List of Tables:

List of Figures:

Table 1 – Phase composition of the cements used in the study.

	CEM I 52.5 N	CEM II/A-LL 42.5 R
Phase	**m.-%**	**m.-%**
C_3S	52.7	53.1
C_2S	26.6	17.5
C_3A	6.6	5.2
C_4AF	2.6	8.2
Free Lime (*Franke*)	0.1	0.3
Anhydrite*	3.5	1.4
Hemihydrate*	1.3	1.1
Dihydrate	0.6	0.1
Calcite	4.2	8.0
Quartz	1.2	0.2
Dolomite	-	2.6
Arcanite	0.6	1.4
Periclase	-	0.9
Total	100	100

* Determined by thermogravimetry

Table 2 – Mixture proportions of the SCC used in the study (w/c = 0.35).

Component	Dry mass [kg]	Dry mass [oz]
0/4 sand	7.960	280.78
4/8 gravel	1.953	68.78
8/16 gravel	5.107	180.14
CEM II/A-LL 42.5 R	3.440	121.34
Fly ash	0.400	14.11
Limestone powder	0.400	14.11
Fresh water	1.204	42.47

Table 3 – Spread flow and V-funnel empty time of SCCs admixed with 50IPEG4.5 and different non-ionic co-dispersants.

System	Spread flow	V-funnel empty time
1.3 % bmoc 50IPEG4.5	750 mm [29.53 in.]	21 sec
1.3 % bmoc 50IPEG4.5 + 1.1 % bmoc DPGDME	750 mm [29.53 in.]	13 sec
1.3 % bmoc 50IPEG4.5 + 1.3 % bmoc DEG	740 mm [29.13 in.]	14 sec

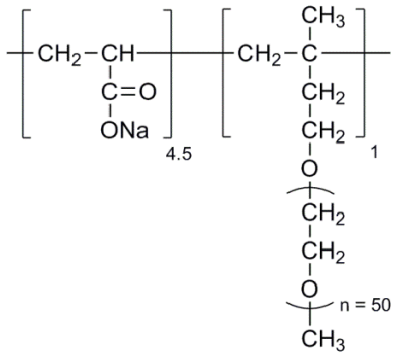

50IPEG4.5

Fig. 1 – Chemical structure of the IPEG PCE sample 50IPEG4.5.

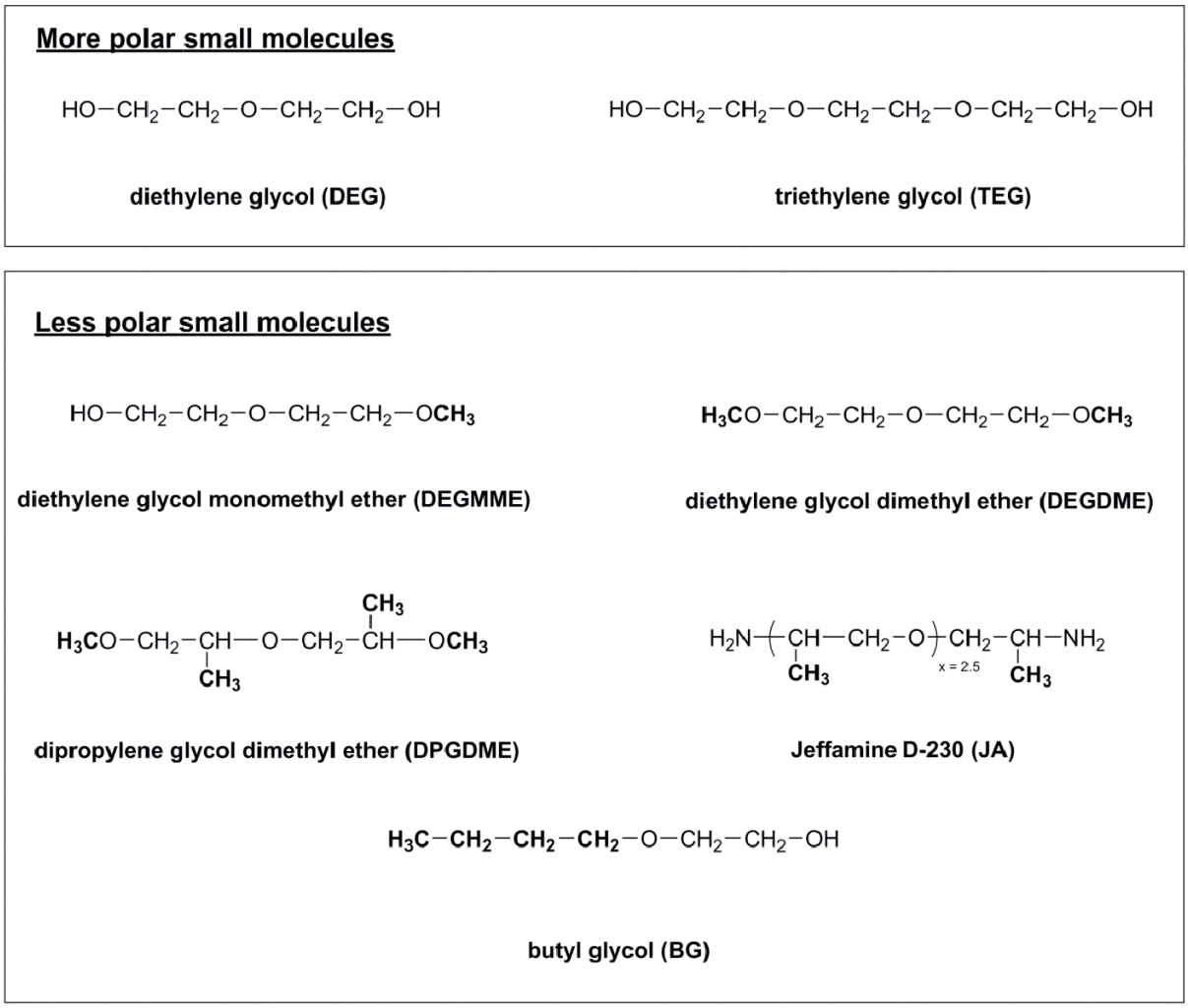

Fig. 2 – Overview of the non-ionic small molecules tested in the study.

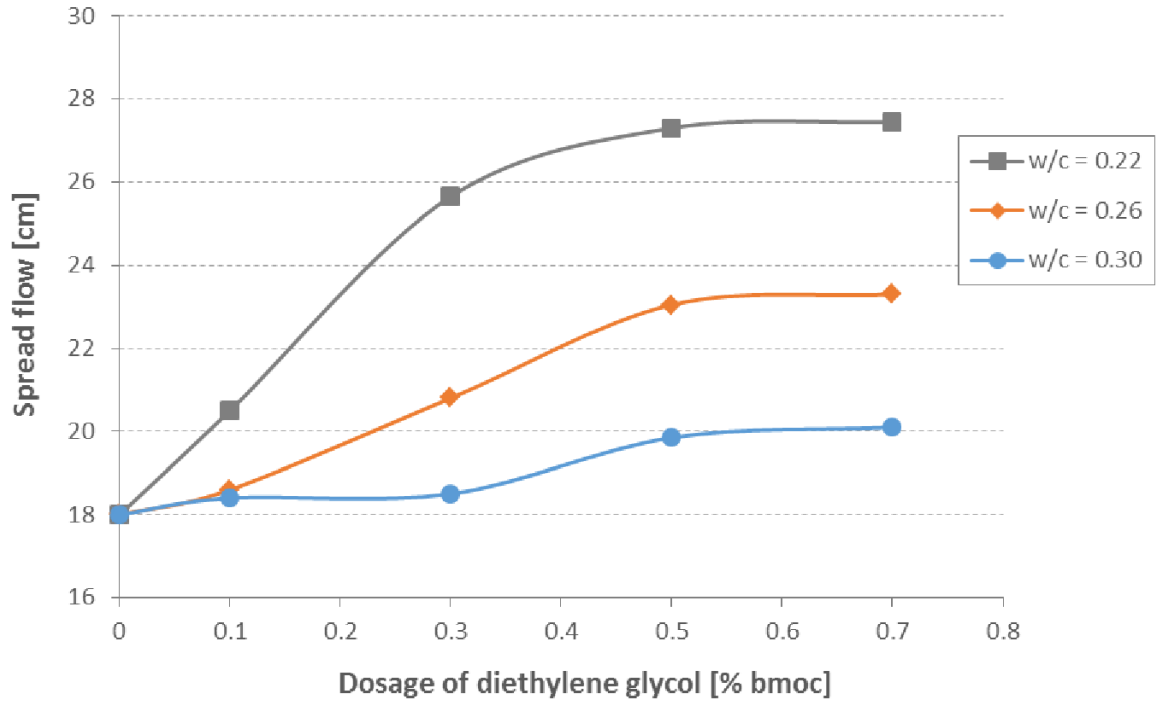

Fig. 3 – Influence of the w/c of cement paste (CEM I 52.5 N) on the spread flow enhancing effect of diethylene glycol in combination with 50IPEG4.5.

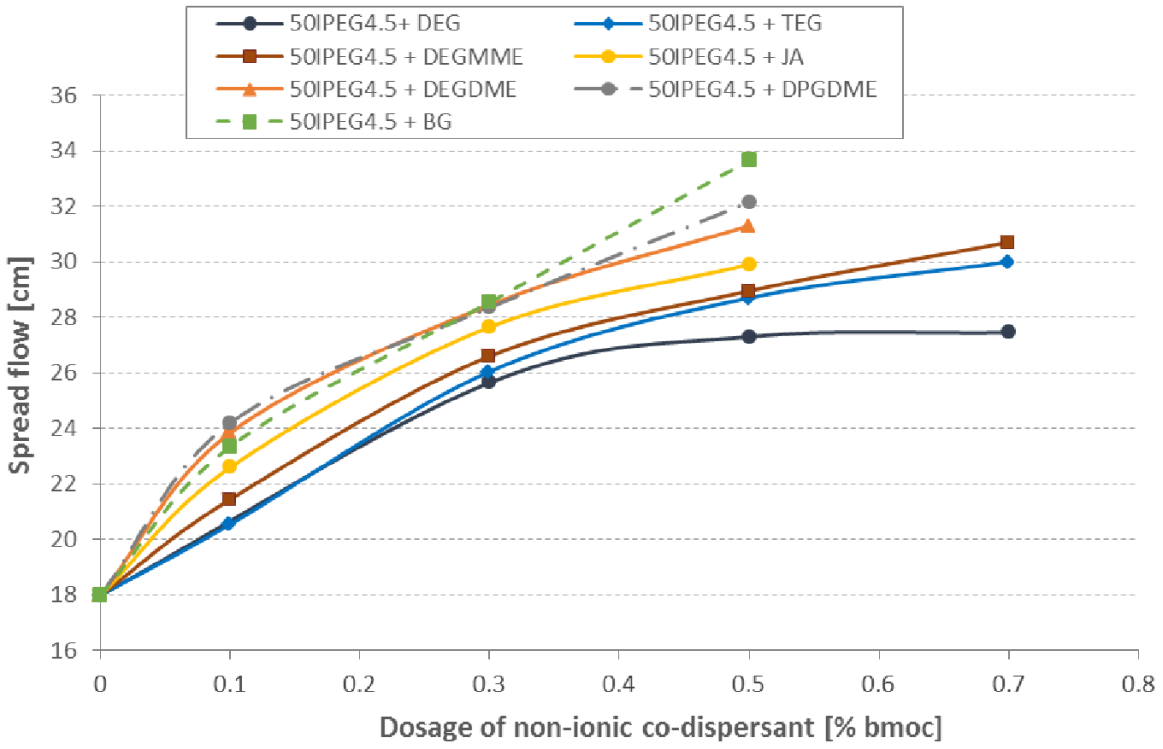

Fig.4 – Spread flow of cement pastes (CEM I 52.5 N, w/c = 0.22) holding 0.215 % bmoc of PCE polymer 50IPEG4.5 and different dosages of the non-ionic glycol compounds.

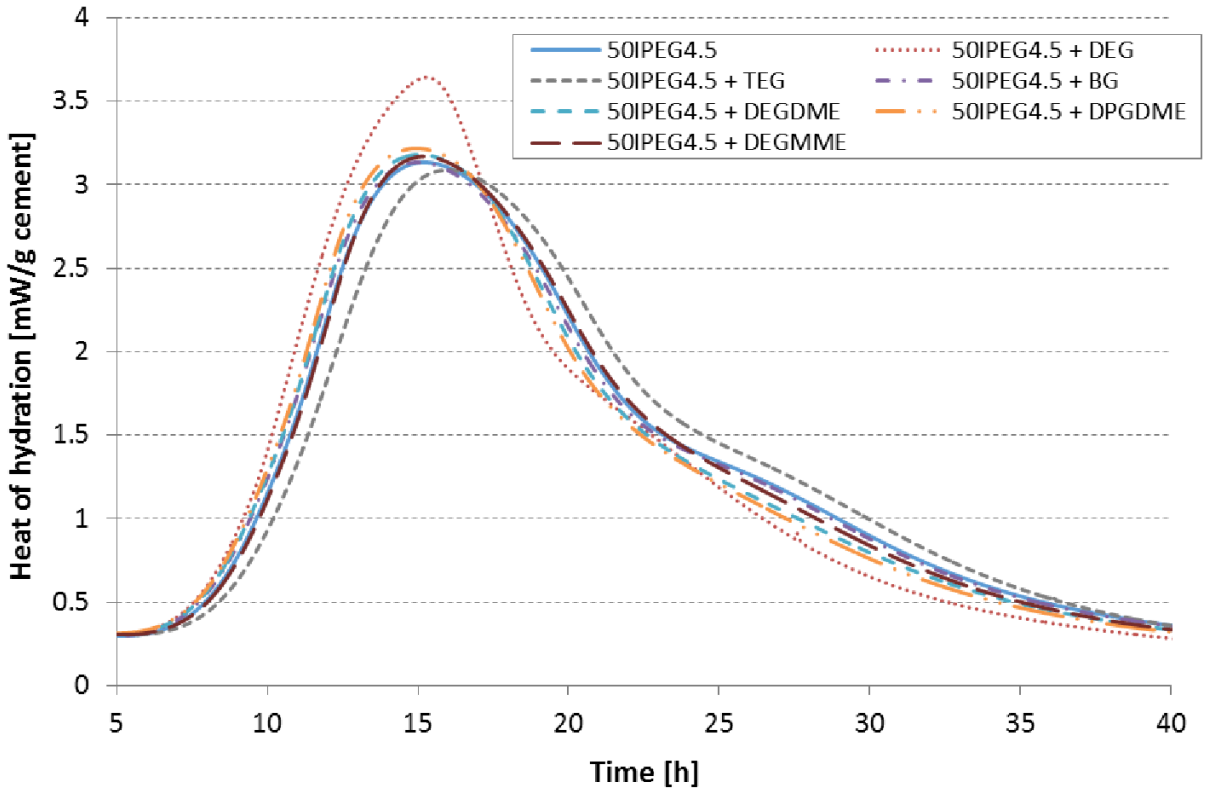

Fig. 5 – Time-dependent heat evolution of cement pastes (CEM I 52.5 N, w/c = 0.22) holding 0.215 % bmoc of 50IPEG4.5 and admixed with 0.30 % bmoc of different non-ionic small molecules.

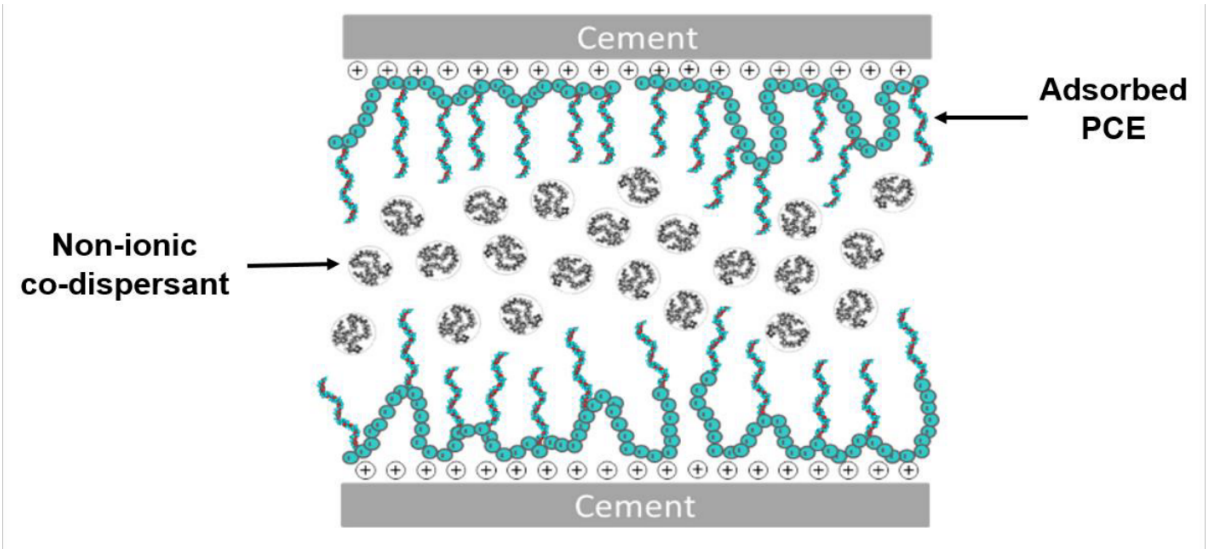

Fig. 6 – Mechanistic model explaining the flow enhancing effect of non-ionic small co-dispersants.

5.1.3. Publikation #3: Non-adsorbing small molecules as auxiliary dispersants for polycarboxylate superplasticizers

In **Publikation #3** wurden die Erkenntnisse aus den vorangegangen Veröffentlichungen aufgegriffen und versucht, das Verständnis zur Wirkungsweise der nicht-adsorbierenden Co-Dispergiermittel durch umfassende mechanistische Untersuchungen weiter zu vertiefen. Es wurden die Fragen adressiert, warum Verbindungen mit einem niedrigen Molekulargewicht sowie einem höheren Anteil an hydrophoben Gruppen jeweils eine bessere Verflüssigung erzielen und weshalb bestimmte PCE-Strukturen mehr von der Zugabe eines nicht-ionischen Additivs profitieren als andere. Dazu wurden MPEG-PCEs mit unterschiedlicher Seitenkettendichte und -länge eingesetzt und in Gegenwart verschiedener nicht-ionischer Moleküle bzw. Polymere getestet.

Es konnte gezeigt werden, dass Polyethylenglykole mit Molmassen zwischen 1000 – 3000 Da im Vergleich zu den niedermolekularen Glykolderivaten nicht so wirksam sind. Über Viskosimetrie wurde festgestellt, dass die Polyethylenglykole eine erhöhte Lösungsviskosität bedingen. Da bei einem niedrigen w/z-Wert das Volumen der Porenlösung äußerst begrenzt ist, führen Polyethylenglykole dort zu einem stark verdickenden Effekt, der eine Verringerung der Fließfähigkeit zur Folge hat. Für ein kurzkettiges Polyethylenglykol (M_w = 300 Da) nahm die Lösungsviskosität hingegen nur minimal zu, weshalb hier ein höheres Fließmaß und somit eine niedrigere Fließgrenze erzielt werden konnten.

Messungen der Oberflächenspannung über die „Hängende-Tropfen"-Methode (*„Pendant drop"*) enthüllten, dass Glykolderivate, die mehrere hydrophobe Strukturmerkmale besitzen, die Oberflächenspannung der Zementporenlösung stärker reduzierten als solche, die vorwiegend hydrophile Eigenschaften vereinen (z.B. Diethylenglykol). Durch die verringerte Oberflächenspannung wird das Benetzungsverhalten des Zements verbessert, wodurch dieser schneller und unmittelbar nach der Wasserzugabe dispergiert werden kann.

Über Fließmaßuntersuchungen wurde herausgefunden, dass auch bei MPEG-PCEs die Seitenkettendichte des Polymers für die Stärke des stabilisierenden Effekts durch die nicht-ionischen Verbindungen entscheidend ist. Zudem konnte die Seitenkettenlänge der PCEs als weiterer entscheidender Paramater identifiziert werden. Insbesondere

PCEs mit einer langen Seitenkette (114 Ethylenoxid-Einheiten) profitierten stark von der Zugabe einer nicht-ionischen Verbindung.

Adsorptionsmessungen wurden schließlich durchgeführt, um den Wirkmechanismus aufzuklären. Hierbei wurde festgestellt, dass PCEs, die besonders stark für die Co-Dispergiermitttel empfänglich sind, nahezu vollständig auf der Zementkornoberfläche adsorbieren und nur ein geringer Teil in der Porenlösung verbleibt. Dies sind hauptsächlich diejenigen PCEs mit einer hohen anionischen Ladung bzw. geringen Seitenkettendichte. Die PCE-Fließmittel mit niedriger anionischer Ladung, für die der Effekt nicht so stark ausgeprägt war, adsorbieren hingegen zu Beginn in einer geringeren Menge, sodass hier das Polymer in einer höheren Konzentration frei in der Porenlösung vorliegt.

Mit Hilfe der gewonnenen Erkenntnisse wurde das mechanistische Modell zur Wirkweise der Co-Dispergiermittel weiter verfeinert (sh. **Abbildung 40**).

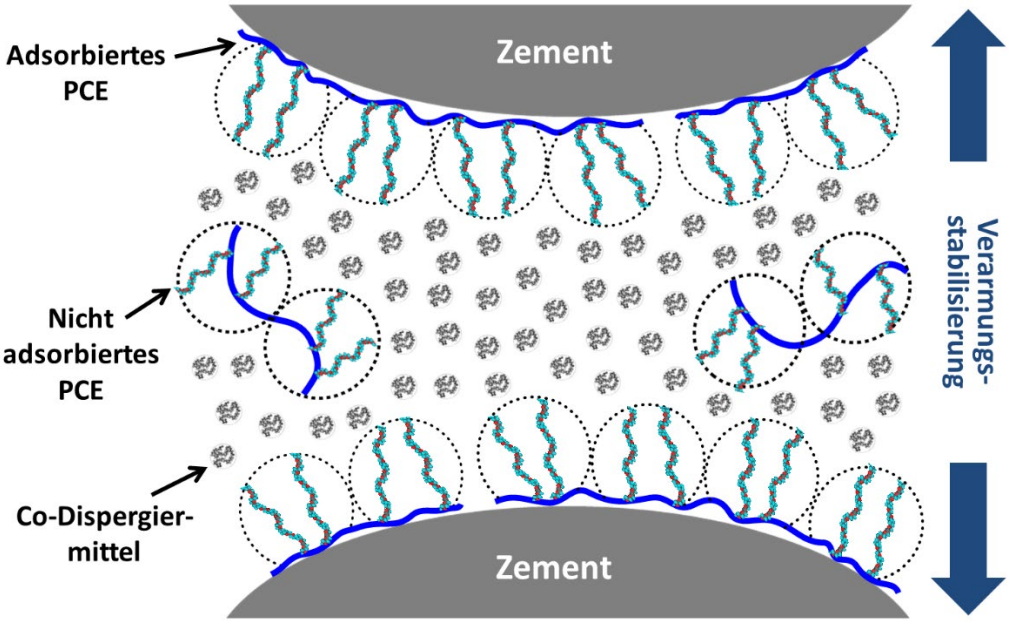

Abbildung 40: Mechanistisches Modell zur Funktionsweise der nicht-ionischen Co-Dispergiermittel.

Demnach halten sich die nicht-ionischen Additive in der Porenlösung zwischen den Seitenketten der adsorbierten PCE-Polymere auf und können für eine Verarmungs-stabilisierung sorgen. Nähern sich die Zementteilchen zu nahe an, würde das Co-Dispergiermittel aus dem Zwischenraum mehrerer Zementpartikel verdrängt, wodurch

eine ungleichmäßige Verteilung der nicht-ionischen Verbindungen resultieren würde. Dies ist aus entropischer Sicht ungünstig und wird deshalb durch die Ausbildung von abstoßenden Kräften verhindert, die neben der elektrosterischen Stabilisierung durch die PCEs zusätzlich zur Dispergierung beitragen. Dieser Effekt tritt nur bei sehr niedrigen w/z-Werten auf, da hier das Porenvolumen äußerst niedrig ist und deshalb sehr hohe Konzentrationen des Co-Dispergiermittels vorherrschen (15 – 135 g/L), die für eine solche Art der Stabilisierung erforderlich sind. Ein vergleichbarer Effekt scheint auch für die nicht-adsorbierten PCE-Polymere möglich zu sein, dass erklären würde, warum die nicht-ionischen Verbindungen keine allzu große Fließmaßverbesserung bei PCEs mit einer hohen Seitenkettendichte erzielen konnten, da diese PCEs zu Beginn weniger adsorbieren und eine höhere nicht-adsorbierte Restmenge in der Porenlösung verbleibt.

Publikation #3

Non-adsorbing small molecules as auxiliary dispersants for polycarboxylate superplasticizers

Manuel Ilg, Johann Plank

Colloids and Surfaces A: Physicochemical and Engineering Aspects
587 (2020) 124307

Doi: 10.1016/j.colsurfa.2019.124307

Colloids and Surfaces A 587 (2020) 124307

Contents lists available at ScienceDirect

Colloids and Surfaces A

journal homepage: www.elsevier.com/locate/colsurfa

Non-adsorbing small molecules as auxiliary dispersants for polycarboxylate superplasticizers

Manuel Ilg, Johann Plank*

Chair for Construction Chemistry, Technische Universität München, Lichtenbergstraße 4, 85748, Garching, Germany

GRAPHICAL ABSTRACT

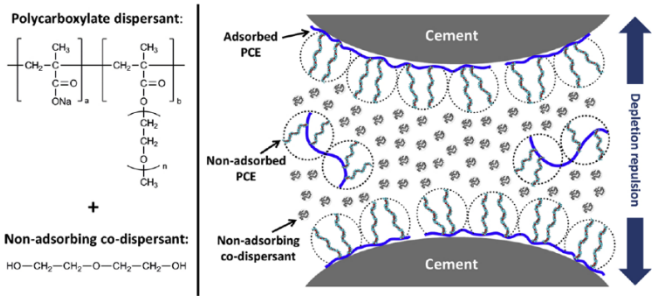

ARTICLE INFO

Keywords:
Dispersion
Non-ionic auxiliary dispersant
Superplasticizer
Adsorption
Polycarboxylate
Cement

ABSTRACT

The dispersing ability of polycarboxylate superplasticizers (PCEs) can be ascribed to the electrostatic and steric stabilization of cement suspensions. For this purpose, PCEs need to adsorb on the cement particle surface to become effective at all. In this study, it is demonstrated that at low water to cement ratios ≤ 0.30, even non-ionic molecules like diethylene glycol or 2-methyl-2,4-pentanediol which do not adsorb on cement, but remain dissolved in the interstitial pore solution, can greatly enhance cement dispersion when combined with PCEs such as conventional methacrylate ester based comb co-polymers. Their effect as co-dispersant is particularly pronounced for PCEs possessing a low side chain density and long side chain length. Relative to the co-dispersants it was found that especially non-polar small molecules like neopentyl glycol greatly enhance the paste fluidity. These molecules significantly reduce the surface tension of the pore solution and thus increase the wettability of cement. Based on results from spread flow tests, adsorption measurements and pendant drop tensiometry it is concluded that in cementitious systems formulated at low w/c ratios, non-adsorbing molecules with a molecular weight of ≤ 1000 g/mol induce repulsive depletion forces which prevent cement particles from agglomeration. This way, such small molecules act as auxiliary or co-dispersant when combined with PCEs.

1. Introduction

Many chemical admixtures which are commonly applied in the construction industry achieve their properties via an adsorptive working mechanism [1–3]. Typical examples are plasticizers and superplasticizers which are added to cement-based materials for dispersion of the solid particles. For this reason, all dispersing additives exhibit anionic groups (e.g. sulfonate, carboxylate, phosphonate or phosphate anchors) to

* Corresponding author.
E-mail address: sekretariat@bauchemie.ch.tum.de (J. Plank).

https://doi.org/10.1016/j.colsurfa.2019.124307
Received 26 September 2019; Received in revised form 22 November 2019; Accepted 30 November 2019
Available online 02 December 2019

facilitate the adsorption on positively charged surface sites through electrostatic attraction [4–7]. The adsorption is a multi-step process including diffusion, accumulation and reorganization of the polymer chains at the solid-liquid interface [8]. It is affected by the molecular properties and architecture of the polymer (e.g. anionic charge amount, chemical nature of anchor group, molecular weight, stereochemistry and conformation of the polymer, etc.), the ion concentration and pH value of the dispersing medium as well as the surface charge of the particles [9–12]. After the adsorption of the polymeric dispersants, attractive *van der Waals* forces are disrupted between the oppositely charged surfaces of the individual clinker and hydrate phases, thus leading to the disagglomeration of cement and to improved fluidity [13–15].

Polycarboxylate superplasticizers (PCEs) are among the most efficient cement dispersants. These comb-shaped (brush-like) polymers consist of a main chain holding anionic carboxylate groups and several linear side chains made up from polyethylene glycols or a mixture of polyethylene/polypropylene oxide units that are attached to the polymer backbone [16,17]. It is well established that the superior dispersing performance of PCEs originates from the electrostatic and steric stabilization of cement particles [4,18]. Due to adsorption of the PCEs, the cement particles become homogeneously negatively charged, thus provoking an electrostatic repulsion. Furthermore, the non-ionic side chains of the PCEs stretch out into the pore solution and create a steric barrier which prevents cement particles from reagglomeration [19]. Generally, the dispersing efficacy of PCEs correlates with the adsorbed amount of polymer, whereas the non-adsorbed portion present in the pore solution determines the time-dependent fluidity properties ("slump retention" behavior) [20–22]. Accordingly, PCEs which adsorb almost quantitatively on cement entail a rapid decrease of the initial flowability, since no free polymer is left for the dispersion of new hydrate phases. However, recent studies suggest that the portion of non-adsorbed PCE not only controls the slump loss behavior, but also can play an important role for the dispersion of concentrated cement suspensions [23]. This was first observed by *Sakai* et al., who investigated the effect of methacrylic acid-*co*-polyethylene glycol methacrylate ester polymers (MPEG-PCEs) on the viscosity of belite-rich low heat Portland cement – silica fume blends at water to powder (w/p) ratios from 0.16 – 0.32. It was found that at low w/p ratios (i.e. 0.16), especially those PCEs were highly effective which only adsorbed in low quantities, while the major part remained in the pore solution. Consequently, in such case the high fluidity cannot be attributed only to the adsorbed amount, but originates more from the portion of non-adsorbed PCE. Further evidence for this effect was given by a follow-up study in which it was demonstrated that the apparent viscosity of cement pastes even decreased at PCE dosages above the saturated adsorption [24]. Moreover, recently *Sun* et al. demonstrated that besides non-adsorbed PCEs, also other components suspended in the pore solution like nano-sized ettringite and other fine matters < 200 nm can contribute to cement dispersion at low w/c ratios [25]. All these previous findings imply that non-adsorbing polymers and nano particles can be quite beneficial for the stabilization of highly particle loaded systems. This was further supported by additional studies showing that other non-ionic polymers such as polyethylene glycol (PEG) of low molecular weight [26,27], hydroxypropyl methyl cellulose [28] or the macromonomers used in the PCE synthesis [26] are capable of improving the dispersing efficacy of PCE superplasticizers. Conversely, polyethylene glycols with a high molecular weight (M_n = 56,000–570,000 g/mol) were found to increase the yield stress and viscosity of cement pastes when combined with a MPEG-type PCE, due to attractive depletion forces which considerably contribute to the flocculation of the particles [29].

Therefore, the question arises how non-ionic molecules with a molecular weight < 1000 g/mol behave and whether such small molecules can induce any dispersion. Thus, the aim of the present study was to investigate the effect of low molecular compounds, namely of glycol and diol derivates, on the fluidity of cement pastes prepared at w/c ratios of 0.22 – 0.40, and to broaden the knowledge about the structure-performance relationship of non-adsorbing additives. Various small molecules were combined with MPEG-PCEs possessing different anionic charge amounts and side chain lengths to identify those PCEs which benefit the most from such a co-dispersant. The effectiveness of the auxiliary dispersants was assessed via spread flow tests, and to elucidate their working mechanism adsorption measurements and pendant drop tensiometry were conducted. Generally, the main purpose of this study was to get a more profound understanding of the role of non-adsorbing molecules for the dispersion of concentrated cement suspensions.

Table 1
Phase composition of the cement sample used in the study.

Phase	wt.%
C_3S	53.3
C_2S	25.7
C_3A_{cubic}	4.2
$C_3A_{orthorhombic}$	4.6
C_4AF	2.6
Free Lime (*Franke*)	0.1
Anhydrite	3.3
Hemihydrate*	0.7
Dihydrate*	0.1
Arcanite (K_2SO_4)	0.5
Calcite	3.9
Quartz	1.0

* determined by thermogravimetry.

2. Materials and methods

2.1. Cement

An ordinary Portland cement CEM I 52.5 N (Milke® classic from HeidelbergCement, Geseke plant, Germany) was used for the experiments. Its phase composition as quantified by X-ray diffraction (Bruker AXS D8 Advance, Karlsruhe, Germany) using *Rietveld* refinement is provided in Table 1. The amounts of hemihydrate ($CaSO_4 \cdot ½\ H_2O$) and gypsum ($CaSO_4 \cdot 2\ H_2O$) were determined by thermogravimetry (Netzsch STA 409 TG-MS, Selb, Germany) and the free lime was quantified according to the *Franke* method.

The average particle size (d_{50} value) of the cement was 13.45 µm (laser granulometry; CILAS 1064 instrument, Cilas, Marseille, France) and the density was 3.19 g/cm^3 (helium pycnometry; Ultrapycnometer 1000, Quantachrome Instruments, Boynton Beach, USA). For the specific surface area (*Blaine* fineness) a value of 3479 cm^2/g was obtained. The particle size distribution of the cement is shown in Fig. 1.

2.2. Non-adsorbing additives

A broad range of glycol and diol derivates was tested as non-adsorbing additives. These compounds were all designated as small molecules because of their low molecular weight between 100–150 g/mol.

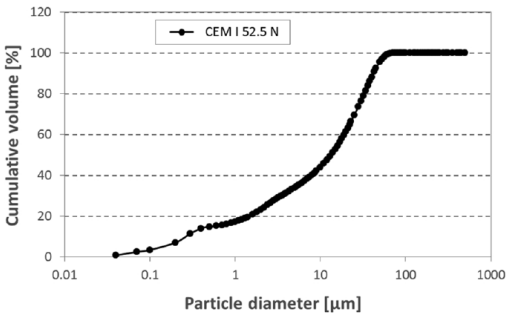

Fig. 1. Particle size distribution of the cement sample.

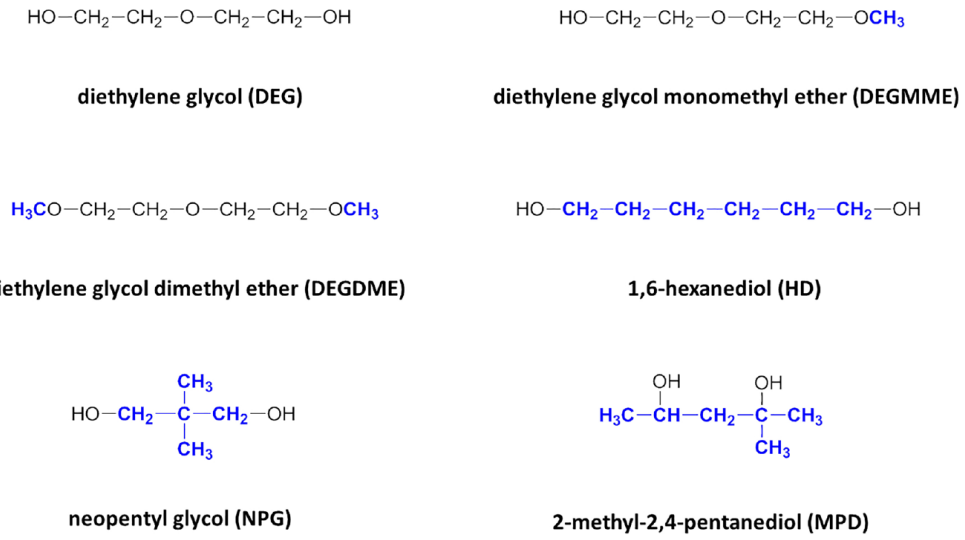

Fig. 2. Chemical structures of the non-adsorbing small molecules tested in the study.

An overview of their chemical structures is presented in Fig. 2. From there it can be seen that the non-ionic co-dispersants comprise quite different amounts of non-polar and hydrophobic groups (shown in bold and blue color).

The non-ionic molecules diethylene glycol (DEG; purity ≥ 99 %), diethylene glycol monomethyl ether (DEGMME; ≥ 99 %) and diethylene glycol dimethyl ether (DEGDME; ≥ 99 %) were provided by Clariant (Burgkirchen, Germany). 1,6-Hexanediol (HD; ≥ 97 %) and neopentyl glycol (NPG; ≥ 98 %) were purchased from Merck (Darmstadt, Germany), while 2-methyl-2,4-pentanediol (MPD; ≥ 98 %) was obtained from Alfa Aesar (Karlsruhe, Germany). These molecules were used to investigate the structure-performance relationship of the non-ionic co-dispersants. In addition, polyethylene glycols with molar masses of 300 (PEG 300; ≥ 99 %), 1000 (PEG 1000; ≥ 99 %) and 3000 g/mol (PEG 3000; ≥ 99 %) were tested to determine the impact of the molecular weight, respectively chain length on the spread flow enhancing capability. The non-ionic character of the co-dispersants was verified by charge titration (see chapter 2.3.2.) in synthetic cement pore solution (SCPS), hence no adsorption through electrostatic attraction was possible. Also note that the non-adsorbing additives do not provoke any fluidity when individually admixed into the cement paste.

2.3. MPEG-type PCE superplasticizers

2.3.1. Synthesis

The dispersing performance of the non-ionic additives was investigated in the presence of seven structurally different MPEG-PCEs. The polymers were synthesized via aqueous free radical copolymerization involving methacrylic acid (> 99 %; Sigma-Aldrich, Steinheim, Germany) and ω-methoxy polyethylene glycol methacrylates (> 98 %; Clariant, Burgkirchen, Germany) at varying molar ratios and side chain lengths of the macromonomer. Sodium persulfate (≥ 99 %; Merck) was used as initiator and 3-mercapto propionic acid (≥ 99 %; Sigma-Aldrich) as chain transfer agent. A detailed description of the synthesis can be found in [16]. In contrast, PCE sample 7PC6 was obtained by grafting a methoxy-terminated polyethylene glycol (Polyglykol M350; ≥ 99 %; Clariant) onto a polymethacrylic acid backbone with M_n = 4700 g/mol at 180 °C under reduced pressure (~ 0.03 mbar) [30]. All synthesized PCEs were designated as xPCy, with x being the number of ethylene oxide (EO) units in the polyethylene glycol side chain (n_{EO} = 7, 25, 45 and 114) and y being the molar ratio of methacrylic acid to ω-methoxy polyethylene glycol methacrylate (2–8 : 1). The synthesized polymer solutions exhibited a pH of ~ 2–3 and were neutralized to pH = 7 with 30 wt.% NaOH to yield aqueous solutions with a solid content of ~ 30 wt.%. The chemical structure of the synthesized MPEG-PCEs is illustrated in Fig. 3.

2.3.2. Polymer characterization

Size exclusion chromatography (SEC) was performed to determine the molar masses and polydispersity (PDI) of the synthesized polymers. A Waters Alliance 2695 separation module coupled with a refractive index detector (2414 module from Waters, Eschborn, Germany) and a Dawn EOS 3 angle static light scattering detector (Wyatt Technology, Santa Barbara, CA) were used for the measurements. Solutions of the PCEs with a concentration of 10 g/L were prepared, filtered through a 0.2 µm syringe filter and injected on a precolumn and three Ultrahydrogel columns (150, 250, 500) for separation. The mobile phase was an aqueous 0.1 M $NaNO_3$ solution (adjusted with NaOH to a pH = 12) which was pumped at a flow rate of 1.0 mL/min. The molar masses were calculated based on the *dn/dc* value of polyethylene glycol (0.135 mL/g) [31].

The anionic charge of the MPEG-PCEs and the non-adsorbing molecules was quantified by polyelectrolyte titration employing a particle charge detector (PCD 03 pH; BTG Instruments, Weßling, Germany). Here, 10 mL of a 0.1 g/L solution of the analyte in synthetic cement

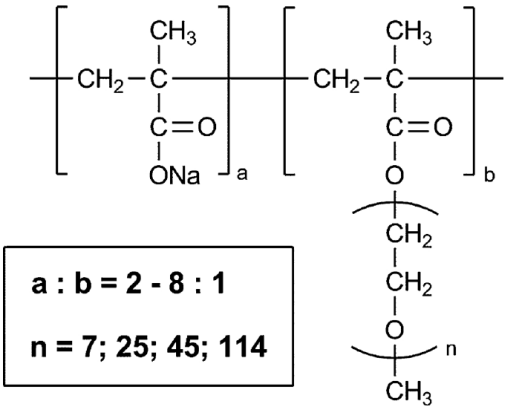

Fig. 3. Chemical composition of the MPEG-based superplasticizers.

pore solution (SCPS) were used and titrated against a cationic 0.001 M poly dimethyl ammonium chloride solution (polyDADMAC) until charge neutralization was achieved (isoelectric point). By means of the volume of consumed polyDADMAC solution, the anionic charge per gram of polymer was calculated. More information about the method and a detailed instruction of the experimental procedure are provided in [32]. The SCPS exhibited a pH of 12.8 and was composed of 1.720 g $CaSO_4 \cdot 2\ H_2O$, 6.959 g Na_2SO_4, 4.757 g K_2SO_4 and 7.120 g KOH dissolved in 1 L of de-ionized (DI) water.

Dynamic light scattering measurements were carried out to ascertain the hydrodynamic radii (R_h) of the polymers. For this purpose, solutions of the PCE samples with a concentration of 10 g/L were prepared using SCPS as solvent, filtered through a 0.2 µm syringe filter into a cuvette and then analyzed with a Zetasizer Nano instrument (Malvern Instruments, Workestershire, United Kingdom). After an equilibration time of 120 s at 25 °C, five independent measurement runs were performed. The hydrodynamic radii were reported as average values, with a standard deviation of ± 0.1 nm.

To understand the structural properties of the PCEs better, also the main and side chain lengths of the polymers were calculated. The length of one EO unit in the polyethylene glycol side chain was assumed to be 0.278 nm, while a value of 0.251 nm was adopted for the C—C—C bond in the polymer backbone [33]. Moreover, the solution conformations of the PCEs were established according to the model proposed by *Gay* and *Raphaël* [34]. Hence, the tested polymers are assigned to the stretched backbone worm (SBW), flexible backbone worm (FBW) and flexible backbone star (FBS) domain, respectively. An overview of the molecular properties of all synthesized MPEG-PCEs is given in Table 2.

2.4. Research methods

2.4.1. Cement dispersion

The effect of the non-adsorbing additives on the rheological properties of cement pastes was investigated by mini slump tests, following the specifications outlined in DIN EN 1015. The experiments were conducted at different w/c ratios ranging from 0.22 – 0.40. At first, the dosage of the PCE was determined to obtain a spread flow of 18 ± 0.5 cm at a given w/c ratio. This dosage was applied for the ensuing experiments, where the dispersing capability of the non-ionic additives was evaluated in the presence of different MPEG-PCEs. The co-dispersants were dissolved in the mixing water at dosages of 0.1 – 0.9 % by weight of cement (bwoc) together with the respective amount of the PCE superplasticizer (dosage of the PCE correlates to a spread flow of 18 cm). The amount of water introduced by the PCE solution was subtracted from the total volume of the mixing water to maintain a constant w/c ratio. The spread flow tests were conducted as follows: within 5 s 400 g cement were added to the mixing water containing the pre-dissolved PCE and non-ionic co-dispersant. The mixture was vigorously stirred for 4 min with a spoon and finally poured into a *Vicat* cone (height 40 mm, top diameter 70 mm, bottom diameter 80 mm) placed on a glass plate. After complete filling, the *Vicat* cone was immediately lifted upwards and retained for 5 s over the spreading cement slurry. The diameter of the cement paste was measured twice with a caliper, the second measurement being in a 90° angle to the first one and averaged to give the spread flow value. All experiments were performed at a temperature of 20 ± 1 °C.

2.4.2. Kinematic and dynamic viscosity

The kinematic and dynamic viscosity of aqueous solutions of PCE sample 45PC6 and of different non-ionic polyethylene glycols in SCPS was measured with an *Ubbelohde* viscometer. The aim of these experiments was to investigate the impact of the non-ionic co-dispersants on the viscosity of the pore solution. To carry out these experiments under similar concentration conditions as prevailing in the cement paste, first the water loss caused by initial wetting and cement hydration was quantified. For this reason, a cement paste which was fluidized with 0.208 % bwoc of 45PC6 (dosage corresponds to a spread flow of 18 cm at w/c = 0.22) was filtrated using a hydraulic press [35] to determine the water volume that is not consumed in the initial cement hydration. This amount of water was considered in the preparation of the samples which were composed of 0.208 % bwoc of 45PC6 and varying dosages of different polyethylene glycols (i.e. 0.1 – 0.9 % bwoc) in SCPS. The polymer solution was filled into the reservoir of a glass capillary (type: 501 10/I from Schott Instruments, Mainz, Germany), equilibrated to 25 °C in a water bath and then the flow time was measured which represents the time the liquid takes to pass a specific distance between two calibration marks. From the viscometer constant K, the flow time t and the flow time dependent *Hagenbach-Couette* correction term ζ, the kinematic viscosity υ was calculated:

$$\upsilon = K \cdot (t - \zeta) \quad (1)$$

Subsequently, the dynamic viscosity η_{dyn} can be obtained by multiplying the kinematic viscosity with the specific density ρ of the solution:

$$\eta_{dyn} = \upsilon \cdot \rho \quad (2)$$

2.4.3. Adsorption measurements

To gain a better understanding of the role of the non-ionic additives in cement dispersion, adsorption measurements were performed using the depletion method. Adsorption isotherms were developed for the individual PCEs, and also the effect of the co-dispersants on the adsorbed amounts of the PCEs was studied. In a typical experiment, 50 g cement, 13 mL DI water (w/c = 0.26) and the respective amount of the dispersants to be tested were added into a 50 mL centrifuge tube, homogenized for 4 min with a vortex mixer and centrifuged for 15 min at 8500 rpm. The supernatant that contains the non-adsorbed compounds was removed, filtered through a 0.2 µm syringe filter and diluted with a 0.1 M HCl to prevent carbonation. Thereafter, the total organic carbon (TOC) content of the solutions was quantified with a LiquiTOC-II instrument (Elementar Analysensysteme; Hanau, Germany). Every sample was measured twice and the received values were reduced by the organic carbon content of a blank cement paste to account for the presence of other organic components such as grinding aids. Finally, the adsorbed amount of the polymer was deduced from

Table 2
Molecular properties of the synthesized PCE superplasticizers.

	45PC2	45PC4	45PC6	45PC8	7PC6	25PC6	114PC6
M_w (g/mol)	39,500	23,700	22,200	19,500	13,400	17,100	82,000
M_n (g/mol)	15,900	12,800	11,200	10,500	6,300	8,800	27,000
PDI (M_w/M_n)	2.5	1.9	2.0	1.9	2.1	1.9	3.0
Conversion of macromonomer (%)	93	94	96	93	93	90	98
Anionic charge in SCPS (µeq/g)	720	1610	2450	2850	4300	1820	1500
R_h (nm)	6.5	5.4	4.5	4.3	3.1	3.5	8.3
Main chain length (nm)	5.3	6.6	7.6	8.6	12.1	9.0	8.4
Side chain length (nm)	12.5	12.5	12.5	12.5	1.9	7.0	31.7
Solution conformation acc. to *Gay*	SBW	FBW	FBW	FBW	FBW	FBW	FBS

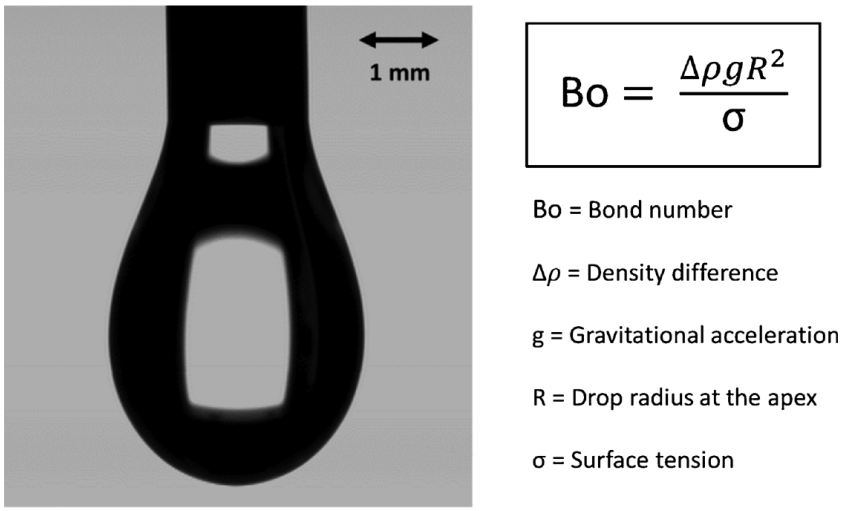

Fig. 4. Surface tension measurement using the pendent drop method.

the difference of the TOC content of the initial polymer solution (= reference) and the supernatant extracted from the cement paste (= residual concentration of the polymers at equilibrium condition).

2.4.4. Pendant drop tensiometry

A drop shape analyzer (DSA100 from Krüss; Hamburg, Germany) was used to assess the impact of the non-ionic additives on the surface tension. In this method, a small droplet of a polymer solution is suspended from a steel needle (capillary tube) and a video image of the pendant drop is recorded with a camera (see Fig. 4). The surface tension can be derived from the fitted contour of the droplet by means of the Bond number Bo that presents the ratio of gravity forces to the surface tension forces which determines the drop shape [36,37].

Mixtures of the PCE polymer 45PC6 and the non-ionic small molecules were prepared in SCPS and filtered through a 0.2 µm syringe filter to remove dust particles. The concentration of the PCE was kept constant at 0.208 % bwoc, while for the co-dispersants different dosages were tested (0.1 – 0.9 % bwoc). Here again, the water consumption owed to the initial cement hydration was taken into account to achieve comparable concentrations of the additives like in the pore solution of the cement paste. For each sample, the surface tension was measured five times at 20 °C and reported as average.

3. Results and discussion

3.1. Relationship between molecular size and effectiveness of non-ionic additives

It has been reported previously that polyethylene glycols with a molecular weight of 2000 g/mol enhance the cement paste fluidity when combined with a MPEG-type PCE [26]. However, no information was provided about the dependence of the dispersing effectiveness from the molecular weight of the co-dispersants. Therefore, spread flow tests were conducted using various polyethylene glycols (PEGs) with molar masses in the range of 300 – 3000 g/mol. As those non-ionic additives do not produce any fluidity when admixed to cement, they always require a PCE superplasticizer to become effective. For this reason, combinations of 0.208 % of PCE sample 45PC6 and varying amounts of the polyethylene glycols were applied in the spread flow tests which were performed at a w/c ratio of 0.22. 45PC6 was used for these investigations as representative superplasticizer due to its median side chain density and side chain length of all synthesized polymers. Throughout the study, the PCE was always dosed in such amounts to obtain a spread flow of 18 cm at a given w/c ratio when no co-dispersant was present. Fig. 5 illustrates the spread flow enhancing effect of the different PEGs as a function of their dosage.

From there it can be seen that the performance of PEG greatly depends on the molecular size. To be more specific, the highest paste fluidities were observed for PEG 300 which exhibits the lowest molecular weight and shortest chain length (n_{EO} = 7). For instance, PEG 300 enhanced the spread flow from 18 to 24 cm at a dosage of 0.5 %, while a smaller increase was attained by PEG 1000 (n_{EO} = 23). In contrast, PEG 3000 (n_{EO} = 68) only slightly improved the spread flow at dosages ≤ 0.5 % bwoc, and higher additions even decreased the fluidity. These results suggest that especially small molecules with a low molecular weight seem to be very powerful co-dispersants which are more suitable to augment the dispersing capability of PCE superplasticizers.

3.2. Effect of non-ionic additives on dynamic viscosity

To elucidate the reasons for the different behavior of the PEG samples in the spread flow tests, viscosity measurements were performed next. Here, the dynamic viscosity of solutions of 45PC6 combined with PEG samples in SCPS were ascertained with an *Ubbelohde* viscometer. To conduct these experiments at similar concentrations such as existing in the cement paste, the amount of water which is consumed by the cement within the first minutes of hydration was

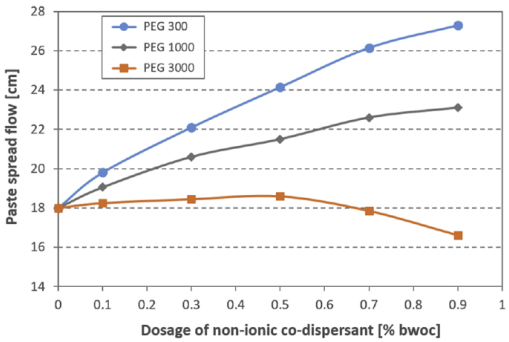

Fig. 5. Effect of the molecular weight of different polyethylene glycols on the dispersing efficacy of PCE 45PC6 in cement (w/c = 0.22).

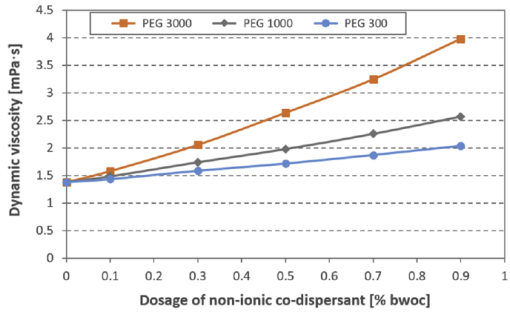

Fig. 6. Dynamic viscosity of synthetic cement pore solutions holding 0.208 % bwoc of PCE 45PC6 and different amounts of PEG samples.

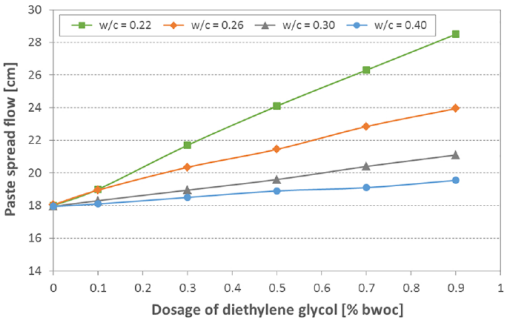

Fig. 7. Impact of the w/c ratio on the spread flow enhancing effect of diethylene glycol in combination with PCE 45PC6; results from cement paste.

considered in the sample preparation. It was found that at a w/c ratio of 0.22, most of the mixing water was already soaked up by the cement after 4 min and only 30 % could be regained by filtration. This already demonstrates that at such low w/c ratios the volume of the interstitial pore solution becomes very small. Fig. 6 shows the dynamic viscosities of the samples for ascending dosages of the non-ionic PEG samples.

As is obvious from the figure, much higher dynamic viscosities were recorded for PEG 3000 compared to the low molecular PEG species. A considerable increase of the dynamic viscosity was observed for PEG 3000 at dosages ≥ 0.5 % (e.g. an increase from 1.4 to 3.2 mPa·s at 0.7 %). Transferring these results to the cement paste it can be inferred that PEG 3000 exerts a thickening effect on the interstitial pore solution and hence increases cement paste viscosity. Since the volume of the interstitial pore solution is quite small at w/c = 0.22, chain entanglements between such long-chain PEG molecules might occur that could induce friction and thus impair fluidity. Such negative interaction would be less possible for PEGs of low molecular weight and with short chain length. Therefore, the highest spread flow values were obtained for PEG 300 which only slightly increased the pore solution viscosity due to its low molecular size.

3.3. Impact of w/c ratio on dispersing effectiveness of co-dispersants

Further mini slump tests were conducted to establish those w/c ratios at which the co-dispersants are most effective. Since the previous investigations have revealed that low molecular compounds are particularly beneficial, diethylene glycol (DEG; M_n = 106 g/mol) was applied as non-ionic additive. In the experiments, PCE sample 45PC6 was combined with different dosages of DEG at w/c ratios from 0.22 – 0.40. At first, the dosages of the PCE superplasticizer were ascertained to achieve a spread flow of 18 cm. This was attained by 0.041 % (w/c = 0.40), 0.11 % (w/c = 0.30), 0.18 % (w/c = 0.26) and 0.208 % (w/c = 0.22), respectively of this PCE. When lowering the w/c ratio, it was noticed that the cement pastes exhibited an increased “sticky” behavior, characterized by a low speed of flow. This was reported before in other studies and ascribed to a high plastic viscosity which originates from the low amount of water and the high solids content of the cement paste [30,38–40]. The above dosages of 45PC6 were then applied in the ensuing mini slump tests in which the spread flow enhancing effect of DEG was studied at different w/c ratios (see Fig. 7).

It can be seen that the dispersing performance of DEG was quite low at w/c ratios from 0.30 – 0.40. High dosages were required to achieve at least a minor increase of the paste fluidity from DEG addition. However, at low w/c ratios (0.22 – 0.26) much higher spread flow values were obtained. Furthermore, it was observed that in the presence of DEG the stickiness of the cement paste was reduced and a “softer” consistency (i.e. a less viscous cement paste) was achieved. Interestingly, at a w/c ratio of 0.22 DEG entailed a similar paste fluidity like PEG 300, thus indicating that a molecular weight between 100–300 g/mol appears to present an optimum for the auxiliary dispersant. These findings signify that the non-ionic co-dispersants become highly effective at low w/c ratios only, where the cement particles are more densely packed and the distance between the binder particles becomes relatively narrow.

3.4. Relationship between PCE molecular structure and spread flow improving effect of DEG

It is well known that the dispersing properties of PCEs are defined by the molecular architecture of the polymers. Depending on the side chain density or the length of the polyethylene glycol pendants, rather different behavior in application is observed [10,41]. Therefore, the question arises whether specific PCE structures can benefit more from the addition of non-ionic co-dispersants. For this purpose, a series of structurally different MPEG-PCEs was synthesized and tested in combination with DEG at w/c = 0.22. First, the spread flow enhancing effect of DEG was probed for PCEs possessing the same side chain length (n_{EO} = 45) but different side chain densities (45PCy polymers) (see Fig. 8). The dosages required from each PCE for a spread flow of 18 cm were found to be 0.49 % (45PC2), 0.193 % (45PC4), 0.208 % (45PC6) and 0.211 % (45PC8), respectively. As is obvious from the figure, not much difference was observed between the PCE samples at dosages ≤ 0.3 %. However, at higher dosages the dispersing efficacy was particularly improved for those PCEs which exhibit a low side chain density and a high anionicity.

Thereafter, spread flow tests were conducted using PCEs of different side chain lengths, but synthesized with the same molar ratio of methacrylic acid to the MPEG macromonomer (xPC6 series). The dosages applied of those PCEs were 0.46 % (7PC6), 0.211 % (25PC6) and 0.223 % (114PC6), respectively. According to Fig. 9, 114PC6 which holds the longest side chain profited most from the addition of DEG, followed by

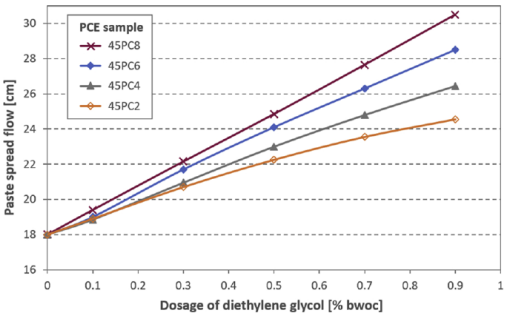

Fig. 8. Impact of side chain density of MPEG-PCE samples possessing the same side chain length (n_{EO} = 45), but different anionicity on the co-dispersing effect of DEG; results from cement paste (w/c = 0.22).

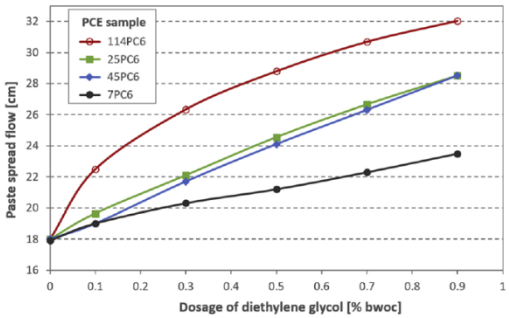

Fig. 9. Impact of the side chain length of different MPEG-PCE samples synthesized with the same molar ratio, on the spread flow enhancing effect of DEG; results from cement paste (w/c = 0.22).

45PC6 and 25PC6 with medium and short length side chains. The least increase in fluidity was recorded for the PCE exhibiting the shortest side chain (7PC6). It is remarkable that the performance of DEG was particularly weak in the presence of PCEs which required relatively high dosages to achieve the initial spread flow value (i.e. 45PC2 and 7PC6). Based on these findings it can be inferred that DEG is a very powerful co-dispersant for PCEs with a low side chain density and long side chains.

3.5. Adsorption measurements

To get more insight into the working mechanism of the non-ionic co-dispersants, adsorption measurements were performed. At first, adsorption isotherms for the individual MPEG-PCEs were developed. This was conducted at a slightly higher w/c ratio of 0.26, because at w/c = 0.22 no sufficient volume of pore solution could be extracted by centrifugation. Fig. 10 displays the *Langmuir*-type adsorption isotherms for all MPEG-PCEs tested. With rising dosages the adsorbed amounts increase up to a plateau value which represents the point of saturated adsorption where the surface sites are completely covered by the polymers.

As expected, the saturated adsorbed amounts increased with higher anionicity (= decreasing side chain density) of the 45PCy polymers (Fig. 10a). This is in agreement with the findings from previous studies [10,11]. For the xPC6 polymers, slightly higher plateau values were found for the PCEs exhibiting shorter side chains (Fig. 10b). Additionally, it was confirmed that diethylene glycol does not show any adsorption when individually admixed to the cement (Fig. 10a). Even negative adsorption values were observed for DEG which originate from the water loss through the cement hydration.

In the following, it was investigated whether DEG exerts any influence on the adsorption of the PCEs. For this purpose, the adsorbed amounts were measured for combinations of different PCEs at increasing dosages of DEG. The adsorption values of the individual PCEs at the dosages for a spread flow of 18 cm were used as reference (i.e. 0. 215 % (45PC2); 0.18 % (45PC6); 0.316 % (7PC6); 0.166 % (114PC6)). As is evident from Fig. 11, DEG did not affect the adsorbed amounts of any PCE, regardless of the DEG dosage applied or the specific molecular structure of the PCE. This clearly suggests that DEG remains freely dissolved in the interstitial pore solution, where it contributes to the dispersion of the particles.

Still, the question remained why certain molecular structures of the PCE benefit more from the addition of DEG. This aspect was investigated by plotting the portion of non-adsorbed PCE as a function of the polymer dosage (see Fig. 12).

It can be seen that a much higher fraction remained non-adsorbed for those PCEs which exhibited a high side chain density (e.g. 74 % (45PC2) vs. 24 % (45PC8) at 0.2 %). This can be attributed to their low anionic character which provokes a low adsorption affinity (e.g. anionic charge amounts 720 µeq/g (45PC2) vs. 2850 µeq/g (45PC8)). Conversely, no big difference was found for the PCEs that were

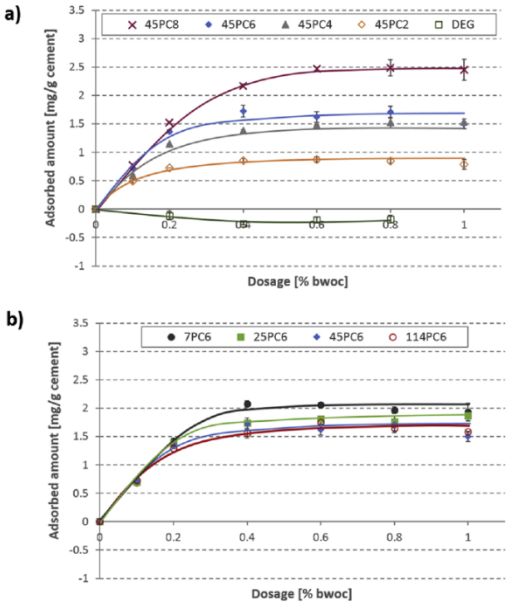

Fig. 10. Adsorption isotherms developed in cement paste at w/c = 0.26 for MPEG-PCEs possessing a) different side chain densities; b) varied side chain lengths.

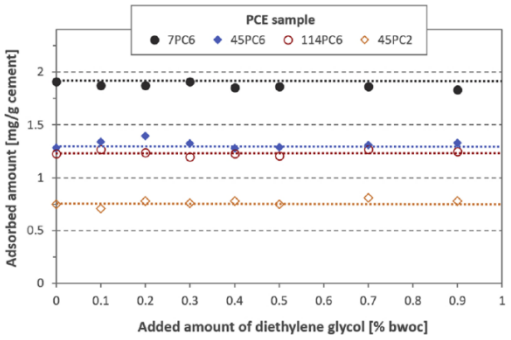

Fig. 11. Effect of different dosages of DEG on the adsorbed amounts of various PCE samples in cement paste (w/c = 0.26).

synthesized at the same molar ratio. Interconnecting these findings with the results from the spread flow tests (Figs. 8 and 9) it can be concluded that DEG especially enhances the fluidity of those PCEs which adsorb almost quantitatively and where only a small portion remains in the pore solution. In contrast, the effect of DEG is rather limited on PCEs which only adsorb in low amounts and thus entail a high residual concentration of non-adsorbed polymer. However, this is not the case for PCEs with varied side chain lengths (xPC6 series). All these PCEs show similar portions of non-adsorbed polymer. This suggests that DEG performs differently with PCEs exhibiting a different side chain length, with longer side chains providing a stronger effect than short ones.

3.6. Co-dispersing performance of structurally different non-ionic co-dispersants

In the next section, several glycol (DEGMME, DEGDME) and diol (HD, NPG, MPD) derivates were tested as non-ionic co-dispersants (see Fig. 2) to probe whether the chemical composition also influences the effectiveness of such auxiliary dispersants. Here, 45PC6 was utilized as

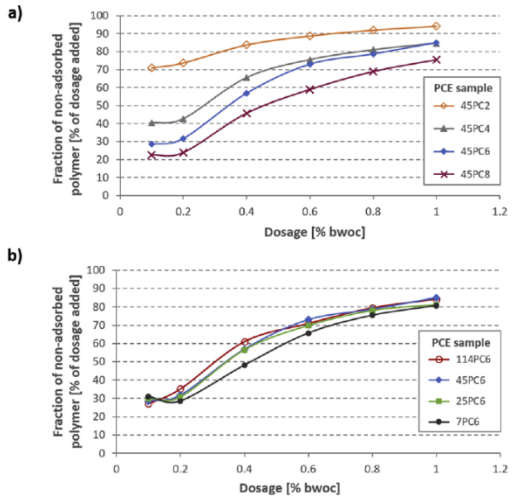

Fig. 12. Fraction of non-adsorbed PCE polymer as a function of the dosage for PCEs exhibiting a) different side chain densities or b) varied side chain lengths; results from cement paste (w/c = 0.26).

superplasticizer and combined with the non-adsorbing molecules at w/c = 0.22.

As evident from Fig. 13, different spread flow values were obtained, depending on the chemical structure of the small molecules. For instance, at a dosage of 0.1 %, MPD increased the spread flow from 18 to 23 cm, while DEGMME only provoked a slight increase to 19 cm. However, all co-dispersants tested produced higher paste fluidities compared to DEG. Most interestingly, the best performance was noticed for the diols MPD, NPG and HD which are commonly applied as shrinkage reducing agents. When taking a closer look at the chemical composition of the co-dispersants, it becomes apparent that especially those compounds with a higher amount of hydrophobic groups were more effective.

3.7. Effect of co-dispersants on surface tension of SCPS

To explain the different performance of the small molecules in the spread flow tests, surface tension measurements were performed using a drop shape analyzer. The aim of these experiments was to study the effect of the co-dispersants on the surface tension of aqueous solutions of superplasticizer 45PC6 in SCPS. Here again, the water loss through the initial cement hydration was taken into account.

At first, the surface tension of the pure SCPS was measured. A value of 71.1 mN/m was recorded which corresponds to the data in the literature [42]. Additionally, the surface tension of SPCS holding 0.208 % of 45PC6 was captured. The PCE decreased the surface tension from 71.1 to 52.4 mN/m. This can be attributed to the surfactancy of the PCE which comprises hydrophilic (e.g. carboxylates, PEG side chains) as well as hydrophobic groups (e.g. methylene bridge, methyl groups). Thereafter, the surface tension was determined for combinations of 45PC6 at different additions of the non-ionic co-dispersants.

From Fig. 14 it can be seen that DEG only caused a minor reduction of the surface tension. However, small molecules with more hydrophobic groups (e.g. methyl, alkyl substituents) than DEG induced a much higher decrease of the surface tension. For example, DEGDME which incorporates two additional methyl groups reduced the surface tension from 52.4 mN/m to 48.8 mN/m at 0.5 %, whereas for HD which possesses a hexyl chain even a lower value (46.3 mN/m) was ascertained. For MPD which represents the most effective co-dispersant, the strongest decline in the surface tension to 41.1 mN/m was observed.

Based on these results it can be concluded that less polar molecules with a higher proportion of hydrophobic groups reduce the surface tension of the pore solution more than molecules which mainly comprise hydrophilic moieties (e.g. hydroxyl, ether, oxyethylene groups). It is known from literature that by lowering the surface tension, the accessibility of water to the cement surface is enhanced which results in a higher fluidity [43–45]. This is in agreement with the observations from the spread flow tests where it was noticed that in systems which contained a less polar co-dispersant the cement paste became much faster fluid during the mixing. Due to the decreased surface tension of the pore solution, the solid-liquid interface energy is reduced which consequently improves the wetting behavior of the particles. It might be argued that the higher spread flow values may possibly originate from air bubbles which are introduced into the cement paste, as it is well known from surfactants that air bubbles induce a ball-bearing effect and hence improve the fluidity [46]. However, when mixing the cement paste no air-entrainment was observed at the dosages tested. Additionally, the same paste fluidities were obtained when a non-ionic, polyether siloxane based defoamer was applied to the cement paste. This suggests that the higher fluidity for the less polar co-dispersants mainly originates from an improved wettability.

3.8. Mechanistic model

Based on the findings achieved so far, a mechanistic model was developed to explain the underlying working mechanism of the co-dispersants (see Fig. 15).

Adsorption measurements have shown that the non-ionic additives do not adsorb on cement nor modify the adsorbed amounts of the PCEs. This indicates that they remain in the interstitial pore solution, where they can implement a spacer effect between the cement particles.

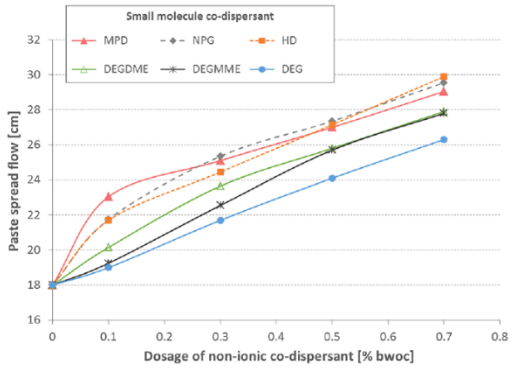

Fig. 13. Spread flow for structurally different co-dispersants, combined with PCE 45PC6; results from cement paste (w/c = 0.22).

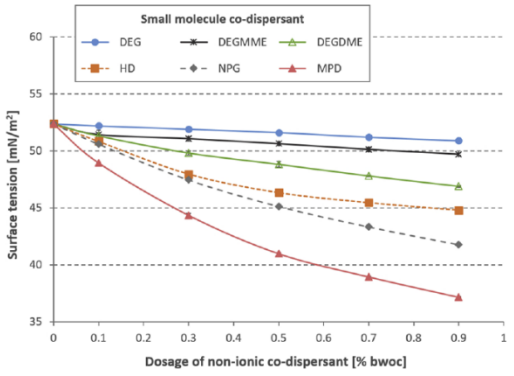

Fig. 14. Surface tension of solutions holding 0.208 % of PCE 45PC6 and different dosages of non-ionic co-dispersants, measured in SCPS.

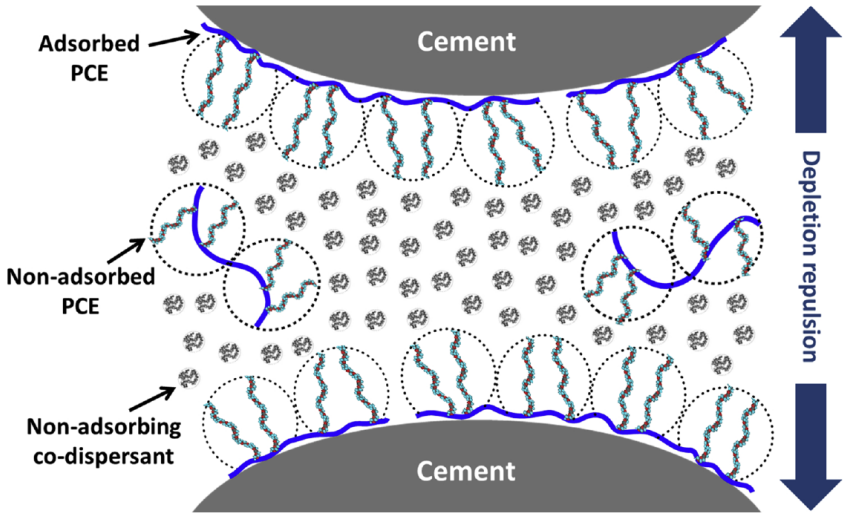

Fig. 15. Conceptual sketch illustrating the working mechanism of the non-adsorbing co-dispersants in cement at low w/c ratios.

According to the model on the solution conformation of comb copolymers from *Gay* and *Raphaël*, it is established that the side chains of PCEs align in form of blobs along the main polymer chain [34,47]. Therefore, we suppose that the co-dispersants exist between those blobs and hinder in this way the cement particles from approaching too close, as otherwise a local depletion of the small molecules would occur. Such condition is entropically unfavorable and therefore avoided through the formation of repulsive depletion forces [48–51]. These repulsive interactions contribute – in addition to the electrosteric stabilization provided by the adsorbed PCEs – also to cement dispersion and thus improve fluidity. However, this is only the case at low w/c ratios, where the cement particles are densely packed and the pore space becomes quite narrow. It was reported in previous studies that depletion repulsion is especially favored at high concentrations of the non-adsorbing polymers [27,52,53]. When we calculate the concentrations of the small molecules in the pore solution considering the water loss through the initial cement hydration at w/c = 0.22, we obtain concentrations in the range of 15–136 g/L for dosages from 0.1 – 0.9 %. This clearly demonstrates that the pore solution is very crowded at such low w/c values with the co-dispersants. Owed to those high concentrations, the small molecules cannot be pushed out very easily from the gap between approaching cement particles, thus creating depletion stabilization.

However, at high w/c ratios the spacer molecules are less or not at all effective due to the larger distance between the particles. Moreover, the spacer effect is less pronounced for PCEs which adsorb less and leave a significant residual concentration non-adsorbed in the pore solution. This implies that repulsive depletion forces also can be induced by non-adsorbed PCEs and explains why polymers that adsorb almost quantitatively benefit more from the addition of the co-dispersants. Furthermore, the depletion effect is particularly strong for PCEs with long side chains signifying that the range and magnitude of the repulsive depletion forces depend on the fraction of non-adsorbed PCE as well as on the specific molecular architecture of the polymer.

4. Conclusion

In this study it was demonstrated that non-ionic additives can be used to augment the dispersing performance of MPEG-PCEs at low w/c ratios. Glycol and diol derivates with a molecular weight ≤ 300 g/mol were found to provide a superior effect over non-adsorbing polymers which were investigated in previous works. Moreover, spread flow tests showed that small molecules exhibiting a higher portion of hydrophobic groups increased paste fluidity more effectively. These small molecules reduce the surface tension of the pore solution and thus improve the water wettability of cement.

Mechanistic investigations revealed that the non-ionic co-dispersants do not alter the adsorbed amounts of the PCEs, but remain dissolved in the pore solution. There, they provide a spacer effect whose range and magnitude depends on the molecular structure of the PCE and the concentration of the non-adsorbed constituents.

Our findings signify that at low w/c ratios other dispersing mechanisms come into play. Here, especially the portion of non-adsorbed compounds becomes crucial for the stabilization of the particles.

Most remarkably, it was observed that the non-ionic small molecules not only increased the spread flow, but also reduced the “sticky” behavior of the cement paste which typically occurs at low w/c values. This specific effect of the co-dispersants on the rheological parameters of cement-based materials will be discussed in another paper.

Author contribution statement

M. Ilg carried out the experiments and wrote the manuscript with support from J. Plank who supervised the project.

Declaration of Competing Interest

The authors declare that they have no known competing financial interests or personal relationships that could have appeared to influence the work reported in this paper.

Acknowledgments

The authors greatly acknowledge the financial support of the German Research Foundation (DFG) (project number: 387082770) within the frame of the SPP 2005 “Opus Fluidum Futurum – Rheology of reactive, multiscale, multiphase construction materials”. Moreover, Clariant and BASF are thanked for providing the non-ionic additives and HeidelbergCement for the supply of the cement.

References

[1] N. Spiratos, M. Page, N.P. Mailvaganam, V.M. Malhotra, C. Jolicoeur, Superplasticizers for Concrete: Fundamentals, Technology, and Practice, Supplementary Cementing Materials for Sustainable Development, Ottawa, 2003.

[2] J. Plank, E. Sakai, C.W. Miao, C. Yu, J.X. Hong, Chemical admixtures – chemistry, applications and their impact on concrete microstructure and durability, Cem. Concr. Res. 78 (2015) 81–99.
[3] J. Liu, C. Yu, X. Shu, Q. Ran, Y. Yang, Recent advance of chemical admixtures in concrete, Cem. Concr. Res. 124 (2019) 105834.
[4] C. Jolicoeur, M.-A. Simard, Chemical admixture-cement interactions: phenomenology and physico-chemical concepts, Cem. Concr. Compos. 20 (1998) 87–101.
[5] F. Dalas, A. Nonat, S. Pourchet, M. Mosquet, D. Rinaldi, S. Sabio, Tailoring the anionic function and the side chains of comb-like superplasticizers to improve their adsorption, Cem. Concr. Res. 67 (2015) 21–30.
[6] L. Coppola, S. Lorenzi, P. Kara, S. Garlati, Performance and compatibility of phosphonate-based superplasticizers for concrete, Buildings 7 (3) (2017) 62.
[7] Y. He, X. Shu, X. Wang, Y. Yang, J. Liu, Q. Ran, Effects of polycarboxylates with different adsorption groups on the rheological properties of cement pastes, J. Disper. Sci. Technol. (2019), https://doi.org/10.1080/01932691.2019.1614029.
[8] T. Nylander, Y. Samoshina, B. Lindman, Formation of polyelectrolyte-surfactant complexes on surfaces, Adv. Colloid Interface Sci. 123-126 (2006) 105–123.
[9] J.A. Lewis, H. Matsuyama, G. Kirby, S. Morissette, J.F. Young, Polyelectrolyte effects on the rheological properties of concentrated cement suspensions, J. Am. Ceram. Soc. 83 (3) (2000) 1905–1913.
[10] F. Winnefeld, S. Becker, J. Pakusch, T. Götz, Effects of the molecular architecture of comb-shaped superplasticizers on their performance in cementitious systems, Cem. Concr. Compos. 29 (2007) 251–262.
[11] A. Zingg, F. Winnefeld, L. Holzer, J. Pakusch, S. Becker, L. Gauckler, Adsorption of polyelectrolytes and its influence on the rheology, zeta potential, and microstructure of various cement and hydrate phases, J. Colloid Interface Sci. 323 (2008) 301–312.
[12] K. Yamada, S. Hanehara, Interaction mechanism of cement and superplasticizers – the roles of polymer adsorption and conditions of aqueous phase, Concrete Sci. Eng. 3 (2001) 135–145.
[13] R.J. Flatt, Dispersion forces in cement suspensions, Cem. Concr. Res. 34 (2004) 399–408.
[14] N. Roussel, A. Lemaitre, R.J. Flatt, P. Coussot, Steady state flow of cement suspensions: a micromechanical state of the art, Cem. Concr. Res. 40 (2010) 77–84.
[15] J. Hot, H. Bessaies-Bey, C. Brumaud, M. Duc, C. Castella, N. Roussel, Adsorbing polymers and viscosity of cement pastes, Cem. Concr. Res. 63 (2014) 12–19.
[16] J. Plank, K. Pöllmann, N. Zouaoui, P.R. Andres, C. Schäfer, Synthesis and performance of methacrylic ester based polycarboxylate superplasticizers possessing hydroxy terminated poly(ethylene glycol) side chains, Cem. Concr. Res. 38 (2008) 1210–1216.
[17] S. Fan, T. Wang, S. Qi, J. Ma, Z. Huang, J. Chen, Q. Ran, Synthesis and performance of polycarboxylate superplasticizers with different propylene oxide contents, Adv. Cem. Res. 31 (5) (2019) 205–213.
[18] H. Uchikawa, S. Hanehara, D. Sawaki, The role of steric repulsive force in the dispersion of cement particles in fresh paste prepared with organic admixture, Cem. Concr. Res. 27 (1997) 37–50.
[19] K. Yoshioka, E. Sakai, M. Daimon, A. Kitahar, Role of steric hindrance in the performance of superplasticizers for concrete, J. Am. Ceram. Soc. 80 (1997) 2667–2671.
[20] Y. Zhang, X. Kong, Correlations of the dispersing capability of NSF and PCE types of superplasticizer and their impacts on cement hydration with the adsorption in fresh cement pastes, Cem. Concr. Res. 69 (2015) 1–9.
[21] C.-Z. Li, N.-Q. Feng, Y.-D. Li, R.-J. Chen, Effects of polyethylene oxide chains on the performance of polycarboxylate-type water-reducers, Cem. Concr. Res. 35 (2005) 867–873.
[22] J.Y. Yoon, J.H. Kim, Evaluation on the consumption and performance of polycarboxylates in cement-based materials, Constr. Build. Mater. 158 (2018) 423–431.
[23] M. Ushiro, D. Atarashi, H. Kawakami, E. Sakai, The effect of superplasticizer present in pore solution on flowability of low water-to-powder cement paste, Cem. Sci. Concr. Technol. 67 (2013) 102–107.
[24] K. Matsuzawa, D. Shimazaki, H. Kawakami, E. Sakai, Effect of non-adsorbed superplasticizer molecules on fluidity of cement paste at low water-powder ratio, Cem. Concr. Compos. 97 (2019) 218–225.
[25] L. Shui, Z. Sun, H. Yang, X. Yang, Y. Ji, Q. Luo, Experimental evidence for a possible dispersion mechanism of polycarboxylate-type superplasticizers, Adv. Cem. Res. 28 (5) (2016) 287–297.
[26] A. Lange, J. Plank, Contribution of non-adsorbing polymers to cement dispersion, Cem. Concr. Res. 79 (2016) 131–136.
[27] L.R. Murray, J.E. Bice, E.G. Soltys, C. Perge, S. Manneville, K.A. Erk, Influence of adsorbed and nonadsorbed polymer additives on the viscosity of magnesium oxide suspensions, J. Appl. Polym. Sci. 153 (3) (2018) 45696.
[28] H.J. Kong, S.G. Bike, V.C. Li, Electrosteric stabilization of concentrated suspensions imparted by a strong anionic polyelectrolyte and a non-ionic polymer, Cem. Concr. Res. 36 (2006) 842–850.
[29] H. Bessaies-Bey, M. Palacios, E. Pustovgar, M. Hanafi, R. Baumann, R.J. Flatt, N. Roussel, Non-adsorbing polymers and yield stress of cement paste: effect of depletion forces, Cem. Concr. Res. 111 (2018) 209–217.
[30] A. Lange, J. Plank, Optimization of comb-shaped polycarboxylate cement dispersants to achieve fast-flowing mortar and concrete, J. Appl. Polym. Sci. 132 (37) (2015) 42529.
[31] S. Kawaguchi, K. Akaike, Z.-M. Zhang, H. Matsumoto, K. Ito, Watersoluble bottlebrushes, Polym. J. 30 (1998) 1004–1007.
[32] J. Plank, B. Sachsenhauser, Experimental determination of the effective anionic charge density of polycarboxylate superplasticizers in cement pore solution, Cem. Concr. Res. 39 (2009) 1–5.
[33] E. Sakai, K. Yamada, A. Ohta, Molecular structure and dispersion-adsorption mechanisms of comb-type superplasticizers used in Japan, J. Adv. Concr. Technol. 1 (2003) 16–25.
[34] C. Gay, E. Raphaël, Comb-like polymers inside nanoscale pores, Adv. Colloid. Interfac. Sci. 94 (1-3) (2001) 229–236.
[35] Ch. Schröfl, M. Gruber, J. Plank, Preferential adsorption of polycarboxylate superplasticizers on cement and silica fume in ultra-high performance concrete (UHPC), Cem. Concr. Res. 42 (2012) 1401–1408.
[36] B. Song, J. Springer, Determination of interfacial tension from the profile of a pendant drop using computer-aided image processing: 1. Theoretical, J. Colloid. Interface Sci. 184 (1996) 64–76.
[37] J.D. Berry, M.J. Neeson, R.R. Dagastine, D.Y.C. Chan, R.F. Tabor, Measurement of surface and interfacial tension using pendant drop tensiometry, J. Colloid Interface Sci. 454 (2015) 226–237.
[38] M. Ilg, J. Plank, Novel admixtures to reduce the stickiness of low w/c concretes, in: J. Liu, Z. Holland, J. Wang, J. Huang, J. Plank (Eds.), Superplasticizers and Other Chemical Admixtures in Concrete, Proceedings Twelfth International Conference, Beijing (China), October 28 – 31, 2018, pp. 77–88 SP-329-07.
[39] P.F.G. Banfill, Additivity effects in the rheology of fresh concrete containing water-reducing admixtures, Constr. Build. Mater. 25 (2011) 2955–2960.
[40] J. Liu, K. Wang, Q. Zhang, F. Han, J. Sha, J. Liu, Influence of superplasticizer dosage on the viscosity of cement paste with low water-binder ratio, Constr. Build. Mater. 149 (2017) 359–366.
[41] R. Abile, A. Russo, C. Limone, F. Montagnaro, Impact of the charge density on the behavior of polycarboxylate ethers as cement dispersants, Constr. Build. Mater. 180 (2018) 477–490.
[42] J. de Reese, P. Lenz, K. Zilch, J. Plank, Influence of type of superplasticizer and cement composition on the adhesive bonding between aged and fresh concrete, Constr. Build. Mater. 48 (2013) 717–724.
[43] M. Li, Y. Wang, H. Jiang, C. Zheng, Z. Guo, Synthesis, characterization and mechanism of polycarboxylate superplasticizer with slump retention capability, IOP Conf. Series: Mater. Sci. Eng. 182 (2017) 012036.
[44] X. Liu, Z. Wang, J. Zhu, Y. Zheng, S. Cui, M. Lan, H. Li, Synthesis, characterization and performance of a polycarboxylate superplasticizer with amide structure, Colloids Surf. A Physicochem. Eng. Asp. 448 (2014) 119–129.
[45] S. Qian, Y. Yao, Z. Wang, S. Cui, X. Liu, H. Jiang, Z. Guo, G. Lai, Q. Xu, J. Guan, Synthesis, characterization and working mechanism of a novel polycarboxylate superplasticizer for concrete possessing reduced viscosity, Constr. Build. Mater. 169 (2018) 452–461.
[46] B. Feneuil, O. Pitois, N. Roussel, Effect of surfactants on the yield stress of cement paste, Cem. Concr. Res. 100 (2017) 32–39.
[47] R.J. Flatt, I. Schober, E. Raphael, C. Plassard, E. Lesniewska, Conformation of adsorbed comb copolymer dispersants, Langmuir 25 (2009) 845–855.
[48] R.I. Feigin, D.H. Napper, Stabilization of colloids by free polymer, J. Colloid Interface Sci. 74 (1980) 567–571.
[49] R.I. Feigin, D.H. Napper, Depletion stabilization and depletion flocculation, J. Colloid Interface Sci. 75 (1980) 525–541.
[50] A.P. Gast, L. Leibler, Interactions of sterically stabilized particles suspended in a polymer solution, Macromolecules 19 (1986) 686–691.
[51] A.L. Ogden, J.A. Lewis, Effect of nonadsorbed polymer on the stability of weakly flocculated suspensions, Langmuir 12 (1996) 3413–3424.
[52] J. Shin, X. Zhang, J. Liu, DNA-functionalized gold nanoparticles in macromolecularly crowded polymer solutions, J. Phys. Chem. B 116 (2012) 13396–13402.
[53] D. Heath, T.F. Tadros, Rheological investigations of the effect of addition of free polymer to concentrated sterically stabilised polystyrene latex dispersions, Faraday Discuss. Chem. Soc. 76 (1983) 203–218.

5.1.4. Publikation #4: Effect of non-ionic auxiliary dispersants on the rheological properties of mortars and concretes of low water-to-cement ratio

In den vorherigen Arbeiten wurde beobachtet, dass die Co-Dispergiermittel nicht nur das Fließmaß von Zementleimen erhöhen, sondern auch die zähe, klebrige Konsistenz reduzieren, die vor allem bei niedrigen w/z-Werten in Erscheinung tritt. Ungeklärt war noch die Frage, welchen Einfluss die nicht-ionischen Moleküle auf die Fließeigenschaften eines Mörtels bzw. Betons haben und wie sie sich konkret auf die rheologischen Paramater – Fließgrenze und plastische Viskosität – auswirken. Dies wurde in **Publikation #4** untersucht. Verschiedene niedermolekulare Verbindungen, wie Diethylenglykol oder 2-Methyl-2,4-pentandiol kamen zum Einsatz und wurden in Gegenwart von 45MPEG4.5 sowie 50IPEG4.5 getestet.

Die Mörtel- und Betonmischungen, die nur mit dem MPEG-PCE verflüssigt wurden, zeigten eine höhere Klebrigkeit und ein stärker kohäsives Verhalten als mit dem IPEG-PCE. In der Literatur wird als Erklärung für dieses Verhalten der unterschiedliche HLB-Wert der Polymere genannt, der das Verhältnis von hydrophilen und hydrophoben Gruppen innerhalb des Polymers wiedergibt. Je niedriger der HLB-Wert, umso viskoser ist der Mörtel bzw. Beton [53]. Bei den Mörtelversuchen wurde zudem festgestellt, dass die nicht-ionischen Additive das Ausbreitmaß vergrößern und die Fließgrenze über den in **Publikation #3** aufgeklärten Mechanismus reduzieren. Ebenfalls wurden die Fließgeschwindigkeiten der Mörtel in einer Fließrinne und die Auslaufzeiten aus einem V-Trichter bestimmt. Hierbei wurden Mörtel verwendet, die auf das gleiche Ausbreitmaß eingestellt waren, sodass die Fließgrenze jeweils vergleichbar war. Als Referenz diente ein Mörtel, der nur mit dem PCE verflüssigt wurde, während die anderen getesteten Systeme stets eine Kombination aus PCE und Co-Dispergiermittel enthielten. Die nicht-ionischen Additive erhöhten die Fließgeschwindigkeit des Mörtels, sodass beispielsweise die Trichterauslaufzeiten um 30 – 40 % reduziert wurden und der Mörtel eine um 10 – 25 % weitere Distanz in der Fließrinne innerhalb von 30 Sekunden zurücklegte. Daraus wurde gefolgert, dass die Co-Dispergiermittel sowohl die Fließgrenze als auch die plastische Viskosität von Mörteln reduzieren.

Ein anderes Bild ergab sich allerdings im Beton. Dort konnten die nicht-ionischen Additive nur die plastische Viskosität senken, sie hatten jedoch keinen Einfluss auf das

Ausbreitmaß bzw. die Fließgrenze. So wurden die Auslaufzeiten bei Kombination der Co-Dispergiermittel mit dem MPEG-PCE um 26 % und im Fall des IPEG-PCEs um 38 % herabgesetzt. Grundsätzlich wiesen alle Betone nach dem Zusatz der Glykol-verbindungen bzw. Diole eine geringere Klebrigkeit auf, wodurch die Handhabung wesentlich erleichtert wurde. Durch ein Kontrollexperiment, bei dem anstelle eines Co-Dispergiermittels Wasser eingesetzt wurde, konnte gezeigt werden, dass die Reduzierung der plastischen Viskosität auf die nicht-ionischen Additive zurückzuführen ist und nicht auf einen Verdünnungseffekt durch eine Verringerung des Feststoffanteils.

Um final aufzuklären, wie die nicht-ionischen Verbindungen die plastische Viskosität reduzieren, wurden weitere Untersuchungen durchgeführt. Da alle getesteten Systeme auf dieselbe Fließgrenze eingestellt waren, konnte zunächst ausgeschlossen werden, dass die Erniedrigung der plastischen Viskosität von einem Abstandseffekt bzw. der Verarmungsstabilisierung herrührt. Wie zuvor beschrieben, halten sich die Co-Dispergiermittel in der Porenlösung auf, weshalb der Fokus auf das frei verfügbare Porenvolumen der Zementleimphase gelegt wurde. Dies ist der Anteil der Porenlösung, der nicht durch die Zementhydratation aufgebraucht wird oder durch physikalische Wechselwirkungen an der Oberfläche gebunden ist, sondern frei zwischen den Zementpartikeln vorliegt. Es wurde gefunden, dass für die Systeme mit den nicht-ionischen Additiven mehr Porenvolumen extrahiert werden konnte als für das Referenzsystem, welches nur mit dem PCE dispergiert wurde. Dies bedeutet, dass im Fall der Co-Dispergiermittel durch Desagglomeration mehr Porenlösung zur Verfügung steht, wodurch der flüssige Film um die Zementpartikel und Gesteinskörnungen stärker ausgeprägt ist (sh. **Abbildung 41**).

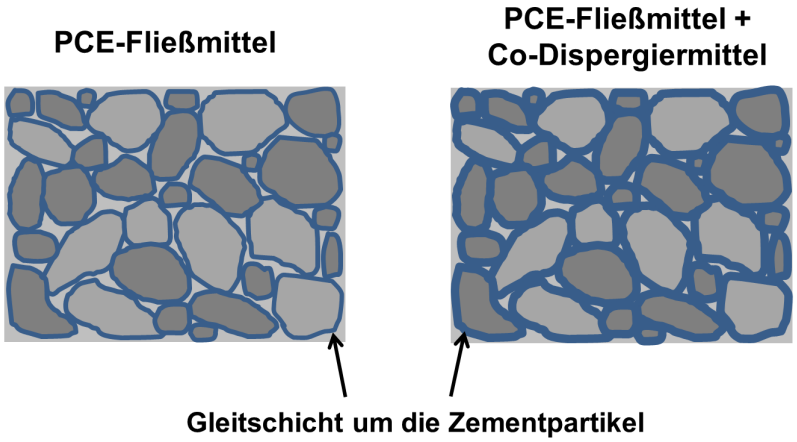

Abbildung 41: Erweitertes mechanistisches Modell zur Funktionsweise der nicht-ionischen Co-Dispergiermittel in Mörtel und Betonen.

Dieser Film besitzt bessere Gleiteigenschaften und kann die Reibung zwischen den Feststoffpartikeln während des Fließens stärker reduzieren und so die Viskosität senken. Wasser besitzt hingegen nicht so gute Gleiteigenschaften wie die nicht-ionischen Additive und kann diesen Effekt im getesteten Dosierbereich nicht erzielen.

Publikation #4

Effect of non-ionic auxiliary dispersants on the rheological properties of mortars and concretes of low water-to-cement ratio

Manuel Ilg, Johann Plank

Construction and Building Materials

259 (2020) 119780

Doi: 10.1016/j.conbuildmat.2020.1197800950

Construction and Building Materials 259 (2020) 119780

Contents lists available at ScienceDirect

Construction and Building Materials

journal homepage: www.elsevier.com/locate/conbuildmat

Effect of non-ionic auxiliary dispersants on the rheological properties of mortars and concretes of low water-to-cement ratio

Manuel Ilg, Johann Plank *

Chair for Construction Chemistry, Technische Universität München, Lichtenbergstraße 4, 85748 Garching, Germany

HIGHLIGHTS

- Sticky behavior of mortar & concrete produced at low w/c ratios is a serious issue.
- Non-ionic co-dispersants are an option to mitigate this problem.
- Such co-dispersants reduce the plastic viscosity when combined with PCEs.
- Reduced stickiness and faster flow can be achieved.
- Thickness of the lubricating layer around the particles is increased.

GRAPHICAL ABSTRACT

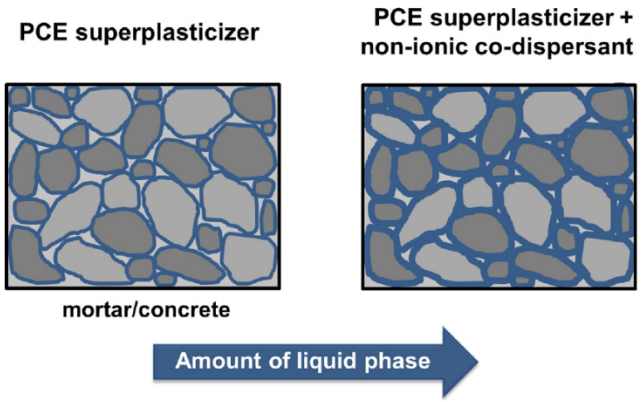

ARTICLE INFO

Article history:
Received 24 February 2020
Received in revised form 11 May 2020
Accepted 30 May 2020

Keywords:
Sticky concrete
Polycarboxylate
Flow speed
Rheology
V-funnel
Superplasticizer
Mortar
Viscosity
Admixture
Self-compacting concrete

ABSTRACT

A high plastic viscosity can be very disadvantageous for the processing of concrete as it often entails a sticky and honey-like consistency. This is especially the case for concretes prepared at low water content and a large amount of fine supplementary cementitious materials (e.g. silica fume). Unfortunately, most of the common polycarboxylate (PCE) superplasticizers cannot effectively reduce the plastic viscosity of such highly particle loaded systems, even though they exhibit strong dispersing capability and can produce high spread flow or slump. In this study, it is demonstrated that non-ionic molecules like diethylene glycol or 2-methyl-2,4-pentane diol can reduce the plastic viscosity when admixed with a PCE superplasticizer. The effect of those auxiliary dispersants on the rheological parameters was investigated by spread flow, flow line and V-funnel tests using mortar and concrete prepared from Portland-limestone cements exhibiting low w/c ratios (0.26 and 0.35, respectively). Moreover, the impact of such non-ionic molecules on the strength development of mortar specimens was tested. Mechanistic investigations revealed that the co-dispersants increase the amount of the liquid phase and hence the thickness of the lubricating layer around the particles. As a result, interparticle friction is reduced and a less sticky material with a higher speed of flow is obtained.

* Corresponding author.
E-mail address: sekretariat@bauchemie.ch.tum.de (J. Plank).

https://doi.org/10.1016/j.conbuildmat.2020.119780
0950-0618/

1. Introduction

Rheology is an important parameter to assess the quality and workability of fresh concrete and mortar. Processing techniques like pumping, pouring, spreading or spraying and properties such as self-leveling, molding or self-compacting are closely linked to rheology [1,2]. The rheological behavior is influenced by many factors like the chemical composition [3,4] and physical properties (e.g. fineness, particle size distribution) [5,6] of the binder, the shape, size and volume fraction of the solid particles [7–11], the volume of water in the mix design [3,12], the temperature [13] and shearing intensity [14]. Besides, rheology can be modified by chemical admixtures to adjust the respective processing conditions. For instance, polycarboxylate superplasticizers (PCEs) are commonly applied to improve the fluidity [15]. It is well known that PCEs work via reduction of the yield stress representing the threshold above which the material starts to flow under gravity [12]. This is achieved by adsorption of the PCEs which lower the attractive interparticle forces through implementation of an electrosteric effect [16–18]. Thus, the agglomerated particles are dispersed and water that was initially entrapped in the flocculated structure is released [19]. The liberated water becomes available for liquefaction and contributes to the flowability of the system.

By using PCEs, even at low w/c ratios high fluidity can be attained, thus enabling to produce concretes with remarkable properties (e.g. high strength, low porosity, long durability etc.) [20,21]. However, at decreasing w/c concretes become increasingly sticky and cohesive. Additionally, some of the concretes exhibit a rather creeping, honey-like flow behavior and require a long period of time to the reach the final spread flow. Such rheology is very undesirable for the placement and can result in insufficient filling of the formwork. For this reason, several studies recently addressed potential solutions to diminish the sticky flow behavior [22–24]. It was found that a high plastic viscosity is the main reason for the stickiness which originates from the high solids content of these concretes at low w/c ratios [12]. Thus, the plastic viscosity has to be reduced in order to obtain a material with lower viscosity and faster flow.

The hydrophilic lipophilic balance (HLB) of a PCE can give a first hint whether the polymer tends to cause a sticky consistency. Accordingly, PCEs which exhibit a high proportion of hydrophobic groups and a low HLB value (~16 – 18) entail a higher plastic viscosity compared to polymers with mainly hydrophilic elements and high HLB value (~18 – 19.5) [23]. To be more specific, it was ascertained that MPEG PCEs provoked a creeping flow behavior, followed by HPEG and IPEG PCEs with a medium speed of flow, while the fastest flow was observed for APEG PCEs [23,25]. These findings imply that a high hydrophilic character of the PCE is necessary to ensure good flow properties. This is further supported by patents describing that a very fast flow behavior can be facilitated by substitution of the polyethylene glycol side chains of the PCEs through more hydrophilic pendant groups like polyvinyl pyrrolidone, polyethylene imine or adducts of ethylene oxide with polyhydric alcohols [26,27]. Additionally, it was reported that also zwitterionic PCEs with cationic lateral chains are quite helpful in reducing the stickiness [28].

An alternative strategy to lower the plastic viscosity is to introduce highly negative phosphate groups into the polymer. Referring to that, polyarylethers were presented some years ago as a new kind of superplasticizer which significantly decreases the sticky behavior at low w/c ratios [24,29]. These polymers comprise an aromatic backbone holding polyethylene glycol side chains as well as phosphate ester groups and are synthesized via polycondensation using formaldehyde. Promising results were also obtained for PCEs modified with hydroxyethylmethacrylate phosphate esters [30,31]. The special property of the phosphate groups to enhance the flow speed is explained by the high hydrophilicity of the phosphated trunk chains which engender a low plastic viscosity. However, since phosphate bearing monomers are expensive and not readily available around the world, alternative concepts need to be identified.

Recently, we reported that non-ionic glycol derivates of low molecular weight can enhance the spread flow of cement pastes when utilized at w/c <0.30 in combination with conventional PCEs [32]. According to our findings, the non-adsorbing molecules remain in the interstitial pore solution and impart a spacer effect which keeps the cement particles separated. Most interestingly, it was noticed that the tested molecules not only improved the spread flow but also produced a less viscous cement paste. Based on those observations, the aim of the present study now was to probe the effect of such auxiliary dispersants on the rheological properties and the flow behavior of mortar and concrete under application conditions. MPEG and IPEG-type PCEs with similar anionicity were chosen as superplasticizers and tested along with different non-ionic glycol and diol derivates. The impact of the small molecules on the yield stress and plastic viscosity was evaluated by spread flow, flow line and V-funnel tests. To get more insights into their mode of action, additionally the amount of pore solution was determined for cement pastes fluidized with the PCEs and co-dispersants. The overall goal of this study was to evaluate whether the flow properties of mortar and concrete can be improved by the addition of such non-ionic auxiliary dispersants.

2. Materials and methods

2.1. Cement

A Portland-limestone blended cement CEM II/A-LL 42.5 N from HeidelbergCement (Ennigerloh plant, Germany) was used for the mortar experiments. This cement was one of the reference materials provided by the central project of the DFG priority program SPP 2005. The mineralogical composition as determined by quantitative X-ray diffraction (Bruker AXS D8 Advance, Karlsruhe, Germany) and *Rietveld* analysis is presented in Table 1. Thermogravimetry (Netzsch STA 409 TG-MS, Selb, Germany) was conducted to ascertain the amounts of the sulfate carriers hemihydrate ($CaSO_4 \cdot ½\ H_2O$) and gypsum ($CaSO_4 \cdot 2\ H_2O$), while the free lime (CaO_{free}) was quantified by the *Franke* method. The specific surface area of the cement was 3,855 cm^2/g (*Blaine* value).

The concrete lab tests were performed at a ready-mix concrete plant using a CEM II/A-LL 42.5 R from Schwenk Zement (Allmendingen plant, Germany). Contrary to the mortar experiments,

Table 1
Phase composition of the cement samples.

Phase	CEM II/A-LL 42.5 N(wt.%)	CEM II/A-LL 42.5 R(wt.%)
C_3S	50.4	53.1
C_2S	11.1	17.5
C_3A	9.0	5.2
C_4AF	5.9	8.2
Free lime (*Franke*)	0.4	0.3
Anhydrite	1.0	1.4
Hemihydrate*	3.0	1.1
Dihydrate*	0.1	0.1
Arcanite	–	1.4
Calcite	15.8	8.0
Quartz	1.1	0.2
Dolomite	0.7	2.6
Periclase	0.5	0.9
Portlandite	1.0	–

* determined by thermogravimetry

the concrete tests were conducted with a cement which is commonly used in this concrete plant to verify the general applicability of the concept of the non-ionic auxiliary dispersants. The phase composition of the cement was provided by the manufacturer and is shown in Table 1. The *Blaine* fineness was found to be 4,697 cm^2/g.

2.2. PCE superplasticizers

Two structurally different PCE superplasticizers were selected for the experiments (see Fig. 1). The MPEG PCE was synthesized via aqueous free radical copolymerization of methacrylic acid (>99%; Sigma-Aldrich, Steinheim, Germany) and ω-methoxy polyethylene glycol methacrylate ester (>98%; Clariant, Burgkirchen, Germany) exhibiting a side chain length of 45 ethylene oxide (EO) units. The polymerization was initiated by ammonium persulfate (≥98%; VWR International, Darmstadt, Germany) and 3-mercapto propionic acid (≥99%; Sigma-Aldrich) was applied as chain transfer agent to control the length of the polymer chains. The synthesis was carried out according to a description from a previous work [33]. The IPEG PCE was an industrial product provided by Nippon Shokubai (Osaka, Japan). It presents a copolymer made up from acrylic acid and ω-methoxy polyethylene glycol isoprenol ether with 50 EO units as lateral chain. Both PCEs were synthesized at a molar ratio of 4.5 : 1 and denoted as x(MPEG/IPEG)y, with x being the number of EO in the polyethylene glycol side chain and y being the molar ratio of the carboxylate bearing monomer and the macromonomer. The PCE samples exhibited a pH of 7 and were used without any further purification.

The molar masses and polydispersity index (PDI) of the polymers as well as the macromonomer conversion were determined by size exclusion chromatography (SEC). Measurements were performed on a Waters Alliance 2695 separation module equipped with a pre-column and three Ultrahydrogel columns (150, 250, 500). Detection was achieved by a refractive index detector (2414 module from Waters, Eschborn, Germany) and a Dawn EOS three angle static light scattering detector (Wyatt Technology, Santa Barbara, CA). A 0.1 M $NaNO_3$ solution (pH = 12; adjusted with sodium hydroxide) was applied as eluent and pumped at a constant flow rate of 1.0 mL/min. The PCE solutions tested exhibited a concentration of 10 g/L and were filtered through a 0.2 μm syringe filter before the measurement. The molar masses M_w and M_n were calculated by means of the *dn/dc* value of polyethylene glycol (0.135 mL/g) [34].

The specific anionic charge amount of the PCEs was assessed via charge titration using a particle charge detector (PCD 03 pH; BTG Instruments, Weßling, Germany). There, a cationic 0.001 M polydiallyl ammonium chloride solution (polyDADMAC) was titrated to 10 mL of a 0.1 g/L PCE solution until the isoelectric point (=0 mV) was reached. To probe the anionicity under different pH values and ion contents, measurements were conducted with solutions of the PCEs in de-ionized (DI) water (pH = 7) and synthetic cement pore solution (SCPS, pH = 12.8). The SCPS was composed of 1.720 g/L $CaSO_4 \cdot 2\,H_2O$, 6.959 g/L Na_2SO_4, 4.757 g/L K_2SO_4 and 7.120 g/L KOH. The anionic charge of the polymers was derived from the consumed volume of polyDADMAC [35]. The molecular properties of the polymers are summarized in Table 2.

It can be seen that both PCEs exhibit a similar anionic charge in both DI water and SCPS. Thus, the polymers are thought to have a comparable adsorption affinity. The lower anionic charge amounts of the PCEs in SCPS originate from the complexation of Ca^{2+} ions by the carboxylate groups.

2.3. Non-ionic auxiliary dispersants

Three different diol derivates and one polyetheramine were tested as auxiliary dispersants (see structures in Fig. 2). Diethylene glycol (DEG; ≥ 99%) and dipropylene glycol dimethylether (DPGDME; ≥ 99%) were provided by Clariant. Jeffamine D-230 (JA; ≥ 99%) was received from Huntsman (Everberg, Belgium) and 2-methyl-2,4-pentanediol (MPD; ≥ 98%) from Alfa Aesar (Karlsruhe, Germany). As evidenced in a previous work, those auxiliary dispersants do not exhibit any charge nor adsorb on cement and therefore remain dissolved in the pore solution [32].

2.4. Mortar tests

2.4.1. Preparation of mortar and spread flow measurements

The mortar used in the study was prepared from 675 g CEM II/A-LL 42.5 N, 1350 g CEN standard sand (cement : sand ratio of 1 : 2) and 175.5 g DI water at a w/c ratio of 0.26. Mixing of the mortar was conducted according to DIN EN 196–1 using an eccentric agitator from Toni Technik (ToniMIX, Baustoffprüfsysteme, Berlin, Germany) [36]. In a typical experiment, the superplasticizer and the non-ionic auxiliary dispersant were added into a stainless steel mixing pot and dissolved in the respective amount of water. Additionally, 0.01 g of a defoamer (Surfynol MD-20, Air Products, the Netherlands) were added to prevent any air introduction by the PCE due to its macro surfactancy. To ensure that all tested mortars exhibited the same w/c ratio, the total amount of mixing water was corrected by the water volume already contained in the aqueous PCE solution. The mortar was prepared as follows: Cement was added into the mixing water and then homogenized for 30 sec at 140 rpm. Subsequently, standard sand was added under continuous stirring over 30 sec and then the mortar was agitated for 30 sec at 285 rpm. After a rest period of 90 sec, mixing was continued

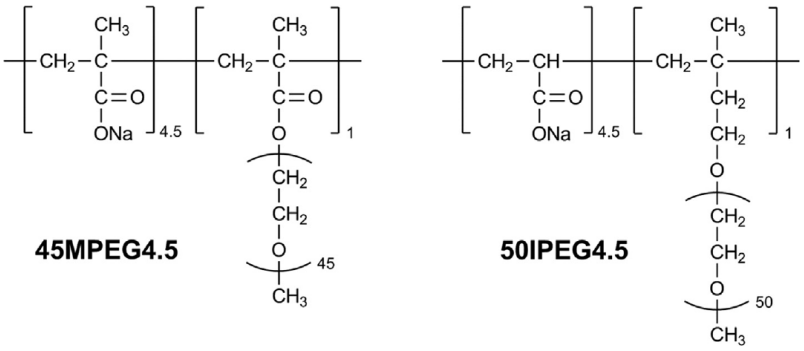

Fig. 1. Chemical structures of the PCE superplasticizers.

Table 2
Molecular properties of the superplasticizer samples.

Polymer	M_w(g/mol)	M_n(g/mol)	PDI(M_w/M_n)	Conversion of macromonomer (%)	Anionic charge amount (μeq/g)	
					SCPS	DI water
45MPEG4.5	18,800	9,100	2.1	94	720	1,780
50IPEG4.5	82,000	36,000	2.3	86	690	1,320

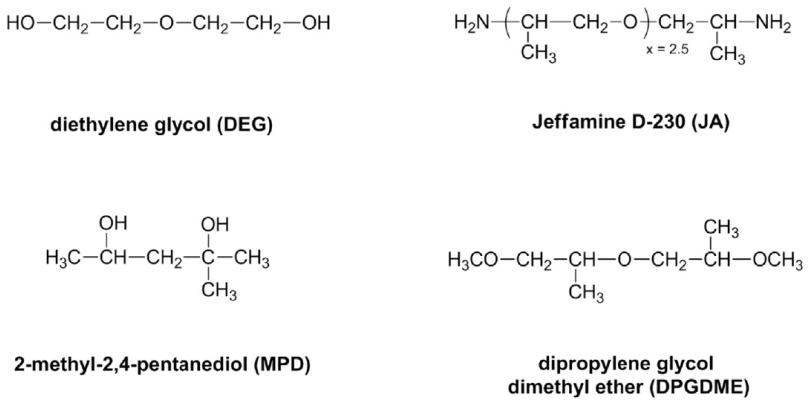

Fig. 2. Chemical structures of the non-ionic co-dispersants.

for additional 60 sec at 285 rpm. The mortar was filled into a *Hägermann* cone (height 60 mm, top diameter 70 mm, bottom diameter 100 mm) positioned on a glass plate. After complete filling, the cone was vertically removed and the diameter of the mortar was measured in two perpendicular directions and averaged. A spread flow of 23 ± 0.5 cm was targeted for the mortars which were applied in the V-funnel and flow line tests. These mortars contained the PCE in a dosage corresponding to a flow diameter of 18 ± 0.5 cm and the non-ionic auxiliary dispersant in such an amount for a final spread flow of 23 ± 0.5 cm. The preparation and testing of the mortar were conducted at a temperature of 20 ± 1 °C and a relative humidity of 40 ± 2%. After measuring the spread flow, the mortar was transferred back into the mixing pot and 5 min after preparation was agitated again for 5 sec at 285 rpm. The flow behavior of the mortar was then investigated in the V-funnel and flow line test, respectively. The chronological sequence of the experiments is illustrated in Fig. 3.

2.4.2. V-funnel Tests

The V-funnel tests were conducted following in principle the specifications of DIN EN 12350–9 [37]. The mortar was filled into a V-shaped funnel (see Fig. 4) whose inside was slightly moistened before. The plug was removed from the bottom outlet and the time which the mortar needed to flow out completely from the funnel was measured.

2.4.3. Flow line tests

The flow line experiments were performed according to DIN EN 13995–2 [38]. The experimental set-up and the dimensions of the flow line are illustrated in Fig. 5. Its design resembles the L-box applied for the testing of self-compacting concrete with the difference that the flow line does not contain any vertical bars as obstacles simulating the reinforcement. For the measurements, a new mortar was prepared and handled in the same way as described in chapter 2.4.1. Five minutes after the preparation, the mortar

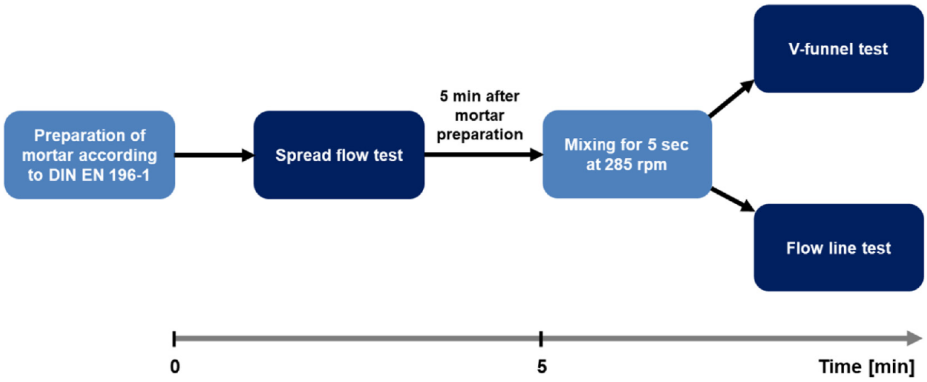

Fig. 3. Chronological order of the test procedure.

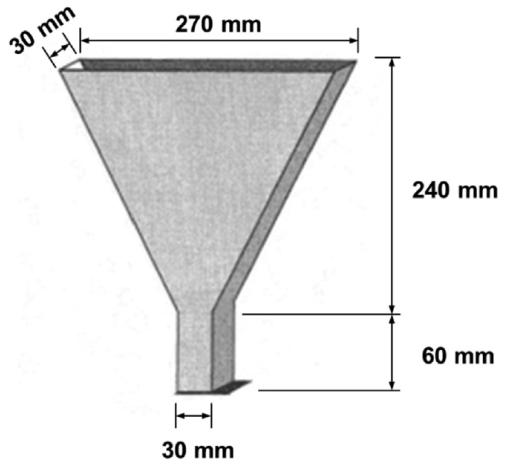

Fig. 4. Geometric dimensions of the V-funnel.

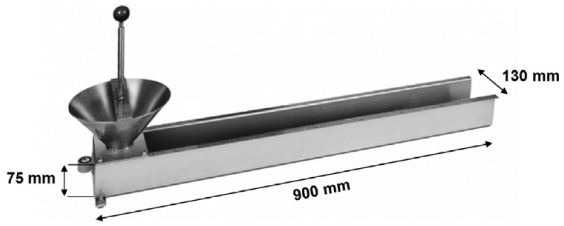

Fig. 5. Experimental set-up of the flow line.

was stirred for 5 sec at 285 rpm and filled into the reservoir of the flow line. The sliding plug was opened and the D30 value which represents the covered distance of the mortar after 30 sec was measured. The final spread flow after stoppage was also noted.

2.4.4. Compressive strength tests

The effect of the non-ionic auxiliary dispersants on the compressive strength of mortar after 1 and 28 d of curing was investigated by crush tests. For this purpose, mortars were prepared at w/c = 0.26 and admixed with the respective dosages of the PCE and the small molecule co-dispersant to adjust an initial spread flow of 23 ± 0.5 cm. Moreover, a mortar only admixed with the PCE was used as reference. The mortars were cast into 40 × 40 × 160 mm steel prism molds, cured at 20 °C and 90% relative humidity in a climate box and demolded after 24 h. The specimens for the 1 d compressive strength were immediately measured, while the other samples were cured in plain water for 28 d until testing commenced [36]. The compressive strength was determined by a compression and bending testing machine (ToniPRAX from Toni Technik) and reported as average value from three mortar prisms.

2.5. Tests in self-compacting concrete

The auxiliary dispersants were also tested in self-compacting concrete (SCC) at w/c = 0.35. The composition of the SCC is shown in Table 3. It was based on a Portland-limestone cement and included fly ash and limestone powder as supplementary cementitious materials.

The SCC was prepared according to the mixing procedure as follows: Sand and gravel were first homogenized with a bucket mixer (Beckel, Schwallungen, Germany) and then one third of the mixing water was added to the aggregates. After a soaking time of 10 min, cement, fly ash and lime stone powder were added and mixed with the residual amount of water. The PCE superplasticizer and auxiliary dispersant were simultaneously admixed after 20 sec and the fresh concrete was further agitated for 5 min. Thereafter, the slump flow of the SCC was determined as specified in DIN EN 12350–8 [39]. The PCE was dosed in such an amount to attain a spread flow of 740 ± 10 mm. After this test, the concrete was transferred back into the mixer and stirred for 2 min. Finally, the V-funnel empty time was measured according to DIN EN 12350–9 [37].

Table 3
Mix proportions of the SCC.

Component	(kg/m^3)
0/4 sand	995
4/8 gravel	244
8/16 gravel	638
CEM II/A-LL 42.5 R	430
Fly ash	50
Limestone powder	50
Fresh water	150

2.6. Amount of pore solution available

For the determination of the amount of pore solution, 50 g cement were filled into centrifuge tubes containing aqueous solutions of the PCE and the non-ionic auxiliary dispersant in such concentrations as utilized in the mortar tests to achieve a spread flow of 23 ± 0.5 cm at w/c = 0.26. The cement slurries were homogenized for 4 min with a vortex mixer and then centrifuged for 5 min at 8,500 rpm. The clear supernatant was removed with a syringe and then the weight of the extracted pore solution was determined. It presents the liquid phase that is not consumed by the cement hydration and is not physically adsorbed onto the surface, but can be collected by centrifugation [40].

3. Results and discussion

3.1. Dispersing performance of the PCE superplasticizers in mortar

At first, the dispersing capacity of the individual PCE polymers was evaluated in mortar. Spread flow tests were conducted at a w/c ratio of 0.26 using dosages in the range from 0.3 to 1.2% bwoc (by weight of cement). As can be seen from Fig. 6, both polymers produced S-shaped curves which are characteristic for PCE

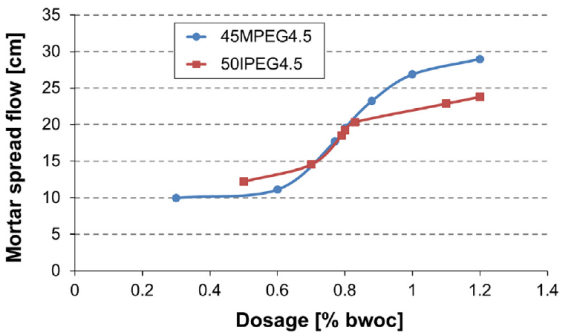

Fig. 6. Spread flow of mortars fluidized with increasing dosages of the PCEs at w/c = 0.26.

superplasticizers. A minimum dosage of the PCE is first required to achieve the onset of the spread flow. Once this dosage has been reached, the fluidity increases linearly with ascending dosage until it levels off due to the saturation of all adsorption sites.

The dispersing performance of both PCEs was rather comparable for dosages $\leq$ 0.8%. However, at higher additions the MPEG PCE performed better. Apart from this, also the corresponding dosages of the PCEs for a spread flow of 18 and 23 ± 0.5 cm were ascertained. This was attained by 0.77% and 0.88% of 45MPEG4.5, while higher dosages of 0.79% and 1.1% were needed from 50IPEG4.5. These dosages were applied in the ensuing experiments.

3.2. Effect of the non-ionic auxiliary dispersants on the spread flow

Recently, we reported that non-ionic molecules can augment the dispersing performance of PCEs and contribute to the dispersion of cement paste at low w/c ratios [32]. A higher fluidity was obtained in these pastes when PCEs were added together with such molecules. This was attributed to a spacing effect of the co-dispersants which remain in the pore solution and hinder the cement particles from agglomeration due to the formation of repulsive depletion forces. In light of this, we first wanted to scrutinize whether the non-ionic molecules are also effective in mortar. To probe this, spread flow tests were carried out where the PCEs were applied in a dosage for a spread flow of 18 cm. Moreover, they were combined with different amounts of the co-dispersants to achieve a spread flow of 23 ± 0.5 cm.

According to Table 4, it is confirmed that the non-ionic molecules also in mortar act as auxiliary dispersants and are capable of enhancing the spread flow there. Since the yield stress is directly related to the spread flow [41], it can be assumed that the small molecules provoke a higher fluidity by lowering the yield stress. To adjust a spread flow of 23 cm, dosages of 0.2 – 0.5% were needed of the co-dispersants. The same fluidity was obtained by using 0.88% 45MPEG4.5 and 1.1% 50IPEG4.5, respectively. This signifies that by means of the auxiliary dispersants also a reduction of the PCE dosage can be facilitated.

3.3. Flow behavior of mortars in the flow line

Next, the spreading ability of the mortars in the flow line was investigated. For the experiments, mortars were utilized holding those dosages of the PCE and co-dispersants as shown in Table 5. Furthermore, mortars which were only fluidized with the PCE superplasticizer were prepared as reference. All mortars tested exhibited a spread flow of 23 ± 0.5 cm. Table 5 summarizes the results of the flow line tests showing the D30 values (=spread flow after 30 sec) and the final spread of the mortars after stoppage.

Generally, it was noticed that 45MPEG4.5 induced a more sticky consistency than 50IPEG4.5. This already became evident during the filling of the mortar into the reservoir of the flow line. Especially the mortar admixed with the MPEG PCE appeared quite tenacious and cohesive. These observations were supported by the D30 value obtained which was lower for the MPEG PCE (8.5 cm vs. 11.7 cm for the IPEG PCE). The mortar fluidized with 45MPEG4.5 showed a creeping flow behavior and only reached a final flow value of 17 cm. However, the mortar comprising the IPEG PCE was much less sticky and obtained a considerably higher final spread flow of 44.1 cm. These results are in agreement with the findings from previous studies [23,25]. Table 5 also displays that the co-dispersants enhanced the D30 values and improved the flow speed of the mortars. To be more specific, the D30 value was increased by ~ 10% for 50IPEG4.5 and ~ 25% in the case of 45MPEG4.5. Additionally, the non-ionic molecules produced higher final spread flow values in the flow line. Based on that, it can be concluded that the non-adsorbing molecules work both as co-dispersant and flow enhancer in mortar.

Table 4
Dosages of the co-dispersants required for a mortar spread flow of 23 cm in the presence of a PCE superplasticizer at w/c = 0.26.

0.77% 45MPEG4.5 …	0.79% 50IPEG4.5 …
… + 0.44% DEG	… + 0.4% DEG
… + 0.43% JA	… + 0.52% JA
… + 0.23% MPD	… + 0.3% MPD
… + 0.36% DPGDME	… + 0.3% DPGMDE

Table 5
Results of the flow line experiments.

System	D30 (cm)	ΔD30 (%)	Final flow (cm)
0.88% 45MPEG4.5 (reference)	8.5	–	17
0.77% 45MPEG4.5 …			
… + 0.44% DEG	10.5	24	21.7
… + 0.43% JA	10.9	28	21.2
… + 0.23% MPD	10.3	22	21.5
… + 0.36% DPGDME	10.5	24	22
1.1% 50IPEG4.5 (reference)	11.7	–	44.1
0.79% 50IPEG4.5 …			
… + 0.4% DEG	12.5	7	51.1
… + 0.52% JA	12.6	8	52
… + 0.3% MPD	13.3	14	53.3
… + 0.3% DPGDME	12.9	10	50.7

3.4. V-funnel Empty times of mortars

Next, V-funnel tests were conducted, to qualitatively capture the impact of the co-dispersants on the plastic viscosity. As described at the beginning, a high plastic viscosity is the primary reason for the sticky consistency occurring at low w/c ratios. The V-funnel empty times were determined for mortars adjusted with the PCE and co-dispersants (see dosages in Table 5) to a spread flow of 23 ± 0.5 cm. The results are illustrated in Figs. 7 and 8.

Principally, it was found that 45MPEG4.5 effecutated longer V-funnel empty times as compared to 50IPEG4.5 (129 sec vs. 77 sec for the referene mortars). This signifies that the mortars fluidized with the MPEG PCE exhibit a relativley high plastic viscosity. Interestingly, after addition of the non-ionic molcules faster V-funnel empty times were achieved for both PCEs. A decrease of ~ 30% was attained for the MPEG PCE whereas for the IPEG PCE the empty times were reduced by ~ 36%. These findings imply that the co-dispersants lower the plastic viscosity and hence decrease the

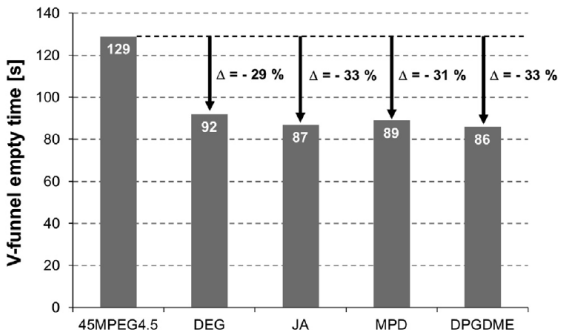

Fig. 7. V-funnel empty times of mortars admixed with 45MPEG4.5 and different non-ionic co-dispersants at w/c = 0.26.

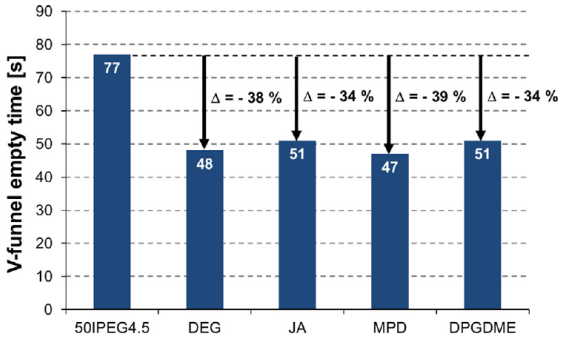

Fig. 8. V-funnel empty times of mortars fluidized with 50IPEG4.5 and different non-ionic co-dispersants at w/c = 0.26.

stickiness. Consequentely, the mortars can be released much faster from the funnel and possess a higher filling ability. Additionally, it was established that the performance of all small molecules tested was quite comparable and did not much depend on their sepecific chemcial composition.

3.5. Effect of the auxiliary dispersants on the compressive strength of mortar

The compressive strengths of mortars admixed with 50IPEG4.5 and the non-ionic small molecules after 1 and 28 d of curing are shown in Fig. 9. The mortars held the same dosages of the additives as utilized in the flow line and V-funnel tests. As can be seen from the figure, the mortar specimens admixed with the PCE and co-dispersants exhibited slightly higher compressive strength values after 1 d of curing for DEG, MPD and DPGDME as compared to the reference that was only fluidized with the PCE. This can be explained by the lower PCE dosage used in the samples when a co-dispersant was present. It is well established that most PCEs retard cement hydration and thus affect early strength development. However, after 28 d of curing, the compressive strengths of the mortars were similar to the reference, except for the sample containing DEG which yielded a slightly reduced compressive strength.

3.6. Effect on flow properties of SCC

Finally, the effect of the auxiliary dispersants on the rheological properties of a self-compacting concrete was investigated by spread flow and V-funnel tests. For the experiments, a SCC was

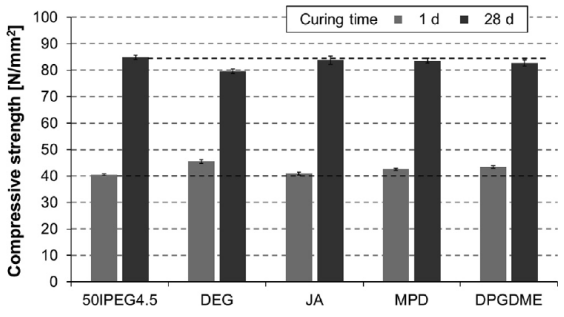

Fig. 9. Compressive strength of mortar specimens admixed with 50IPEG4.5 and various non-ionic co-dispersants, measured after 1 and 28 d of curing.

used which was prepared from Portland-limestone cement at a w/c ratio of 0.35. First, the dosages of the individual PCEs were ascertained for a spread flow of 740 ± 10 mm. This was achieved by 0.8% 45MPEG4.5 and 1.3% 50IPEG4.5, respectively. Even though the SCC could be highly fluidized with the PCEs, it exhibited a sticky and cohesive consistency. Similar as in mortar, again a more pronounced stickiness was observed for the MPEG PCE. This became evident from a higher V-funnel empty time (see Table 6). After addition of the co-dispersants, the SCC appeared less tenacious and discharged much faster from the funnel. The V-funnel empty times were reduced from 23 to 17 sec for the MPEG PCE, signifying a decrease of 26% which is attributable to the addition of the co-dispersants. For the IPEG PCE, the empty times were even shortened from 21 to 13 sec (i.e. decline of 38%). This clearly confirms that the non-ionic co-dispersants decrease the plastic viscosity. Thus, a concrete with improved rheological properties is obtained which can be processed easier at the construction site. Remarkably, the small molecules did not affect the spread flow (yield stress) of the concrete, but only the plastic viscosity. This differs from the results obtained in mortar where the co-dispersants influenced both, the spread flow and the plastic viscosity. In a control experiment, the amount of non-ionic co-dispersant was substituted by the same amount of water to probe whether the reduced plastic viscosity merely derives from decreasing the solid volume fraction. It was found that the addition of 0.8% bwoc water had no effect on the spread flow and V-funnel empty time. This suggests that the higher speed of flow can be attributed to the presence of the auxiliary dispersants. Obviously, the addition of an equivalent amount of water is insufficient to reduce the viscous consistency of the concrete and to affect the plastic viscosity.

3.7. Mechanistic investigation

Still, the question remained how the non-ionic auxiliary dispersants reduce the plastic viscosity. Since all mortars/concretes tested exhibited the same spread flow it can be excluded that the lower plastic viscosities mainly originate from a spacing effect of the co-dispersants that particularly would affect the yield stress. Taking into consideration that the small molecules remain non-adsorbed in the interstitial pore solution, we decided to take a closer look on the available amount of pore solution that can be extracted by centrifugation. According to [40,42], this includes the amount of the liquid phase that is not chemically consumed by cement hydration nor physically adsorbed on the surface of cement particles or hydration products. The amount of pore solution was quantified for cement pastes admixed with the dosages applied in the mortar tests.

Table 6
Spread flow and V-funnel empty times of SCCs fluidized with the PCE and co-dispersants at w/c = 0.35.

System	Concrete spread flow (cm)	V-funnel empty time (s)
0.8% 45MPEG4.5 (reference)	745	23
0.8% 45MPEG4.5 ...		
... + 0.8% DEG	740	17
... + 0.8% MPD	750	17
... + 0.8% DPGDME	740	17
... + 0.8% water	740	23
1.3% 50IPEG4.5 (reference)	745	21
1.3% 50IPEG4.5 ...		
... + 1.3% DEG	740	14
... + 1.0% MPD	750	13
... + 1.1% DPGDME	750	13

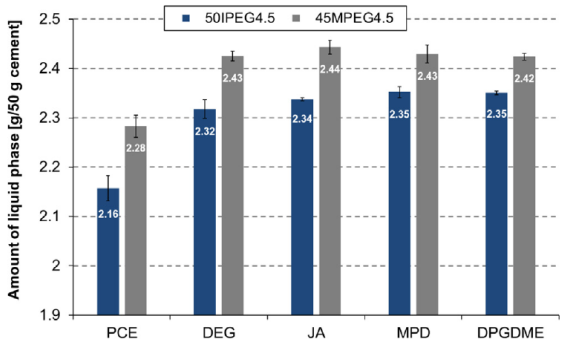

Fig. 10. Amount of liquid phase in cement pastes (w/c = 0.26) holding the corresponding dosages of the PCE and non-ionic co-dispersants as utilized in the mortar tests.

Fig. 10 reveals that a higher amount of pore solution was extracted from the cement pastes holding the combination of PCE and co-dispersant than from the reference paste admixed with PCE only. The paste fluidized with the IPEG PCE exhibited a lower amount of pore solution because this polymer binds more water due to its higher molecular weight. Relating these amounts of the liquid phase collected from 50 g cement to 675 g (as in the mortar), it was found that through the addition of the co-dispersants the amount of pore solution increased by 2.4 g for 50IPEG4.5 and 2 g for 45MPEG4.5, respectively. This corroborates that the liquid film surrounding the particles increases which minimizes unfavorable contact interactions [43–45]. Fig. 11 schematically illustrates this working mechanism of the small molecules. Moreover, the previous results that all co-dispersants tested produced very similar values in the flow line and V-funnel tests (see Table 5 and Figs. 7 and 8) is now explained by their comparable amounts of the liquid phase. To conclude, the lower plastic viscosities originate from a higher amount of the pore solution which increases the thickness of the liquid layer around the particles and hence reduces the friction during flow owed to a better lubrication. Considering the results from the concrete test, it can be inferred that only the auxiliary dispersants are capable of producing superior lubrication, whereas the addition of water had no impact on the plastic viscosity for the dosage tested.

4. Conclusions

The present study investigated the effect of non-ionic molecules when combined with PCE superplasticizers on the rheological parameters of mortar and concrete. It was found that the small molecules reduce both the yield stress and plastic viscosity in mortar, while in concrete they only decrease the plastic viscosity. Thus, the sticky behavior which typically appears at low w/c ratios and high solids volume fractions is reduced and a higher flow speed is achieved. Through addition of the small molecules, the D30 values of mortars were lowered by 10 – 30% and the V-funnel empty times of mortars and concretes were decreased by 25 – 40%. Compressive strength tests confirmed that the small molecules did not negatively impact the strength development of mortar. The reduced plastic viscosities of mortar and concrete can be attributed to the enhanced lubrication of the particles by the co-dispersants.

Generally, the addition of non-ionic molecules represents a viable option for reducing the plastic viscosity at low w/c ratios and for formulating mortars and concretes with improved rheological behavior which facilitate an easier and faster processing. In this respect, the concept of the non-ionic auxiliary dispersants might be promising for ultra-high performance concrete (UHPC) which commonly exhibits a viscous consistency and a slow flow behavior, originating from the extremely low water to binder ratio ($\leq$0.22) and the high solids content. First results suggest that the non-ionic molecules can also reduce the stickiness of UHPC prepared from cement/silica blends and hence improve its flow properties resulting in a concrete which appears less cohesive and spreads out faster.

CRediT authorship contribution statement

Manuel Ilg: Conceptualization, Investigation, Writing - original draft, Writing - review & editing, Visualization, Funding acquisition. **Johann Plank:** Conceptualization, Investigation, Writing - original draft, Writing - review & editing, Supervision, Funding acquisition.

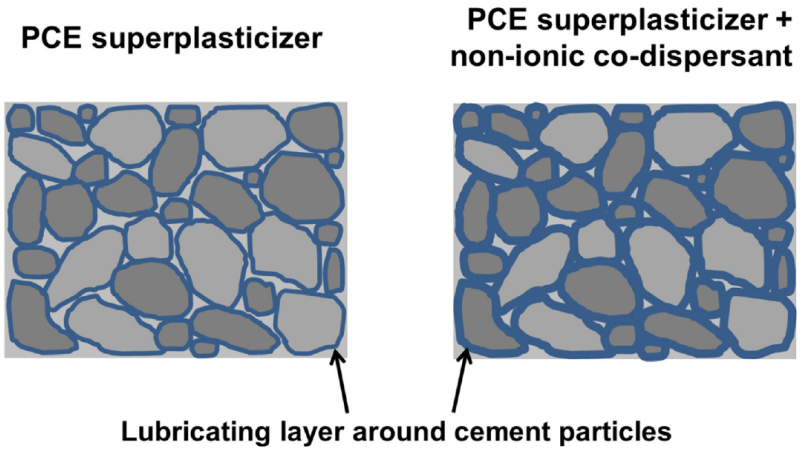

Fig. 11. Conceptual sketch of the mode of action of the non-ionic co-dispersants.

Declaration of Competing Interest

The authors declare that they have no known competing financial interests or personal relationships that could have appeared to influence the work reported in this paper.

Acknowledgments

The authors would like to greatly acknowledge the financial support received by the German Research Foundation (Deutsche Forschungsgemeinschaft) (project number: 387082770) within the frame of the SPP 2005 "Opus Fluidum Futurum – Rheology of reactive, multiscale, multiphase construction materials". Additionally, BASF, Clariant and Huntsman are thanked for providing the non-ionic auxiliary dispersants. A special thank also goes to Schwenk Zement for their great support during the concrete lab tests which we performed in their ready-mix concrete plant in Ludwigsfeld (Munich).

References

[1] C.F. Ferraris, P. Billberg, R. Ferron, D. Feys, J. Hu, S. Kawashima, E. Koehler, M. Sonebi, J. Tanesi, N. Tregger, Role of rheology in achieving successful concrete performance, ACI Committee 238 (2017) 43–51.
[2] P.F.G. Banfill, Rheology of fresh cement and concrete, Rheology Reviews (2006) 61–130.
[3] J. Golaszewski, J. Szwabowski, Influence of superplasticizers on rheological behaviour of fresh cement mortars, Cem. Concr. Res. 34 (2004) 235–248.
[4] C.R. Robert, D. Sathyan, K.B. Anand, Effect of superplasticizers on the rheological properties of fly ash incorporated cement paste, Mater. Today:. Proc. 5 (2018) 23955–23963.
[5] D.P. Bentz, C.F. Ferraris, M.A. Galler, A.S. Hansen, J.M. Guynn, Influence of particle size distributions on yield stress and viscosity of cement-fly ash pastes, Cem. Concr. Res. 42 (2012) 404–409.
[6] J.J. Chen, A.K.H. Kwan, Superfine cement for improving packing density, rheology and strength of cement paste, Cem. Concr. Compos. 34 (2012) 1–10.
[7] J. Hu, K. Wang, Effect of coarse aggregate characteristics on concrete rheology, Constr. Build. Mater. 25 (2011) 1196–1204.
[8] M.R. Geiker, M. Brandl, L.N. Thrane, L.F. Nielsen, On the effect of coarse aggregate fraction and shape on the rheological properties of self-compacting concrete, Cem, Concr. Aggr. 24 (2002) 3–6.
[9] K. Ostrowski, L. Sadowski, D. Stefaniuk, D. Walach, T. Gawenda, K. Oleksik, I. Usydus, The effect of the morphology of coarse aggregate on the properties of self-compacting high-performance fibre-reinforced concrete, Materials 11 (2018) 1372.
[10] F. Mahaut, S. Mokeddem, X. Chateau, N. Roussel, G. Ovarlez, Effect of coarse particle volume fraction on the yield stress and thixotropy of cementitious materials, Cem. Concr. Res. 38 (2008) 1276–1285.
[11] O.H. Wallevik, J.E. Wallevik, Rheology as a tool in concrete science: The use of rheographs and workability boxes, Cem. Concr. Res. 41 (2011) 1279–1288.
[12] P.F.G. Banfill, Additivity effects in the rheology of fresh concrete containing water-reducing admixtures, Constr. Build. Mater. 25 (2011) 2955–2960.
[13] J.-Y. Petit, K.H. Khayat, E. Wirquin, Coupled effect of time and temperature on variations of plastic viscosity of highly flowable mortar, Cem. Concr. Res. 39 (2009) 165–170.
[14] D. Han, R.D. Ferron, Effect of mixing method on microstructure and rheology of cement paste, Constr. Build. Mater. 93 (2015) 278–288.
[15] J. Plank, E. Sakai, C.W. Miao, C. Yu, J.X. Hong, Chemical admixtures – Chemistry, applications and their impact on concrete microstructure and durability, Cem. Concr. Res. 78 (2015) 81–99.
[16] H. Uchikawa, S. Hanehara, D. Sawaki, The role of steric repulsive force in the dispersion of cement particles in fresh paste prepared with organic admixture, Cem. Concr. Res. 27 (1997) 37–50.
[17] Q. Ran, P. Somasundaran, C. Miao, J. Liu, S. Wu, J. Shen, Effect of the length of the side chains of comb-like copolymer dispersants on dispersion and rheological properties of concentrated cement suspensions, J. Colloid Interface Sci. 336 (2009) 624–633.
[18] N. Roussel, A. Lemaitre, R.J. Flatt, P. Coussot, Steady state flow of cement suspensions: A micromechanical state of the art, Cem. Concr. Res. 40 (2010) 77–84.
[19] J. Björnström, S. Chandra, Effect of superplasticizers on the rheological properties of cements, Mater. Struct. 36 (2003) 685–692.
[20] J. Liu, K. Wang, Q. Zhang, F. Han, J. Sha, J. Liu, Influence of superplasticizer dosage on the viscosity of cement paste with low water-binder ratio, Constr. Build. Mater. 149 (2017) 359–366.
[21] C. Shi, Z. Wu, J. Xiao, D. Wang, Z. Huang, Z. Fang, A review on ultra high performance concrete: Part I. Raw materials and mixture design, Constr. Build. Mater. 101 (2015) 741–751.
[22] S. Qian, Y. Yao, Z. Wang, S. Cui, X. Liu, H. Jiang, Z. Guo, G. Lai, Q. Xu, J. Guan, Synthesis, characterization and working mechanism of a novel polycarboxylate superplasticizer for concrete possessing reduced viscosity, Constr. Build. Mater. 169 (2018) 452–461.
[23] A. Lange, J. Plank, Optimization of comb-shaped polycarboxylate cement dispersants to achieve fast-flowing mortar and concrete, J. Appl. Polym. Sci. 132 (2015) 42529.
[24] A. Kraus, O. Mazanec, J. Dengler, N. Hillesheim, J. Bokern, Influence of PAE, SMD and PCE superplasticizers on the rheological properties of mortars and concretes, in: V. Mechtcherine, C. Schroefl (Eds.), International Conference on Application of Superabsorbent Polymers and Other New Admixtures in Concrete Construction, Dresden (Germany), September 14 – 17, 2014, RILEM Publications S.A.R.L., Proceedings PRO 95, pp. 115-126.
[25] A. Lange, T. Hirata, J. Plank, Influence of the HLB value of polycarboxylate superplasticizers on the flow behavior of mortar and concrete, Cem. Concr. Res. 60 (2014) 45–50.
[26] T. Yuasa, T. Nishikawa, N. Sakamoto, T. Hirata, H. Izukashi, T. Ueta, H. Tanaka, Y. Onda, T. Uno, Polycarboxylic acid copolymer, production method and use thereof, US 7,405,264 B2, (assigned to Nippon, Shokubai Co LTD), 2008.
[27] T. Yuasa, H. Tanaka, N. Sakamoto, T. Nishikawa, H. Izukashi, T. Uno, T. Hirata, T. Ueta, Y. Onda, Cement admixture and production method thereof, US 7,662,884 B2 (2010) (assigned to Nippon Shokubai Co LTD).
[28] E. Sakai, A. Ishida, A. Ohta, New trends in the development of chemical admixtures in Japan, J. Adv. Concr. Technol. 4 (2) (2006) 211–223.
[29] S.D. Bauchkar, H.S. Chore, Effect of PCE superplasticizers on rheological and strength properties of high strength self-consolidating concrete, Adv. Concr. Constr. 6 (2018) 561–583.
[30] J. Stecher, J. Plank, Phosphated comb polymers – A new generation of highly effective superplasticizers, in: K. H. Khayat (Ed.), 8th International RILEM Symposium on Self-Compacting Concrete – SCC 2016, Washington, D.C. (USA), May 15 – 18, 2016, pp. 61-71.
[31] Y. He, X. Shu, X. Wang, Y. Yang, J. Liu, Q. Ran, Effects of polycarboxylates with different adsorption groups on the rheological properties of cement paste, J. Disper. Sci. Technol. (2019), https://doi.org/10.1080/01932691.2019.1614029.
[32] M. Ilg, J. Plank, Non-adsorbing small molecules as auxiliary dispersants for polycarboxylate superplasticizers, J. Colloid. Surf. A 587 (2020) 124307.
[33] J. Plank, K. Pöllmann, N. Zouaoui, P.R. Andres, C. Schäfer, Synthesis and performance of methacrylic ester based polycarboxylate superplasticizers possessing hydroxy terminated poly(ethylene glycol) side chains, Cem. Concr. Res. 38 (2008) 1210–1216.
[34] S. Kawaguchi, K. Akaike, Z.-M. Zhang, H. Matsumoto, K. Ito, Watersoluble bottlebrushes, Polym. J. 30 (1998) 1004–1007.
[35] J. Plank, B. Sachsenhauser, Experimental determination of the effective anionic charge density of polycarboxylate superplasticizers in cement pore solution, Cem. Concr. Res. 39 (2009) 1–5.
[36] DIN EN 196-1:2016 Methods of testing cement – Part 1: Determination of strength.
[37] DIN EN 12350-9:2010 Testing fresh concrete – Part 9: Self-compacting concrete – V-funnel test.
[38] DIN EN 13395-2:2002 Products and systems for the protection and repair of concrete structures - Test methods - Determination of workability - Part 2: Test for flow of grout or mortar.
[39] DIN EN 12350-8:2019 Testing fresh concrete – Part 8: Self compacting concrete – Slump flow test.
[40] S. Han, P.Y. Yan, X.M. Kong, Study on the compatibility of cement-superplasticizer system based on the amount of free solution, Sci. China Tech. Sci. 54 (2011) 183–189.
[41] H. Bessaies-Bey, R. Baumann, M. Schmitz, M. Radler, N. Roussel, Organic admixtures and cement particles: Competitive adsorption and its macroscopic rheological consequences, Cem. Concr. Res. 80 (2016) 1–9.
[42] L. Shui, Z. Sun, H. Yang, X. Yang, Y. Ji, Q. Luo, Experimental evidence for a possible dispersion mechanism of polycarboxylate-type superplasticizers, Adv. Cem. Res. 28 (5) (2016) 287–297.
[43] Y. Ghasemi, M. Emborg, A. Cwirzen, Effect of water film thickness on the flow in conventional mortars and concrete, Mater. Struct. 52 (2019) 62.
[44] M. Zhao, X. Zhang, Y. Zhang, Effect of free water on the flowability of cement paste with chemical or mineral admixtures, Constr. Build. Mater. 111 (2016) 571–579.
[45] L.G. Li, A.K.H. Kwan, Mortar design based on water film thickness, Constr. Build. Mater. 25 (2011) 2381–2390.

Folgeversuche zu Publikation #4:

In Ergänzung zu den in **Publikation #4** dargelegten Untersuchungen wurden weitere Rheologieversuche mit den nicht-ionischen Co-Dispergiermitteln durchgeführt. Diese Versuche erfolgten am Zentrum für Baustoffe und Materialprüfung der TU München. Als Testsystem wurde ein selbstverdichtender Beton mit einem w/z-Wert von 0,25 eingesetzt. Die Zusammensetzung dieses Betons sowie die Beschreibung der Anmischmethode sind in **Abbildung 42** dargestellt. 50IPEG4.5 wurde als Fließmittel verwendet und Diethylenglykol bzw. Jeffamin D-230 als Co-Dispergiermittel.

Zusammensetzung SVB

CEM I 42.5 R	14,00 kg
Sand 0/2 mm	14,27 kg
Kies 4/8 mm	6,74 kg
Kies 8/16 mm	10,18 kg
Frischwasser	3,41 kg

Ausbreitmaß: 730 mm; w/z = 0,25

PCE: 50IPEG4.5
Co-Dispergiermittel: Diethylenglykol, Jeffamin D-230

Anmischmethode (Eirich Betonmischer)

- Homogenisierung der Ausgangsstoffe für 30 sec (CEM I 42.5 R, Sand und Kies)
- Zugabe des Anmachwassers innerhalb von 30 sec
- Anschließende Zugabe des Fließmittels + Co-Dispergiermittels binnen 30 sec
- Durchmischen des Frischbetons für 2 min

Abbildung 42: Formulierung des SVBs und Beschreibung der Anmischmethode.

Beim Einstellen des SVBs auf ein Ausbreitmaß von 730 mm zeigte sich erneut, dass die nicht-ionischen Additive keinen Einfluss auf die Fließgrenze haben. Über Messungen mit einem Vane Rheometer (ICAR Rheometer von Germann Instruments; **Abbildung 43**) konnten die Ergebnisse aus den V-Trichter-Versuchen in **Publikation #4** bestätigt werden, dass die Co-Dispergiermittel im Beton ausschließlich die plastische Viskosität verringern (sh. **Tabelle 1**). So nahm die Viskosität durch die Zugabe von Diethylenglykol von 144 auf 84 Pa•s und für Jeffamin D-230 auf 79 Pa•s ab. Dies entspricht in beiden Fällen einer Reduzierung um mehr als 40 %.

Tabelle 1: Additivdosierungen in den SVBs für ein Ausbreitmaß von 730 mm sowie Übersicht der durch Vane Rheometrie gemessenen plastischen Viskositäten.

Zusatzmittel	**SVB 1**	**SVB 2**	**SVB 3**
50IPEG4.5 [% bwoc]	0,6	0,6	0,6
Diethylenglykol [% bwoc]	-	0,6	-
Jeffamin D-230 [% bwoc]	-	-	0,6
Plastische Viskosität [Pa•s]	144	84	79

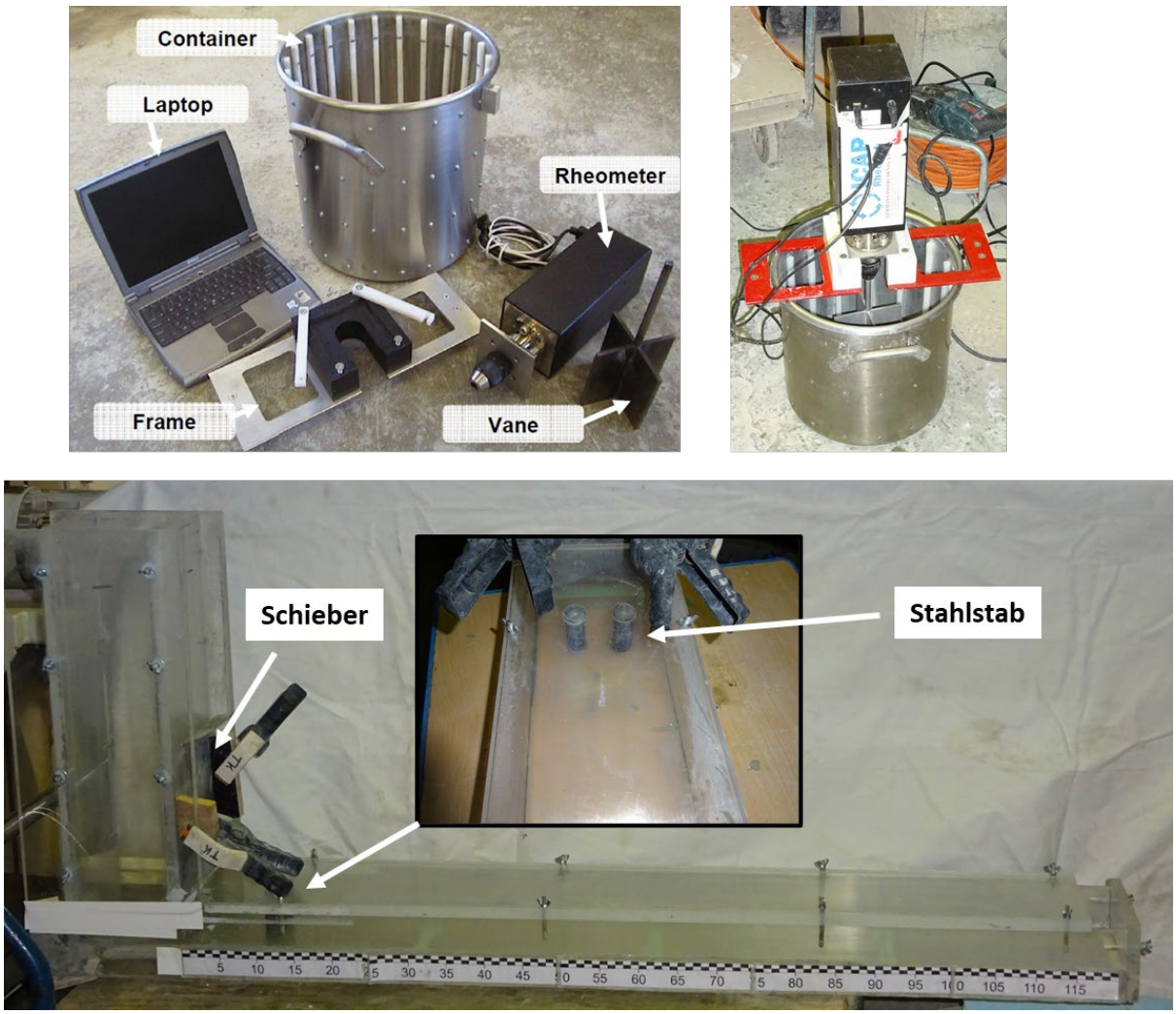

Abbildung 43: Experimenteller Aufbau des Vane Rheometers (oben) und der L-Box (unten); Abbildung links oben aus [245].

Weitere Erkenntnisse zur Rheologie sollten über L-Box-Versuche gewonnen werden. Bei diesen Tests wurde das Fließverhalten und die Blockierneigung des SVBs untersucht. Die L-Box ist eine Testvorrichtung, die aus zwei Kammern besteht, die durch einen Schieber voneinander getrennt sind (sh. **Abbildung 43**). Der Beton wird in die vertikale Kammer gefüllt und der Schieber danach geöffnet, sodass der Beton in den horizontalen Bereich fließen kann. Um die Blockierneigung zu untersuchen, sind zusätzlich Stahlstäbe im Übergangsbereich der Kammern angebracht, welche die Effekte einer Bewehrung simulieren sollen. Anhand der L-Box-Versuche konnte gezeigt werden, dass der SVB mit den Co-Dispergiermitteln eine deutlich schnellere Fließgeschwindigkeit besitzt und eine weitere Distanz in einem bestimmten Zeitintervall zurücklegt. So weisen beide SVBs in **Abbildung 44** das gleiche Ausbreitmaß auf, jedoch benötigt der Beton, der nur mit dem Fließmittel dispergiert wurde, eine deutlich längere Zeit um den Endwert zu erreichen.

Diese Versuche belegen, dass durch die Reduzierung der plastischen Viskosität die Fließeigenschaften erheblich verbessert werden und sich der SVB dadurch leichter verarbeiten lässt (z.B. schnelleres und problemloses Einbringen des Betons in Schalungen aufgrund eines besseren Formfüllungsverhaltens). Basierend auf diesen Beobachtungen wurde gefolgert, dass das Konzept der nicht-ionischen Co-Dispergiermittel auch in der Praxis gut umsetzbar ist und rheologische Optimierungen von Betonformulierungen damit vorgenommen werden können.

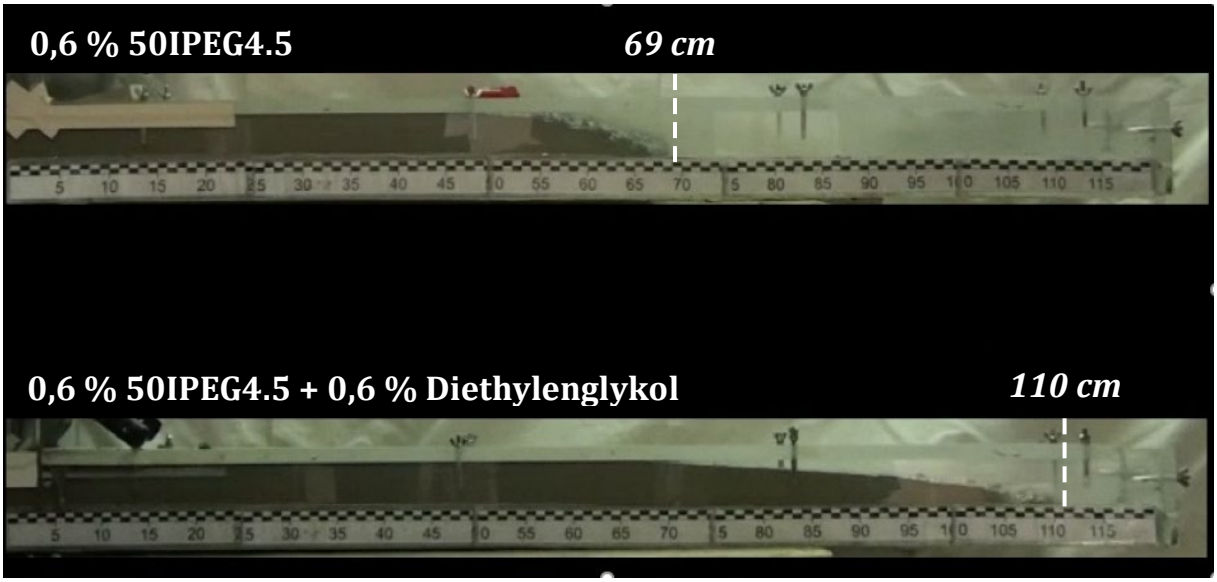

Abbildung 44: Betonfließmaß nach 60 Sekunden in der L-Box; der obere SVB wurde mit 0,6 % 50IPEG4.5 verflüssigt, der untere mit einer Mischung aus 0,6 % 50IPEG4.5 und 0,6 % Diethylenglykol.

5.1.5. Weitere Veröffentlichungen

Die **Publikationen #5** und **#6** wurden als Tagungsbeiträge verfasst und thematisieren ebenfalls die verflüssigende Wirkung von nicht-ionischen kleinen Molekülen. In beiden Arbeiten wird das neue Dispergierkonzept vorgestellt und die Ergebnisse aus den ersten Untersuchungen geschildert. Die Erkenntnisse und Schlussfolgerungen dieser Arbeiten sind analog zu den zuvor diskutierten Veröffentlichungen.

5.1.5.1. Publikation #5: A New Dispersing Mechanism For Cement Augmented by Non-Adsorbing Molecules

Publikation #5

A New Dispersing Mechanism For Cement Augmented by Non-Adsorbing Molecules

Manuel Ilg, Johann Plank

2nd International Conference on the Chemistry of Construction Materials (ICCCM), Munich (Germany)

GDCh Monographie 50 (2016) 63 – 66

Chemical Admixtures

A New Dispersing Mechanism For Cement Augmented by Non-Adsorbing Molecules

M. Ilg, J. Plank
Technische Universität München, Chair for Construction Chemistry, Lichtenbergstraße 4, 85747 Garching, Germany

Introduction

Fresh cement pastes can be regarded as concentrated colloidal suspensions of polydisperse particles ranging from only a few nanometers to several micrometers in water. Due to the polydispersity, the rheological behavior of cementitious systems is governed by interparticle forces (e.g. colloidal interactions, hydrodynamic and contact forces) /1/.
However, the poor workability of cement pastes can primarily be attributed to electrostatic attractive forces between the heterogeneous surface charge domains of cement /2/. To overcome those attractive forces, superplasticizers including polycarboxylate ethers (PCEs) are added. It is well established that PCEs can disperse cement through a combination of electrostatic repulsion as described by the DLVO theory and a steric hindrance effect which is influenced by the adsorbed layer thickness /3/. Both dispersion mechanisms require that the polymers used as dispersant adsorb onto the particle surface.
Oppositely, less attention has been devoted to the portion of non-adsorbed polymer remaining in the pore solution. Recently it has been reported that at low w/c ratios (< 0.3), even non-adsorbed polymers (PCEs and other macromolecules) can contribute to cement dispersion /4, 5/. Based on these findings, a new concept for cement dispersion is proposed here by combining an IPEG-PCE with different non-adsorbing small molecules which should help to improve the flowability of cement pastes at low w/c ratios.

Materials and methods

As superplasticizer, a commercial isoprenolether (IPEG) based PCE was utilized, comprising the monomers acrylic acid and poly (ethylene glycol) isoprenol ether possessing 50 ethylene oxide units. Molar ratio of the monomers was 4.5:1 and molecular properties were: M_w 82,000 g/mol, M_n 36,000 g/mol resulting in a PDI of 2.3. The polymer's specific anionic charge was 689 µeq/g in synthetic cement pore solution, thus facilitating its adsorption on cement. As non-adsorbing molecules, diethylene glycol and Jeffamine® D-230, a di-functional primary amine, were tested (see

Fig. 1 and **Fig. 2**). Adsorption measurements confirmed that both molecules do not adsorb on cement when individually added to cement. The non-ionic character was also verified by anionic charge measurements.
The effect of the small molecules on cement dispersion was ascertained by performing mini slump tests using a CEM I 52.5 N sample. A detailed description of the test procedure can be found in /5/. Note that the non-adsorbing molecules were always pre-dissolved in the mixing water together with the IPEG-PCE.

Results and discussion

The enhancement of the plasticizing effect of the IPEG-PCE through non-adsorbing molecules was investigated at different w/c ratios. First, the dosage of the superplasticizer was adjusted to attain a slump flow of 18 ± 0.5 cm. As expected, higher dosages of the PCE are needed as the w/c ratio decreases. Consequently, the dosage rose from 0.1 % bwoc at w/c = 0.3 to 0.145 % bwoc (w/c = 0.26) and finally to 0.215 % bwoc (w/c = 0.22). Next, diethylene glycol and Jeffamine® D-230 were admixed to the IPEG-PCE in ascending dosages from 0.1 – 0.9 % bwoc and their impact on paste fluidity was analyzed by mini slump tests (**Fig. 1** and **Fig. 2**).

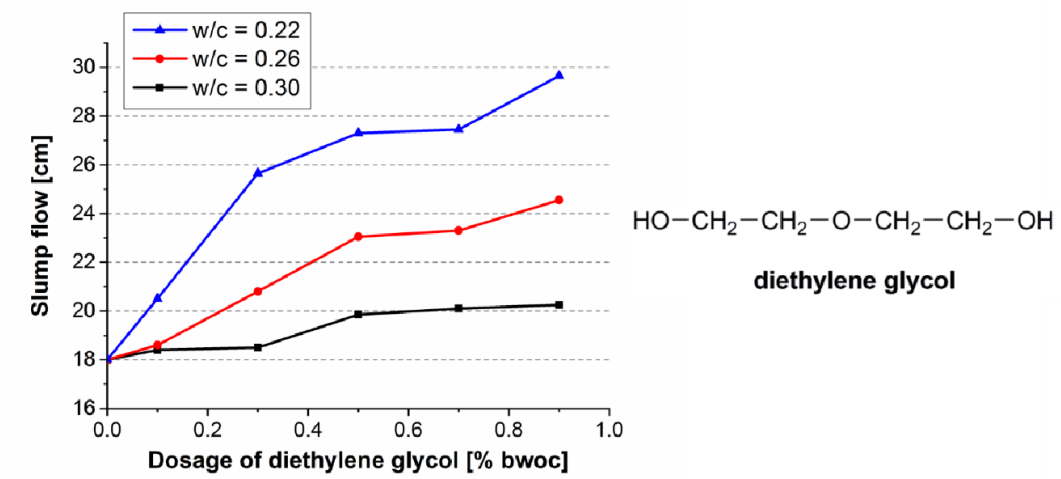

Fig. 1: Slump flow of cement pastes holding the respective dosage of IPEG-PCE for an initial slump flow of 18 cm, admixed with 0.1 – 0.9 bwoc % of diethylene glycol at different w/c ratios.

As is obvious from the figures, at a w/c ratio of 0.3 the improvement in flowability provided by the non-adsorbing molecules is rather limited. High dosages of the small molecules (> 0.5 % bwoc) are required to

observe at least a minor increase of the spread flow. However, the effect becomes very significant when the w/c ratio is reduced to 0.22. For instance, by adding 0.3 % bwoc diethylene glycol, the slump flow can be enhanced from the initial 18 cm to almost 26 cm at w/c = 0.22. In contrast, Jeffamine® D-230 produces a slightly minor plasticizing effect at dosages < 0.5 % bwoc, but becomes extremely effective at higher dosages (e.g. slump flow of 30 cm at 0.7 % bwoc).

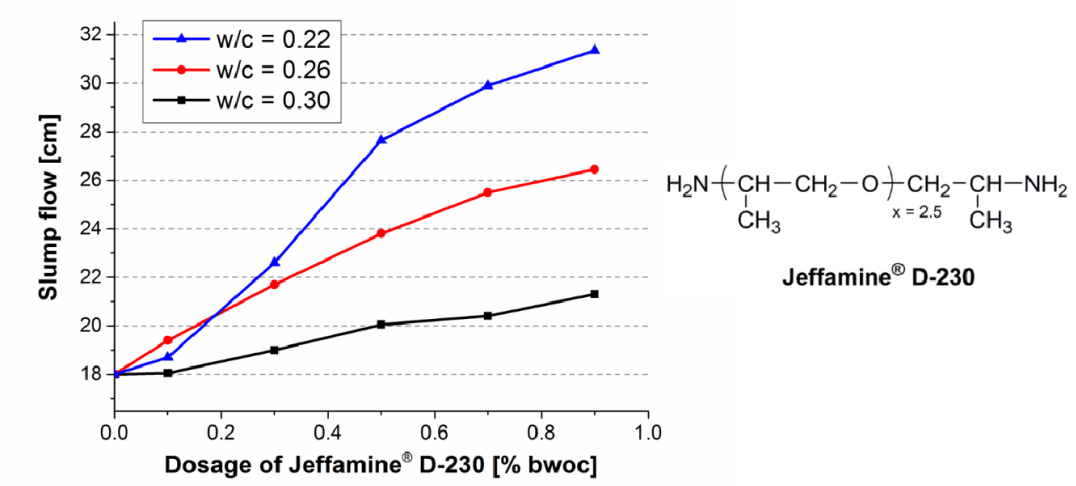

Fig. 2: Slump flow of cement pastes holding the respective dosage of IPEG-PCE for a slump flow of 18 cm, admixed with 0.1 – 0.9 bwoc % of Jeffamine® D-230 at different w/c ratios.

Apparently, only the combination of non-adsorbing molecules with the IPEG-PCE produces a significant increase of paste fluidity, especially at high solid volume fractions. Individually, the non-adsorbing molecules do not produce any fluidity when solely admixed to cement, although a more creamy consistency was observed (particularly at w/c = 0.3).
To gain more insight into the working mechanism of the small molecule co-dispersants, adsorption measurements were carried out. The amount of Jeffamine® sorbed in presence of the IPEG polymer was determined by measuring the total organic carbon and nitrogen content of the non-adsorbed portion of polymer present in cement pore solution using the depletion method. It was found that the Jeffamine® does not adsorb when combined with the PCE, it remains dissolved in the pore solution. Similar results were found for diethylene glycol.

Conclusion

The results suggest that non-adsorbing small molecules such as diethylene glycol and Jeffamine® D-230 can augment the dispersing

performance of IPEG-PCEs. This effect is most pronounced at low w/c ratios, where the cement particles are densely packed and the distance between adjacent cement grains is small. Based on this, a mechanistic model is proposed, whereby the non-adsorbing small molecules act as osmotic spacer (**Fig. 3**). The non-ionic molecules present in the pore solution provide a steric hindrance effect which keeps cement particles apart from each other and adds to the electrosteric dispersion originating from the PCEs. Agglomeration of cement particles is prevented through osmotic forces because then some parts of the pore solution will be depleted from the non-ionic compound which would be entropically unfavorable. This model can explain why the effect occurs only at low w/c ratios. Such synergistic interaction between PCEs and non-ionic small molecules is proposed as a new kind of dispersing mechanism.

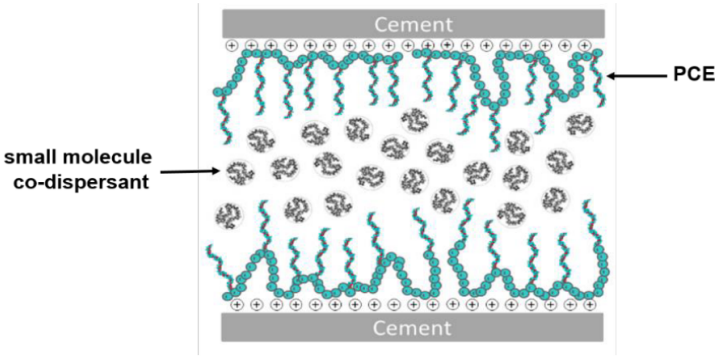

Fig. 3: Conceptual sketch of the new dispersing mechanism for PCEs augmented by non-adsorbing molecules.

Bibliographical references

/1/ N. Roussel, A. Lemaitre, R.J. Flatt, P. Coussot:
"Steady state flow of cement suspensions: A micromechanical state of the art"
Cem. Concr. Res. (2010) 40, 77-84.

/2/ R.J. Flatt:
"Dispersion forces in cement suspensions"
Cem. Concr. Res. (2004) 34, 399-408.

/3/ K. Yoshioka, E. Sakai, M. Daimon, A. Kitahara:
"Role of steric hindrance in the performance of superplasticizers for concrete"
J. Am. Ceram. Soc. (1997) 80, 2667-2671.

/4/ M. Ushiro, D. Atarashi, H. Kawakami, E. Sakai:
"The effect of superplasticizer present in pore solution on flowability of low water-to-powder cement paste"
Cem. Sci. Concr. Technol. (2013) 67, 102-107.

/5/ A. Lange, J. Plank:
"Contribution of non-adsorbing polymers to cement dispersion"
Cem. Concr. Res. (2016) 79, 131-136.

5.1.5.2. Publikation #6: Improving the flow properties of concretes prepared at low w/c ratio by using small molecule-based co-dispersant admixtures

Publikation #6

Improving the flow properties of concretes prepared at low w/c ratio by using small molecule-based co-dispersant admixtures

Manuel Ilg, Johann Plank

2nd International RILEM Conference on Rheology and Processing of Construction Materials (RheoCon2)
Dresden (Germany), 2019, Proceedings

Improving the flow properties of concretes prepared at low w/c ratio by using small molecule-based co-dispersant admixtures

Manuel Ilg[1], Johann Plank[1]
[1]*Chair for Construction Chemistry, Technische Universität München, Germany*

Abstract
The poor workability of fresh cementitious systems can be attributed to attractive Van der Waals forces between the heterogeneous surface charge domains of cement and the first hydration products. To overcome those interparticle interactions, superplasticizers including polycarboxylate ethers (PCEs) are typically added. It is well established that PCEs can disperse cement through a combination of electrostatic repulsion as described by the DLVO theory and a steric hindrance effect which is influenced by the adsorbed layer thickness. Both dispersion mechanisms require that the polymers used as dispersant adsorb onto the particle surface. Less attention has been devoted to non-adsorbing compounds which remain in the interstitial pore solution.
Now, it has been found that non-adsorbing small molecules (a) significantly improve the fluidity of cementitious materials at low water-to-cement ratios (< 0.30) and (b) eliminate the well-known "stickiness" and creeping flow behavior of such concretes when admixed with a conventional PCE superplasticizer. A big variety of different non-ionic glycol derivatives such as diethylene glycol (DEG), diethylene glycol dimethyl ether (DEGDME), dipropylene glycol dimethylether (DPGME) etc. were screened for their effectiveness as co-dispersants and the most powerful ones were identified. It was found that especially those glycol compounds with a high content of non-polar moieties performed as highly efficient co-dispersants. Based on adsorption measurements a mechanistic model explaining the reasons for the enhanced flow behavior is presented. Finally, some selected co-dispersants were tested in a ready-mix concrete plant to verify the practical applicability of these glycol compounds in concrete.

Keywords: Flow enhancer; co-dispersant; rheology; sticky concrete; self-compacting concrete.

1. Introduction

Concretes prepared at low w/c ratios exhibit outstanding material properties. Though such concretes can be highly fluidized with PCEs, applicators often report a honey-like consistency for them. These concretes creep rather than flow and exhibit a low speed of flow during placement at the construction site. This rheological behavior which becomes increasingly worse as w/c decreases is not desirable for placement and consolidation of the concrete into formworks or in elements containing densely packed reinforcement. The "stickiness" of these concretes can result in insufficient filling and induce voids and defects in the hardened concrete structure. Thus, academia and industry are actively researching

the reasons behind these rheological properties in order to find new concepts which mitigate this creeping flow behavior [1, 2].
Previous studies suggest that the stickiness derives from a high plastic viscosity owed to the high solid volume fractions of these concretes. Accordingly, a high speed of flow can be achieved by decreasing the plastic viscosity. Additionally, it was found that the hydrophilic-lipophilic balance (HLB) value of the PCE superplasticizer seems to present a key parameter which influences the plastic viscosity of concretes with w/c of 0.30 or less. To obtain a high speed of flow, the PCE must be as hydrophilic as possible, whereas hydrophobic groups (e.g. methyl groups) should be avoided in the structure [2].
Some studies imply that for concretes exhibiting high solids contents the conventional models for dispersion like the DLVO theory (electrostatic stabilization) or the Ottewill-Walker equation (steric stabilization) are no longer exclusively applicable [3]. Instead, the portion of non-adsorbed PCE polymer remaining in the pore solution seems to contribute to the cement dispersion [4, 5]. This concept was first described by *Sakai* et al. who investigated the fluidity of low heat Portland cement – silica blends using different PCE superplasticizers at water-to-powder ratios ranging from 0.16 – 0.32 [4]. According to their results, the high paste fluidity at low w/p ratios (i.e. 0.16) cannot be ascribed only to a steric hindrance effect of adsorbed PCE polymers, but is linked to un-adsorbed PCE polymers remaining in the interstitial pore solution.
More recent findings from our group confirm that specific non-ionic polymers (e.g. common polyethylene glycol PEG-2000) can significantly augment the dispersing performance of PCE superplasticizers at low w/c (e.g. 0.30) and enhance the paste fluidity of such systems [6]. Such combinations of the non-ionic polymers with PCEs lead to an increase in fluidity whereas the individual non-ionic polymers do not produce any fluidity at all. In a consecutive study it was found that especially non-ionic small molecules like diethylene glycol are even more effective co-dispersants than the polymers [7].
This work here addresses the role of different non-ionic small molecules on the fluidity of cementitious systems exhibiting low w/c (e.g. 0.22). The main goal of this study was to further investigate this new type of dispersing mechanism and to elucidate the correlation between the chemical composition and the dispersing effectiveness of the small molecule co-dispersants. Additionally, adsorption measurements were carried out to gain a more profound understanding of the working mechanism. Finally, concrete lab test were performed to verify whether the findings obtained for the co-dispersants in cement paste are also applicable in concrete.

2. Experimental part

2.1. Materials

For the screening of the non-ionic molecules an ordinary Portland cement CEM I 52.5 N (Milke classic®, HeidelbergCement) was utilized. The concrete lab tests were performed with a Portland/limestone cement CEM II/A-LL 42.5 R from Schwenk Cement. The flow-enhancing effect of the non-ionic molecules was tested in the presence of a commercial

IPEG-type PCE. This PCE is composed of acrylic acid and isoprenolether polyethylene glycol (IPEG) in a molar ratio of 4.5 : 1 and comprises 50 ethylene oxide units in the side chain, thus designating the polymer as 50IPEG4.5. The IPEG PCE exhibits a M_n = 36,000 g/mol and M_w = 82,000 g/mol which results in a PDI of 2.3. The anionic charge amount of the PCE was 1,320 µeq/g in deionized (DI) water (pH = 7) and 689 µeq/g in synthetic cement pore solution (SCPS) (pH = 12.8).
A large number of different glycol derivatives was screened for their effectiveness as non-ionic co-dispersants including diethylene glycol (DEG), triethylene glycol (TEG), diethylene glycol monomethyl ether (DEGMME), diethylene glycol dimethyl ether (DEGDME) and dipropylene glycol dimethyl ether (DPGDME). Furthermore, a di-functional polyether amine (Jeffamine® D-230; JA) was tested. Charge titration experiments of the small molecules in SCPS confirmed their non-ionic character, thus no electrostatically driven interaction between the small molecules and the cement surface should occur. An overview of the chemical structures of the different small molecules tested are illustrated in **Figure 1**.

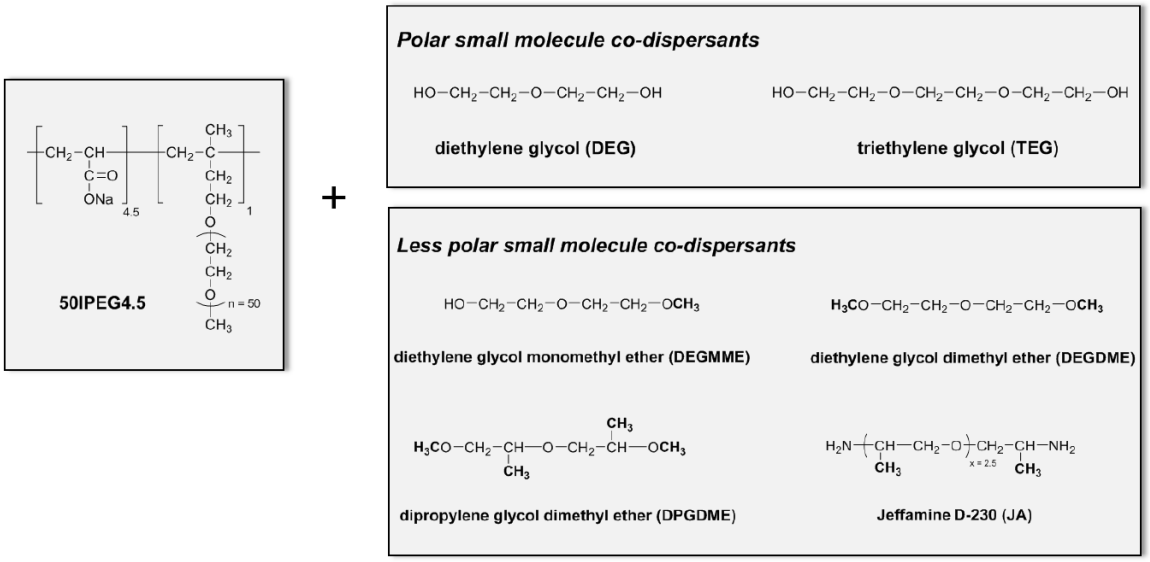

Figure 1. Combination of 50IPEG4.5 with different non-ionic small molecule co-dispersants.

2.2. Cement dispersion

The dispersing efficacy of the non-ionic molecules was evaluated with a series of mini slump tests which were performed according to DIN EN 1164. A detailed description of the experimental procedure can be found in [7]. All experiments were carried out at a temperature of 20 °C and a relative humidity of 30 % to ensure the reproducibility of the results.

2.3. Adsorption measurements

To gain a better understanding of the role of the non-ionic co-dispersants on the adsorption behavior of the IPEG-PCE, adsorption measurements were carried out using the depletion method as described in [7]. Adsorption isotherms of the individual IPEG-PCE and the non-ionic small molecule Jeffamine® D-230 as well as of combination of both additives were captured at a w/c ratio of 0.30.

2.4. Concrete lab tests

To investigate the effect of the co-dispersants on the flow properties of a SCC, concrete lab tests were performed in a ready mix concrete plant. The concrete comprised a Portland/limestone cement CEM II/A-LL 42.5 R as well as fly ash and limestone powder as supplementary cementitious materials and was prepared at a w/c ratio of 0.35. The mix proportion of the SCC is shown in **Table 1**:

Table 1: Mix proportion of the SCC used in the study.

0/4 sand	4/8 gravel	8/16 gravel	Cement	Fly ash	Limestone powder	Water
7.960 kg	1.953 kg	5.107 kg	3.440 kg	0.400 kg	0.400 kg	1.204 kg

The SCC was prepared as follows: First, sand and the coarse aggregates were added to a bucket mixer and homogenized for one minute. Consequently, one third of the fresh water was added and the aggregates were soaked for 10 min. Fly ash, limestone powder and cement were then added to the aggregates and mixed with the remaining amount of water. The superplasticizer and the non-ionic co-dispersant were added simultaneously after 20 sec to the concrete and mixing was continued for additional 5 min. Next, the slump flow of the SCC was determined according to DIN EN 12350-8. The PCE was dosed in such an amount to achieve a spread flow of ~ 750 mm. After the spread flow test, the concrete was transferred back into the bucket mixer and stirred for 2 min. Finally, the SCC was poured into a V-funnel and the empty time was recorded according to DIN EN 12350-9.

3. Results and discussion

3.1. Influence of polarity of non-ionic small molecules on dispersing effectiveness

First, 50IPEG4.5 was combined with various non-ionic glycol compounds in cement pastes at w/c = 0.22 to investigate the impact of the chemical structure of the co-dispersant on the paste fluidity. A wide range of different glycol derivatives was tested whose structures are presented in **Figure 1**. The glycol compounds were selected to exhibit different proportions of non-polar moieties in their structure in order to evaluate if any benefit can be achieved from the incorporation of hydrophobic groups into these molecules. The mini slump tests were conducted using combinations of 0.215 % bwoc of

50IPEG4.5 (= dosage corresponds to a spread flow of 18 ± 0.5 cm) and different amounts of the non-ionic small molecules. The results of the tests are illustrated in **Figure 2**.

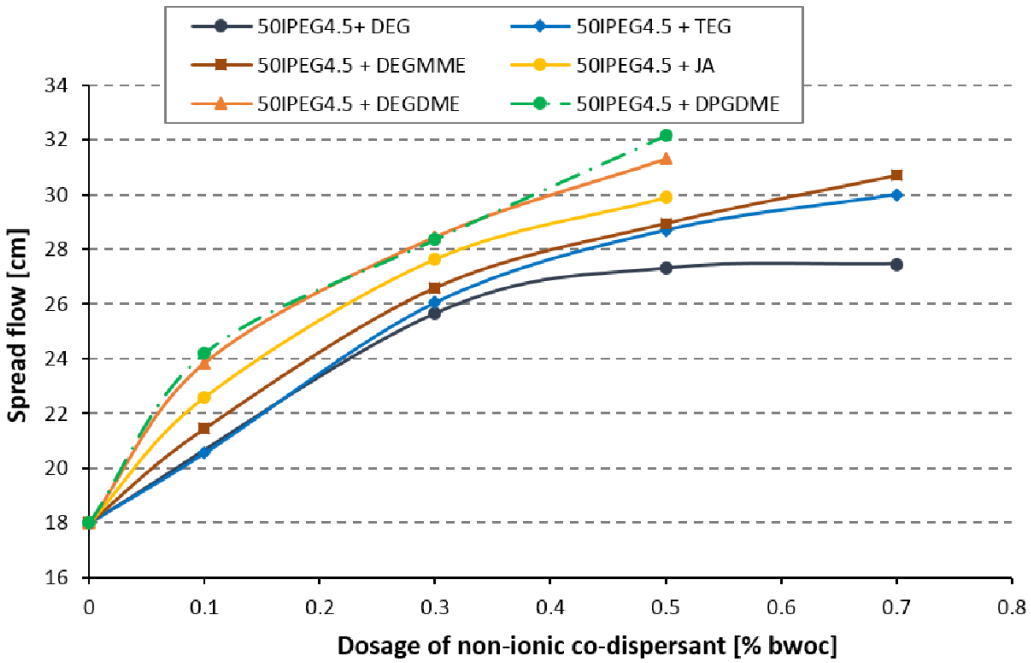

Figure 2. Spread flow of cement pastes admixed with 0.215 % bwoc of 50IPEG4.5 and different dosages of the non-ionic co-dispersants at w/c = 0.22.

As shown in **Figure 2**, the less polar glycol derivatives (e.g. DEGDME, DPGDME, JA) are more effective co-dispersants than the more polar ones (e.g. DEG, TEG, DEGMME). For instance, by admixing 0.1 % bwoc DPGDME a significant improvement of the slump flow from 18 cm to 24 cm can be attained. For all less polar molecules, comparable paste fluidities can be observed at smaller dosages (0.1 – 0.3 % bwoc), whereas at higher dosages (e.g. 0.5 % bwoc) the differences become more pronounced. Here, a clear relationship between the amount of non-polar moieties in the structure and the flow enhancing effect can be identified. The less polar glycol derivatives can be arrayed according to their dispersing effectiveness in following order: DPGDME > DEGDME > DEGMME. The performance of the co-dispersants declines in this sequence as fewer hydrophobic and more polar groups are incorporated. To be more specific, DPGDME represents the most powerful small molecule at a dosage of 0.5 % bwoc (spread flow increase: 14 cm) as it contains four non-polar and hydrophobic methyl groups, while DEGMME is less effective since it exhibits only one hydrophobic methyl functionality (spread flow increase: 11 cm). These results clearly suggest that via the polarity of the small molecules, their spread flow enhancing effect can be manipulated specifically.

3.2. Adsorption measurements

To further elucidate the working mechanism of the non-ionic small molecules adsorption measurements were carried out. First, the individual adsorption isotherms of 50IPEG4.5 and the non-ionic co-dispersant Jeffamine® D-230 were developed at w/c = 0.30.

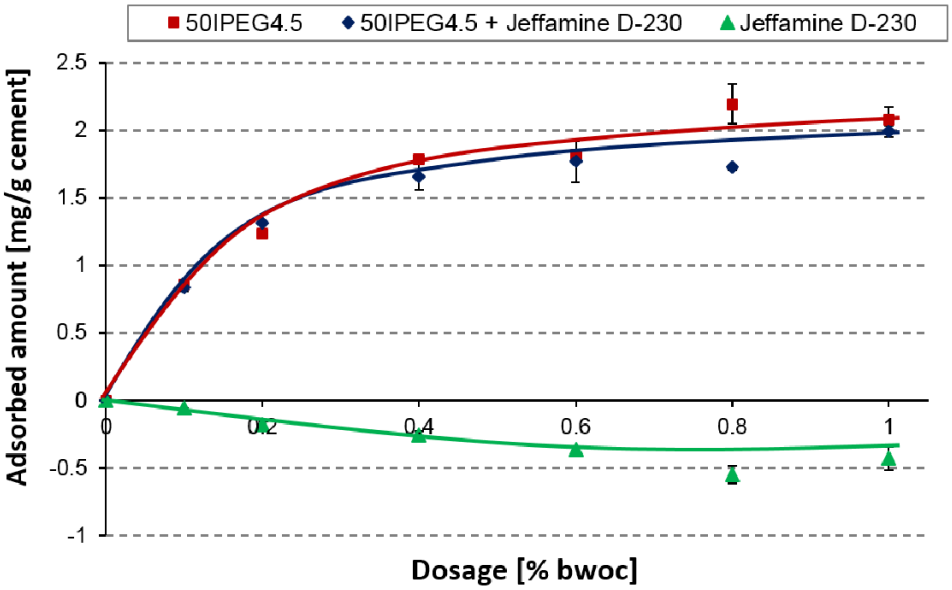

Figure 3. Adsorption isotherms on CEM I 52.5 N (w/c= 0.30) of 50IPEG4.5 and Jeffamine® D-230 as well as of 1 : 1 (wt/wt) combinations.

It can be seen from **Figure 3** that the IPEG PCE exhibits a saturated adsorbed amount of ~ 2 mg/g cement whereas for individual Jeffamine® no adsorption was detected. Even negative adsorption values were found which can be attributed to the water loss resulting from initial wetting and hydration of the cement. Furthermore, the effect of Jeffamine® on the adsorption behavior of 50IPEG4.5 was ascertained by using 1 : 1 (wt/wt) mixtures of the non-ionic co-dispersant and the superplasticizer for the measurement. The amount of Jeffamine® adsorbed in the presence of the IPEG PCE was quantified via the nitrogen content (amine groups). It was found that Jeffamine® does not adsorb on cement nor shows any concomitant adsorption when admixed to the PCE. Moreover, the Jeffamine® does not affect adsorption of 50IPEG4.5, as almost the same values for the saturated adsorbed amount were found in the presence and absence of the co-dispersant. These results clearly imply that the spread flow enhancing effect solely derives from the non-ionic molecules which remain dissolved in the interstitial pore solution.

3.3. Impact of the non-ionic glycol compounds on the V-funnel empty time of SCCs

Next, concrete lab tests were carried out in a ready mix concrete plant to investigate the performance of some selected co-dispersants in SCC with respect to the flow speed as

presented by the empty time from the V-funnel. The SCC used for the experiments comprised a Portland/limestone cement and was prepared at a w/c of 0.35. A dosage of 1.3 % bwoc of 50IPEG4.5 was needed to achieve the targeted slump flow of 750 mm. Although this SCC exhibited a high final slump flow value, it showed a very sticky, honey-like consistency combined with a creeping flow behavior. However, when admixing combinations of the non-ionic co-dispersants (e.g. DEG, DPGDME) and the PCE to the concrete, the stickiness was reduced and a more flowable concrete was obtained. This effect became evident by much faster empty times of the SCC from the V-funnel. After addition of the co-dispersants, the empty times were reduced from 21 sec to 13 sec which corresponds to a decrease of almost 40 % (see results in **Table 2**). It is obvious that such concretes can be processed much easier and faster at the construction site. Most interestingly, it was established here that the non-ionic molecules do not affect the fluidity (= spread flow) of the SCC, but only decrease the plastic viscosity which results in faster flow. These results differ from those obtained in cement paste where the co-dispersants also increased the fluidity of the lime phase and thus induced a higher spread flow value (see **Figure 2**).

Table 2. Spread flow and V-funnel empty times of SCCs admixed with 50IPEG4.5 and different non-ionic co-dispersants.

System	Spread flow	V-funnel empty time
1.3 % bwoc 50IPEG4.5	750 mm	21 sec
1.3 % bwoc 50IPEG4.5 + 1.1 % bwoc DPGDME	750 mm	13 sec
1.3 % bwoc 50IPEG4.5 + 1.3 % bwoc DEG	740 mm	14 sec

3.4. Mechanistic model for the effect of the non-ionic small molecules

Finally, a mechanistic model was developed which can explain the working mechanism of the non-ionic co-dispersants. Since adsorption measurements have proven that the non-ionic small molecules do not adsorb onto the cement surface nor increase the adsorbed amount of the PCE superplasticizer, it became clear that they remain freely dissolved in the pore solution. There, they can act as osmotic spacer molecules which prevent the cement particles from approaching each other. Otherwise, this would lead to depletion of the non-ionic molecules from some parts of the pore solution which is entropically unfavorable and therefore is avoided. For this mechanism, low w/c are necessary (≤ 0.26) so that the co-dispersants can implement their osmotic spacer effect. At higher w/c, the effect of local depletion of the non-ionic co-dispersants is less significant, because there the cement particles are not so densely packed. By generating a lubricating layer around the cement particles holding adsorbed PCE polymers, the friction during the flow is reduced which entails a much decreased stickiness of the concrete.

4. Summary and conclusion

This study demonstrates that non-ionic glycol derivatives can be used as co-dispersants to reduce the stickiness of cementitious systems formulated at low w/c. In cement paste the small molecules reduce both the yield value and the plastic viscosity of the lime phase, whereas in concrete only the plastic viscosity is decreased. Mini slump tests revealed that less polar glycol species are more effective to enhance paste fluidity. Adsorption measurements confirmed that the co-dispersants do not influence the adsorbed amounts of the PCE, but remain dissolved in the pore solution where they act as an osmotic spacer. Additionally, they can provide lubrication between adjacent cement particles which reduces the friction and leads to much shorter V-funnel empty times. The findings signify that at such low w/c different mechanisms for cement dispersion come into play.

5. Acknowledgement

The authors would like to thank Stefan Schmidt from Schwenk's ready-mix concrete plant in Munich for his support during the concrete tests. Furthermore, the authors are very grateful to Clariant, BASF and Huntsman for providing the different non-ionic glycol compounds. Moreover, the authors greatly acknowledge the financial support of DFG (project number: 387082770) within the frame of the SPP 2005 "Opus Fluidum Futurum – Rheology of reactive, multiscale, multiphase construction materials".

References

[1] J. Liu, K. Wang, Q. Zhang, F. Han, J. Sha, J. Liu, Influence of superplasticizer dosage on the viscosity of cement paste with low water-binder ratio, Constr. Build. Mater. 149 (2017) 359-366.

[2] A. Lange, T. Hirata, J. Plank, Influence of the HLB value of polycarboxylate superplasticizers on the flow behavior of mortar and concrete, Cem. Concr. Res. 60 (2014) 45-50.

[3] W. Schmidt, J. Brouwers, H. C. Kühne, B. Meng, Effects of superplasticizer and viscosity-modifying agent on fresh concrete performance of SCC at varied ambient temperatures; Design, Production and Placement of Self-Consolidating Concrete, RILEM Bookseries 1 (2010) 65-77.

[4] M. Ushiro, D. Atarashi, H. Kawakami, E. Sakai, The effect of superplasticizer present in pore solution on flowability of low water-to-powder cement paste, Cement Science and Concrete Technology 67 (2013) 102-107.

[5] L. Shui, Z. Sun, H. Yang, X. Yang, Y. Ji, Q. Luo, Experimental evidence for a possible dispersion mechanism of polycarboxylate-type superplasticizers, Adv. Cem. Res. 28 (2016) 287-297.

[6] A. Lange, J. Plank, Contribution of non-adsorbing polymers to cement dispersion, Cem. Concr. Res. 79 (2016) 131-136.

[7] M. Ilg, J. Plank, Non-ionic small molecules as flow-enhancers for cementitious systems prepared at low w/c ratios, Proceedings of the 2nd International Confrence on Polycarboxylate Superplasticizers (PCE 2017), Garching (Germany), pp. 235-250.

5.2. Synthese und Charakterisierung eines hyperverzweigten Polycarboxylat-Fließmittels

5.2.1. Publikation #7: Synthesis and Properties of a Polycarboxylate Superplasticizer with a Jellyfish-Like Structure Comprising Hyperbranched Polyglycerols

Polycarboxylat-Fließmittel sind Kammpolymere, die aus einer Hauptkette mit anionischen Carboxylat-Gruppen und mehreren Seitenketten auf Polyethylenglykol-Basis bestehen. Fließmittel mit stark verzweigten Strukturmerkmalen sind in der Literatur bisher wenig bekannt. In dieser Publikation wurde ein solches Fließmittel über drei Reaktionsschritte dargestellt und die Anwendungseigenschaften untersucht. Das neuartige Fließmittel setzt sich aus zwei Strukturblöcken zusammen: wichtigster Baustein ist ein carboxymethyliertes Polyglycerol, das am Ausgangspunkt der Verzweigung zusätzlich eine lineare Polyetheramin-Seitenkette enthält. Aufgrund seiner spezifischen Struktur wurde dieses Polymer auch als „Quallen-förmiges" (*„jellyfish"*) Fließmittel bezeichnet. Um die Eigenschaften sowie den sterischen Effekt der einzelnen Strukturbausteine zu ermitteln, wurden zusätzlich ein hyperverzweigtes Polymer ohne Seitenkette sowie ein lineares, unverzweigtes Dicarboxylat synthetisiert.

Die erfolgreiche Synthese des Fließmittels konnte über NMR- und FTIR-Spektroskopie nachgewiesen werden. Durch die Anwendung der *„Slow Monomer Addition"*-Strategie wurde ein Polymer mit einer einheitlichen Molmassenverteilung und einer niedrigen Polydispersität (PDI = 1,4) erhalten. Untersuchungen im Zementleim ergaben, dass das hyperverzweigte PCE im Gegensatz zu einem kammförmigen MPEG-PCE eine langanhaltende Fließwirkung ermöglicht und eine hohe Sulfatrobustheit aufweist, das heißt, dass die Dispergierwirkung nicht durch Sulfationen beeinträchtigt wird, die in einer kompetitiven Adsorption zum Fließmittel stehen. Zudem ist das hyperverzweigte Fließmittel dosierungseffizienter als das lineare Dicarboxylat und das carboxymethylierte hyperverzweigte Polyglycerol. Dies verdeutlich, dass sowohl die Seitenkette als auch das Polyglycerolgerüst erforderlich sind, um eine ausreichend gute sterische Stabilisierung zu erzielen. Aufgrund der spezifischen Polymerstruktur adsorbiert das Fließmittel hauptsächlich über die endständigen Carboxylatgruppen auf der Zementkornoberfläche, wobei die lineare Polyetheraminseitenkette nahezu

senkrecht in die Porenlösung ragt („*Tail*"-Adsorptionsmodus). Diese Adsorptionskonformation erfordert eine höhere Dosierung für eine effektive Oberflächenbelegung als bei einem kammförmigen PCE, welches sich bevorzugt in einer Schleifenkonformation auf der Oberfläche anlagert und dadurch mehrere Bereiche gleichzeitig besetzen kann. Dies wurde aus den Ergebnissen der Adsorptionsmessungen über die Berechnung der Anzahl an Carboxylat-Gruppen pro Flächeneinheit hergeleitet (sh. **Abbildung 45**). Außerdem ergaben Untersuchungen im Wärmeflusskalorimeter, dass das hyperverzweigte Fließmittel die Zementhydratation mehr verzögert als das MPEG-PCE. Dies wurde auf drei Effekte zurückgeführt. Zum einen besitzt das Polymer wegen der vielen Carboxylat-Gruppen eine hohe Bereitschaft Ca^{2+}-Ionen zu binden, andererseits wird durch den speziellen Adsorptionsmodus die Oberfläche stärker abgeschirmt. In der Folge wird der Wasserzutritt zu den oberflächennahen Bereichen erschwert und die Zementhydratation dadurch verlangsamt. Zudem konnte über Kalorimetrieversuche mit Polymerzwischenstufen gezeigt werden, dass die Hydroxylgruppen des Polyglycerols ebenfalls einen verzögernden Effekt haben.

Unter Berücksichtigung aller Ergebnisse wurde gefolgert, dass das hyperverzweigte Polyglycerol-basierte Fließmittel für Anwendungen interessant ist, in denen lange Verarbeitungszeiten benötigt werden (z.B. Transportbeton). Außerdem kann die verzögernde Wirkung des Fließmittels in heißen Ländern ein Vorteil sein. Dort werden üblicherweise Verzögerer zusätzlich eingesetzt, um die Zementhydratation zu verlangsamen und eine gute Verarbeitbarkeit über einen längeren Zeitraum sicherzustellen.

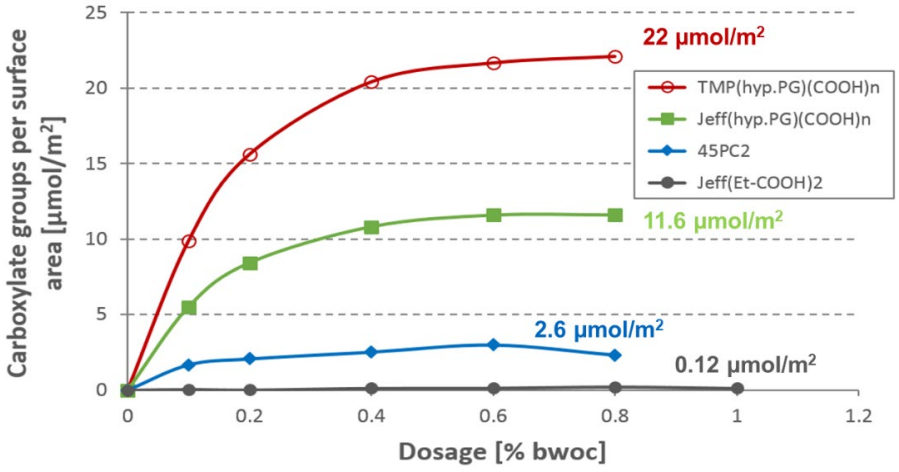

Abbildung 45: Anzahl der Carboxylat-Gruppen pro Flächeneinheit der in der Arbeit synthetisierten Polymere [246].

Publikation #7

Synthesis and Properties of a Polycarboxylate Superplasticizer with a Jellyfish-Like Structure Comprising Hyperbranched Polyglycerols

Manuel Ilg, Johann Plank

Industrial & Engineering Chemistry Research

58 (29) (2019) 12913 – 12926

Doi: 10.1021/acs.iecr.9b02077

I&EC research
Industrial & Engineering Chemistry Research

Article

Cite This: Ind. Eng. Chem. Res. 2019, 58, 12913−12926

pubs.acs.org/IECR

Synthesis and Properties of a Polycarboxylate Superplasticizer with a Jellyfish-Like Structure Comprising Hyperbranched Polyglycerols

Manuel Ilg and Johann Plank*

Chair for Construction Chemistry, Technische Universität München, Lichtenbergstraße 4, Garching 85748, Germany

Supporting Information

ABSTRACT: Polycarboxylate superplasticizers (PCEs) are comb-shaped polymers with an anionic backbone and several nonionic pendant chains, which typically are comprised of polyethylene glycols. In this study, the synthesis of a new type of superplasticizer is presented, which does not exhibit the typical comb-shaped form of PCEs but is built up from a linear polyetheramine and a hyperbranched polyglycerol scaffold, which was carboxymethylated in the periphery. $^{1}H/^{13}C$ NMR and FT-IR spectroscopy and size exclusion chromatography were employed for the characterization of the polymers. Furthermore, their dispersing performance and "slump retention" capability were investigated in cement pastes. Adsorption and zeta potential measurements as well as heat flow calorimetry were conducted to gain more insight into the interaction of the polymers with cement. It was found that such non-comb-shaped polymers are highly effective cement dispersants. Moreover, the hyperbranched superplasticizers exhibited high robustness toward alkali sulfates and maintained the fluidity much longer, compared to a conventional comb-shaped PCE.

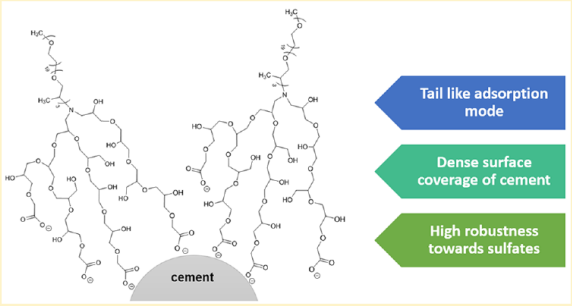

1. INTRODUCTION

Polycarboxylate superplasticizers (PCEs) emerged as one of the most important superplasticizers for concrete due to their superior performance.[1,2] Compared to other products like polycondensates, they fluidize cement even at low water to cement ratios, require relatively low dosages, and exhibit a long slump retention capability.[3−5] The high dispersing efficacy of PCEs can be ascribed to the nonionic side chains, which stretch out into the pore solution and act as a steric barrier to keep the cement particles apart.[6] Moreover, due to the adsorption of the PCEs, a negative surface charge is induced, which also provokes electrostatic repulsion between cement particles.[7] However, a key parameter for effective dispersion represents the adsorbed layer thickness of the PCEs on the cement surface.[8−10] According to the Ottewill Walker equation, a high steric stabilization of particulate suspensions especially can be achieved by polymers which adsorb by forming a particularly thick layer.[11] Therefore, it is assumed that bulky, outstretched, and sterically demanding polymers might produce an even stronger steric effect than comb-shaped PCEs. This hypothesis was confirmed by Liu et al., who showed that star-shaped PCEs are superior over comb-shaped analogues due to their multi-arm structure composed of acrylic acid-*co*-isoprenyloxy polyethylene glycol ether (IPEG), which allows the polymer to reach out far more into the pore solution, thus creating a higher layer thickness.[12] Similar results were also reported for PCEs with a branched topological structure synthesized by free radical copolymerization of acrylic acid, polyethylene glycol methallyl ether (HPEG), and a branched monomer, which was prepared in a two-step synthesis from diallylamine, methyl acrylate, and trimethylolpropane.[13] Even the incorporation of branched lateral chains into comb-shaped PCEs can effectuate a higher steric hindrance effect as was demonstrated by Li and co-workers.[14] They found that the dispersing performance of IPEG-PCEs was considerably improved after the introduction of hyperbranched polyamidoamine side chains synthesized from ethylene diamine and methyl acrylate. All these previous findings suggest that branched structures seem to be very beneficial for the steric stabilization, which is why such motifs are attractive elements for the development of new superplasticizers. Unfortunately, their preparation often involves multiple synthesis steps being tedious and time-consuming.[15−17] Hence, branched polymer structures are needed, which can be formed in just a few reaction steps.

In light of this, hyperbranched polyglycerols represent a promising candidate as they can be obtained in one single step.[18] They are synthesized by anionic ring opening multibranching polymerization (ROMP) of glycidol yielding branched polyether polyols with a globular structure and numerous hydroxyl functionalities in the inner and outer

Received: April 16, 2019
Revised: June 17, 2019
Accepted: June 22, 2019
Published: June 23, 2019

DOI: 10.1021/acs.iecr.9b02077
Ind. Eng. Chem. Res. 2019, 58, 12913−12926

sphere.[19] Hyperbranched polyglycerols have gained much attention over the last years due to their outstanding properties. They are nontoxic and highly water-soluble and exhibit a high chemical stability and low intrinsic viscosity, and their molecular weight can be tuned over a broad range.[18,20] From a chemical perspective, they are highly interesting because the hydroxyl groups in the periphery can be derivatized by various functional groups.[21] Owing to their excellent biocompatibility, hyperbranched polyglycerols are widely used in biomedical and pharmaceutical applications such as in polymer therapeutics, for controlled drug release, in the fabrication of antifouling surfaces, in tissue engineering, or as imaging agent.[20,22] Meanwhile, they were also applied for other purposes such as for the biomimetic crystallization of calcium carbonate[23] or as an additive in aqueous printing inks to improve the color fastness.[24] Hitherto, hyperbranched polyglycerols have not been considered as a structural motif for superplasticizers. Therefore, this study aims to present the synthesis of a new type of superplasticizer, which contains a hyperbranched polyglycerol scaffold, and to evaluate the dispersing properties of such moieties in cement. On the basis of previous work from Frey and co-workers, the hyperbranched polymer was synthesized from a polyether monoamine (Jeffamine) and glycidol using the slow monomer addition approach.[25] Thereafter, some of the hydroxyl groups in the periphery of the polyglycerol scaffold were carboxymethylated to facilitate the adsorption of the polymer on cement. In this way, a polymer was obtained whose structure resembles a jellyfish made up from a linear polyetheramine side chain and a hyperbranched polyglycerol unit. To ascertain the steric effect of this superplasticizer, additionally, a carboxymethylated hyperbranched polyglycerol without any side chain as well as a linear non-hyperbranched molecule with two carboxylate groups were synthesized as reference compounds. The dispersing performance and slump retention ability of all synthesized polymers were investigated via mini-slump tests and compared with the results obtained for a conventional comb-shaped PCE. Isothermal heat flow calorimetry as well as adsorption and zeta potential measurements were performed to elucidate the working mechanism of the novel hyperbranched superplasticizer. The overall goal of this study was to find out whether hyperbranched polyglycerols can provoke a sufficient steric hindrance effect.

2. MATERIALS AND METHODS

2.1. Cement. An ordinary Portland cement CEM I 52.5 N ("Milke classic" from HeidelbergCement, plant Geseke, Germany) was used in the study. Its phase composition as obtained by quantitative X-ray diffraction analysis (Q-XRD) using the Rietveld method is shown in Table 1.

The amount of anhydrite ($CaSO_4$) and calcium sulfate hemihydrate ($CaSO_4 \cdot 1/2H_2O$) was determined by thermogravimetry, and the free lime content was assessed according to the method of Franke. The cement exhibited a d_{50} value of 13.45 μm (determined by laser granulometry) and a specific surface area (Blaine value) of 3479 cm^2/g. The density of the cement was 3.19 g/cm^3 (helium pycnometry).

2.2. Chemicals. Glycidol (purity ≥96%) was received from Arcos Organics, and potassium methoxide (KOMe; ≥90%) was from Alfa Aesar, while trimethylolpropane (TMP; ≥99%), sodium chloroacetate (≥98%), methyl acrylate (≥99%), imidazole (≥99%), phthalic anhydride (≥98%), and sodium hydroxide (≥98%) were obtained from Merck (Darmstadt, Germany).

Table 1. Phase Composition of the Cement Sample As Determined by Q-XRD

phase	wt %
C_3S	53.3
C_2S	25.7
C_3A	8.8
C_4AF	2.6
free lime (Franke)	0.1
anhydrite[a]	3.3
hemihydrate[a]	0.7
dihydrate	0.1
calcite	3.9
quartz	1.0
arcanite	0.5
total	100

[a]Determined by thermogravimetry.

Jeffamine M-1000, which represents a ω-methoxy terminated polyether monoamine with an average molar mass of ~1000 g/mol, was provided by Huntsman (Everberg, Belgium). The Jeffamine contains ethylene (EO) and propylene oxide (PO) units at a molar ratio of 19:3.

Tetrahydrofuran (THF) and methanol were purified via vacuum distillation and stored over a molecular sieve with a pore size of 4 Å. Pyridine (≥99%) was obtained from VWR Chemicals (Darmstadt, Germany) and used as is. The deionized (DI) water was additionally purified by a Diamond water filtration system.

For the synthesis of the reference PCE superplasticizer, sodium persulfate (≥99%) from Merck and 3-mercaptopropionic acid (≥99%) from Sigma-Aldrich were utilized. The MPEG macromonomer (Polyglykol MA 2000) was supplied by Clariant (Burgkirchen, Germany).

2.3. Synthesis of the Hyperbranched Superplasticizer Jeff(hyp.PG)(COOH)$_n$. The hyperbranched superplasticizer (denoted as Jeff(hyp.PG)$(COOH)_n$) was synthesized in a three step synthesis starting from Jeffamine M-1000 (see Scheme 1).

The synthesis was performed in flame-dried glass equipment under argon using a standard Schlenk technique. First, Jeffamine M-1000 was reacted with two equivalents of glycidol to obtain a bis-glycidolized intermediate that contains four hydroxyl groups per molecule.[25] For this purpose, 30 g (30 mmol) of Jeffamine M-1000 was added under argon into a Schlenk flask and heated to 120 °C in an oil bath. Within 30 min, 4 mL (60 mmol, 4.44 g) of glycidol was injected using a syringe over a septum and stirred overnight. The mixture was cooled down from 120 °C to ambient temperature to obtain the bis-glycidolized Jeffamine.

Next, 10% of the hydroxyl groups of the adduct was deprotonated by adding 1.41 mL (5.2 mmol, 0.4 equiv) of a 3.7 M potassium methoxide solution in methanol to 15 g (13.1 mmol, 1 equiv) of the bis-glycidolized Jeffamine and then stirred for 2 h at 70 °C. Thereafter, methanol was completely removed under high vacuum, and the partially deprotonated Jeffamine based intermediate was transferred into a three necked round-bottom flask equipped with a stirrer and a Dean–Stark apparatus using 50 mL of anhydrous THF. The solution was heated up to 120 °C, and THF was evaporated to yield a rather pure deprotonated intermediate. Next, a solution

DOI: 10.1021/acs.iecr.9b02077
Ind. Eng. Chem. Res. 2019, 58, 12913−12926

Scheme 1. Synthesis of the Jellyfish-Like Superplasticizer Jeff(hyp.PG)(COOH)$_n$

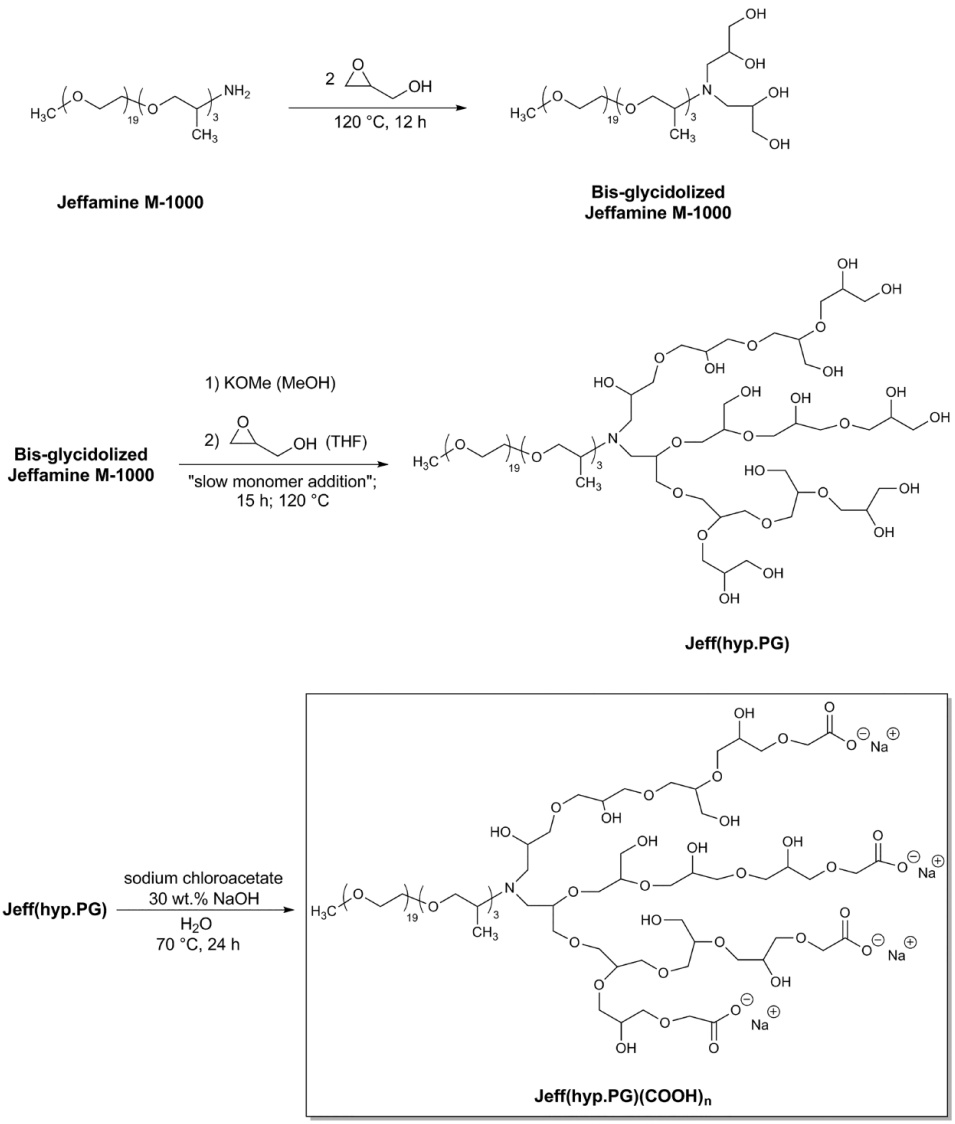

of 35 mL (38.9 g, 525 mmol, 40 equiv) of glycidol in 120 mL of THF was slowly added over 15 h using a peristaltic pump. After addition was complete, 60 mL of THF was added, and the solution was stirred for another 2 h at 100 °C. THF was finally evaporated under reduced pressure to obtain brownish, highly viscous Jeff(hyp.PG) polymer as the intermediate.

The hydroxyl groups of the polyglycerol scaffold were then carboxymethylated as a final step. At first, 37 g (corr. to 373 mmol of OH groups) of Jeff(hyp.PG) was dissolved in aqueous NaOH solution prepared from 25.4 g of NaOH and 80 mL of DI water. Subsequently, a solution of 73.9 g (634 mmol) of sodium chloroacetate in 95 mL of DI water was added within 30 min at ambient and heated to 80 °C for 20 h. The solution was cooled to ambient temperature, and the pH was adjusted from 11.7 to 6.0 using 37 wt % HCl. The product was purified via dialysis using dialysis membranes (Spectra/Por7 from Spectrum Laboratories) with a molecular weight cut off (MWCO) of 1 kDa. Dialysis was performed in 2 L of DI water that was exchanged every 2 h over a period of 12 h. The aqueous solution of the purified Jeff(hyp.PG)(COOH)$_n$ was concentrated under vacuum to a solid content of 30 wt %. The hyperbranched superplasticizer was obtained as a yellowish, slightly viscous polymer solution with a pH of 5.1.

2.4. Synthesis of TMP(hyp.PG)(COOH)$_n$. Moreover, a carboxymethylated hyperbranched polyglycerol was synthesized that does not comprise a linear EO/PO side chain. This polymer was denoted as TMP(hyp.PG)(COOH)$_n$ and prepared in a two-step synthesis from trimethylol propane (TMP) and glycidol (see Scheme 2).

Synthesis was performed following the general procedure presented for the hyperbranched Jeff(hyp.PG)(COOH)$_n$, and a detailed description can be found in refs 19 and 23. The anionic ring opening polymerization of glycidol was initiated by the partially deprotonated (10%) TMP and carried out in

DOI: 10.1021/acs.iecr.9b02077
Ind. Eng. Chem. Res. 2019, 58, 12913−12926

Scheme 2. Synthesis Route for TMP(hyp.PG)(COOH)$_n$ Starting from Trimethylol Propane

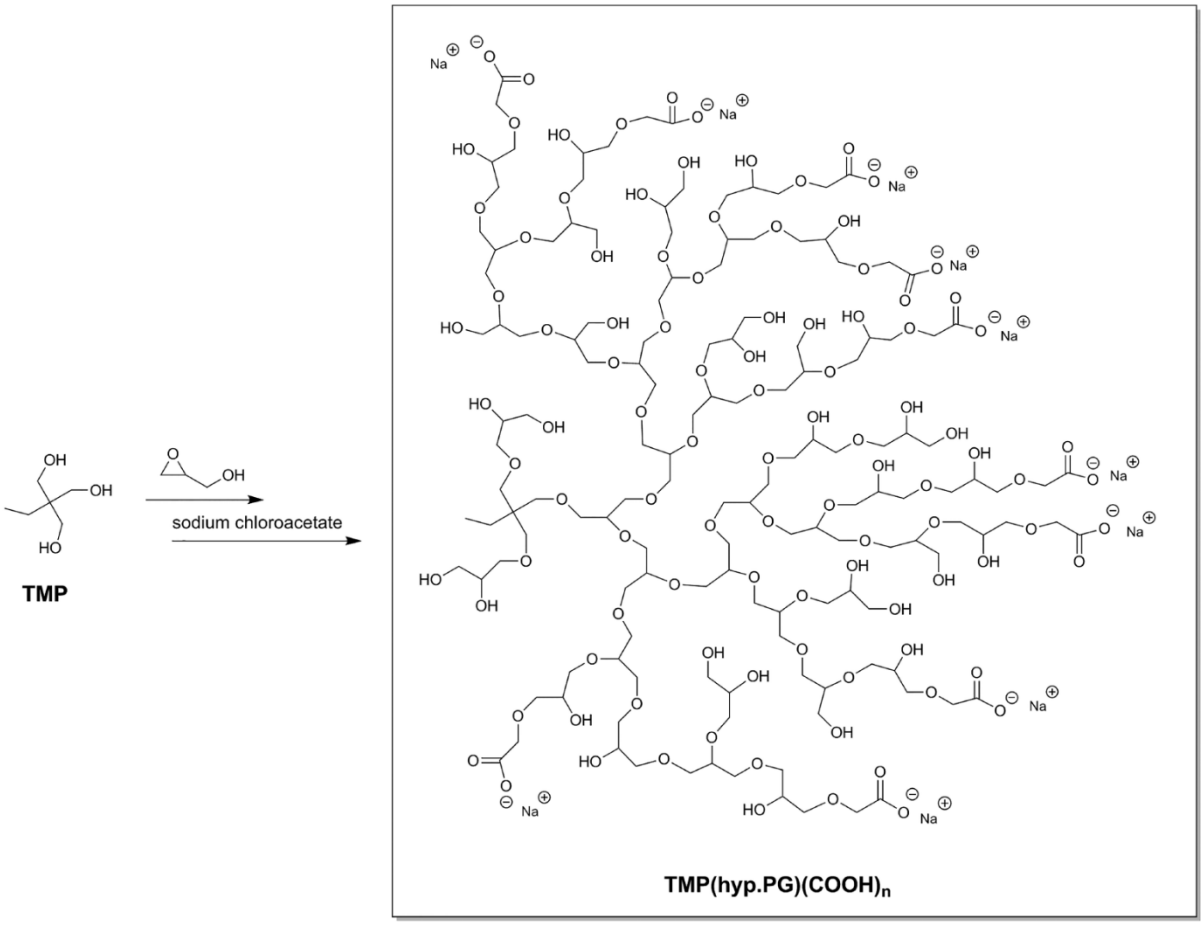

Scheme 3. Synthesis of the Linear, Non-hyperbranched Jeff(Et-COOH)$_2$

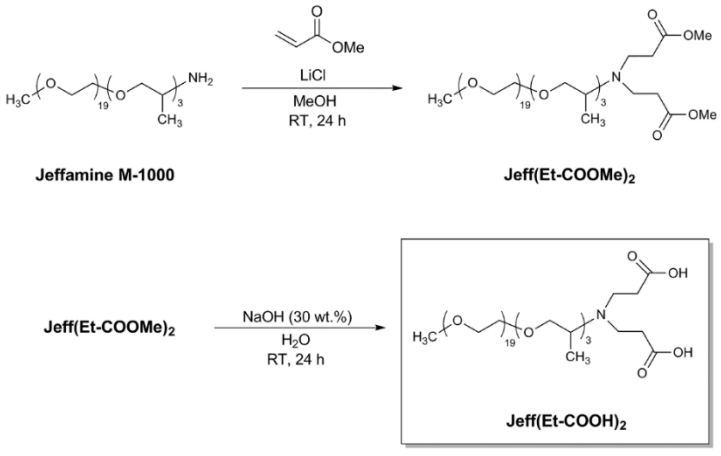

bulk. The molar ratio of glycidol to TMP was 40:1. For the carboxymethylation, 45 g (corr. to 641 mmol of OH groups) of TMP(hyp.PG) was used, dissolved in a NaOH solution prepared from 43.6 g of NaOH in 125 mL of DI water, and then, a sodium cloroacetate solution (127 g in 160 g of DI water, 1.09 mol) was added dropwise over 2 h at ambient temperature. After a reaction time of 20 h at 80 °C and purification of the product via dialysis, TMP(hyp.PG)-(COOH)$_n$ was obtained as a pale yellowish, slightly viscous solution with a solid content of 27 wt % and a pH of 5.8.

DOI: 10.1021/acs.iecr.9b02077
Ind. Eng. Chem. Res. 2019, 58, 12913−12926

Scheme 4. Synthesis of the Comb-Shaped PCE 45PC2

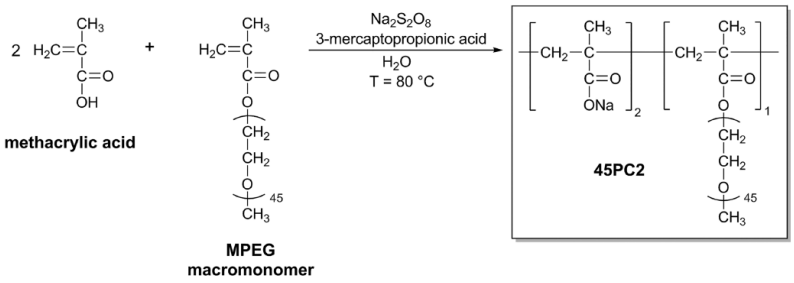

2.5. Synthesis of the linear Jeff(Et-COOH)$_2$. As reference, also a linear, non-hyperbranched molecule was synthesized via a Michael-type reaction of Jeffamine M-1000 and methylacrylate (see Scheme 3).

At first, 100 g (100 mmol, 1 equiv) of Jeffamine M-1000 and 300 mg (7 mmol) of LiCl were dissolved in 80 mL of MeOH and cooled to 0 °C in an ice−water bath. Thereafter, 30.1 g (350 mmol, 3.5 equiv) of methyl acrylate was added over 10 min and stirred for 1 day at ambient. After MeOH was removed under reduced pressure, alkaline hydrolysis of the ester functionalities was carried out. First, the residue was dissolved in 70 g of DI water; then, 55 g of a 30 wt % NaOH solution was added, and the aqueous solution was stirred for another day at ambient. Purification was carried out via dialysis according to the procedure presented above. Finally, the aqueous purified Jeff(Et-COOH)$_2$ solution was concentrated under vacuum, and a cationic exchange resin (Dowex 50WX8 hydrogen form, 200−400 mesh) was added to adjust to a slightly acidic pH of 6. The solution was stirred overnight, and the exchange resin was removed by vacuum filtration. After evaporation of the solvent under reduced pressure, Jeff(Et-COOH)$_2$ remained as a white, wax-like solid.

2.6. Synthesis of the Comb-Shaped PCE Superplasticizer. The comb-shaped superplasticizer was synthesized by aqueous free radical copolymerization of methacrylic acid and ω-methoxypolyethylene glycol methacrylate (MPEG macromonomer comprising 45 ethylene oxide units) (see Scheme 4).

The PCE was prepared at a molar ratio of methacrylic acid to MPEG macromonomer of 2:1; thus, it was designated as 45PC2. Synthesis was carried out as follows: 45 g of DI water was added into a five necked round-bottom flask equipped with a stirrer, inlet for N_2 gas, reflux condenser, and thermometer, purged with N_2 for 1 h, and subsequently heated to 80 °C. Next, two solutions were prepared. Solution I presented a mixture of 19 g (221 mmol, 2 equiv) of methacrylic acid, 402 g (111 mmol, 1 equiv) of MPEG macromonomer (55 wt % solution) and 2.34 g (22 mmol, 0.2 equiv) of 3-mercaptopropionic acid (= chain transfer agent) in 20 g of DI water, while solution II consisted of 2.63 g (11 mmol, 0.1 equiv) of sodium persulfate (= initiator) in 80 g of water. Both solutions were fed continuously over 4 h (solution I) or 5 h (solution II) into the reaction vessel using two peristaltic pumps. After addition was complete, the polymer solution was stirred for one more hour at 80 °C and cooled to ambient. Finally, a pH of 7 was adjusted by using 30 wt % NaOH to obtain a yellowish, slightly viscous polymer solution with a solid content of 31.9 wt % as final product.

2.7. Characterization of the Polymers. *2.7.1. Titration According to Elder and Co-Workers.*[26] The number of hydroxyl groups in the polyglycerol scaffold of TMP/Jeff(hyp.PG) was determined by the titration method established by Elder and co-workers.[26] On the basis of this value, the amount of sodium chloroacetate was calculated. A detailed description of the procedure can be found in the Supporting Information.

2.7.2. NMR and FT-IR Analysis. ^{1}H and ^{13}C NMR spectra were recorded on an AVANCE-III 400 MHz NMR spectrometer (Bruker BioSpin GmBH, Karlsruhe, Germany). The chemical shifts were referenced to the residual non-deuterated solvent signal (D_2O: ^{1}H NMR δ = 4.79 ppm). Infrared spectra were measured on a Vertex 70 FT-IR spectrometer (Bruker) using a diamond ATR unit.

2.7.3. Size Exclusion Chromatography. The molar masses (M_w, M_n) and the polydispersity (PDI) of the polymer samples were determined by size exclusion chromatography (SEC) using a Waters separation module equipped with a refractive index detector (2414 module from Waters, Eschborn, Germany) and a Dawn EOS 3 angle static light scattering detector (Wyatt Technology, Clinton, IA). Solutions of the polymers with a concentration of 10 g/L were prepared using 0.1 M $NaNO_3$ as solvent (adjusted with NaOH to pH = 12), which was also applied as eluent for the SEC instrument. The solutions were filtered through a 0.2 μm syringe filter and separated on a precolumn and three Ultrahydrogel columns (150, 250, 500) at a flow rate of 1.0 mL/min. For the calculation of M_w and M_n, a dn/dc of 0.12 mL/g (value for polyglycerol) was adopted,[27] whereas for the comb-shaped and linear polymer, a dn/dc of 0.135 mL/g (value of poly(ethylene oxide)) was utilized.[28]

2.7.4. Anionic Charge Amount. For the quantitative determination of the anionic charge amount, a polyelectrolyte titration was conducted using a particle charge titrator (PCD 03 pH from BTG Instruments, Herrsching, Germany). The streaming potential of the anionic polymers was captured through titration of a cationic polyelectrolyte (polyDADMAC) until charge neutralization was achieved. At first, aqueous solutions of the superplasticizer samples (conc. 0.1 g/L) were prepared using a synthetic cement pore solution (SCPS; pH = 12.8) and 0.1 M NaOH (pH = 13) as solvent. The SCPS was prepared from 1.720 g of $CaSO_4 \cdot 2H_2O$, 6.959 g of Na_2SO_4, 4.757 g of K_2SO_4, and 7.120 g of KOH in 1 L of DI water, whose ion content represents the typical composition of the pore solution of an ordinary Portland cement. For the measurement, 10 mL of the polymer solution was pipetted into the measuring cell of the instrument, and a 0.001 M polydiallyldimethylammonium chloride (polyDADMAC) sol-

DOI: 10.1021/acs.iecr.9b02077
Ind. Eng. Chem. Res. 2019, 58, 12913−12926

ution was titrated to the sample until the isoelectric point (= 0 mV) was reached. Every sample was measured three times, and the values obtained were averaged. The anionic charge amount of the polymers was calculated from the amount of consumed polyDADMAC as described in ref 29.

2.7.5. Hydrodynamic Radius. The hydrodynamic radius (R_h) of the polymers was measured via dynamic light scattering (DLS) using a Zetasizer Nano instrument (Malvern Instruments, Worchestershire, UK). Aqueous solutions of the polymers with a concentration of 10 g/L were prepared in SCPS and filtered through a 0.2 μm syringe filter into a cuvette to remove dust particles, which could impair the measurement due to their high light scattering intensity. The cuvette was placed into the instrument and equilibrated for 120 s at 25 °C before the measurement was started. The hydrodynamic radius was captured five times for every sample, and the average was reported.

2.8. Test Methods. *2.8.1. Dispersing Efficacy.* The dispersing performance of the polymers was ascertained via mini slump tests, which were performed according to DIN EN 1015. First, the water-to-cement ratio (w/c) of the neat cement paste for a spread flow of 18 ± 0.5 cm was established. This value was used for all consecutive experiments. The mini slump tests were conducted as follows: At first, the superplasticizer was predissolved at a respective dosage (0.1−1.2% bwoc) in the mixing water contained in a porcelain cup. The water content of the superplasticizer solution was subtracted from the total amount of mixing water to perform all experiments at the same w/c ratio. Then, 300 g of cement was added over 1 min to the mixing water, soaked for 1 min, and subsequently agitated manually for 2 min with a spoon. Next, the cement slurry was transferred into a Vicat cone (height of 40 mm, top diameter of 70 mm, bottom diameter of 80 mm) placed on a glass plate and filled to the brim. The cone was immediately lifted upward and kept for 5 s over the spreading cement paste. The diameter of the cement slurry was measured twice with a caliper, the first measurement being vertically to the second one, and averaged to obtain the spread flow value. The mini slump tests were carried out at a temperature of 20 ± 1 °C.

Additionally, time-dependent mini slump tests were performed to ascertain the evolution of the paste fluidity over time. For these experiments, 500 g of cement was used and admixed at a w/c ratio of 0.50 with the corresponding dosage of the superplasticizers for a spread flow of 26 ± 0.5 cm. The cement slurry was prepared according to the procedure presented above and, after each measurement, was transferred back into the porcelain cup. The porcelain cup was covered with a wet towel to avoid any desiccation of the cement paste. Prior to each mini slump test, the cement paste was vigorously stirred for 2 min with a spoon. The slump (= fluidity) retaining capability of the polymers was investigated over a total period of 8 h.

2.8.2. Adsorption Measurements. Adsorbed amounts of the polymers on cement were determined via the depletion method. Here, the amount of polymer remaining in the interstitial pore solution at the equilibrium condition after the contact with the cement was quantified by measuring the total organic carbon (TOC) content of cement pastes admixed with different dosages of the superplasticizers (i.e., 0.1−1.0% bwoc). In a typical experiment, 15 g of cement was added to 7.5 mL of DI water (w/c = 0.50) and the respective amount of polymer, placed in a centrifuge tube, homogenized for 2 min with a vortex mixer, and centrifuged for 10 min at 8500 rpm (BioFuge, Haereus). Afterward, the supernatant was filtered through a 0.2 μm syringe filter and diluted with 0.1 M HCl to avoid any carbonation of the sample. The carbon content of the supernatant was quantified using a LiquiTOC-II apparatus from Elementar Analysensysteme GmbH (Hanau, Germany). The measurement was repeated twice for every sample, and the obtained values were averaged and corrected by the blank TOC value found for the neat cement to consider the organic carbon content stemming, e.g., from grinding agents. The adsorbed amount of the polymer was calculated from the difference of the TOC content in the supernatant and the initial polymer solution.

2.8.3. Zeta Potential Measurements. The zeta potential of cement slurries admixed with different amounts of the superplasticizers was determined on a model DT 1200 electroacoustic spectrometer from Dispersion Technology (Bedford Hills, NY, USA). For the measurement, a cement paste was prepared at a w/c ratio of 0.50. Increasing dosages of the polymers (0.01−1.0% bwoc) were added to the slurry under constant stirring in 60 incremental steps via a dosing pump.

2.8.4. Isothermal Heat Flow Calorimetry. To investigate the effect of the polymers on the hydration of cement, heat flow calorimetric measurements were carried out using a TAM Air Thermostat (TA Instruments, Järfälla, Sweden). Four grams of cement was filled into 20 mL glass ampules and mixed with aqueous solutions of the polymer samples to attain a w/c ratio of 0.50. After the addition, the glass ampules were sealed with an aluminum lid, homogenized for 2 min with a vortex mixer, and placed into the calorimeter that was precalibrated at 20 °C. The heat released from cement hydration was captured until the heat evolution subsided completely.

3. RESULTS AND DISCUSSION

3.1. Structural Analysis of the Polymers. The hyperbranched structure of the jellyfish-like superplasticizer was achieved by anionic ring opening polymerization of glycidol using a partially deprotonated bis-glycidolized Jeffamine as initiator. Thus, a diblock copolymer was obtained, composed of one linear polyetheramine side chain and a hyperbranched polyglycerol moiety. The initiator for the ring opening polymerization was synthesized from Jeffamine and two equivalents of glycidol, yielding a bis(2,3-dihydroxypropyl) adduct with four terminal hydroxyl groups.[25] This reaction was quantitative, and the formation of the product was confirmed by ^{1}H/^{13}C NMR spectroscopy (see Figures S6 and S7).

The key step of the synthesis comprised an anionic ring opening multibranching polymerization of glycidol. The hydroxyl groups of the bis-glycidolized Jeffamine were partially deprotonated by potassium methoxide to create nucleophilic initiating sites for the polymerization. After the addition of glycidol, the initiator attacks the unsubstituted end of the epoxide ring causing the ring to open and the formation of a secondary alkoxide and primary hydroxyl group. The fast cation exchange equilibrium between the primary and secondary alcohol group ensures that chain propagation also proceeds from the primary hydroxyl functionalities. The consecutive reaction of the terminal alkoxide groups with glycidol results in the successive formation of the polyglycerol scaffold. To synthesize hyperbranched polyglycerols with controlled molecular weight, low polydispersity, and a high

DOI: 10.1021/acs.iecr.9b02077
Ind. Eng. Chem. Res. 2019, 58, 12913−12926

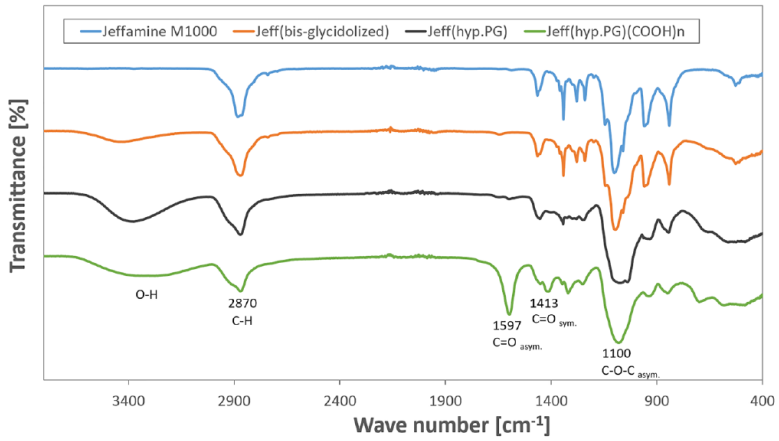

Figure 1. FT-IR spectra of Jeffamine M-1000, the intermediate products, and Jeff(hyp.PG)$(COOH)_n$.

degree of branching, the simultaneous growth of all chain ends has to be ensured. This was achieved by partial deprotonation of the initiator as well as slow monomer addition of glycidol.[19] Contrary to other works in which diglyme or dixoane was used as reaction solvent, the polymerization was carried out here in bulk.[19,25,27] When applying diglyme, we observed a multimodal molecular weight distribution of the polyglycerol with almost no incorporation of the Jeffamine due to solubility problems of this rather polar core unit in the aprotic solvent.

Finally, the hydroxyl groups in the periphery of the polyglycerol scaffold were carboxymethylated. This derivatization was performed under highly alkaline conditions using an excess of sodium chloroacetate (1.7-fold relative to the hydroxyl groups) to ensure a high degree of substitution. Successful introduction of the carboxymethyl functionalities was evidenced by ^{13}C NMR spectroscopy via the signals for the carboxylate group at δ = 177.7 ppm and the carbon atom next to it at δ = 76.9 ppm (see Figure S12). Additionally, the FT-IR spectrum of Jeff(hyp.PG)$(COOH)_n$ showed characteristic absorption bands at 1597 and 1413 cm^{-1}, which can be attributed to the asymmetric and symmetric C═O stretching vibration of the carboxylate group, respectively (Figure 1).

Besides, the absorption band at 2870 cm^{-1} derives from the C−H stretching vibration, and the peak at 1100 cm^{-1} is owed to the asymmetric stretching vibration of the ether linkages (C−O−C) present in the polyetheramine side chain and the polyglycerol moiety. A comparison of the FT-IR spectra of all intermediates and the final product revealed that the intensity of the absorption band of the stretching vibration of the hydroxyl group at ∼3400 cm^{-1} increased from Jeff(bis-glycidolized) to Jeff(hyp.PG) and then decreased and broadened for Jeff(hyp.PG)$(COOH)_n$, thus indicating that some of the hydroxyl groups were indeed consumed and converted into carboxymethyl functionalities.

The carboxymethylated hyperbranched polyglycerol TMP-(hyp.PG)$(COOH)_n$ that exhibits an ethyl group as the "side chain" at the main branching point was synthesized from the trifunctional TMP. The results obtained from FT-IR and NMR analysis (spectra in the Supporting Information) confirmed its formation and are in compliance with data from other studies.[23,30]

The non-hypyerbranched, linear molecule Jeff$(Et\text{-}COOH)_2$ was prepared by a Michael-type reaction of Jeffamine M-1000 and methyl acrylate using catalytic amounts of LiCl to enhance the electrophilic character of the carbonyl carbon atom. Carboxylate groups were then introduced by the alkaline hydrolysis of the methyl ester groups. As a result, the absorption band of the C═O stretching vibration of the ester disappeared at 1736 cm^{-1} and a new band emerged in the FT-IR spectrum at 1595 cm^{-1}, originating from the C═O stretching vibration of the carboxylate group. The $^1H/^{13}C$ NMR and FT-IR spectra of the synthesized Jeff$(Et\text{-}COOH)_2$ are provided in the Supporting Information.

Thus, analysis confirmed that the targeted compounds Jeff(bis-glycidolized), Jeff(hyp.PG), Jeff(hyp.PG)$(COOH)_n$, TMP(hyp.PG)$(COOH)_n$, and Jeff$(Et\text{-}COOH)_2$ were successfully achieved.

3.2. Molecular Characteristics of the Polymers.

Molecular properties of the synthesized polymers were ascertained by SEC. The weight and number-average molecular weights as well as the polydispersity (PDI) of the polymer samples are summarized in Table 2.

Table 2. Molar Masses, Polydispersity (PDI), and Hydrodynamic Radii (R_h) of the Polymers

polymer sample	M_w [g/mol]	M_n [g/mol]	PDI	R_h [nm]
Jeff(hyp.PG)$(COOH)_n$	5250	3790	1.4	6.7 ± 0.2
TMP(hyp.PG)$(COOH)_n$	6840	4720	1.4	5.5 ± 0.5
Jeff$(Et\text{-}COOH)_2$	1360	1330	1.0	1.0 ± 0.1
45PC2	39 780	16 460	2.4	6.5 ± 0.1

The SEC spectra (Figure S1) confirm that the anionic ring opening polymerization of glycidol had indeed produced rather uniform products. Both hyperbranched polymers show an almost monodisperse molecular weight distribution indicated by a narrow polydispersity index of 1.4. In comparison, the free radical copolymerization in the PCE synthesis also produced a homogeneous product (macromonomer conversion of 93%) but with a higher PDI of 2.4. Generally, the hyperbranched polymers exhibit relatively low molar masses compared to the comb-shaped PCE. For instance, the M_w of the jellyfish-like superplasticizer lies at 5250 g/mol, whereas for 45PC2, a value of 39 780 g/mol was found. The dynamic light scattering signal in the SEC spectrum of TMP(hyp.PG)$(COOH)_n$ revealed that the polymer contains a small fraction (<0.1%) of a high

DOI: 10.1021/acs.iecr.9b02077
Ind. Eng. Chem. Res. 2019, 58, 12913−12926

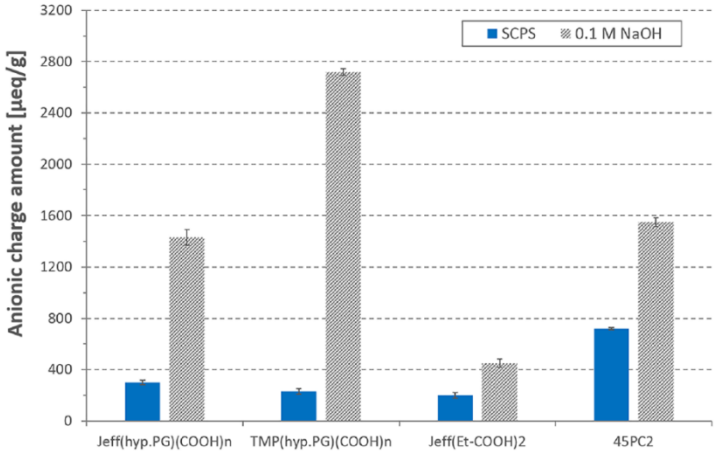

Figure 2. Anionic charge amounts of the synthesized polymers in SCPS and 0.1 M NaOH.

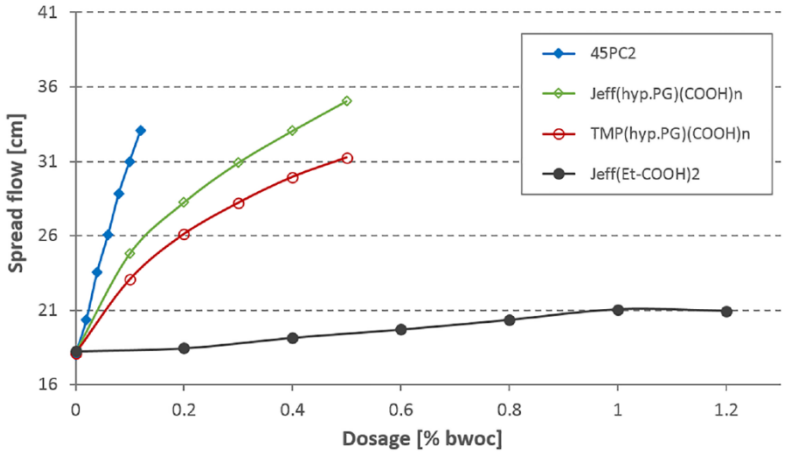

Figure 3. Dosage-dependent effect of the synthesized polymers on cement paste fluidity.

molecular weight compound, which presents a homopolymerized hyperbranched polyglycerol that was presumably formed due to the relatively high viscosity of the reaction mixture. Considering the molar masses of the polymers, it became apparent that TMP(hyp.PG)$(COOH)_n$ holds a higher proportion of the carboxymethylated hyperbranched polyglycerol skeleton than the jellyfish-like superplasticizer.

The hydrodynamic radii of the synthesized polymers are presented in Table 2. According to these results, Jeff(hyp.PG)-$(COOH)_n$ exhibits a higher R_h than TMP(hyp.PG)$(COOH)_n$ and Jeff(Et-$COOH)_2$ as it combines the structural features of both polymers (i.e., hyperbranched polyglycerol scaffold + linear polyetheramine side chain). Surprisingly, the hydrodynamic radius of the comb-shaped PCE 45PC2 was similar to that of the jellyfish-like superplasticizer, in spite of its considerably higher molecular weight. These findings indicate that the comb-shaped PCE has a rather coiled solution conformation, whereas the hyperbranched polymers are more stretched due to the globular structure of the hyperbranched polyglycerol. Also, the propylene oxide units in the Jeffamine slightly contribute to a certain stiffness of the polyetheramine side chain.

Anionicity of the polymers was quantified via charge titration. As can be seen from Figure 2, all polymers tested showed the highest anionic charge amount in 0.1 M NaOH because there the carboxylate groups are fully deprotonated. Much lower values were obtained in SCPS, due to the complexation of Ca^{2+} ions by the carboxylate functionalities. The anionic charge amounts of the jellyfish-like superplasticizer and the comb-shaped PCE were comparable in 0.1 M NaOH, lying at ~1500 μeq/g. However, the highest anionic charge amount was found for TMP(hyp.PG)-$(COOH)_n$ (i.e., 2700 μeq/g in 0.1 M NaOH), implying that there is a large number of carboxylate groups present in the hyperbranched polyglycerol skeleton. Contrary to this, the linear non-hyperbranched Jeff(Et-$COOH)_2$ exhibited a low anionicity because of only two carboxylate groups per molecule. Moreover, the experiments disclosed that both hyperbranched polymers have a high affinity to chelate calcium ions, since a significant decrease of the anionic charge amount was observed in SCPS.

3.3. Dispersing Performance in Cement. The dispersing efficacy of the synthesized polymers was investigated by mini slump tests. Here, different dosages of the polymers (i.e.,

DOI: 10.1021/acs.iecr.9b02077
Ind. Eng. Chem. Res. 2019, 58, 12913−12926

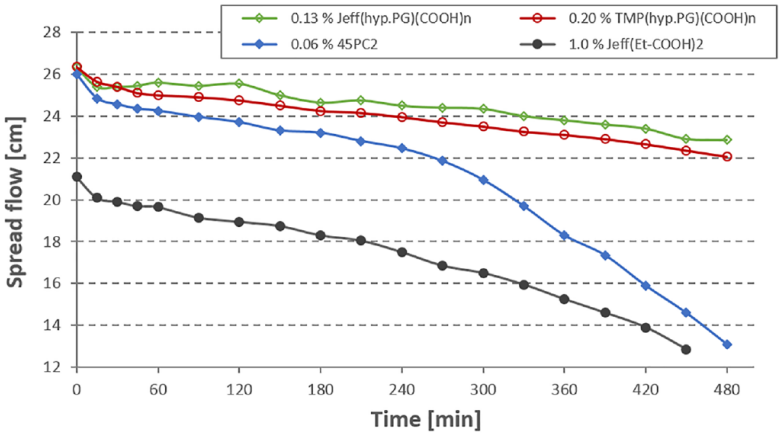

Figure 4. Time-dependent evolution of the spread flow of cement pastes admixed with the synthesized polymers (w/c = 0.50).

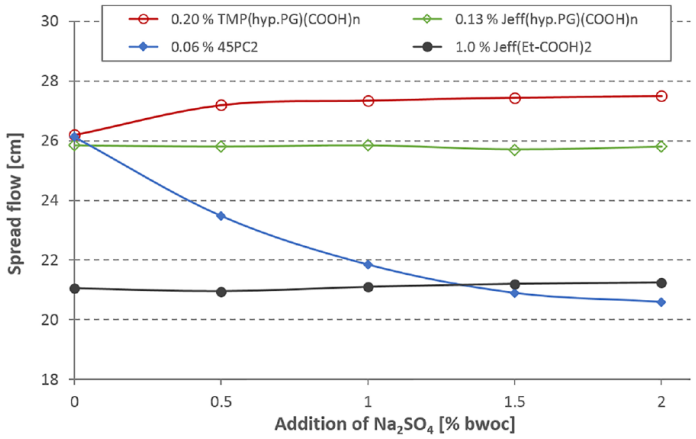

Figure 5. Impact of sodium sulfate additions on the dispersing performance of the polymers.

0.02−1.2% by weight of cement, bwoc) were probed, and their effect on the paste fluidity was ascertained at a w/c ratio of 0.50 (Figure 3). In this way, it was hoped to achieve a better understanding of the relationship between the topological structure of the polymers and their dispersing performance. As is evident from Figure 3, the dispersing ability of the linear, non-hyperbranched molecule Jeff(Et-COOH)$_2$ was rather limited. High dosages were necessary to achieve at least a slight increase of the fluidity (e.g., from 18 to 21 cm at 1.0%). Clearly, the hyperbranched polymers were superior over the linear, non-hyperbranched Jeff(Et-COOH)$_2$. For instance, a dosage of only 0.20% was required for TMP(hyp.PG)-(COOH)$_n$ to achieve a spread flow of 26 cm, while Jeff(hyp.PG)(COOH)$_n$ attained this value already at 0.13%. The higher efficiency of the jellyfish-like superplasticizer can be attributed to the additional steric effect imparted by the linear polyetheramine side chain (see also the higher R_h value in Table 2). The comb-shaped PCE was even more effective and required only 0.06% dosage to achieve a 26 cm spread flow. The higher dispersing efficacy of this polymer can be attributed to its significantly higher side chain density and thus its enhanced steric hindrance effect, compared to the jellyfish dispersant.

3.4. Slump Retention Capability. In the following, the time-dependent fluidity retention of the polymers, which presents an important aspect in actual application, was tested. For this purpose, cement pastes were fluidized with the respective dosages of the polymers to achieve a spread flow of 26 cm, and the evolution of paste fluidity was measured over time.

According to Figure 4, the linear, non-hyperbranched Jeff(Et-COOH)$_2$ showed a very poor slump retention ability even at a dosage as high as 1.0%. Opposite to this, Jeff(hyp.PG)(COOH)$_n$ maintained the initial fluidity over two hours before paste fluidity declined very slowly. Most remarkably, even six hours after the preparation, the cement slurry still exhibited a spread flow of 23.8 cm. A similar behavior was observed for the other hyperbranched polymer TMP(hyp.PG)(COOH)$_n$. However, fluidity of the cement paste admixed with 45PC2, which represents a PCE which is designed to provide particularly long fluidity retention, already within the first 4 h decreased from 26 to 22.5 cm and then declined rapidly, while the hyperbranched polymers still were able to maintain high cement fluidity.

3.5. Dispersing Performance in the Presence of Sulfate. It has been established that the dispersing performance of PCEs often is much lower in cement samples with a

DOI: 10.1021/acs.iecr.9b02077
Ind. Eng. Chem. Res. 2019, 58, 12913−12926

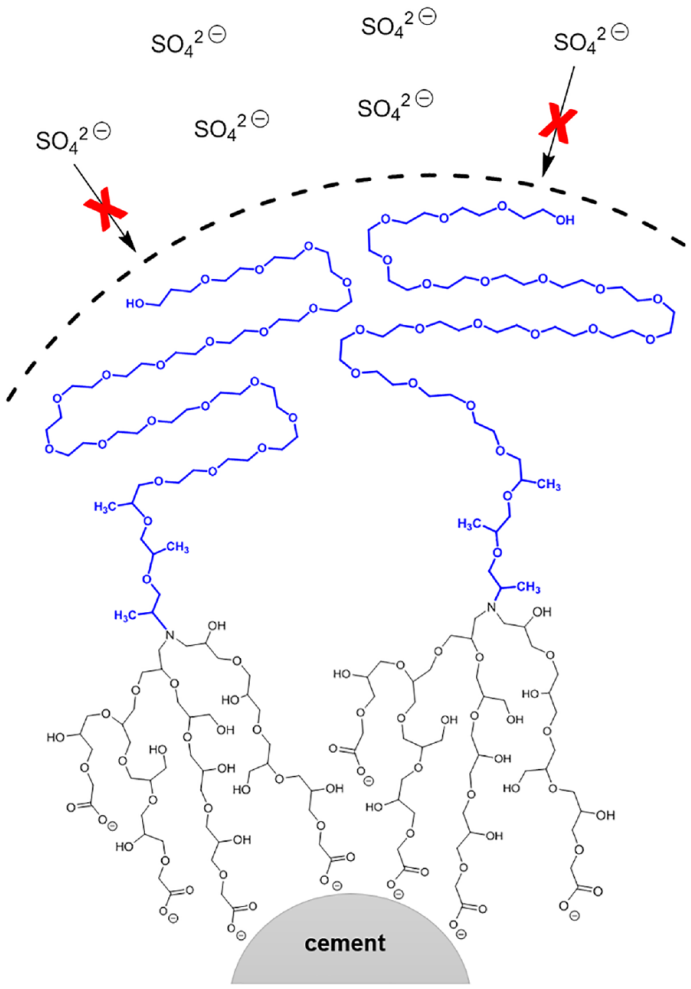

Figure 6. Schematic representation of the tail-like adsorption mode of Jeff(hyp.PG)$(COOH)_n$ and the hindered access of sulfate ions to the surface of the cement.

high content of immediately soluble sulfates (e.g., α-, β-hemihydrate, alkali sulfates).[31] It was found that this behavior primarily derives from competitive adsorption between the PCEs and the sulfate ions for adsorption sites.[32] Therefore, in recent years, several attempts were made to develop superplasticizers that exhibit higher robustness in the presence of sulfates.[33,34] To investigate the sulfate tolerance of the polymers synthesized here, different amounts of sodium sulfate (i.e., 0.5−2.0% bwoc) were dissolved in the mixing water together with the polymers and mini slump tests were carried out (w/c = 0.50).

According to Figure 5, the dispersing performances of the hyperbranched polymers as well as of the linear, non-hyperbranched Jeff(Et-$COOH)_2$ are not impaired by sulfate ions. Contrary, the comb-shaped PCE 45PC2 showed a remarkably low sulfate tolerance (e.g., decrease of the spread flow from 26 to 20.6 cm at Na_2SO_4 addition of 2%). The high robustness of the hyperbranched polymers and of Jeff(Et-$COOH)_2$ can be attributed to their specific molecular architecture. Since all these polymers exhibit terminal carboxylate groups, they presumably adsorb in a tail (= brush)-like conformation. This means that they anchor via their chain end on the cement surface, while the rest of the structure stretches out into the pore solution. In this way, a more dense surface coverage is obtained, and a barrier for the access of hydrated sulfate ions forms, which prevents the desorption of the adsorbed polymers from the cement surface (see the illustration in Figure 6).

A similar mechanism was reported earlier for linear polyoxyethylene diphosphonate dispersants that also adsorb via their phosphonate groups in a tail-like conformation and exhibit high robustness toward soluble sulfates.[35] However, the comb-shaped structure of the PCE from our study apparently favors a loop-shaped conformation, whereby only some segments of the polymer chain are attached to the cement surface. As a result of this adsorption mode, the surface is not so densely covered by the polymer and is more accessible to sulfate ions. Interestingly, the highest sulfate robustness was found for TMP(hyp.PG)$(COOH)_n$ even though it does not comprise a linear polyether side chain. This can be attributed to its high anionicity (i.e., 2700 μeq/g in 0.1 M NaOH), which provokes a strong anchoring on the cement surface, thus impeding the desorption of the polymer by soluble sulfates.

DOI: 10.1021/acs.iecr.9b02077
Ind. Eng. Chem. Res. 2019, 58, 12913−12926

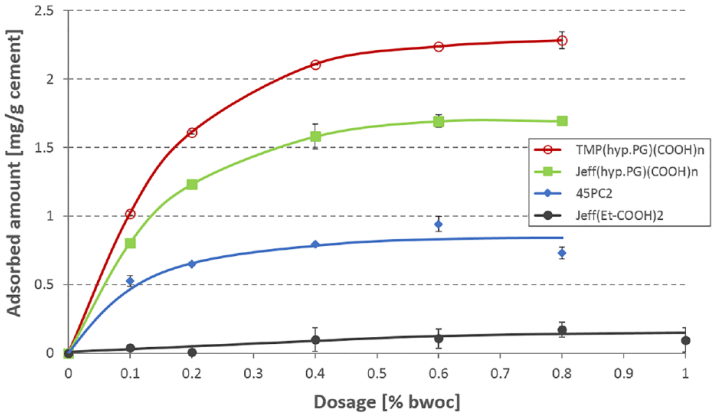

Figure 7. Adsorption isotherms on cement developed for the individual polymers at w/c = 0.50.

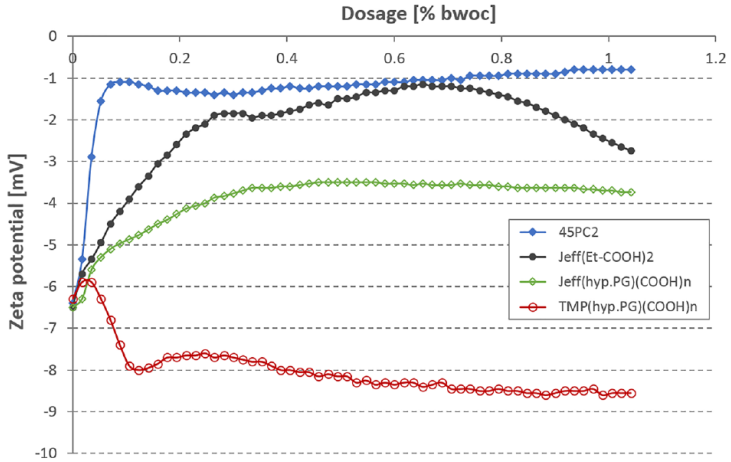

Figure 8. Zeta potential of cement slurries (w/c = 0.50) admixed with increasing polymer dosages.

3.6. Adsorption Measurements. To gain information about the adsorption of the polymers on cement, individual adsorption isotherms were developed at a w/c ratio of 0.50. As can be seen from Figure 7, all polymers except for Jeff(Et-COOH)$_2$ showed a Langmuir-type adsorption isotherm characterized by a steep increase of the adsorbed amount at low dosages until it gradually levels off at the saturation point where all surface sites are completely covered by a monolayer of the polymer.

Generally, significantly higher adsorbed amounts were found for the hyperbranched polymers compared to the PCE. To be more specific, Jeff(hyp.PG)(COOH)$_n$ and TMP(hyp.PG)-(COOH)$_n$ reached the saturated adsorption at 1.7 and 2.3 mg/g cement, respectively, while 45PC2 attained the plateau at 0.84 mg/g cement only. These findings suggest that the hyperbranched polymers indeed adsorb in a tail-like conformation, which allows a more dense packing of the polymer and a higher loading of the surface. This result further supports the previous observation of a higher sulfate tolerance for these polymers. In comparison, the comb-shaped PCE occupies a much higher surface area per molecule, with its main chain spread out on the surface (loop-shaped conformation) and therefore achieves saturated adsorption already at low addition. This was confirmed by converting the adsorbed amounts in mg/g cement into carboxylate groups (COO^-) available for adsorption per m^2 and plotting it against the applied polymer dosage (see Figure S19). From there, it can be seen that for the comb-shaped PCE only 2.6 μmol of COO^- is anchored per m^2 at saturated adsorption, while significantly higher values were obtained for Jeff(hpy.PG)(COOH)$_n$ and TMP(hyp.PG)-(COOH)$_n$ (11.6 and 22 μmol/m^2, respectively). For the linear non-hyperbranched Jeff(Et-COOH)$_2$, only low adsorbed amounts were found (e.g., 0.1 mg/g cement and 0.12 μmol/m^2 at 1.0%, respectively), which provide only partial surface coverage. This is the reason for the poor dispersing performance of this molecule.

3.7. Impact of the Polymers on Zeta Potential. The interaction of the polymers with cement was investigated by zeta potential measurements. Here, cement slurries (w/c = 0.50) were admixed with increasing dosages of the polymers, and the zeta potential of the cement particles was captured using the electroacoustic method.

As is obvious from Figure 8, the polymers, which comprise linear polyether side chains, showed an increase of the zeta potential at ascending dosages until they reached a plateau. It is well established for PCE superplasticizers that this increase stems from the steric effect of the polyether side chains, which shift the shear plane of the zeta potential toward the isoelectric

DOI: 10.1021/acs.iecr.9b02077
Ind. Eng. Chem. Res. 2019, 58, 12913−12926

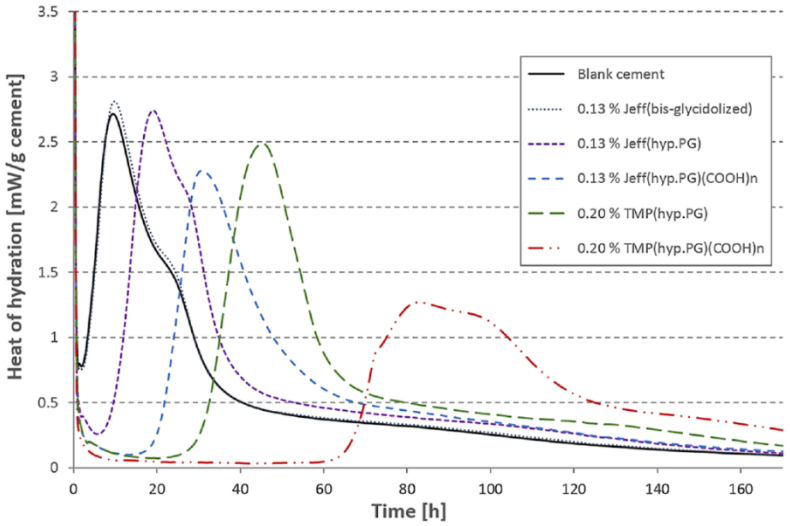

Figure 9. Time-dependent evolution of the hydration heat released from cement slurries (w/c = 0.50) admixed with different polymers.

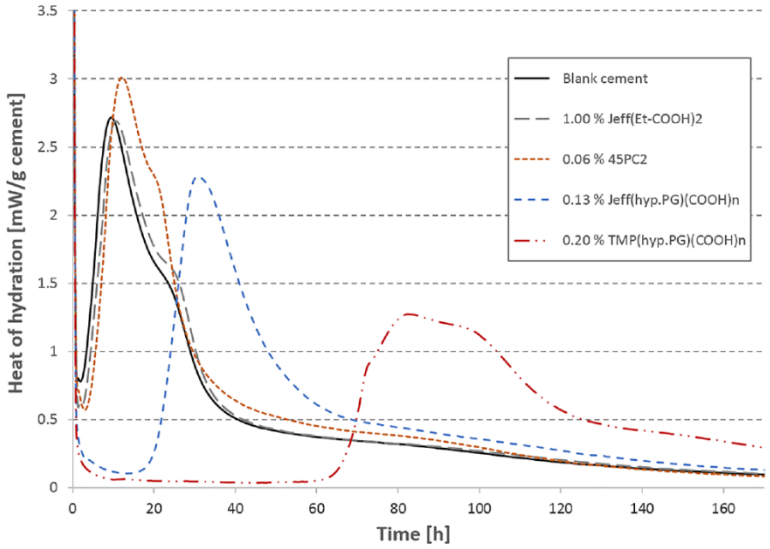

Figure 10. Time-dependent evolution of the hydration heat released from cement slurries (w/c = 0.50) admixed with different intermediates from the polymer syntheses.

point.[36] Since 45PC2 possesses a longer side chain than Jeff(hyp.PG)$(COOH)_n$ (45 EO units vs 19 EO + 3 PO units), more positive zeta potential values were obtained for the comb-shaped PCE. Furthermore, it can be seen from the figure that 45PC2 approached the plateau level at a much lower dosage than Jeff(hyp.PG)$(COOH)_n$, while for Jeff(Et-$COOH)_2$, no plateau value was found at all. However, TMP(hyp.PG)$(COOH)_n$ slightly decreased the zeta potential from −6.2 to −8.8 mV, signifying that the individual hyperbranched polyglycerol scaffold imparts a lower steric hindrance effect compared to 45PC2 or Jeff(hyp.PG)-$(COOH)_n$. On the basis of the zeta potential measurements, it also can be concluded that all synthesized polymers interact with the cement surface via physisorption.

3.8. Heat Flow Calorimetry. Finally, the impact of the synthesized polymers on cement hydration was investigated via isothermal heat flow calorimetry. The time-dependent heat release from cement pastes (w/c = 0.5) admixed with the respective dosages of the polymers required for a spread flow of 26 cm is illustrated in Figure 9.

According to this, the linear non-hyperbranched Jeff(Et-$COOH)_2$ and the comb-shaped PCE delay the main peak of cement hydration only slightly compared to the blank cement (e.g., 3 h for 45PC2). For both hyperbranched polymers, a much stronger retardation was found. The addition of 0.13% Jeff(hyp.PG)$(COOH)_n$ resulted in a retardation of 21 h, while 0.20% TMP(hyp.PG)$(COOH)_n$ delayed the cement hydration even for 78 h, which explains the exceptional fluidity retention of the cement pastes containing these polymers (see Figure 4).

DOI: 10.1021/acs.iecr.9b02077
Ind. Eng. Chem. Res. 2019, 58, 12913−12926

To further elucidate the retarding properties of the polymers, heat flow calorimetry was also conducted for the intermediate products occurring in the syntheses.

Figure 10 confirms that the bis-glycidolized Jeffamine does not affect the cement hydration, whereas for Jeff(hyp.PG) and TMP(hyp.PG), strong retardation was evidenced (e.g., 36 h for TMP(hyp.PG)). However, their retarding effect was less severe than for the carboxymethylated products. These findings suggest that the retardation of the hyperbranched polymers stems not only from the carboxylate groups but also from the hyperbranched polyglycerol skeleton. Generally, retardation can be ascribed to different mechanisms:[37] (a) adsorption of the polymer on the surface of cement, which reduces the access of water to facilitate hydration; (b) adsorption on initial hydration products, which blocks their further growth; (c) complexation of Ca^{2+} ions by the polymer and consequently reduced formation of the hydrate phases; (d) precipitation of the polymer, which acts as a diffusion barrier on the cement surface. The retarding effect of the hyperbranched polymers can be explained as follows: Through adsorption of the polymers on cement and the initial hydration products, a densely packed polymer layer is formed. As a result, the dissolution of the clinker phases and the ion transport at the solid−liquid interface as well as the growth of the initial hydrate phases are inhibited. Moreover, Jeff(hyp.PG)-$(COOH)_n$ and TMP(hyp.PG)$(COOH)_n$ exhibit a high ability to complex Ca^{2+} ions, as was evidenced by the charge titration experiments in Section 3.2 (see Figure 2), whereas precipitation of the polymer by Ca^{2+} can be excluded since no precipitate was observed in SCPS.

4. CONCLUSION

In this study, a new type of superplasticizer was successfully synthesized by anionic ring opening multibranching polymerization of glycidol. Contrary to conventional PCEs, this polymer exhibits a linear hyperbranched diblock structure composed of a carboxmethylated hyperbranched polyglycerol moiety and one linear polyetheramine side chain at the branching point.

The terminal carboxylate groups present in the periphery of the hyperbranched polyglycerol skeleton effectuate a perpendicular (tail-like) adsorption mode, which entails higher polymer dosages required for the complete surface coverage of cement compared to conventional comb-shaped PCEs. Moreover, our study about the structure−performance relationship of the different synthesized polymers signifies that superplasticizers need at least one component that can provide a powerful steric hindrance effect and additionally must exhibit a sufficient anionic charge amount to facilitate the adsorption on cement.

The results from the time-dependent fluidity tests show that carboxymethylated hyperbranched polyglycerols provoke a superior slump loss behavior and therefore behave more favorably in applications such as ready-mix concrete where a fluid consistency has to be retained over a longer period of time until delivery at the construction site has been achieved. Considering the retarding effect of the hyperbranched superplasticizer, we suggest that such polymers might be very beneficial, e.g., for concreting at high temperatures (>30 °C) where strong retardation actually is required or in oil well cementing where cement slurries are pumped over long distances at temperatures as high as 200 °C. Future research should focus on novel hybrid structures by incorporating hyperbranched polyglycerols as side chains into comb-shaped PCEs and studying whether such branched lateral chains are more effective than the linear ones present in conventional PCEs.

■ ASSOCIATED CONTENT

Supporting Information

The Supporting Information is available free of charge on the ACS Publications website at DOI: 10.1021/acs.iecr.9b02077.

Titration according to Elder and co-workers,[26] SEC spectra, FT-IR spectra, ^1H and ^{13}C NMR data, and the adsorption measurement (PDF)

■ AUTHOR INFORMATION

Corresponding Author

*E-mail: sekretariat@bauchemie.ch.tum.de.

ORCID

Johann Plank: 0000-0002-4129-4784

Notes

The authors declare no competing financial interest.

■ ACKNOWLEDGMENTS

The authors would like to thank Huntsman for generously providing the Jeffamine sample and HeidelbergCement for supplying the cement.

■ REFERENCES

(1) Spiratos, N.; Page, M.; Mailvaganam, N. P.; Malhotra, V. M.; Jolicoeur, C. *Superplasticizers for Concrete: Fundamentals, Technology, and Practice*; Supplementary Cementing Materials for Sustainable Development: Ottawa, 2003.

(2) Plank, J.; Sakai, E.; Miao, C. W.; Yu, C.; Hong, J. X. Chemical admixtures − Chemistry, applications and their impact on concrete microstructure and durability. *Cem. Concr. Res.* **2015**, *78*, 81−99.

(3) Äitcin, P.-C.; Flatt, R. J. *Science and Technology of Concrete Admixtures*, 1st ed.; Woodhead Publishing, 2016.

(4) Yamada, K.; Takahashi, T.; Hanehara, S.; Matsuhisa, M. Effects of the chemical structure on the properties of polycarboxylate-type superplasticizer. *Cem. Concr. Res.* **2000**, *30*, 197−207.

(5) Zhang, Y.; Kong, X. Correlations of the dispersing capability of NSF and PCE types of superplasticizer and their impacts on cement hydration with the adsorption in fresh cement pastes. *Cem. Concr. Res.* **2015**, *69*, 1−9.

(6) Uchikawa, H.; Hanehara, S.; Sawaki, D. The role of steric repulsive force in the dispersion of cement particles in fresh paste prepared with organic admixture. *Cem. Concr. Res.* **1997**, *27*, 37−50.

(7) Jolicoeur, C.; Simard, M.-A. Chemical admixture-cement interactions: Phenomenology and physico-chemical concepts. *Cem. Concr. Compos.* **1998**, *20*, 87−101.

(8) Yoshioka, K.; Sakai, E.; Daimon, M.; Kitahara, A. Role of steric hindrance in the performance of superplasticizers for concrete. *J. Am. Ceram. Soc.* **1997**, *80* (10), 2667−2671.

(9) Houst, Y. F.; Bowen, P.; Perche, F.; Kauppi, A.; Borget, P.; Galmiche, L.; Le Meins, J. F.; Lafuma, F.; Flatt, R. J.; Schober, I.; Banfill, P. F.G.; Swift, D. S.; Myrvold, B. O.; Petersen, B. G.; Reknes, K. Design and function of novel superplasticizers for more durable high performance concrete (superplast project). *Cem. Concr. Res.* **2008**, *38*, 1197−1209.

(10) Hirata, T.; Ye, J.; Branicio, P.; Zheng, J.; Lange, A.; Plank, J.; Sullivan, M. Adsorbed conformations of PCE superplasticizers in cement pore solution unraveled by molecular dynamics simulations. *Sci. Rep.* **2017**, *7*, 16599.

(11) Ottewill, R. H.; Walker, T. The influence of non-ionic surface active agents on the stability of polystyrene latex dispersions. *Colloid Polym. Sci.* **1968**, *227* (1−2), 108−116.

DOI: 10.1021/acs.iecr.9b02077
Ind. Eng. Chem. Res. 2019, 58, 12913−12926

(12) Liu, X.; Guan, J.; Lai, G.; Wang, Z.; Zhu, J.; Cui, S.; Lan, M.; Li, H. Performances and working mechanism of a novel polycarboxylate superplasticizer synthesized through changing molecular topological structure. *J. Colloid Interface Sci.* **2017**, *504*, 12−24.
(13) Ao, L.; Zhao, W.; Lei, Q.; Wang, D.; Guan, Y.; Liu, K.; Guo, T.; Fan, X.; Wei, X. Synthesis of a novel polycarboxylate superplasticizer with hyperbranched structure. *Chemistry Select* **2018**, *3*, 13493−13496.
(14) Zhu, Q.-H.; Zhang, L.-Z.; Min, X.-M.; Yu, Y.-X.; Zhao, X.-F.; Li, J.-H. Comb-typed polycarboxylate superplasticizer equipped with hyperbranched polyamide teeth. *Colloids Surf., A* **2018**, *553*, 272−277.
(15) Kong, X.; Hou, S.; Lu, Z. Effect of dendrimeric polyamide on fluidity of cement paste, cement hydration and their adsorption in cement paste. *J. Chin. Ceram. Soc.* **2014**, *42* (11), 1355−1361.
(16) Shou, C.; Xiao, W. Hyper-branched polycarboxylate high-efficiency water reducing agent and preparation method thereof. China Patent CN 101580353 B, 2012.
(17) Li, S.; Wu, Q.; Wang, X.; Kong, C.; Zhu, H.; Zhang, C.; Yang, T.; Wang, C.; Xu, F.; Liu, Y.; Fan, S. Hyperbranched polycarboxylate water reducer and preparation method thereof. China Patent CN 107325296 A, 2017.
(18) Gheybi, H.; Sattari, S.; Bodaghi, A.; Soleimani, K.; Dadkhah, A.; Adeli, M. Polyglycerols. In *Engineering of Biomaterials for Drug Delivery Systems: Beyond Polyethylene Glycol*; Woodhead Publishing Series in Biomaterials, 2018; pp 103−171.
(19) Sunder, A.; Hanselmann, R.; Frey, H.; Mülhaupt, R. Controlled synthesis of hyperbranched polyglycerols by ring-opening multibranching polymerization. *Macromolecules* **1999**, *32*, 4240−4246.
(20) Abbina, S.; Vappala, S.; Kumar, P.; Siren, E. M. J.; La, C. C.; Abbasi, U.; Brooks, D. E.; Kizhakkedathu, J. N. Hyperbranched polyglycerols: recent advances in synthesis, biocompatibility and biomedical applications. *J. Mater. Chem. B* **2017**, *5*, 9249−9277.
(21) Frey, H.; Haag, R. Dendritic polyglycerol: a new versatile biocompatible material. *Rev. Mol. Biotechnol.* **2002**, *90*, 257−267.
(22) Wilms, D.; Stiriba, S.-E.; Frey, H. Hyperbranched Polyglycerols: From the Controlled Synthesis of Biocompatible Polyols to Multipurpose Applications. *Acc. Chem. Res.* **2010**, *43* (1), 129−141.
(23) Wang, G.; Li, L.; Lan, J.; Chen, L.; You, J. Biomimetic crystallization of calcium carbonate spherules controlled by hyperbranched polyglycerols. *J. Mater. Chem.* **2008**, *18*, 2789−2797.
(24) Zolek-Tryznowska, Z.; Tryznowski, M.; Krolikowska, J. Hyperbranched polyglycerol as an additive for water-based printing ink. *J. Coat. Technol. Res.* **2015**, *12* (2), 385−392.
(25) Istratov, V.; Kautz, H.; Kim, Y.-K.; Schubert, R.; Frey, H. Linear-dendritic nonionic poly(propylene oxide)-polyglycerol surfactants. *Tetrahedron* **2003**, *59*, 4017−4024.
(26) Carey, M. A.; Wellons, S. L.; Elder, D. K. Rapid method for measuring the hydroxyl content of polyurethane polyols. *J. Cell. Plast.* **1984**, *20*, 42−48.
(27) Kainthan, R. K.; Muliawan, E. B.; Hatzikiriakos, S. G.; Brooks, D. E. Synthesis, characterization, and viscoelastic properties of high molecular weight hyperbranched polyglycerols. *Macromolecules* **2006**, *39*, 7708−7717.
(28) Kawaguchi, S.; Aikaike, K.; Zhang, Z.-M.; Matsumoto, K.; Ito, K. Watersoluble bottlebrushes. *Polym. J.* **1998**, *30*, 1004−1007.
(29) Plank, J.; Sachsenhauser, B. Experimental determination of the effective anionic charge density of polycarboxylate superplasticizers in cement pore solution. *Cem. Concr. Res.* **2009**, *39*, 1−5.
(30) Barriau, E.; Frey, H.; Kiry, A.; Stamm, M.; Gröhn, F. Negatively charged hyperbranched polyether-based polyelectrolytes. *Colloid Polym. Sci.* **2006**, *284*, 1293−1301.
(31) Magarotto, R.; Moratti, F.; Zeminian, N. Influence of sulfates content in cement on the performance of superplasticizers. In *Proceedings of the 8th CANMET/ACI Conference on Superplasticizers and Other Chemical Admixtures in Concrete*; Malhotra, V. M., Ed., Sorrento, Italy, 2006; SP-239-15; pp 215−229.
(32) Han, S.; Plank, J. Mechanistic study on the effect of sulfate ions on polycarboxylate superplasticizers in cement. *Adv. Cem. Res.* **2013**, *25* (4), 200−207.
(33) Pourchet, S.; Liautaud, S.; Rinaldi, D.; Pochard, I. Effect of the repartition of the PEG side chains on the adsorption and dispersion behaviors of PCP in presence of sulfate. *Cem. Concr. Res.* **2012**, *42*, 431−439.
(34) Habbaba, A.; Lange, A.; Plank, J. Synthesis and performance of a modified polycarboxylate dispersant for concrete possessing enhanced cement compatibility. *J. Appl. Polym. Sci.* **2013**, *129*, 346−353.
(35) Mosquet, M.; Chevalier, Y.; Brunel, S.; Guicquero, J. P.; Le Perchec, P. Polyoxyethylene di-phosphonates as efficient dispersing polymers for aqueous suspensions. *J. Appl. Polym. Sci.* **1997**, *65*, 2545−2555.
(36) Plank, J.; Sachsenhauser, B. Impact of molecular structure on zeta potential and adsorbed conformation of α-allyl-ω-methoxypolyethylene glycol-maleic anhydride superplasticizers. *J. Adv. Concr. Technol.* **2006**, *4* (2), 233−239.
(37) Cheung, J.; Jeknavorian, A.; Roberts, L.; Silva, D. Impact of admixtures on the hydration kinetics of Portland cement. *Cem. Concr. Res.* **2011**, *41*, 1289−1309.

DOI: 10.1021/acs.iecr.9b02077
Ind. Eng. Chem. Res. 2019, 58, 12913−12926

Supporting Information

Synthesis and Properties of a Polycarboxylate Superplasticizer with a Jellyfish-Like Structure Comprising Hyperbranched Polyglycerols

Manuel Ilg and Johann Plank*

Chair for Construction Chemistry, Technische Universität München,

Lichtenbergstraße 4, Garching 85748, Germany

* Corresponding author:

Tel: +49-89-289-13151; Fax: +49-89-289-13152

E-mail address: sekretariat@bauchemie.ch.tum.de (J. Plank)

Titration according to *Elder*:

In a typical experiment, 1 g of the polymer (m_{sample}) was dissolved in 25 mL of a reagent solution prepared from 28.4 g phthalic anhydride and 4.3 g imidazole in 175 mL pyridine. The solution was heated up to 98 °C, stirred there for 15 min and then cooled to ambient. 10 mL of DI water and 0.5 mL of a 1 wt.% phenolphthalein solution in pyridine were added and titrated against a 0.5 M NaOH solution (c_{NaOH}) until the color changed from colorless to slightly violet (= equivalence point). Additionally, a titration with no polymer present was conducted to assess the maximum amount of carboxylate groups of the reagent solution (= blank value). By using **equation 1**, the hydroxyl number was calculated from the volume of the NaOH titrant needed for the reference ($V_{NaOH,blank}$) and polymer sample ($V_{NaOH,sample}$).

$$\text{Hydroxyl number}\left[\frac{\text{mmol}}{\text{g polymer}}\right] = \frac{(V_{NaOH,blank} - V_{NaOH,sample})\cdot c_{NaOH}}{m_{sample}} \quad (1)$$

Size exclusion chromatography (SEC):

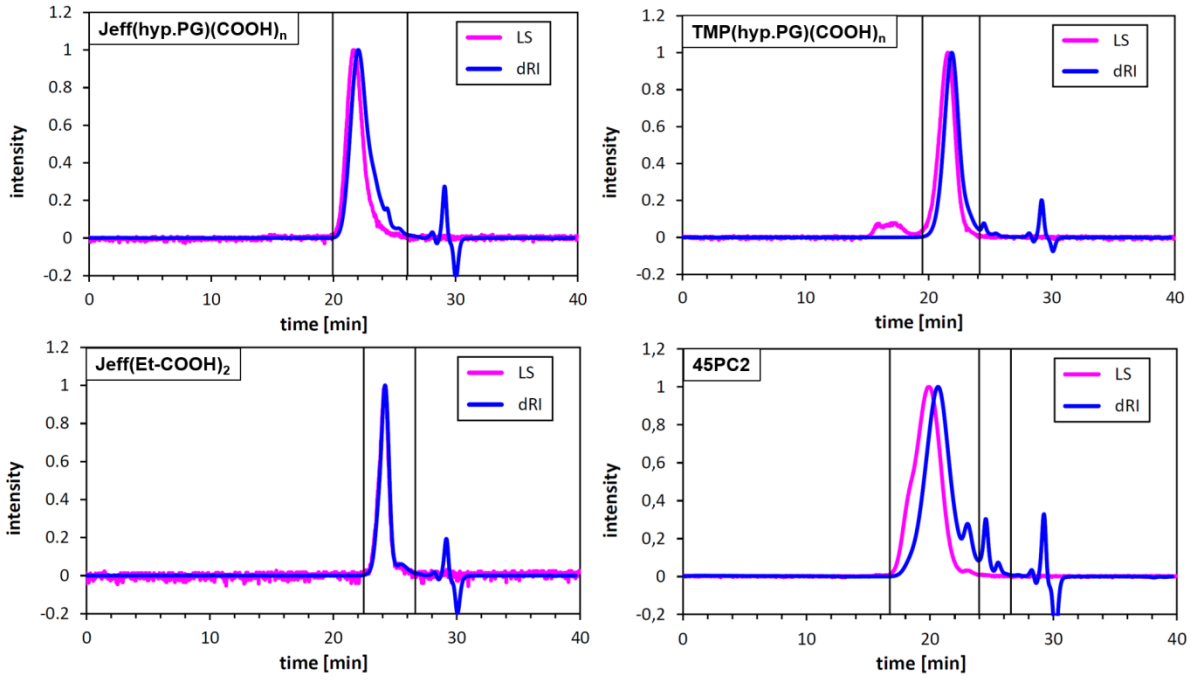

Figure S1: SEC spectra of the synthesized polymers

FT-IR spectroscopy:

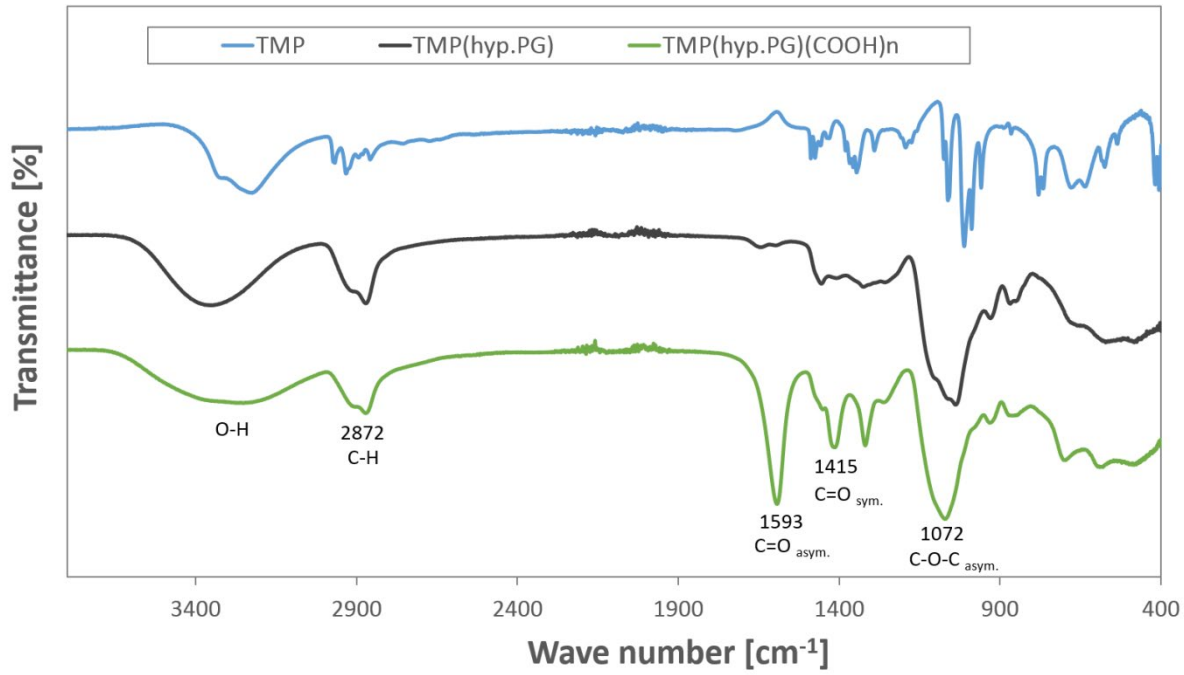

Figure S2: FT-IR spectra of TMP, TMP(hyp.PG) and TMP(hyp.PG)$(COOH)_n$

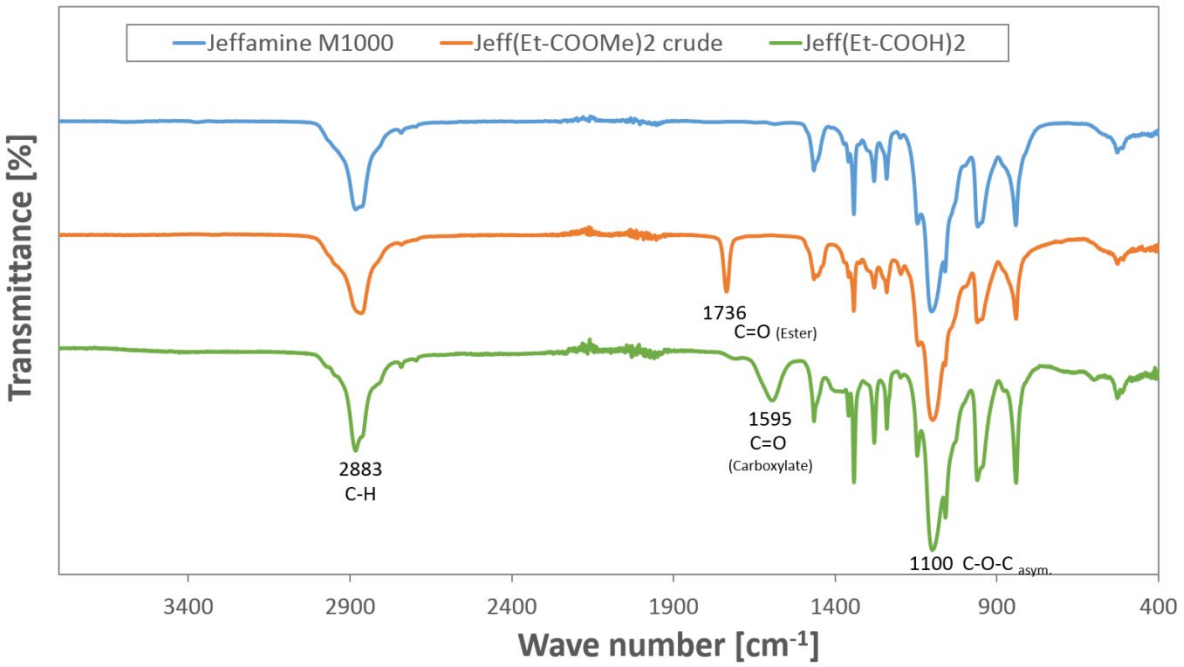

Figure S3: FT-IR spectra of Jeffamine M-1000, Jeff(Et-COOMe)$_2$ and Jeff(Et-COOH)$_2$

^{1}H and ^{13}C NMR spectroscopy:

- **Jeffamine M-1000**:

^{1}H NMR spectrum (400 MHz, D_2O):

δ [ppm] = 1.04 (d, 3H, -CH_2-$CHCH_3$-NH_2), 1.18 (d, 5H, CH_3 PPO), 2.99 – 3.18 (m, 1H, -$CHCH_3$-NH_2), 3.22 – 3.37 (m, 1H, CH PPO), 3.41 (s, 3H, -OCH_3), 3.46 – 3.94 (m, 84H, CH_2 PEO, CH_2 PPO, -CH_2-$CHCH_3$-NH_2, CH PPO)

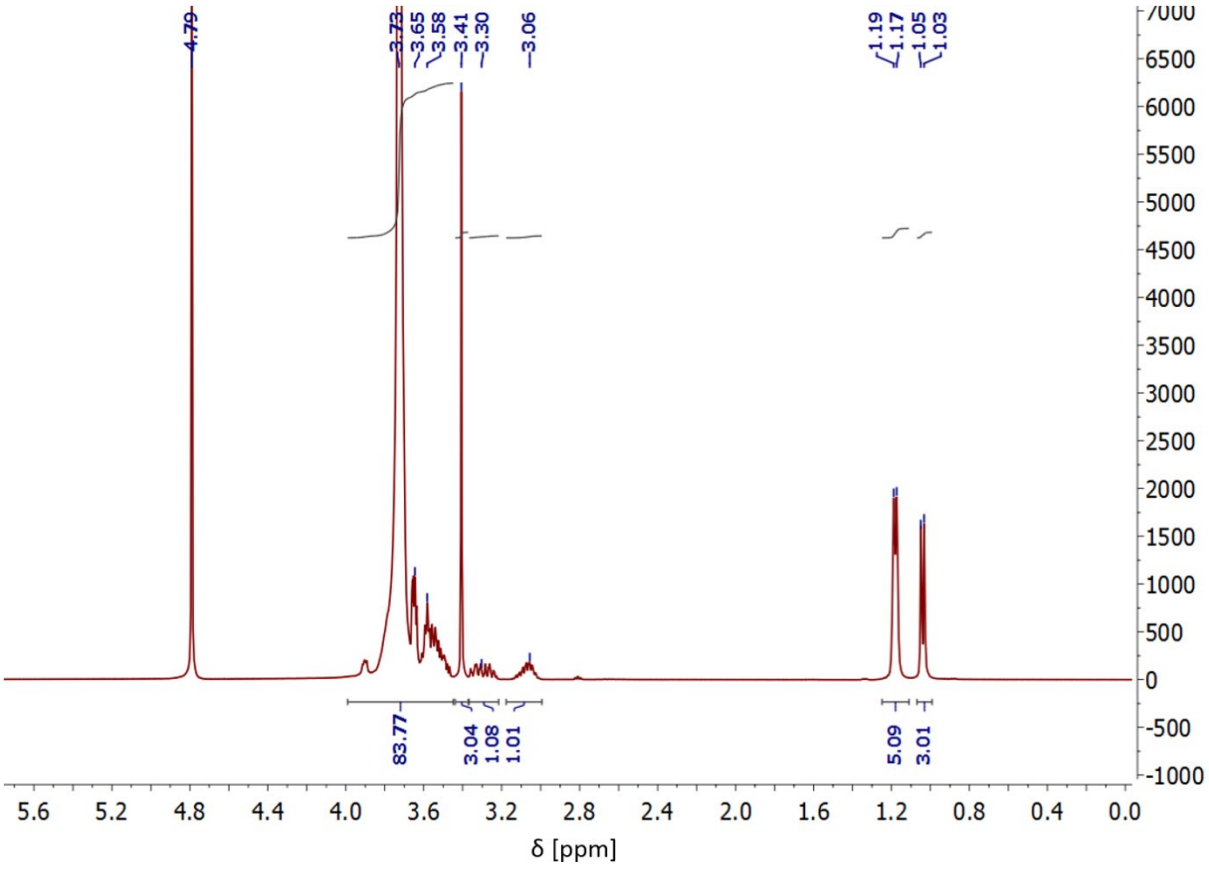

Figure S4: ^{1}H NMR spectrum of Jeffamine M-1000 in D_2O

^{13}C NMR spectrum (101 MHz, D_2O):

δ [ppm] = 15.81 (CH_3 PPO), 18.16 (-CH_2-$CH\underline{C}H_3$-NH_2), 45.14 – 45.71 (-CH_2-$\underline{C}HCH_3$-NH_2), 58.08 (-OCH_3), 69.61 (CH_2 PEO), 71.94 – 72.23 (-$\underline{C}H_2$-$CHCH_3$-NH_2), 74.08 (CH_2 PPO), 74.63 – 75.42 (CH PPO)

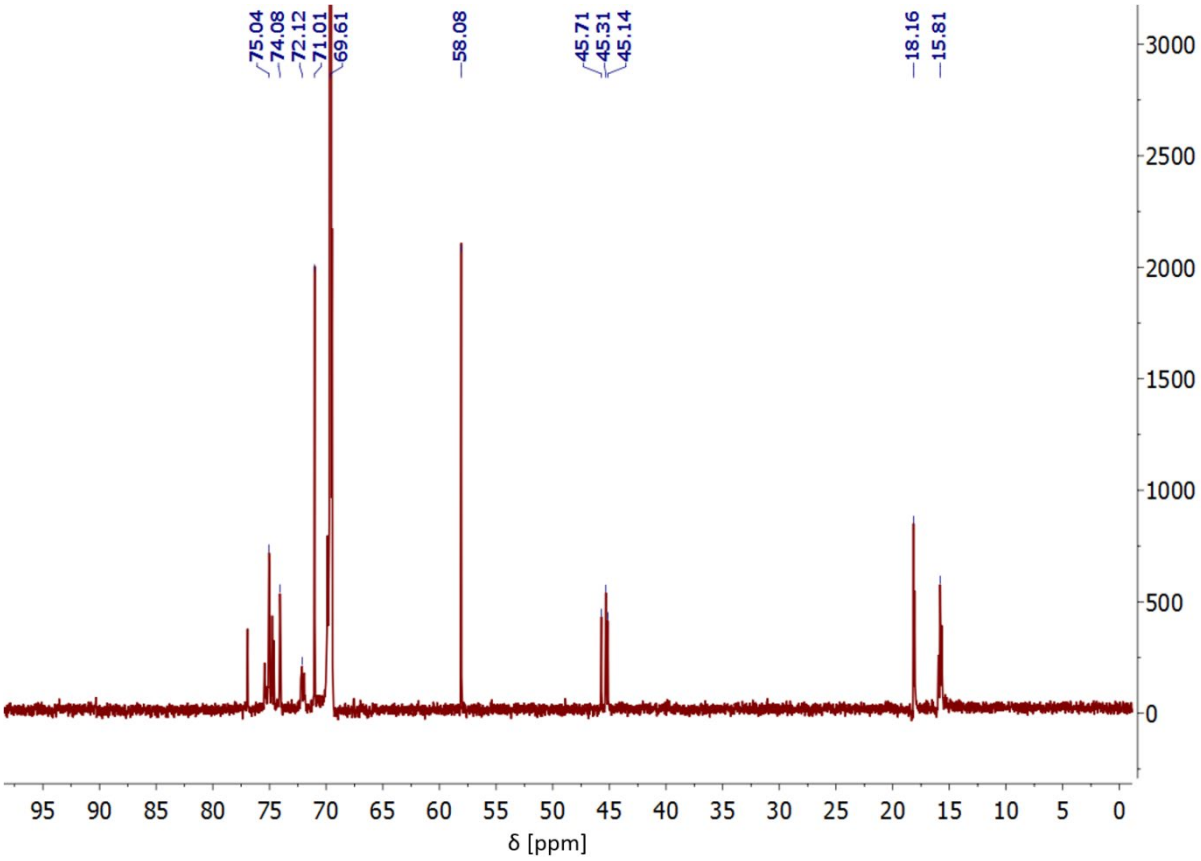

Figure S5: ^{13}C NMR spectrum of Jeffamine M-1000 in D_2O

- **Bis-glycidolized Jeffamine M-1000:**

^{1}H NMR spectrum (400 MHz, D_2O):

δ [ppm] = 1.02 (d, 3H, -CH_2-CHC<u>H</u>$_3$-N-), 1.17 (d, 5H, CH_3 PPO), 2.46 – 2.80 (m, 4H, -N-C<u>H</u>$_2$-CHOH-), 2.99 – 3.19 (m, 1H, -CH_2-C<u>H</u>CH_3-N-), 3.40 (s, 3H, -OCH_3), 3.43 – 3.95 (m, 91H, CH_2 PEO, CH_2 PPO, -C<u>H</u>$_2$-CHCH$_3$-N-, CH PPO, -N-CH_2-CHOH-C<u>H</u>$_2$-OH, -N-CH_2-C<u>H</u>OH-CH_2-OH)

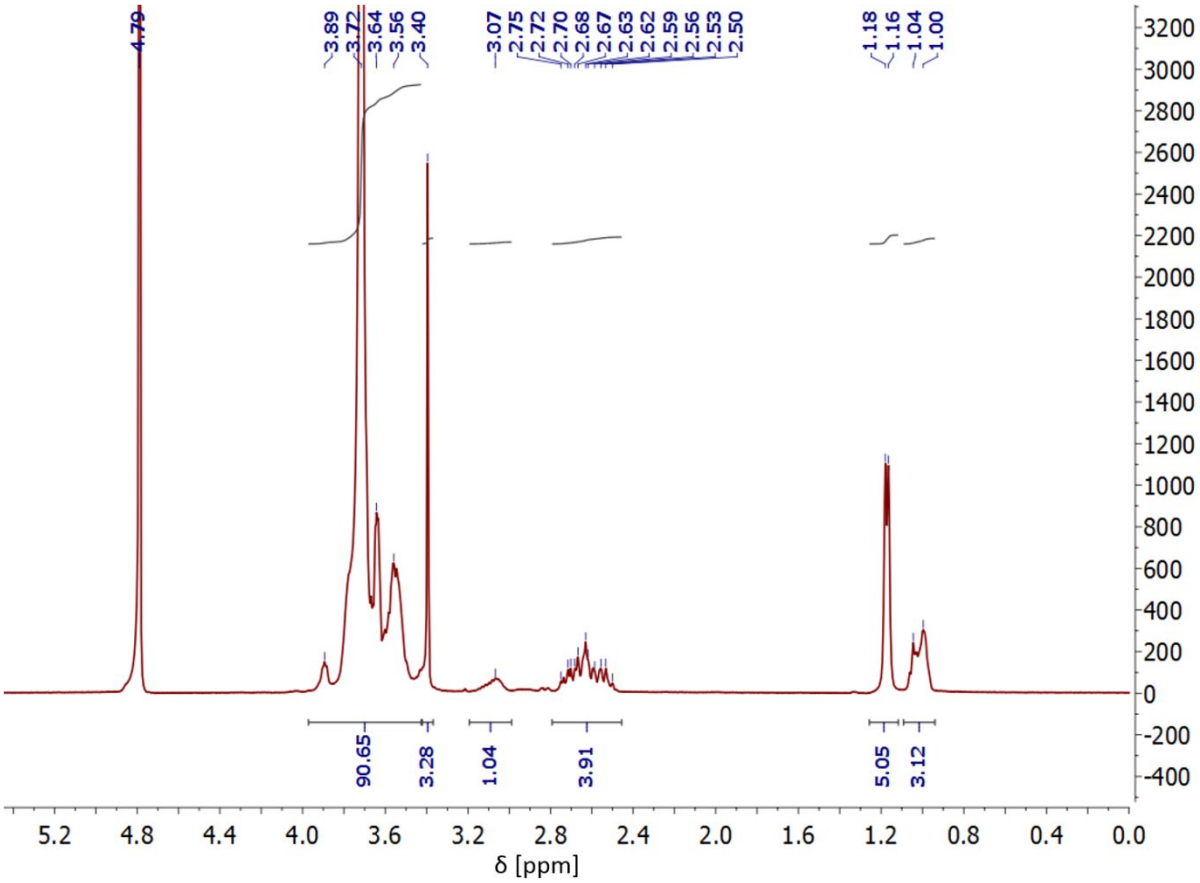

Figure S6: ^{1}H NMR spectrum of the bis-glycidolized Jeffamine M-1000 in D_2O

^{13}C NMR spectrum (101 MHz, D_2O):

δ [ppm] = 10.55 (-CH_2-$CHCH_3$-N-), 15.84 (CH_3 PPO), 52.70 – 54.01 (-N-CH_2-CHOH-), 55.94 (-$CHCH_3$-N-), 58.08 (OCH_3), 63.71 – 64.28 (-N-CH_2-CHOH-CH_2-OH), 69.12 (-N-CH_2-CHOH-), 69.61 (CH_2 PEO), 71.87 – 72.25 (-CH_2-$CHCH_3$-N-), 74.07 (CH_2 PPO), 74.69 – 75.20 (CH PPO)

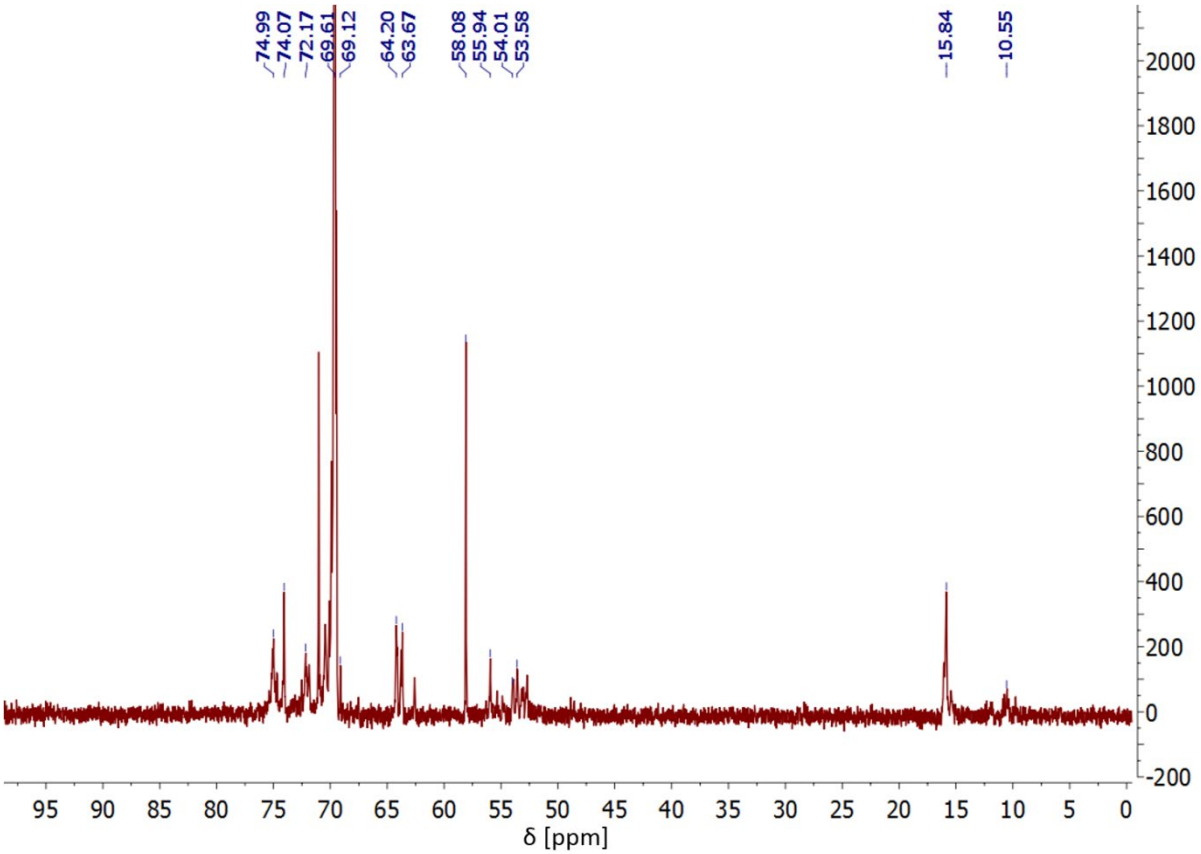

Figure S7: ^{13}C NMR spectrum of the bis-glycidolized Jeffamine M-1000 in D_2O

- **Jeff(hyp.PG):**

^{1}H NMR spectrum (400 MHz, D_2O):

δ [ppm] = 1.02 (d, 3 H, -CH_2-CHC<u>H</u>$_3$-N-), 1.18 (d, 4 H, CH_3 PPO), 2.49 – 2.79 (m, 4 H, -N-<u>C</u>H_2-CHOH-), 2.96 – 3.13 (m, 1 H, -CH_2-C<u>H</u>CH_3-N-), 3.40 (s, 3 H, -OCH_3), 3.43 – 4.21 (m, 167 H, CH_2 PEO, CH_2 PPO, CH PPO, CH and CH_2 polyglycerol scaffold)

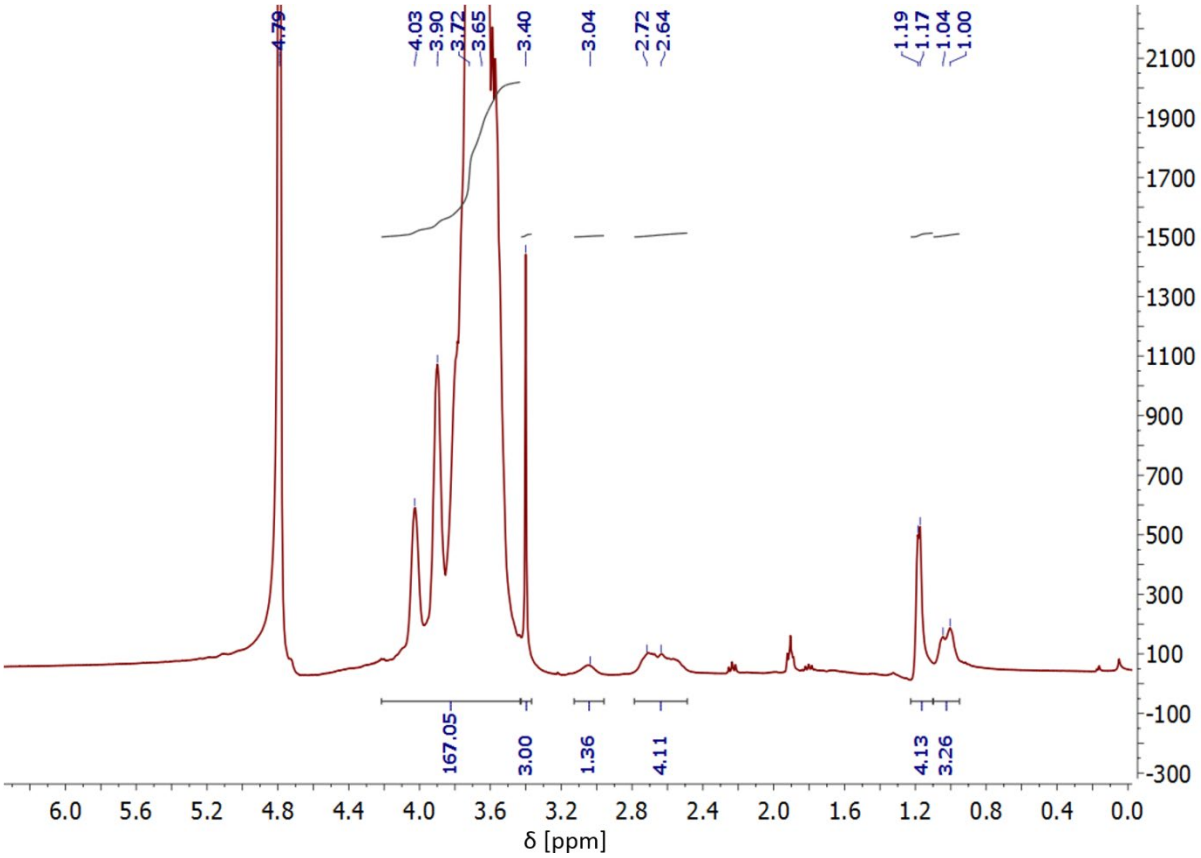

Figure S8: ^{1}H NMR spectrum of the crude product Jeff(hyp.PG) in D_2O

^{13}C NMR spectrum (101 MHz, D_2O):

δ [ppm] = 15.97 (CH_3 PPO), 58.08 (-O<u>C</u>H_3), 60.74 (L_{13}), 62.59 (T), 68.84 (L_{14}), 69.14 (L_{13}), 69.59 (CH_2 PEO), 70.10 – 71.10 (2 D, 2 T), 72.09 (2 L_{14}), 74.04 (CH_2 PPO), 77.88 (D), 79.40 (L_{13})

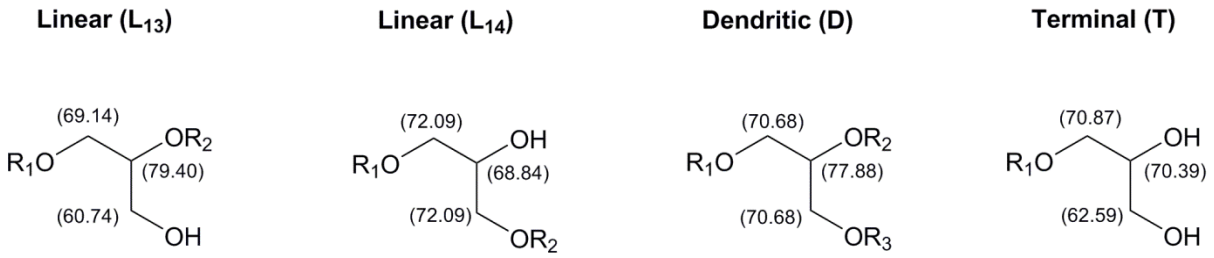

Figure S9: Structural units contained in the polyglycerol scaffold and the chemical shifts of the corresponding individual carbon atoms

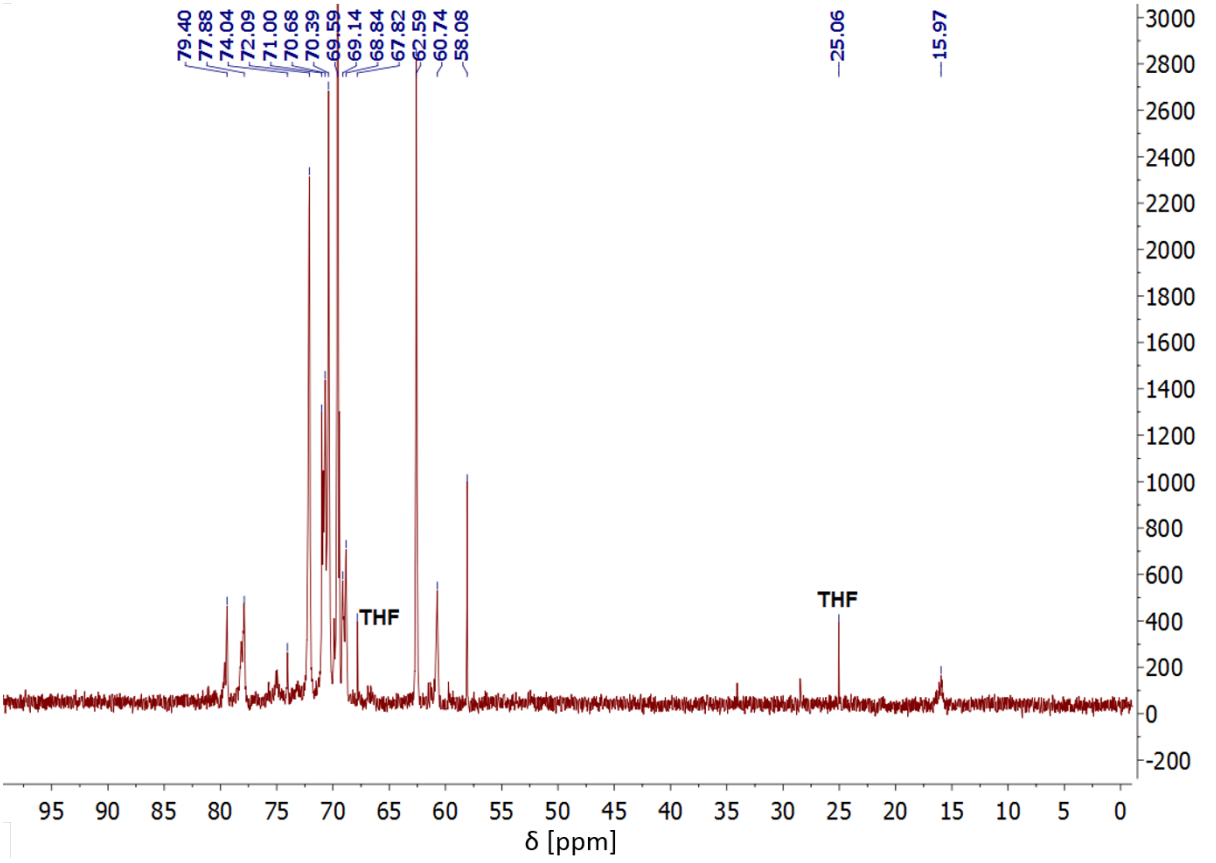

Figure S10: ^{13}C NMR spectrum of the crude product Jeff(hyp.PG) in D_2O

- **Jeff(hyp.PG)(COOH)$_n$:**

^{1}H NMR spectrum (400 MHz, D_2O):

δ [ppm] = 1.20 (s, 6 H, CH_3 PPO), 1.36 (s, 3 H, -CH_2-CHC$\underline{H}_3$-N-), 3.19 – 4.35 (m, 228 H, -OCH_3, CH_2 PEO, CH_2 PPO, CH PPO, -C$\underline{H}_2$-COOH, CH and CH_2 polyglycerol scaffold)

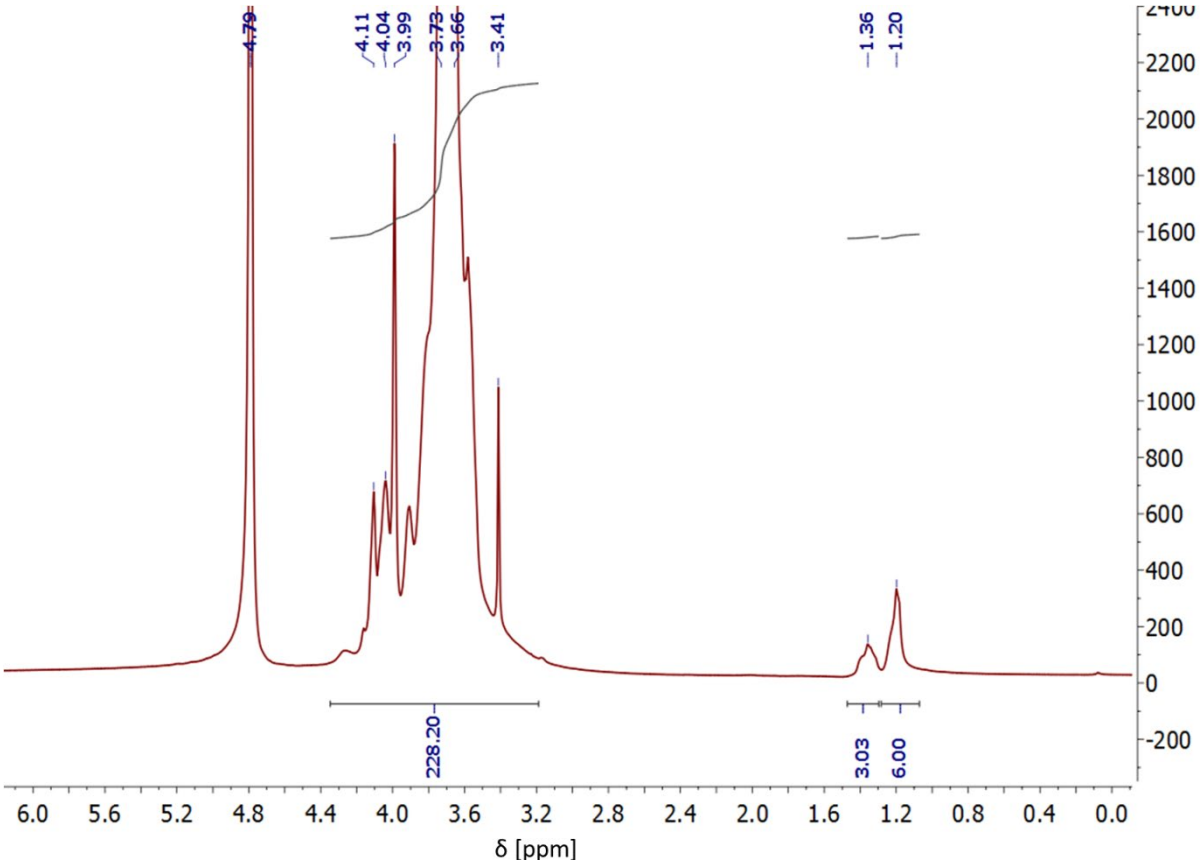

Figure S11: ^{1}H NMR spectrum of Jeff(hyp.PG)(COOH)$_n$ in D_2O

^{13}C NMR spectrum (101 MHz, D_2O):

δ [ppm] = 15.85 (CH_3 PPO), 58.08 (-O<u>C</u>H_3), 60.75 (L_{13}), 62.58 (T), 68.76 (L_{14}), 69.04 (L_{13}), 69.53 (CH_2 PEO), 69.98 – 71.17 (2 D, 2 T), 72.10 (2 L_{14}), 73.96 (CH_2 PPO), 76.92 (-<u>C</u>H_2-COOH), 77.82 (D), 79.35 (L_{13}), 177.67 (-COOH)

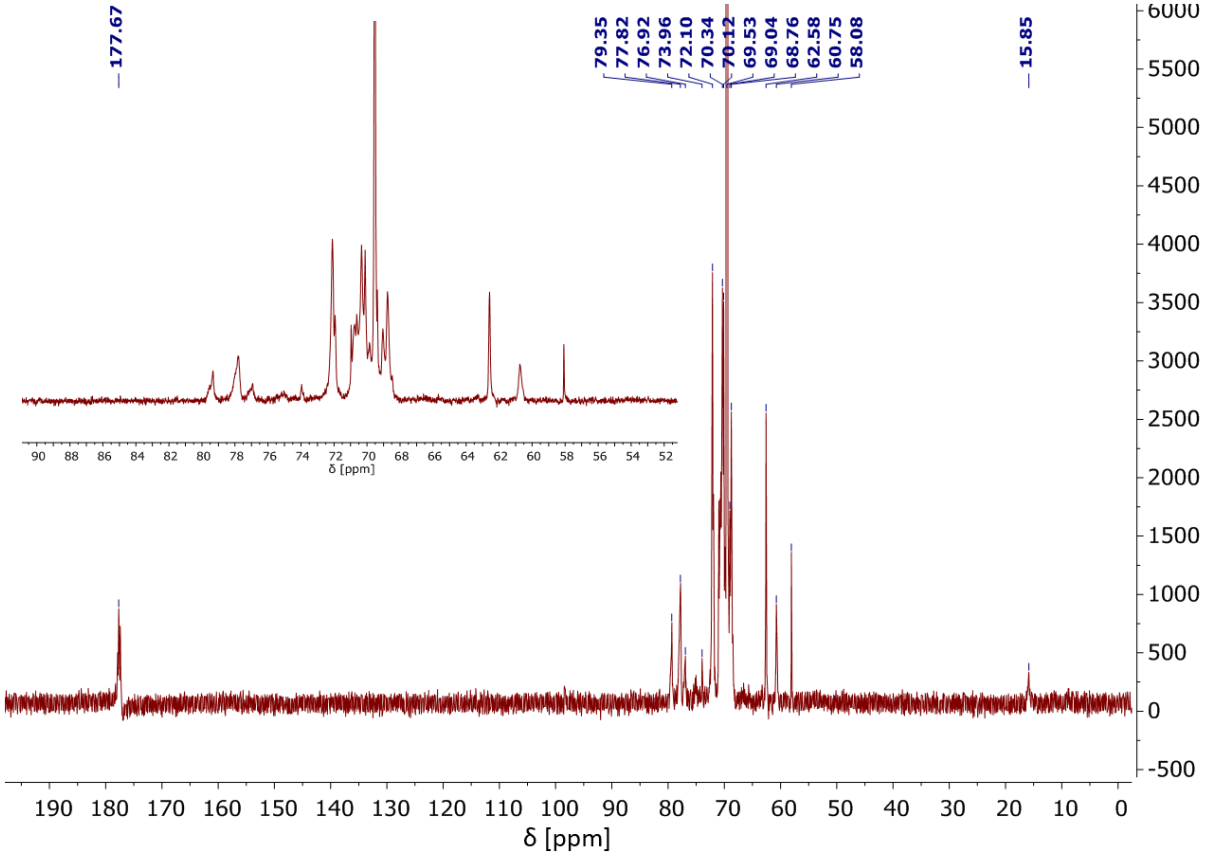

Figure S12: ^{13}C NMR spectrum of Jeff(hyp.PG)$(COOH)_n$ in D_2O

- **TMP(hyp.PG):**

<u>^{1}H NMR spectrum (400 MHz, D_2O):</u>

δ [ppm] = 0.84 (s, 3 H, -C<u>H</u>$_3$ TMP), 1.35 (s, 2 H, -C<u>H</u>$_2$-CH$_3$ TMP), 3.35 – 4.05 (m, 191 H, CH and CH_2 polyglycerol scaffold)

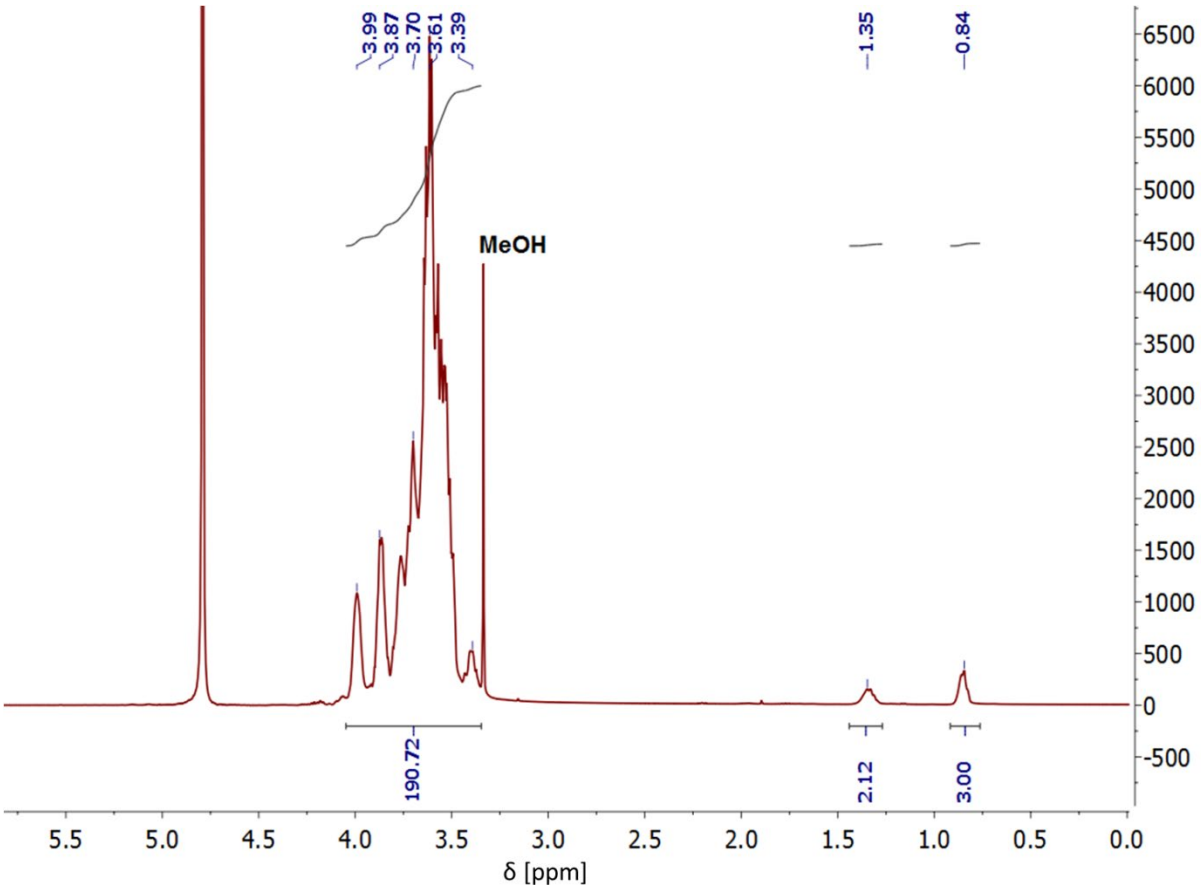

Figure S13: ^{1}H NMR spectrum of the crude product TMP(hyp.PG) in D_2O

^{13}C NMR spectrum (101 MHz, D_2O):

δ [ppm] = 6.80 (-CH_3 TMP), 21.95 (-CH_2 TMP), 43.12 (-C- TMP), 60.75 (L_{13}), 62.52 (T), 68.84 (L_{14}), 69.14 (L_{13}), 70.04 – 71.17 (2 D, 2 T), 72.09 (2 L_{14}), 77.89 (D), 79.41 (L_{13}).

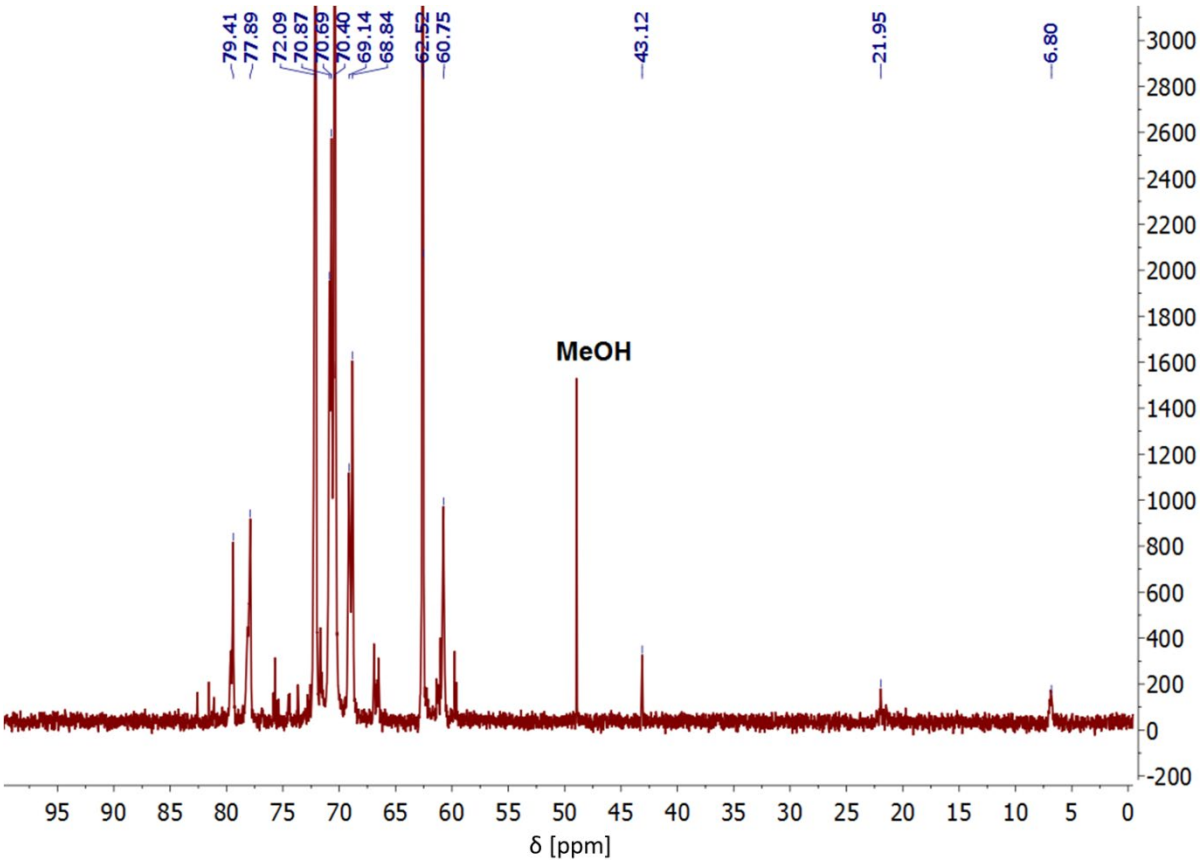

Figure S14: ^{13}C NMR spectrum of the crude product TMP(hyp.PG) in D_2O

- **TMP(hyp.PG)(COOH)$_n$:**

^{1}H NMR spectrum (400 MHz, D_2O):

δ [ppm] = 0.88 (s, 3 H, -CH_3 TMP), 1.38 (s, 2 H, -CH_2-CH_3 TMP), 3.13 – 4.25 (m, 239 H, -CH_2-COOH, CH and CH_2 polyglycerol scaffold)

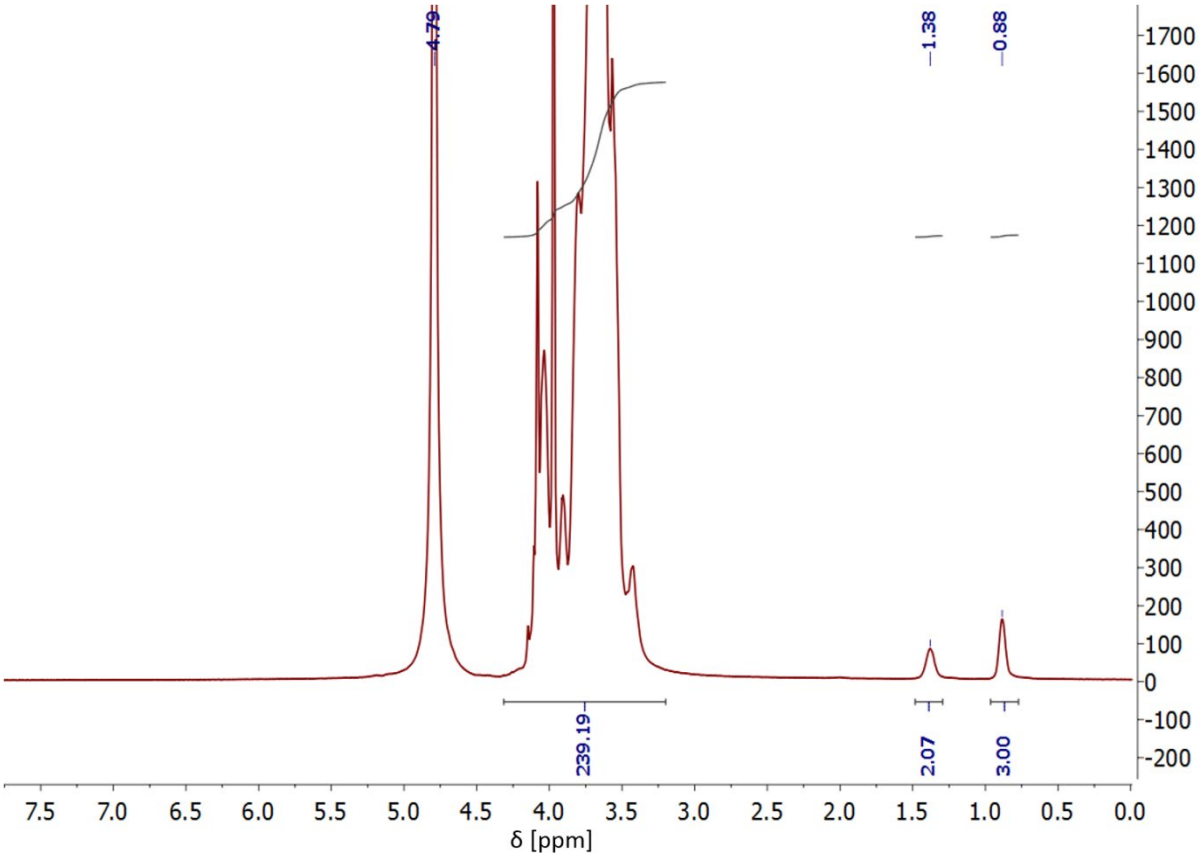

Figure S15: ^{1}H NMR spectrum of TMP(hyp.PG)(COOH)$_n$ in D_2O

^{13}C NMR spectrum (101 MHz, D_2O):

δ [ppm] = 6.73 (-CH_3 TMP), 22.03 (-CH_2 TMP), 43.11 (-C- TMP), 60.79 (L_{13}), 62.63 (T), 68.84 (L_{14}), 69.15 (L_{13}), 69.50 – 71.19 (2 D, 2 T), 72.18 (2 L_{14}), 77.01 (-CH_2-COOH), 77.88 (D), 79.39 (L_{13}), 178.07 (-COOH)

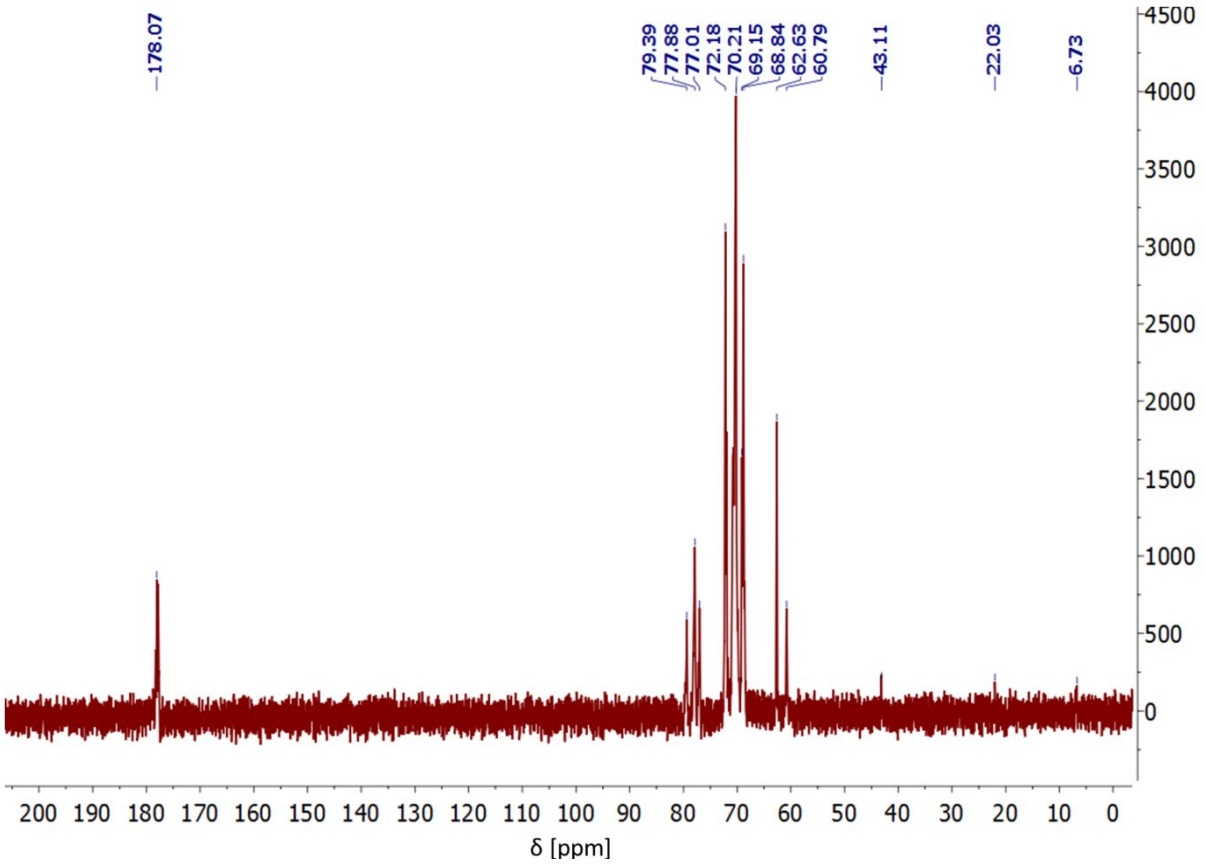

Figure S16: ^{13}C NMR spectrum of TMP(hyp.PG)$(COOH)_n$ in D_2O

- **Jeff(Et-COOH)$_2$:**

^{1}H NMR spectrum (400 MHz, D_2O):

δ [ppm] = 1.11 – 1.26 (s, 5H, CH_3 PPO), 1.26 – 1.42 (d, 3 H, -CH_2-CHC$\underline{H}_3$-N-), 2.52 – 2.77 (m, 3H, -N-CH_2-C$\underline{H}_2$-COOH), 3.09 – 3.27 (m, 1H, -CH_2-C$\underline{H}$$CH_3$-N-), 3.29 – 3.37 (m, 1 H, CH PPO), 3.40 (s, 3H, -OCH_3), 3.42 – 4.02 (m, 89 H, CH_2 PEO, CH_2 PPO, -C$\underline{H}_2$-$CHCH_3$-N-, -N-C$\underline{H}_2$-CH_2-COOH -, CH PPO).

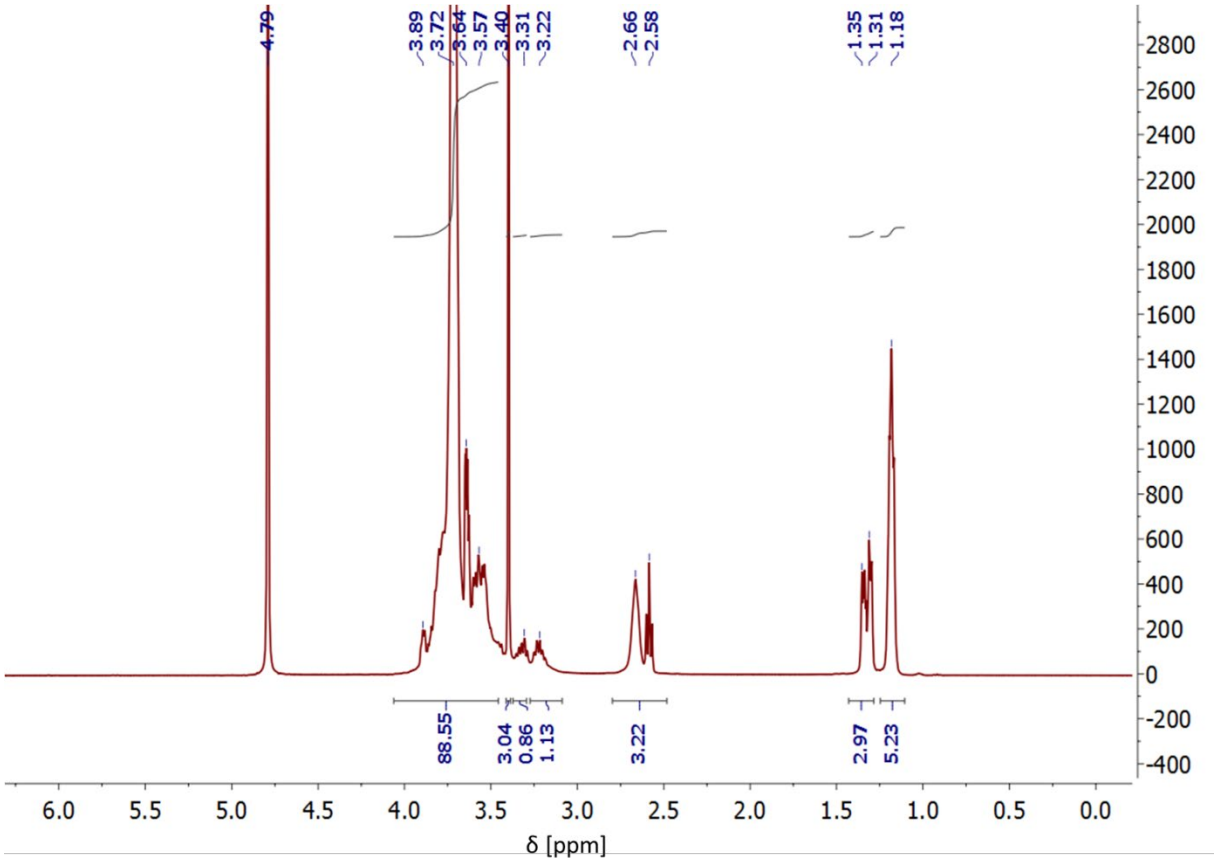

Figure S17: ^{1}H NMR spectrum of Jeff(Et-COOH)$_2$ in D_2O

^{13}C NMR spectrum (101 MHz, D_2O):

δ [ppm] = 9.33 (CH_3 PPO), 12.52 (CH_3 PPO), 15.65 (CH_3 PPO), 32.26 (-N-CH_2-CH_2-COOH), 41.49 (-N-CH_2-CH_2-COOH), 53.64 (-CH_2-$CHCH_3$-N-), 58.08 (OCH_3), 69.60 (CH_2 PEO), 71.01 (-CH_2-$CHCH_3$-N-), 74.01 (CH_2 PPO), 74.60 – 75.70 (CH PPO), 177.41 (COOH)

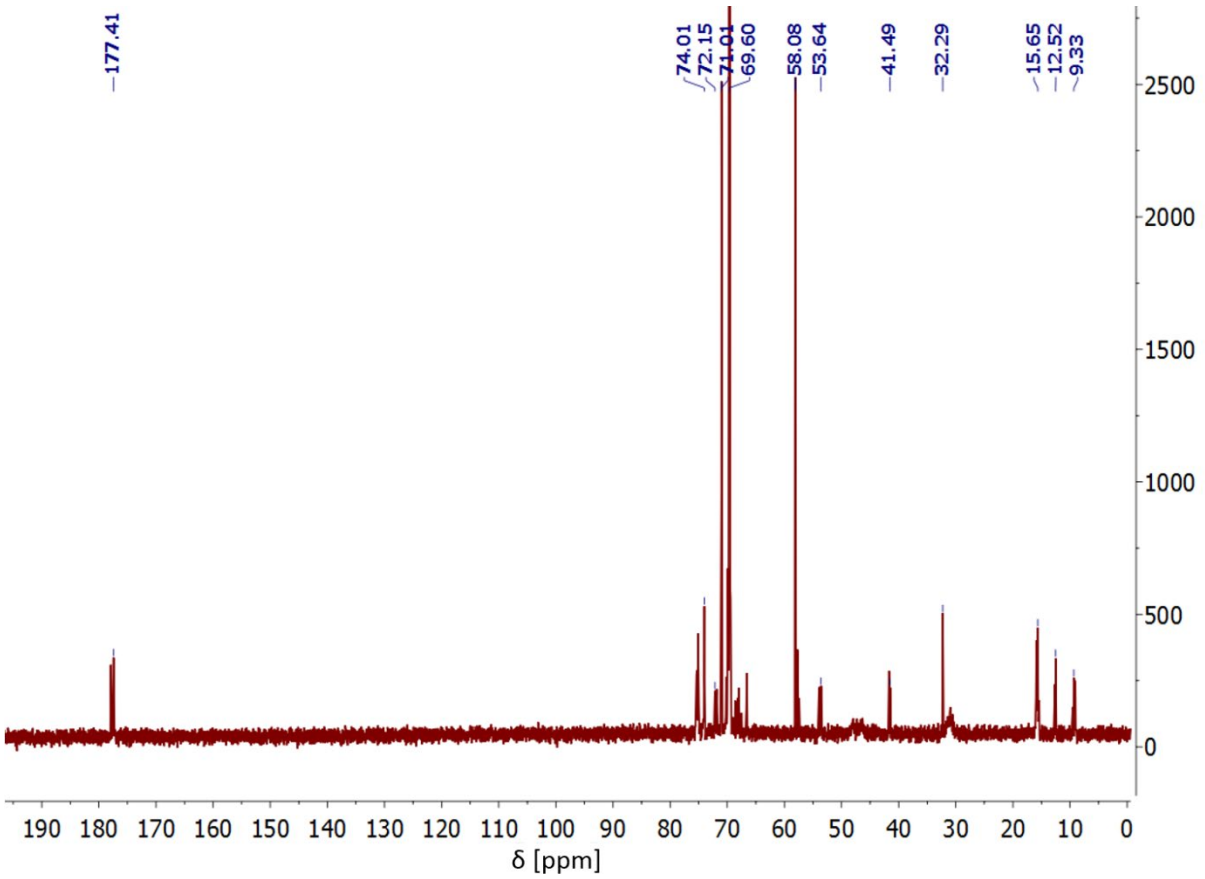

Figure S18: ^{13}C NMR spectrum of Jeff(Et-COOH)$_2$ in D_2O

Adsorption measurement:

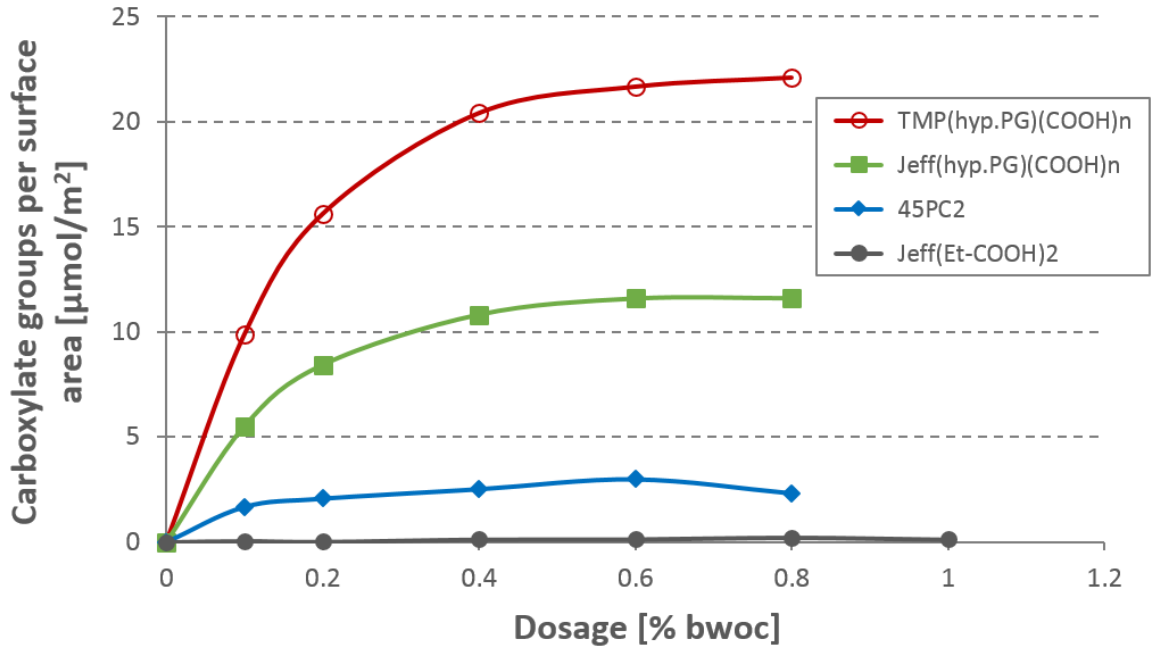

Figure S19: Adsorption isotherms of the individual polymers at w/c = 0.50, plotted as carboxylate groups available per surface area in dependence of the polymer dosage

5.2.2. Weitere Veröffentlichungen

Die **Publikationen #8** und **#9** beschreiben erste Versuche zur Synthese eines hyperverzweigten Fließmittels. Im Gegensatz zu **Publikation #7** wurde in diesen Arbeiten Jeffamin M-2070 als Initiator für die anionische Ringöffnungspolymerisation von Glycidol verwendet. Jeffamin M-2070 ist ein höhermolekulares Polyetheramin, welches aus 31 Ethylenoxid und 10 Propylenoxid-Einheiten besteht. Ein wirksames Fließmittel konnte auch ausgehend von diesem Initiator synthetisiert werden, allerdings resultierte eine breitere Molmassenverteilung, da sich die Polymerisationskontrolle durch das höhere Molekulargewicht von Jeffamin M-2070 als schwieriger erwies. Außerdem wurden aufgrund der höheren Anzahl an unpolaren Propylenoxid-Einheiten Löslichkeitsprobleme während der Polymerisation beobachtet, weshalb die Synthese auf das kurzkettige Jeffamin M-1000 umgestellt wurde, das nur drei Propylenoxid-Einheiten beinhaltet und daher hydrophiler ist.

5.2.2.1. Publikation #8: Synthesis and Characterization of a Novel Kind of Superplasticizer with Jellyfish-Like Structure Based on Hyperbranched Polyglycerols

Publikation #8

Synthesis and Characterization of a Novel Kind of Superplasticizer with Jellyfish-Like Structure Based on Hyperbranched Polyglycerols

Manuel Ilg, Johann Plank

20. Internationale Baustofftagung (ibausil)

Weimar (Germany), 2018

Tagungsband 1, 835 – 842

Ilg, M.; Plank, J.

Synthesis and Characterization of a Novel Kind of Superplasticizer with Jellyfish-Like Structure Based on Hyperbranched Polyglycerols

1. Introduction

With a production volume of more than four million tons per year, polycarboxylate superplasticizers (PCEs) represent one of the most important kind of concrete admixtures. They can disperse cement even at low w/c ratios and require much lower dosages compared to polycondensate based superplasticizers. A main advantage of the PCE technology is their high chemical variability which allows to synthesize PCE variants with quite different molecular structures [1]. It is well established that the dispersing efficacy and thus the application properties of PCEs can be tuned by various structural parameters (e.g. repartition of the monomers, anionic charge amount, side chain density and length). Therefore, much effort has been made over the last years to develop new PCE molecules and to further elucidate the correlation between structure and dispersing performance. Generally, PCEs are comb-shaped polymers with a main chain holding anionic carboxylate groups and side chains which most often contain polyethylene glycol (PEG) units [1]. Typically, they are synthesized by aqueous free radical copolymerization of carboxylate bearing monomers (e.g. acrylic or methacrylic acid, maleic anhydride etc.) and macromonomers comprising non-ionic PEG side chains (e.g. MPEG, APEG, VPEG, IPEG, HPEG). The superior efficacy of PCEs can be attributed to a steric hindrance effect imparted by the non-adsorbing PEG chains which protrude freely into the pore solution and thus prevent the cement particles from agglomeration. The steric effect depends on various parameters which are described by the *Ottewill-Walker* equation. Accordingly, a high dispersing efficacy can be achieved by PCE polymers which adsorb with a high layer thickness on the cement particle surface. This is in agreement with findings that PCEs with longer side chains are more powerful superplasticizers than those with shorter ones [2]. Furthermore, the adsorbed conformation and an effective surface coverage are also highly relevant for the dispersion of cement.

Recent studies suggest that star-shaped PCEs are more effective than comb-shaped polymers as they produce a much higher layer thickness due to their branched multi-arm structure [3]. Therefore, the question arises whether dendrimeric or hyperbranched structural motifs can also provide a much stronger steric stabilization. Until now, hyperbranched structures have found little consideration and their effect in cement paste is rather unknown. Only a very limited number of patents present vague examples for such PCE polymers or describe in general the synthesis of branched macromonomers [4-6]. To close this gap, a new type of superplasticizer which is composed of a hyperbranched polyglycerol scaffold with carboxylate groups in the outer sphere and one single side chain with ethylene as well as propylene oxide subunits at the branching point was synthesized in this work. The hyperbranched superplasticizer whose structure resembles a jellyfish was synthesized in a three step synthesis from a polyether amine and glycidol. The polyglycerol scaffold was built up by anionic ring opening polymerization (ROP) of glycidol using the slow monomer addition technique [7]. In the following, the hyperbranched superplasticizer was

characterized with respect to its molecular properties and anionic charge amount. Additionally, the dispersing performance of the polymer was assessed *via* mini slump tests and compared with that of a linear, non-hyperbranched small molecule. The sulfate tolerance, slump retention over time and the effect of the jellyfish-like polymer on cement hydration were also investigated. The overall aim of this study was to elucidate the properties of hyperbranched motifs in cement paste and to gain more information on the structure-performance relationship of PCE superplasticizers.

2. Materials and methods

An ordinary Portland cement CEM I 52.5 N from HeidelbergCement was used for the experiments. Quantitative X-ray diffraction with subsequent *Rietveld* analysis resulted in following phase composition: 53.3 wt. % C_3S, 25.7 wt. % C_2S, 8.8 wt. % C_3A, 2.6 wt. % C_4AF, 0.1 wt. % free lime, 3.3 wt. % anhydrite, 0.7 wt. % hemihydrate, 0.1 wt. % dihydrate, 3.9 wt. % calcite, 1.0 wt. % quartz and 0.5 wt. % arcanite. The specific surface area (*Blaine* value) of the cement was 3,479 cm^2/g and the d_{50} value as determined by laser granulometry was found to be 13.5 µm.

For the synthesis of the hyperbranched superplasticizer, a polyether amine commercially available under the proprietary name Jeffamine® M-2070 (Huntsman) was utilized as starting compound. This methoxy terminated polyether amine exhibits a M_w of ~ 2,300 g/mol and comprises ethylene and propylene oxide units at a molar ratio of 31 : 10. The bis-glycidolization of the Jeffamine® as well as the anionic ring opening polymerization of glycidol were carried out under an inert argon atmosphere using standard *Schlenk* line techniques to avoid any side reaction of the highly reactive glycidol.

The molecular properties (i.e. molar masses, PDI) of the synthesized polymers were determined by size exclusion chromatography (Waters 2695 separation module equipped with three Ultrahydrogel™ columns and one guard column). For this purpose, polymer solutions holding a concentration of 10 g/L were prepared using 0.1 M $NaNO_3$ (adjusted with NaOH to pH = 12) as solvent. The hydrodynamic radius of the polymers was measured *via* dynamic light scattering (Zetasizer Nano from Malvern Instruments). Solutions exhibiting a concentration of 10 g/L were prepared by dissolving the respective amount of the polymer in synthetic cement pore solution, SCPS (1.72 g $CaSO_4 \cdot 2\ H_2O$, 6.96 g Na_2SO_4, 4.75 g K_2SO_4 and 7.12 g KOH in 1 L DI water). The samples were filtrated through a 0.2 µm syringe filter before measurement to remove any dust particles. Additionally, the anionicity of the polymers was quantified under different pH and electrolyte conditions (deionized (DI) water, 0.1 M NaOH and SCPS, respectively) by using a particle charge titrator (PCD 03 pH from BTG Instruments). A cationic 0.001 M poly dimethyl ammonium chloride solution was titrated to 10 mL of the polymer solutions (concentration of 0.1 g /L) until charge neutralization.

The dispersing performance of the polymers was assessed by mini-slump tests following the specifications outlined in DIN EN 1015. A detailed description of the procedure is provided in [8]. The impact of the polymers on the kinetics of cement hydration was investigated by isothermal heat flow calorimetry (TAM Air Thermostat). Here, 4 g cement were filled into 20 mL glass ampoules, mixed with the respective amounts of the polymer solutions and placed into the calorimeter. The heat released from the cement hydration was recorded until it subsided completely.

3. Results and discussion

3.1 Synthesis and characterization of the hyperbranched superplasticizer

The hyperbranched superplasticizer was synthesized *via* a three step synthesis starting from Jeffamine® M-2070. At first, Jeffamine® was reacted with two equivalents glycidol to achieve a bis-glycidolized intermediate which exhibits four terminal hydroxyl groups. After partial deprotonation of 10 % of the hydroxyl groups with potassium methoxide, the hyperbranched polyglycerol scaffold was gradually built up by slow monomer addition of glycidol [7]. The partially deprotonated bis-glycidolized intermediate acts like an initiator which can attack the unsubstituted end of the oxirane ring of glycidol, thus leading to the ring opening and the formation of a primary and secondary alkoxide group. Subsequent reaction of these highly reactive sites with glycidol induces step by step the formation of the hyperbranched polyglycerol motif. Glycidol was slowly added to guarantee a controlled polymerization and to finally obtain a polyglycerol with controlled molecular weight and low polydispersity. The polyglycerol scaffold exhibits numerous primary and secondary hydroxyl groups which can be quantified by the titration according to *Elder* [9]. Their number was needed for the final synthesis step where carboxylate groups were incorporated in the outer sphere of the polyglycerol by carboxymethylation using sodium chloroacetate. This reaction was carried out under highly alkaline conditions to guarantee a high degree of derivatization. As product, a slightly viscous, orange colored polymer solution with a solid content of 29 wt.% and a pH of 6.5 was obtained For the polymer tested in this study, a molar ratio of glycidol to the bis-glycidolized Jeffamine® of 30 : 1 was applied, thus designating this polymer as Jeff(hyp.PG30)$(COOH)_n$. The chemical structure of the hyperbranched superplasticizer whose structure resembles a jellyfish is illustrated in **Figure 1**.

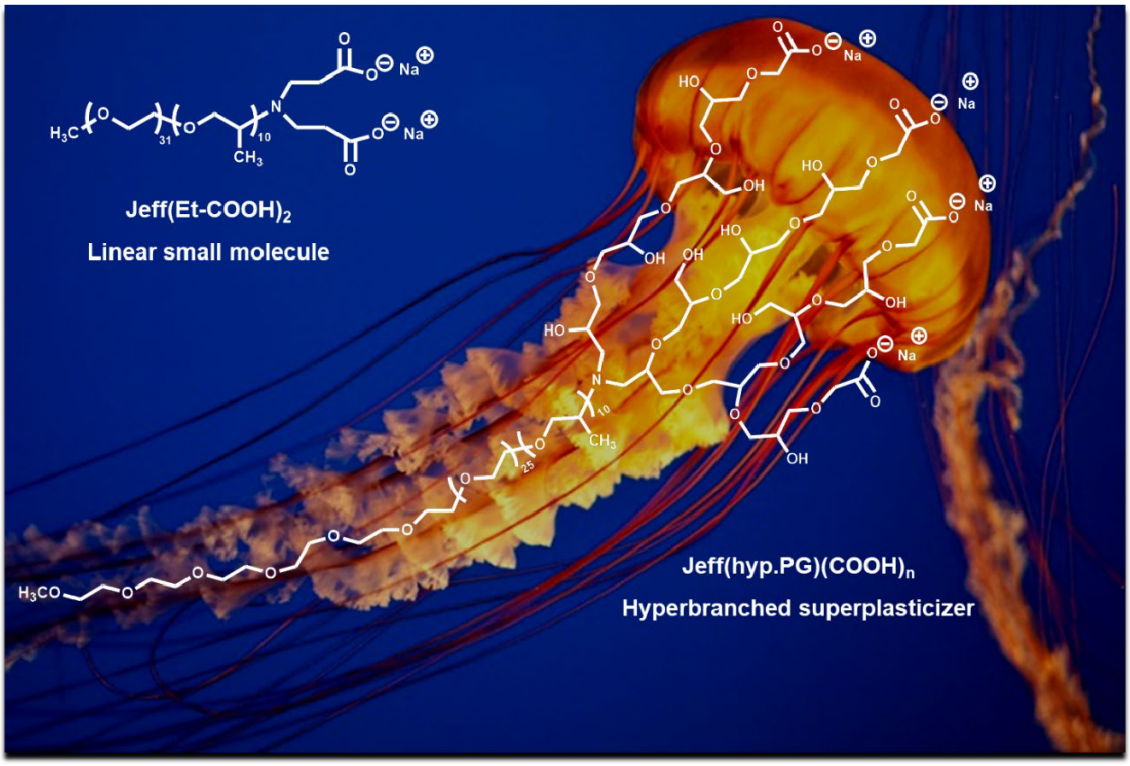

Figure 1: Chemical structures of the jellyfish-like superplasticizer as well as the linear, non-hyperbranched small molecule.

Additionally, a linear, non-hyperbranched small molecule with two terminal carboxylate groups was synthesized to ascertain the effect of the hyperbranched polyglycerol scaffold on the dispersing properties. This molecule was obtained by a *Michael* type addition of Jeffamine® to methyl acrylate and subsequent acid hydrolysis of the ester functionalities using an excess of formic acid. The final product was a highly viscous, yellowish polymer solution with a solid content of 85 wt.% and a pH of 3.4. The chemical structure of this linear small molecule which is designated as Jeff(Et-COOH)$_2$ is also depicted in **Figure 1**.

The synthesized polymers were first characterized by size exclusion chromatography and their hydrodynamic radii were measured *via* dynamic light scattering (see results in **Table 1**).

Table 1: Molar masses, PDI and hydrodynamic radii (R_h) of the synthesized polymers.

Polymer sample	M_w (g/mol)	M_n (g/mol)	PDI (M_w/M_n)	R_h (nm)
Jeff(Et-COOH)$_2$	2,660	2,610	1.0	3.2 ± 0.3 nm
Jeff(hyp.PG30)(COOH)$_n$	6,420	3,730	1.7	9.7 ± 0.1 nm

The hyperbranched polymer exhibits relatively low molar masses (e.g. M_w of 6,420 g/mol) which are much lower compared to the values known for common PCE polymers. Moreover, the slow monomer addition of glycidol resulted in a low polydispersity (PDI) which implies that the anionic ring opening polymerization indeed occurred in a very controlled manner. The molecular weights of the incorporated polyglycerol scaffold are also in good agreement with the values reported in the literature [10]. The dynamic light scattering measurements confirmed that Jeff(hyp.PG30)(COOH)$_n$ possesses a much higher hydrodynamic radius than the linear, non-hyperbranched small molecule (9.7 nm *vs.* 3.2 nm). This can be attributed to a much higher steric demand of the polyglycerol scaffold.

Table 2: Anionic charge amounts of the polymers in DI water, 0.1 M NaOH and SCPS.

Polymer sample	DI water (µeq/g)	0.1 M NaOH (µeq/g)	SCPS (µeq/g)
Jeff(Et-COOH)$_2$	~ 0	430	20
Jeff(hyp.PG30)(COOH)$_n$	925	1,020	220

Next, the anionic charge amounts of the polymers were determined in DI water, 0.1 M NaOH and SCPS. From **Table 2** it can be seen that the hyperbranched superplasticizer in all tested solutions produced a higher anionic charge amount than the linear, non-hyperbranched Jeff(Et-COOH)$_2$. This can be explained by the larger amount of carboxylate groups prevailing in the periphery of the polyglycerol scaffold. The highest anionic charge amount was found for both polymers in 0.1 M NaOH since all carboxylate functionalities are fully deprotonated there. Moreover, it can be noticed from **Table 2** that both polymers have a high tendency to complex Ca^{2+} ions, as a significant decline of the anionic charge amount was found in SCPS.

3.2. Dispersing performance of the hyperbranched superplasticizer

The dispersing performance of Jeff(Et-COOH)$_2$ and Jeff(hyp.PG30)(COOH)$_n$ was ascertained *via* mini slump tests. For these experiments, a w/c ratio of 0.5 was applied which results in a spread flow of 18 cm when no polymer was present. In the following, mini slump tests were conducted to determine the increase of the spread flow with polymer dosage.

It becomes obvious from **Figure 2** that Jeff(Et-COOH)$_2$ only effectuated a minor increase of the paste fluidity (e.g. spread flow of 20.7 cm at 0.2 % bwoc). The maximum achievable spread flow value was 22 cm at 0.6 % bwoc, even higher dosages did not enhance the paste fluidity any further. Contrary to this, Jeff(hyp.PG30)(COOH)$_n$ showed a much higher dispersing ability. For instance, at a dosage of 0.19 % bwoc a spread flow value of 26 cm was achieved. Based on these results it can be concluded that the hyperbranched polymer is a much more powerful superplasticizer compared to the linear, non-hyperbranched small molecule as it engenders a much stronger steric effect due to the hyperbranched polyglycerol scaffold.

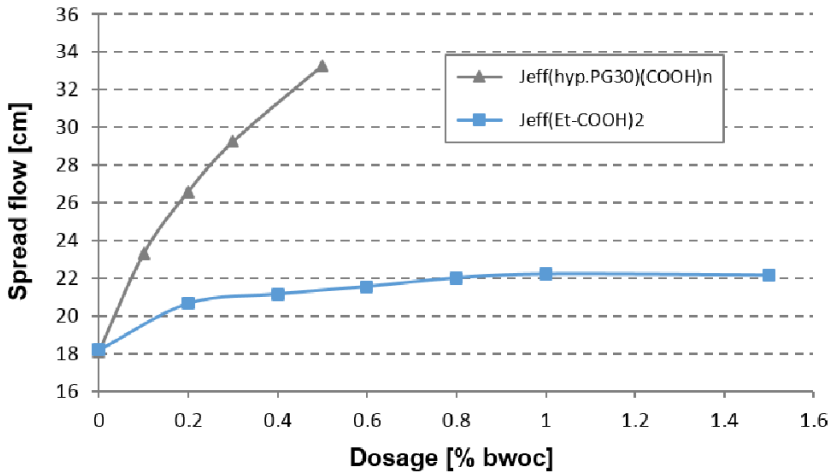

Figure 2: Spread flow of cement pastes (w/c = 0.5) admixed with different dosages of the synthesized polymers.

3.3 Time dependent slump loss behavior

Next, the time dependent evolution of the spread flow of cement pastes admixed with the synthesized polymers was investigated. Two cement pastes (w/c = 0.5) were fluidized with 0.19 % bwoc of Jeff(hpy.PG30)(COOH)$_n$ (spread flow of 26 cm) and 0.8 % bwoc Jeff(Et-COOH)$_2$ (spread flow of 22 cm) respectively and their slump loss behavior over time was determined.

According to **Figure 3** the spread flow of the cement paste containing the linear, non-hyperbranched small molecule quickly decreased from 22 cm to 18.3 cm within two hours. Opposite to this, the hyperbranched superplasticizer caused a much slower slump loss. The cement paste fluidized with Jeff(hyp.PG30)(COOH)$_n$ still exhibited a spread flow of 22.6 cm after four hours. This demonstrates that the hyperbranched polymer can provide long slump retention which enables to utilize this superplasticizer for applications where principally long processing times are needed.

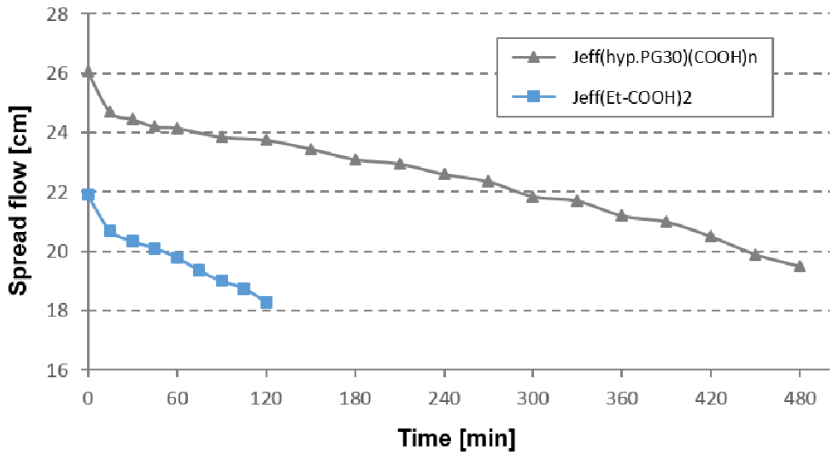

Figure 3: Slump loss behavior of cement slurries admixed with 0.19 % bwoc Jeff(hyp.PG30)$(COOH)_n$ and 0.8 % bwoc Jeff(Et-$COOH)_2$.

3.4. Effect of sulfate ions on the dispersing performance

The dispersing efficacy of the synthesized polymers was also tested in the presence of sodium sulfate. Generally, the performance of common PCE based superplasticizers is impaired by sulfate ions as they compete with the PCE molecules for adsorption sites on the cement surface. To probe into the sulfate tolerance, different amounts (i.e. 0.5 – 2.0 % bwoc) of sodium sulfate were pre-dissolved in the mixing water together with the polymers and mini slump tests were conducted.

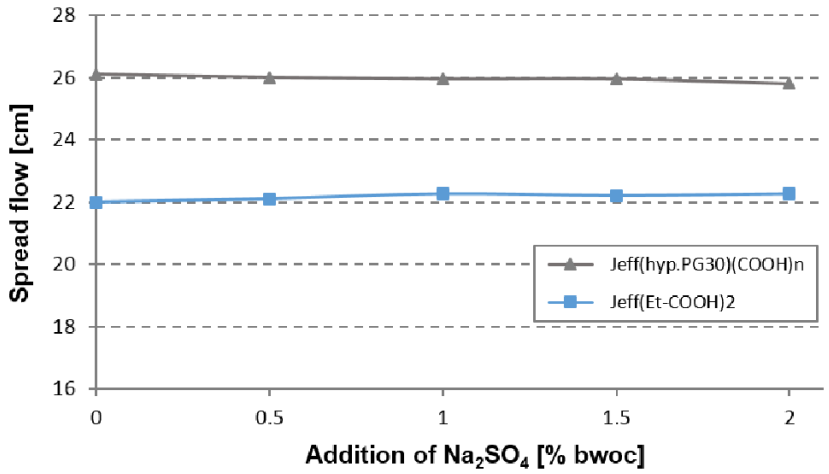

Figure 4: Impact of different Na_2SO_4 dosages on the spread flow of cement pastes holding 0.19 % bwoc of Jeff(hyp.PG30)$(COOH)_n$ and 0.8 % bwoc Jeff(Et-$COOH)_2$.

From **Figure 4** it can be seen that both polymers exhibit a high robustness towards sulfate ions, as for sodium sulfate additions of up to 2 % bwoc the spread flow remained constant. This can be explained by the specific structure of both polymers. Since Jeff(Et-$COOH)_2$ and Jeff(hyp.PG30)$(COOH)_n$ exhibit carboxylate groups at one end, they presumably will adsorb on the cement surface in a tail like conformation while the sidechain will stretch out almost vertically into the pore solution. Consequently, a

much denser surface coverage as well as a strong steric effect result which impede the sulfate ions from replacing and desorbing already adsorbed PCE molecules.

3.5 Impact of the hyperbranched superplasticizer on cement hydration

The effect of the synthesized polymers on cement hydration was investigated by isothermal heat flow calorimetry. Here, the heat evolution from a cement paste (w/c = 0.5) admixed with different amounts of the synthesized polymers was captured over time (see **Figure 5**). The linear, non-hyperbranched small molecule Jeff(Et-COOH)$_2$ did not notably affect cement hydration. However, for the hyperbranched superplasticizer increased retardation at higher dosages was observed. For instance, 0.2 % bwoc of Jeff(hyp.PG30)(COOH)$_n$ resulted in a retardation of almost 18.5 h compared to the neat cement paste. The retardation can be ascribed to the hyperbranched polyglycerol scaffold which causes a densely packed polymer layer around the cement particles, thus hindering the ingress of water and consequently delaying the ion transport from the cement surface. Another reason is the high calcium complexing ability of the hyperbranched superplasticizer, as seen from the charge titration experiments.

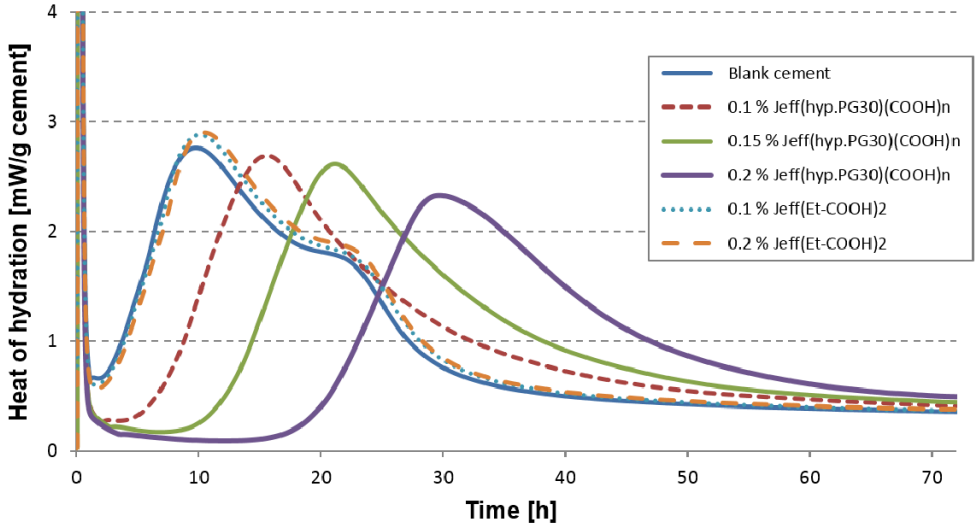

Figure 5: Heat evolvement from cement pastes (w/c = 0.5) holding different dosages of the synthesized polymers.

4. Conclusion

In this study, the synthesis of a new kind of superplasticizer with jellyfish-like structure based on hyperbranched polyglycerols was presented. Contrary to common PCE superplasticizers, this polymer was synthesized by anionic ring opening polymerization of glycidol using the slow monomer addition technique. This way a hyperbranched polymer with low polydispersity and controlled molecular weight was obtained. The hyperbranched superplasticizer exhibits a much higher dispersing ability compared to its linear, non-hyperbranched small molecule counterpart, due to its much stronger steric hindrance effect imparted by the polyglycerol scaffold. Additionally, the hyperbranched polymer shows a high robustness towards sulfate ions and effectuates long slump retention. Our results signify that in general hyperbranched scaffolds

represent a very promising motif also for PCE polymers. However, more research needs to be carried out to realize the full potential of these structures.

5. References

[1] Plank, J.; Lei, L.: *Future perspectives of PCE technology*, in: J. Plank, L. Lei, eds., 2nd International Conference on Polycarboxylate Superplasticizers (PCE 2017), Munich (Germany), Conference proceedings, 2017, pp. 19-62.

[2] Houst, Y.F.; Bowen, P.; Perche, F.; Kauppi, A.; et al.: *Design and function of novel superplasticizers for more durable high performance concrete (superplast project)*, Cement and Concrete Research 38 (2008), pp. 1197-1209.

[3] Liu, X.; Wang, Z.; Zhu, J.; Zhao, M.; Liu, W.; Yin, D.: *Preparation and characterization of star-shaped polycarboxylate superplasticizer*, Eleventh ACI International Conference on Superplasticizers and Other Chemical Admixture in Concrete, sp-302-14, 2015, Ottawa (Canada), pp. 183-198.

[4] Shou, C.; Xiao, W.: *Hyper-branchend polycarboxylate high-efficiency water reducing agent and preparation method thereof*, CN 101580353 B, 2012.

[5] Miao, C.; Qiao, M.; Ran, Q.; Liu, J.; Zhou, D.; Yang, Y.; Mao, Y.: *Preparation method of hyperbranched polycarboxylic acid type copolymer cement dispersant*, US 20130102749 A1, 2013.

[6] Raether, R.B.; Flakus, S.; Dengler, J.; Zeminian, N.; Ros, I.: *Branched polycarboxylate ethers*, EP 2774941 A1, 2014.

[7] Sunder, A.; Hanselmann, R.; Frey, H.; Mülhaupt, R.: *Controlled synthesis of hyperbranched polyglycerols by ring-opening multibranching polymerization*, Macromolecules 32 (1999), pp. 4240-4246.

[8] Habbaba, A.; Lange, A.; Plank, J.: *Synthesis and performance of a modified polycarboxylate dispersant for concrete possessing enhanced cement compatibility*, Journal of Applied Polymer Science 129 (2013), pp. 346-353.

[9] Carey, M.A.; Wellons, S.L.; Elder, D.K.: *Rapid method for measuring the hydroxyl content of polyurethane polyols*, Journal of Cellular Plastics 20 (1984), pp. 42-48.

[10] Wang, G.; Li, L.; Lan, J.; Chen, L.; You, J.: *Biomimetic crystallization of calcium carbonate spherules controlled by hyperbranched polyglycerols*, Journal of Materials Chemistry 18 (2008), pp. 2789-2797.

Authors

M.Sc. Manuel Ilg manuel.ilg@bauchemie.ch.tum.de
Prof. Dr. Johann Plank sekretariat@bauchemie.ch.tum.de

Technische Universität München
Lehrstuhl für Bauchemie
Lichtenbergstraße 4
85747 Garching

5.2.2.2. Publikation #9: A New Type of Superplasticizer Possessing Dendrimeric Structure

Publikation #9

A New Type of Superplasticizer Possessing Dendrimeric Structure

Manuel Ilg, Johann Plank

In: J. Liu, Z. Wang, T. C. Holland, J. Huang, J. Plank (Eds.),
Superplasticizers and Other Chemical Admixtures in Concrete,
Proceedings Twelfth International Conference, Beijing (China), 2018
SP-329-08, 89 – 102

A NEW TYPE OF SUPERPLASTICIZER POSSESSING DENDRIMERIC STRUCTURE

Manuel Ilg and Johann Plank

Technische Universität München, Chair for Construction Chemistry,

Lichtenbergstraße 4, 85747 Garching, Germany

Biography:

Manuel Ilg studied chemistry and received his B.Sc. and M.Sc. degrees in chemistry from Technische Universität München. Since 2014 he is a Ph.D. student at the Chair for Construction Chemistry in Garching where he works on polycarboxylate superplasticizers with a focus on novel PCE structures and concepts, e.g. to overcome the "stickiness" of concretes prepared at low water-cement ratios.

Johann Plank is a full Professor at the Institute of Inorganic Chemistry of Technische Universität München, Germany. Since 2001, he holds the Chair for Construction Chemistry there. His research interests include cement chemistry, concrete admixtures, organic-inorganic composite and nano materials, concrete, dry-mix mortars and oil well cementing. In 2015 he received the *A. Aignesberger* Award of ACI for his outstanding contributions to the research and development of superplasticizers and other chemical admixtures.

ABSTRACT

In this study, the synthesis of a new superplasticizer is described which is composed of a hyperbranched polyglycerol scaffold with multiple carboxylate groups in the periphery and one single side chain comprised of ethylene oxide as well as propylene oxide subunits at the

branching point. This hyperbranched superplasticizer was obtained *via* a three step synthesis from Jeffamine and glycidol by anionic ring-opening polymerization. Additionally, a linear small molecule was synthesized as reference using a *Michael* type reaction to assess the effect of the dendrimeric structural motif on the dispersing capability and application properties (e.g. slump retention, sulfate tolerance). Both polymers were characterized by SEC and their anionicity was captured by charge titration. Furthermore, mini-slump tests and heat flow calorimetric measurements were conducted. For the hyperbranched superplasticizer a superior dispersing performance was found compared to the reference, resulting from improved steric hindrance induced by the dendrimeric polyglycerol.

Keywords: Hyperbranched superplasticizer, Polyglycerol, Dendrimeric structure, Dispersion, Calorimetry, Sulfate tolerance, Small molecule, Admixture

INTRODUCTION

In developed countries, ninety percent of the concrete manufactured nowadays contain chemical admixtures which are typically added in small quantities (< 2 wt.%) to improve the material properties in the fresh and hardened state [1, 2]. For instance, polycarboxylate superplasticizers (PCEs) are applied to increase the workability and/or to enhance the durability due to a much lower amount of water that is principally required to attain a specific flowability [3, 4].

The invention of PCEs in 1981 marks a milestone in modern admixture technology. After the introduction of PCEs it was possible to fluidize concrete even at very low w/c ratios and to maintain a fluid consistency over several hours which fostered the development of high performance concretes (e.g. SCC or UHPC) in the following years. Compared to conventional polycondensate based superplasticizers like BNS or MFS, a big advantage of the PCEs is their

high chemically variability. Their dispersing performance can be tuned by numerous structural parameters (e.g. anionic charge amount, side chain density, repartition of monomers etc.) thus allowing to tailor PCE products which exhibit quite different properties in individual applications [5]. Depending on the chemical nature of the monomers a broad range of PCE variants can be obtained (e.g. MPEG-, APEG-, IPEG-, HPEG-, VPEG-, OSi- or XPEG-PCEs) [6].

Generally, PCEs exhibit a comb like structure with a main chain holding anionic anchor groups and non-ionic side chains which are typically composed of polyethylene glycol units. It is well established that the superior dispersing efficacy of PCEs can be attributed to a steric hindrance effect generated by those lateral chains which keep the cement particles apart and prevent them from agglomeration [7]. The steric effect is directly proportional to the thickness of the adsorbed polymer layer, as described by the *Ottewill-Walker* equation. The significance of the adsorbed layer thickness for the steric stabilization is supported by findings that PCEs possessing longer side chains are more effective dispersants than those exhibiting shorter ones [8]. Additionally, the adsorbed conformation of the polymer attached to the particle surface (e.g. train, loop, tail) greatly determines the layer thickness [9].

The relevance of the adsorbed layer thickness in the steric stabilization inspires to develop PCEs with dendrimeric, respectively hyperbranched structures to research whether such products can provide a much stronger steric hindrance effect. Unfortunately, hyperbranched structural motifs have found only little entrance into PCE technology so far and their dispersing effectiveness in cement is rather unknown. Only a few patents are existing which propose principal structures for such PCE molecules [10, 11]. To our knowledge, the first example for a hyperbranched PCE was presented by *Shou* and *Xiao* in 2012. This PCE is composed of a main polymer chain comprising methyl allyl sulfonate, polyethylene glycol ally ether and *tert.*-butyl acrylate and hyperbranched polyamide side chains at both ends of the

main chain (a “dumbbell” like structure) [10]. In the outer sphere of the hyperbranched molecule carboxylate groups are present to facilitate the adsorption onto the cement surface.

The aim of the present study was to develop a synthesis route towards a novel hyperbranched polycarboxylate superplasticizer and to present first results on the properties of an admixture possessing such structural motif. This new type of superplasticizer does not exhibit the typical comb-shaped structure, but consists of a hyperbranched polyglycerol with carboxylate groups in the periphery. At the branching point a polyether amine containing ethylene and propylene oxide units is attached to provide an additional steric hindrance effect. The hyperbranched polymer was characterized with respect to its molecular properties (M_w, M_n, R_h) and its anionic charge amount. The dispersing performance of the hyperbranched polymer was assessed *via* mini slump testing and compared with the efficiency of a linear, non-hyperbranched small molecule. Furthermore, its sulfate tolerance and slump retaining ability were ascertained. The effect of the hyperbranched superplasticizer on the kinetics of the cement hydration was finally assessed by heat flow calorimetry.

RESEARCH SIGNIFICANCE

PCE superplasticizers exhibit a comb-shaped structure comprising a main chain holding anionic anchor groups and non-ionic side chains which are predominantly composed of polyethylene glycol units. However, less attention has been given to hyperbranched motifs so far. This study aims to investigate the properties of dendrimeric scaffolds and to evaluate potential benefits which can be drawn from the incorporation of such hyperbranched structures. The information obtained here about the relationship between the structure and dispersing efficacy could help to develop even more powerful superplasticizers in the future.

EXPERIMENTAL PART

Cement

The experiments carried out in this study were performed with an ordinary Portland cement CEM I 52.5 N. Its mineralogical composition as determined by *Q-XRD* and *Rietveld* analysis is shown in **Table 1**. For the specific surface area a *Blaine* value of 3,479 cm^2/g was measured and the density was found to be 3.19 g/cm^3 (He pycnometry). The d_{50} *value* of the cement lies at 13.5 µm (laser granulometer).

Polymer samples

The chemical structures of the synthesized polymers are illustrated in **Fig. 1**. The hyperbranched superplasticizer *Jeff(hyp.PG)(COOH)*$_n$ was synthesized in a three step synthesis starting from a polyether amine (Jeffamine M-2070). This starting compound is a monoamine with an average molar mass M_w of ~ 2,300 g/mol and contains ethylene as well as propylene oxide units in a molar ratio of 31 : 10.

In the first step of the synthesis, the Jeffamine was converted with glycidol to a bis-glycidolized intermediate which was then partially deprotonated with potassium methoxide. Next, the polyglycerol scaffold was built up by anionic ring-opening polymerization of glycidol initiated by the deprotonated intermediate. Finally, carboxylate anchor groups were introduced into the periphery of the polyglycerol scaffold *via* carboxymethylation using sodium chloroacetate. As final product, an orange colored, slightly viscous polymer solution exhibiting a solid content of 29 wt.% and a pH of 6.5 was obtained.

Additionally, a linear, non-hyperbranched small molecule *Jeff(Et-COOH)*$_2$ with two terminal carboxylate groups was synthesized as a reference polymer. This compound can be formed in a two-step synthesis *via* a *Michael* type reaction of Jeffamine and methyl acrylate. The carboxylate groups were introduced in the final step by acid hydrolysis of the ester groups

using an excess of formic acid. Here, a highly viscous, yellowish polymer solution with a solid content of 85 wt. % and a pH of 3.4 was obtained. A detailed description of the syntheses will be presented in another paper which is currently under preparation.

Size exclusion chromatography (SEC)

The molar masses (M_w and M_n) of the polymers were determined by size exclusion chromatography. The instrument is equipped with a RI detector and a three angle static light scattering detector. Solutions of the polymer samples holding a concentration of 10 g/L were prepared, filtrated through a 0.2 µm syringe filter and separated on a pre-column and three columns using a 0.1 M $NaNO_3$ solution (adjusted with NaOH to a pH of 12) as an eluent at a flow rate of 1.0 mL/min. For the calculation of M_w and M_n a *dn/dc* value of 0.135 mL/g (value for polyethylene oxide) was adopted.

Anionic charge amount

The anionic charge amount of the polymer samples was quantified *via* polyelectrolyte titration using a particle charge detector. First, solutions of the polymer samples holding a concentration of 0.1 g/L were prepared using either DI water, synthetic cement pore solution (SCPS) or 0.1 M NaOH as solvent to determine the anionicity under different pH and polyelectrolyte conditions. The SCPS was prepared by dissolving 1.72 g [0.061 oz] $CaSO_4 \cdot 2H_2O$, 6.96 g [0.246 oz] Na_2SO_4, 4.75 g [0.168 oz] K_2SO_4 and 7.12 g [0.251 oz] KOH in 1 L [33.8 fl oz] DI water. For the experiment, 10 mL [0.338 fl oz] of the solution were pipetted into the PTFE measuring cell of the instrument and a 0.001 M poly diallyl dimethyl ammonium chloride (polyDADMAC) solution was added until charge neutralization (= isoelectric point) was reached. The measurements were repeated three times for each solution and the obtained values were averaged. Finally, from the amount of consumed polyDADMAC the anionic charge per gram of polymer was calculated.

Hydrodynamic radius

The hydrodynamic radius R_h of the polymer samples was determined by dynamic light scattering using a Zetasizer Nano. Solutions exhibiting a concentration of 10 g/L were prepared by dissolving the respective amount of polymer in SCPS. The polymer solutions were filtrated through a 0.2 µm syringe filter into a cuvette which was then transferred to the instrument. The measurement was repeated for each sample five times and the average value was calculated. Each test consisted of a 10 s light scattering run taken at a temperature of 25 °C [77 °F].

Cement dispersion

The dispersing efficiency of the synthesized polymers was investigated with a modified mini-slump test following in principle the guidelines specified in DIN EN 1015. First, the w/c ratio of the neat cement slurry was ascertained which is required for an initial slump flow of 18 ± 0.5 cm [7.1 ± 0.2 in.]. This w/c ratio was utilized in the following experiments where the dispersing performance of the individual polymers was tested. The polymers were pre-dissolved at different dosages in the mixing water, whereby the amount of water contained in the polymer solution was subtracted from the total amount of mixing water to keep a constant w/c ratio. The mini slump tests were carried out as follows: 300 g [10.6 oz] cement were added within 60 sec to the mixing water contained in a porcelain cup and then soaked for further 60 sec. Next, the cement/water mixture was vigorously stirred for 2 min with a spoon and subsequently poured into a *Vicat* cone (height 40 mm [1.57 in.], top diameter 70 mm [2.76 in.], bottom diameter 80 mm [3.15 in.] placed on a glass plate. After complete filling, the cone was vertically removed. The diameter of the spread cement paste was measured at two perpendicular axes and averaged to get the final spread flow value.

Furthermore, a time dependent mini slump test was conducted to investigate the slump loss behavior of the synthesized polymers. For this purpose, 500 g [17.6 oz] cement were mixed

with the required amount of water and polymer to achieve the targeted spread flow value. The mini slump test was carried out according to the procedure presented above. After each measurement the cement slurry was transferred back into the porcelain cup and covered with a wet towel to avoid desiccation. Prior to each subsequent measurement, the cement slurry was manually stirred for 2 min again.

Heat flow calorimetry

To ascertain the impact of the synthesized polymers on the kinetics of cement hydration, isothermal heat flow calorimetric measurements were performed. In a typical experiment, 4 g [0.141 oz] cement were filled into 20 mL [0.68 fl oz] glass ampoules and mixed with the respective amount of the aqueous polymer solutions (w/c = 0.5). The heat release from a neat cement paste was also captured as reference. After addition of the polymer solutions, the glass ampoules were capped with an aluminum lid, homogenized for 2 min with a vortex mixer and subsequently placed into the calorimeter. The measurement was continued until the heat evolution from the hydration reaction subsided completely.

RESULTS AND DISCUSSION

Synthesis and molecular properties of the synthesized polymers

The hyperbranched superplasticizer was synthesized *via* anionic ring-opening polymerization of glycidol using a partially deprotonated (10 %) bis-glycidolized Jeffamine as initiator. Glycidol represents a highly reactive hydroxyl epoxide which easily polymerizes to dendrimeric polyglycerols that exhibit numerous primary as well as secondary hydroxyl groups. The partially deprotonated Jeffamine initiator can attack the unsubstituted end of the epoxide ring of glycidol, thus leading to ring opening and the formation of a primary and secondary alkoxide group. The reaction of these highly reactive sites with glycidol leads to

the gradually formation of the polyglycerol scaffold. The addition of glycidol to the Jefamine based initiator was carried out according to the slow monomer addition approach which enables to synthesize well-defined polyglycerols with controlled molecular weights, low polydispersity and a high degree of branching, as is described in the literature [12]. The synthesis of hyperbranched polyglycerols according to the slow monomer addition technique was first introduced by *Frey* et al. who carried out various studies on the controlled polymerization of glycidol [12, 13]. In the final step the terminal carboxylate groups were incorporated *via* carboxymethylation under highly alkaline conditions using an excess of sodium chloroacetate to achieve a high degree of substitution of the terminal hydroxyl groups [14].

For comparison, a linear, non-hyperbranched small molecule was synthesized. This molecule was obtained by a *Michael* addition of Jeffamine to methyl acrylate and subsequent acid hydrolysis of the ester functionalities using formic acid. The composition of both polymers was clearly confirmed by FTIR and NMR spectroscopy (spectra not shown here).

First, the molecular properties of the synthesized polymers were determined by SEC and dynamic light scattering. The molar masses and the hydrodynamic radii of the polymers are summarized in **Table 2**.

From the data it becomes obvious that the hyperbranched polymer exhibits relatively low molar masses of 6,420 g/mol (M_w) and 3,730 g/mol (M_n), respectively. Furthermore, *Jeff(hyp.PG)(COOH)*$_n$ exhibits a narrow molecular weight distribution with a low PDI of 1.7 which indicates that the anionic ring-opening polymerization indeed had proceeded under very controlled conditions. The SEC spectra of the synthesized polymers are displayed in **Fig. 2**. The molecular weight found for the incorporated polyglycerol scaffold is in good agreement with values presented in other studies for such hyperbranched polyglycerols [12, 14].

As expected, the hydrodynamic radius R_h of the hyperbranched polymer is larger than the value for the linear small molecule (9.7 nm *vs.* 3.2 nm), resulting from the higher steric demand of the polyglycerol unit. Most interestingly, *Jeff(hyp.PG)(COOH)$_n$* also possesses a higher R_h value than a conventional MPEG type PCE superplasticizer (e.g. R_h of 45PC6: 4.5 ± 0.1 nm).

Next, the anionic charge amounts of the synthesized polymers were determined in DI water, 0.1 M NaOH and SCPS. The results are presented in **Table 3**. Generally, the hyperbranched polymer exhibits a higher anionicity compared to the linear *Jeff(Et-COOH)$_2$*, because of much more carboxylate groups existing in the outer sphere of the polyglycerol unit. The highest anionic charge amounts were found for both polymers in 0.1 M NaOH, as a consequence of complete deprotonation of the carboxylate groups there. However, the anionic charge amount significantly decreases in SCPS due to the complexation of Ca^{2+} ions which signifies a high binding affinity of the polymers to these ions. Based on these results it can be concluded that both synthesized polymers are negatively charged, thus allowing them to adsorb on the surface of the cement particles *via* electrostatic interactions.

Cement dispersion

The dispersing efficacy of the polymers was investigated by a series of mini slump tests where the increase of the spread flow as a function of the polymer dosage added was ascertained. At first the w/c ratio of a neat cement paste without any polymer was set to obtain a spread flow of 18 cm ± 0.5 cm [7.1 ± 0.1 in.]. This was achieved at a w/c ratio of 0.5. In the following, the effect of different dosages of the polymers on the spread flow was determined. The results are illustrated in **Fig. 3**. As can be seen there, the dispersing effect of the linear molecule *Jeff(Et-COOH)$_2$* is rather limited. For instance, after the addition of 0.4 % bwoc *Jeff(Et-COOH)$_2$* the spread flow only increased from 18 cm [7.1 in.] to ~ 21.2 cm [8.3 in.]. At

a dosage of 0.8 % bwoc already the maximum spread flow value of 22 cm [8.7 in.] was attained. However, higher dosages of the non-branched molecule did not enhance paste fluidity any further.

Opposite to this, the hyperbranched polymer *Jeff(hyp.PG)(COOH)$_n$* showed a much higher dispersing ability compared to the linear species. Already at a dosage of 0.2 % bwoc an increase of the spread flow to 26.6 cm [10.5 in.] was observed and addition of higher dosages resulted in even much higher spread flow values (e.g. 33.3 cm [13.1 in.] at 0.5 % bwoc). These results clearly demonstrate that the hyperbranched polymer presents a much more powerful superplasticizer compared to the linear one, as it can induce a much stronger steric hindrance effect due to the hyperbranched polyglycerol scaffold (see higher R_h value for the hyperbranched species).

Time-dependent development of the spread flow

Additionally, the slump retention of cement pastes admixed with the synthesized superplasticizers was determined at a w/c of 0.5. For this purpose, two cement pastes holding 0.19 % bwoc of *Jeff(hyp.PG)(COOH)$_n$* (spread flow of 26 cm [10.2 in.]) and of 0.8 % bwoc *Jeff(Et-COOH)$_2$* (spread flow of 22 cm [8.7 in.]) respectively were prepared and the spread flow over time was captured (see results in **Fig. 4**).

The spread flow of the cement paste fluidized with the linear molecule quickly (i.e. within two hours) decreased from 22 cm [8.7 in.] to 18.3 cm [7.2 in.]. However, the hyperbranched polymer maintained the workability for a longer period of time. For instance, even after five hours the cement paste admixed with *Jeff(hyp.PG)(COOH)$_n$* still exhibited a spread flow of ~ 22 cm [8.7 in.]. To sum up, the hyperbranched superplasticizer favors a very slow decline of the fluidity which engenders long processing times.

Sulfate tolerance of the polymers

It is well established that sulfate ions can perturb the dispersing efficiency of polycarboxylate superplasticizers. Numerous studies have been carried out over the last years to investigate this effect and to develop strategies how this problem can be mitigated [15 – 17]. To elucidate whether the synthesized polymers are also affected by sulfate ions, mini slump test were carried out whereby different dosages of sodium sulfate (ranging from 0.5 – 2.0 % bwoc) together with respective amounts of the synthesized polymers were pre-dissolved in the mixing water.

It can be seen from **Fig. 5** that the dispersing performance of *Jeff(hyp.PG)(COOH)$_n$* as well as of *Jeff(Et-COOH)*$_2$ is not impeded by sulfate ions. At sodium sulfate additions of up to 2 wt.%, the spread flow remained the same. The high sulfate tolerance might be explained with their specific molecular structure. Since both polymers exhibit carboxylate groups at the end of the backbone, they probably will adsorb in a tail like conformation which leads to a much denser surface coverage of the cement particles. This way, sulfate ions are hindered from replacing and desorbing polymers from the cement surface. Additionally, the non-ionic side chain will stretch out almost vertically from the surface into the pore solution, thus providing a significant steric hindrance effect. Similar results were reported several years ago for polyoxyethylene diphosphonate based superplasticizers which also can adsorb *via* the terminal anchor groups in a brush (= tail) like conformation on cement which effectuates high robustness of the polymer towards soluble sulfates [18].

Effect on cement hydration

Finally, heat flow calorimetry measurements were carried out to assess the effect of the linear and hyperbranched polymer on the kinetics of cement hydration. A cement paste holding different dosages of the polymers was prepared at w/c = 0.5 and the heat released from the hydration reaction was recorded over time (see **Fig. 6**).

The linear molecule *Jeff(Et-COOH)*$_2$ does not significantly impact cement hydration, since similar curves as for the reference were obtained for the heat evolvement. However, for the hyperbranched superplasticizer retardation of cement hydration was observed which becomes even more pronounced with increasing dosages. For instance, when adding 0.2 % bwoc of *Jeff(hyp.PG)(COOH)*$_n$ the peak of the heat release was delayed by ~ 18.5 h compared to the neat cement paste. The retardation can be ascribed to the polyglycerol scaffold which probably impedes the dissolution of cement by generating a densely packed polymer layer around the cement particles. Thus, the ingress of water and consequently the transport of ions from the surface are decelerated.

CONCLUSION

A new type of superplasticizer with dendrimeric structure has been synthesized *via* anionic ring-opening polymerization of glycidol. By applying the slow monomer addition technique a hyperbranched polymer with controlled molecular weight and low polydispersity was achieved. Mini slump tests revealed that the hyperbranched superplasticizer is superior over a linear small molecule due to a much higher steric hindrance effect induced by the polyglycerol motif. Furthermore, the hyperbranched superplasticizer produced long slump retention and a high tolerance towards sulfate ions.

This new concept for a superplasticizer is highly promising as it includes a specific modification of the molecular structure. In future products, different side chain lengths or molecular weights of the polyglycerol scaffold can be selected. Furthermore, the outer sphere of the polyglycerol structure could be modified with various functional groups (e.g. sulfonate, phosphate) in order to vary the affinity of the polymer to the cement surface. The influence of these parameters on the dispersing performance should be investigated in further studies.

Based on the results it is suggested that this new superplasticizer might be useful in special applications such as concreting in hot climates (there, the retardation from the hyperbranched polymer is beneficial), or for applications which require long slump retention such as for the pumping of concrete over long distances.

ACKNLOWEDGMENT

The authors would like to thank Huntsman for generously providing the Jeffamine sample.

REFERENCES

1. Fonds der Chemischen Industrie im Verband der Chemischen Industrie e.V. (FCI), “From Caves to Skyscrapers”, Brochure, 1st Edition, Schmidt printmedien (Ginsheim-Gustavsburg), 2015.

2. Plank, J., Sakai, E., Miao, C.W., Yu, C., Hong, J.X., “Chemical admixtures – Chemistry, applications and their impact on concrete microstructure and durability”, *Cement and Concrete* Research, Vol. 78, 2015, pp. 81-99.

3. Ramachandran, V. S., Malhotra, V. M., Jolicoeur, C., Spiratos, N., “Superplasticizers: Properties and applications in concrete”, CANMET, Ottawa, Canada, 1998.

4. Spiratos, N., Page, M., Mailvaganam, N. P., Malhotra, V. M., Jolicoeur, C., “Superplasticizers for Concrete: Fundamentals, Technology, and Practice”, Supplementary Cementing Materials for Sustainable Development, Ottawa, Canada, 2003.

5. Äitcin, P.-C., Flatt, R., “Science and Technology of Concrete Admixtures (1st Edition)”, Woodhead Publishing, 2016.

6. Plank, J., Lei, L., “Future perspectives of PCE technology”, in: J. Plank, L. Lei, eds., 2nd International Conference on Polycarboxylate Superplasticizers (PCE 2017), Munich (Germany), Conference proceedings, 2017, pp. 19-62

7. Yoshioka, K., Sakai, E., Daimon, M., Kitahar, A., “Role of steric hindrance in the performance of superplasticizers for concrete”, *Journal of the American Ceramic Society*, Vol. 80, 1997, pp. 2667-2671.

8. Houst, Y.F., Bowen, P., Perche, F., Kauppi, A., Borget, P., Galmiche, L., Le Meins, J.-F., Lafuma, F., Flatt, R.J., Schober, I., Banfill, P.F.G., Swift, D.S., Myrvold, B.O., Petersen, B.G., Reknes, K., "Design and function of novel superplasticizers for more durable high performance concrete (superplast project)", *Cement and Concrete Research*, Vol. 38, 2008, pp. 1197-1209.

9. Hirata, T., Ye, J., Branicio, P., Zheng, J., Lange, A., Plank, J., Sullivan, M., "Adsorbed conformations of PCE superplasticizers in cement pore solution unraveled by molecular dynamics simulations", *Scientific Reports*, Vol. 7, 2017, 16599.

10. Shou, C., Xiao, W., "Hyper-branchend polycarboxylate high-efficiency water reducing agent and preparation method thereof", CN 101580353 B, 2012.

11. Miao, C., Qiao, M., Ran, Q., Liu, J., Zhou, D., Yang, Y., Mao, Y., "Preparation method of hyperbranched polycarboxylic acid type copolymer cement dispersant", US 20130102749 A1, 2013.

12. Sunder, A., Hanselmann, R., Frey, H., Mülhaupt, R., "Controlled synthesis of hyperbranched polyglycerols by ring-opening multibranching polymerization", *Macromolecules*, Vol. 32, 1999, pp. 4240-4246.

13. Sunder, A., Türk, H., Haag, R., Frey, H., "Copolymers of glycidol and glycidyl ethers: design of branched polyether polyols by combination of latent cyclic AB_2 and ABR monomers", *Macromolecules*, Vol. 33, 2000, pp. 7682-7692.

14. Wang, G., Li, L., Lan, J., Chen, L., You, J., "Biomimetic crystallization of calcium carbonate spherules controlled by hyperbranched polyglycerols", *Journal of Materials Chemistry*, Vol. 18, 2008, pp. 2789-2797.

15. Pourchet, S., Liautaud, S., Rinaldi, D., Pochard, I., "Effect of the repartition of the PEG side chains on the adsorption and dispersion behaviors of PCP in presence of sulfate", *Cement and Concrete Research*, Vol. 42, 2012, pp. 431-439.

16. Zimmermann, J., Hampel, C., Kurz, C., Frunz, L., Flatt, R.J., "Effect of polymer structure on the sulfate-polycarboxylate competition", Ninth ACI International Conference on Superplasticizers and Other Chemical Admixture in Concrete, sp-262-12, 2009, Sevilla (Spain), pp. 165-176.

17. Habbaba, A., Lange, A., Plank, J., "Synthesis and performance of a modified polycarboxylate dispersant for concrete possessing enhanced cement compatibility", *Journal of Applied Polymer Science*, Vol. 129, 2013, pp. 346-353.

18. Mosquet, M., Chevalier, Y., Brunel, S., Guicquero, J.P., "Polyoxyethylene di-phosphonates as efficient dispersing polymers for aqueous suspensions", *Journal of Applied Polymer Science*, Vol. 65, 1997, pp. 2545-2555.

TABLES AND FIGURES

List of Tables:

List of Figures:

Table 1 – Mineralogical composition of the CEM I 52.5 N sample.

Phase	wt.%
C_3S	53.3
C_2S	25.7
C_3A	8.8
C_4AF	2.6
Free Lime (*Franke*)	0.1
Anhydrite*	3.3
Hemihydrate*	0.7
Dihydrate	0.1
Calcite	3.9
Quartz	1.0
Arcanite	0.5
Total	100

* Determined by thermogravimetry

Table 2 – Molar masses, PDI and hydrodynamic radii of the synthesized polymers.

Polymer sample	M_n (g/mol)	M_w (g/mol)	PDI (M_w/M_n)	R_h (nm)
Jeff(Et-COOH)$_2$	2,610	2,660	1.0	3.2 ± 0.3 nm
Jeff(hyp.PG)(COOH)$_n$	3,730	6,420	1.7	9.7 ± 0.1 nm

Table 3 – Anionic charge amounts of the polymer samples in DI water, 0.1 M NaOH and SCPS.

Polymer sample	DI water (µeq/g)	0.1 M NaOH (µeq/g)	SCPS (µeq/g)
Jeff(Et-COOH)$_2$	~ 0	430	20
Jeff(hyp.PG)(COOH)$_n$	925	1,020	220

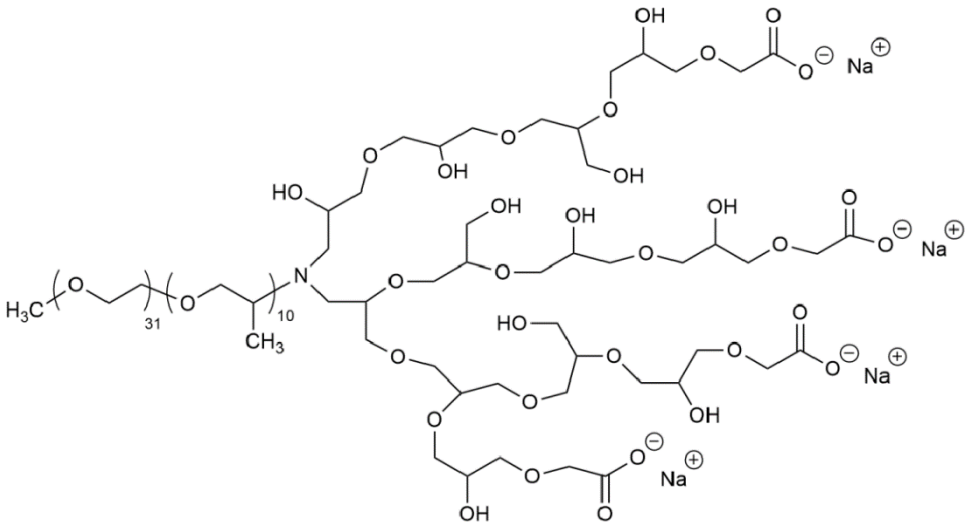

Jeff(hyp.PG)(COOH)$_n$

Hyperbranched superplasticizer

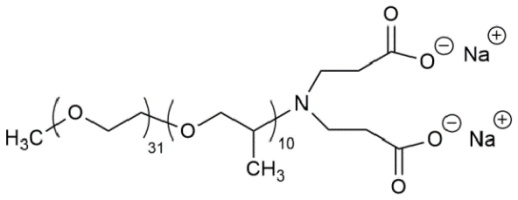

Jeff(Et-COOH)$_2$

Linear small molecule

Fig. 1 – Chemical structures of the synthesized hyperbranched and linear polymers.

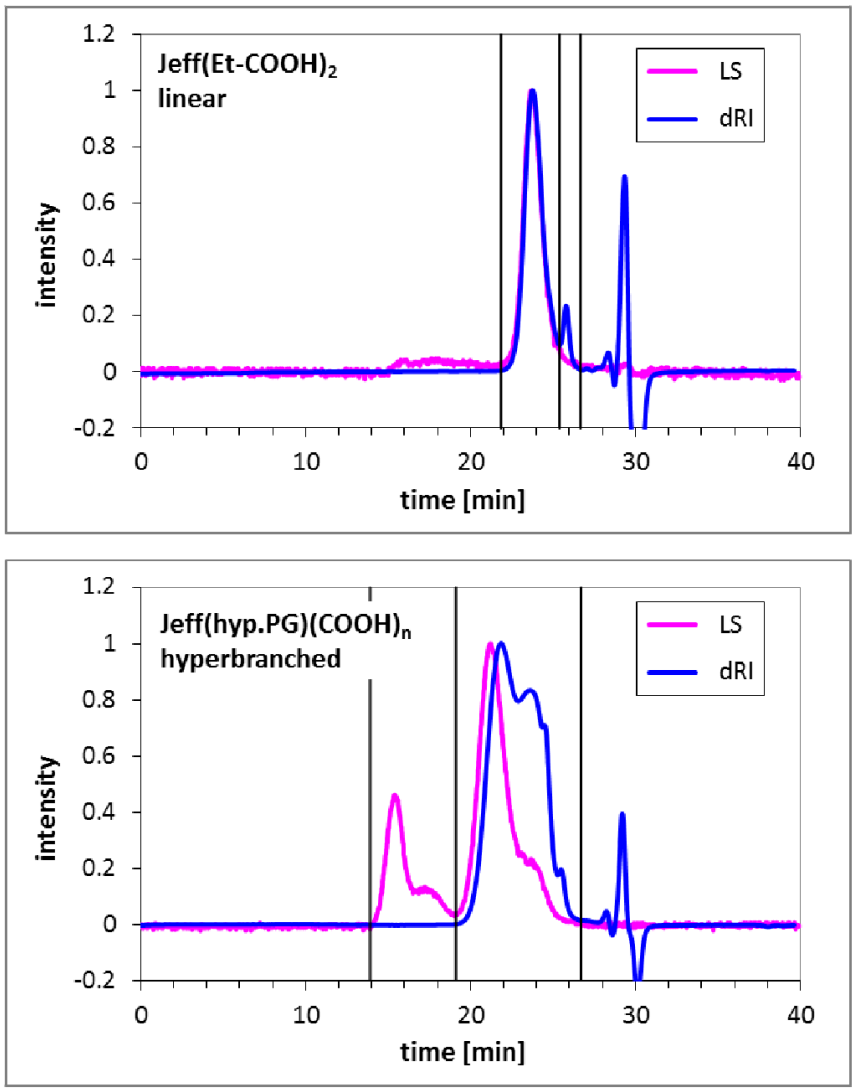

Fig. 2 – SEC spectra of the synthesized linear and hyperbranched polymers.

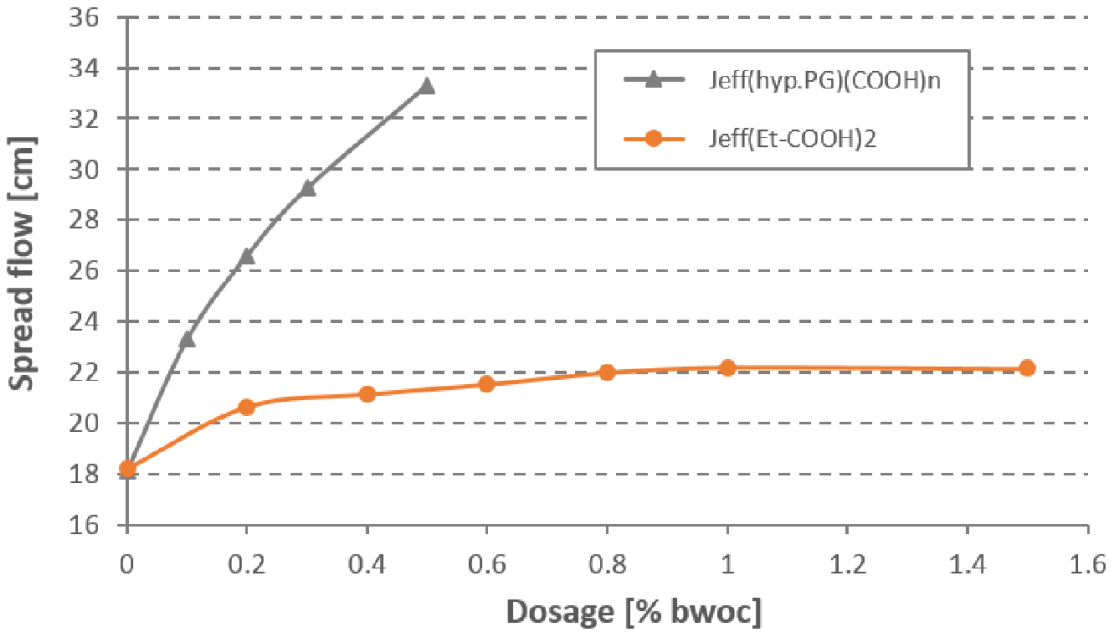

Fig. 3 – Spread flow of cement pastes (w/c = 0.5) admixed with different dosages of the linear and the hyperbranched polymer.

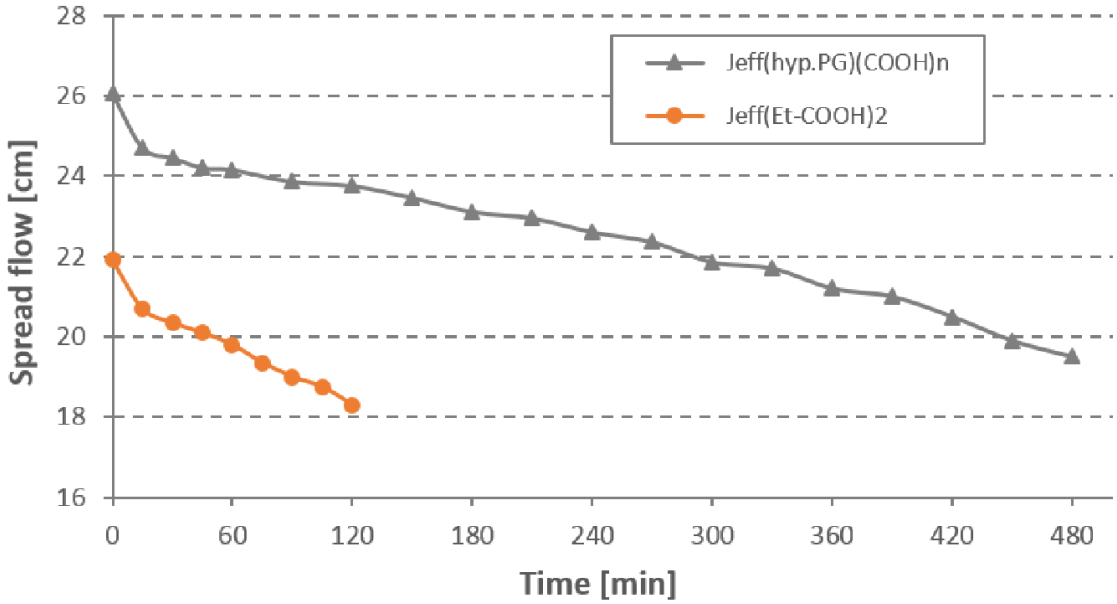

Fig. 4 – Time dependent evolution of the spread flow of cement pastes admixed with 0.19 % bwoc *Jeff(hyp.PG)(COOH)$_n$* and 0.8 % bwoc *Jeff(Et-COOH)$_2$*.

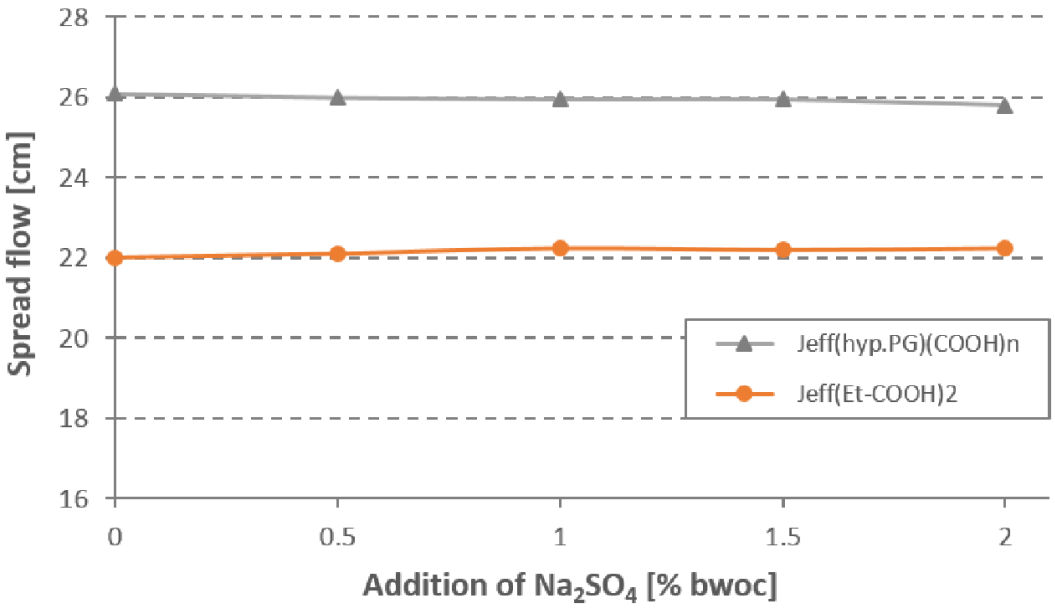

Fig. 5 – Effect of various additions of Na_2SO_4 on the spread flow of cement pastes containing 0.19 % bwoc of *Jeff(hyp.PG)(COOH)$_n$* and 0.8 % bwoc *Jeff(Et-COOH)$_2$*.

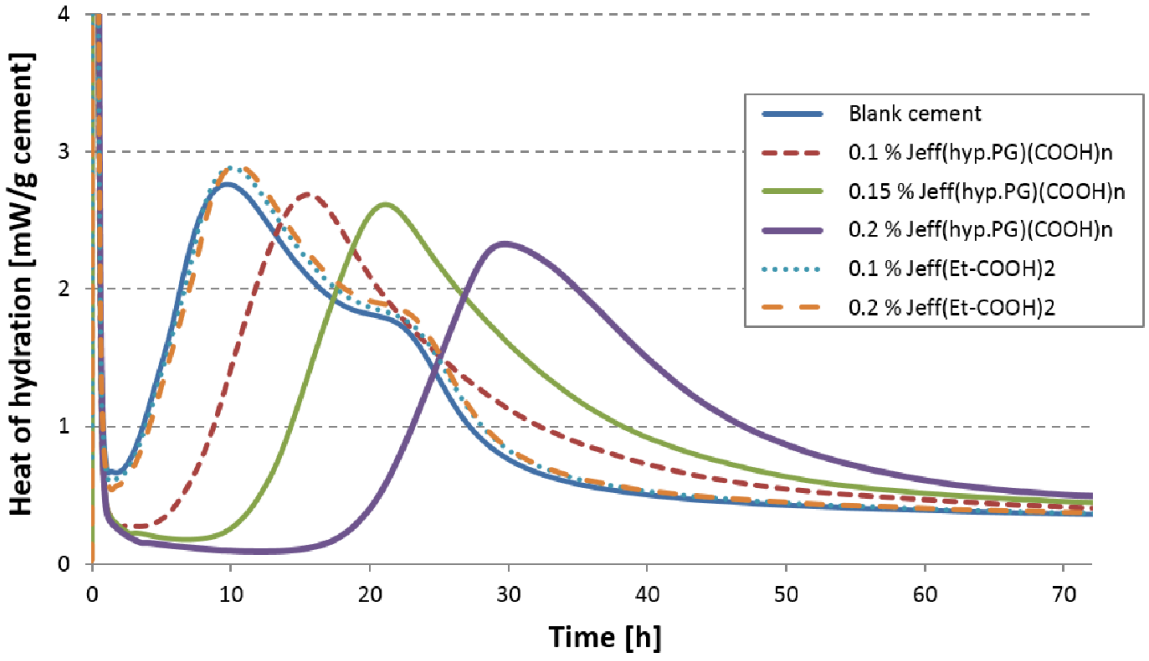

Fig. 6 – Time dependent heat evolution from cement pastes (w/c = 0.5) admixed with different dosages of the synthesized polymers.

5.3. Synthese und Eigenschaften von Lignit-basierten Fließmitteln

Fließmittel sind lineare oder kammförmige Polymere, die in der Regel aus einer aliphatischen Hauptkette bestehen, in der anionische Ankergruppen vorliegen, über die das Polymer auf der Bindemitteloberfläche adsorbiert. In den **Publikationen #10** und **#11** wurde ein neuartiges Fließmittel synthetisiert, dessen Struktur sich aus einer relativ starren aromatischen Hauptkette und mehreren geladenen Seitenketten mit Sulfonat- und Carboxylatgruppen zusammensetzt (sh. **Abbildung 46**). Als Polymerrückgrat wurden Humin- und Fulvinsäuren verwendet, die in **Publikation #10** aus Braunkohle extrahiert wurden, während das Fließmittel in **Publikation #11** ausgehend von einem kommerziellen Lignit mit einem erhöhten Huminsäure-Anteil (sog. Superlignit) dargestellt wurde. Durch die Zugabe des Initiators Natriumpersulfat wurden H-Atome von den funktionellen Gruppen (z.B. OH-Gruppen) der Huminsäuren abstrahiert, wodurch Radikalstellen gebildet wurden, von denen aus eine Pfropfcopolymerisation mit den Monomeren ATBS und Acrylsäure erfolgte.

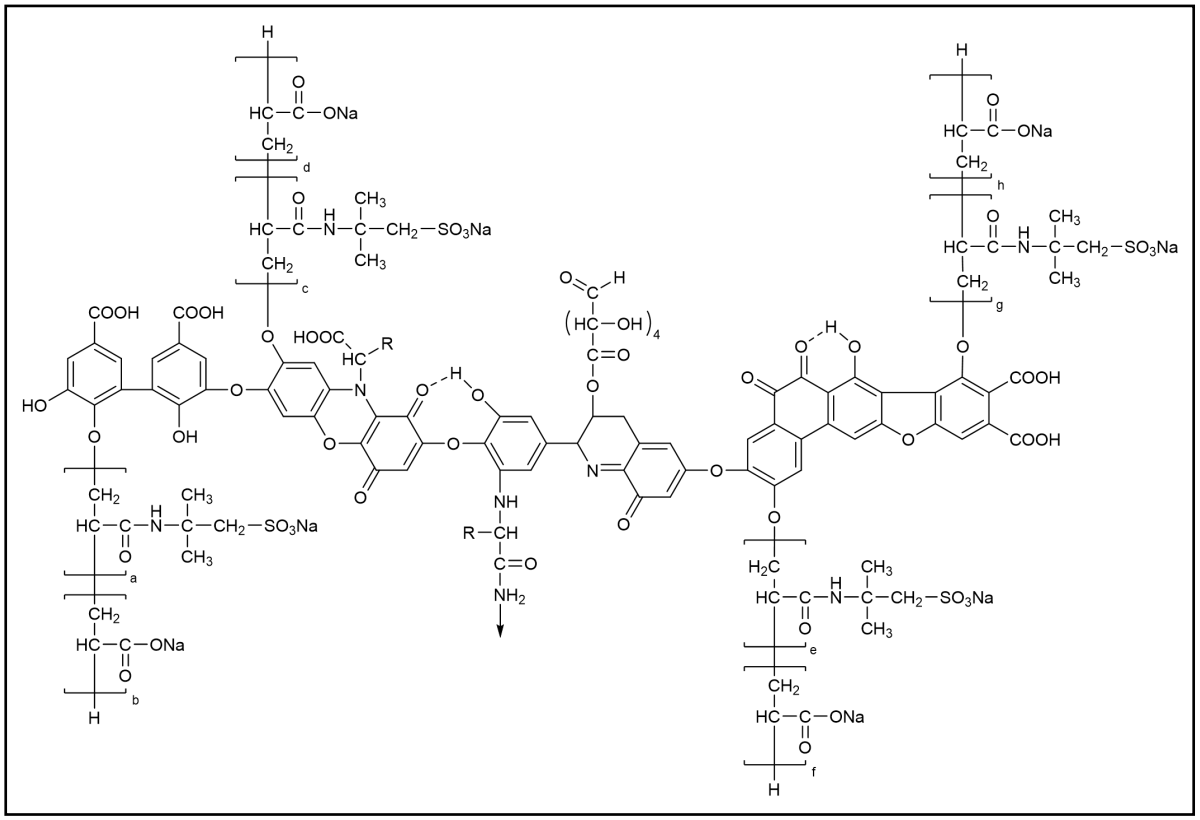

Abbildung 46: Chemische Struktur des Lignit-basierten Fließmittels.

Darüber hinaus wurde ein ATBS-Acrylsäure-Copolymer synthetisiert, welches im Vergleich zu den Lignit-Polymeren aus einer aliphatischen Hauptkette besteht und sich

daher durch eine höhere konformationelle Flexibilität auszeichnet. Als weiteres Referenzpolymer wurde ein BNS Polykondensat-Fließmittel eingesetzt, welches ebenfalls eine starrere Konformation besitzt, da es aus β-Napthalinsulfonsäure-Einheiten aufgebaut ist, die über Methylenbrücken miteinander verbunden sind. Beide Publikationen befassen sich mit der Charakterisierung der Lignit-basierten Fließmittel und mit Untersuchungen ihrer Dispergiereigenschaften sowie dem Nachweis, dass die Monomere erfolgreich auf das Huminsäure-Rückgrat aufgepfropft wurden.

Erste Hinweise auf eine erfolgreiche Synthese des Fließmittels konnten aus den GPC Messungen abgeleitet werden. Die Lignit-basierten Polymere zeigten ein höheres Molekulargewicht und größere Polymerradien als das ATBS-Acrylsäure-Copolymer, welches unter den gleichen Reaktionsbedingungen wie das Lignit-Pfropfcopolymer synthetisiert wurde. In **Publikation #10** wurde ein ATBS-Acrylsäure-Verhältnis von 1 : 0,15 gewählt, wohingegen in **Publikation #11** das Monomerverhältnis von 1 : 0,15 – 1 : 1,5 variiert wurde. Insbesondere die Lignit-basierten Polymere mit einem ATBS-Acrylsäure-Verhältnis von 1 : 0,15 zeichneten sich durch niedrige Polydispersitäten (≤ 2,0) und einheitliche Molmassenverteilungen aus. Höhere Acrylsäure-Anteile führten hingegen zu einem Anstieg der Polydispersität und zu niedrigeren Molekulargewichten, was darauf hindeutet, dass im Polymer zunehmend kürzere Seitenketten vorliegen und ein gewisser Anteil nicht aufgepfropft wurde. Über Ladungstitration konnte gezeigt werden, dass durch die Modifizierung des Lignits mit ATBS und Acrylsäure stark negativ geladene Polymere resultieren (Ladungsmenge > 4000 µeq/g in 0,1 M NaOH), die in der Lage sind über Physisorption mit der Zementkornoberfläche zu wechselwirken.

Untersuchungen zur Dispergierwirkung ergaben, dass insbesondere die Polymere mit einem hohen Acrylsäure-Anteil höher dosiert werden müssen, um ein bestimmtes Zementfließmaß zu erzielen. So nahm die Dosierung des Superlignit-basierten Fließmittels bei Änderung des ATBS-Acrylsäure-Verhältnisses von 1 : 0,15 auf 1 : 1,5 von 0,25 % auf 0,47 % zu. Mit steigender Acrylsäure-Menge wurden verstärkt Polyacrylate gebildet, die nicht auf die Huminsäure aufgepfropft wurden. Niedrigere Acrylsäure-Mengen sind daher vorteilhafter, da die Fließmittel weniger polydispers sind und längere aufgepfropfte Seitenketten für die Adsorption vorliegen. Interessanterweise war das Fließmittel, welches aus dem Braunkohleextrakt synthetisiert wurde (**Publikation #10**) geringfügig effizienter als die Superlignit-basierten Polymere aus **Publikation #11**. Zudem wurde festgestellt, dass die Lignit-Pfropfcopolymere

wirkungsvollere Fließmittel im Vergleich zu BNS sind (0,3 %), jedoch höher dosiert werden müssen als das ATBS-Acrylsäure-Copolymer (0,19 %). Die verflüssigende Wirkung der Lignit-basierten Fließmittel beruht hauptsächlich auf den aufgepfropften Seitenketten, da weder die Na-Salze der Braunkohle noch das Superlignit eine Dispergierung hervorrufen konnten. Außerdem wurde gefunden, dass das Superlignit-haltige Fließmittel das Fließmaß über eine Stunde konstant halten kann, während die Verarbeitbarkeit sowohl für das ATBS-*co*-Acrylsäure-Polymer als auch das BNS Polykondensat bereits nach 15 Minuten stark reduziert war. TOC Messungen offenbarten, dass vom Lignit-Polymer unmittelbar nach der Zugabe eine höhere Restmenge in der Porenlösung verbleibt, wodurch eine langanhaltende Fließwirkung möglich ist. Das ATBS-*co*-Acrylsäure-Polymer und BNS adsorbieren hingegen nahezu vollständig zu Beginn, sodass nur noch wenige Polymere in der Lösung vorhanden sind und daher die Fließfähigkeit rasch über die Zeit abnimmt, da neu gebildete Hydratphasen nicht mehr ausreichend dispergiert werden.

Die Lignit-Pfropfcopolymere wirken kaum verzögernd und ihr Effekt auf die Zementhydratation ist ähnlich zu dem des ATBS-*co*-Acrylsäure-Polymers und BNS. Über Zeta-Potential Messungen wurde zudem nachgewiesen, dass die Lignit-Pfropf-copolymere auf der Bindemitteloberfläche adsorbieren und eine stark negative Oberflächenladung hervorrufen (-28 mV), die zu einer elektrostatischen Abstoßung der Zementteilchen führt. Außerdem wirken die Lignit-Fließmittel zu einem gewissen Anteil über einen sterischen Effekt, das über Schichtdickenmessungen der Polymere gezeigt wurde. Für die Lignit-basierten Fließmittel wurden deutlich höhere Schichtdicken gefunden (~ 6,5 – 6,7 nm) als für das ATBS-*co*-Acrylsäure-Polymer (~ 1,7 nm), BNS (~ 0,3 nm) sowie die Na-Salze der Braunkohle (~ 2,5 nm) bzw. Superlignit (~ 1,3 nm) (sh. **Abbildung 47**). Ferner konnte mit Hilfe der Schichtdickenmessung bekräftigt werden, dass die Monomere ATBS und Acrylsäure auf die löslichen Lignitbestandteile aufgepfropft wurden und keine Mischung aus einem ATBS-*co*-Acrylsäure-Polymer und dem Lignit vorliegt. Die hohen Schichtdicken der Pfropfcopolymere werden durch die starre Anordnung der Huminsäure und die aufgepfropften Seitenketten verursacht. Allerdings benötigen die Lignit-Fließmittel eine höhere Dosierung um die Oberfläche zu belegen, was darauf hindeutet, dass die Polymere nur über einzelne Seitenketten auf der Oberfläche adsorbieren, während der Rest des Polymers in die Porenlösung zeigt. Durch die starre und gestreckte Lösungskonformation ist die Fähigkeit der Lignit-Polymere

eingeschränkt sich entsprechend auf der Oberfläche auszurichten, um mehrere Bereiche gleichzeitig zu besetzen. Das ATBS-*co*-Acrylsäure-Polymer ist hingegen flexibler und in der Lage sich so anzuordnen, sodass mehrere Stellen belegt werden, weshalb hier eine höhere Dosiereffizienz resultiert. Aufgrund der spezifischen Adsorptionsweise und der damit einhergehenden höheren adsorbierten Schichtdicke zeigte das Lignit-basierte Fließmittel eine höhere Robustheit gegenüber Sulfationen. Die Pfropfcopolymere schirmen die Oberfläche stärker als das ATBS-Acrylsäure-Copolymer ab und können daher nicht so einfach von der Oberfläche verdrängt werden.

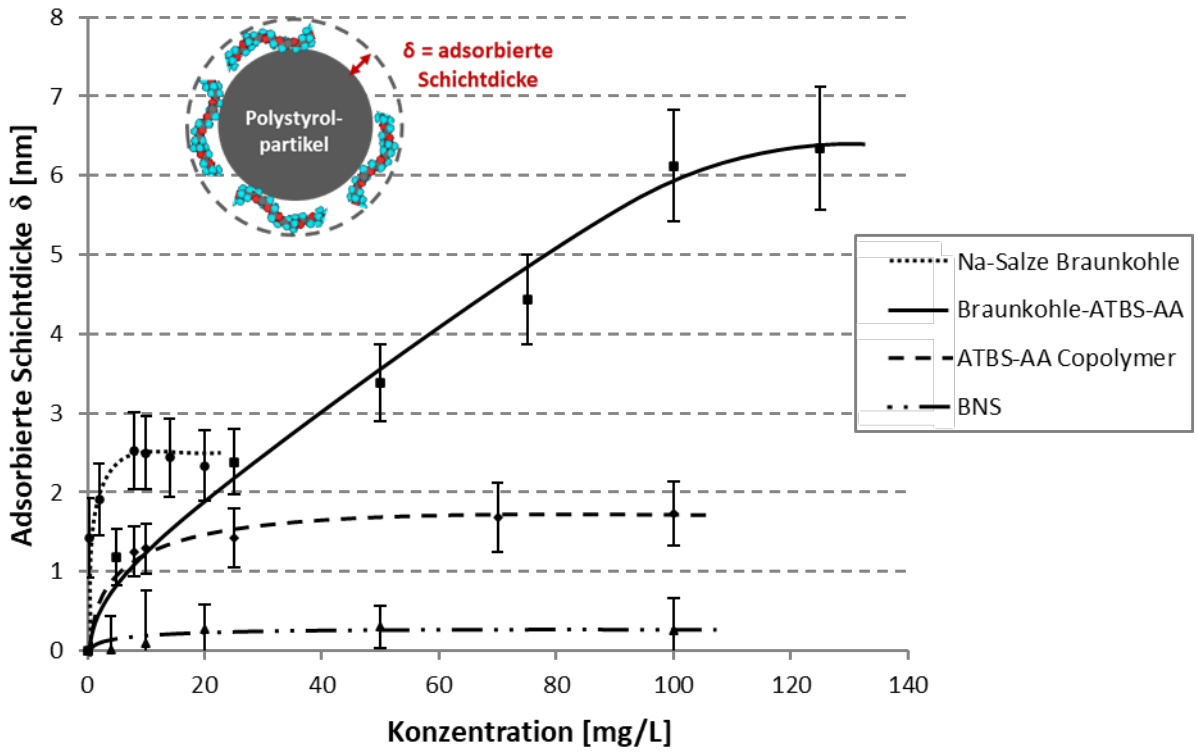

Abbildung 47: Adsorbierte Schichtdicken der in **Publikation #10** untersuchten Polymere.

5.3.1. Publikation #10: Synthesis of a Novel Superplasticizer Prepared from Brown Coal

Publikation #10

Synthesis of a Novel Superplasticizer Prepared from Brown Coal

Manuel Ilg, Johann Plank

In: V. M. Malhotra, P. R. Gupta, T. C. Holland (Eds.),
11th CANMET/ACI Conference on Superplasticizers and Other Chemical Admixtures in Concrete, Ottawa (Canada), 2015
ACI SP-302-05, 63 – 76

SYNTHESIS OF A NOVEL SUPERPLASTICIZER PREPARED FROM BROWN COAL

By

Manuel Ilg, Johann Plank

Prof. Dr. Johann Plank

Chair for Construction Chemistry, Technische Universität München

Lichtenbergstraße 4

85747 Garching, Germany

Tel: 0049 (0)89 289-13151

Fax: 0049 (0)89 289-13152

E-mail: sekretariat@bauchemie.ch.tum.de

#SP-015

SYNTHESIS OF A NOVEL SUPERPLASTICIZER PREPARED FROM BROWN COAL

Manuel Ilg, Johann Plank

Synopsis: Polycondensates and polycarboxylates are known to be effective superplasticizers. Here, the synthesis of a novel, brown coal based superplasticizer by grafting acrylic acid (AA) and 2-acrylamido-2-tert.butyl sulfonic acid (ATBS) onto the alkali soluble components of brown coal (lignite) as backbone using free radical copolymerization technique is described. Furthermore, an ATBS-acrylic acid copolymer was synthesized to investigate the influence of the graft chains on the performance of the lignite copolymer. Successful grafting was confirmed by size exclusion chromatography (SEC) and comparison of the adsorbed layer thicknesses of the brown coal substrate and the grafted product. The dispersing performance of the graft copolymer was probed via mini slump tests and compared with that of BNS. Additionally, slump flow retention and sulfate tolerance were determined. It was found that the graft copolymer possesses higher dispersion effectiveness than BNS and exhibits high sulfate tolerance.

Keywords: admixture; adsorbed layer thickness; brown coal; graft copolymer; lignite; superplasticizer

Manuel Ilg studied chemistry and received his B.Sc. and M.Sc. from Technische Universität München. He is currently a Ph.D. student at the Chair for Construction Chemistry in Garching where he works on new structural concepts for superplasticizers.

Johann Plank is a full Professor at the Institute of Inorganic Chemistry of Technische Universität München, Germany. Since 2001, he holds the Chair for Construction Chemistry there. His research interests include cement chemistry, concrete admixtures, organic-inorganic composite and nano materials, concrete, dry-mix mortars and oil well cementing.

INTRODUCTION

Superplasticizers are an important part of modern concrete technology to improve the workability of fresh concrete. With the help of these admixtures the water-to-cement ratio can be reduced, thus obtaining cementitious building materials with higher strength and durability[1,2]. Although polycondensates and polycarboxylates represent very effective polymers, new structures and concepts are still investigated[3]. In recent years, natural polymers became increasingly popular as a starting material for the synthesis of new admixtures[4]. A main reason is that natural polymers offer novel structural motifs and often bear a high diversity of functional groups. In literature, a number of examples already exist where through functionalization and modification of natural polymers, novel superplasticizers have been synthesized[5,6]. Ordinary brown coal (often referred to as lignite) also presents a promising candidate for the development of new superplasticizers, because of its global abundance and its low cost.

Brown coal is a combustible sedimentary rock that was built million years ago from dead plant material through a process called coalification[7]. In flooded areas such as swamps the main constituents of plant residues, lignin and cellulose, were decomposed gradually to humic substances (peat). Burial by sediments and subsequent tectonic pressure over millions of years led to an increase of the temperature causing compaction of the decomposition products. In this process, peat was successively metamorphosed into brown coal under release of water and gases such as methane and carbon dioxide[7].

In this study, a caustic extract of brown coal containing humic and fulvic acids as main constituents was utilized[8-10]. Such alkali extracts are commercially available and widely used in different industries including agriculture (as fertilizer)[10] and in oil well drilling as drilling fluid (the so-called “lignite” mud)[11]. However, up to date no brown coal based concrete superplasticizer has been developed. Here, we report on the synthesis of a novel superplasticizer prepared by grafting acrylic acid and ATBS monomers onto the alkali soluble components of brown coal. Generally, humic and fulvic acids possess a large number of functional groups (i.e. aliphatic/aromatic carboxylate, carbonyl, amino, phenolic and ketone groups) which present a perfect substrate for graft copolymerization reactions[12,13].

The synthesized brown coal-ATBS-acrylic acid graft copolymer was characterized with respect to its molecular properties (M_w, M_n) and its anionic charge amount. Its dispersing effectiveness and slump retention behavior was compared with that of an industrial grade β-naphthalene sulfonate (BNS) sample. Additionally, the sulfate tolerance of the graft copolymer was studied and heat flow calorimetry measurements were performed to assess its effect on cement hydration. To prove successful grafting, the adsorbed layer thicknesses of the brown coal substrate and the graft copolymer were measured via dynamic light scattering utilizing cationic polystyrene nanoparticles as adsorbent[14]. Finally, the working mechanism of the superplasticizer was clarified via zeta potential measurements.

RESEARCH SIGNIFICANCE

A novel brown coal based superplasticizer has been synthesized using graft copolymerization technique. From a commercial brown coal the alkali soluble fraction (mainly humic and fulvic acids) was extracted and utilized as backbone. Up to date, coal and natural gas are the only readily available alternatives to petroleum. Therefore, the different constituents of brown coal could be an alternative feedstock in the production of superplasticizers to save the more precious resources of petroleum. The overall goal of this study was to validate new structural motifs and to offer a synthetic route to highly economical, brown coal based superplasticizers.

EXPERIMENTAL PROCEDURE

Materials

Brown coal – The used brown coal was mined in the Lusatia brown coal mining district near Cottbus, Germany.

Chemicals – 2-Acrylamdio-2-tert.butyl sulfonic acid (ATBS), acrylic acid (AA), sodium hydroxide (NaOH), sodium peroxodisulfate ($Na_2S_2O_8$), sodium pyrosulfite ($Na_2S_2O_5$) and EDTA were used as per obtained.

Industrial superplasticizer sample – A spray dried powder BNS superplasticizer was used as an industrial grade reference sample.

Cement – The cement used for this study was an ordinary Portland cement CEM I 52.5 N. Its phase composition as determined by X-ray diffraction and subsequent *Rietveld* refinement is illustrated in **Table 1**. Its specific surface area was 3,583 cm^2/g (*Blaine* method) and its particle size (d_{50} value) was 11.5 µm [$45.3 \cdot 10^{-5}$ in.] (laser granulometer). The density as obtained by helium pycnometry was 3.15 g/cm^3.

Extraction of brown coal

The individual steps performed in the extraction process are schematically presented in **Fig. 1**. First, chunks of brown coal were coarsely crushed with a hammer and the residue was sieved to < 250 µm [$9.84 \cdot 10^{-3}$ in.] to obtain a brown coal powder exhibiting a narrow particle size distribution and a high specific surface area. For extraction of the alkali soluble components, 70 g [2.47 oz.] of the brown coal powder were mixed with 700 mL [23.7 fl. oz.] of 0.5 M NaOH placed in a 1 L [33.8 fl. oz.] round-bottom flask[9]. The mixture was refluxed for three hours at 90 °C [194 °F] under constant stirring. Next, the dark solution was cooled to ambient temperature and centrifuged two times for 10 minutes at 8,500 rpm. The supernatant was separated from the residue and freeze dried, yielding 21.7 g [0.765 oz.] of a black solid (theor. yield 31 %). It is noteworthy that many coal producers offer such extracts in liquid or powder form designated as “caustic lignite”.

Synthesis of brown coal-ATBS-acrylic acid graft copolymer

The novel brown coal-ATBS-acrylic acid graft copolymer was synthesized by aqueous free radical copolymerization using sodium peroxodisulfate as initiator. Here, 2-acrylamido-2-tert.butyl sulfonic acid (ATBS) and acrylic acid were grafted onto the extracted alkali soluble components (i.e. humic and fulvic acid) of brown coal. The molar ratio between ATBS and acrylic acid was 1 : 0.15 and the weight ratio between the brown coal and the grafted monomers was 20 : 80 (wt/wt). In a five necked, 1 L [33.8 fl. oz.] round-bottom flask equipped with stirrer, thermometer, reflux condenser and inlet for N_2 gas, 13.2 g [0.466 oz.] of the dry alkali soluble components were dissolved in 206 mL [6.97 fl. oz.] DI water. Thereafter, 8.8 g [0.31 oz.] NaOH pellets were added to adjust a pH of 12 and then cooled to 18 °C [64 °F]. Next, 50.0 g [1.76 oz.] ATBS (241 mmol, 1.0 eq) were dissolved stepwise and the temperature was kept constantly under 25 °C [77 °F] to avoid homopolymerization of ATBS. 2.60 g [0.092 oz.] acrylic acid (36.1 mmol, 0.15 eq), 600 mg [0.021 oz.] EDTA and 1.00 g [0.035 oz.] of an organo-modified polysiloxane defoamer were added and the mixture was purged with N_2 for 1 h at room temperature. After heating to 50 °C [122 °F] the first portion of sodium peroxodisulfate initiator was added (8 g [0.282 oz.]) and the reaction mixture was stirred for 50 minutes at this temperature. The second part of initiator was added (8 g [0.282 oz.]) and the polymerization continued for additional 70 minutes at 50 °C [122 °F]. Then the temperature was increased to 60 °C [140 °F] and kept there for 1 h. Finally, the reaction flask was heated to 80 °C [176 °F], 3.60 g [0.127 oz.] of sodium pyrosulfite were added to quench remaining radicals and stirring continued for 1 h at 80 °C [176 °F]. The solution was cooled to room temperature to obtain a viscous, dark brownish polymer solution with a solid content of 29 wt.% and a pH of 2.5. The polymer solution was used without any further purification.

Synthesis of ATBS-acrylic acid copolymer

An ATBS-acrylic acid copolymer was synthesized according to the procedure described above except that no alkali soluble components were present. Here, a pale yellowish, 27.6 wt.% aqueous solution with low viscosity and a pH of 2.5 was obtained. This polymer was used for comparison.

Characterization of polymers

Size exclusion chromatography – Molecular weights (M_w and M_n) and polymer radii ($R_{h(z)}$ and $R_{g(z)}$) of all synthesized polymers were determined by size exclusion chromatography. The instrument is equipped with a RI detector and an 18 angle dynamic light scattering detector. Polymer solutions exhibiting a concentration of 2 g/L were prepared for the SEC analysis. The polymers were separated on a precolumn and two columns using 0.2 M $NaNO_3$ solution (adjusted with NaOH to pH 9) as an eluent at a flow rate of 1.0 mL/min. The value of *dn/dc* used to calculate M_w and M_n was 0.218 mL/g (value for lignin)[15].

Anionic charge amount of the polymers – The anionic charge of the polymers was determined via polyelectrolyte titration using a particle charge detector. 0.001 M cationic polydiallyl dimethyl ammoniumchloride (polyDADMAC) solution was employed as titrator. Polymer solutions with a concentration of 0.1 g/L were prepared in DI water, in 0.1 M NaOH and in cement pore solution (CPS). Cement pore solution was freshly prepared by vacuum filtration of neat cement slurries using a water-to-cement ratio of 0.455. In a typical experiment, 10 mL [0.34 fl. oz.] of the polymer solution were pipetted into a PTFE cylinder with an oscillating PTFE piston in the center. The dissolved polymers can adsorb via *Van der Waals* forces on the surface of the cylinder and the piston. Because of the oscillating movement of the piston, counter ions are removed from the immobilized polymers and a streaming current results which can be measured by two platinum electrodes located within the PTFE cylinder. The polyDADMAC solution was titrated until the isoelectronic point was reached. For every polymer sample the measurement was repeated three times and the values were averaged. From the consumption of polyDADMAC the amount of negative charge per gram of polymer was calculated.

Heat flow calorimetry – To investigate the influence of the synthesized polymers on cement hydration, isothermal heat flow calorimetric measurements were carried out. There, 4 g [0.141 oz.] cement were filled into 20 mL [0.68 fl. oz.] glass ampoules and mixed with the respective amount of aqueous polymer solution to obtain a water-to-cement ratio of 0.455. The ampoules were sealed, homogenized for 1 min in a wobbler and then placed into the isothermal conduction calorimeter. Data logging was continued until heat evolution from the hydration reaction subsided completely.

Performance of the synthesized polymers

Mini slump test – The dispersing effectiveness of the synthesized polymers was assessed utilizing a mini slump test following in principle DIN EN 1015, but with some modifications. At first, the water-to-cement ratio required to reach a slump flow of 18 ± 0.5 cm [7.1 ± 0.2 in.] was established for the cement paste without polymers. At this specific water-to-cement ratio, the dosage of the polymers was determined to attain a spread flow of 26 ± 0.5 cm [10.2 ± 0.2 in.]. In a typical experiment, the superplasticizer was dissolved in the required amount of mixing water placed in a porcelain cup. The amount of water contained in the polymer solution was subtracted from the amount of mixing water. 300 g [10.6 oz.] of cement were added to the mixing water over a period of 1 min, then rested for 1 min and subsequently were stirred manually for 2 min with a spoon. Immediately after the end of stirring, the cement slurry was poured into a *Vicat* cone (height 40 mm [1.57 in.], top diameter 70 mm [2.76 in.], bottom diameter 80 mm [3.15 in.]) placed on a glass plate, filled to the brim and the cone was lifted vertically. The resulting paste spread was measured twice, the second measurement being perpendicular to the first one and averaged to obtain the slump flow value.

Time dependent mini slump test – Development of dispersing performance over time was investigated via time dependent mini slump testing. Here, 400 g [14.1 oz.] cement were mixed with the required amount of water and polymer to achieve an initial slump flow of 26 ± 0.5 cm. The procedure was the same as described above. After each measurement the cement paste was transferred back into the porcelain cup and covered with a wet towel to avoid desiccation. Prior to each measurement the cement paste was vigorously stirred for two minutes. Measurements were conducted every 15 minutes over a total period of 120 minutes.

Adsorbed layer thickness

The adsorbed layer thickness of the polymers was captured by dynamic light scattering. Here, monodisperse polystyrene nanoparticles exhibiting an average particle size of 75.5 ± 0.5 nm [$2.97 \cdot 10^{-6}$ in.] were utilized as adsorbent. Starting from a 150 mg/L stock solution of each polymer in 0.1 M NaOH, different concentrations were prepared by dilution (diluent 0.1 M NaOH). Prior to the measurements, the solutions were filtered through a 0.2 µm [$7.9 \cdot 10^{-6}$ in.] filter to remove undesired dust particles that can disturb measurements because of their high scattering intensity. Next, 50 µL [$1.7 \cdot 10^{-3}$ fl. oz.] of a suspension of cationic polystyrene nanoparticles

(for preparation see[14]) were added and sonicated for 5 min. The polymer solution was filled into a glass cuvette and then placed in the instrument. Every measurement was repeated 150 times per sample and the average value was calculated. Each test consisted of a 10 s light scattering run taken at a temperature of 25 °C [77 °F]. Measurements were continued at increasing polymer concentrations until a stable, final value was reached that was regarded as the point of saturated adsorption. The adsorbed layer thickness was calculated using **equation 1**.

$$\text{adsorbed layer thickness [nm]} = \frac{d_{ads}\,[\text{nm}] - d_{polystyrene}\,[\text{nm}]}{2} \qquad (1)$$

where d_{ads} represents the particle size of the polystyrene nanoparticle holding adsorbed polymer, and $d_{polystyrene}$ represents the particle size of the native polystyrene particle.

Zeta potential measurement

Zeta potential measurements were performed at room temperature on an electro acoustic spectrometer. This instrument measures a vibration current induced by an acoustic wave which causes the aqueous phase to move relative to the cement particles. From that, a potential difference results which can be measured and designated as zeta potential. Immediately after mixing, the freshly prepared cement slurries holding the respective dosage of the polymer samples required for a slump flow of 26 ± 0.5 cm were filled into the cup of the instrument and measured under continuous stirring for a total period of 30 min.

EXPERIMENTAL RESULTS AND DISCUSSION

Characterization of brown coal-ATBS-acrylic acid graft copolymer

The synthesized graft copolymer and the ATBS-acrylic acid copolymer were characterized using SEC. The molar masses and polymer radii are listed in **Table 2**. According to these data, the brown coal-ATBS-acrylic acid graft copolymer exhibits a significantly higher molar mass (M_w ~ 443,300 g/mol) than the ATBS-acrylic acid copolymer (M_w ~ 183,300 g/mol). This result is a first indication that grafting was successful. Furthermore it was observed that the hydrodynamic and gyration radii increased from 14.5 nm [$5.71 \cdot 10^{-7}$ in.] and 23.9 nm [$9.41 \cdot 10^{-7}$ in.] respectively for the ATBS-acrylic acid copolymer to 22.1 nm [$8.70 \cdot 10^{-7}$ in.] and 37.2 nm [$1.46 \cdot 10^{-6}$ in.] resp. after the grafting process. In comparison, BNS possesses a much lower molar mass (M_w ~ 140,000 g/mol) than the graft copolymer. In summary, the graft copolymerization process produces a relatively homogeneous graft copolymer that exhibits a quite narrow polydispersity index of ~ 2.0 (see SEC spectrum of graft copolymer in **Fig. 2**).

Next, the anionic charge amounts of the polymers were determined in DI water, cement pore solution (CPS) and in 0.1 M NaOH solution. The results are summarized in **Table 3**. Generally, the graft copolymer possesses a highly anionic character (charge amount e.g. in CPS 3,964 µeq/g), owed to the carboxylate and sulfonate groups present in the graft chains. Such high anionic charge promotes adsorption of the graft copolymer onto positively charged surfaces of cement. The ATBS-acrylic acid copolymer exhibits an even higher anionic charge while BNS possesses a much lower anionic charge than the brown coal based graft copolymer and the ATBS-acrylic acid copolymer.

For the chemical structure of the graft copolymer, the model as follows was developed: Humic acid which presents the main component in the alkali extract possesses numerous functional groups (i. e. phenolic and carboxylate groups) in its structure which provide perfect docking sites for the grafting reaction. After addition of an initiator (e.g. sodium peroxodisulfate), macroradicals can form through abstraction of hydrogen from these functional groups. Consequently, ATBS and acrylic acid monomers can be grafted onto these free radical sites. Simultaneously, side chain propagation can continue. As a result, a graft copolymer is formed that is composed of a humic acid backbone and grafted ATBS-*co*-acrylic acid side chains. A structural model of the graft copolymer is proposed in **Fig. 3**. Note that for humic acid, only model structures exist[16] due to complexity of composition and abundant natural variants. Generally, humic acid contains a number of condensed aromatic rings, and thus attains a relatively stiff, linear conformation. In contrast to this, the ATBS-*co*-acrylic acid graft chains exhibit high conformational flexibility and are coiled in solution. These differences in solution conformation were confirmed by the *Burchard* parameters (ratio of $Rg_{(z)}/R_{h(z)}$). There, a value of 1.7 was obtained for the graft copolymer which represents a linear, stretched random coil[17].

Cement dispersion

The dispersing performance of the brown coal based graft copolymer was determined using a mini slump test. Here, the dosages were established to reach a paste flow of 26 ± 0.5 cm. The water-to-cement ratio of the neat cement paste without superplasticizer was set to produce a slump flow of 18 ± 0.5 cm (w/c ratio of 0.455). This water-to-cement value was applied for all measurements. For the brown coal-ATBS-acrylic acid graft copolymer a dosage of 0.21 % bwoc was required to reach the desired slump flow of 26 ± 0.5 cm. Thus, the novel graft copolymer was even more effective than a commercial BNS reference sample (dosage 0.30 % bwoc). Additional mini slump testing carried out for the ATBS-acrylic acid copolymer revealed that this polymer was slightly better (dosage 0.19 % bwoc) than the graft copolymer itself. The results suggest that the dispersing effect mainly originates from the ATBS-*co*-acrylic acid graft chains. This was confirmed further via mini slump tests, evidencing that the alkaline brown coal extract does not disperse cement.

Furthermore, the time dependent slump loss behavior of a cement paste prepared at a water-to-cement ratio of 0.455 containing the polymers at dosages required for a slump flow of 26 ± 0.5 cm was investigated. The results of these measurements are displayed in **Fig. 4**. Starting from an initial slump flow of 26 ± 0.5 cm, fluidity was monitored every 15 min for a period of 120 min. According to **Fig. 4**, the dispersing performance of the brown coal-ATBS-acrylic acid graft copolymer quickly decreases in the first 30 min (slump flow 21.4 cm [8.43 in.]). Afterwards, the decrease becomes very slow. In contrast, the ATBS-acrylic acid copolymer exhibits better slump retention and behaves more similar than the commercial BNS superplasticizer.

Sulfate tolerance of graft copolymer

The presence of alkali sulfates (i.e. K_2SO_4, Na_2SO_4) in cement can have a significant impact on the dispersing performance of superplasticizers. This phenomenon (the so-called “sulfate effect”) has been observed mainly for polycarboxylates. In literature, two mechanisms are discussed for the negative impact of sulfate on PCEs: competitive adsorption between sulfate ions and PCEs[18] and shrinkage of PCE molecules[19]. To investigate whether the brown coal based graft copolymer is also affected by sulfate ions, mini slump tests at increasing additions of sodium sulfate were carried out. The graft copolymer was applied at a dosage of 0.21 % bwoc (slump flow 26 ± 0.5 cm). The results are illustrated in **Fig. 5**. There, it was observed that the graft copolymer is not much affected by the presence of different concentrations of sulfate, thus confirming high sulfate tolerance for the grafted product. In contrast, the ATBS-acrylic acid copolymer shows strong sensitivity to sulfate. At increasing Na_2SO_4 additions, its initial slump flow of 26.3 cm [10.4 in.] quickly drops to 20.9 cm [8.22 in.]. Furthermore, a physical blend of 20 wt.% brown coal extract and 80 wt.% of the ATBS-acrylic acid copolymer (as present in the graft copolymer) was tested. It was found that this physical mixture exhibits the same poor sulfate tolerance than the ATBS-acrylic acid copolymer, thus providing further evidence that in fact a chemical reaction had occurred between the brown coal substrate and the monomers. A potential explanation for the different behaviors of the brown coal-ATBS-acrylic acid graft copolymer and the ATBS-acrylic acid copolymer are the different molar masses of the polymers. The graft copolymer possesses a higher M_w than the copolymer, so its adsorption is mainly driven by entropic effects (desorption of a huge amount of ions and water molecules adsorbed on the surface of cement), thus producing a high *Gibbs* energy of adsorption[20]. Whereas sulfate ions, whose energy of adsorption results from an enthalpic contribution only and is comparatively low cannot displace already adsorbed polymers from the surface of cement.

Adsorbed layer thickness

Additional experiments were carried out to prove successful grafting of ATBS and acrylic acid monomers onto the alkaline extract of brown coal. For this purpose, the adsorbed layer thicknesses of the graft copolymer, the ATBS-acrylic acid copolymer and the brown coal extract were measured and compared. Monodisperse, spherical cationic polystyrene nanoparticles were taken as adsorbent and layer thicknesses were determined using dynamic light scattering. This method allows facile determination of the adsorbed layer thickness of negatively charged polyelectrolytes at high pH conditions such as in cement pore solution[14]. Layer thicknesses were measured as a function of polymer concentration until the point of saturated adsorption was reached. The results are displayed in **Fig. 6**. The alkaline extract of brown coal reaches the point of saturated adsorption at an adsorbed layer thickness of ~ 2.5 nm [$9.8 \cdot 10^{-8}$ in.] only whereas the brown coal-ATBS-acrylic acid graft polymer exhibits a substantially higher layer thickness of ~ 6.4 nm [$2.5 \cdot 10^{-7}$ in.]. Contrary to this, the ATBS-acrylic acid copolymer produces an adsorbed layer thickness of ~ 1.7 nm [$6.7 \cdot 10^{-8}$ in.] only. These values signify that grafting of the monomers onto the brown coal substrate has indeed occurred, and that the graft product possesses pendants of ATBS-*co*-acrylic acid. However, BNS shows a very low adsorbed layer thickness of only ~ 0.3 nm.

Effect on cement hydration

The influence of the superplasticizers on cement hydration was tested by means of isothermal heat flow calorimetry. The heat evolution from cement hydration was monitored for cement pastes prepared at a water-to-cement ratio of 0.455 holding 0.25 % bwoc of the brown coal-ATBS-acrylic acid graft copolymer, of ATBS-acrylic acid copolymer and of BNS respectively. The results are illustrated in **Fig. 7**. It was observed that the brown coal-ATBS-acrylic acid graft copolymer causes very minor retardation, apparently caused by the ATBS-*co*-acrylic acid pendant groups.

Mechanism of dispersion

Adsorption of superplasticizers on cement particles can be tracked via zeta potential measurements. Here, the zeta potential of cement slurries holding different polymer samples was measured. Concentrations of the polymer samples were those required for a slump flow of 26 ± 0.5 cm. The neat cement paste exhibited a slightly negative zeta potential of – 3.3 mV. After addition of the polymer samples, the zeta potentials of all cement slurries decreased to similar values: brown coal-ATBS-acrylic acid graft copolymer – 28.0 mV; ATBS-acrylic acid copolymer – 27.3 mV and BNS – 29.3 mV. These results signify that the brown coal-ATBS-acrylic acid graft copolymer adsorbs and also achieves dispersion through an electrostatic repulsion effect.

CONCLUSIONS

An alkali brown coal extract holding humic and fulvic acids was successfully used as substrate for the synthesis of a brown coal based superplasticizer. Acrylic acid and ATBS were successfully grafted onto the extracted lignite, as was confirmed via SEC analysis and measurements of the adsorbed layer thicknesses of the graft copolymer and an ATBS-acrylic acid copolymer prepared under comparable conditions. A structural model for the novel graft copolymer suggests that humic/fulvic acid backbones hold grafted chains of ATBS-acrylic acid copolymer. The synthesized brown coal-ATBS-acrylic acid graft copolymer presents an effective cement dispersant which is superior over industrial BNS and exhibits excellent sulfate tolerance. Its working mechanism relies on a combination of a strong electrostatic and a minor steric effect.

The study shows that caustic lignite extracts present interesting and low-cost starting materials for the development of novel superplasticizers holding unique structural motifs. Future research should focus on the replacement of the ATBS monomer by less expensive alternatives such as e.g. itaconic, methacrylic, styrene sulfonic, allyloxy hydroxy propyl sulfonic acid or esters thereof. Due to the chemical variability of brown coal and the number of natural variants, different brown coal types should be tested as well. We consider our work as an initial study which may stimulate further ideas to exploit the potential of this concept, especially in countries where more sophisticated monomers are not available.

ACKNOWLEDGEMENTS

The authors would like to thank Vatenfall Europe Mining AG for providing the brown coal samples and Lubrizol for the supply of the ATBS monomer.

REFERENCES

1. Ramachandran, V. S., Malhotra, V. M., Jolicoeur, C., Spiratos, N., “Superplasticizers: Properties and applications in concrete”, CANMET, Ottawa, Canada, 1998.

2. Spiratos, N., Page, M., Mailvaganam, N. P., Malhotra, V. M., Jolicoeur, C., “Superplasticizers for Concrete: Fundamentals, Technology, and Practice”, *Supplementary Cementing Materials for Sustainable Development*, Ottawa, Canada, 2003.

3. Plank, J., “PCE Superplasticizers – Chemistry, Applications and Perspectives”, 18. ibausil, Weimar, Germany, 12-15 September 2012, Vol.1, pp. 91-102.

4. Plank, J., "Applications of Biopolymers in Construction Engineering, *Biopolymers*, Vol. 10, 2003, pp. 29-95.

5. Lv, S., Gao, R., Cao, Q., Li, D., Duan, J., "Preparation and characterization of poly-carboxymethyl-β-cyclodextrin superplasticizer", *Cement and Concrete Research*, Vol. 42, 2012, pp. 1356-1361.

6. Zhang, D.F., Ju, B. Z., Zhang, S. F., He, L., Yang, J. Z., "The study on the dispersing mechanism of starch sulfonates as a water-reducing agent for cement", *Carbohydrate Polymers*, Vol. 70, No. 4, 2007, pp 363-368.

7. Hatcher, P. G., Clifford, D. J., The organic geochemistry of coal: from plant materials to coal", *Organic Geochemistry*, Vol. 27, No. 5/6, 1997, pp. 251-274.

8. Ashida, R., Morimoto, M., Makino, Y., Umemoto, S., Nakagawa, H., Miura, K., Saito, K., Kato, K., "Fractionation of brown coal by sequential high temperature solvent extraction", *Fuel*, Vol. 88, 2009, pp. 1485-1490.

9. Pang, L. S. K., Vassallo, A. M., Wilson, M. A., "Chemistry of alkali extraction of brown coals – I. Kinetics, characterization and implications to coalification", *Organic Geochemistry*, Vol. 16, 1990, pp. 853-864.

10. Garcia, D., Cegarra, J., Abad, M., Fornes, F., "Effects of the extractants on the characteristics of humic fertilizer obtained from lignite", *Bioresource Technology*, Vol. 43, 1993, pp. 221-225.

11. Caenn, R., Chillingar, G. V., "Drilling fluids: state of the art", *Journal of Petroleum Science and Engineering*, Vol. 14, 1996, pp. 221-230.

12. Pehlivan, E., Arslan, G., "Comparison of adsorption capacity of young brown coals and humic acids prepared from different coal mines in Anatolia", *Journal of Hazardous Materials*, Vol. B138, 2006, pp. 401-408.

13. Krol-Domanska, K., Smolinska, B., "Advantages of lignite addition in purification process of soil polluted by heavy metals", *Biotechnology and Food Sciences*, Vol. 76, No. 1, 2012, pp. 51-58.

14. Tiemeyer, C., Lange, A., Plank, J., "Determination of the adsorbed layer thickness of functional anionic polymers utilizing chemically modified polystyrene nanoparticles", *Colloids and Surfaces A: Physiochemical and Engineering Aspects*, Vol. 456, 2014, pp. 139-145.

15. Gupta, P. R., Goring, D. A. I., "Physicochemical Studies of Alkali Lignins III: Size and Shape of the Macromolecule", *Canadian Journal of Chemistry*, Vol. 38, No. 2, 1960, pp. 270-279.

16. Stevenson, F. J., "Humus Chemistry: Genesis, Composition, Reactions", *John Wiley & Sons*, New York, USA, 2nd Edition, 1994.

17. Burchard, W., "Static and dynamic light scattering from branched polymers and biopolymers", *Advances in Polymer Science*, Vol. 48, 1983, pp. 1-124.

18. Han, S., Plank, J., "Mechanistic study on the effect of sulfate ions on polycarboxylate superplasticizers in cement", *Advances in Cement Research*, Vol. 25, No. 4, 2013, pp. 200-207.

19. Yamada, K., Ogawa, S., Hanehara, S., "Controlling of the adsorption and dispersing force of polycarboxylate-type superplasticizer by sulfate ion concentration in aqueous phase", *Cement and Concrete Research*, Vol. 31, 2001, pp. 375-383.

20. Plank, J., Sachsenhauser, B., de Reese, J., "Experimental determination of the thermodynamic parameters affecting the adsorption behaviour and dispersion effectiveness of PCE superplasticizers", *Cement and Concrete Research*, Vol. 40, 2010, pp. 699-709.

TABLES AND FIGURES

List of Tables

List of Figures

Table 1 – Phase composition of the CEM I 52.5 N sample determined by Q-XRD using *Rietveld* refinement.

Phase	wt.%
C_3S, m	54.14
C_2S, m	26.63
C_3A, c	3.28
C_3A, o	4.26
C_4AF, o	2.45
Free Lime (*Franke*)	0.10
Periclase (MgO)	0.03
Anhydrite	2.64
Hemihydrate*	1.21
Dihydrate*	0.02
Calcite	3.61
Quartz	1.16
Arcanite (K_2SO_4)	0.46

* determined by thermogravimetry

Table 2 – Molar masses, polydispersity index (PDI) and polymer radii of the synthesized polymers and of BNS as reference superplasticizer sample.

Polymer	M_w [g/mol]	M_n [g/mol]	PDI	$R_{g(z)}$ [nm]	$R_{h(z)}$ [nm]
Brown coal-ATBS-AA	443,300	216,100	2.0	37.2	22.1
ATBS-AA copolymer	183,300	93,460	2.0	23.9	14.5
BNS	140,000*	-	-	-	-

* = batch measurement

Table 3 – Anionic charge amounts of the polymer samples in DI water, CPS and 0.1 M NaOH solution.

Polymer	DI water [µeq/g]	CPS [µeq/g]	0.1 M NaOH [µeq/g]
Brown coal-ATBS-AA	3,347	3,964	4,765
ATBS-AA copolymer	4,241	3,974	4,855
BNS	3,643	2,713	3,989

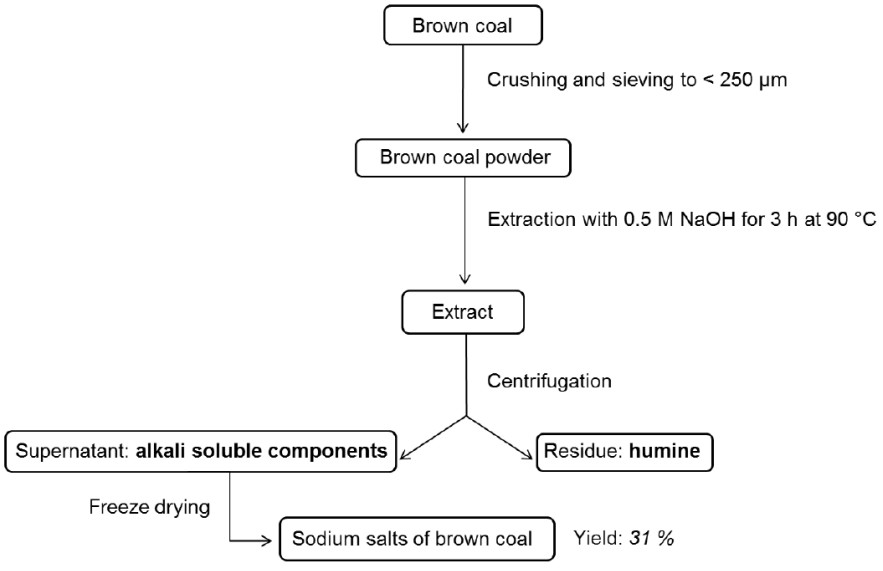

Fig. 1 – Scheme for extraction of alkali soluble components from brown coal.

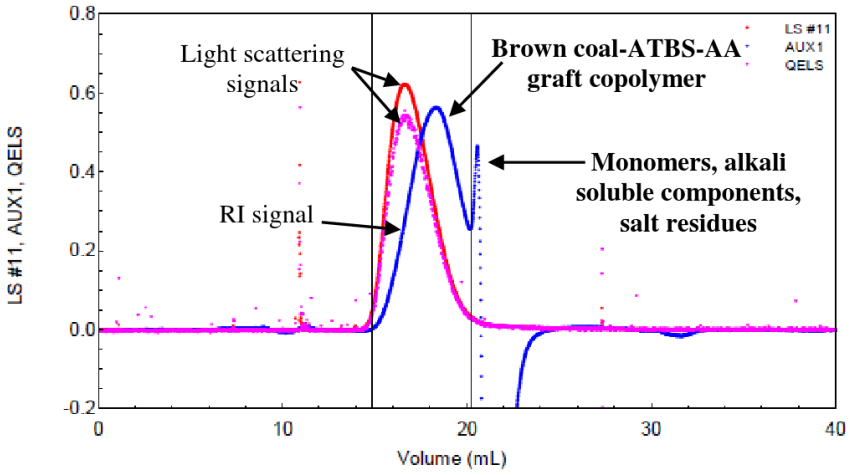

Fig. 2 – SEC spectrum of the brown coal-ATBS-AA graft copolymer.

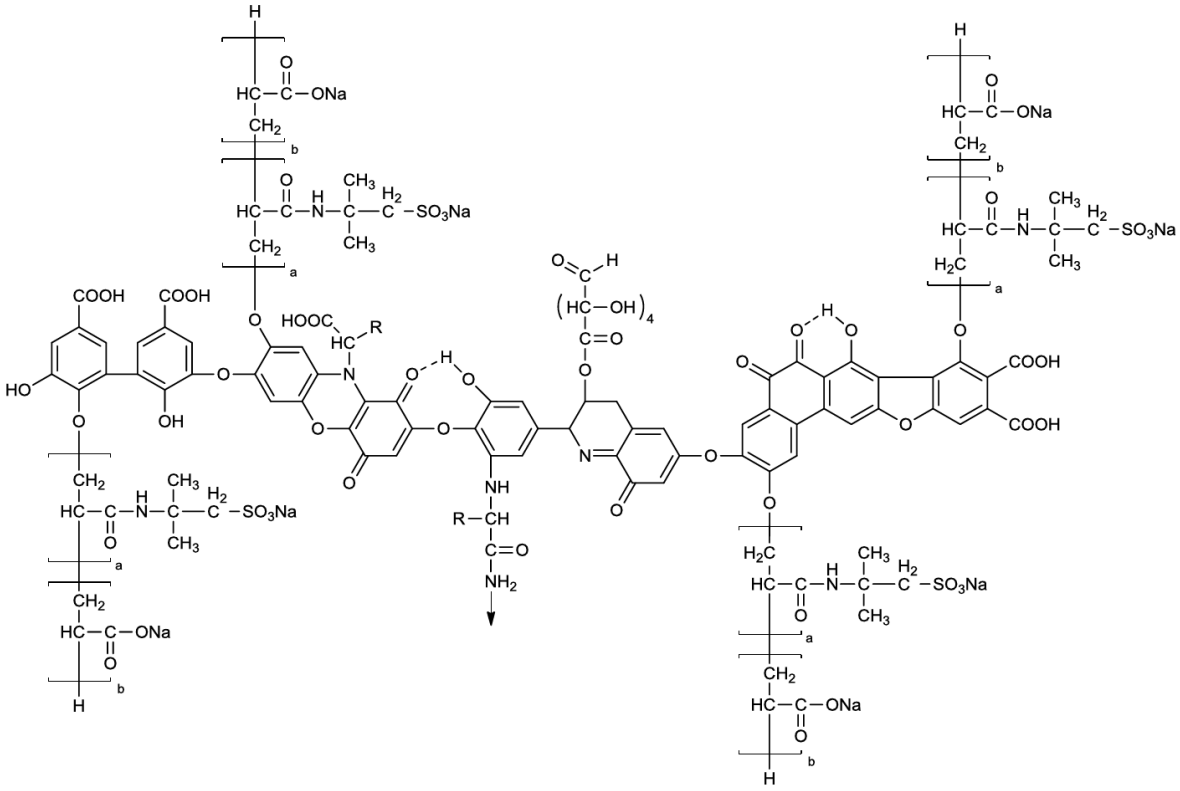

Fig. 3 – Proposed chemical structure of the brown coal-ATBS-AA graft copolymer.

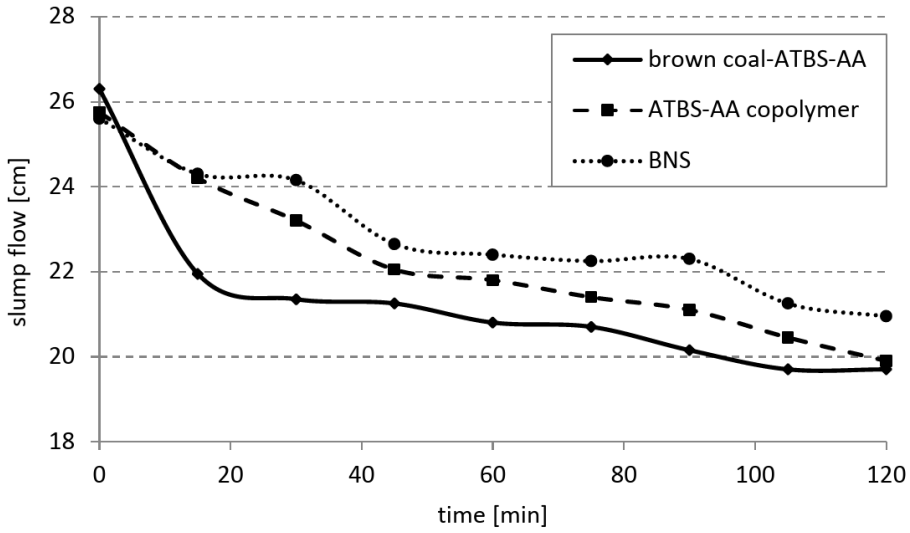

Fig. 4 – Time dependent development of the slump flow of a cement slurry (w/c = 0.455) containing 0.21 % bwoc of brown coal-ATBS-AA graft copolymer, 0.19 % bwoc of ATBS-AA copolymer and 0.3 % bwoc of BNS respectively.

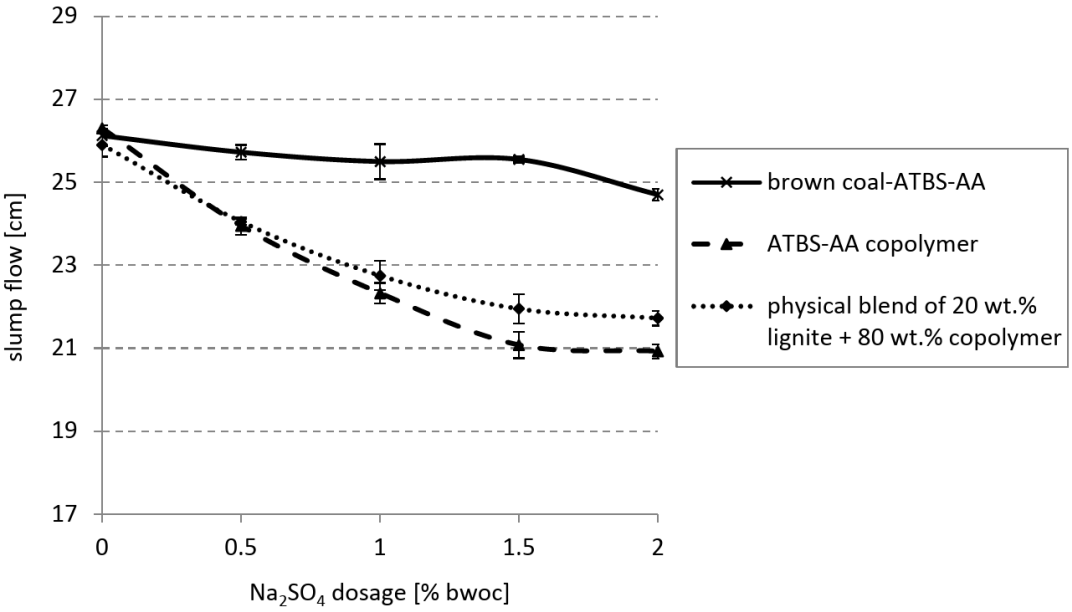

Fig. 5 – Effect of different Na_2SO_4 dosages on the slump flow of cement pastes (w/c = 0.455) holding different polymer samples.

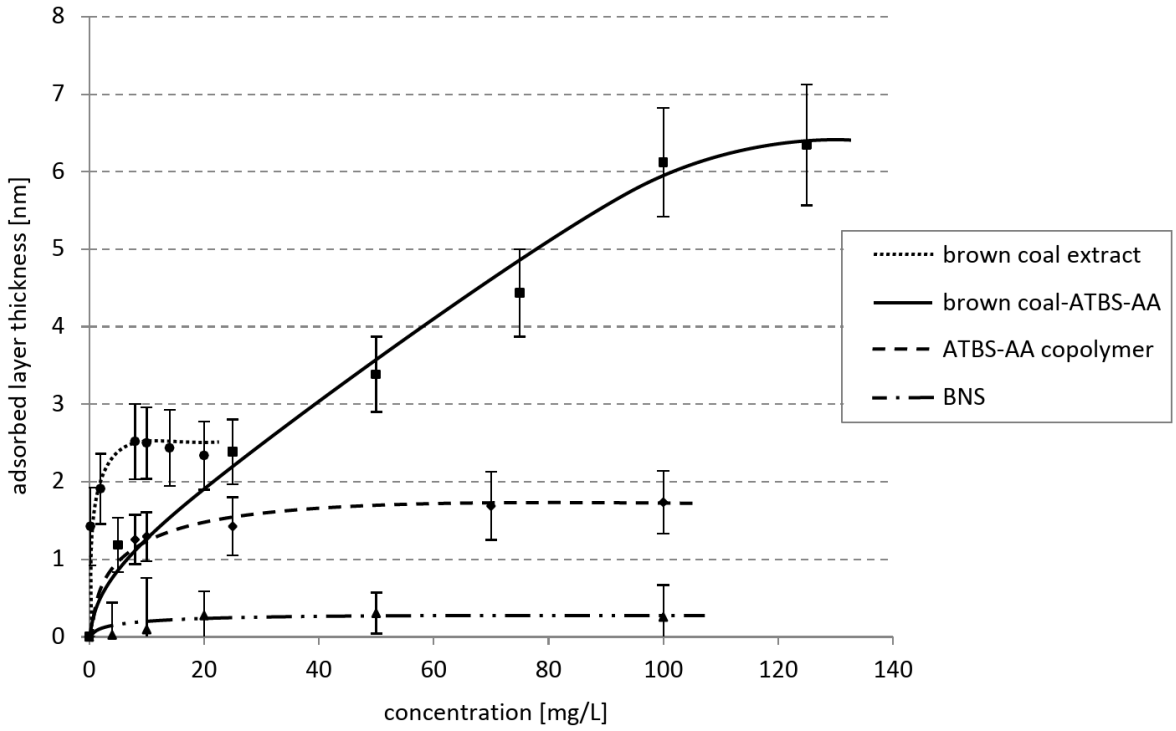

Fig. 6 – Concentration-dependent adsorbed layer thicknesses of the brown coal-ATBS-AA graft copolymer, of ATBS-AA copolymer, of the alkaline brown coal extract and BNS.

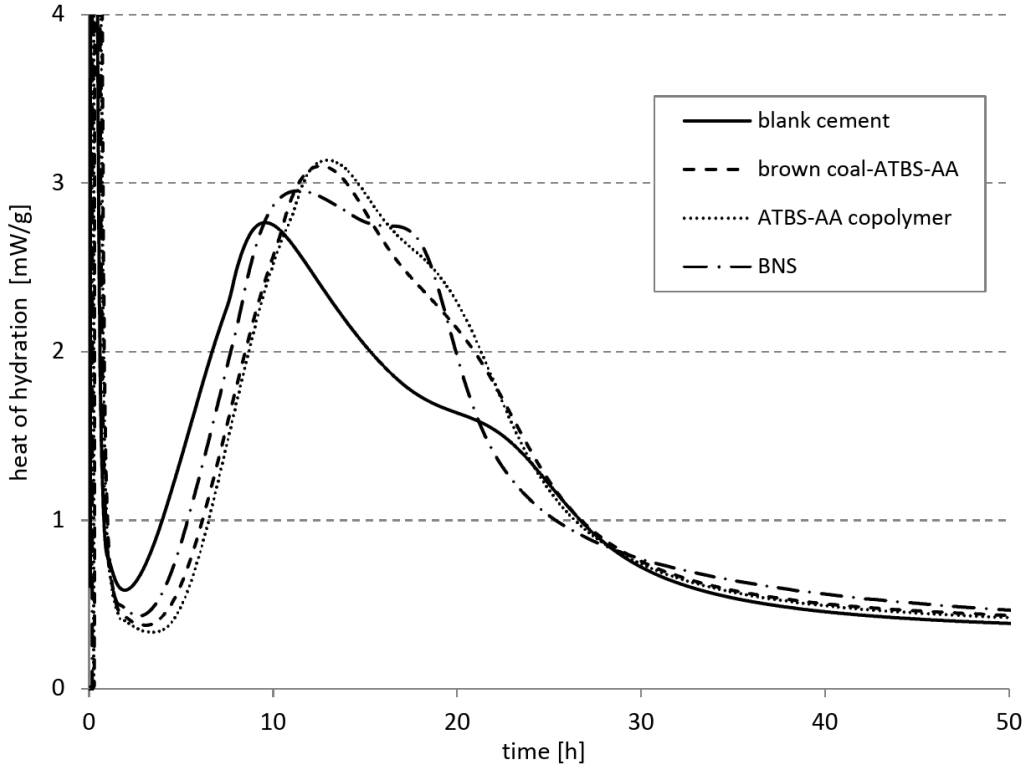

Fig. 7 – Isothermal heat flow calorimetry of cement slurries (w/c = 0.455) holding 0.25 % bwoc of brown coal-ATBS-AA graft copolymer, ATBS-AA copolymer and BNS respectively.

5.3.2. Publikation #11: A novel kind of concrete superplasticizer based on lignite graft copolymers

Publikation #11

A novel kind of concrete superplasticizer based on lignite graft copolymers

Manuel Ilg, Johann Plank

Cement and Concrete Research

79 (2016) 123 – 130

Doi: 10.1016/j.cemconres.2015.09.004

Cement and Concrete Research 79 (2016) 123–130

Contents lists available at ScienceDirect

Cement and Concrete Research

journal homepage: http://ees.elsevier.com/CEMCON/default.asp

A novel kind of concrete superplasticizer based on lignite graft copolymers

Manuel Ilg, Johann Plank *

Chair for Construction Chemistry, Technische Universität München, Lichtenbergstraße 4, Garching 85747, Germany

ARTICLE INFO

Article history:
Received 27 February 2015
Accepted 8 September 2015
Available online 9 October 2015

Editor: Keith Baldie

Keywords:
Dispersion (A)
Characterization (B)
Admixture (D)
Concrete (E)
Lignite

ABSTRACT

A novel superplasticizer was synthesized by grafting 2-acrylamido-2-tert.butyl sulfonic acid (ATBS) and acrylic acid (AA) monomers onto a lignite backbone using free radical copolymerization technique. Different molar ratios of ATBS:acrylic acid were tested to investigate the influence of the acrylic acid content on the dispersing performance of the graft copolymer. The synthesized polymers were characterized relative to their molecular properties and their dispersing performance in cement. It was found that especially the graft copolymer with an ATBS:acrylic acid molar ratio of 1:0.15 exhibits high dispersing force, long slump retention, high sulfate tolerance and only minor cement retardation. The polymer is more effective than industrial grade BNS. Successful grafting of the monomers was confirmed by size exclusion chromatography and measurement of the adsorbed layer thicknesses.

1. Introduction

Concrete presents the most common man-made building material at present. It constitutes the fundamental element of our modern architecture and infrastructure [1,2]. A key factor for its widespread use is its unprecedented versatility. For example, it can be utilized for the construction of skyscrapers and bridges, in the manufacturing of prefabricated concrete elements, as shotcrete in tunneling or as drymix concrete [3]. Other important advantages include the ubiquitous availability of the raw materials (cement, sand, gravel and water), its simple fabrication, its stability and durability as well as its relatively low price. The variability of concrete properties also results from the application of chemical admixtures such as, e.g., superplasticizers [4]. These chemical admixtures are added in small amounts to the cement to enhance its workability (increased flowability and pumpability) and to improve the material properties of the hardened concrete (higher compressive and bending tensile strength) [5]. Superplasticizers facilitate the reduction of the water-to-cement ratio, thus enabling the production of concrete with higher strength and durability.

Since the invention of superplasticizers in the 1960s, this group of chemical admixtures experienced a rapid growth. Nowadays, different kinds of superplasticizers can be identified: polycondensates, polycarboxylates, small molecules and biopolymers [6]. Although the present kinds of polycondensates and polycarboxylates represent highly effective superplasticizers, still new structures and concepts are targeted by scientific and industrial researchers [7]. A new approach for the synthesis of superplasticizers is the utilization of natural polymers as a starting material [8]. They can offer novel structural motifs and often possess a high density of functional groups. Therefore, they can present perfect substrates for chemical modifications, including graft copolymerization reactions. Some examples have already been reported in the literature, where novel superplasticizers have been synthesized through functionalization (i.e., *via* sulfonation or carboxymethylation) of natural polymers [9–11]. Lignite, a synonym used in the scientific literature for ordinary brown coal, presents an outstanding starting material for such preparations because of its global abundance, low cost and its high structural diversity.

Lignite is a sedimentary type of coal often occurring near the surface of earth that formed million years ago through coalification [12,13]. This process was initiated in flooded areas such as swamps whereby plant residues (i.e., roots, leaves and spores) were submerged in water, thus preventing the aerobic degradation of the plant material. The high bioproduction rates prevailing under the primeval subtropical climate conditions ensured that more plant residues were deposed than degraded [13]. As a result, plant material was accumulated and partially decomposed to peat. Burial of these humic substances over millions of years by sediments and geological changes (e.g., tectonic movements) caused an increased pressure leading to drainage and the release of gases like methane or carbon dioxide [14]. This process caused the plant residues to successively metamorphose into lignite. Depending on the degree of coalification, four different coal types are distinguished: lignite, sub-bituminous coal, bituminous coal and anthracite. According

* Corresponding author. Tel.: + 49 89 289 13151; fax: + 49 89 289 13152.
E-mail address: sekretariat@bauchemie.ch.tum.de (J. Plank).

http://dx.doi.org/10.1016/j.cemconres.2015.09.004
0008-8846/

to this classification, lignite presents a coal of low quality possessing the highest water and the lowest carbon content.

Chemically, lignite constitutes a complex, inhomogeneous mixture containing a variety of organic and inorganic compounds. The organic components include bitumen (wax, resins), humic substances and incompletely charred lignin and cellulose residues. The humic substances can be divided according to their solubility in aqueous solution in humin, fulvic and humic acids [15]. The organic constituents that are insoluble over the entire pH range are designated as humin, while the fulvic acid fraction includes the substances that are soluble under all pH conditions. Contrary, humic acids are only soluble in alkaline media, but insoluble in strongly acidic environments (pH <1). Humic and fulvic acid represent the main part of the organic constituents (up to 80 wt.%). They can be extracted by treating lignite with alkali hydroxide solution [16,17]. The alkali-soluble components of lignite are commercially available as "caustic lignite," which for example is used in millions of tons as fertilizer in agriculture [15,18] or as drilling fluid additive by the oil industry [19]. However, up to date, no lignite-based superplasticizer has been developed.

In recent work, we already have described the synthesis of a graft copolymer from ordinary brown coal mined in Germany [20]. Due to its high amount of insoluble components, an alkaline extraction was first performed to remove all non-reactive components (e.g., humin, ashes, minerals, etc.) and to isolate the fraction which contains the humic and fulvic acids because only they can be utilized as starting material for the grafting process. In contrast, the lignite sample studied here had been purified already and was selected for a high content of humic acids, which is particularly advantageous for the grafting reaction. Therefore, one purpose of the paper here was to prove the applicability of our process to commercial purified lignite samples.

In this study, we report on the synthesis of a novel superplasticizer prepared by grafting ATBS and acrylic acid onto the alkali-soluble constituents of lignite. The lignite sample differs in its chemical composition from the previously studied brown coal regarding its higher amount of humic acids.

The alkali-soluble constituents exhibit a high number of functional groups (i.e., aliphatic/aromatic carboxylate, amino, hydroxyl and phenolic groups) and thus represent an ideal substrate for graft copolymerization reactions [21]. Through the addition of an initiator, the different functionalities allow the formation of free radical sites. Vinyl monomers can be grafted onto these sites leading to a polymer with lateral graft chains and lignite as backbone. Different lignite{ATBS-*co*-AA} graft copolymers were synthesized and the molar ratio of the monomers ATBS and acrylic acid was varied from 1:0.15 to 1.50 to investigate the influence of the acrylic acid content on the dispersing power. To ascertain the contribution of the lignite backbone to the dispersing effect, an ATBS-acrylic acid copolymer was synthesized as comparative sample to the respective lignite{ATBS-*co*-AA} graft copolymer. Furthermore, the overall aim of this study was to evaluate new structural motifs and concepts for the synthesis of potent new superplasticizer molecules.

2. Materials and methods

2.1. Cement

An ordinary Portland cement CEM I 52.5N (*Milke®classic* from HeidelbergCement, Geseke plant, Germany) was used in this study. The phase composition of the cement as determined by Q-XRD and subsequent *Rietveld* refinement is illustrated in Table 1. Its specific surface area as obtained by the *Blaine* method was 3,583 cm^2/g. For the average particle size (d_{50} value; determined by laser granulometry using a CILAS 1064 instrument, Cilas, Marseille, France), a value of 11.5 μm was found, and the density of the cement was 3.15 g/cm^3 (Helium pycnometer from Toni Technik, Berlin, Germany).

Table 1
Phase composition of the CEM I 52.5N sample as determined by Q-XRD using *Rietveld* refinement.

Phase	wt.%
C_3S, m	54.14
C_2S, m	26.63
C_3A, c	3.28
C_3A, o	4.26
C_4AF, o	2.45
Free lime (*Franke*)	0.10
Periclase (MgO)	0.03
Anhydrite	2.64
Hemihydrate[a]	1.21
Dihydrate[a]	0.20
Calcite	3.61
Quartz	1.16
Arcanite (K_2SO_4)	0.46

[a] Determined by thermogravimetry.

2.2. Chemicals

2-Acrylamido-2-tert.butyl sulfonic acid (ATBS; AMPS® 2404 monomer; >99% purity) was received from Lubrizol (Rouen, France). AMPS® is a registered trademark of the Lubrizol Corporation (Wickliffe, Ohio). Acrylic acid (AA; >99%), sodium hydroxide (NaOH; >98%), sodium peroxodisulfate ($Na_2S_2O_8$; >99%) and sodium pyrosulfite ($Na_2S_2O_5$; >99%) were purchased from Merck (Darmstadt, Germany), while ethylenediamine tetraacetic acid (EDTA; purity >99.5%) came from Sigma-Aldrich (Munich, Germany). All chemicals were used without further purification.

Melcret® 500 F, a spray dried β-naphthalenesulfonate (BNS)-based superplasticizer powder received from BASF Construction Polymers GmbH (Trostberg, Germany), was used as an industrial reference sample.

2.3. Lignite sample

Superlignite, an untreated lignite supplied as a dark brown powder which exhibits a pH of 5.7 in 10 wt.% aqueous solution, was obtained from American Colloid Company (Hofmann Estates, Illinois, USA). This lignite sample is mined in North Dakota; it contains a high amount of humic acids and was used as is. The data obtained from the elemental analysis of the lignite sample are tabulated in Table 2. Superlignite exhibits a carbon content of only 42.30 wt.%, which confirms its low degree of coalification. The molecular weights of this lignite as determined by size exclusion chromatography where found at 36,000 g/mol (M_w) and 30,000 g/mol (M_n), respectively. The chemical composition of the sample was quantified according to an experimental procedure described in literature [16]. It was found that superlignite contains about 41 wt.% alkali-insoluble components (i.e., humin and inorganic matter), while the main part represents the alkali-soluble fraction (57 wt.% humic acid; 2 wt.% fulvic acid). Furthermore, anionic charge measurements revealed a slightly anionic character of the raw material in DI water (183 μEq/g), and a higher charge in 0.1 M NaOH (464 μEq/g).

2.4. Preparation of the lignite{ATBS-co-AA} graft copolymers

The lignite{ATBS-*co*-AA} graft copolymers were synthesized by aqueous free radical copolymerization using sodium peroxodisulfate

Table 2
Elemental analysis data of the lignite sample.

Element	C	H	N	S	Na	K	O[a]
[wt.%]	42.30	3.73	0.95	1.65	2.00	0.20	49.17

[a] O content calculated as difference to 100%.

as initiator. Five different ATBS:acrylic acid molar ratios were tested (1:0.15–1.50). A reaction scheme illustrating the synthesis of the graft copolymers is displayed in Fig. 1. In the following, the general preparation procedure is described for a graft copolymer where the ATBS:acrylic acid molar ratio was 1:0.15. For all copolymerizations, the weight ratio of lignite:grafted monomers was 20:80 (wt/wt). In a five-necked, 1 L round bottom flask equipped with a mechanical stirrer, reflux condenser, thermometer and inlet for N_2 gas, 13.2 g of lignite was dissolved in 206 mL DI water before 13.6 g of NaOH pellets was added to adjust a pH of 12 to solubilize the lignite. Thereafter, 50.0 g ATBS (241 mmol, 1.0 Eq.) was added stepwise while the temperature was kept under 18 °C to prevent the undesired homopolymerization of ATBS. Next, 2.60 g acrylic acid (36.1 mmol, 0.15 Eq.), 600 mg EDTA and 1.00 g of a defoamer (e.g., TEGO ANTIFOAM MR. 2123, an organo-modified polysiloxane from Evonik, Essen, Germany) were added, and the mixture was purged with N_2 for 1 h at room temperature. Then the temperature was raised to 50 °C and the first amount of sodium peroxodisulfate initiator (8 g) was added. Within a few minutes, a significant increase of the viscosity can be observed. After stirring the mixture for 50 min, the second half of the initiator (8 g) was added and the polymerization was continued for 70 min at 50 °C. Next, the temperature was increased to 60 °C and kept at this temperature for one additional hour. After heating to 80 °C, 3.6 g sodium pyrosulfite was added to quench remaining radicals, and the solution was stirred at this temperature for 1 h. Finally, the polymer solution was cooled to ambient yielding a dark brown, viscous product with a solid content of 30.3 wt.% and a pH of 2.2. In all further investigations, the polymer solutions were used as is without any additional purification.

2.5. Preparation of ATBS-acrylic acid copolymer

The ATBS-acrylic acid copolymer was synthesized (molar ratio ATBS:AA = 1:0.15) according to the procedure for the lignite{ATBS-*co*-AA} graft copolymer except that no lignite was present. Here, a pale yellowish, slightly viscous, 27.6 wt.% polymer solution (pH 2.5) was received as a final product. Again, this polymer solution was applied without further purification.

2.6. Characterization of the polymers

2.6.1. Specific anionic charge amount

The anionic charge of the polymers was measured *via* polyelectrolyte titration using a particle charge detector PCD 03 pH (BTG Mütek GmbH, Herrsching, Germany). Charge titration was carried out with a

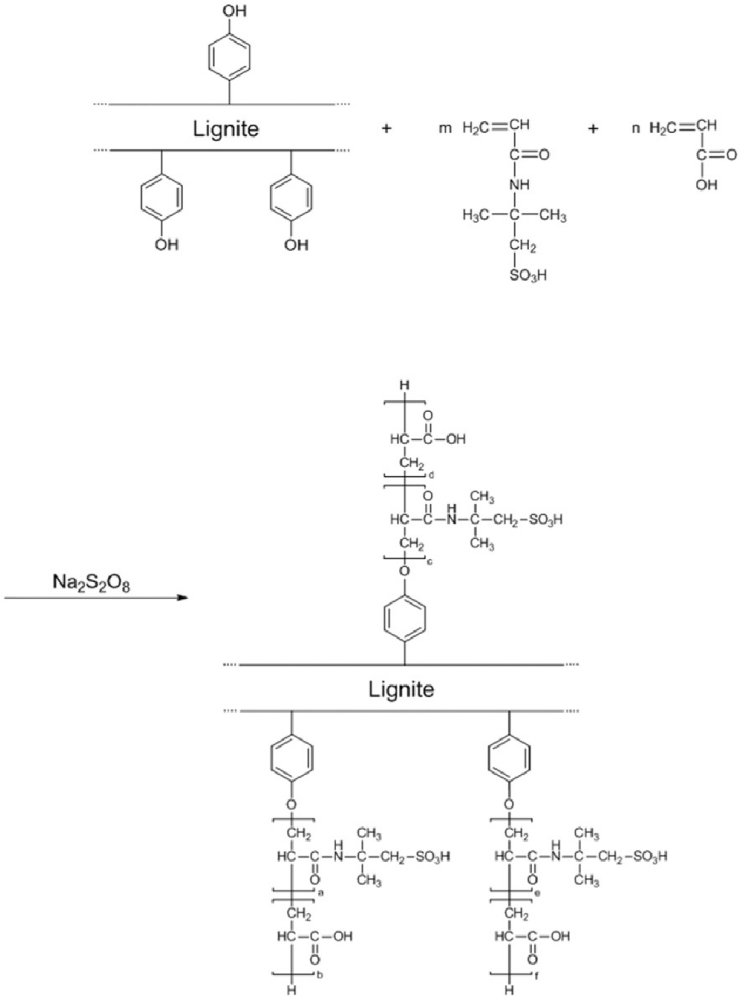

Fig. 1. Schematic illustration of grafting reaction yielding the lignite{ATBS-*co*-AA} graft copolymer.

cationic 0.001 M polydiallyl dimethyl ammonium chloride solution (polyDADMAC). Measurements of the polymer samples (concentration of 0.1 g/L) were performed in DI water, cement pore solution and 0.1 M NaOH. Cement pore solution was freshly prepared by vacuum filtration of a neat cement paste, mixed at a water-to-cement ratio of 0.455. In a typical experiment, 10 mL of the polymer solution was pipetted into the PTFE cylinder of the instrument, and a 0.001 M polyDADMAC solution was titrated against it until the isoelectronic point was reached. The measurements were repeated three times and the obtained values were averaged. By means of the amount of polyDADMAC consumed, the specific anionic charge amount (anionic charge per gram of polymer) can be calculated.

2.6.2. Size exclusion chromatography

Molecular weights (M_w, M_n) and polymer radii ($R_{g(z)}$, $R_{h(z)}$) of the synthesized polymers were measured *via* size exclusion chromatography (SEC). Measurements were performed on a Waters 2695 separation module equipped with RI detector 2414 (Waters, Eschborn, Germany) and an 18-angle light scattering detector (Dawn EOS from Wyatt Technologies, Santa Barbara, CA, USA). The concentration of the polymer solutions was 2 g/L. The separation of the polymers was facilitated on a precolumn and two Aquagel-OH 60 columns (Polymer Laboratories, distributed by Varian, Darmstadt, Germany) using 0.2 M aqueous $NaNO_3$ solution (adjusted with NaOH to a pH of 9) as an eluent at a flow rate of 1.0 mL/min. The differential index of refraction (dn/dc) used to calculate M_w and M_n of superlignite was 0.218 mL/g (value for lignin), while for the lignite-based graft copolymers and the ATBS-acrylic acid copolymer, a value of 0.156 mL/g (value for polyacrylamide) was applied [22,23].

2.6.3. Dispersing performance

The dispersing power of the polymers was determined by means of a 'mini slump' test performed according to DIN EN 1015, but with some modifications [24]. At first, the water-to-cement ratio required to reach a slump flow of 18 ± 0.5 cm without admixture was established. This specific water-to-cement ratio (0.455) was applied to determine the polymer dosages required for a slump flow of 26 ± 0.5 cm. The experimental procedure was as follows. First, the polymer sample was dissolved in the required amount of mixing water placed in a porcelain cup. The amount of water contained in the polymer solution was regarded and subtracted from the amount of mixing water. Then, 300 g of cement was added to the mixing water over a period of 1 min, rested for 1 min and finally stirred manually for 2 min with a spoon. Subsequently, the cement paste was poured into a *Vicat* cone (height 40 mm, top diameter 70 mm, bottom diameter 80 mm) placed on a glass pate, filled to the rim and the cone was vertically removed. The resulting diameter was measured twice, the second measurement being perpendicular to the first one and averaged to attain the slump flow value.

For time-dependent paste flow testing, 400 g of cement was mixed with the respective amount of water and the polymer sample to obtain an initial slump flow of 26 ± 0.5 cm. The experimental procedure was analogue to that as described above. After each measurement, the cement slurry was transferred back into the porcelain cup and covered with a wet towel to prevent desiccation. Prior to each test, the cement slurry was again vigorously stirred for 2 min. Measurements were performed every 15 min over a period of 60 min.

2.6.4. Adsorbed layer thickness

To confirm successful grafting, the thickness of the adsorbed layer of graft copolymer was determined. The adsorbed layer thickness was measured *via* dynamic light scattering utilizing a Zetasizer Nano ZS (Malvern Instruments, Worcestershire, England). Cationic, monodisperse polystyrene nanoparticles with an average particle size of 75.5 ± 0.5 nm were used as an adsorbent. The nanoparticles were synthesized according to a procedure described in the literature and modified with zinc palmitate to attain a positive surface charge [25]. Prior to the measurement, different concentrations of the polymers were prepared by dilution (diluent 0.1 M NaOH) starting from a 150 mg/L stock solution. The solutions were filtered through a 0.2 μm syringe filter to remove undesired dust particles that can disturb the measurement. Fifty microliters of the polystyrene nanoparticle dispersion was added and sonicated for 5 min. The solution was poured into a cuvette and placed in the Zetasizer Nano ZS instrument. Data logging was repeated 150 times per sample, and the values obtained were averaged. Each test consisted of a 10 s light scattering run taken at a temperature of 25 °C. Measurements were performed until a stable, final value representing the point of saturated adsorption was reached. The adsorbed layer thickness of the polymer was calculated according to Eq. (1).

$$\text{adsorbed layer thickness [nm]} = \frac{d_{\text{ads}}\ [\text{nm}] - d_{\text{polystyrene}}\ [\text{nm}]}{2} \quad (1)$$

where d_{ads} denotes the particle size of the polystyrene nanoparticle holding the adsorbed polymer and $d_{\text{polystyrene}}$ represents the size of the native polystyrene particle.

2.6.5. Isothermal heat flow calorimetry

Potential retardation of cement was investigated by isothermal heat flow calorimetry using a TAM Air Thermostat (TA Instruments, Järfälla, Sweden). The calorimeter consists of an eight-channel twin-type block, meaning that on one side the heat flow of the sample is monitored while the reference is on a parallel sensor. The difference in heat flow between the sample and the reference is registered and represents the isothermal heat flow. For the measurements, 4 g of cement was weighed into 20 mL glass ampoules, and aqueous polymer solutions were added at the respective dosages to obtain a water-to-cement ratio of 0.455. The ampoules were capped, homogenized in a wobbler for 1 min and then placed in the calorimeter. Measurements were carried out until the release of heat from the hydration reaction subsided completely.

3. Results and discussion

3.1. Molecular properties of the lignite{ATBS-co-AA} graft copolymers

At first, the anionic charge amounts of the graft copolymers were determined *via* charge titration. The anionic charge amount provides a first information about the interaction of the polymers with cement. Measurements were performed in DI water (pH 7), in 0.1 M NaOH (pH 13) as well as in cement pore solution (pH 13.5), to investigate the polymers under different pH and electrolyte conditions. The results are displayed in Fig. 2.

Generally, all lignite{ATBS-*co*-AA} graft copolymers possess high anionic charge amounts, resulting from the sulfonate and carboxylate groups present in the graft chains, whereas the lignite starting material only shows a very minor anionic charge amount (e.g., 183 μEq/g in DI water vs. ~3,500 μEq/g for the grafted products). As can be seen from Fig. 2, in DI water, the anionic charges of all graft copolymers are quite comparable at 3,500 μEq/g and increase significantly to ~4,400–6,100 μEq/g in 0.1 M NaOH because of complete deprotonation of the acid groups. Furthermore, the anionic charges increase steadily with ascending acrylic acid content. In cement pore solution, the graft copolymers exhibit lower anionic charges due to complexation of calcium ions by the carboxylate groups. For comparison, the anionic charge of lignite-free ATBS-*co*-acrylic acid (ATBS:AA = 1:0.15) was measured. As expected, this copolymer shows a higher anionic charge amount than the corresponding lignite{ATBS-*co*-AA} graft copolymer. This result confirms that in the graft copolymer, the graft chains represent the critical part which contribute to the charge of the polymers.

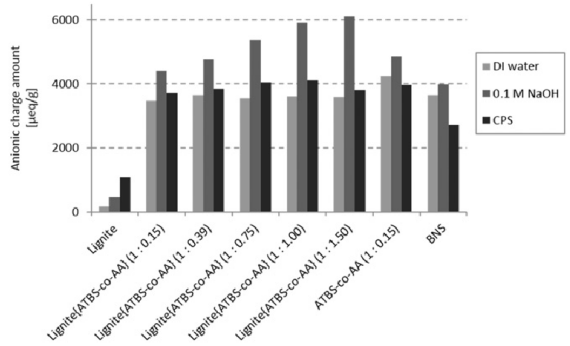

Fig. 2. Anionic charge amounts of the lignite{ATBS-*co*-AA} graft copolymers, of ATBS-*co*-AA and of BNS in DI water, 0.1 M NaOH and cement pore solution (CPS).

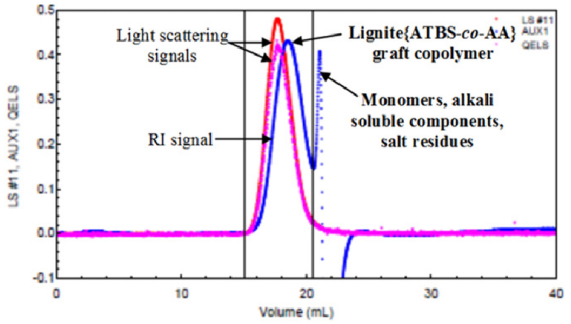

Fig. 3. SEC spectrum of the lignite{ATBS-*co*-AA} graft copolymer (molar ratio ATBS:AA = 1:0.15).

Next, the molecular weights of the synthesized polymers were ascertained using size exclusion chromatography (SEC). The results are summarized in Table 3. According to these data, the lignite{ATBS-*co*-AA} graft copolymers principally possess high molecular weights (>200,000 g/mol). As an example, the SEC spectrum of the graft copolymer prepared at a molar ratio of ATBS:acrylic acid of 1:0.15 is displayed in Fig. 3. There, it is noticeable that the graft copolymerization produces a relatively homogeneous polymer with a narrow molecular weight distribution. A PDI of 1.6 was found for this graft copolymer. When increasing the acrylic acid content, the PDI rises up to 2.8, and the molecular weights show a tendency to decrease. Thus, higher acrylic acid contents seem to favor the formation of shorter graft chains. For comparison, the ATBS-AA copolymer (ATBS:AA = 1:0.15) was analyzed as well (Table 3). Generally, molar masses and polymer radii of the copolymer were lower than for the lignite-based graft copolymer. These results provide a first indication for successful grafting of the ATBS and acrylic acid monomers onto the lignite backbone. However, as a typical polycondensate-based superplasticizer, BNS exhibits a molecular weight of only ~140,000 g/mol (M_w).

Relative to the grafting mechanism, the considerations as follows were made: under the impact of heat, the initiator sodium peroxodisulfate decomposes into sulfate radicals, which react further with water to hydrogen sulfate and hydroxyl radicals. These radicals can abstract hydrogen from functional groups (e.g., phenolic or carboxylate) contained in humic and fulvic acid, thus leading to free radical sites on the lignite backbone which then represents a macroradical. ATBS and acrylic acid can be grafted onto these sites leading to successive chain propagation initiated, e.g., from the humic acid backbone. This way, a graft copolymer is obtained with a lignite backbone and ATBS-*co*-acrylic acid as pendant groups. Based on these considerations, the chemical structure as shown in Fig. 4 is proposed for the lignite{ATBS-*co*-AA} graft copolymer. Note that for humic acid several structural models exist in the literature because of the complexity of its composition and the numerous natural variants. For our model, the structure as presented by *Stevenson* [26] was adopted. As is apparent from the figure, humic acid includes several condensed aromatic ring systems. This favors the formation of a nearly linear structure. In contrast, the ATBS-*co*-AA graft chains exhibit high conformational flexibility. This was ascertained from the *Burchard* parameters (ratio of $R_{g(z)}/R_{h(z)}$; see Table 3) of the lignite{ATBS-*co*-AA} graft copolymers which exhibit *Burchard* parameters of ~2.0–2.2. Such values correspond to molecular conformations lying between that of a random coil and a rigid chain [27].

3.2. Dispersion effectiveness

The dispersing performance of the synthesized graft copolymers was assessed by means of a 'mini slump' test. There, the dosages of the polymer samples required to reach a slump flow of 26 ± 0.5 cm were determined for cement pastes prepared at a water-to-cement ratio of 0.455. Without any superplasticizer, this water-to-cement value produces a slump flow of 18 ± 0.5 cm.

As can be seen from Fig. 5, the lowest dosage (0.25% by weight of cement, bwoc) was found for the graft copolymers prepared at ATBS:acrylic acid molar ratios of 1:0.15 and 1:0.39, respectively. When the acrylic acid content was increased, then the dosages rose from 0.25% to 0.47% bwoc (the latter for the polymer containing ATBS:acrylic acid of a molar ratio of 1:1.50). Apparently, higher acrylic acid contents do not result in a better dispersing effect. For comparison, the ATBS-acrylic acid copolymer (molar ratio 1:0.15) was tested as well. It required a lower dosage (0.19% bwoc) than the respective lignite-based graft copolymer. This observation suggests that the dispersing ability of the graft copolymer mainly results from the grafted ATBS-*co*-acrylic acid pendant groups. Additional tests using pure lignite confirmed this finding because no dispersing effect was observed for individual lignite. The increase of dosages at higher acrylic acid contents can be attributed to the shorter side chains present in such graft copolymers, as evidenced by the lower molecular weights (see Table 3).

Finally, performance of the graft copolymers was compared with that of an industrial grade BNS reference sample. The measurements revealed that the graft copolymers prepared at an ATBS:acrylic acid molar ratio of 1:0.15–0.75 are more effective dispersants than the commercial BNS reference sample (dosage: 0.30% bwoc).

Table 3
Molar masses, polydispersity index (PDI) and polymer radii of the synthesized polymers and of BNS as reference superplasticizer sample.

Polymer (molar ratio)	M_w [g/mol]	M_n [g/mol]	PDI	$R_{g(z)}$ [nm]	$R_{h(z)}$ [nm]
Lignite{ATBS-*co*-AA} (1:0.15)	288,100	178,700	1.6	31.8	17.0
Lignite{ATBS-*co*-AA} (1:0.39)	375,600	147,800	2.5	49.8	22.5
Lignite{ATBS-*co*-AA} (1:0.75)	208,100	91,480	2.3	35.1	17.8
Lignite{ATBS-*co*-AA} (1:1.00)	268,900	95,810	2.8	44.2	20.3
Lignite{ATBS-*co*-AA} (1:1.50)	215,000	90,750	2.4	36.0	18.5
ATBS-*co*-AA (1:0.15)	183,300	93,460	2.0	23.9	14.5
BNS	140,000[a]	–	–	–	–

[a] Batch measurement.

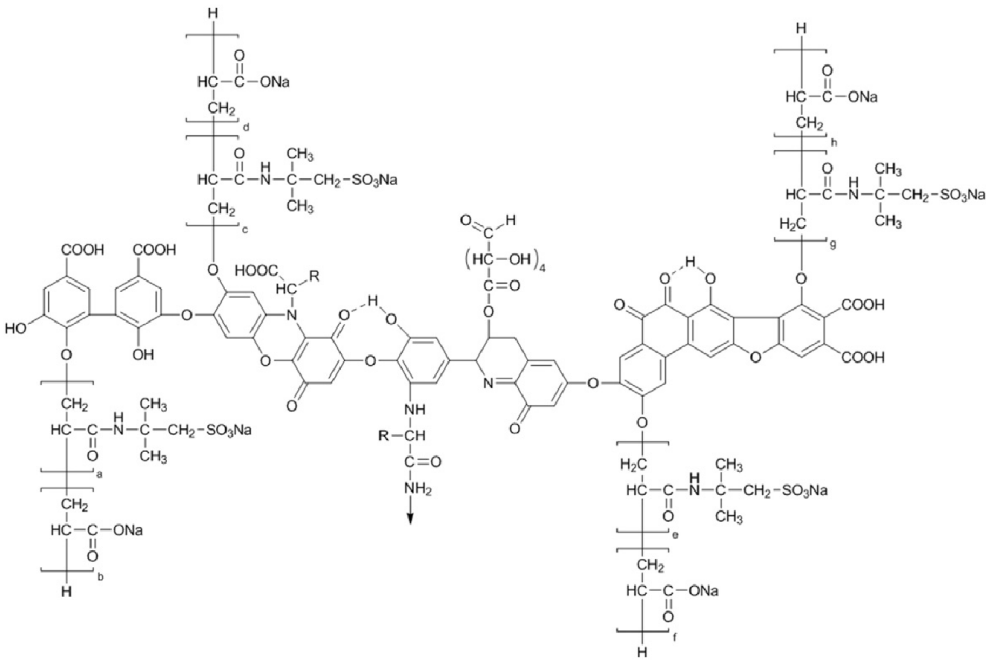

Fig. 4. Proposed chemical structure of the lignite{ATBS-*co*-AA} graft copolymer.

Note that in all further experiments, the lignite{ATBS-*co*-AA} graft copolymer prepared at an ATBS:acrylic acid molar ratio of 1:0.15 was used because of its superior dispersing performance.

3.3. Slump retention behavior

Next, the time-dependent slump flow behavior was investigated. For this purpose, the slump flow of the best performing lignite{ATBS-*co*-AA} graft copolymer, of the ATBS-acrylic acid copolymer and BNS was looked at over a period of 1 h. The polymer dosages applied were the same as in the 'mini slump' tests before (see Section 3.2). The water-to-cement ratio was 0.455. The results are shown in Fig. 6.

As can be seen there, the lignite{ATBS-*co*-AA} graft copolymer (molar ratio ATBS:AA = 1:0.15) is well able to hold its slump flow constant over 1 h. This behavior instigates that the lignite{ATBS-*co*-AA} graft copolymer does not quantitatively adsorb on the surface of cement after it has been added to the paste. Apparently, a certain portion remains in the cement pore solution and can later adsorb on newly formed cement hydrates, thus leading to continued dispersion over 1 h. Contrary to this, within the 60 min, the slump flow of the ATBS-acrylic acid copolymer decreases rapidly from 26 cm to 22 cm, similar to that of a commercial BNS polycondensate. According to these results, a significant difference exists between the lignite-based graft product and the ATBS-acrylic acid copolymer.

To investigate the reason behind the strong dispersing ability of the graft copolymer, its adsorption on cement was determined. As expected, it was found that from the total dosage added, only ~45% had anchored on cement while a major quantity remained in solution and

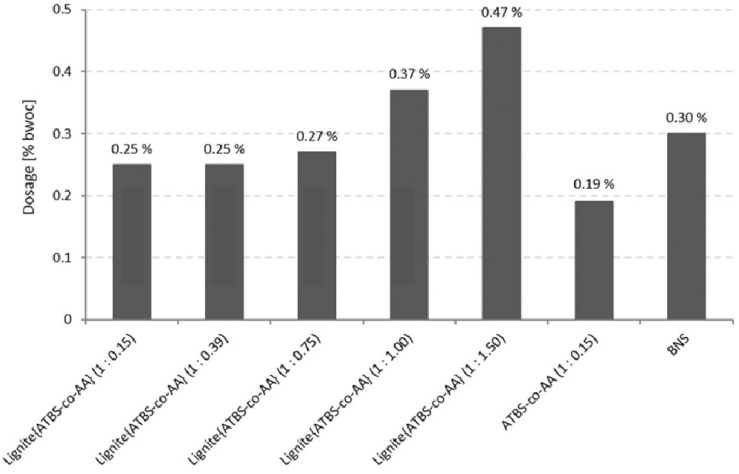

Fig. 5. Dosages of the lignite{ATBS-*co*-AA} graft copolymers required for a slump flow of 26 ± 0.5 cm (w/c ratio = 0.455).

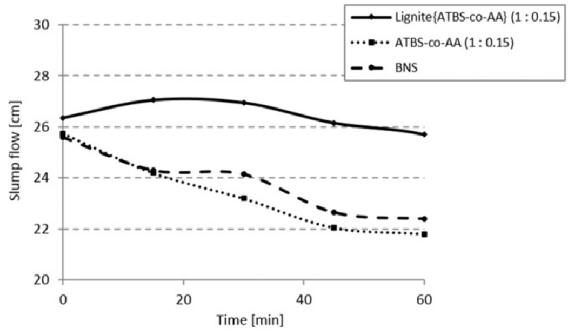

Fig. 6. Time-dependent evolution of the slump flow of a cement paste (w/c = 0.455) holding 0.25% bwoc of a lignite{ATBS-*co*-AA} graft copolymer (molar ratio ATBS:AA = 1:0.15), 0.19% bwoc of ATBS-*co*-AA and 0.3% bwoc of BNS, respectively.

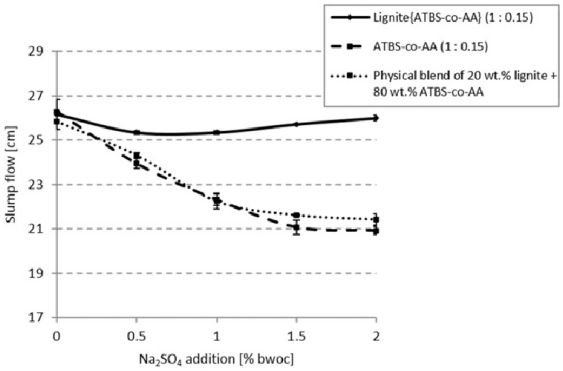

Fig. 7. Effect of different Na_2SO_4 additions on the slump flow of cement pastes (w/c = 0.455) containing different polymer samples.

could adsorb later. Contrary to this, for the ATBS-acrylic acid copolymer and BNS, about ~73% and 88%, respectively, of dosage added were adsorbed immediately, thus leaving not much polymer in solution which could provide a slump retaining effect. The results strongly suggest that the graft copolymer does not constitute a mere mixture of lignite and the ATBS-acrylic acid copolymer and that indeed a specific chemical reaction leading to a new structure has taken place. Furthermore, the slump retention behavior of the other lignite containing polymers was tested as well. Their slump retaining capacity was slightly less than for the lignite graft copolymer possessing an ATBS:AA molar ratio of 1:0.15, thus suggesting that this composition presented an optimum.

3.4. Sulfate tolerance of the graft copolymer

It is well established that sulfate ions can perturb the dispersing effect of superplasticizers. This phenomenon known as "sulfate effect" is especially observed for polycarboxylate superplasticizers. In scientific literature, two different mechanisms were presented: According to *Yamada* et al., polycarboxylates coil and shrink at high sulfate concentrations, thus making their adsorption on cement more difficult [28]. However, more recent results indicate that competitive adsorption between polycarboxylates and sulfate ions underlies the "sulfate effect" and that the detailed polymer structure (i.e., grafting density, side chain length) as well as the kind of anionic anchor group are more important for the sulfate sensitivity of PCEs [29–31].

To assess whether the lignite{ATBS-*co*-AA} graft copolymer is also negatively affected by sulfate ions, 'mini slump' tests were performed at increased Na_2SO_4 additions to the paste (up to 2.0 wt.% bwoc). The graft copolymer was applied at a dosage of 0.25% bwoc. The results are illustrated in Fig. 7.

Generally, the dispersion effectiveness of the lignite{ATBS-*co*-AA} graft copolymer is not much influenced by sulfate ions whereas the non-grafted ATBS-acrylic acid copolymer experiences a strong reduction in performance by sulfate. To probe whether lignite perhaps is responsible for the sulfate tolerance, a physical mixture of 80 wt.% of the ATBS-acrylic acid copolymer (molar ratio ATBS:AA = 1:0.15) and 20 wt.% of lignite (material composition of the graft copolymer) was also tested. For this physical blend, the slump flow decreased in the manner as for the lignite-free copolymer. This different behavior provides further evidence that a grafting reaction onto lignite has occurred.

3.5. Adsorbed layer thickness of lignite graft copolymer

To further verify successful grafting of ATBS and acrylic acid onto lignite, the adsorbed layer thicknesses of the lignite{ATBS-*co*-AA} graft copolymer (molar ratio ATBS:AA = 1:0.15), of the ATBS-acrylic acid copolymer and the lignite backbone were compared. For the measurements, cationic, monodisperse and spherical polystyrene nanoparticles were used as adsorbent. This method enables the facile determination of the adsorbed layer thickness of functional polymers under highly alkaline pH conditions such as prevailing in cement pore solution [25]. Measurements were performed at increasing polymer concentrations until the point of saturated adsorption was reached.

The results are illustrated in Fig. 8. As can be seen there, the lignite{ATBS-*co*-AA} graft copolymer exhibits a saturated adsorbed layer thickness of ~6.5 nm, while the ATBS-acrylic acid copolymer shows a layer thickness of 1.6 nm only. Non-grafted lignite produces an even smaller layer thickness of 1.3 nm. Therefore, it can be assumed that grafting of ATBS and acrylic acid onto lignite has indeed occurred.

3.6. Effect on cement hydration

To investigate the influence of the lignite{ATBS-*co*-AA} graft copolymer on cement hydration, isothermal heat flow calorimetry measurements were carried out. For this purpose, cement pastes containing 0.25% bwoc of the lignite{ATBS-co-AA} graft copolymer were prepared (w/c = 0.455). Heat evolution was measured over a total period of 50 h, as illustrated in Fig. 9.

Generally, the lignite{ATBS-*co*-AA} graft copolymer causes only minor retardation of cement. Additional experiments involving the ATBS-acrylic acid copolymer revealed that the copolymer retards slightly more than the graft copolymer. Moreover, retardation caused by the lignite{ATBS-*co*-AA} graft copolymer is slightly higher than for BNS. It is noticeable that for all superplasticizers tested the shoulder on the main peak of cement hydration occurs earlier than in neat cement

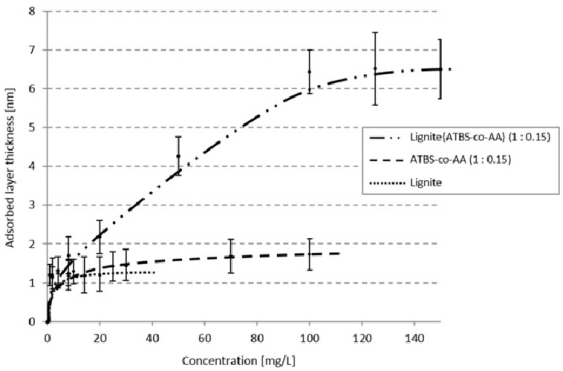

Fig. 8. Concentration-dependent adsorbed layer thicknesses of the lignite{ATBS-*co*-AA} graft copolymer, ATBS-*co*-AA (1:0.15) and lignite.

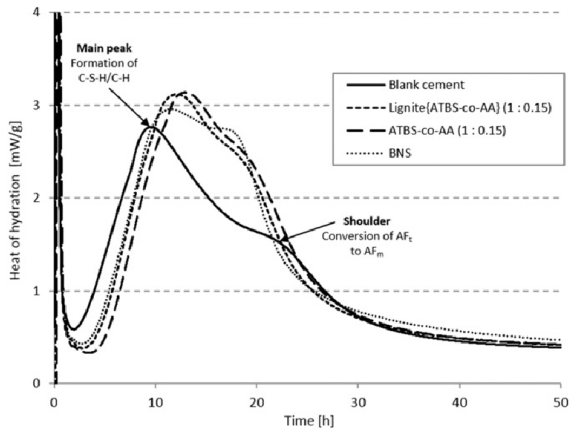

Fig. 9. Development of the heat of hydration of cement slurries (w/c = 0.455) holding 0.25% bwoc of lignite{ATBS-*co*-AA} graft copolymer (1:0.15), ATBS-*co*-AA (1:0.15) and of BNS, respectively.

(see Fig. 9). This reaction is usually attributed to the conversion of ettringite to mono sulfoaluminate. However, this process is currently discussed controversially in the scientific literature [32]. Additionally, the total heat released during the first 20 h of hydration is higher for the samples that contain the superplasticizer than for the neat cement paste. This effect can be explained by the disagglomeration of the cement particles, which is achieved by the dispersants. As a result, more of the clinker surface becomes exposed to water and can hydrate.

4. Conclusions

A new type of superplasticizer was synthesized by grafting the monomers ATBS and acrylic acid onto lignite, an extract from ordinary brown coal. The results signify that graft copolymerization constitutes a general method suitable for the targeted modification of lignite. As an example, an ATBS-*co*-acrylic acid grafted lignite copolymer presents an effective dispersant with good slump flow retention and high sulfate tolerance in cement. Successful grafting of the monomers onto the lignite backbone was evidenced by several independent methods, including measurement of the adsorbed layer thickness. It can be concluded that lignite represents an interesting, abundant and inexpensive starting material for the synthesis of novel superplasticizers and other admixtures, among other because of its chemical diversity.

Furthermore, the use of lignite presents an alternative to the more precious and scarce resources of petroleum or natural gas which currently constitute the main raw materials for the production of concrete admixtures. The work here should be considered as a first approach to synthesize such low cost admixtures. Future research should concentrate on substituting the relatively expensive ATBS with more versatile monomers.

Acknowledgments

The authors would like to thank Lubrizol for providing the ATBS monomer and American Colloid Company (Hoffman Estates, Illinois) for the supply of the superlignite.

References

[1] V. Smil, Making the modern world—materials and dematerialization, first ed. John Wiley & Sons, 2014.
[2] P.C. Aïtcin, Cements of yesterday and today—concrete of tomorrow, Cem. Concr. Res. 30 (2000) 1349–1359.
[3] J.T. Sentowski, Concrete Materials: Properties, Performance and Applications, Material Science and Technologies, 2009.
[4] V.S. Ramachandran, V.M. Malhotra, C. Jolicoeur, N. Spiratos, Superplasticizers: Properties and Applications in Concrete, CANMET, Ottawa, Canada, 1998.
[5] N. Spiratos, M. Page, N.P. Mailvaganam, V.M. Malhotra, C. Jolicoeur, Superplasticizers for concrete: fundamentals, technology and practice, Supplementary Cementing Materials for Sustainable Development, Ottawa, Canada, 2003.
[6] J. Plank, Current developments on concrete admixtures in Europe, Proceedings of the Symposium Chemical Admixtures in Concrete, Dalian, China, 2004, pp. 13–27.
[7] J. Plank, PCE Superplasticizers—Chemistry, Applications and Perspectives, ZKG International 67, Drymix Special,1 (2014) 48–59.
[8] J. Plank, Applications of biopolymers in construction engineering, Biopolymers 10 (2003) 29–95.
[9] Q. Song, P. Zheng, Studies on the graft copolymerization of acrylonitrile onto humic acid, Acta Polym. Sin. 1 (5) (1987) 388–392.
[10] D.F. Zhang, B.Z. Ju, S.F. Zhang, L. He, J.Z. Yang, The study on the dispersing mechanism of starch sulfonates as a water-reducing agent for cement, Carbohydr. Polym. 70 (4) (2007) 363–368.
[11] S. Lv, R. Gao, Q. Cao, D. Li, J. Duan, Preparation and characterization of polycarboxymethyl-β-cyclodextrin superplasticizer, Cem. Concr. Res. 42 (2012) 1356–1361.
[12] L. Thomas, Coal Geology, 2nd ed. John Wiley & Sons, 2012.
[13] M. Teichmüller, The genesis of coal from the viewpoint of coal petrology, Int. J. Coal Geol. 12 (1–4) (1989) 1–87.
[14] P.G. Hatcher, D.J. Clifford, The organic geochemistry of coal: from plant materials to coal, Org. Geochem. 27 (5/6) (1997) 251–274.
[15] E.M. Pena-Mendez, J. Havel, J. Patocka, Humic substances—compound of still unknown structure: applications in agriculture, industry, environment, and biomedicine, J. Appl. Biomed. 3 (2005) 13–24.
[16] L.S.K. Pang, A.M. Vassallo, M.A. Wilson, Chemistry of alkali extraction of brown coals—I. Kinetics, characterization and implications to coalification, Org. Geochem. 16 (1990) 853–864.
[17] D. Garcia, J. Cegarra, M. Abad, F. Fornes, Effects of the extractants on the characteristics of humic fertilizer obtained from lignite, Bioresour. Technol. 43 (1993) 221–225.
[18] R.L. Mikkelsen, Humic materials for agriculture, Better Crops 89 (3) (2005) 6–10.
[19] R. Caenn, G.V. Chillingar, Drilling fluids: state of the art, J. Pet. Sci. Eng. 14 (1996) 221–230.
[20] M. Ilg, J. Plank, Synthesis of a Novel Superplasticizer Prepared from Brown Coal, 11th International Conference on Superplasticizers and Other Chemical Admixtures in Concrete (CANMET/ACI) July 12–15 2015, pp. 63–76 (Ottawa/Canada, Proceedings).
[21] J. Peuravuori, A.J. Simpson, B. Lam, P. Zbankova, K. Pihlaja, Structural features of lignite humic acid in light of NMR and thermal degradation experiments, J. Mol. Struct. 826 (2007) 131–142.
[22] P.R. Gupta, D.A.I. Goring, Physicochemical studies of alkali lignins III: size and shape of the macromolecule, Can. J. Chem. 38 (2) (1960) 270–279.
[23] M.B. Huglin, in: J. Brandrup, E.H. Immergut (Eds.), Polymer Handbook, 3rd ed.Wiley, New York, 1989.
[24] DIN EN 1015–3:2007–05, Methods of Test for Mortar for Masonry—Part 3: Determination of Consistence of Fresh Mortar, DIN, Berlin/Germany, 2007.
[25] C. Tiemeyer, A. Lange, J. Plank, Determination of the adsorbed layer thickness of functional anionic polymers utilizing chemically modified polystyrene nanoparticles, Colloids Surf. A 456 (2014) 139–145.
[26] F.J. Stevenson, Humus Chemistry: Genesis, Composition, Reactions, 2nd ed., John Wiley & Sons, 1994.
[27] W. Burchard, Static and dynamic light scattering from branched polymers and biopolymers, Adv. Polym. Sci. 48 (1983) 1–124.
[28] K. Yamada, S. Ogawa, S. Hanehara, Controlling of the adsorption and dispersing force of polycarboxylate-type superplasticizer by sulfate ion concentration in aqueous phase, Cem. Concr. Res. 31 (2001) 375–383.
[29] F. Dalas, A. Nonat, S. Pourchet, M. Mosquet, D. Rinaldi, S. Sabio, Tailoring the anionic function and the side chains of comb-like superplasticizers to improve their adsorption, Cem. Concr. Res. 67 (2015) 21–30.
[30] S. Pourchet, S. Liautaud, D. Rinaldi, I. Pochard, Effect of the repartition of the PEG side chains on the adsorption and dispersion behaviors of PCP in presence of sulfate, Cem. Concr. Res. 42 (2012) 431–439.
[31] J. Zimmermann, C. Hampel, C. Kurz, L. Frunz, R.J. Flatt, Effect of polymer structure on the sulfate-polycarboxylate competition, Ninth ACI International Conference on Superplasticizers and Other Chemical Admixture in Concrete, SP-262-12 2009, pp. 165–176 (Sevilla/Spain).
[32] J.W. Bullard, H.M. Jennings, R.A. Livingston, A. Nonat, G.W. Scherer, J.S. Schweitzer, K.L. Scrivener, J.J. Thomas, Mechanisms of cement hydration, Cem. Concr. Res. 41 (2011) 1208–1223.

6. Zusammenfassung und Ausblick

Im Rahmen dieser Arbeit wurden vier verschiedene Themenblöcke behandelt. Der erste Teil beschäftigte sich mit der Frage, wie nicht-adsorbierte Verbindungen zur Zementdispergierung beitragen. Gemäß früheren Studien von *Sakai* et al. können in der Porenlösung vorhandene nicht-adsorbierte PCEs in bestimmten Fällen ebenfalls für einen stabilisierenden Effekt sorgen. Diese Beobachtungen wurden in der Arbeit weiter vertieft, um ein besseres Verständnis zur Rolle und Wirkungsweise derartiger nicht-adsorbierter Komponenten zu erhalten. Durch Kombination strukturell verschiedener PCE-Fließmittel mit einer großen Bandbreite nicht-ionischer Moleküle und Polymere auf Glykol- sowie Diolbasis wurde festgestellt, dass auch nicht-ionische Verbindungen zur Stabilisierung beitragen können und sowohl Fließmaß als auch Fließgeschwindigkeit von Zementleimen erhöhen. Die wichtigsten Beobachtungen zu diesem Thema waren wie folgt:

- Nicht-ionische Verbindungen fungieren als Co-Dispergiermittel, d.h. sie sind nur in Gegenwart eines PCE-Fließmittels wirksam
- Ihre dispergierende Wirkung ist besonders stark bei niedrigen w/z-Werten < 0,26
- PCE-Fließmittel mit hoher anionischer Ladung und langen Seitenketten profitieren mehr von der Zugabe nicht-ionischer Additive
- Nicht-ionische Polymere erhöhen die Viskosität der Porenlösung, wodurch die Fließfähigkeit nachteilig beeinflusst wird
- Co-Dispergiermittel mit Molmassen ≤ 300 Da sind wirkungsvoller als Polymere (z.B. PEGs mit Molmassen ≥ 1000 Da)
- Co-Dispergiermittel mit einem höheren Anteil an unpolaren Gruppen ergeben eine stärkere Verflüssigung
  → Oberflächenspannung der Porenlösung wird stärker reduziert und dadurch das Benetzungsverhalten des Zements verbessert
- Der Anteil nicht-adsorbierter PCEs entscheidet, wie stark der stabilisierende Effekt der Co-Dispergiermittel ist
  → PCEs, die stark adsorbieren und von denen eine nur geringe Restmenge in der Porenlösung verbleibt, profitieren stärker von der Zugabe nicht-ionischer Additive

Durch Adsorptionsmessungen wurde aufgeklärt, dass die Co-Dispergiermittel in der Porenlösung vorliegen und dort keinen Einfluss auf die Adsorption des PCEs haben. Vielmehr agieren sie als Abstandshalter, die neben der elektrosterischen Stabilisierung durch die PCEs zusätzlich einen Beitrag zur Dispergierung leisten. Dieser Effekt tritt nur bei niedrigen w/z-Werten auf, da hier der Abstand zwischen den Zementpartikeln äußerst gering ist. Nähern sich die Zementteilchen zu nahe an, wird ein Teil des Co-Dispergiermittels aus dem Porenraum zwischen den Partikeln verdrängt, wodurch ein Konzentrationsgradient entsteht. Dieser Zustand ist unter entropischen Gesichtspunkten unvorteilhaft und wird deshalb durch das Auftreten zusätzlicher stabilisierender Kräfte (sog. Verarmungsstabilisierung) verhindert. Diese Art der Stabilisierung erfordert eine hohe Konzentration des Co-Dispergiermittels, die nur bei niedrigen w/z-Werten erreicht werden kann, da hier das Volumen der frei zur Verfügung stehenden Porenlösung äußerst begrenzt ist. Ferner deuten die Ergebnisse darauf hin, dass auch nicht-adsorbierte PCEs eine solche Stabilisierung hervorrufen können, was erklärt, warum die Co-Dispergiermittel insbesondere bei PCE-Fließmitteln wirksam sind, von denen nur eine geringe Menge in der Porenlösung verbleibt.

Im zweiten Teil der Arbeit wurde untersucht, wie sich die Co-Dispergiermittel auf die Rheologie von Mörtel und Betonen auswirken. Im Mörtel konnten die nicht-ionischen Additive die Fließgrenze und plastische Viskosität reduzieren, während sie im Beton nur die plastische Viskosität verringerten. Der Stabilisierungseffekt durch die Co-Dispergiermittel scheint im Beton nicht ausreichend genug zu sein, um dort die Fließgrenze zu senken. Es muss berücksichtigt werden, dass im Beton im Vergleich zu Zementpasten und Mörteln gröbere Gesteinskörnungen vorhanden sind und daraus eine viele höhere Fließgrenze resultiert. Durch die Reduzierung der plastischen Viskosität wurde jedoch das zähe und kriechende Fließverhalten, das insbesondere bei den niedrigen w/z-Werten in Erscheinung trat, erheblich verbessert. Kürzere Trichterauslaufzeiten und höhere Fließgeschwindigkeiten wurden erhalten. Die Erniedrigung der plastischen Viskosität wurde darauf zurückgeführt, dass die Co-Dispergiermittel das frei verfügbare Volumen der Porenlösung erhöhen. Dadurch wird die Dicke des flüssigen Films um die Feststoffteilchen erhöht, wodurch die Reibung zwischen den Partikeln während des Fließens reduziert wird. Die nicht-ionischen Additive weisen bessere Gleiteigenschaften als Wasser auf, das nicht in der Lage war in

Dosierungen, die denen der Co-Dispergiermittel entsprechen, die plastische Viskosität zu reduzieren.

Diese Resultate verdeutlichen, dass mit dem Konzept der Co-Dispergiermittel die rheologischen Eigenschaften von zementären Systemen erheblich verbessert werden können, ohne einen negativen Einfluss auf das Abbindeverhalten oder die Festigkeitsentwicklung zu haben. Dies ermöglicht es Betonformulierungen, die sich durch ein stark kohäsives (klebriges) Verhalten auszeichnen und nur schwer zu verarbeiten sind, zu optimieren.

Als Nächstes sollten die Co-Dispergiermittel in ultrahochfesten Betonen getestet werden. Hier könnte das Konzept ebenfalls sehr interessant sein, da im UHPC sehr niedrige w/z-Werte < 0,2 zum Einsatz kommen und Mikrosilika zur Festigkeitssteigerung zugegeben wird, woraus ein hoher Feststoffanteil und ein klebriges Verhalten resultieren. Erste Voruntersuchungen in UHPC-Pasten deuten darauf hin, dass das Konzept auch hier zu Vorteilen führen kann. Darüber hinaus sollten die Co-Dispergiermittel in alternativen Bindemittelsystemen wie calcinierten Tonen oder Portlandkompositzementen getestet werden, die aufgrund ihrer geringeren CO_2-Bilanz zunehmend von Interesse sind und ebenfalls Konzepte für eine effiziente Verflüssigung benötigen.

Im dritten Teil der Arbeit wurde ein neuartiges hyperverzweigtes Fließmittel synthetisiert. Dieses Fließmittel enthält als charakteristisches Strukturmerkmal ein hyperverzweigtes Polyglycerol, das im Gegensatz zu vielen ähnlichen verzweigten Strukturen in einem Syntheseschritt darstellbar ist. Das hyperverzweigte Polyglycerol wurde über eine anionische Ringöffnungspolymerisation von Glycidol erhalten, bei der als Initiator ein bisglycidoliertes Polyetheramin verwendet wurde. Einige terminale OH-Gruppen des Polyglycerols wurden carboxymethyliert, damit das Polymer auf der Zementkornoberfläche adsorbieren kann. Das neue Fließmittel setzt sich so aus einem carboxymethylierten Polyglycerolgerüst und einer linearen Polyetheraminkette am Hauptverzweigungspunkt zusammen, die für einen zusätzlichen sterischen Effekt sorgen soll.

Wie bei herkömmlichen PCEs ist auch bei diesem Fließmittel die Strukturvariabilität gegeben. So lässt sich die Seitenkettenlänge des Polyetheramins sowie die Größe des

Polyglycerols variieren, auch können verschiedene Ankergruppen über eine Funktionalisierung der OH-Gruppen eingebracht werden.

Durch die Anwendung der *„Slow Monomer Addition“*-Strategie, bei der Glycidol langsam zugegeben wurde, verlief die Polymerisation unter kontrollierten Bedingungen, sodass ein Polymer mit einer engen Molmassenverteilung und einem niedrigen PDI erhalten wurde. Messungen des hydrodynamischen Radius ergaben, dass das hyperverzweigte Fließmittel trotz seines geringeren Molekulargewichts eine ähnliche Größe wie das kammförmige Referenz-PCE (45MPEG2) besitzt. Dies suggerierte, dass das hyperverzweigte Fließmittel eine gestreckte Lösungskonformation wegen der globulären Struktur des hyperverzweigten Polyglycerols einnimmt, während das MPEG-PCE vorwiegend als Polymerknäuel vorliegt. Durch Vergleich der Dispergier-eigenschaften des Fließmittels mit anderen synthetisierten Polymerstrukturen konnte festgestellt werden, dass sowohl die Polyetheraminseitenkette als auch das hyper-verzweigte Polyglycerolgerüst einen Beitrag zur sterischen Stabilisierung leisten. Aufgrund der terminalen Carboxylatgruppen adsorbiert das Fließmittel hauptsächlich in einem *„Tail“*-Adsorptionsmodus, bei dem die Seitenkette und das Polyglycerolgerüst nahezu senkrecht in die Porenlösung zeigen. Diese Adsorptionsweise führt neben einer höheren Robustheit des Polymers gegenüber Sulfationen auch dazu, dass im Vergleich zu einem kammförmigen PCE eine höhere Dosierung für eine effektive Oberflächenbelegung benötigt wird.

Ein Vorteil des hyperverzweigten Fließmittels ist, dass es die Fließfähigkeit durch die verzögernde Wirkung über einen längeren Zeitraum aufrechterhalten kann, weshalb es beispielsweise im Transportbeton oder bei Betonagen in heißen Ländern verwendet werden könnte.

Aufbauend auf den Untersuchungen dieser Arbeit wäre ein interessanter Ansatz, ein hyperverzweigtes Polyglycerol als Seitenkette in ein kammförmiges PCE einzubringen und zu untersuchen, wie sich für ein solches Hybridpolymer die Eigenschaften verändern. Außerdem könnte auf Basis des hyperverzweigten Fließmittels ein hantelförmiges Polymer dargestellt werden, wenn anstelle eines methoxy-terminierten Polyetheramins ein Diamin verwendet wird, bei dem an beiden Enden ein verzweigtes Polyglycerolgerüst vorliegen würde.

Der letzte Teil der Arbeit beschäftigte sich mit der Synthese und Charakterisierung eines neuen Fließmittels auf Lignit-Basis, welches durch die chemische Modifizierung von Humin- und Fulvinsäuren dargestellt wurde. Auf die alkali-löslichen Komponenten des Lignits wurden Seitenketten aus ATBS und Acrylsäure Monomeren über eine radikalische Polymerisation aufgepfropft, wodurch ein kammförmiges Polymer mit einer Huminsäure-Hauptkette und mehreren ATBS-*co*-Acrylsäure-Polymeren als Seitenketten erhalten wurde. Da sich die Humin- und Fulvinsäuren aus mehreren kondensierten aromatischen Strukturbausteinen zusammensetzen, weist das neue Fließmittel eine starre Hauptkette auf, wohingegen die Seitenketten über eine hohe konformationelle Flexibilität verfügen. Das Fließmittel konnte sowohl ausgehend von einer kommerziellen Lignit-Probe mit einem hohen Huminsäure-Anteil als auch aus den Na-Salzen von Braunkohle synthetisiert werden, die zuvor aus Braunkohlestücken extrahiert wurden. Die besten Eigenschaften wurden für ein ATBS-Acrylsäure-Verhältnis von 1 : 0,15 gefunden, da hier die Fließmittel die geringste Polydispersität, die größten Polymerradien und die längsten aufgepfropften Seitenketten aufwiesen. Durch Vergleich der molekularen Eigenschaften des Lignit-Pfropfcopolymers und des ATBS-*co*-Acrylsäure-Referenzpolymers sowie über Messungen der adsorbierten Schichtdicke konnte auf eine erfolgreiche Pfropfung der Monomere geschlossen werden.

Weitere Untersuchungen ergaben, dass die Lignit-Fließmittel nur minimal verzögernd sind und die Dispergierung über einen elektrostatischen Mechanismus erzielen. Dabei adsorbieren die Fließmittel über die Sulfonat- und Carboxylatgruppen der Seitenketten auf der Zementkornoberfläche, wodurch ein stark negatives Zeta-Potential resultiert, vergleichbar mit den Werten für das ATBS-*co*-Acrylsäure-Polymer und BNS. Da die kammförmige Polymerstruktur sowie die gestreckte Lösungskonformation zu einer höheren Schichtdicke führen, wirkt das Polymer zu einem gewissen Anteil auch über einen sterischen Effekt. Aufgrund des starren Huminsäure-Rückgrats kann sich das Fließmittel allerdings nicht so gut auf der Oberfläche ausrichten, wodurch die Adsorption nur über einzelne Seitenketten erfolgt. Daher benötigt das Lignit-Fließmittel höhere Dosierungen als das ATBS-*co*-Acrylsäure-Polymer, das durch die hohe konformationelle Flexibilität mehrere Oberflächenbereiche belegen kann. Durch die kammförmige Struktur sind die Lignit-Polymere dennoch wirkungsvoller als ein BNS Polykondensat-Fließmittel, das aus einer linearen Hauptkette besteht und nur eine geringe adsorbierte Schichtdicke erzielt.

Abschließend kann gefolgert werden, dass durch eine starre Hauptkette die Adsorptionseigenschaften wesentlich beeinflusst werden und damit einhergehend auch Merkmale wie die Dosiereffizienz oder die Robustheit gegenüber Sulfationen. Im Gegensatz zum ATBS-*co*-Acrylsäure-Polymer nahm beispielsweise die Dispergierwirkung der Lignit-basierten Fließmittel nicht in der Gegenwart von Sulfationen ab. Eine gestreckte Polymerkonformation und eine hohe adsorbierte Schichtdicke scheinen daher für eine hohe Sulfatrobustheit vorteilhaft zu sein.

Als Nächstes sollte untersucht werden, wie sich die Eigenschaften des Fließmittels verändern würden, wenn ein kurzkettiges PEG-haltiges Makromonomer in die Seitenkette des Lignit-Polymers eingebaut wird. Außerdem wäre es interessant, weniger reaktive Monomere wie Maleinsäureanhydrid, Itaconsäure oder Methacrylsäure anstelle von Acrylsäure zu verwenden und zu untersuchen, ob diese Monomere bei höheren Mengen einfacher auf die Huminsäure aufgepfropft werden können, ohne dass unerwünschte Nebenreaktionen stattfinden.

7. Summary and outlook

Within the scope of the thesis, four different topics were addressed. The first part covers the question, how non-adsorbed compounds can contribute to cement dispersion. According to a previous study by *Sakai* et al., the portion of non-adsorbed PCEs remaining in the interstitial pore solution can also provoke a stabilizing effect under certain conditions. These findings were looked at in more depth within this work to gain a better understanding of the function of non-adsorbed constituents in cement dispersion. By combining structurally different PCEs with a large variety of non-ionic molecules and polymers based on glycol and diol chemistry it was established that also non-ionic compounds can impart a stabilization and improve cement paste fluidity. The key findings from this topic were as follows:

- Non-ionic additives can act as auxiliary dispersants, becoming only effective in presence of a PCE superplasticizer
- Their dispersing performance is particularly powerful at low w/c ratios < 0.26
- PCE polymers possessing a high anionic charge and long side chain length benefit more from the addition of the non-ionic additives
- Non-ionic polymers increase the viscosity of the interstitial pore solution, thus negatively affecting the cement paste fluidity
- Auxiliary dispersants with molar masses ≤ 300 Da are more effective than polymers (e.g. PEGs with molecular weight ≥ 1000 Da)
- Auxiliary dispersants with a higher content of non-polar groups induce a higher fluidity
  → Surface tension of the pore solution is strongly decreased, hence improving the wettability of cement
- The residual concentration of non-adsorbed PCEs in the pore solution impacts how strong the effect of the auxiliary dispersants is
  → PCEs with a lower residual polymer concentration benefit more from the addition of the co-dispersants

By means of adsorption measurements via TOC it was found that the non-ionic co-dispersants remain freely in the pore solution and do not have any influence on the adsorbed amounts of the PCEs. They act as spacer molecules which contribute, besides to the electrosteric stabilization by the PCEs, also to dispersion. This effect only occurs at

low w/c ratios because here, the distance between the individual cement grains becomes quite narrow. If the cement particles are approaching each other too close, a part of the co-dispersant is squeezed out from the space between the particles, thus causing a concentration gradient. From an entropic point of view, this condition is highly disadvantageous and therefore prevented by the implementation of an additional stabilizing force (depletion stabilization). However, this stabilization requires a relatively high concentration of the co-dispersant which is the case only at low w/c ratios since here the volume of the freely available amount of pore solution is rather limited. Moreover, the findings suggest that non-adsorbed PCEs can also provoke such a kind of stabilization which explains why non-ionic additives work particularly well in presence of PCEs with a lower residual concentration in the pore solution.

The second part of the work deals with investigations on the effect of the co-dispersants on the rheology of mortar and concrete. The auxiliary dispersants can reduce the yield stress and plastic viscosity of mortars, while in concrete they only decrease the plastic viscosity. Obviously, the stabilizing effect of the non-ionic additives is too insufficient to reduce the yield point of concrete. It must be considered that compared to cement pastes and mortar, concrete contains coarse aggregates and therefore exhibits a much higher yield point value. However, by lowering the plastic viscosity, the honey-like and creeping flow behavior that particularly occurs at low w/c ratios is improved. Shorter empty times from the V-funnel and a higher speed of flow were obtained. The decrease of the plastic viscosity by the co-dispersants was explained by an increase of the amount of the freely available pore solution. In this way, the thickness of the liquid film around the solid particles is increased, thus leading to a strong reduction of the friction between the particles during flow. The co-dispersants provide better lubrication as compared to water that was not capable of lowering the plastic viscosity when being applied in the same amount as the non-ionic additives.

These findings signify that the concept of the co-dispersants can improve the rheological properties of cementitious systems without negatively affecting the setting behavior or the strength development. This allows to optimize challenging concrete formulations with a tenacious consistency and difficult workability. As one of the next steps, the performance of the auxiliary dispersants should also be investigated in ultra-high performance concrete. There, the concept can be of great interest as well, since UHPC is prepared at low w/c ratios < 0.2 and contains micro silica to enhance the compressive

strength causing a high solids content and sticky consistency. First investigations in UHPC pastes indicate that the co-dispersants might also be advantageous there. Additionally, the non-ionic additives should be tested in alternative binder systems like calcined clays or Portland-limestone cements which are more challenging with regard to achieving high fluidity. It is expected that these kinds of binder systems are going to become more important in the upcoming years due to their lower CO_2 footprint.

The third part of the thesis is about the synthesis of a new hyperbranched superplasticizer. The polymer exhibits a hyperbranched polyglycerol as a characteristic structural feature that unlike to other branched structures can be synthesized in only one synthesis step. The hyperbranched polyglycerol was obtained by anionic ring opening polymerization of glycidol using a bis-glycidolized polyether amine as initiator. Some of the terminal OH groups of the polyglycerol scaffold were carboxymethylated to facilitate the adsorption of the polymer on the cement surface. Thus, the new superplasticizer comprises a carboxymethylated polyglycerol and one linear polyether amine side chain at the branching point to induce an additional steric effect.

Like for conventional comb shaped PCEs also the new superplasticizer allows high variability of the structure. Referring to this, the side chain length of the polyether amine as well as the size of the polyglycerol can be varied, and different anchor groups can also be incorporated through the functionalization of the OH groups. By using the *"slow monomer addition approach"* the polymerization proceeded under controlled conditions, yielding a polymer with a narrow molecular weight distribution and a low PDI. Measurements of the hydrodynamic radii via dynamic light scattering revealed that the hyperbranched polymer exhibits a similar value as the comb shaped reference PCE (45MPEG2), despite of its lower molar mass. This indicates that the hyperbranched superplasticizer possesses a rather stiff conformation due to the globular structure of the polyglycerol whereas the MPEG PCE exhibits a more coiled conformation. By comparing the dispersing properties of the hyperbranched superplasticizer with those of other synthesized polymers it was established that the polyether amine as well as the hyperbranched polyglycerol contribute to the steric stabilization. Due to the terminal carboxylate groups, the polymer adsorbs in a tail-like adsorption mode in which the side chain and the polyglycerol scaffold point almost vertically into the pore solution. This adsorption mode entails a higher robustness of the polymer towards sulfate ions, but

also requires a higher dosage for an effective surface coverage compared to the comb shaped reference PCE.

A big advantage of the new superplasticizer is its long slump retention capability owed to its retardation. Therefore, the hyperbranched polymer might be interesting for ready mix concrete applications or concretes used in countries with hot climate conditions.

Based on the investigations within the scope of this work, it might be interesting to incorporate a hyperbranched polyglycerol moiety as side chain into a comb shaped PCE and to study the properties of such a hybrid polymer. Furthermore, starting from the hyperbranched superplasticizer a dumbbell-shaped polymer could be obtained when a diamine is used instead of the methoxy-terminated polyether amine so that a hyperbranched polyglycerol scaffold could be built up in this case from both sides.

The last part of the thesis is about the synthesis and characterization of a novel lignite-based superplasticizer, which was obtained through chemical modification of humic and fulvic acids from brown coal. Side chains comprised of the monomers ATBS and acrylic acid were grafted onto these alkali-soluble components, thus yielding a comb shaped polymer with a humic acid backbone and several ATBS-*co*-acrylic acid polymers as lateral chains. As the humic and fulvic acids are composed of condensated aromatic structural units, the new superplasticizer exhibits a relatively stiff main chain, whereas the side chains show a high conformational flexibility. The superplasticizer was synthesized from a commercial lignite sample possessing a high content of humic acids as well as from the sodium salts of brown coal, which were priorly extracted from brown coal samples. The optimum properties were found for an ATBS-acrylic acid ratio of 1 : 0.15. At this specific ratio, the polymers exhibited the lowest polydispersity, the highest polymer radii, and the longest grafted side chains. Successful grafting of the monomers onto the humic acid backbone was concluded after comparing the molecular properties of the lignite graft copolymer with the ATBS-*co*-acrylic acid reference polymer as well as after measurement of the adsorbed layer thickness.

Further investigations revealed that the lignite-based superplasticizers show only minor retardation and achieve dispersion through an electrostatic effect by adsorption of the polymers via the sulfonate and carboxylate groups of the side chains. Thus, a highly negative zeta potential results, which is in a similar range as for the ATBS-*co*-acrylic acid polymer and BNS. Since the comb shaped polymer structure and the stretched solution

conformation favor a more pronounced adsorbed layer thickness, the polymer also acts via a steric effect. However, owed to the stretched humic acid backbone, the superplasticizer cannot easily align on the surface, which is why the adsorption only occurs through a few side chains. Therefore, the lignite-based superplasticizer requires a higher dosage than the ATBS-*co*-acrylic acid polymer that can occupy more surface areas due to its higher flexibility. Nevertheless, the lignite polymers are more effective compared to a BNS polycondensate superplasticizer, which is composed of one linear chain and effectuates only a low adsorbed layer thickness.

Finally, it can be concluded that a stiff main chain has a significant impact on the adsorption properties and hence on features such as the dosing efficiency or the robustness of the polymer towards sulfate ions. For instance, the dispersing performance of the lignite-based superplasticizer was not affected by the presence of sulfate ions in contrast to the ATBS-*co*-acrylic acid polymer. Thus, a stretched solution conformation and a high adsorbed layer thickness seem to be beneficial for an enhanced sulfate robustness.

Next, it should be investigated how the properties will change when a macromonomer with a short PEG chain is incorporated into the side chain of the lignite polymer. It would also be interesting to use less reactive monomers like maleic anhydride, itaconic acid or methacrylic acid instead of acrylic acid and to probe whether these monomers can be easier grafted onto the humic acid backbone at higher ratios without the occurrence of side reactions.

8. Literaturverzeichnis

[1] A. N. Beris, A. Jeffrey Giacomin, *Πάντα Ῥεῖ: Everything Flows*, Applied Rheology 24 (5) **(2014)** 52918.

[2] K. Walters*, History of rheology*, In: C. Gallegos, K. Walters (Eds.), Rheology: encyclopedia of life support systems (EOLSS), UNESCO. Eolss, Oxford, **2010**, 15–30.

[3] D. Doraiswamy, *The origins of rheology: a short historical excursion*, Rheology Bulletin 71(1) **(2002)** 1-9.

[4] R. I. Tanner, K. Walters, *Rheology: An historical perspective*, Rheology Series 7, Elsevier Science, **1998**, 53-72.

[5] E. B. Burov, *Rheology and strength of the lithosphere*, Marine and Petroleum Geology 28 (8) **(2011)** 1402-1443.

[6] J. Jackson, D. McKenzie, K. Priestley, B. Emmerson, *New views on the structure and rheology of the lithosphere*, Journal of Geological Society 165 (2) **(2008)** 453-465.

[7] B. M. Minchew, C. R. Meyer, A. A. Robel, G. H. Gudmundsson, M. Simons, *Process controlling the downstream evolution of ice rheology in glacier shear margins: case study on Rutford Ice Stream, West Antarctica*, Journal of Glaciology 64 (246) **(2018)** 583-594.

[8] W. F. Budd, T. H. Jacka, *A review of ice rheology for ice sheet modelling*, Cold Regions Science and Technology 16 (2) **(1989)** 107-144.

[9] B. P. Hubbard, A. Hubbard, H. M. Mader, J.-L. Tison, K. Grust, P. W. Nienow, *Spatial variability in the water content and rheology of temperate glaciers: Glacier de Tsanfleuron, Switzerland*, Annals of Glaciology 37 **(2003)** 1-6.

[10] C. Verdier, J. Etienne, A. Duperray, L. Preziosi, *Review: Rheological properties of biological materials*, Comptes Rendus Physique 10 (8) **(2009)** 790-811.

[11] D. T. N. Chen, Q. Wen, P. A. Janmey, J. C. Crocker, A. G. Yodh, *Rheology of Soft Materials*, Annual Review of Condensed Matter Physics 1 **(2010)** 301-322.

[12] N. D. Polychronopoulos, J. Vlachopoulos, *Polymer Processing and Rheology*, In: M. A. J. Mazumder, H. Sheardown, A. Al-Ahmed (Eds.), Functional Polymers, Polymers and Polymeric Composites: A Reference Series, Springer, **2018**, 133-180.

[13] K.-J. Min, M. Lee, J. Son, J.-H. Lee*, Rheology as a powerful tool for industrial material development*, Korea-Australia Rheology Journal 22 (1) **(2010)** 1-10.

[14] M. Gahleitner, *Rheology as a quality control instrument*, Journal of Macromolecular Science, Part A 36 (11) **(1999)** 1731-1741.

[15] P. Fischer, E. J. Windhab, *Rheology of food materials*, Current Opinion in Colloid & Interface Science 16 (1) **(2011)** 36-40.

[16] R. Brummer, S. Godersky, *Rheological studies to objectify sensations occurring when cosmetic emulsions are applied to the skin*, Colloids and Surfaces A: Physicochemical and Engineering Aspects 152 (1-2) **(1999)** 89-94.

[17] R. R. Eley, *Applied rheology and architectural coating performance*, Journal of Coatings Technology and Research 16 **(2019)** 263-305.

[18] C. H. Lee, V. Moturi, Y. Lee, *Thixotropic property in pharmaceutical formulations*, Journal of Controlled Release 136 (2) **(2009)** 88-98.

[19] C. D. Han, *Rheology and Processing of Polymeric Materials, Volume I Polymer Rheology*, Oxford University Press, **2007**.

[20] C. F. Ferraris, P. Billberg, R. Ferron, D. Feys, J. Hu, S. Kawashima, E. Koehler, M. Sonebi, J. Tanesi, N. Tregger, *Role of Rheology in Achieving Successful Concrete Performance*, Concrete International 39 (6) **(2017)** 43-51.

[21] A. Bacigalupe, Z. He, M. M. Escobar, *Effects of Rheology and Viscosity of Bio-based Adhesives on Bonding Performance*, In: Z. He (Ed.), Bio-based Wood Adhesives, Preparation, Characterization and Testing (1st Edition), CRC Press, **2017**, 293-309.

[22] S. Croll, *Overview of Developments in the Paint Industry since 1930*, In: T. J. S. Learner, P. Smithen, J. W. Krueger, M. R. Schilling (Eds.), Modern Paints Uncovered, Proceedings from the Modern Paints Uncovered Symposium, London (UK), **2006**, 17-29.

[23] J. Plank, *Applications of biopolymers and other biotechnological products in building materials*, Applied Microbiology and Biotechnology 66 **(2004)** 1-9.

[24] a) https://www.indiamart.com/northernlubetechnology/lubricating-oil.html (abgerufen: 01.09.21)

b) https://wiki.anton-paar.com/de-de/grundlagen-der-rheologie/rheologische-untersuchung-von-polymeren/ (abgerufen: 01.09.21)

c) https://wiki.anton-paar.com/de-de/grundlagen-der-rheologie/rheologische-untersuchung-von-lebensmitteln/ (abgerufen: 01.09.21)

d) https://wiki.anton-paar.com/de-de/grundlagen-der-rheologie/rheologische-untersuchung-von-kosmetik-und-pharmaprodukten/ (abgerufen: 01.09.21)

e) https://wiki.anton-paar.com/de-de/grundlagen-der-rheologie/rheologische-untersuchung-von-baustoffen/ (abgerufen: 01.09.21)

f) https://gafacom.website/degradation-in-pharmaceutical-creams/ (abgerufen: 01.09.21)

[25] P.-C. Äitcin, R. J. Flatt, *Science and Technology of Concrete Admixtures (1st Edition)*, Woodhead Publishing, **2016**.

[26] V. S. Ramachandran, V. M. Malhotra, C. Jolicoeur, N. Spiratos, *Superplasticizers: Properties and applications in concrete,* CANMET, Ottawa, Canada, **1998**.

[27] Beton.org, *Betonzusätze – Zusatzmittel und Zusatzstoffe*, Zement-Merkblatt, Betontechnik B 3, **2014**.

[28] J. Plank, *Bauchemie*, In: K. Zilch, C. J. Diederichs, K. J. Beckmann, C. Gertz, A. Malkwitz, C. Moormann, W. Urban, F. Valentin (Eds.), Handbuch für Bauingenieure, Springer Vieweg, **2019**, 1-57.

[29] N. Schröter, P. Fischer, *Entwicklung und Trends bei Betonzusatzmitteln*, Deutsche Bauchemie, Sonderdruck, **2010**.

[30] a) https://www.swr.de/swr2/wissen/deshalb-ist-beton-ein-echter-klimakiller-100.html (abgerufen: 01.09.21)

b) https://festival.bergamoscienza.it/it/calendario/53702/calore-e-temperatura?datainizio=01/01/2021&datafine=31/05/2021&target=&disponibilita=False (abgerufen: 01.09.21)

c) R. König, S. Dittmar, *Der perfekte Mix. Moderne Betonzusatzmittel und ihr Einfluss auf den Mischprozess*, Vortrag BFT Fachforum, **2019**, Folie 18.

d) https://www.bauen.de/putz.html (abgerufen: 01.09.21)

e) https://www.borchers.com/product/borchers-af-1270/ (abgerufen: 01.09.21)

f) https://www.master-builders-solutions.com/de-de/produkte/masterair (abgerufen: 01.09.21)

g) https://www.presyn.ch/media/web/presyn.ch/media/downloads/de/publikationen/12pre_47.4_infoblatt_schwinden_presyn_d_wu.pdf (abgerufen: 01.09.21)

[31] N. Spiratos, M. Page, N. P. Mailvaganam, V. M. Malhotra, C. Jolicoeur, *Superplasticizers for Concrete: Fundamentals, Technology, and Practice*. Supplementary Cementing Materials for Sustainable Development, Ottawa, **2003**.

[32] S. Zheng, T. Liu, G. Jiang, C. Fang, B. Qu, P. Gao, L. Li, Y. Feng, *Effects of water-to-cement ratio on pore structure evolution and strength development of cement slurry based on HYMOSTRUC3D and micro-CT*, Applied Sciences 11 (7) **(2021)** 3063.

[33] B. Felekoglu, S. Türkel, B. Baradan, *Effect of water/cement ratio on the fresh and hardened properties of self-compacting concrete*, Building and Environment 42 (4) **(2007)** 1795-1802.

[34] G. De Schutter, P. J. M. Bartos, P. Domone, J. Gibbs, *Self-Compacting Concrete*, Whittles Publishing, **2008**.

[35] H. G. Russell, B. A. Graybeal, *Ultra-High Performance Concrete: A State-of-the-Art Report for the Bridge Community*, U.S. Department of Transportation, Federal Highway Administration, **2013**.

[36] M. Benaicha, A. Hafidi Alaoui, O. Jalbaud, Y. Burtschell, *Dosage effect of superplasticizer on self-compacting concrete: correlation between rheology and strength*, Journal of Materials Research and Technology 8 (2) **(2019)** 2063-2069.

[37] C. Schröfl, M. Gruber, J. Plank, *Preferential adsorption of polycarboxylate superplasticizers on cement and silica fume in ultra-high performance concrete (UHPC)*, Cement and Concrete Research 42 **(2012)** 1401-1408.

[38] J. Plank, E. Sakai, C.W. Miao, C. Yu, J.X. Hong, *Chemical admixtures – Chemistry, applications and their impact on concrete microstructure and durability*, Cement and Concrete Research 78 **(2015)** 81-99.

[39] S. Sha, M. Wang, C. Shi, Y. Xiao, *Influence of the structures of polycarboxylate superplasticizer on its performance in cement-based materials – A review*, Construction and Building Materials 233 **(2020)** 117257.

[40] F. Dalas, A. Nonat, S. Pourchet, M. Mosquet, D. Rinaldi, S. Sabio, *Tailoring the anionic function and the side chains of comb-like superplasticizers to improve their adsorption*, Cement and Concrete Research 67 **(2015)** 21-30.

[41] F. Dalas, S. Pourchet, A. Nonat, D. Rinaldi, S. Sabio, M. Mosquet, *Fluidizing efficiency of comb-like superplasticizers: The effect of the anionic function, the side chain length and the grafting degree*, Cement and Concrete Research 71 **(2015)** 115-123.

[42] E. Janowska-Renkas, *The effect of superplasticizers' chemical structure on their efficiency in cement pastes*, Construction and Building Materials 38 **(2013)** 1204-1210.

[43] F. Winnefeld, S. Becker, J. Pakusch, T. Götz, *Effects on the molecular architecture of comb-shaped superplasticizers on their performance in cementitious systems*, Cement and Concrete Composites 29(4) **(2007)** 251-262.

[44] H. Uchikawa, S. Hanehara, D. Sawaki, *The role of steric repulsive force in the dispersion of cement particles in fresh paste prepared with organic admixture*, Cement and Concrete Research 27 **(1997)** 37-50.

[45] K. Yoshioka, E. Sakai, M. Daimon, A. Kitahar*, Role of steric hindrance in the performance of superplasticizers for concrete*, Journal of American Ceramic Society 80 **(1997)** 2667-2671.

[46] K. Yoshioka, E. Tazawa, K. Kawai, T. Enohata, *Adsorption characteristics of superplasticizers on cement component minerals*, Cement and Concrete Research 32 (10) **(2002)** 1507-1513.

[47] K. Yamada, S. Hanehara*, Interaction mechanism of cement and superplasticizers – The roles of polymer adsorption and conditions of aqueous phase*, Concrete Science and Engineering 3 **(2001)** 135-145.

[48] J. Plank, D. Vlad, A. Brandl, P. Chatziagorastou, *Colloidal chemistry examination of the steric effect of polycarboxylate superplasticizers*, Cement International 2 **(2005)** 100-110.

[49] J. Hot, H. Bessaies-Bey, C. Brumaud, M. Duc, C. Castella, N. Roussel, *Adsorbing polymers and viscosity of cement pastes*, Cement and Concrete Research 63 **(2014)** 12-19.

[50] A. Lange, J. Plank, *A Study on the Cement Compatibility of PCE Superplasticizers*, In: V. M. Malhotra, P. R. Gupta, T. C. Holland (Eds.), Superplasticizers and Other Chemical Admixtures in Concrete, Proceedings Eleventh International Conference, Ottawa, **2015**, SP-302-30, 401-414.

[51] K. Yamada, S. Ogawa, S. Hanehara, *Controlling of the adsorption and dispersing force of polycarboxylate-type superplasticizer by sulfate ion concentration in aqueous phase*, Cement and Concrete Research 31 **(2001)** 375-383.

[52] L. Lei, J. Plank, *A study on the impact of different clay minerals on the dispersing force of conventional and modified vinyl ether based polycarboxylate superplasticizers*, Cement and Concrete Research 60 **(2014)** 1-10.

[53] A. Lange, T. Hirata, J. Plank, *Influence of the HLB value of polycarboxylate superplasticizers on the flow behavior of mortar and concrete*, Cement and Concrete Research 60 **(2014)** 45-50.

[54] L. Ferrari, J. Kaufmann, F. Winnefeld, J. Plank, *Interaction of cement model systems with superplasticizers investigated by atomic force microscopy, zeta potential, and adsorption measurements*, Journal of Colloid and Interface Science 347 **(2010)** 15-24.

[55] J. A. Lewis, H. Matsuyama, G. Kirby, S. Morissette, J. F. Young, *Polyelectrolyte effects on the rheological properties of concentrated cement suspensions*, Journal of American Ceramic Society 83 (8) **(2000)** 1905-1913.

[56] M. Ushiro, D. Atarashi, H. Kawakami, E. Sakai, *The effect of superplasticizer present in pore solution on flowability of low water-to-powder cement paste*, Cement Science and Concrete Technology 67(1) **(2013**) 102-107.

[57] K. Matsuzawa, D. Shimazaki, H. Kawakami, E. Sakai, *Effect of non-adsorbed superplasticizer molecules on fluidity of cement paste at low water-powder ratio*, Cement and Concrete Composites 97 **(2019)** 218-225.

[58] A. Lange, J. Plank, *Contribution of non-adsorbing polymers to cement dispersion*, Cement and Concrete Research 79 **(2016)** 131-136.

[59] A. Lange, J. Plank, *Optimization of comb-shaped polycarboxylate cement dispersants to achieve fast-flowing mortar and concrete*, Journal of Applied Polymer Science 132 **(2015)** 42529.

[60] S. D. Bauchkar, H. S. Chore, *Effect of PCE superplasticizers on rheological and strength properties of high strength self-consolidating concrete*, Advances in Concrete Construction 6 **(2018)** 561-583.

[61] T. Nawa, *Effect of chemical structure on steric stabilization of polycarboxylate-based superplasticizer*, Journal of Advanced Concrete Technology 44 **(2006)** 225-232.

[62] E. Sakai, K. Yamada, A. Ohta, *Molecular structure and dispersion-adsorption mechanisms of comb-type superplasticizers used in Japan*, Journal of Advanced Concrete Technology 1 **(2003)** 16-25.

[63] Y. F. Houst, P. Bowen, F. Perche, A. Kauppi, P. Borget, L. Galmiche, J.-F. Le Meins, F. Lafuma, R. J. Flatt, I. Schober, P. F. G. Banfill, D. S. Swift, B. O. Myrvold, B. G. Petersen, K. Reknes, *Design and function of novel superplasticizers for more durable high performance concrete (superplast project)*, Cement and Concrete Research 38 **(2008)** 1197-1209.

[64] R. J. Flatt, I. Schober, E. Raphael, C. Plassard, E. Lesniewska, *Conformation of adsorbed comb copolymer dispersants*, Langmuir 25 **(2009)** 845-855.

[65] K. Yamada, T. Takahashi, S. Hanehara, M. Matsuhisa, *Effects of the chemical structure on the properties of polycarboxylate-type superplasticizer*, Cement and Concrete Research 30 **(2000)** 197-207.

[66] X. Liu, Z. Wang, J. Zhu, M. Zhao, W. Liu, D. Yin, *Preparation and Characterization of Star-Shaped Polycarboxylate Superplasticizer*, In: V. M. Malhotra, P. R. Gupta, T. C. Holland (Eds.), Superplasticizers and Other Chemical Admixtures in Concrete, Proceedings Eleventh International Conference, Ottawa, **2015**, SP-302-14, 183-198.

[67] H. Zhao, B. Liao, K. Wang, Y. Zhao, F. Nian, Y. Meng, H. Pang, *Synthesis, characterization, and performance of a novel polycarboxylate superplasticizer with a crosslinked topological structure*, Journal of Applied Polymer Science 135 (45) **(2018)** 46716.

[68] P. F. G. Banfill, *Rheology of fresh cement and concrete*, Rheology Reviews **(2006)** 61-130.

[69] N. Roussel, *Rheological Admixtures, Chapter 19*, In: Y. Mouton (Ed.), Organic Materials for Sustainable Civil Engineering, ISTE Ltd., **2011**, 433-446.

[70] N. Roussel, A. Lemaitre, R. J. Flatt, P. Coussot, *Steady state flow of cement suspensions: A micromechanical state of the art*, Cement and Concrete Research 40 **(2010)** 77-84.

[71] R. J. Flatt, *Towards a prediction of superplasticized concrete rheology*, Materials and Structures 37 **(2004)** 289-300.

[72] P. F. G. Banfill, *Rheological methods for assessing the flow properties of mortar and related materials*, Construction and Building Materials 8 **(1994)** 43-50.

[73] T. G. Mezger, *Das Rheologie Handbuch: Für Anwender von Rotations- und Oszillations-Rheometern*, 2. Auflage, Vincentz Network, **2006**.

[74] R. Shaughnessy, P. E. Clark, *The rheological behavior of fresh cement pastes*, Cement and Concrete Research 18 **(1988)** 327-341.

[75] P. F. G. Banfill, *Additivity effects in the rheology of fresh concrete containing water-reducing admixtures*, Construction and Building Materials 25 **(2011)** 2955-2960.

[76] X. W. Zhang, L. W. Kong, A. W. Yang, H. M. Sayem, *Thixotropic mechanism of clay: A microstructural investigation*, Soils and Foundations 57 (1) **(2017)** 23-35.

[77] S. J. Manion, L. L. Johnson, R. H. Fernando, *Shear-thickening in aqueous surfactant-associative thickener mixtures*, Journal of Coatings Technology and Research 8 **(2011)** 299-309.

[78] W. H. Herschel, R. Bulkley, *Konsistenzmessungen von Gummi-Benzollösungen*, Kolloid-Zeitschrift 39 (4) **(1926)** 291-300.

[79] R. Lapasin, A. Papo, S. Rajgelj, *Flow behavior of fresh cement pastes. A comparison of different rheological instruments and techniques*, Cement and Concrete Research 13 **(1983)** 349-356.

[80] N. Roussel, *A thixotropy model for fresh fluid concretes: Theory, validation and applications,* Cement and Concrete Research 36 **(2006)** 1797-1806.

[81] N. Roussel, G. Ovarlez, S. Garrault, C. Brumaud, *The origins of thixotropy of fresh cement pastes*, Cement and Concrete Research 42 **(2012)** 148-157.

[82] F.-J. Rubio-Hernandez, *Rheological Behavior of Fresh Cement Pastes*, Fluids 3 (4) **(2018)** 106.

[83] O. H. Wallevik, J. E. Wallevik, *Rheology as a tool in concrete science: The use of rheographs and workability boxes*, Cement and Concrete Research 41 (12) **(2011)** 1279-1288.

[84] D. Jiao, C. Shi, Q. Yuan, X. An, Y. Liu, H. Li, *Effect of constituents on rheological properties of fresh concrete – A review,* Cement and Concrete Composites 83 **(2017)** 146-159.

[85] J. Hu, K. Wang, *Effect of coarse aggregate characteristics on concrete rheology*, Construction and Building Materials 25 **(2011)** 1196-1204.

[86] M. R. Geiker, M. Brandl, L. N. Thrane, L. F. Nielsen, *On the effect of coarse aggregate fraction and shape on the rheological properties of self-compacting concrete*, Cement, Concrete and Aggregates 24 **(2002)** 3-6.

[87] K. Ostrowski, L. Sadowski, D. Stefaniuk, D. Walach, T. Gawenda, K. Oleksik, I. Usydus, *The effect of the morphology of coarse aggregate on the properties of self-compacting high-performance fibre-reinforced concrete*, Materials 11 **(2018)** 1372.

[88] F. Mahaut, S. Mokeddem, X. Chateau, N. Roussel, G. Ovarlez, *Effect of coarse particle volume fraction on the yield stress and thixotropy of cementitious materials*, Cement and Concrete Research 38 **(2008)** 1276-1285.

[89] J. Golaszewski, J. Szwabowski, *Influence of superplasticizers on rheological behaviour of fresh cement mortars*, Cement and Concrete Research 34 **(2004)** 235-248.

[90] J.-Y. Petit, K. H. Khayat, E. Wirquin, *Coupled effect of time and temperature on variations of plastic viscosity of highly flowable mortar*, Cement and Concrete Research 39 **(2009)** 165-170.

[91] B. Feneuil, O. Pitois, N. Roussel, *Effect of surfactants on the yield stress of cement paste*, Cement and Concrete Research 100 **(2017)** 32-39.

[92] L. J. Struble, Q. Jiang, *Effects of Air Entrainment on Rheology*, ACI Materials Journal 101 (6) **(2004)** 448-456.

[93] D. A. Williams, A. W. Saak, H. M. Jennings, *The influence of mixing on the rheology of fresh cement paste*, Cement and Concrete Research 29 **(1999)** 1491-1496.

[94] D. Han, R. D. Ferron, *Effect of mixing method on microstructure and rheology of cement paste*, Construction and Building Materials 93 **(2015)** 278-288.

[95] J. J. Chen, A. K. H. Kwan, *Superfine cement for improving packing density, rheology and strength of cement paste*, Cement and Concrete Composites 34 **(2012)** 1-10.

[96] L. Struble, G. K. Sun, *Viscosity of Portland cement pastes as a function of concentration*, Advanced Cement Based Materials 2 **(1995)** 62-69.

[97] D. P. Bentz, C. F. Ferraris, M. A. Galler, A. S. Hansen, J. M. Guynn, *Influence of particle size distributions on yield stress and viscosity of cement-fly ash pastes*, Cement and Concrete Research 42 **(2012)** 404-409.

[98] C. R. Robert, D. Sathyan, K. B. Anand, *Effect of superplasticizers on the rheological properties of fly ash incorporated cement paste*, Materials Today: Proceedings 5 **(2018)** 23955-23963.

[99] Y. J. Kim, B.-Y. Cho, S.-J. Lee, J. Hu, J. W. Wilde, *Investigation of Rheological Properties of Blended Cement Pates Using Rotational Viscometer and Dynamic Shear Rheometer*, Advances in Materials Science and Engineering **(2018)** 6303681.

[100] J. Newman, B. S. Choo, *Advanced Concrete Technology 2: Concrete Properties*, 1st Edition, Butterworth-Heinemann, **2003**, 352.

[101] N. Roussel, C. Stefani, R. Leroy, *From mini-cone test to Abrams cone test: measurement of cement-based materials yield stress using slump tests*, Cement and Concrete Research 35 **(2005)** 817-822.

[102] N. Roussel, P. Coussot, *"Fifty-cent rheometer" for yield stress measurements: from slump to spreading flow*, Journal of Rheology 49(3) **(2005)** 705-718.

[103] N. Roussel, *Rheology of fresh concrete: from measurements to predictions of casting process*, Materials and Structures 40 (10) **(2007)** 1001-1012.

[104] N. Roussel, *Correlation between yield stress and slump: comparison between numerical simulations and concrete rheometers results*, Materials and Structures 39 **(2006)** 501-509.

[105] S. Pandey, A. Dalvi, A. Patel, B. Chaurasia, N. Mishra, *A Review on the Study of Principle Characteristics, Composition Mixture and Durability of Self-Compacting Concrete with Different Techniques*, International Journal of Scientific Engineering and Science 2 (1) **(2018)** 10-13.

[106] G. Ramesh, *Self-Compacting Concrete: A Review*, Indian Journal of Structure Engineering (IJSE) 1 (2) **(2021)** 9-12.

[107] J. Plank, *On the correct chemical nomenclature of C_3S, tricalcium oxy silicate*, Cement and Concrete Research 130 **(2020)** 105957.

[108] A. Michael Harrisson, *Constitution and Specification of Portland Cement*, In: P. C. Hewlett, M. Liska (Eds.), Lea's Chemistry of Cement and Concrete, Butterworth-Heinemann, 5. Ausgabe, **2019**, 94-101.

[109] F. Ridi, E. Fratini, P. Baglioni, *Cement: A two thousand year old nano-colloid*, Journal of Colloid and Interface Science 357 **(2011)** 255-264.

[110] C. Jolicoeur, M.-A. Simard, *Chemical admixture-cement interactions: Phenomenology and Physico-chemical concepts*, Cement and Concrete Composites 20 **(1998)** 87-101.

[111] J. Plank, D. Stephan, C. Hirsch, *Bauchemie*, In: Chemische Technik – Prozesse und Produkte, Band 7: Industrieprodukte, Winnacker/Küchler, Wiley-VCH Verlag, 5. Auflage, **2004**.

[112] J. Beaudoin, I. Odler, *Hydration, Setting and Hardening of Portland Cement*, In: P. C. Hewlett, M. Liska (Eds.), Lea's Chemistry of Cement and Concrete, Butterworth-Heinemann, 5. Ausgabe, **2019**, 157-250.

[113] J. Plank, C. Hirsch, *Impact of zeta potential of early cement hydration phases on superplasticizer adsorption*, Cement and Concrete Research 37 **(2007)** 537-542.

[114] R. J. Flatt, *Dispersion forces in cement suspensions*, Cement and Concrete Research 34 **(2004)** 399-408.

[115] A. Zingg, L. Holzer, A. Kaech, F. Winnefeld, J. Pakusch, S. Becker, L. Gauckler, *The microstructure of dispersed and non-dispersed fresh cement pastes – New insight by cryo-microscopy*, Cement and Concrete Research 38 **(2008)** 522-529.

[116] J. Björnström, S. Chandra, *Effect of superplasticizers on the rheological properties of cements*, Materials and Structures 36 **(2003)** 685-692.

[117] H. Uchikawa, D. Sawaki, S. Hanehara*, Influence of kind and added timing of organic admixture on the composition, structure and property of fresh cement paste*, Cement and Concrete Research 25 **(1995)** 353-364.

[118] M. Y. A. Mollah, W. J. Adams, R. Schennach, D. L. Cocke, *A review of cement-superplasticizer interactions and their models*, Advances in Cement Research 12 (4) **(2000)** 153-161.

[119] T. Nylander, Y. Samoshina, B. Lindman, *Formation of polyelectrolyte-surfactant complexes on surfaces*, Advances in Colloid and Interface Science 123-126 **(2006)** 105-123.

[120] B. Derjaguin, L. Landau, *Theory of the stability of strongly charged lyophobic sols and of the adhesion of strongly charged particles in solutions of electrolytes,* Progress in Surface Science 43 (1-4) **(1993)** 30-59.

[121] E. J. W. Verwey, J. T. G. Overbeek, *Theory of the stability of lyophobic colloids*, Journal of Physical Chemistry 51 (3) **(1947)** 631-636.

[122] R. J. Flatt, P. Bowen, *Electrostatic repulsion between particles in cement suspensions: domain of validity of linearized Poisson-Boltzmann equation for non-ideal electrolytes*, Cement and Concrete Research 33 **(2003)** 781-791.

[123] Q. Ran, P. Somasundaran, C. Miao, J. Liu, S. Wu, J. Shen, *Effect of the length of the side chains of comb-like copolymer dispersants on dispersion and rheological properties of concentrated cement suspensions*, Journal of Colloid and Interface Science 336 **(2009)** 624-633

[124] Y. Zhang, X. Kong, *Correlations of the dispersing capability of NSF and PCE types of superplasticizer and their impacts on cement hydration with the adsorption in fresh cement pastes*, Cement and Concrete Research 69 **(2015)** 1-9.

[125] R. H. Ottewill, T. Walker, *The influence of non-ionic surface active agents on the stability of polystyrene latex dispersions*, Kolloid-Zeitschrift und Zeitschrift für Polymere 227 **(1968)** 108-116.

[126] X. Shu, Q. Ran, J. Liu, H. Zhao, Q. Zhang, X. Wang, Y. Yang, J. Liu, *Tailoring the solution conformation of polycarboxylate superplasticizer toward the improvement of dispersing performance in cement paste*, Construction and Building Materials 116 **(2016)** 289-298.

[127] R. J. Flatt, Y. F. Houst, *A simplified view on chemical effects perturbing the action of superplasticizers*, Cement and Concrete Research 31 **(2001)** 1169-1176.

[128] P. G. de Gennes, *Polymers at an interface; a simplified view*, Advances in Colloid and Interface Science 27 **(1987)** 189-209.

[129] P. G. de Gennes, *Conformations of polymers attached to an interface*, Macromolecules 13 **(1980)** 1069-1075.

[130] A. Kauppi, K. M. Andersson, L. Bergström, *Probing the effect of superplasticizer adsorption on the surface forces using the colloidal probe AFM technique*, Cement and Concrete Research 35 **(2005)** 133-140.

[131] J. Liu, C. Yu, X. Shu, Q. Ran, Y. Yang, *Recent advance of chemical admixtures in concrete*, Cement and Concrete Research 124 **(2019)** 105834.

[132] T. Hirata, J. Ye, P. Branicio, J. Zheng, A. Lange, J. Plank, M. Sullivan, *Adsorbed Conformations of PCE Superplasticizers in Cement Pore Solution Unraveled by Molecular Dynamics Simulations*, Scientific Reports 7 **(2017)** 16599.

[133] T. Hirata, P. Branicio, J. Ye, J. Zheng, Y. Tomike, A. Lange, J. Plank, M. Sullivan, *Atomistic dynamics simulation to solve conformation of model PCE superplasticizers in water and cement pore solution*, Advances in Cement Research 29 (10) **(2017)** 418-428.

[134] H. Zhao, Y. Wang, Y. Yang, X. Shu, H. Yan, Q. Ran, *Effect of hydrophobic groups on the adsorption conformation of modified polycarboxylate superplasticizer investigated by molecular dynamics simulation*, Applied Surface Science 407 **(2017)** 8-15.

[135] P.-H. Chuang, Y.-H. Tseng, Y. Fang, M. Gui, X. Ma, J. Luo, *Effect of Side Chain Length on Polycarboxylate Superplasticizer in Aqueous Solution: A Computational Study*, Polymers 11 (2) **(2019)** 346.

[136] J.-H. Chen, L-Q. Lu, H.-X. Zhao, Y. Yang, X. Shu, Q.-P. Ran, *Conformational Properties of Comb-shaped Polyelectrolytes with Negatively Charged Backbone and Neutral Side Chains Studied by a Generic Coarse-grained Bead-and Spring Model*, Chinese Journal of Polymer Science 38 **(2020)** 371-381.

[137] S. Zhang, P.-H. Chuang, Y. Ke, Y. Fang, *Conformation and Adsorption Properties in Aqueous Solution for Polycarboxylate Superplasticizers with Different Main Chain Lengths*, International Conference on Artificial Intelligence and Electromechanical Automation (AIEA) **(2020)** 670-674.

[138] Q. Ran, P. Somasundaran, C. Miao, J. Liu, S. Wu, J. Shen, *Adsorption Mechanism of Comb Polymer Dispersants at the Cement/Water Interface*, Journal of Dispersion Science Technology 31 (6) **(2010)** 790–798.

[139] J. Y. Yoon, J. H. Kim, *Evaluation on the consumption and performance of polycarboxylates in cement-based materials*, Construction and Building Materials 158 **(2018)** 423-431.

[140] R. Abile, A. Russo, C. Limone, F. Montagnaro, *Impact of the charge density on the behavior of polycarboxylate ethers as cement dispersants*, Construction and Building Materials 180 **(2018)** 477-490.

[141] L. Shui, Z. Sun, H. Yang, X. Yang, Y. Ji, Q. Luo, *Experimental evidence for a possible dispersion mechanism of polycarboxylate-type superplasticizers*, Advances in Cement Research 28 (5) **(2016)** 287-297.

[142] H. Bessaies-Bey, M. Palacios, E. Pustovgar, M. Hanafi, R. Baumann, R. J. Flatt, N. Roussel, *Non-adsorbing polymers and yield stress of cement paste: Effect of depletion forces*, Cement and Concrete Research 111 **(2018)** 209-217.

[143] J. Plank, M. Ilg, *The Role of Chemical Admixtures in the Formulation of Modern Advanced Concrete*, In: W. Boshoff, R. Combrinck, V. Mechtcherine. M. Wyrzykowski (Eds.), 3rd International Conference on the Application of Superabsorbent Polymers (SAP) and Other New Admixtures Towards Smart Concrete, SAP 2019, RILEM Bookseries 24 **(2020)** 143-157.

[144] J. Plank, K. Pöllmann, N. Zouaoui, P. R. Andres, C. Schaefer, *Synthesis and performance of methacrylic ester based polycarboxylate superplasticizers possessing hydroxy terminated poly(ethylene glycol) side chains,* Cement and Concrete Research 38 **(2008)** 1210-1216.

[145] M. Liu, J. Lei, X. Du, B. Huang, L. Chen, *Synthesis and properties of methacrylate-based and allylether-based polycarboxylate superplasticizer in cementitious system*, Journal of Sustainable Cement-Based Materials 2 (3-4) **(2013)** 218-226.

[146] J. Plank, B. Sachsenhauser, *Impact of molecular structure on zeta potential and adsorbed conformation of α-allyl-ω-methoxypolyethylene glycol - maleic anhydride superplasticizers*, Journal of Advanced Concrete Technology 4 (2) **(2006)** 233-239.

[147] Y. Li, C. Yang, Y. Zhang, J. Zheng, H. Guo, M. Lu, *Study on dispersion, adsorption and flow retaining behaviors of cement mortars with TPEG-type polyether kind polycarboxylate superplasticizers*, Construction and Building Materials 64 **(2014)** 324-332.

[148] J. Plank, H. Li, M. Ilg, J. Pickelmann, W. Eisenreich, Y. Yao, Z. Wang, *A microstructural analysis of isoprenol ether-based polycarboxylates and the impact of structural motifs on the dispersing effectiveness*, Cement and Concrete Research 84 **(2016)** 20-29.

[149] M. Schmid, J. Plank, *Dispersing performance of different kinds of polycarboxylate (PCE) superplasticizers in cement blended with a calcined clay*, Construction and Building Materials 258 **(2020)** 119576.

[150] L. Lei, H.-K. Chan, *Investigation into the molecular design and plasticizing effectiveness of HPEG-based polycarboxylate superplasticizers in alkali-activated slag*, Cement and Concrete Research 136 **(2020)** 106150.

[151] Y. Shao, G. Lai, Y. Fang, Y. Guo, *Process design and optimization of VPEG-PCEs*, IOP Conference Series: Earth and Environmental Science 358 **(2019)** 032014.

[152] G. Liu, X. Wei, Z. Wang, J. Ren, *Study on the activity difference of macromonomers for preparing polycarboxylic superplasticizers*, Journal of Applied Polymer Science 137 (26) **(2020)** 48844.

[153] T. Amaya, A. Ikeda J. Imamura, A. Kobayashi, K. Saito, W. Danzinger, T. Tomoyose, *Cement Dispersant and Concrete Composition containing the Dispersant*, WO 0,039,045 (Patent), **2000**.

[154] H. Tahara, H. Ito, Y. Mori M. Mizushima, *Cement Additive, Method for Producing the same, and Cement Composition*, US 5,476,885 (Patent), **1995**.

[155] S. Xiang, Y. Gao, C. Shi, *Progress in Synthesis of Polycarboxylate Superplasticizer*, Advances in Civil Engineering **(2020)** 8810443.

[156] X. Liu, X. Bai, Q. Xu, C. Xia, G. Lai, J. Guan, *Synthesis and Application Performances of Solid Polycarboxylate Superplasticizers using Different Initiators*, Materials Science Forum 993 **(2020)** 1367-1372.

[157] Z.M. Wang, Y. Xu, H. Wu, X. Liu, F. Y. Zheng, H. Q. Li, S. P. Cui, M. Z. Lan, Y. L. Wang, *A Room Temperature Synthesis Method for Polycarboxylate Superplasticizer*, CN 101974135 B (Patent), **2013**.

[158] S. Xiang, Y. Gao, C. Shi, *Synthesis of a New Polycarboxylate at Room Temperature and Its Influence on the Properties of Cement Pastes with Different Supplementary Cementitious Materials*, Advances in Civil Engineering **(2020)** 8854422.

[159] G. Wang, L. X. Liang, *Study on Synthesis of Polycarboxylate Superplasticizer at Room Temperature*, Applied Mechanics and Materials 672-674 **(2014)** 688-690.

[160] A. Tajbakhshian, M. R. Saeb, S. H. Jafari, F. Najafi, H. A. Khonakdar, M. Ayoubi, F. H. Asl, *High-performance carboxylate superplasticizers for concretes: Interplay between the polymerization temperature and properties*, Journal of Applied Polymer Science 134 (23) **(2017)** 44908.

[161] L. Zhang, W. Du, D. Wang, F. Wang, K. Fang, J. Yu, B. Sheng, *Syntheses of polycarboxylate superplasticizers: Microwave induction versus conventional thermal induction*, Composites Part B: Engineering 207 **(2021)** 108560.

[162] X. Wang, Y. Yang, X. Shu, Y. Wang, Q. Ran, J. Liu, *Tailoring polycarboxylate architecture to improve the rheological properties of cement paste*, Journal of Dispersion Science and Technology 40 (11) **(2019)** 1567-1574.

[163] S. Pourchet, S. Liautaud, D. Rinaldi, I. Pochard, *Effect of the repartition of the PEG side chains on the adsorption and dispersion behaviors of PCP in presence of sulfate*, Cement and Concrete Research 42 **(2012)** 431-439.

[164] Y.-R. Zhang, X.-M. Kong, Z.-B. Lu, Z.-C. Lu, S.-S. Hou, *Effects of the charge characteristics of polycarboxylate superplasticizers on the adsorption and the retardation in cement pastes*, Cement and Concrete Research 67 **(2015)** 184-196.

[165] J. Ma, Y. Shang, C. Peng, H. Liu, S. Zheng, Y. Wang, S. Qi, Q. Ran, *Synthesis and properties of comb-like and linear polymers: Effects of dispersant structure on the bubble structure, surface activity, adsorption, and rheological performance*, Colloids and Surfaces A: Physicochemical and Engineering Aspects 562 **(2019)** 336-344.

[166] T. M. Vickers Jr., S. A. Farrington, J. R. Bury, L. E. Brower, *Influence of dispersant structure and mixing speed on concrete slump retention*, Cement and Concrete Research 35 (10) **(2005)** 1882-1890.

[167] B. Yu, Z. Zeng, Q. Ren, Y. Chen, M. Liang, H. Zou, *Study on the performance of polycarboxylate-based superplasticizers synthesized by reversible addition-fragmentation chain transfer (RAFT) polymerization*, Journal of Molecular Structure 1120 **(2016)** 171-179.

[168] Q. Ran, X. Wang, X. Shu, Q. Zhang, Y. Yang, J. Liu, *Effects of sequence structure of polycarboxylate superplasticizers on the dispersion behavior of cement paste*, Journal of Dispersion Science and Technology 37 **(2016)** 431-441.

[169] J. Weidmann, L. Frunz, J. Zimmermann, *Block Copolymer*, WO2015/144886 A1 (Patent), **2015**.

[170] Q. Ran, X. Wang, J. Jiang, Y. Yang, *Synthesis of block polycarboxylate copolymer and its application in a cement system*, Advances in Cement Research 28 (3) **(2016)** 202-208.

[171] M. Ezzat, X. Xu, K. El Cheikh, K. Lesage, R. Hoogenboom, G. De Schutter, *Structure-property relationships for polycarboxylate ether superplasticizers by means of RAFT polymerization*, Journal of Colloid and Interface Science 553 **(2019)** 788-797.

[172] J. Weidmann, J. Zimmermann, K. Shindo, K. Saitoh, *New PCE class enables short mixing times in high performance applications*, In: J. Plank, L. Lei (Eds.), Conference Proceedings of 3rd International Conference on Polycarboxylate Superplasticizers (PCE 2019), Garching (Germany), **2019**, 41-49.

[173] W. C. Griffin, *Classification of surface active agents by HLB*, Journal of the Society of Cosmetic Chemists 1 **(1949)** 311-326.

[174] W. C. Griffin, *Calculation of HLB values of non-ionic surfactants*, Journal of the Society of Cosmetic Chemists 5 **(1954)** 249-256.

[175] J. Stecher, J. Plank, *Phosphated comb polymers – A new generation of highly effective superplasticizers*, in: K. H. Khayat (Ed.), 8th International RILEM Symposium on Self-Compacting Concrete – SCC 2016, Washington (USA), **2016**, 61-71.

[176] J. Stecher, J. Plank, *Novel concrete superplasticizers based on phosphate esters*, Cement and Concrete Research 119 **(2019)** 36-43.

[177] Y. He, X. Shu, X. Wang, Y. Yang, J. Liu, Q. Ran, *Effects of polycarboxylates with different adsorption groups on the rheological properties of cement paste*, Journal of Dispersion Science and Technology 41 (6) **(2020)** 873-883.

[178] A. Kraus, O. Mazanec, J. Dengler, N. Hillesheim, J. Bokern, *Influence of PAE, SMD and PCE superplasticizers on the rheological properties of mortars and concretes*, In: V. Mechtcherine, C. Schroefl (Eds.), International Conference on Application of Superabsorbent Polymers and Other New Admixtures in Concrete Construction, Dresden (Germany), RILEM Publications S.A.R.L., Proceedings PRO 95 **(2014)** 115-126.

[179] M. L. Vo, J. Plank, *Dispersing effectiveness of a phosphated polycarboxylate in α- und β-calcium sulfate hemihydrate systems*, Construction and Building Materials 237 **(2020)** 117731.

[180] H. Qi, B. Ma, H. Tan, Y. Su, Z. Jin, C. Li, X. Liu, Q. Yang, Z. Luo, *Polycarboxylate superplasticizer modified by phosphate ester in side chain and its basic properties in gypsum plaster*, Construction and Building Materials 271 **(2021)** 121566.

[181] M. L. Vo, J. Plank, *Evaluation of phosphated superplasticizers in high-performance α-calcium sulfate hemihydrate-based floor screeds*, Journal of Building Engineering 41 **(2021)** 102787.

[182] S.-H. Lv, R.-J. Gao, J.-P. Duan, D. Li, Q. Cao, *Effects of β-Cyclodextrin Side Chains on the Dispersing and Retarding Properties of Polycarboxylate Superplasticizers*, Journal of Applied Polymer Science 125 (1) **(2012)** 396-404.

[183] H. Xu, S. Sun, J. Wei, Q. Yu, Q. Shao, C. Lin, *β-Cyclodextrin as Pendant Groups of a Polycarboxylate Superplasticizer for Enhancing Clay Tolerance*, Industrial & Engineering Chemistry Research 54 (37) **(2015)** 9081-9088.

[184] Y. Ma, C. Shi, L. Lei, S. Sha, B. Zhou, Y. Liu, Y. Xiao, *Research progress on polycarboxylate based superplasticizers with tolerance to clays – A review*, Construction and Building Materials 225 **(2020)** 119386.

[185] S. Ng, J. Plank, *Interaction mechanisms between Na montmorillonite clay and MPEG-based polycarboxylate superplasticizers*, Cement and Concrete Research 42 **(2012)** 847-854.

[186] H. Tan, B. Gu, S. Jian, B. Ma, Y. Guo, Z. Zhi, *Improvement of polyethylene glycol in compatibility with polycarboxylate superplasticizer and poor-quality aggregates containing montmorillonite*, Journal of Materials in Civil Engineering 29 (9) **(2017)** 04017131.

[187] R. B. Raether, S. Flakus, J. Dengler, N. Zeminian, I. Ros, *Branched polycarboxylate ethers*, EP 2774941 A1 (Patent), **2014**.

[188] Q.H. Zhu, L.-Z. Zhang, X.-M. Min, Y.-X. Yu, X.-F. Zhao, J.-H. Li, *Comb-typed polycarboxylate superplasticizer equipped with hyperbranched polyamide teeth*, Colloids and Surfaces A: Physicochemical and Engineering Aspects 553 **(2018)** 272-277.

[189] J. M. Ren, T. G. McKenzie, Q. Fu, E. H. H. Wong, J. Xu, Z. An, S. Shanmugam, T. P. Davis, C. Boyer, G. G. Qiao, *Star Polymers*, Chemical Reviews 116 (12) **(2016)** 6743-6836.

[190] X. Liu, Z. Wang, J. Zhu, M. Zhao, Y. Zheng, *Synthesis, Characterization and Performance of Superplasticizer with a Multi-arm Structure*, Materials Science Forum 815 **(2015)** 594-600.

[191] X. Liu, J. Guan, G. Lai, Z. Wang, J. Zhu, S. Cui, M. Lan, H. Li, *Performances and working mechanism of a novel polycarboxylate superplasticizer synthesized through changing molecular topological structure*, Journal of Colloid and Interface Science 504 **(2017)** 12-24.

[192] L. Ao, W. Zhao, Q. Lei, D. Wang, Y. Guan, K. Liu, T. Guo, X. Fan, X. Wei, *Synthesis of a Novel Polycarboxylate Superplasticizer with Hyperbranched Structure*, Chemistry Select 3 **(2018)** 13493-13496.

[193] K. Wang, H. Pang, H. Huang, L. Song, J. Huang, Y. Zhao, *Study on the dispersion, adsorption and early hydration behavior of cement pastes containing multi-armed polycarboxylate superplasticizers*, Journal of Dispersion Science and Technology 41(2) **(2020)** 277-288.

[194] J. Chen, S. Zhang, Y. Jiang, L. Li, M. Zhou, T. Jiang, *A New Type of Clay Resistant Polycarboxylate Superplasticizers with a Snowflake-shaped Molecular Structure*, International Conference on Advanced Chemical Engineering and Environmental Sustainability (ICACEES) **(2018)** 351-364.

[195] X. Lin, M. Zhou, S. Wang, H. Lou, D. Yang, X. Qui, *Synthesis, Structure, and Dispersion Property of a Novel Lignin-Based Polyoxyethylene Ether from Kraft Lignin and Poly(ethylene)glycol*, ACS Sustainable Chemistry and Engineering 2 **(2014)** 1902-1909.

[196] T. Zheng, D. Zheng, X. Qiu, D. Yang, L. Fan, J. Zheng, *A novel branched claw-shape lignin-based polycarboxylate superplasticizer: Preparation, performance and mechanism*, Cement and Concrete Research 119 **(2019)** 89-101.

[197] Z. Huang, Y. Yang, Q. Ran, J. Liu, *Preparing hyperbranched polycarboxylate superplasticizers possessing excellent viscosity-reducing performance through in situ redox initialized polymerization method*, Cement and Concrete Composites 93 **(2018)** 323-330.

[198] X. Lin, B. Liao, J. Li, J. Huang, M. Lu, H. Pang, *Effect of crosslinked polycarboxylate superplasticizers with varied structures on cement dispersion performance*, Journal of Applied Polymer Science 138 (11) **(2020)** 50012.

[199] N. Zeng, Y. Yu, J. Chen, X. Meng, L. Peng, Y. Dan, L. Jiang, *Facile synthesis of branched polyvinyl acetate via redox-initiated radical polymerization*, Polymer Chemistry 23 (9) **(2018)** 3215-3222.

[200] K. Si, X. Q. Guo, K. Y. Qiu, *Initiation Mechanism of Radical Polymerization Using Ammonium Persulfate and Polymerizable Amine Redox Initiators*, Journal of Macromolecular Science Part A 32 **(1995)** 1149-1159.

[201] X. Lin, B. Liao, J. Zhang, S. Li, J. Huang, H. Pang, *Synthesis and characterization of high-performance cross-linked polycarboxylate superplasticizers*, Construction and Building Materials 210 **(2019)** 162-171.

[202] C. Shou, W. Xiao, *Hyper-branched polycarboxylate high-efficiency water reducing agent and preparation method thereof*, CN 101580353 B (Patent), **2012**.

[203] H. Frey, H. Kautz, *Hyperverzweigte Polymere: von baumartigen Makromolekülen zu Funktionsmaterialien*, Nachrichten aus der Chemie 50 (11) **(2002)** 1218-1224.

[204] E. Abbasi, S. F. Aval, A. Akbarzadeh, M. Milani, H. T. Nasrabadi, S. W. Joo, Y. Hanifehpour, K. Nejati-Koshki, R. Pashaei-Asl, *Dendrimers: synthesis, applications, and properties*, Nanoscale Research Letters 9 **(2014)** 247.

[205] B. Voit, *New developments in hyperbranched polymers*, Journal of Polymer Science Part A: Polymer Chemistry 38 (14) **(2000)** 2505-2525.

[206] A. Sunder, R. Hanselmann, H. Frey, R. Mülhaupt, *Controlled synthesis of hyperbranched polyglycerols by ring-opening multibranching polymerization*, Macromolecules 32 **(1999)** 4240-4246.

[207] M. Schömer, C. Schüll, H. Frey, *Hyperbranched aliphatic polyether polyols*, Journal of Polymer Science, Part A: Polymer Chemistry 51 **(2013)** 995-1019.

[208] E. Moore, H. Thissen, N. H. Voelcker, *Hyperbranched polyglycerols at the biointerface*, Progress in Surface Science 88 **(2013)** 213-236.

[209] D. Wilms, S.-E. Stiriba, H. Frey, *Hyperbranched Polyglycerols: From the Controlled Synthesis of Biocompatible Polyols to Multipurpose Applications*, Accounts of Chemical Research 43 (1) **(2010)** 129-141.

[210] S. Abbina, S. Vappala, P. Kumar, E. M. J. Siren, C. C. La, U. Abbasi, D. E. Brooks, J. N. Kizhakkedathu, *Hyperbranched polyglycerols: recent advances in synthesis, biocompatibility and biomedical applications*, Journal of Materials Chemistry B 5 **(2017)** 9249-9277.

[211] R. K. Kainthan, E. B. Muliawan, S. G. Hatzikiriakos, D. E. Brooks, *Synthesis, Characterization, and Viscoelastic Properties of High Molecular Weight Hyperbranched Polyglycerols*, Macromolecules 39 **(2006)** 7708-7717.

[212] D. Wilms, F. Wurm, J. Nieberle, P. Böhm, U. Kemmer-Jonas, H. Frey, *Hyperbranched polyglycerols with elevated molecular weights: A facile two-step synthesis protocol based on polyglycerol macroinitiators*, Macromolecules 42 (9) **(2009)** 3230-3236.

[213] H. Frey, R. Haag, *Dendritic polyglycerol: a new versatile biocompatible material*, Reviews in Molecular Biotechnology 90 **(2002)** 257-267.

[214] E. Barriau, H. Frey, A. Kiry, M. Stamm, F. Gröhn, *Negatively charged hyperbranched polyether-based polyelectrolytes*, Colloid and Polymer Science 284 (11) **(2006)** 1293-1301.

[215] M. Weinhart, D. Gröger, S. Enders, J. Dernedde, R. Haag, *Synthesis of Dendritic Polyglycerol Anions and Their Efficiency Towards L-Selectin Inhibition*, Biomacromolecules 12 **(2011)** 2502-2511.

[216] H. Gheybi, S. Sattari, A. Bodaghi, K. Soleimani, A. Dadkhah, M. Adeli, *Polyglycerols*, In: A. Parambath (Ed.), Engineering of Biomaterials for Drug Delivery Systems: Beyond Polyethylene Glycol, Woodhead Publishing Series in Biomaterials, **2018**, 103-172.

[217] G. Wang, L. Li, J. Lan, L. Chen, J. You, *Biomimetic crystallization of calcium carbonate spherules controlled by hyperbranched polyglycerols*, Journal of Materials Chemistry 18 **(2008)** 2789-2797.

[218] M. Balz, E. Barriau, V. Istratov, H. Frey, W. Tremel, *Controlled crystallization of $CaCO_3$ on hyperbranched polyglycerol adsorbed to self-assembled monolayers*, Langmuir 21 **(2005)** 3987-3991.

[219] Y. Chen, H. Frey, R. Thomann, S.-E. Stiriba, *Optically active amphiphilic hyperbranched polyglycerols as templates for palladium nanoparticles*, Inorganica Chimica Acta 359 (6) **(2006)** 1837-1844.

[220] Y. Shen, G. He, Y. Guo, H. Xie, W. Fang, *Modified Hyperbranched Polyglycerol as Dispersant for Size Control and Stabilization of Gold Nanoparticles in Hydrocarbons*, Nanoscale Research Letters 12 **(2017)** 525.

[221] Z. Zolek-Tryznowska, M. Tryznowski, J. Krolikowska, *Hyperbranched polyglycerol as an additive for water-based printing ink*, Journal of Coatings Technology and Research 12 (2) **(2015)** 385-392.

[222] V. Istratov, H. Kautz, Y.-K. Kim, R. Schubert, H. Frey, *Linear-dendritic nonionic poly(propylene oxide)-polyglycerol surfactants*, Tetrahedron 59 **(2003)** 4017-4024.

[223] M. A. Carey, S. L. Wellons, D. K. Elder, *Rapid method for measuring the hydroxyl content of polyurethane polyols*, Journal of Cellular Plastics 20 **(1984)** 42-48.

[224] M. Böse, J. Ehlers, F. Lehmkuhl, *Das Tertiär – nicht nur Braunkohle*, Deutschlands Norden, Springer Verlag, **2018**, 41-50.

[225] F. Rosendahl, *Die Entstehung der Kohle im Lichte der chemischen und biologischen Forschung*, Naturwissenschaften 19 (13) **(1931)** 281-289.

[226] J. Grotzinger, T. Jordan, *Press/Siever Allgemeine Geologie, Kapitel 23: Mensch und Umwelt*, 7. Auflage, Springer Spektrum, **2017**, 657.

[227] W. H. Orem, R. B. Finkelman, *Coal Formation and Geochemistry*, Treatise on Geochemistry 7 **(2003)** 191-222.

[228] P. G. Hatcher, D. J. Clifford, *The organic geochemistry of coal: from plant materials to coal*, Organic Geochemistry 27 (5/6) **(1997)** 251-274.

[229] S. P. Schweinfurth, *Coal – A Complex Natural Resource, An overview of factors affecting coal quality and use in the United States*, U.S. Geological Survey Circular 1143, **2003**, 1-39.

[230] K. Krol-Domanska, B. Smolinska, *Advantages of lignite addition in purification process of soil polluted by heavy metals*, Biotechnology and Food Sciences 76 (1) **(2012)** 51-58.

[231] J. P. Mathews, A. L. Chaffee, *The molecular representations of coal – A review*, Fuel 96 **(2012)** 1-14.

[232] E. A. Wolfrum, *Correlations Between Petrographical Properties, Chemical Structure, and Technological Behavior of Rhenish Brown Coal*, In: H. Schobert (Ed.), The Chemistry of Low-Rank Coals, Chapter 2, ACS Symposium Series 264, **1984**, 15-37.

[233] M. Mikos-Szymanska, S. Schab, P. Rusek, K. Borowik, P. Bogusz, M. Wyzinska, *Preliminary Study of a Method for Obtaining Brown Coal and Biochar Based Granular Compound Fertilizer*, Waste and Biomass Valorization 10 **(2019)** 3673-3685.

[234] F. J. Stevenson, *Humus Chemistry: Genesis, Composition, Reactions*, 2nd Edition, Wiley, **1994**.

[235] E. M. Pena-Mendez, J. Havel, J. Patocka, *Humic substances – compounds of still unknown structure: applications in agriculture, industry, environment, and biomedicine*, Journal of Applied Biomedicine 3 **(2005)** 13-24.

[236] D. Eifler, *Charakterisierung von Huminstoffen durch Fraktionierung und Metallgehaltsbestimmung mittels eines gekoppelten Systems Kapillarelektrophorese – induktiv gekoppeltes Plasma Massenspektrometer*, Dissertation, Universität Hamburg, **2005**, 9.

[237] L. S. Pang, A. M. Vassallo, M. A. Wilson, *Chemistry of alkali extraction of brown coals – I. Kinetics, characterisation and implications to coalification*, Advances in Organic Geochemistry 16 (4-6) **(1990)** 853-864.

[238] D. Garcia, J. Cegarra, M. Abad, F. Fornes, *Effects of the extractants on the characteristics of a humic fertilizer obtained from lignite*, Bioresource Technology 43 **(1993)** 221-225.

[239] F. J. Stevenson, J. H. A. Butler, *Chemistry of Humic Acids and Related Pigments*, In: G. Eglinton, M. T. J. Murphy (Eds.), Organic Geochemistry, Springer-Verlag, **1969**, 534-557.

[240] J. Buffle, F.-L. Greter, W. Haerdi, *Measurement of Complexation Properties of Humic and Fulvic Acids in Natural Waters with Lead and Copper Ion-Selective Electrodes*, Analytical Chemistry 49 (2) **(1977)** 216-222.

[241] a) https://www.indiamart.com/proddetail/humic-acid-13204176933.html (abgerufen: 01.09.21)

b) https://www.indiamart.com/proddetail/25kg-fulvic-acid-20538725712.html (abgerufen: 01.09.21)

[242] J. D. Berry, M. J. Neeson, R. R. Dagastine, D. Y. C. Chan, R. F. Tabor, *Measurement of surface and interfacial tension using pendant drop tensiometry*, Journal of Colloid and Interface Science 454 **(2015**) 226-237.

[243] C. Tiemeyer, A. Lange, J. Plank, *Determination of the adsorbed layer thickness of functional anionic polymers utilizing chemically modified polystyrene nanoparticles,* Colloids and Surfaces A: Physicochemical and Engineering Aspects 456 **(2014)** 139-145.

[244] W. Burchard, *Static and dynamic light scattering from branched polymers and biopolymers*, Advances in Polymer Science 48 **(1983)** 1-124.

[245] http://www.avantech.in/products/icar-rheometer-self-compacting-concrete-rheology.aspx (abgerufen: 01.09.21)

[246] M. Ilg, J. Plank, *Synthesis and Properties of a Polycarboxylate Superplasticizer with a Jellyfish-Like Structure Comprising Hyperbranched Polyglycerols*, Industrial & Engineering Chemistry Research 58 (29) **(2019)** 12913-12926.

9. Anhang

Im Folgenden sind noch weitere Publikationen dargestellt, die während der Promotionszeit entstanden sind.

9.1. Veröffentlichung aus der Mitarbeit an Projekten anderer Doktoranden

Publikation #12 resultierte aus der Zusammenarbeit (Teamarbeit) mit anderen Doktoranden am Lehrstuhl sowie einer Arbeitsgruppe in China. Sie beschreibt die Mikrostrukturanalyse von IPEG-PCEs durch ^{13}C NMR-Spektroskopie und Gelpermeationschromatographie. Über ^{13}C NMR-Spektroskopie wurde die Häufigkeit spezifischer Monomersequenzen (Triaden) im PCE-Polymer aufgeklärt. Mit Hilfe dieser Ergebnisse sowie jenen aus der GPC zur Molmassenverteilung und Einheitlichkeit des Polymers wurde die Mikrostruktur hergeleitet.

Auf diese Weise konnte die Monomerabfolge innerhalb der einzelnen PCEs aufgeklärt und ein besseres Verständnis darüber erhalten werden, welche spezifischen Mikrostrukturen bei bestimmten Verhältnissen von Acrylsäure und IPEG-Makromonomer im Polymer tatsächlich vorliegen. Abschließend wurde der Einfluss der Mikrostrukturen auf die Dispergierwirkung der PCEs untersucht.

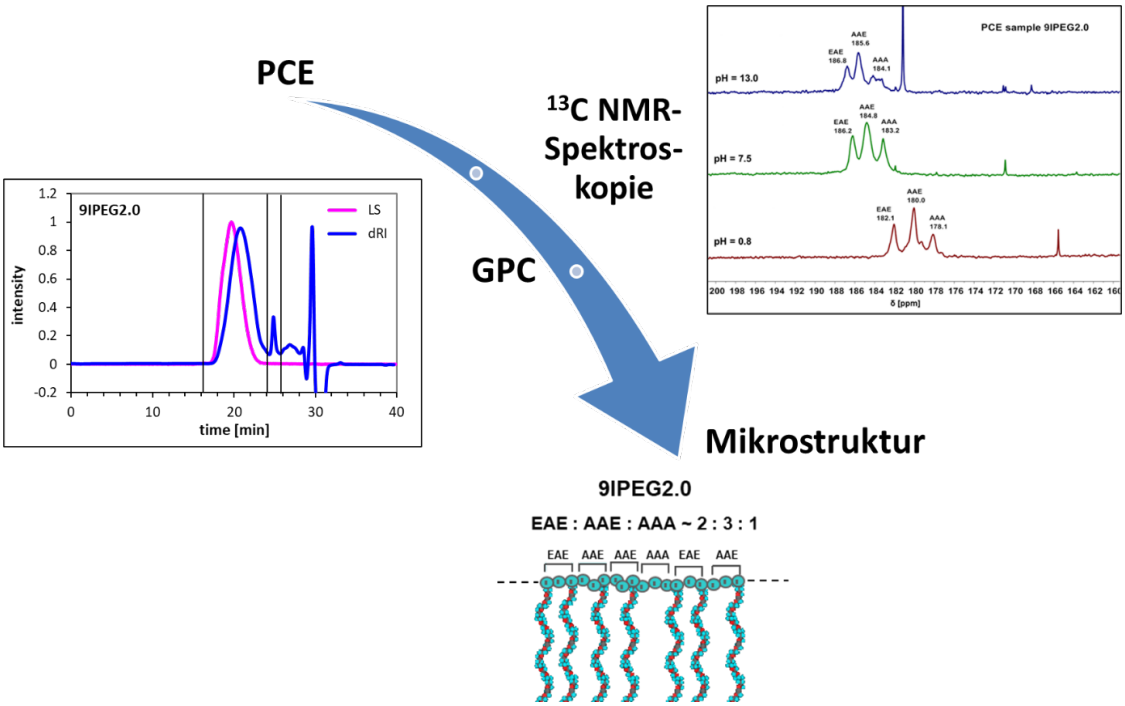

Abbildung A1: Mikrostrukturanalyse von IPEG-PCEs über eine Kombination von ^{13}C NMR-Spektroskopie und GPC-Messungen; Abbildungen aus [148].

9.1.1. Publikation #12: A microstructural analysis of isoprenol ether-based polycarboxylates and the impact of structural motifs on the dispersing effectiveness

Publikation #12

A microstructural analysis of isoprenol ether-based polycarboxylates and the impact of structural motifs on the dispersing effectiveness

Johann Plank, Huiqun Li, Manuel Ilg, Julia Pickelmann,

Wolfgang Eisenreich, Yan Yao, Ziming Wang

Cement and Concrete Research

84 (2016) 20 – 29

Doi: 10.1016/j.cemconres.2016.02.010

Cement and Concrete Research 84 (2016) 20–29

Contents lists available at ScienceDirect

Cement and Concrete Research

journal homepage: www.elsevier.com/locate/cemconres

A microstructural analysis of isoprenol ether-based polycarboxylates and the impact of structural motifs on the dispersing effectiveness

Johann Plank [a,*], Huiqun Li [a,b,d], Manuel Ilg [a], Julia Pickelmann [a], Wolfgang Eisenreich [c], Yan Yao [d], Ziming Wang [b]

[a] Technische Universität München, Chair for Construction Chemistry, 85747 Garching, Lichtenbergstraße 4, Germany
[b] Beijing University of Technology, College of Materials Science and Engineering, 100124 Beijing, China
[c] Technische Universität München, Chair for Biochemistry, 85747 Garching, Lichtenbergstraße 4, Germany
[d] China Building Materials Academy, State Key Laboratory of Green Building Materials, 100024 Beijing, China

ARTICLE INFO

Article history:
Received 7 August 2015
Accepted 17 February 2016
Available online 14 March 2016

Keywords:
Admixture (D)
Microstructure (B)
^{13}C NMR spectroscopy (B)
Polycarboxylate superplasticizer
Polymers (D)

ABSTRACT

Generally, polycarboxylate superplasticizers (PCEs) are synthesized via aqueous free radical copolymerization. The conditions during copolymerization such as relative reactivity and feeding mode and ratio of monomers can cause different monomer sequences in the final product. In this study, the sequence of monomers in PCE polymers synthesized from acrylic acid and isoprenyloxy polyethylene glycol (IPEG) macromonomer was characterized by ^{13}C nuclear magnetic resonance (NMR) spectroscopy. Three different triads of monomer sequences (EAE, AAE and AAA; E = ether, A = acid monomer) were detected. It was found that IPEG PCEs predominantly contain the structural motifs of AAE and EAE, and less of AAA. Higher additions of acrylic acid do not incorporate into the structure of PCE, but convert to HMW polyacrylate as by-product instead. A PCE with optimal dispersing effectiveness was achieved at high contents of IPEG macromonomer, a molecular weight (M_w) around 40,000 Da and narrow molecular weight distribution.

1. Introduction

Polycarboxylate superplasticizers (PCEs) have become an essential admixture for the concrete industry since their invention in 1981 [1]. They can significantly improve fluidity, compressive strength and durability of concrete [2,3]. The designable structure of PCE endows them various preferential properties arising from specific microstructures.

It is known to those skilled in the art that in PCE copolymers, the feeding molar ratios of the macromonomers do not necessarily represent the actual molar ratios present in the final product. In fact, when combining such highly reactive monomers like acrylic acid or methacrylic acid with macromonomers, then copolymers of non-homogeneous composition are formed. In aqueous radical copolymerization the monomers can arrange randomly, alternating, in block or in graft chains. An overview of the different possibilities existing for a system composed of two monomers, A and B respectively, is shown in Fig. 1.

The sequence of monomers in copolymers can be predicted by the value of the monomer reactivity ratios. If the value of r_1 is higher than 1, then A tends to react with itself, thus forming a homopolymer or – in the case of two monomers – a block copolymer. For example, if r_1 is greater than 1 and r_2 less than 1, then a copolymer with blocks as shown in Fig. 2 is formed [4].

Exactly this situation occurs when acrylic acid and isoprenyloxy polyethylene glycol (IPEG) macromonomer are copolymerized, as it is well established that the reactivity of acrylic acid is much higher than that of the IPEG macromonomer [5]. Obviously, it is highly desirable to understand the actual sequence of monomers present in a synthesized PCE copolymer, as it may directly affect its adsorption behavior and dispersing power in cement paste. Thus, a suitable analytical method allowing precise determination of the monomer sequence in a PCE copolymer is most essential.

^{13}C NMR spectroscopy reflects the resonance of the ^{13}C nucleus to the external magnetic field which is affected by the electron density in the proximity. Thus, in a certain functional group the resonance of the ^{13}C nucleus varies with different neighboring monomers connected. This effect has been utilized to determine the monomer sequences present in methacrylate ester copolymers [6,7] and in hydrolyzed polyacrylamides [8]. Relative to PCEs, *Belloto* and *Rozzoni* have applied this method to methacrylate ester (MPEG)-based PCEs and revealed interesting details on the microstructural composition of these copolymers [9]. In the present study, this method was applied to analyze specifically synthesized IPEG PCE copolymers with the aim to compare the actual monomer sequence with that derived statistically from the molar feeding ratios.

* Corresponding author. Tel.: +49 89 289 13151; fax: +49 89 289 13152.
E-mail address: sekretariat@bauchemie.ch.tum.de (J. Plank).

http://dx.doi.org/10.1016/j.cemconres.2016.02.010
0008-8846/

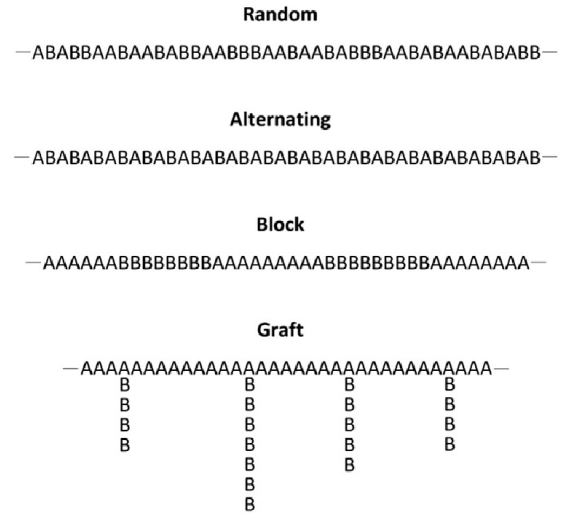

Fig. 1. Potential monomer sequences formed in free radical copolymerization of two monomers, A and B.

Theoretically, and assuming that the PCE polymer is prepared at a molar excess of acrylic acid over the IPEG macromonomer, then the monomer sequences expressed as triads as shown in Fig. 3 can occur in the PCE polymers. Note that sequence EEE was considered as unlikely and therefore excluded on the grounds of the relatively lower concentration and reactivity of the macromonomer compared to acrylic acid, as will be shown later. Similarly, AEA which presents a variation of the structural motif AAE was not considered here because later in the evaluation of the ^{13}C NMR spectra, no indication for occurrence of this monomer sequence was found.

The goal of this study was to determine the microstructure of four different IPEG PCE samples synthesized at varied molar ratios of acrylic acid to macromonomer (1:1, 2:1, 3:1 and 4.5:1) at a constant side chain length of 9 EO units in the macromonomer. Moreover, size exclusion chromatography (SEC) was applied to characterize the molecular properties and residual amounts of non-reacted IPEG macromonomer or acrylic acid homopolymer present in the final product.

PCE molecules can disperse cement particles effectively based on the combined effects of electrostatic repulsion and steric hindrance (an "electrosteric" effect) [10,11]. The sequence of monomers reflects the arrangement of the anchor and the pendant groups present in the PCE polymers. Apparently, such arrangement can have significant effect on the dispersing effectiveness of a PCE product. Therefore, the dispersing power of the synthesized copolymers was determined by using a mini slump test involving cement paste. The results were correlated with those obtained from the microstructural analysis, and a model was sought which can identify the microstructure which is optimal for the dispersion of cement.

2. Materials and experiments

2.1. Materials

The macromonomers isoprenyloxy polyethylene glycol ether with $M_w = 500$ Da and 1100 Da (abbreviated as IPEG-500 and IPEG-1100) containing 9 and 25 ethylene oxide units, respectively, were provided by Clariant Deutschland GmbH, Burgkirchen, Germany. These short-chain macromonomers were chosen to ensure a high content of the trigger carbon atoms in acrylic acid and IPEG macromonomer which is essential for the accuracy of the results from ^{13}C NMR spectroscopy. Sodium polyacrylate (Sokalan® PA 40) with a degree of polymerization (DP) of 40 was provided by BASF SE, Ludwigshafen, Germany. Acrylic acid, ammonium persulfate and sodium methyallyl sulfonate were all purchased from Sigma-Aldrich Chemie GmbH, Steinheim, Germany and used as is.

For the dispersing tests, a CEM I 52.5 N (Milke® Classic from HeidelbergCement, Geseke plant, Germany) was used. Its phase composition determined by quantitative X-ray diffraction including *Rietveld* refinement (Bruker axs D8) is shown in Table 1. Its average particle size (d_{50} value) was found at 11.5 μm (laser granulometer Cilas 1064, Cilas, Marseille, France) and its specific surface area (*Blaine* instrument, Toni Technik, Berlin, Germany) was 5383 cm^2/g.

2.2. Synthesis of PCE copolymers

A series of polycarboxylate superplasticizers with different molar ratios of acrylic acid to IPEG was synthesized by aqueous free radical copolymerization. The polymers were designated as xIPEGy.0, whereby x represents the degree of polymerization of ethylene oxide in the macromonomer; while y represents the molar ratio of acrylic acid to the macromonomer. Ammonium persulfate was used as initiator and sodium methallyl sulfonate as chain transfer agent. As an example, the preparation of 9IPEG2.0 polymer is described: 50.0 g of IPEG-500 macromonomer was dissolved in 80.0 g DI water and placed in a five neck round bottom flask with a mechanical stirrer and heated to 60 °C using a water bath. Then 14.4 g acrylic acid and 4.74 g of sodium methallyl sulfonate were dissolved in 15.0 g DI water. This mixture was designated as solution A. Next, 3.87 g of ammonium persulfate was dissolved in 15.0 g DI water and labeled as solution B. Solution A and B were fed separately and continuously into the reaction flask over a period of 3 h, followed by post treatment for 2 h at 60 °C. The reaction mixture was cooled to ambient and adjusted from pH ~ 1.5 to 7.5 with aqueous 30 wt.% NaOH solution, yielding a yellowish aqueous PCE solution with a solid content of 39 wt.%.

2.3. Size exclusion chromatography (SEC)

PCE solutions of 10 g/L concentration were used in the size exclusion chromatography (SEC) measurements. A Waters 2695 Separation Module equipped with three Ultrahydrogel™ columns (120, 250, 500) and a Ultrahydrogel™ guard column from Waters, Eschborn, Germany, and a three angle static light scattering detector ("mini Dawn" from Wyatt Technology Corp., Santa Barbara, CA, USA) was used in the measurements. Polymer concentration was recorded with a differential refractive index detector (RI 2412, Waters, Eschborn, Germany). Molecular weight, polydispersity index and hydrodynamic radius of the PCE polymers were obtained from the light scattering detector. As eluent, 0.1 N $NaNO_3$ adjusted to pH 12.0 pumped at a flow rate of 1.0 mL/min was used. For calculation of M_w and M_n a value of dn/dc of 0.135 mL/g (the value for polyethylene glycol) was adopted [12].

2.4. ^1H and ^{13}C NMR spectroscopic analysis

^1H NMR spectroscopy was used to calculate the actual molar ratio of monomers present in the synthesized PCE polymers. For these measurements, an AVANCE-III 400 MHz NMR spectrometer (Bruker BioSpin

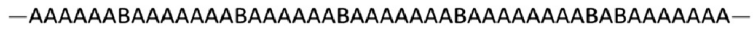

Fig. 2. Sequence of monomers A and B in a copolymer obtained when $r_1 > 1$ and $r_2 < 1$.

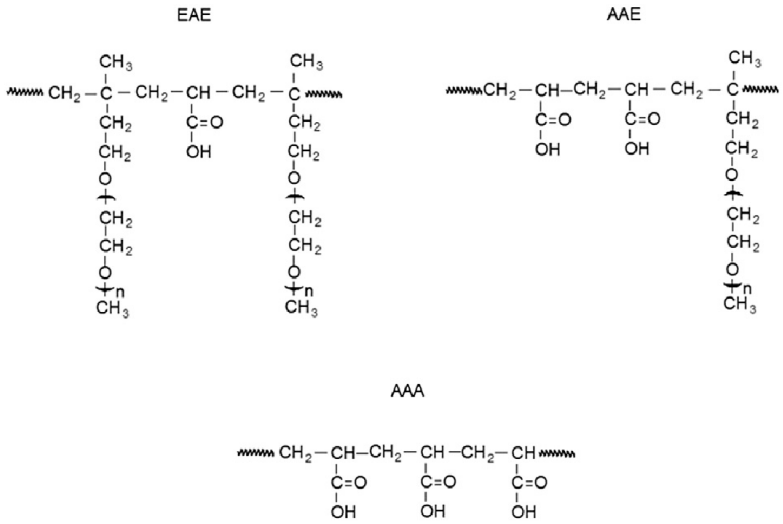

Fig. 3. Theoretically possible monomer sequences which can occur in PCE copolymers synthesized from acrylic acid and IPEG macromonomer (A = acrylic acid, E = IPEG macromonomer).

GmbH, Karlsruhe, Germany) operating with 16 scans and 1 s relaxation delay was utilized. Samples were prepared by dissolving the powdered PCE in D_2O at a concentration of 0.1 g/mL.

^{13}C NMR spectroscopy was employed to identify the microstructure (monomer sequences) present in the PCE copolymers. All ^{13}C NMR spectra for acrylic acid and sodium polyacrylate were recorded at 300 K on an AVANCE-III 400 MHz NMR spectrometer (Bruker BioSpin GmbH) operating at 100.6 MHz with 8200 scans, 2 s relaxation delay and under continuous ^{1}H radiation (cross polarization). Acrylic acid, sodium polyacrylate and the IPEG macromonomers were measured as references to determine the chemical shift of the marker carbon atoms (carboxyl carbon in acrylic acid and isoprenyl carbon directly attached to the ether oxygen in the macromonomer).

In analysis of the pH-dependent microstructure of PCE copolymer sample 9IPEG2.0 and 25IPEG2.0, the instrument parameters were 12,000 scans and 4 s relaxation delay on a 500 MHz NMR spectrometer (Bruker BioSpin GmbH) operating at 125.8 MHz which was equipped with a He cryo-cooled probehead (QNP CryoProbe). This higher frequency and the probehead optimized for ^{13}C detection were necessary to obtain a higher resolution with an improved signal-to-noise ratio. Furthermore, the FIDs were rocessed with mild Gaussian apodization in order to further enhance resolution.

Table 1
Phase composition of the CEM I 52.5 N sample as determined by Q-XRD using *Rietveld* refinement.

Phase	wt.%
C_3S, m	54.1
C_2S, m	26.6
C_3A, c	3.3
C_3A, o	4.3
C_4AF, o	2.5
Free lime (*Franke* method)	0.1
Periclase (MgO)	0.0
Anhydrite	2.6
$CaSO_4$-hemihydrate[a]	1.21
Gypsum[a]	0.02
Calcite	3.6
Quartz	1.2
Arcanite (K_2SO_4)	0.5

[a] Determined by thermogravimetry.

2.5. Dispersing effectiveness

Fluidity of cement pastes was determined in a modified mini slump test according to DIN EN 1015 at a w/c ratio of 0.3 [13]. The dosage of PCE was adjusted to achieve a spread flow of 26 ± 0.5 cm for the cement paste. The mini slump test was conducted as follows: In a porcelain cup the PCE solution was dissolved in DI water and then within one minute 300 g of cement were added to the mixing water which was allowed to soak for one minute, followed by two minutes of continuous manual stirring and subsequent transfer into a *Vicat* cone (height 40 mm, top diameter 70 mm, bottom diameter 80 mm) placed on a glass plate. The cone was then lifted vertically and the final flow spread was recorded as the average of two perpendicular diameters of the cement paste.

3. Results and discussion

3.1. Molecular properties of synthesized PCE polymers

The molecular properties of the 9IPEGy.0 polymer series were analyzed by size exclusion chromatography (SEC). The respective spectra are shown in Fig. 4 and the results are tabulated in Table 2.

Analysis of the SEC data reveals that with increasing acrylic acid content, the initially monomodal polymer distribution present in 9IPEG1.0 and 9IPEG2.0 turns into a bimodal (for 9IPEG3.0) and even a trimodal distribution for 9IPEG4.5. This suggests that at increased acrylic acid contents, a mixture of copolymers is produced with presumably quite different compositions. For the PCE polymers 9IPEG1.0 and 9IPEG2.0, M_w values of 13,600 and 36,600 g/mol were found which are characteristic for PCE products [14]. Whereas for copolymer 9IPEG3.0, a peak at M_w = 40,600 g/mol signifying the PCE copolymer and another peak at M_w = 211,000 g/mol likely containing a large amount of acrylic acid or even representing homopolymerized acrylic acid were detected. Finally, the polymer 9IPEG4.5 even exhibits a third fraction (shoulder) at M_w ~ 1.4 mio. g/mol, thus indicating that such high contents of acrylic acid lead to increasingly inhomogeneous products.

The reactivity of the IPEG macromonomer is lower than that of acrylic acid, because of higher stability of the radical and the steric hindrance induced by the bulky monomer during polymerization. To account for this, in the PCE synthesis the IPEG macromonomer

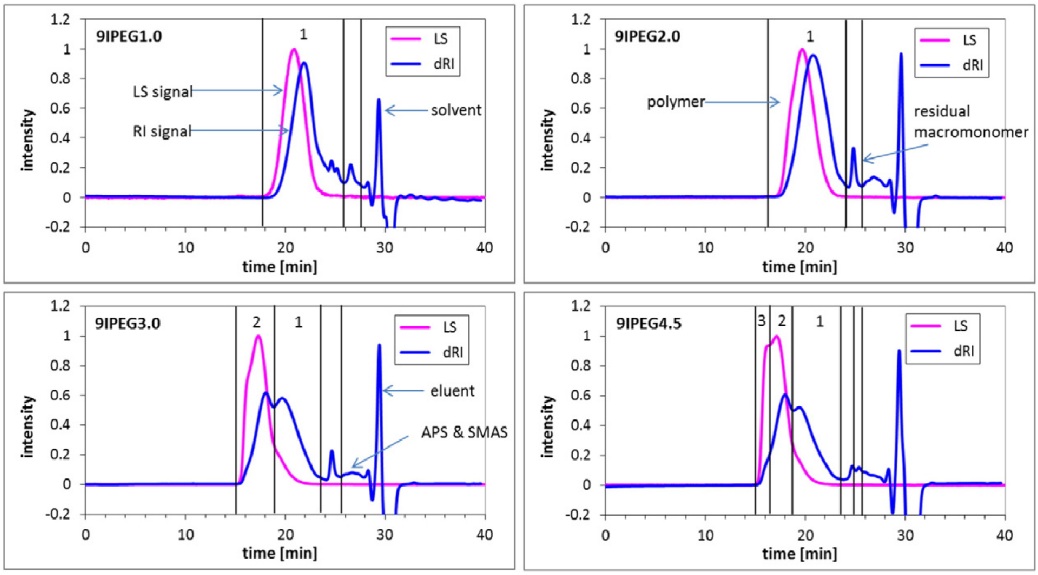

Fig. 4. SEC spectra of the 9IPEGy.0 polymer series (y = 1; 2; 3; 4.5).

was placed in the reactor from the beginning while acrylic acid was dropped in continuously, thus providing acrylic acid with the possibility to polymerize in an excess of macromonomer. Through this method, a higher conversion of the macromonomer was achieved, as is evidenced from the data presented in Table 2 (90.2–94.3%). As expected, the conversion increased when more acrylic acid was used.

3.2. Monomeric composition of the PCE samples

A quantitative analysis of the PCE polymers via ^{1}H NMR spectroscopy (as an example the spectrum for 9IPEG3.0 is displayed in Fig. 5) revealed that for all polymer samples, the actual molar ratios of acrylic acid to IPEG macromonomer were slightly higher than the feeding ratios (Table 3), as was derived already from the SEC data and the IPEG conversion values shown in Table 2. These data again confirm a higher reactivity for acrylic acid than for the macromonomer. Note that all polymer compositions obtained from ^{1}H NMR analysis as exhibited in Table 3 were calculated by subtracting the amount of non-reacted IPEG macromonomer as determined via SEC (Table 2). Furthermore, for 9IPEG1.0 and 9IPEG2.0 the molar ratios displayed in Table 3 present the actual compositions of the PCE molecules because they consist of one polymer fraction only whereas the values obtained for 9IPEG3.0 and 9IPEG4.5 refer to the entire reaction product which presents a mixture of different polymers (see Fig. 11).

Table 2
Molecular parameters and macromonomer conversion for the 9IPEGy.0 polymer series.

Polymer sample	M_w average[a] (g/mol)	PDI (M_w/M_n)	M_w (g/mol)			Conversion of IPEG macrom. (%)
			Peak #1	Peak #2	Peak #3	
9IPEG1.0	13,600	2.5	13,600	–	–	90.2
9IPEG2.0	36,600	2.6	36,600	–	–	91.6
9IPEG3.0	81,700	3.0	40,600	211,100	–	94.3
9IPEG4.5	261,000	4.8	46,600	329,000	1,430,000	94.0

[a] Average across all polymer peaks.

3.3. ^{13}C NMR spectroscopy

The monomer sequence present in the synthesized PCE copolymers was assessed via ^{13}C NMR spectroscopy.

3.3.1. Analysis of AA and PAA

At first, the pH dependent appearances of the ^{13}C signals of acrylic acid were examined. For this purpose, acrylic acid was dissolved in D_2O at pH values of 1.0; 7.5 and 13.0, and the spectra were recorded. Generally, when acrylic acid is neutralized with a base then the carboxylic acid becomes deprotonated, thus leading to an increased electron density at the carboxyl carbon. Accordingly, the chemical shift of the carboxyl carbon should be pH dependent.

As can be seen from Fig. 6, a significant low field shift from 170.0 ppm to 175.5 ppm was indeed observed for the carboxyl carbon when the pH value increased from 1.0 to 13.0, thus confirming that the resonance of the carboxyl carbon in acrylic acid is strongly pH dependent [15]. Conversely, the chemical shifts of the methylene and methine groups contained in acrylic acid shift only slightly (~1 ppm) as the pH value increases. This observation is in accordance with earlier reports in the literature [16].

The ^{13}C NMR spectroscopic data confirm that most of the acrylic acid (pK_a value 4.25) is deprotonated when the pH value was adjusted to 7.5, and that only a few carboxylic acid molecules were left to be deprotonated from pH 7.5 to 13.0. Consequently, the resonance of the carboxyl carbon exhibited a major shift when the pH value was modulated from 1.0 to 7.5, and only a minor shift when the pH value was further increased from 7.5 to 13.0.

Additionally, the ^{13}C NMR spectrum of sodium polyacrylate was recorded in D_2O at pH = 1.0; 7.5 and 13.0, respectively (Fig. 7). At pH = 1.0, a signal attributed to the carboxyl carbon is observed at δ = 178.7 ppm which is in accordance with the results from a previous study [17]. Whereas, at pH = 7.5 and 13.0 the signal splits as a result of the tacticity of the carboxylate functionality along the polymer chain. Apparently, at pH = 1 the chemical shift of the carboxyl carbon present in polyacrylic acid appears at ~179 ppm which is ~9 ppm higher than in monomeric acrylic acid at the same pH value. This indicates that

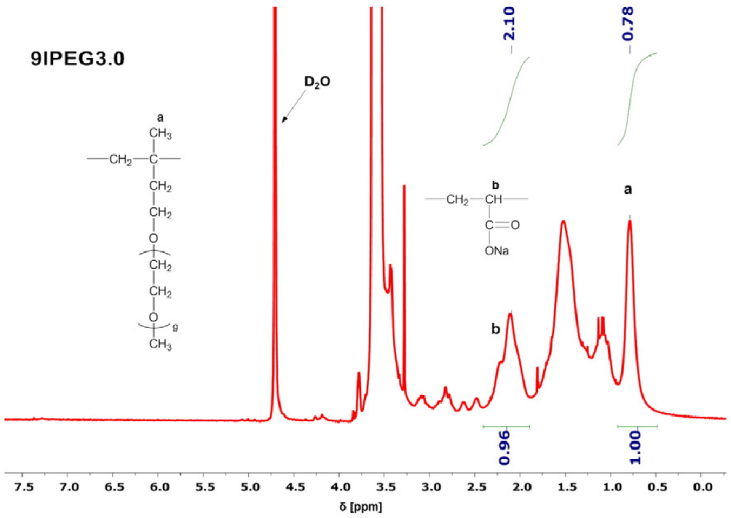

Fig. 5. ^{1}H NMR spectrum of PCE sample 9IPEG3.0.

the electron density in the vicinity of the carbonyl carbon changes as a result of the change from the CC double bond in acrylic acid to a C–C single bond present in the polymerized form. Thus, the ^{13}C NMR signal provides information about the electronic environment (chemical bond and type of functionality/substituent) around the carboxyl carbon. This effect can be utilized for a more detailed microstructural analysis of PCE copolymers.

Another difference between acrylic acid and sodium polyacrylate is that for the latter, the chemical shifts of the ^{13}C signal of the carboxyl carbon are (within the accuracy of the instrument) identical at pH 7.5 and 13.0, respectively, whereas a noticeable change was observed for monomeric acrylic acid (Fig. 6).

3.3.2. Analysis of the monomer sequence

As presented above, the ^{13}C nucleus in a specific group is impacted by the neighboring monomers. In PCEs, the interesting point is the repartition of pendant groups along the main chain, because different repartitions can lead to quite different behaviors, e.g. with respect to adsorption, and sulfate tolerance. [18,19]. Previously, we have studied the repartition of side chains in methacrylate ester-based PCE copolymers by using ^{13}C NMR spectroscopic analysis [20]. Here, this technique was applied to study the synthesized IPEG PCE polymers.

As an example, the ^{13}C NMR spectra relating to the carboxyl carbon of acrylic acid incorporated into the 9IPEG2.0 polymer is discussed (Fig. 8). Similar to pure acrylic acid, a clear pH dependence of the signals can be observed, whereby the major shift to low field occurs when the pH is increased from 0.8 to 7.5. This finding again suggests that when conducting the microstructural analysis, then all samples should be examined at the same pH value to allow proper comparison.

Table 3
Molar ratios of acrylic acid to IPEG-500 macromonomer in the 9IPEG polymers as found via SEC and ^{1}H NMR spectroscopy.

Sample	Molar ratio of acrylic acid: macromonomer		
	Theoretical	From SEC	From ^{1}H NMR
9IPEG1.0	1.0	1.11	1.11
9IPEG2.0	2.0	2.18	2.31
9IPEG3.0	3.0	3.18[a]	3.03[a]
9IPEG4.5	4.5	4.79[a]	4.62[a]

[a] Average value across all polymer fractions.

Furthermore, at all pH values the PCE samples generally exhibit three distinct signals for the carboxyl carbon which represent the three potential monomer sequences (triads) occurring in this PCE, as shown in Fig. 3. The methyl carbon connected to the quaternary carbon present in the backbone of the IPEG PCE acts as an electron donor group. This effect increases the electron density around the carboxyl carbon as well as its chemical shift in the ^{13}C NMR spectrum. Therefore, the resonances recorded in the ^{13}C NMR spectrum of 9IPEG2.0 can be assigned as follows (pH = 13.0): δ (EAE) = 186.8 ppm; δ (AAE) = 185.6 ppm; δ (AAA) = 184.1 ppm. Obviously, based on signal intensity the monomer sequence AAE is the most frequent one in the molecule. Whereas the two other sequences, AAA and EAE are less frequent, but do occur in the PCE molecule. Accordingly, it is demonstrated that the repartition of side chains along the polymer trunk by no means is homogeneous, as is often assumed. Instead, during copolymerization a random distribution occurs, with a statistically higher occurrence of the idealized composition AAE.

For comparison, the ^{13}C NMR spectrum of PCE polymer 25IPEG2.0 exhibiting a longer side chain (25 EO units *versus* 9 in 9IPEG2.0) was recorded (Fig. 9). There, polymer 25IPEG2.0 exhibits the same three resonances representing the monomer sequences EAE, AAE and AAA, as detected before for polymer 9IPEG2.0 (Fig. 8). Furthermore, the relative intensities of the triad signals are identical with those of 9IPEG2.0. This finding suggests that more bulky macromonomers seem to possess similar reactivity like their shorter analogs, and thus do not much impact the repartition of the side chains along the main chain.

3.3.3. Monomer sequence in PCE samples 9IPEGy.0

The ^{13}C NMR spectra displaying the carboxyl carbon contained in the 9IPEGy.0 series of polymers representing the different molar feeding ratios of acrylic acid to IPEG macromonomer of 1:1, 2:1, 3:1 and 4.5:1 are shown in Fig. 10. The spectra clearly reveal that the molar feeding ratio of the monomers determines the monomer sequence in the 9IPEGy.0 polymer series. For example, in 9IPEG1.0 the main unit is EAE, followed by very minor amounts of the sequences AAE and AAA. However, in the ^{13}C NMR spectrum of sample 9IPEG2.0, AAE represents the most frequent unit while EAE and especially AAA are less dominant. The same behavior was found for polymer 9IPEG3.0, with the only difference being that the signal for triad AAA broadened and increased as a consequence of the higher feeding amount of acrylic acid. The broadening of the signal can be attributed to the presence of two different polymers

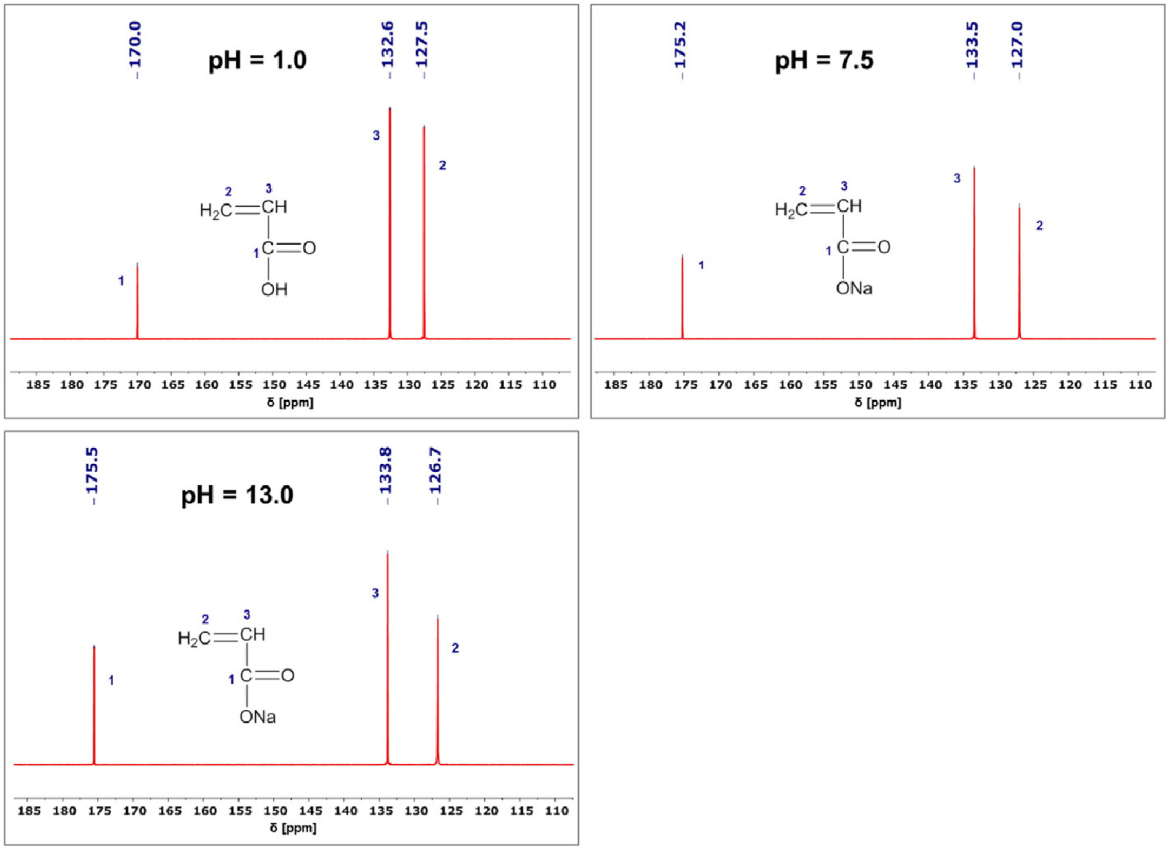

Fig. 6. ^{13}C NMR spectra of acrylic acid in D_2O at pH 1.0; 7.5 and 13.0, respectively.

now, one being the PCE copolymer and the second a homopolymer of acrylic acid, as will be shown later. Finally, in polymer sample 9IPEG4.5 the structural unit AAA had become the prevalent one now, while the sequence representing EAE had almost disappeared from the spectrum.

The ^{13}C NMR spectra of the 9IPEGy.0 polymer series allow to develop an idea of the actual average composition and microstructure of these polymers as a function of the feeding ratios of the monomers. According to SEC analysis (Fig. 4), the polymer distribution in samples 9IPEG1.0 and 2.0 is monomodal, i.e. they contain a relatively uniform polymer species. Based on this information, structural models for both polymers can be derived whereby the frequency of each structural motif was adjusted to comply with the ^{13}C NMR data as shown in Fig. 10. The result is displayed in Fig. 11.

The microstructural analysis of the 9IPEG3.0 and 9IPEG4.5 polymer samples is more complicated, because they clearly represent mixtures of polymers as is obvious from their SEC spectra (Fig. 4). Polymer 9IPEG3.0 constitutes a binary mixture of polymers, and sample 9IPEG4.5 even contains a very minor portion of a third, extremely high molecular weight component (see Table 2). Considering the low field shift of the AAA signal with increasing acrylic acid content (from $\delta = 183.9$ ppm in 9IPEG1.0 to 184.5 ppm in 9IPEG4.5) which is identical with that of sodium polyacrylate ($\delta = 184.5$ ppm, see Fig. 7) one can assume that the high molecular weight portions present in both polymers are sodium polyacrylate which is also suggested by the chemical shift of the AAA motif, while the remainder is a typical PCE copolymer with AAE as the main unit. Hence, for 9IPEG3.0 the supposed average composition of EAE:AAE:AAA is around 1:4:1 for the main fraction and polyacrylate as a second minor fraction (Fig. 11). Sample 9IPEG4.5 consists mainly of a densely grafted PCE copolymer in which the structural unit AAE is dominant and a sparsely grafted PCE and pure sodium polyacrylate represent minor constituents (Fig. 11).

It is therefore most remarkable that higher additions of acrylic acid lead to a more uniform PCE as the main product while at the same time minor amounts of pure PAA and of a low grafted PCE occur as by-products.

3.4. Dispersing effectiveness in cement

The impact of the different microstructures on the dispersing performance of these PCE copolymers in cement paste was evaluated. Both the initial flow value as well as time-dependent slump retention were tested with the aim to check whether a correlation exists between individual microstructures and dispersing effectiveness.

The dosages required for 9IPEG2.0 and 9IPEG3.0 samples to achieve an initial spread flow of 26 ± 0.5 cm were 0.27% and 0.42% by weight of cement (bwoc) respectively. As is shown in Fig. 12, the cement paste containing sample 9IPEG2.0 performed best with respect to dosage and also exhibited excellent slump retention over no less than 3 h which is considered to be excellent. On the contrary, the flow spread resulting from sample 9IPEG3.0 already decreased significantly after 0.5 h and provided no more workability after 1.5 h.

For the polymer samples 9IPEG1.0 and 9IPEG4.5 respectively, dosages in excess of 1.0% bwoc were required to achieve the flow spread of 26 ± 0.5 cm, far inferior to the two other PCE polymers. This finding

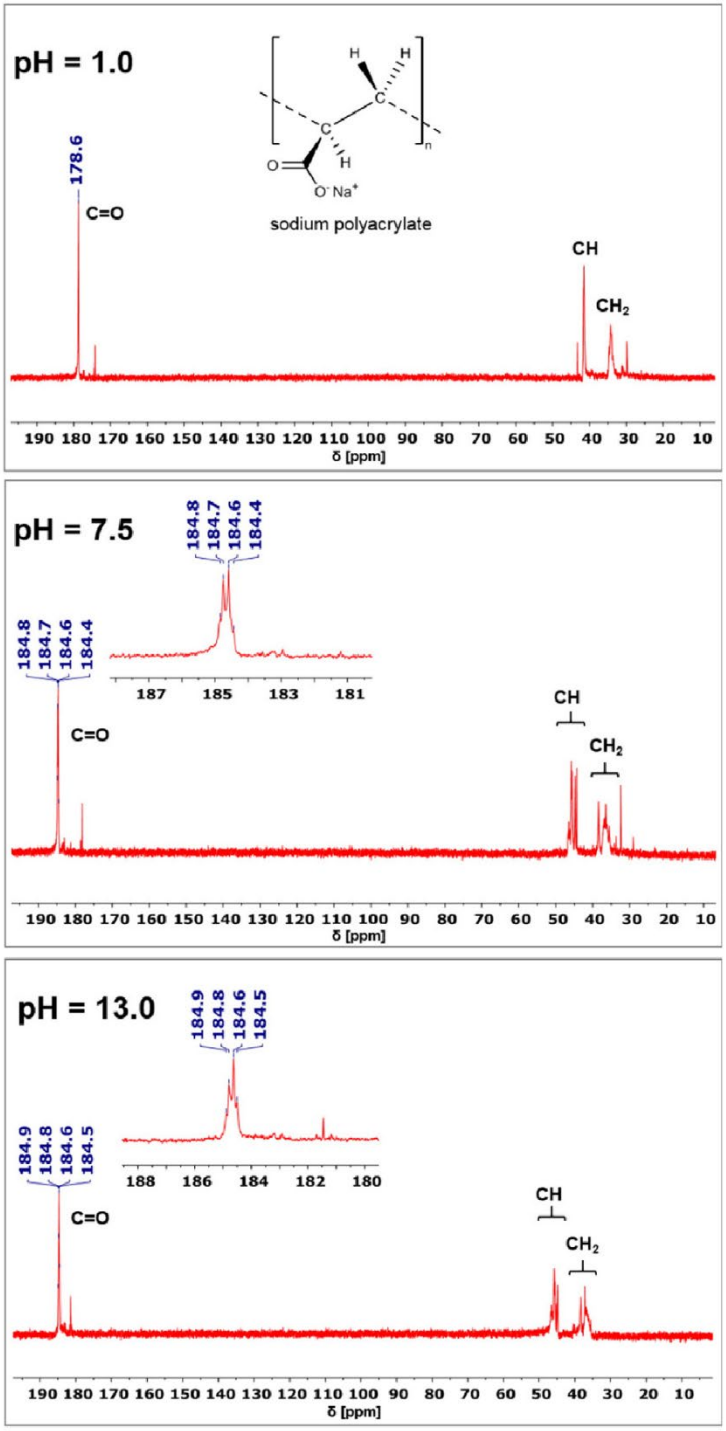

Fig. 7. pH-dependent ^{13}C NMR spectra of sodium polyacrylate at pH 1.0; 7.5 and 13.0, measured in D_2O.

suggests that in 9IPEG1.0, the amount of acrylic acid and hence its anionic character is too low to achieve a sufficiently high adsorbed amount which is required for effective dispersion [21]. Whereas, in 9IPEG4.5 the major constituent of the sample is polyacrylate of high molecular weight, which functions as a viscosifier and thus even counteracts the dispersing effect of the minor constituent PCE.

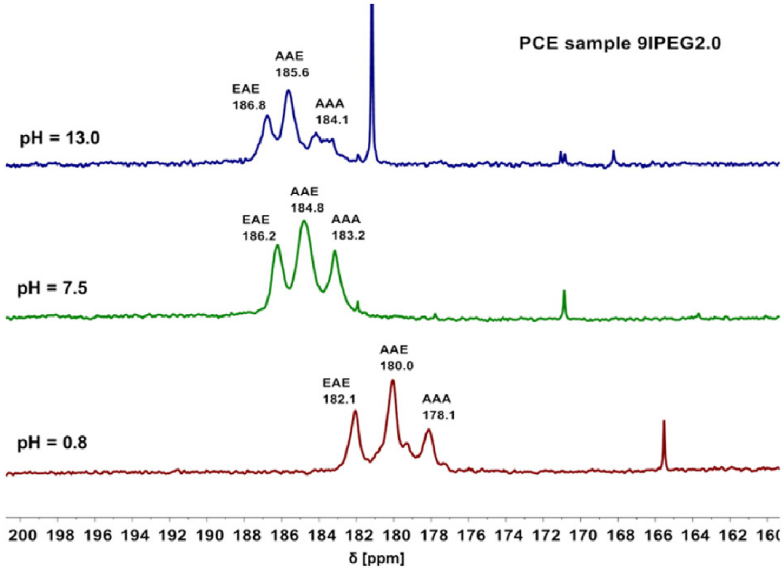

Fig. 8. pH-dependent ^{13}C NMR spectra of PCE product 9IPEG2.0 measured in D_2O at pH = 0.8; 7.5 and 13.0, revealing the monomer sequence present in the polymer.

Furthermore, the data also suggest that to achieve optimal dispersing efficiency a polymer predominantly comprised of AAE building units is preferable for the IPEG PCEs studied here, although some EAE and AAA motifs may be contained as well.

On a general note, when connecting dispersing performance characteristics with the molecular structure of PCEs one has to consider also the uniformity of the polymer product to allow specific conclusions. First, a thorough SEC analysis is required to differentiate single polymers from polymer mixtures; and second, it needs to be considered that depending on the synthesis process chosen the repartition of monomers along the main chain might differ within a polymer fraction, especially when higher values for the PDI are found. In such case it is impossible to extract from the data which polymer fraction is actually responsible for optimal dispersing performance.

4. Conclusions

In this study, the microstructure of PCE copolymers synthesized from acrylic acid and a short-chain IPEG macromonomer at molar ratios of AA to IPEG of 1:1 to 4.5 was investigated using ^{13}C NMR spectroscopy. The resonance of the carboxyl carbon present in acrylic acid was selected as the marker atom which can be used to identify and quantify the three potential structural motifs expressed as AAA, AAE and EAE.

It was found that this technique presents a semi-quantitative method to identify the actual microstructure (i. e. monomer sequence) occurring in these PCE copolymers. However, it is necessary to consider data from other methods, especially size exclusion chromatography, which provide information on the uniformity of the polymer to avoid misinterpretation. Following this approach, a relatively realistic concept of the

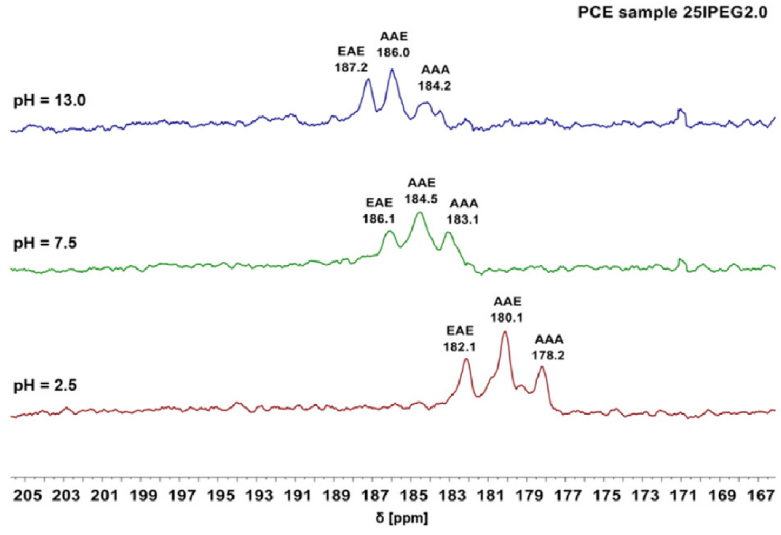

Fig. 9. pH dependent ^{13}C NMR spectra of PCE sample 25IPEG2.0, measured in D_2O at pH = 2.5; 7.5 and 13.0.

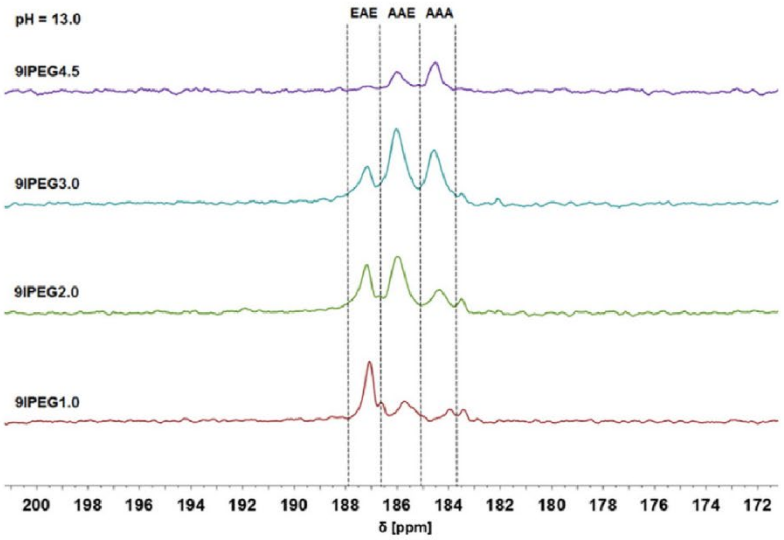

Fig. 10. ^{13}C NMR spectra of the 9IPEGy.0 polymer series, measured in D_2O at pH = 13.0.

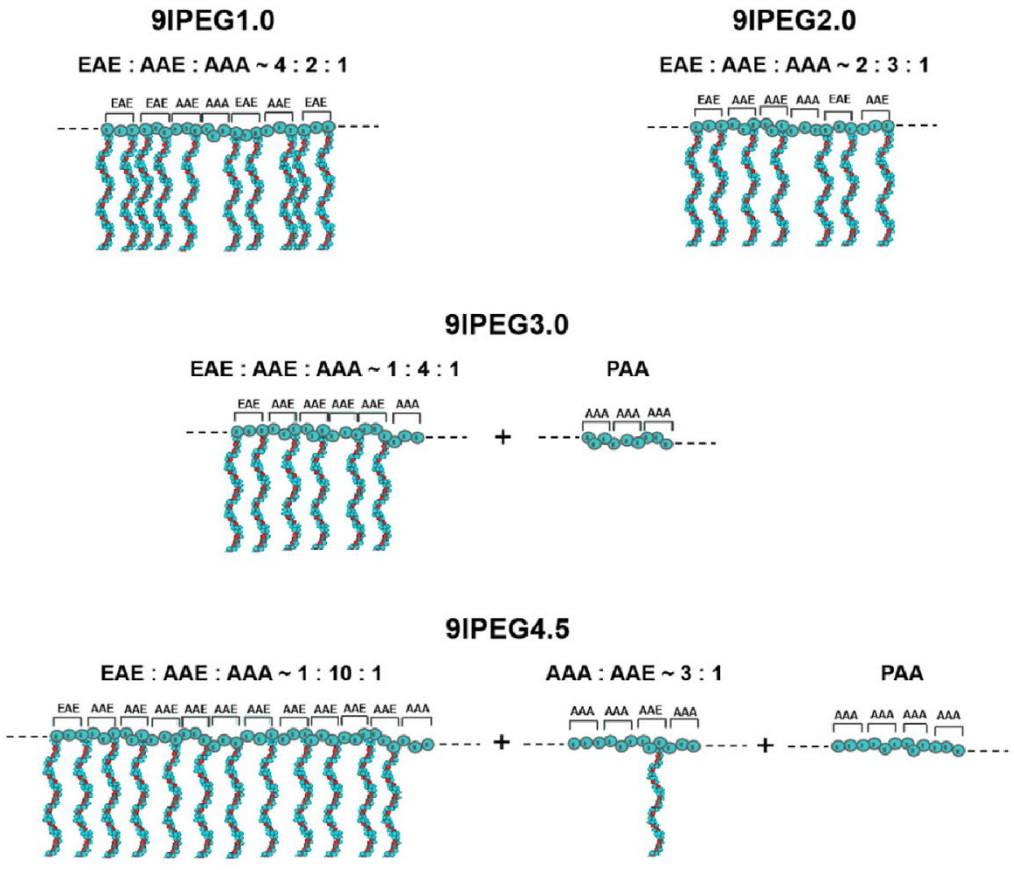

Fig. 11. Schematic illustration of the average actual composition of the synthesized PCE polymer samples 9IPEGy.0.

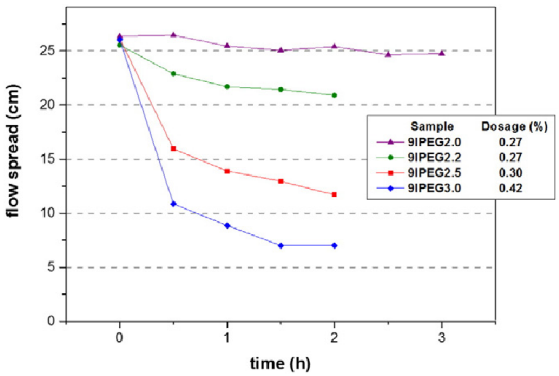

Fig. 12. Flow spread of cement pastes (w/c = 0.3) containing the synthesized 9IPEGy.0 polymer samples.

actual polymer composition which might be completely different from the theoretical one can be obtained. Combining this information with dispersion tests in cement helps to understand which structural motifs are the most effective ones with respect to dispersion effectiveness, and which should be targeted in synthesis work.

In future studies, the influence of other parameters including the side chain length, the feeding method during copolymerization and the type of chain-transfer agent and initiator used on the microstructure of PCE polymers should be considered as well.

Acknowledgment

Huiqun Li would like to thank the "Center for Advanced PCE Studies" of Technische Universität München for generous financial support of her research stay. The authors also wish to thank Clariant Deutschland GmbH for providing the isoprenyloxy polyethylene glycol ether macromonomer samples.

References

[1] T. Hirata, Japanese Patent JP 84 (1981) 2022 (S59-018338).
[2] E. Sakai, A. Ishida, A. Otha, New trends in the development of chemical admixtures in Japan, J. Adv. Concr. Technol. 4 (2) (2006) 211–223.
[3] J. Plank, PCE superplasticizers — chemistry, applications, and perspectives, ZKG International 67, Drymix Special 1 (2014) 48–59.
[4] C.E. Carraher Jr., Copolymerization, Polymer Chemistry, CRC Press, Boca Raton 2007, pp. 207–212.
[5] J. Brandrup, E.H. Immergut, E.A. Grulke (Eds.), Polymer Handbook, 4th Ed.Wiley, New York, 2005.
[6] G. Nguyen, D. Nicole, M. Swistek, Sequence distribution of the methyl methacrylate-ethyl acrylate copolymers by ^{13}C N.M.R. spectroscopy, Polym 38 (1997) 3455–3461.
[7] Y. Kin, H.J. Harwood, Analysis of sequence distribution in methyl methacrylate–methyl acrylate copolymers by ^{13}C NMR spectroscopy, Polym. 43 (2002) 3229–3237.
[8] F. Halverson, J.E. Lancaster, M.N. O'Connor, Sequence distribution of carboxyl groups in hydrolyzed polyacrylamide, Macromolecules 18 (1985) 1139–1144.
[9] A. Rozzoni, M. Bellotto, Configurational NMR Study of Sodium Polymethacrilate-G-PEO Comb Polymers, 14th International Congress on the Chemistry of Cement, Madrid, 2011.
[10] H. Uchikawa, S. Hanehara, D. Sawaki, The role of steric repulsive force in the dispersion of cement particles in fresh paste prepared with organic admixture, Cem. Concr. Res. 27 (1997) 37–50.
[11] C.Z. Li, N.Q. Feng, Y.D. Li, R.J. Chen, Effects of polyethylene oxide chains on the performance of polycarboxylate-type water-reducers, Cem. Concr. Res. 35 (2005) 867–873.
[12] M. Teresa, R. Laguna, R. Medrano, M.P. Plana, M.P. Tarazona, Polymer characterization by size-exclusion chromatography with multiple detection, J. Chromatogr. A 919 (2001) 13–19.
[13] DIN EN 1015-3:2007–05, Methods of Test for Mortar for Masonry — Part 3: Determination of Consistence of Fresh Mortar, DIN, Berlin/Germany, 2007.
[14] L. Lei, J. Plank, A concept for a polycarboxylate superplasticizer possessing enhanced clay tolerance, Cem. Concr. Res. 42 (2012) 1299–1306.
[15] P. Borget, L. Gaomiche, J.F. Le Meins, F. Lafuma, Microstructural characterization and behavior in different salt solutions of sodium polymethacrylate-g-PEO comb copolymers, Colloids Surf. A: Eng. Aspects 260 (2005) 173–182.
[16] C. Elvira, J.S. Roman, Synthesis and stereochemistry of isomeric methacrylic polymers derived from 4- and 5-aminosalicylic acids, Polym. 38 (1997) 4743–4750.
[17] C. Chang, D.D. Muccio, T.St. Pierre, Determination of the tacticity and analysis of the pH titration of poly(acrylic acid) by ^{1}H and ^{13}C NMR, Macromolecules 18 (1985) 2154–2157.
[18] S. Pourchet, S. Liautaud, D. Rinaldi, I. Pochard, Effect of the repartition of the PEG side chains on the adsorption and dispersion behaviors of PCP in presence of sulfate, Cem. Concr. Res. 42 (2012) 431–439.
[19] W. Fan, F. Stoffelbach, J. Rieger, L. Regnaud, A. Vichot, B. Bresson, N. Lequeux, A new class of organosilane-modified polycarboxylate superplasticizers with low sulfate sensitivity, Cem. Concr. Res. 42 (2012) 166–172.
[20] J. Pickelmann, H.Q. Li, R. Baumann, J. Plank, A ^{13}C NMR spectroscopic study on the repartition of acid and ester groups in MPEG type PCEs prepared via radical copolymerization and grafting techniques, 11th CANMET/ACI International Conference on Superplasticizers and Other Chemical Admixtures in Concrete, Ottawa/ON, Canada 2015, pp. 25–37 SP-302-02.
[21] A. Zingg, F. Winnefeld, L. Holzer, J. Pakusch, S. Becker, L. Gauckler, Adsorption of polyelectrolytes and its influence on the rheology, zeta potential, and microstructure of various cement and hydrate phases, J. Colloid Interface Sci. 323 (2008) 301–312.

9.2. Review Beiträge

Im Folgenden sind Übersichtsartikel dargestellt, die ebenfalls während der Promotionszeit verfasst wurden. Die Veröffentlichungen thematisieren unter anderem die neuesten Entwicklungen auf dem Gebiet der PCE-Technologie (**Publikation #13**), sie beschreiben welche Anforderungen an neue Zusatzmittel in alternativen Bindemittelsystemen mit einem niedrigen CO_2-Fußabdruck gestellt werden (**Publikation #14**) und geben einen allgemeinen Überblick zu möglichen Interaktionen von PCE-Fließmitteln mit Zement (**Publikation #15**). Außerdem wird in den Beiträgen diskutiert, welche wichtige Rolle bauchemische Zusatzmittel heutzutage in der Formulierung von Hochleistungsbaustoffen einnehmen (**Publikation #16**) und welche Möglichkeiten bestehen, die plastische Viskosität von Betonen mit niedrigen w/z-Werten zu reduzieren (**Publikation #17**).

9.2.1. Publikation #13: Next Generation of PCE Superplasticizers

Publikation #13

Next Generation of PCE Superplasticizers

Johann Plank, Manuel Ilg

47th Annual ICT Convention Symposium, London (UK), 2019

ICT Yearbook 2019/2020

Next Generation of PCE Superplasticizers

Johann Plank, Prof. Dr.
Professor
Technische Universität München
Chair for Construction Chemistry
Garching, Germany

Manuel Ilg, M.Sc.
Ph.D. student
Technische Universität München
Chair for Construction Chemistry
Garching, Germany

Johann Plank is full professor for Construction Chemistry and head of the Institute for Inorganic Chemistry at Technische Universität München. He studied chemistry in Regensburg, Germany and in 1980 earned a Ph.D. degree there. He then joined SKW Trostberg as a research group leader, construction polymers and founded SKW's oilfield chemical business before he became General Manager of SKW Construction Polymers GmbH in 1997. In 2001, he joined Technische Universität München, Germany, as a full professor for Construction Chemistry. His current research interests include cement and admixture chemistry for concrete, gypsum, mortar and oil well cementing. Prof. Plank has published about 400 scientific papers, holds 40 patents in the field of construction admixtures and has received many awards and honorary professorships from universities in Japan, China, Singapore and Thailand.

Manuel Ilg studied chemistry and received his B.Sc. and M.Sc. degrees in chemistry from Technische Universität München. Since August 2014 he is a Ph.D. student at the Chair for Construction Chemistry where he works on polycarboxylate superplasticizers with a main focus on novel PCE structures and concepts how the "stickiness" of concretes prepared at low water-cement ratios can be reduced.

ABSTRACT

Polycarboxylate superplasticizers (PCEs) became an indispensable part in many modern concrete formulations as they allow to produce concretes with outstanding material properties in the fresh and hardened state (e.g. high fluidity, long slump retention, outstanding durability etc.). However, since their invention in 1981, PCEs have experienced a rapid development so that by now a huge variety of chemically different polymers is available with significant variances in performance characteristics. Nevertheless, industrial and academic researchers continue to develop new and improved polymers, despite of the great diversity of already existing products. In this paper the chemistry and properties of such new PCE superplasticizers will be presented and an outlook into potential future developments will be given.

Keywords: Superplasticizers, Polycarboxylates, Clay-tolerant PCEs, Defoamer, Flow speed, Green binders

INTRODUCTION

The invention of polycarboxylate superplasticizers clearly represents a major milestone in concrete technology [1]. With their help it was now possible to formulate highly sophisticated concrete products such as ultrahigh strength concrete (UHSC) which can attain compressive strength values > 150 MPa, or self-compacting concrete (SCC) which no longer requires compaction via vibration [2, 3].

Prior to the invention of PCEs, all superplasticizers available at this time were based on a polycondensation reaction involving formaldehyde. The most important products of this family were β-naphthalene sulfonate formaldehyde (BNS) and melamine-formaldehyde-sulfite (MFS). While those polycondensates already marked a big step forward in concrete technology, they had some fundamental problems such as the rapid slump loss behavior, poor dispersing effectiveness at low water-to-cement ratios, dependence of their performance on the addition mode and the free formaldehyde content.

Because of all these shortcomings, several companies endeavored to develop new, improved superplasticizers. The first break-through came when in 1983 National Starch developed a polymer which no longer was based on a polycondensation reaction, but on aqueous free radical copolymerization. Their product ("Narlex LD-31") consisted of a copolymer of acrylic acid and hydroxyethyl methacrylate ester. Despite of the excellent dispersing performance, the product suffered from strong air-entrainment into concrete as a highly undesirable side effect. This problem was never solved to satisfaction, which made Narlex LD-31 to become a niche product in the market.

The final break-through for superplasticizers synthesized via radical copolymerization came with the introduction of comb polymers made from (meth)acrylic acid and the polyethylene glycol esters of methacrylic acid. This technology (developed by Nippon Shokubai) utilized the concept of dispersion via steric hindrance between the cement particles and thus delivered products of vastly superior performance over the hitherto used polycondensates which only relied on an electrostatic dispersion mechanism [4]. This new generation of admixtures also worked well at low w/c ratios (e.g. 0.30) and was free of formaldehyde. Moreover, when later the concepts of specific PCE molecules providing long slump retention, but without negative effect on the early strength of concrete were presented, it became clear that PCEs would much encroach on the market for polycondensates and replace them. In Europe this trend accelerated much beginning in 2005, however, it took a break around 2012 when applicators realized the sensitivity of specific PCEs to certain cements. It prompted local PCE producers to focus their development on more robust PCE polymers, and to this day has resulted in a ~ 80 % replacement of polycondensate superplasticizers.

The overwhelming success of PCEs still came as a surprise. Although at the market introduction of the polycarboxylates in the early 1990s it was obvious that this technology would become significant, nobody expected it to reach such a high volume ever. The constant improvement in product performance and – most important – the steady trend to lower costs for the PCEs have made this possible. According to a market survey in 2017, the global volume of PCE produced already surpassed 4 mio. tons, based on 40 wt. % liquid. However, still large entire regions such as Central Asia and parts of Africa do not use PCEs at all.

As of today, a great diversity of chemically very different PCE products is existing which includes MPEG-, APEG-, IPEG-, HPEG-, VPEG-, XPEG- and PAAM-type PCEs. The chemical structures of these PCEs variants are illustrated in **Figure 1**.

Even though those PCEs represent very powerful superplasticizers, the chemical and admixture industry are still heavily engaged in the development of new PCE structures and concepts which aim to improve the application properties of PCEs even more. In the following, some recent innovations in the field of PCE superplasticizers are presented. This includes for instance strategies how the deleterious effect of clay impurities on the dispersing effectiveness of PCEs can be mitigated. Furthermore, concepts for new superplasticizers are discussed which exhibit a long shelf life in blends with a defoamer. Moreover, several approaches are described how the flow speed of mortar and concrete can be significantly improved at low water-to-cement ratios (< 0.30). Finally, this paper presents PCE structures which are highly effective in alternative binder systems such as calcined clay blended cements.

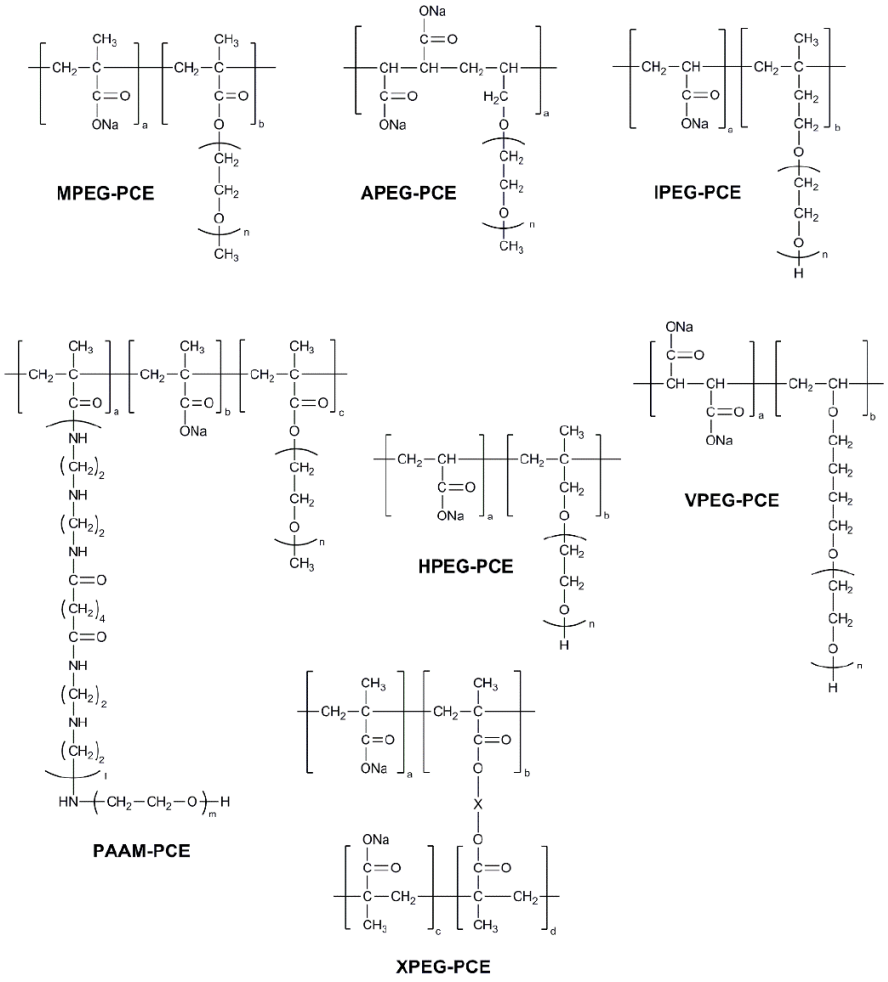

Figure 1: Chemical structures of commonly applied PCE polymers.

SUPERPLASTICZERS WITH A REDUCED SENSITIVITY TO CLAY IMPURITIES

Over the last years, applicators have observed that PCE superplasticizers – unlike polycondensates – exhibit a pronounced sensitivity to clay and silt contaminants. Those impurities are more prevalent now, as aggregates (sand, gravel) no longer are washed carefully or even are not available anymore in good quality. For example, we have received sand samples from construction sites which contained as much as 12 wt. % of clay minerals. Additionally, the limestone powders which are blended into cement nowadays often contain 0.5 – 5 wt. % of clay minerals. As a result, PCE performance is greatly reduced or the PCEs become entirely ineffective. Clays and clay minerals which frequently occur in aggregates include montmorillonite (bentonite), kaolinite, illite and mica. Montmorillonite, a 2:1 smectite clay, has been found to be more harmful than any other clay such as kaolinite [5, 6]. Generally, the capacity of clays to sorb water, hydrate and swell always viscosifies cement pastes. This effect results in a loss of workability or a higher water demand, independent of whether a superplasticizer is present or not. Previous research has established that in cement pore solution, the surfaces of bentonite clay particles become positively charged as a result of Ca^{2+} adsorption onto the negative alumosilicate layers. Onto these ion layers, polyanionic superplasticizers such as polycondensates or polycarboxylates will adsorb, thus resulting in a partial depletion of superplasticizer which then no longer is available for cement dispersion. This way, clay competes with cement for superplasticizer. Moreover, when PCE polymers are present, they can intercalate chemically into the interlayer space between the individual alumosilicate layers, resulting in an organo-mineral phase whereby their poly(ethylene glycol) side chains occupy the interlayer space, as is shown in **Figure 2**. This reaction with clay is specific for PCEs and is a consequence of their PEO side chains, as was evidenced by XRD measurements [7]. Consequently, PCEs can be used up by clay by both surface adsorption and chemical sorption (the latter consumes considerably more PCE than surface adsorption) whereas

polycondensates such as BNS only are consumed by surface interaction [7, 8]. This explains why PCEs are significantly more affected by clay than polycondensates.

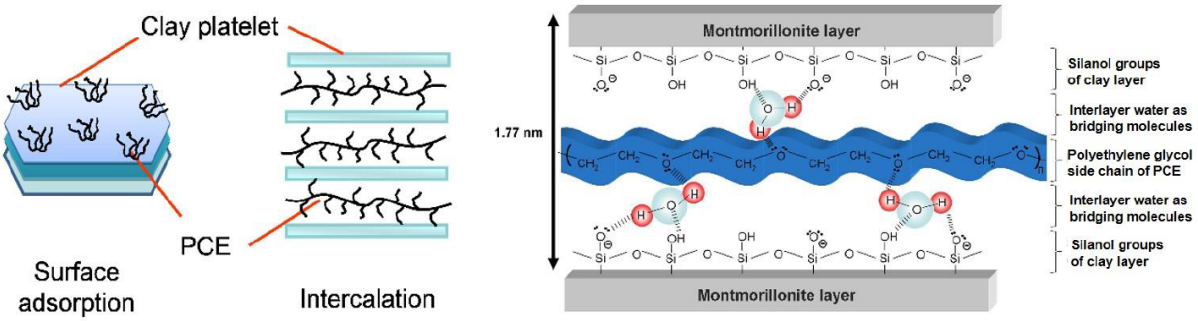

Figure 2: Fundamental types of interaction between PCE and clay (left) and chemical sorption (intercalation) of a poly(ethylene glycol) side chain in between alumosilicate layers (right).

Currently, the industry applies several strategies to mitigate the negative effects of clay on PCEs:

(a) Use of sacrificial agents: Pure PEG or MPEG are utilized as sacrificial agents to occupy the interlayer spaces while the PCE molecule is preserved and can thus interact with cement to achieve dispersion. Hence, admixture companies developed mixtures of PEG with PCEs which provide a more clay-tolerant superplasticizer. Another remedy includes the application of cationic polymers which can inhibit the swelling of clay entirely [9]. This method offers the advantage of zero water consumption because the clay will not hydrate. Additionally, the interlayer spacing will not be accessible for the PCEs. The disadvantage of this concept is that the cationic polymer must be added separately to the concrete because it will precipitate the PCE polymer from the admixture solution.

(b) Introduction of novel PCE structures: obviously, the best solution to the problem of the limited clay tolerance of PCEs would be a novel PCE structure which does not contain PEO side chains. Recently, such polymers have been synthesized using hydroxyl alkyl esters of (meth)acrylic acid as side chain bearing macromonomers [10]. Good results were also reported for PCE polymers synthesized from vinylacetate and the monomeric adduct of sulfanilic acid to maleic anhydride (see **Figure 3**) [11]. Utilizing XRD analysis, it was found that indeed these novel polycarboxylates do not intercalate into the clay structure and sorb on clay surfaces in small quantity only. Consequently, they exhibit a more robust performance even in the presence of montmorillonite as contaminant. However, the incorporation of non-polar moieties into the polymer structure seems to be a promising approach how clay tolerant PCEs can be obtained. It is assumed that hydrophobic and bulky components might impede the intercalation of the PCEs into the hydrophilic alumosilicate layers of the clay minerals. Referring to this, more research is necessary to provide the industry with even less clay-sensitive PCE products.

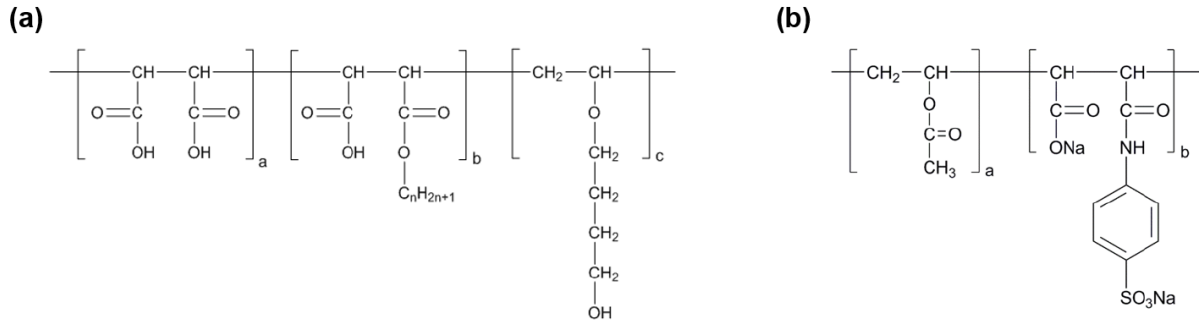

Figure 3: Chemical structures of clay-tolerant PCEs: (a) Terpolymer synthesized from maleic anhydride, monoalkyl maleate and 4-hydroxy butyl vinyl ether (HBVE); (b) Copolymer composed of vinyl acetate and the adduct of sulfanilic acid to maleic anhydride.

STABLE PCE-DEFOAMER COMBINATIONS

PCE superplasticizers have a high foaming tendency [12] and therefore always need to be formulated with a defoamer to avoid the introduction of air voids into the concrete. However, a main problem of defoamers is their poor miscibility in the aqueous PCE solution. Usually, the defoamer starts to separate after some time on the surface of the superplasticizer solution. To overcome this problem, PCEs have been recently developed which contain a chemically bound defoamer molecule (e.g. an alcohol) that has been grafted onto the backbone of the PCE via an ester. Under the alkaline conditions prevailing in the fresh concrete, hydrolysis of the ester occurs and the defoamer molecule gets released. An alternative concept is to physically blend the PCE solution with a defoamer that exhibits a terminal amino group (e.g. Jeffamine®). In PCE solutions with a pH of 4 – 5, the amino group is protonated as $-NH_3^+$ and forms a so-called ion pair bond with the negative $-COO^-$ group of the PCE. In this way, the defoamer is connected via an electrostatic interaction to the PCE molecule and cannot separate during the storage. When this superplasticizer is added to the cement, deprotonation of the $-NH_3^+$ group occurs due to the very high pH in the cement and the ion-pair bond between the PCE molecule and defoamer is removed. Consequently, the defoamer molecule is released and becomes effective. The two different approaches for stable PCE-defoamer combinations are illustrated in **Figure 4**.

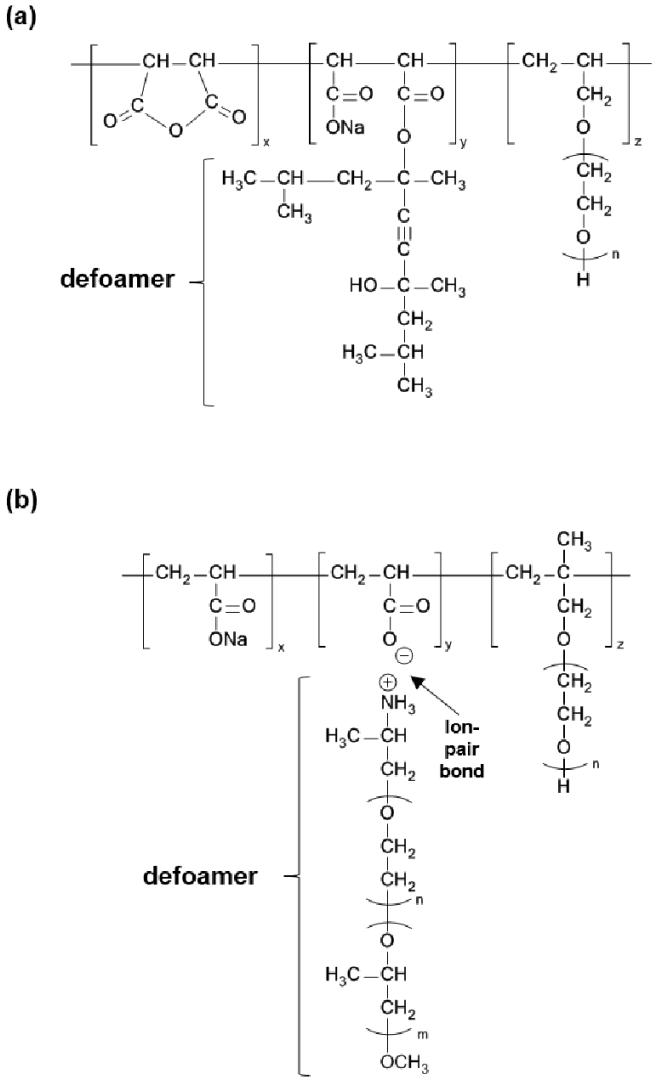

Figure 4: Concepts for stable PCE-defoamer combinations: (a) Chemical bond between the defoamer and the PCE molecule; (b) Ion-pair bond between the PCE and defoamer. In the alkaline environment of the cement, both defoamers are then released by ester hydrolysis (a) or removal of the ion-pair bond (b).

CONCEPTS FOR FAST FLOWING CONCRETE

Since long it has been known that concretes prepared at low w/c ratio (especially < 0.30) exhibit a slow flow which makes it very difficult to achieve fast placement on construction sites. In fact, such concretes creep like honey rather than flow, which made construction workers to designate these concretes as "sticky". Still, these concretes can produce a high slump or spread flow value, they just take very long to achieve the final spread. The mechanism behind this effect has been investigated thoroughly and is believed to stem from an excessively high plastic viscosity of the lime phase [13]. This rheological parameter controls the flow speed of concrete and mortar. However, at low w/c ratios it is generally not possible to lower the plastic viscosity substantially by using polycarboxylates. Bearing this concept in mind, we have systematically investigated the behavior of all types of PCEs in this respect and found that also here the HLB value (i.e. hydrophilic lipophilic balance) plays a critical role (see **Table 1**).

Table 1: Impact of the HLB value of different PCE polymers on the flow speed of concrete.

PCE Polymer	Chemistry	HLB Value	Plastic Viscosity [mPa·s]	Flow speed of concrete
MPEG-7	Methacrylate Ester	16.4	1,806	very low
MPEG-10	Methacrylate Ester	16.7	1,550	low
MPEG-25	Methacrylate Ester	17.8	1,388	low
MPEG-45	Methacrylate Ester	18.2	1,400	medium
MPEG-114	Methacrylate Ester	18.8	1,310	medium
IPEG-25	Isoprenyl Ether	18.8	1,276	medium
IPEG-50	Isoprenyl Ether	18.6	1,299	medium
APEG-23	Allyl Ether	19.3	1,296	high
APEG-34	Allyl Ether	19.5	1,146	very high
APEG-70	Allyl Ether	19.7	1,221	high

According to **Table 1**, PCEs exhibiting a low HLB value (e.g. MPEG PCEs) produce particularly "sticky" concretes whereas those possessing high HLB values (e.g. APEG and IPEG PCEs) can facilitate faster flow [14]. Thus, the hydrophilic character of the PCE polymer is of pivotal importance to achieve good flow properties. However, in certain countries the kind of PCE which can impart a fast flow is unavailable. For that reason, we have investigated possibilities to adapt those PCEs of low HLB value also for this application. One concept involves to include a more negatively charged anchoring group into the PCE which replaces the carboxylate group. A viable candidate for this purpose is the phosphate functionality. Recently, such new types of comb polymers were introduced on the market which contain phosphate functionalities instead of carboxylates. These novel polymers consist of a polyaromatic backbone holding polyethylene glycol side chains as well as phosphate ester groups and is prepared via a polycondensation reaction involving a phenolethoxylate, a phenol ethoxy phosphate ester, phenol and formaldehyde (see **Figure 5 (a)**) [15]. An alternative, CH_2O-free synthesis is based on aqueous free radical copolymerization and involves hydroxyethylmethacrylate phosphate ester (HEMAP) and the macromonomer known from the MPEG-PCE synthesis, the MPEG ester of methacrylic acid (**Figure 5 (b)**) [16]. The phosphated comb polymers were shown to exhibit excellent cement dispersing properties which are often superior to that of conventional PCE copolymers [17]. Furthermore, they stand out because of their robustness in the presence of sulfate and other adsorbing admixtures, the reason for this can be attributed to their high calcium binding capacity. The most striking feature of polyphosphate superplasticizers is their ability to increase

the flow speed of concrete and to reduce the well-known "stickiness" at low w/c ratios. This special property of the phosphate comb polymer can be attributed to the higher hydrophilic character of the trunk chain resulting from the divalent phosphate groups, which leads to a lower plastic viscosity of the lime phase in the concrete. Moreover, by the introduction of phosphate groups into MPEG-PCEs a significant improvement of the flow properties can be effectuated compared to the unmodified counterpart. Through this modification, even MPEG-PCEs which usually effectuate a low speed of low can produce a fast flowing concrete.

Generally, phosphate-based PCEs have already proven its benefits, and commercial products are used in Japan and Europe. The successful commercialization of this type of PCE is much supported by the relatively easy availability of the monomer HEMAP. However, considering the additional costs for the phosphate bearing monomer, other strategies for a high flow speed were investigated.

(a) phosphated phenolethoxylate

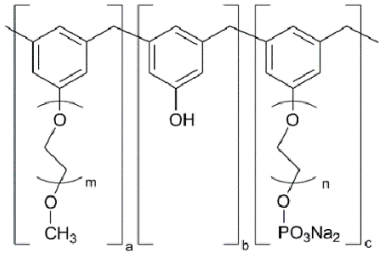

(b) phosphated MPEG-PCE

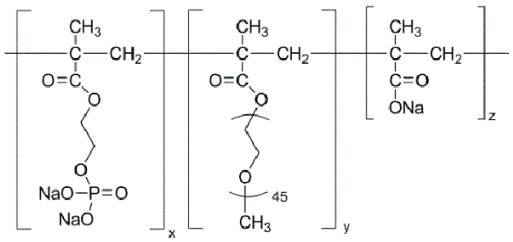

Figure 5: Chemical structures of phosphate-group modified superplasticizers: (a) phosphate polyphenylethoxylate and (b) methacrylate-ester PCE containing phosphate groups.

Most interestingly, we have found that even simple blends of non-ionic molecules including glycol compounds (e.g. diethylene glycol (DEG) or triethylene glycol (TEG)) or polyether amines with common PCE superplasticizers can substantially enhance the paste fluidity, but also notably increase the flow speed, as was evidenced by shorter empty times of mortar and concrete from the V-funnel [18, 19]. Note that such non-ionic compounds do not provide any fluidity at all when applied individually without PCE. The effect increases with decreasing w/c ratio and is particularly strong for PCEs with high anionicity (see **Figure 6**). For example, an IPEG PCE prepared from a molar ratio of ~ 6:1 of acrylic acid : macromonomer benefits much more from the non-ionic molecules than the less hydrophilic polymer synthesized at a molar ratio of ~ 2.0:1. Also, the effect is much more pronounced at a low w/c ratio (e.g. 0.22). However, typical dosages of the non-ionic co-dispersant range between 0.3 and 0.5 % by weight of cement and often exceed that of the PCE.

Mechanistically, the staggering effect of non-ionic compounds on the flow speed of concrete can be explained by a lubricating layer which forms in the pore solution between two adjacent cement particles. Apparently, at low w/c ratios the conventional dispersing mechanisms which are based on electrostatic and steric repulsion no longer exclusively are responsible for fluidity. Instead, in such systems possessing an extremely high volume fraction of solids another mechanism applies. It involves a lubricating interlayer between the particles which are kept apart through an additional osmotic and entropic effect [18].

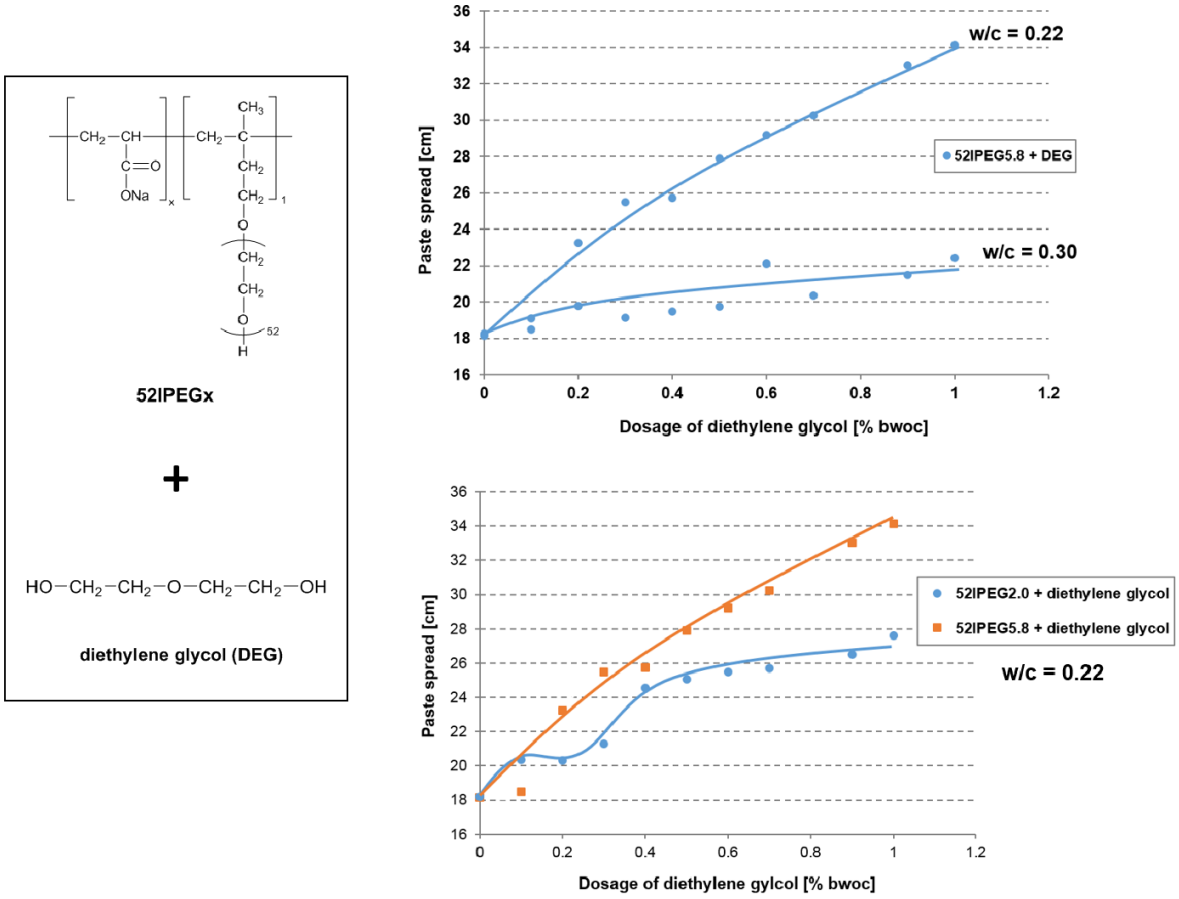

Figure 6: Effectiveness of diethylene glycol as co-dispersant on the dispersing performance of IPEG-PCEs at different w/c ratios.

PCES FOR NEW BINDER SYSTEMS

The discussion on climate change originating from increased levels of CO_2 in the atmosphere also has affected the cement industry which emits no less than ~ 7 % of the anthropogenic CO_2. As a result, governments press the cement industry to reduce the clinker factor by blending Portland cement clinker with SCMs such as fly ash, ground granulated blast furnace slag, burnt oil shale, trass etc. However, those SCMs are not available everywhere which is why other binder materials appear on the market now (e.g. calcium sulfoaluminate cements, geopolymer binders such as fly ash, rice husk ash, slags etc., calcium hydrosilicates, thermally activated clays or special binders like α-, α'-belite or ternesite) [20].

Widespread acceptance of any of those novel binder materials will greatly depend on their ability to work with chemical admixtures which allow to control fluidity, set behavior, air entrainment, defoaming, water-retention etc. Relative to superplasticizers, it is well established that they work through surface adsorption which involves a physical interaction with specific surfaces (typically ion layers on mineral surfaces). However, considering the huge diversity of novel binder systems it is most unlikely that the current PCE portfolio can satisfy all needs. As an example, it is well-known that the currently existing arsenal of PCE polymers does not work well in geopolymer binders, presumably because of the extremely high pH value. Whereas cationic surfactants have shown good performance. Likewise, it is established that specific calcined clays do not respond well to existing PCEs. Interestingly, our research produced surprisingly good results when using amphoteric polymers synthesized from methacrylic acid (MA), MPEG macromonomer and 3-trimethylammonium propyl methacrylamide chloride (MAPTAC) to disperse calcined clay blended cements [21]. According to our study, the amphoteric polymer with the lowest content of the cationic monomer MAPTAC and with the longest polyethylene glycol sidechain (n_{EO} = 113) produced the best dispersing performance and was even better than a conventional MPEG-type PCE (45PC6) (see results in **Figure 7**).

Further investigations on the dispersion of alkali-activated slag pastes revealed that APEG-PCEs with a low side chain length (n_{EO} = 7) and a molecular weight > 30,000 Da are highly efficient superplasticizers in such systems [22]. This can be attributed to the high calcium complexing ability of those PECs owed to the neighboring carboxylate groups in the maleic anhydride monomer. All this points out that in the future, significantly modified PCEs or entirely new superplasticizer polymers may be needed to cope with the demands of such new binder systems.

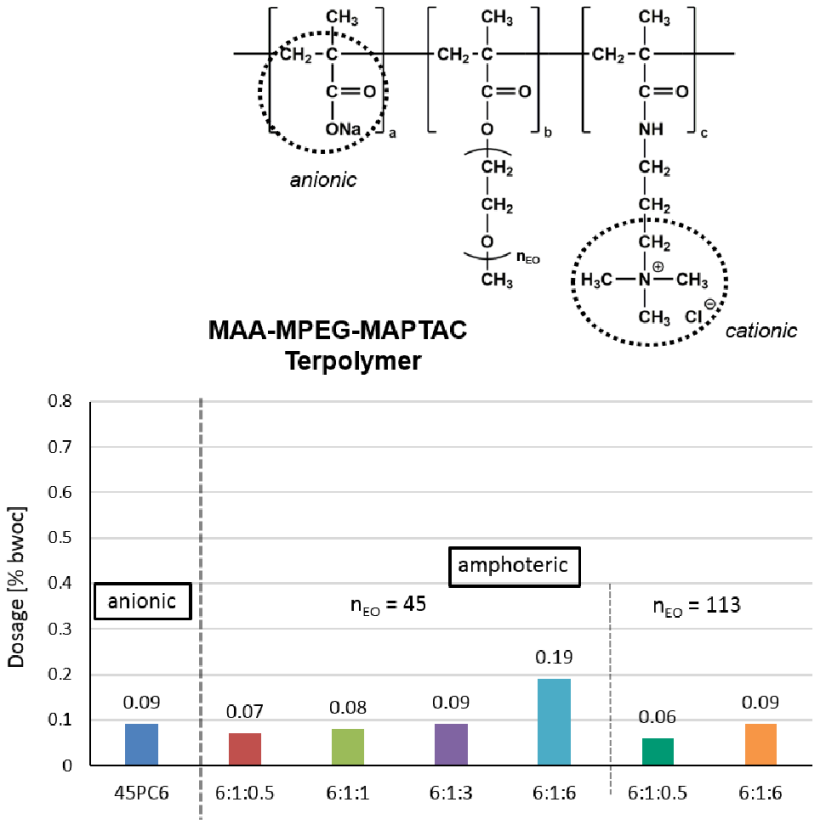

Figure 7: Dosages of amphoteric MAA-MPEG-MAPTAC terpolymers with varying molecular composition and side chain length for a spread flow of 26 cm in calcined clay blended cements.

CONCLUSION

The invention of PCE superplasticizers has truly revolutionized modern concrete technology. They present a major driver for innovation in concrete and will continue to do so for many years to come. However, the main focus will be in the upcoming years on the development of new superplasticizers which can ensure a high fluidity and good workability of alternative binder systems. The introduction of such new superplasticizers is a prerequisite for the successful implementation of low carbon cement systems in the construction industry. Additionally, the current PCE superplasticizers will be refined further to become even more effective, and they will be tailored more specifically to distinct applications. Moreover, completely new technologies (e.g. nitrogen-containing macromonomers, branched side chains etc.) are already on the horizon which can have a significant impact on future building technology.

REFERENCES

1. Plank J., Sakai E., Miao C. W., Yu C., Hong J. X., Chemical Admixtures – Chemistry, Applications and Their Impact on Concrete Microstructure and Durability. *Cement and Concrete Research*, Vol. 78, 2015, pp. 81 – 99.

2. Shi C., Wu Z., Xiao J., Wang D., Huang Z., Fang Z., A review on ultra high performance concrete: Part I. Raw materials and mixture design. *Construction and Building Materials*, Vol. 101 (1), 2015, pp. 741 – 751.

3. Khayat K. H., Workability, Testing, and Performance of Self-Consolidating Concrete. *ACI Materials Journal*, Vol. 96 (3), 1999, pp. 346 – 353.

4. Yoshioka K., Sakai E., Daimon M., Kitahar A., Role of Steric Hindrance in the Performance of Superplasticizers for Concrete. *Journal of the American Ceramic Society*, Vol. 80, 1997, pp. 2667 – 2671.

5. Sakai E., Atarashi D., Daimon M., Interaction between Superplasticizers and Clay Minerals. 6th CANMET/ACI International Symposium on Concrete Technology for Sustainable Development, Xi'an/China, American Concrete Institute, 2006, pp. 1560 – 1566.

6. Jeknavorian A. A., Jardine L., Ou C. C., Koyata H., Folliard K. J., Interaction of Superplasticizers with Clay-Bearing Aggregates. 7th CANMET/ACI International Conference on Superplasticizers and Other Chemical Admixtures in Concrete, Berlin/Germany, American Concrete Institute, SP–217, 2003, pp. 1293 – 1316.

7. Ng S., Plank J., Study on the Interaction of Na-montmorillonite clays with Polycarboxylate based superplasticizers", 10th CANMET/ACI Conference on Superplasticizers and Other Chemical Admixtures in Concrete (supplementary papers), Prague/CZ, American Concrete Institute, 2012, pp. 377 – 384.

8. Atarashi D., Sakai E., Obinata R., Daimon M., Interactions between Superplasticizers and Clay Minerals. *Cement Science and Concrete Technology*, Vol. 58, 2004, pp. 387 – 392.

9. Jacquet A., Villard E., Watt O., Method for Inerting Impurities. WO patent 2,006,032,785 (2006).

10. Lei L., Plank J., A Concept for a Polycarboxylate Superplasticizer Possessing Enhanced Clay Tolerance. *Cement and Concrete Research*, Vol. 42, 2012, pp. 1299 – 1306.

11. Sulser U., Huber A., Widmer J., Water-soluble copolymers of vinylacetate and maleamic acids and use as fluidizers high-range water-reducers for aqueous suspensions. US patent 5,633,310 (1997).

12. Lange A., Plank J., Study on the foaming behavior of allyl ether-based polycarboxylate superplasticizers. *Cement and Concrete Research*, Vol. 42, 2012, pp. 484 – 489.

13. Lange A., Hirata T., Plank J., Influence of the HLB Value of Polycarboxylate Superplasticizers on the Flow Behavior of Mortar and Concrete. *Cement and Concrete Research*, Vol. 60, 2014, pp. 45 – 50.

14. Lange A., Plank J., Optimization of Comb-Shaped Polycarboxylate Cement Dispersants to Achieve Fast-Flowing Mortar and Concrete. *Journal of Applied Polymer Science*, Vol. 132, 2015, 42529.

15. Wieland P., Kraus A., Albrecht G., Becher K., Grassl H., Polycondensation product based on aromatic or heteroaromatic compounds, method for the production thereof and use thereof. WO/2006/042709 A1 (2006).

16. Stecher J., Plank J., Novel concrete superplasticizers based on phosphate esters. *Cement and Concrete Research*, 2019, in print.

17. Stecher J., Plank J., Phosphated comb polymers – A new generation of highly effective superplasticizers. International Concrete Sustainability Conference (SCC 2016), Washington/USA, 2016, Proceedings, pp. 61 – 71.

18. Ilg M., Plank J., Improvement of SCC flow properties through addition of non-adsorbing small molecule co-dispersants. International Concrete Sustainability Conference (SCC 2016), Washington/USA, 2016, Proceedings, pp. 49 – 59.

19. Ilg M., Plank J., Novel Admixtures To Reduce The Stickiness Of Low W/C Concretes. Superplasticizers and Other Chemical Admixtures in Concrete, Proceedings Twelfth International Conference, Beijing/China, 2018, SP-329-07, pp. 77 – 88.

20. Gartner E., Sui T., Alternative cement clinkers. *Cement and Concrete Research*, Vol. 114, 2018, pp. 27 – 39.

21. Schmid M., Beuntner N., Thienel K.-Ch., Plank J., Amphoteric Superplasticizers for Cements Blended with a Calcined Clay. Superplasticizers and Other Chemical Admixtures in Concrete, Proceedings Twelfth International Conference, Beijing/China, 2018, SP-329-04, pp. 41 – 54.

22. Conte T., Plank J., Impact of molecular structure and composition of polycarboxylate comb polymers on the flow properties of alkali-activated slag. *Cement and Concrete Research*, Vol. 116, 2019, pp. 95 – 101.

9.2.2. Publikation #14: Chemical Admixtures for Low Carbon Cement Systems

Publikation #14

Chemical Admixtures for Low Carbon Cement Systems

Johann Plank, Manuel Ilg

1st International Conference on Innovation in Low-Carbon Cement and Concrete Technology (ILCCC)

London (UK), 2019

Proceedings

1st INTERNATIONAL CONFERENCE ON INNOVATION IN LOW-CARBON CEMENT & CONCRETE TECHNOLOGY

Chemical Admixtures for Low Carbon Cement Systems

Johann Plank[1]*, Manuel Ilg[1]

ABSTRACT

Low carbon cements will reduce the CO_2 footprint of the construction industry and therefore will become more dominant in the future. Such binders include geopolymer binders such as alkali-activated slags (AAS), calcined clays, ternesite cement, α-C_2SH and CSA cement, to name a few. However, their future acceptance and widespread use much depends on the availability of chemical admixtures which allow to control their workability, set behaviour, strength development etc.

This article will give an overview on some experimental results of chemical admixtures in low carbon cement systems. First, new insights will be presented on the behaviour of polycarboxylate superplasticizers in alkali-activated slags. Moreover, data on the performance of superplasticizers in α-C_2SH - a new type of hydraulic binder with a 50 % lower CO_2 footprint than OPC – will be outlined. Finally, C-S-H-PCE nanocomposites will be introduced as a novel kind of early strength enhancer for slag and calcined clay blended cements.

Keywords: chemical admixtures; superplasticizers; early strength accelerators; low carbon binders

1| INTRODUCTION

The production of Portland cement accounts for about 7 % of the total anthropogenic emissions of carbon dioxide which mainly originates from the de-carbonation of limestone, the calcination and the milling process [1]. Large amounts of CO_2 are also emitted through the firing of fossil fuels or waste materials (e.g. vehicle-tires and sludges) which are burned to heat the rotary kilns up to temperatures of 1450 °C. Around 900 kg of CO_2 are released for every ton of clinker produced which underlines the necessity to establish concepts and strategies how the CO_2 emissions can be significantly reduced [1, 2]. The Paris Agreement that limits the rise of the global average temperature below to 2 °C by 2050 can only be successfully implemented when also the cement industry takes measures to mitigate its greenhouse gas emissions.

In light of this, much research was carried out in the last years on the development of new binders where cement is partially or completely substituted by other readily available materials [3]. These supplementary cementitious materials (SCMs) are often industrial by-products such as silica fume, fly ash, granulated ground blast furnace slag or other mineral admixtures like limestone or metakaolin [1]. Blended cements such as CEM II/III are already adopted in many fields of the construction industry and will increasingly replace Portland cements (CEM I) in the years to come. When SCMs are blended with cement some of these materials, namely fly ash, slag and calcined clay, can induce similar or even better long-term properties (mechanical resistance, durability) than pure Portland cement based concrete. However, a drawback of such blended cements is their slow early strength development, owed to the slow pozzolanic reaction of the SCMs. Therefore, admixtures have to be found which boost the hydration reactions of cement as well as of the SCMs to effectuate a higher early strength without any sacrifices in the final strength. Moreover, a good workability is another important factor which has to be guaranteed. For this purpose, potent superplasticizers need to be identified to ensure an effective dispersion and consequently good processing properties of the low carbon cement systems.

In this context, the article will present some results on the performance of superplasticizers in low carbon binder systems, namely alkali-activated slags and α-C_2SH. For the AAS system it was found that specific molecular parameters provoke a high fluidity. Furthermore, early strength accelerators based on C-S-H-PCE nanocomposites are presented for CEM II/III and their underlying working mechanism will be discussed.

2| PCE SUPERPLASTICICIZERS FOR AAS

Ground granulated blast furnace slag (GGBFS) – a waste product from the steel industry – has already been widely implemented as SCM allowing cement replacement levels of 30 – 70 wt.%. Due to its latent hydraulic character, an alkaline activation (using e.g. sodium hydroxide, carbonate, sulfate or silicate) is required to achieve similar hydration rates as for OPC. Concretes made from AAS exhibit a high durability and enhanced material properties like a high resistance towards corrosion and the attack of acids or sulfate ions [4]. Unfortunately, the workability of most AAS is inferior compared to that of cement-based materials. Therefore, polymer admixtures have to be found which can substantially improve their flowability.
Polycarboxylate superplasticizers (PCEs) – comb-shaped polymers that are composed of an anionic backbone holding carboxylate anchor groups and several non-ionic polyethylene glycol side chains – seem to be a promising candidate for AAS due to their well-known superior dispersing performance in cement (see structures in Fig. 1).

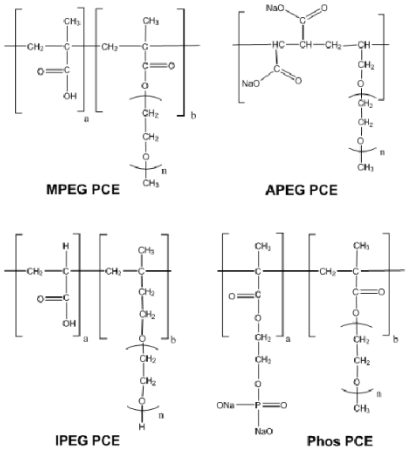

Fig. 1 | Molecular structure of PCE based superplasticizers.

(1) Chair for Construction Chemistry, Technical University of Munich, Garching, Germany.
* Corresponding author(s): sekretariat@bauchemie.ch.tum.de

However, two requirements have to be met first to facilitate the applicability of PCEs also in AAS systems. First, the PCE polymer needs to be soluble in the highly alkaline environment of the activator. Low solubility of the polymer becomes apparent when a solution of the PCE turns turbid which is regarded as the so-called "cloud point". Secondly, the PCE needs to adsorb on the slag surface which is determined by the calcium ion concentration present on the surface of the slag particles and the calcium complexing ability of the PCE.

Taken all these points into account, solubility experiments were performed, to identify those structural parameters of PCEs which provoke a high solubility in an aqueous solution of the activator (i.e. NaOH resp. Na_2CO_3) [5]. For this purpose, a 0.1 wt.% solution of the PCE was prepared in DI water and NaOH or Na_2CO_3 was added in incremental steps until the solution became turbid which signifies the "cloud point". Fig. 2 shows the concentration of the alkaline activator necessary to reach the cloud point of various MPEG-type PCEs that exhibit the same side chain length (45 ethylene oxide units) but different side chain densities (i.e. acid to side chain ratio was varied from 2:1 to 20:1). As evident from the figure, the solubility of the MPEG PCEs decreased with increasing side chain length. It has to be noted, that except for 45MPEG2 the maximum solubility of the tested PCEs was higher than the NaOH concentration typically applied for the activation of GGBFS. In the Na_2CO_3 solution all PCE polymers tested showed a lower solubility than in NaOH. Furthermore, the solubility slightly increased with lower side chain density. Even for the high acid to side chain ratio of 20:1 the solubility was still lower than the Na_2CO_3 concentration needed to activate GGBFS (1.67 mol/L) which means that all these PCEs cannot induce any fluidity when added into a slag paste.

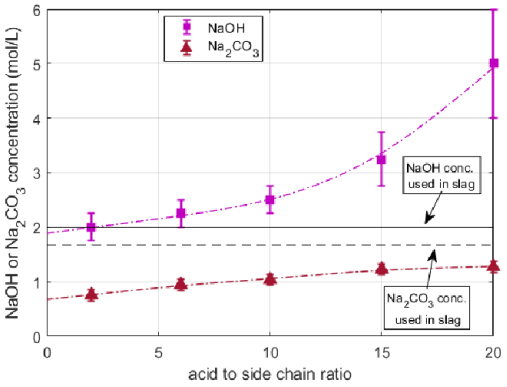

Fig. 2 | Concentrations of NaOH and Na_2CO_3 required to reach the cloud point of MPEG PCEs as a function of their acid to side chain ratio.

Furthermore, the concentration of the alkaline activator required to reach the "cloud point" for MPEG PCEs with the same side chain density (acid to side chain ratio of 10) but different side chain length (i.e. 25 – 114 EO units) was measured (Fig. 3). The solubility of the MPEG PCEs decreased when the side chain length increases. For the NaOH activated system, the solubility of all PCEs was above 2 mol/L. On the contrary, for the Na_2CO_3 system only the solubility of the MPEG PCE with a short side chain length (i.e. 25 EO units) was above the activator concentration.
Based on those experiments, it can be concluded that PCE variants with short side chain length and a high content of carboxylate groups may present the optimal structure for the dispersion of AAS [5].

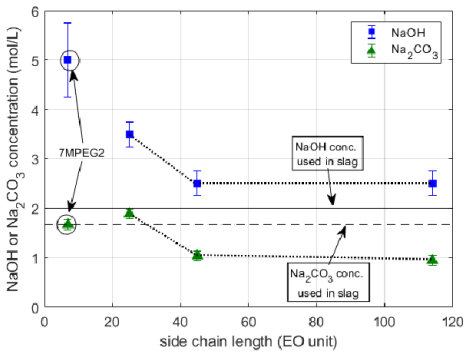

Fig. 3 | Concentrations of NaOH and Na_2CO_3 required to reach the cloud point of MPEG PCEs as a function of their side chain length.

However, spread flow tests of NaOH activated slag pastes admixed with different MPEG type PCEs revealed that all of the tested polymers only slightly improved the paste fluidity (Fig. 4). The best performance was found for 45MPEG20 which increased the spread flow from 15.7 cm to 18.1 cm. Anyway, the trend for the dispersing efficacy of the MPEG PCEs was in perfect agreement with the results of the solubility experiments in NaOH hence the fluidity increased there from 45MPEG2 to 45MPEG20 with rising anionicity.

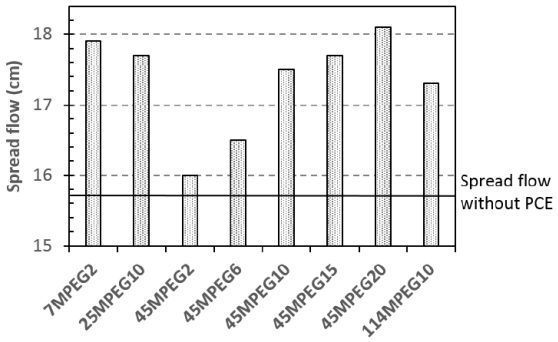

Fig. 4 | Spread flow of NaOH activated slag pastes containing 0.05 wt. % of different MPEG type PCEs at w/b = 0.5.

Next, the dispersing capability of PCEs exhibiting a different chemical composition but the same side chain length (n = 7 EO) was probed in AAS. According to Fig. 5, the MPEG, IPEG and phosphate based PCE variants did not provoke any considerable increase of the paste fluidity. On the contrary, the APEG PCE effectuated an exceptional rise of the spread flow from 15.7 cm to 33.7 cm which signifies an increase of ~ 120 %. One reason for this behaviour seems to be the high Ca^{2+} complexing affinity of 7APEG2 (i.e. anionic charge declines from 3700 µeq/g to 300 µeq/g in the presence of Ca^{2+}) which originates from the vicinal carboxylate groups in the maleic anhydride.

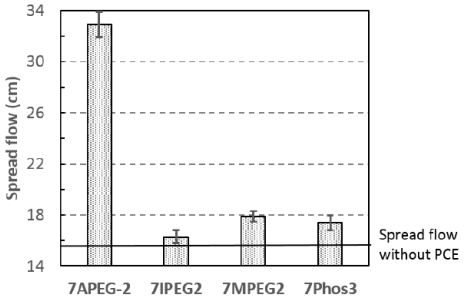

Fig. 5 | Spread flow of NaOH activated slag pastes admixed with 0.05 wt.% of PCE polymers exhibiting short side chain length.

Moreover, further experiments disclosed that especially those APEG PCEs provoke a high fluidity in the NaOH activated slag pastes which exhibit a short side chain length (n = 7 EO) and a molecular weight M_w > 30,000 Da [5].

3| ADMIXTURES FOR α-C_2SH based binders

Hydraulic calcium hydrosilicates (α-C_2SH) present a further example for a sustainable binder system which seems to be very promising as the production causes up to 50 % less CO_2 compared to OPC [6]. It can be synthesized from lime and quartz in a hydrothermal synthesis at 200 °C in an autoclave. However, the formed α-C_2SH is crystalline due to hydrogen bondings in the structure and hence exhibits no hydraulic reactivity. Therefore, a mechanochemical activation has to be carried out. This is achieved by intergrinding the α-C_2SH with 50 wt.% of a siliceous filler like quartz or blast furnace slag. Thus, the material becomes amorphous and a reactive layer around the filler particles is produced which reacts after the contact with water to C-S-H phases whose composition is similar to that which are formed in the hydration of OPC. Mortar samples prepared from this binder displayed in first test series good material properties like an adequate compressive strength of 80 N/mm² after 28 days as well as a low content of capillary pores [6].

In spite of everything, rheology measurements of α-C_2SH pastes revealed that its water demand is exceptionally higher in contrast to OPC. As can be seen from Fig. 6, high w/b ratios are necessary (e.g. 1.0) to obtain at least a reasonable fluidity. Such rheological properties are usually obtained for OPC based systems at much lower w/b ratios (i.e. 0.4 – 0.7). The high water demand can be mainly ascribed to the high fineness of the material (Blaine value ~ 10,000 cm²/g).

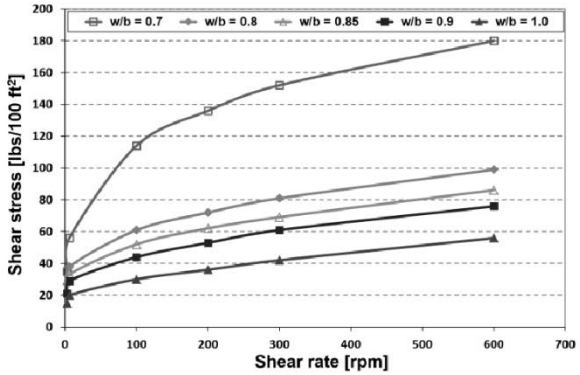

Fig. 6 | Rheology of α-C_2SH slurries prepared at different w/b ratios.

The rheology of α-C_2SH slurries (w/b ratio = 0.7) admixed with different dosages of a superplasticizer, namely an AFS-based polycondensate is depicted in Fig. 7. It was found that the binder particles can be efficiently dispersed even by a conventional superplasticizer albeit relatively high dosages are needed. Yet again, the high surface area of the α-C_2SH and the high content of the filler are the principal reasons why the admixture needs to be highly dosed to effectuate a good fluidity at all. Most important, all common superplasticizers such as PCEs or poly-condensates which are typically applied for the dispersion of OPC can be also used for α-C_2SH based systems, so there is no need to develop new chemical admixtures here.

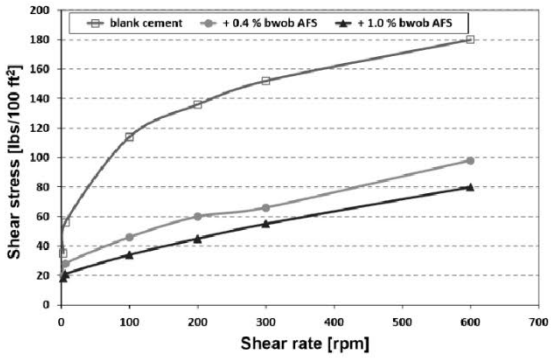

Fig. 7 | Rheology of α-C_2SH slurries prepared at w/b = 0.7 admixed with different dosages of a polycondensate-based superplasticizer.

4| C-S-H-PCE NANOCOMPOSITES AS EARLY STRENGTH ACCELERATORS FOR CEM II/III

From a world-wide perspective, calcined clays present by far the most attractive pathway to reduce the CO_2 emissions from cement manufacturing, as they allow to reduce the clinker factor by as much as 34 %. However, this reduction comes with a significantly decelerated early strength development, compared to OPC. This disadvantage might be solved by the addition of an early strength enhancer that is based on C-S-H-PCE nanofoils which act as a seeding (nucleation) material for the growth of C-S-H phases. This seeding material can be synthesized by co-precipitation of calcium nitrate and sodium silicate in the presence of a PCE superplasticizer. The formed C-S-H-PCE nano-composites exhibit a foil-like morphology with an average length of ~ 50 nm and a thickness of ~ 5 nm as can be seen from TEM imaging (Fig. 8).

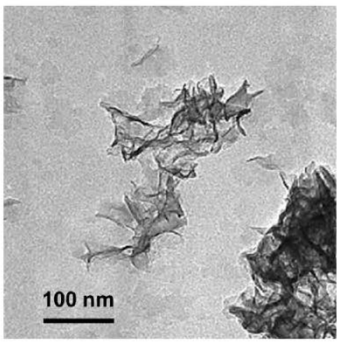

Fig. 8 | TEM image of a C-S-H-PCE nanocomposite.

It is well known that such C-S-H-PCEs are excellent accelerators for OPC [7]. However, as evident from Fig. 9 the addition of these nanocomposites also promotes the early strength development of mortars prepared from calcined clay blended (35 wt.%) cements [8]. Especially within the first 24 hours a considerably increase of the compressive strength can be effectuated compared to the reference sample without any C-S-H-PCE. The compressive strength values obtained between 6-24 hours were even higher than the corresponding values for a mortar sample prepared from OPC. After 7-28 days of curing the increase of the early strength varied between 10 – 20 % compared to that of the calcined clay cement without the C-S-H-PCE. These results clearly demonstrate that C-S-H-PCEs even can enhance the early strength development of calcined clay cements significantly.

Besides, similar or even better results for the accelerating effect can be also achieved in other CEM II/III based cements which contain fly ash or slags as SCMs [8, 9].

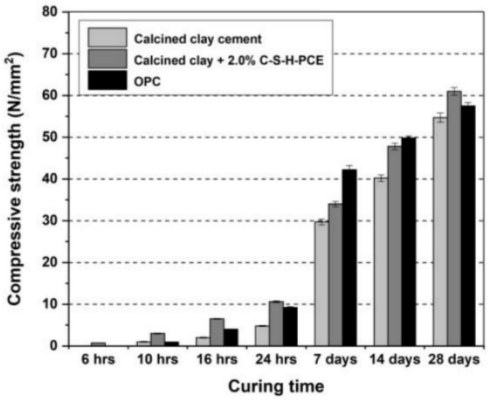

Fig. 9 | Compressive strength of mortars prepared from calcined clay cement after 6, 10, 16, 24 hours, 7, 14 and 28 days of curing.

To gain more insights into the working mechanism of the C-S-H PCEs, in-situ XRD measurements were conducted to monitor the formation of the hydration products in the calcined clay cements. For this purpose, the time-dependent relative intensities of the XRD reflections of Portlandite (Fig. 10) and hemicarbo aluminate (Fig. 11) were compared for calcined clay blended cements hydrated without and in the presence of a C-S-H-PCE [9].

.

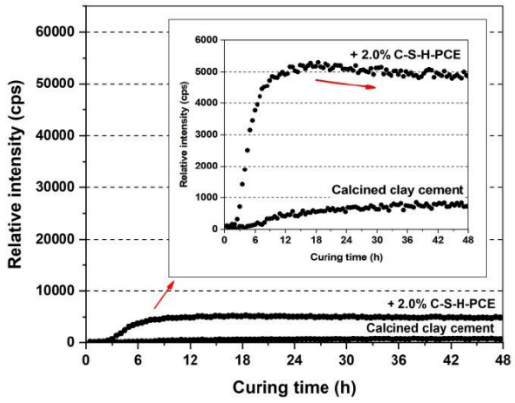

Fig. 10 | Time-dependent intensities of the Portlandite reflection, recorded from in-situ XRD measurements of calcined clay cements hydrated with and without of a C-S-H-PCE nanocomposite.

According to Fig. 10, the Portlandite formation starts much later in the calcined clay cement as compared to the sample containing the C-S-H-PCE. Additionally, the Portlandite concentration starts to decline after ~ 18 h for the seeded sample, thus corraborating an accelerated pozzolanic reaction to occur between the calcined clay and Portlandite. Furthermore, the addition of the C-S-H-PCE results in a higher production of hemicarbo alumiante (Hc) which also starts earlier than in the untreated calcined clay cement.
Based on that, it can be concluded that in the calcined clay blended cement which contains the C-S-H-PCE, Portlandite is used up by two different reactions: first, via the pozzolanic reaction of the calcined clay which produces C-S-H and second via the formation of Hc. Obviously, the C-S-H-PCE first accelerates the hydration of the silicate phases of cement and additionally promotes the pozzolanic reaction of the calcined clay which then starts earlier and becomes more intense and third it leads to the formation of Hc which is known to reduce the porosity in the matrix and therefore favors a higher compressive strength [9].

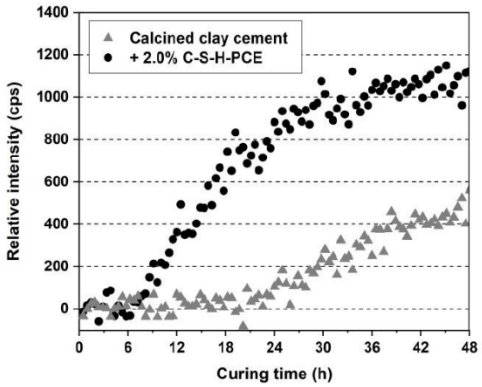

Fig. 11 | Time-dependent intensities of the hemicarbo aluminate reflection, obtained from in-situ XRD measurements of calcined clay cements hydrated with and without of a C-S-H-PCE.

5 | CONCLUSION

To conclude, the admixtures currently applied in OPC work in most cases also for low carbon cement based systems, however, some specific gaps exist which need to be filled by new chemistries (e.g. suitable structures for PCEs which engender a high solubility in Na_2CO_3 activated AAS). Successful development of those admixtures presents the key for wide-spread utilization of any alternative binder material.

REFERENCES

[1] UN Environment, Srivener, K.L., John, V.M., Gartner, E.M., 2018. Eco-efficient cements: Potential economically viable solutions for a low-CO_2 cement based materials industry. Cement and Concrete Research, 114:2-26.

[2] Gartner, E.M., Macphee, D.E., 2011. A physico-chemical basis for novel cementitious binders. Cement and Concrete Research, 41:736-749.

[3] Gartner, E., Sui, T., 2018. Alternative cement clinkers. Cement and Concrete Research, 114:27-39.

[4] Ding, Y., Dai, J.-G., Shi, C.-J., 2016. Mechanical properties of alkali-activated concrete: A state-of-the-art review. Construction and Building Materials, 127:68-79.

[5] Conte, T., Plank, J., 2019. Impact of molecular structure and composition of polycarboxylate comb polymers on the flow properties of alkali-activated slag. Cement and Concrete Research, 116:95-101.

[6] Stemmermann, P., Beuchle, G., Garbev, K., Schweike, U., 2011. Celitement® – A new sustainable hydraulic binder based on calcium hydrosilicates. Proceedings of the 13th ICCC (Vol.46).

[7] Kanchanason, V., Plank, J., 2017. Role of pH on the structure, composition and morphology of C-S-H-PCE nanocomposites and their effect on early strength development of Portland cement. Cement and Concrete Research, 102:90-98.

[8] Kanchanason, V., Plank, J., 2018. Effectiveness of a calcium silicate hydrate – polycarboxylate ether (C-S-H-PCE) nanocomposite on early strength development of fly ash cement. Construction and Building Materials, 169:20-27.

[9] Kanchanason, V., Plank, J., 2019. Effect of calcium silicate hydrate-polycarboxylate ether (C-S-H-PCE) nanocomposite as accelerating admixture on early strength enhancement of slag and calcined clay blended cements. Cement and Concrete Research.

9.2.3. Publikation #15: Interaction of Superplasticizers with Cement from the Point of View of Colloid Chemistry

Publikation #15

Interaction of Superplasticizers with Cement from the Point of View of Colloid Chemistry

Johann Plank, Manuel Ilg

In: V. Mechtcherine, K. Khayat, E. Secrieru (Eds.),
Rheology and Processing of Construction Materials,
RheoCon 2019, SCC 2019
RILEM Bookseries 23 (2020) 134 – 141

Doi: 10.1007/978-3-030-22566-7_16

Interaction of Superplasticizers with Cement from the Point of View of Colloid Chemistry

Johann Plank(✉) and Manuel Ilg

Chair for Construction Chemistry, Technische Universität München, Munich, Germany
sekretariat@bauchemie.ch.tum.de

Abstract. When cement is mixed with water, the clinker phases immediately start to dissolve and a large amount of ions is released into the pore solution. As a result, the ion concentration rapidly increases until the aqueous phase is supersaturated, at which first hydration products are precipitated. As the dissolution, crystallization and the initial hydration reactions all occur at the solid-liquid interface, it is appropriate to consider early cement hydration from the aspects of colloid and interface science.

Generally, fresh cement pastes constitute a thermodynamically unstable colloidal dispersion of mesoscopic particles and hydrate phases in water. The rheological properties (e.g. viscosity, yield stress) and the stability are affected by colloidal and interparticle interactions (e.g. Brownian effects, hydrodynamic and contact forces). However, the poor workability of cement suspensions can be attributed to attractive van der Waals forces between cationic and anionic surface areas. To overcome those forces, superplasticizers are added which disperse cement by imparting an electrostatic (polycondensates) or steric (polycarboxylates) effect. Superplasticizers can interact with cement via adsorption (=physisorption), chemisorption (=intercalation into early hydrate phases) or at low water-to-cement ratios even through repulsive depletion forces induced by the portion of non-adsorbed polymers remaining in the pore solution.

In light of this, the aim of the paper is to give an overview of the different kinds of interactions of superplasticizers with cement from a colloid chemistry point of view. It will be shown, to which thermodynamic parameters the adsorption process is subjected and how the chemical composition of the polymers affects the adsorption behavior. Additionally, experimental methods will be presented that are commonly applied for the investigation of cement-superplasticizer interactions (adsorption and zeta potential measurements). Finally, the role of non-adsorbed superplasticizer molecules on the dispersion of cementitious systems with high solid volume fractions will be discussed.

Keywords: Dispersion · Adsorption · Superplasticizer · Colloid chemistry · Adsorbed layer thickness

V. Mechtcherine et al. (Eds.): RheoCon 2019/SCC 2019, RILEM Bookseries 23, pp. 134–141, 2020.
https://doi.org/10.1007/978-3-030-22566-7_16

1 Dispersion Mechanism of Superplasticizers

Ordinary Portland cement comprises silicate (C_3S, C_2S) and aluminate phases (C_3A, C_4AF) as well as sulfate carriers (e.g. gypsum) for the regulation of the set behavior. When suspended in water, the clinker phases develop a heterogeneous surface charge which leads to the flocculation of the cement particles [1]. Thus, some of the mixing water is entrapped resulting in a high viscosity. However, the agglomerates can be dissipated by the addition of superplasticizers like polycondensates or polycarboxylates (PCEs) which modify the interparticle forces.

It is well established that polycondensates disperse cement through an electrostatic effect, while PCEs achieve dispersion through a combination of electrostatic and steric repulsive forces [2, 3]. To achieve dispersion the superplasticizers need to adsorb at the solid-liquid interface. After adsorption the particles exhibit a negative surface charge which provokes an electrostatic repulsion whose magnitude is much stronger for polycondensates due to their higher anionicity. The electrostatic stabilization of colloidal suspensions is described by the DLVO theory developed by Derjaguin, Landau, Verwey and Overbeek. According to this model, the dimension of the electrostatic effect depends on the electric charge and the Debye length that represents the thickness of the ion cloud surrounding the suspended particles. In contrast to polycondensates, PCEs additionally impart a steric effect induced by their polyethylene glycol side chains [2]. These non-ionic lateral chains protrude into the pore solution and prevent cement particles from approaching each other too close. The steric effect correlates with the thickness of the adsorbed polymer layer, as obvious from the Ottewill-Walker equation:

$$V_{\text{steric}}(a) = \frac{4\pi kTC_v^2}{3v_1^2\rho_2^2}(\psi_1 - \kappa_1)(\delta - a)^2\left(3R + 2\delta + \frac{a}{2}\right)$$

where C_v is the concentration of the adsorbed polymer, v_1 is the molecular volume of the solvent molecules, δ is the adsorbed layer thickness, ρ_2 is the density of the adsorbate (polymer), ψ_1 is the entropy, κ_1 is the enthalpy, R is the radius of the adsorbate, and a is the distance between two adsorbate particles.

The importance of the adsorbed layer thickness for the steric stabilization is supported by findings from Houst et al. who showed that PCEs with longer side chains are more powerful dispersants than those exhibiting shorter ones [4]. Therefore, knowing the layer thickness can help to better understand the differences in the performance characteristics of superplasticizers. Unfortunately, the experimental determination is not very easy because no direct measurement on cement particles is possible due to the continuous changes of their surface composition during the hydration reactions. So far, the layer thicknesses of only a limited number of PCE products have been assessed, most often by atomic force microscopy (AFM) using non-reactive substrates like quartz, mica or magnesium oxide (MgO) [5]. This method produced relatively low values for the layer thickness (1 nm–4 nm) which are far below the values calculated for ideally stretched side chains. For example, many common PCEs exhibit lateral side chains made up of 45 ethylene oxide units which in an ideally stretched conformation

would spread over ∼12.5 nm. The low values for the layer thickness are often ascribed to compression of the polymer layer by the negatively charged AFM tip. Based on those results, it is argued that AFM is an appropriate method to determine the actual adsorbed layer thickness of PCEs. Thus, more reliable information from additional methods is required to obtain a better understanding of the actual dimensions of the adsorbed layer thickness.

Recently, molecular dynamics simulations (MDS) were carried out to investigate the adsorption behavior of PCEs (MPEG-, APEG- and IPEG-PCE) on MgO in synthetic cement pore solution [6]. It was found that the adsorbed conformation is sensitive to the initial orientation of the polymers against the MgO surface. To be more specific, a parallel orientation favored a train like conformation, whereas a perpendicular one was more beneficial for a loop or tail shaped adsorption mode. Depending on the chemical composition of the PCEs quite different conformations were obtained (Fig. 1). According to the results of the MD simulations, the MPEG-PCE adsorbs in a rather flat conformation (=train) covering a large surface area that results in a thin layer thickness. However, the APEG-PCE provokes a medium but dense polymer layer. The highest layer thickness was observed for the IPEG-PCE that adsorbs in a tail like conformation mode. By interconnecting these findings with results from adsorption and fluidity tests it was inferred that a layer thickness higher than 6 nm is necessary for a high dispersing efficacy at a standard dosage of the PCE [6].

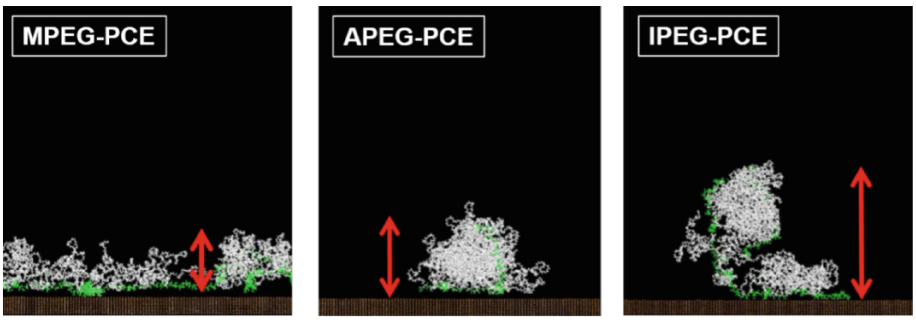

Fig. 1. Adsorbed conformations of different PCEs on MgO as obtained by MD simulations.

2 Adsorption Behavior of Superplasticizers

The working mechanism of superplasticizers relies on physical adsorption (=physisorption) of the anionic polymers on oppositely charged surface areas. Generally, adsorption is a dynamic process with three fundamental steps including the diffusion of the polymers to the solid-liquid interface, the physical attachment to the surface and the final rearrangement of the polymer layer until a maximum number of binding points is achieved [7]. From an energetic perspective, adsorption spontaneously occurs when the Gibbs free energy of adsorption ΔG is negative in sign. According to the Gibbs Helmholtz equation ($\Delta G = \Delta H - T \cdot \Delta S$) this is the case, when heat is released ($\Delta H < 0$) and/or the entropy of the system increases ($\Delta S > 0$). However, depending on

the molecular composition of the superplasticizer, enthalpy or entropy may be the prevalent parameter which instigates adsorption [8]. The experimental determination of ΔH and ΔS for polycondensates revealed that their adsorption is mainly driven by enthalpic contributions resulting from strong electrostatic interactions of the highly anionic polymers with the particle surface. For PCEs, adsorption primarily derives from a huge gain in entropy owed to the release of a large amount of ions and water molecules from the particle surface and the hydrate shell of the polymer [8].

The adsorption behavior of superplasticizers can be modified by the molecular weight, chemical composition and the overall polymer structure. It is well known, that differences in the adsorption properties entail quite diverging performance characteristics (e.g. slump retention capability). For instance, the high anionic character of polycondensates (e.g. BNS, MFS) favors an immediate and almost quantitative adsorption on cement. Consequently, the fluidity rapidly decreases within the first 30 min because no polymer remains in the pore solution to disperse newly formed hydration products. The adsorption properties of PCEs are influenced by the anionic charge amount and the side chain density. Principally, two generic types are differentiated (Fig. 2). PCE variants with a high side chain density and short side chains are favorable for ready mix concrete, whereas products with a high anionicity and a long side chain length are mainly used for precast concrete. The PCE with a low anionic charge amount initially adsorbs only in a small quantity (20%–30% of dosage). The reserve of polymer remaining in the pore solution can then gradually adsorb over time which leads to a long slump retention. Because of this mechanism, such PCEs require a relatively high dosage. Oppositely, PCEs for precast concrete adsorb in a high amount (70%–80%) which engenders a fast decrease of the initial fluidity due to a much smaller depot effect of the non-adsorbed polymers.

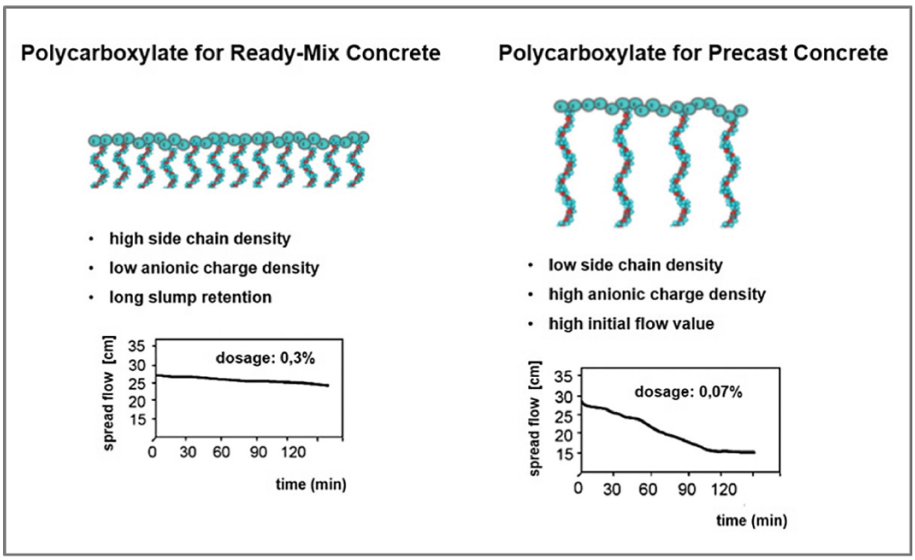

Fig. 2. Structural composition of PCEs applied in ready-mix and precast concrete.

3 Methods for Investigating Cement-Superplasticizer Interactions

Usually, the interaction of superplasticizers with cement is investigated by adsorption measurements using the depletion method. Here, the amount of polymer remaining in the pore solution after contact with cement at equilibrium condition is quantified by total organic carbon (TOC) analysis. Adsorbed amounts are determined for increasing polymer additions until a plateau value is reached (=saturated adsorption) signifying full surface coverage. Adsorption isotherms can be developed then by plotting the depleted amount of polymer as a function of the initial polymer concentration. The adsorption isotherms obtained for polycondensate and PCE based superplasticizers generally comply with the Langmuir adsorption model. However, it has to be noted that this analytical method is incapable of distinguishing the amount of polymer adsorbed via physical attraction from the portion which was consumed by absorption (=chemical intercalation) or precipitation. Therefore, data obtained from adsorption measurements should be interpreted in a prudent way since this method only gives an indication about the depleted amount of polymer.

Actual adsorption of superplasticizers can be corroborated by zeta potential measurements of cement slurries using the electroacoustic method. The zeta potential represents the electric potential at the shear plane between the Stern layer (stationary layer) and the diffuse ion layer of a colloidal particle. Though zeta potential does not correspond to the actual surface charge, it provides useful information about the colloidal stability and the working mechanism of superplasticizers. The typical zeta potential curves for a polycondensate and PCE based superplasticizer are illustrated in Fig. 3. As can be seen there, rising additions of the polycondensate gradually decreases the zeta potential to highly negative values (~ -55 mV) until to the saturated adsorption. At this point, the zeta potential remains constant because no polymer can adsorb on the surface anymore. The highly negative zeta potential induces an electrostatic repulsion of the cement particles.

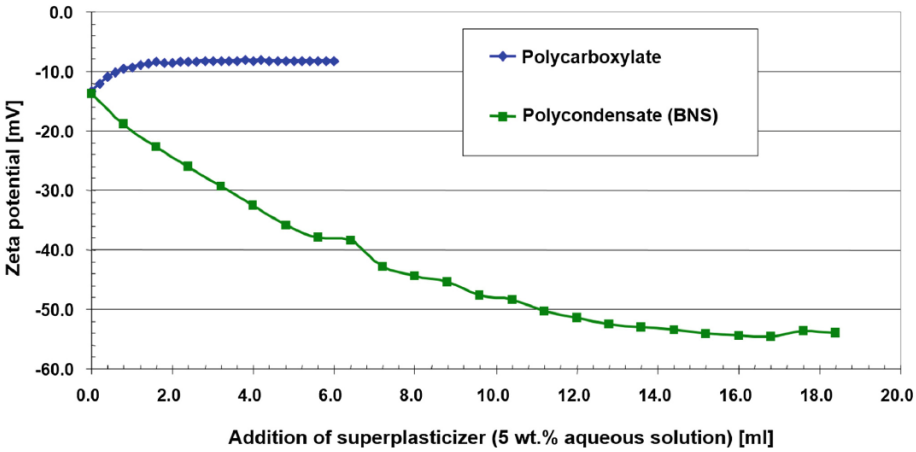

Fig. 3. Zeta potential of cement slurries admixed with different types of superplasticizers.

Adsorption of PCEs generally provokes an increase of the zeta potential. This can be attributed to a displacement of the shear plane by the polyethylene glycol side chains. PCEs with a long side chain length ($n_{EO} \geq 20$) move the shear plane to greater distances away from the cement surface thus causing a more positive value [9].

However, still the question remains on which surface areas superplasticizers adsorb. Yoshioka et al. found that a much higher quantity adsorbs on the aluminate phases (C_3A, C_4AF) than on the silicates (C_3S, C_2S) [2]. This was attributed to the different zeta potentials of the pure cement minerals. C_3A and C_4AF exhibit a positive zeta potential, whereas C_3S and C_2S develop a negative one. A further study revealed that also the adsorbed amount of superplasticizers on the surface of early hydration products is quite different [10]. High adsorbed amounts were especially found for those hydrate phases with a positive zeta potential (i.e. ettringite and mono sulfoaluminate). No adsorption occurred on syngenite, portlandite and gypsum because their zeta potential is zero or negative. This means that superplasticizers are mainly concentrated on surface areas where hydration products with a positive zeta potential crystallize. Thus, a mosaic structure results with an uneven distribution of the polymers on the surface area of the hydrating cement grain (Fig. 4) [10].

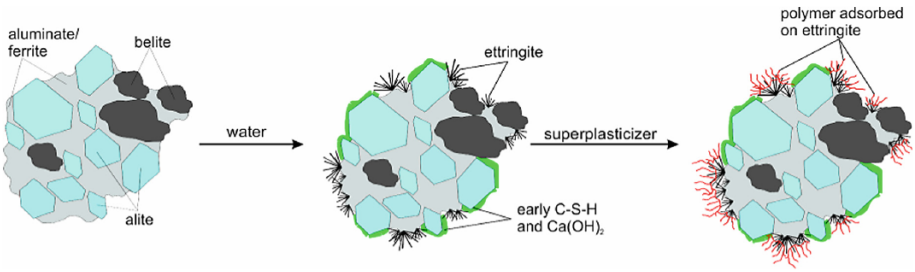

Fig. 4. Schematic presentation of the preferential adsorption sites of superplasticizers on a hydrating cement grain [10].

4 Chemisorption of Superplasticizers

Superplasticizers can interact with cement not only via surface adsorption, also intercalation (chemisorption) of a part of the polymer into the layered structure of calcium aluminate hydrates (C-A-H) may occur during cement hydration. This reaction is highly undesirable because after intercalation the polymer can no longer induce any fluidity. It was found that such intercalates (=organo-mineral phase) form instantaneously upon contact of cement with water when little or no sulfate is initially available for the hydration of C_3A [11]. For cements possessing a high content of alkali sulfates no intercalation was observed. The reaction patterns of C_3A are illustrated for different sulfate concentrations in Fig. 5. Generally, intercalation can be prevented by using alkali sulfates which immediately dissolve or by a delayed addition mode of the superplasticizer.

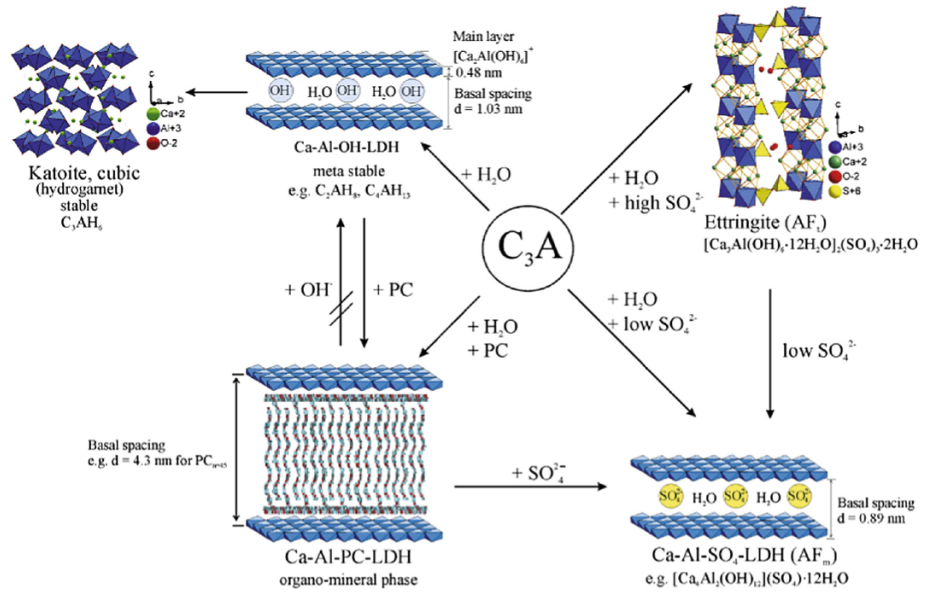

Fig. 5. Reaction patterns of C_3A hydrated at different sulfate concentrations in the absence and presence of a PCE superplasticizer [11].

5 Dispersion Forces at Low w/c-Ratios

Some studies suggest that at low w/c ratios the conventional models for dispersion like the DLVO theory and the Ottewill-Walker equation are no longer exclusively applicable. Instead, the portion of non-adsorbed polymers remaining in the pore solution seems to contribute to cement dispersion as well. This was first described by Sakai et al. who investigated the fluidity of low heat Portland cement – silica blends using different PCE superplasticizers at water-to-powder ratios from 0.16–0.32 [12]. According to their results, the paste fluidity at low w/p ratios (i.e. 0.16) cannot derive only from a steric effect of adsorbed PCE polymers, but is linked to non-adsorbed PCEs that remain in the pore solution. More recent studies showed that even specific non-ionic polymers and glycol compounds can augment the dispersing performance of PCEs at w/c ratios ≤ 0.30 [13]. It is assumed that such co-dispersants might induce repulsive depletion forces between the cement particles. However, more research is necessary to elucidate in more detail the role of non-adsorbed polymers to cement dispersion.

6 Summary

Superplasticizers can adsorb on cement, chemisorb into lamellar C-A-H phases or remain in the pore solution. The macroscopic properties of cement suspensions (e.g. rheology) are affected by those interactions. Adsorption of the superplasticizers on the

surface of the first hydration products is essential for cement dispersion. Depending on the chemical composition of the polymer dispersion is achieved by an electrostatic and/or steric effect. Chemisorption mainly occurs when cement is undersulfated. A low amount of highly soluble sulfates during the first seconds of the hydration of C_3A usually entails an intercalation of the superplasticizer into C-A-H phases. Thus, the polymer becomes ineffective and the fluidity decreases. However, non-adsorbed polymers that remain in the pore solution seem to contribute to cement dispersion especially at low w/c ratios.

References

1. Yoshioka K, Tazawa E, Kawai K, Enohata T (2002) Adsorption characteristics of superplasticizers on cement component minerals. Cem Concr Res 32:1507–1513
2. Yoshioka K, Sakai E, Daimon M, Kitahar A (1997) Role of steric hindrance in the performance of superplasticizers for concrete. J Am Ceram Soc 80:2667–2671
3. Flatt RJ (2004) Dispersion forces in cement suspensions. Cem Concr Res 34:399–408
4. Houst YF, Bowen P, Perche F, Kauppi A et al (2008) Design and function of novel superplasticizers for more durable high performance concrete (superplast project). Cem Concr Res 38:1197–1209
5. Flatt RJ, Schober I, Raphael E, Plassard C, Lesniewska E (2009) Conformation of adsorbed comb polymers dispersant. Langmuir 25(2):845–855
6. Hirata T, Ye J, Branicio P, Zheng J, Lange A, Plank J, Sullivan M (2017) Adsorbed conformations of PCE superplasticizers in cement pore solution unraveled by molecular dynamics simulations. Sci Rep 7:16599
7. Nylander T, Samoshina Y, Lindman B (2006) Formation of polyelectrolyte-surfactant complexes on surfaces. Adv Colloid Interfac 123–126:105–123
8. de Reese J, Plank J (2011) Adsorption of polyelectrolytes on calcium carbonate – Which thermodynamic parameters are driving this process? J Am Ceram Soc 94:3515–3522
9. Plank J, Vlad D, Brandl A, Chatziagorastou P (2005) Colloidal chemistry examination of the steric effect of polycarboxylate superplasticizers. Cem Int 2:100–110
10. Plank J, Hirsch C (2007) Impact of zeta potential of early cement hydration phases on superplasticizer adsorption. Cem Concr Res 37:537–542
11. Plank J, Dai Z, Keller H, von Hoessle F, Seidl W (2010) Fundamental mechanisms for polycarboxylate intercalation into C_3A hydrate phases and the role of sulfate present in cement. Cem Concr Res 40:45–57
12. Ushiro M, Atarashi D, Kawakami H, Sakai E (2013) The effect of superplasticizer present in pore solution on flowability of low water-to-powder cement paste. Cem Sci Concr Technol 67:102–107
13. Lange A, Plank J (2016) Contribution of non-adsorbing polymers to cement dispersion. Cem Concr Res 79:131–136

9.2.4. Publikation #16: The Role of Chemical Admixtures in the Formulation of Modern Advanced Concrete

Publikation #16

The Role of Chemical Admixtures in the Formulation of Modern Advanced Concrete

Johann Plank, Manuel Ilg

In: W. Boshoff, R. Combrinck, V. Mechtcherine, M. Wyrzykowski (Eds.), 3rd International Conference on the Application of Superabsorbent Polymers (SAP) and Other New Admixtures Towards Smart Concrete, SAP 2019

RILEM Bookseries 24 (2020) 143 – 157

Doi: 10.1007/978-3-030-33342-3_16

The Role of Chemical Admixtures in the Formulation of Modern Advanced Concrete

Johann Plank(✉) and Manuel Ilg

Chair for Construction Chemistry, Technische Universität München, Lichtenbergstraße 4, 85747 Garching, Germany
sekretariat@bauchemie.ch.tum.de

Abstract. Chemical admixtures constitute indispensable ingredients for the production of modern advanced concrete. In developed countries, at least 80% of the concrete produced contains one or several admixtures. They include plasticizers, superplasticizers, retarders, accelerators, stabilizers, defoamers, foamers and shrinkage reducers, to name the most important classes. With their help it is possible to optimize the properties of fresh and hardened concrete in such way as to adapt better to local climate and processing conditions and to enhance the mechanical properties and durability. Furthermore, highly sophisticated products such as ultra-high strength concrete (UHPC) or self-levelling and self-compacting concrete (SCC) became possible only with the invention of specific high performance admixtures.

This article gives an overview of major classes of chemical admixtures (e.g. PCE superplasticizers, C-S-H-PCE nanocomposites, stabilizers for SCC, shrinkage-reducing agents) and their current status of development. The main technologies will be described and their role in the formulation of modern advanced concrete will be highlighted. Finally, an outlook on potential developments in the future (e.g. improved curing agents, admixtures which enhance the ductility of concrete) will be provided.

Keywords: Admixtures · PCE superplasticizers · Shrinkage-reducing agents · C-S-H-PCE nanocomposites · Viscosity modifying agents

1 Polycarboxylate (PCE) Superplasticizers

1.1 Current PCE Technology

Polycarboxylate superplasticizers are added to the fresh concrete for the dispersion of the cement particles. They produce a highly flowable concrete which can be placed at the construction site much easier. Additionally, lower w/c ratios can be applied thus facilitating the manufacturing of building materials with high mechanical strength and long durability. PCE-based admixtures have taken an unprecedented rise since their invention in 1981 (Hirata 1981). It is estimated that in 2014, the global volume of PCE produced exceeded 3 mio. tons, based on 30% liquid concentration. Meanwhile, the term “PCE” includes a huge variety of chemically often substantially different

W. P. Boshoff et al. (Eds.): SAP 2019, RILEM Bookseries 24, pp. 143–157, 2020.
https://doi.org/10.1007/978-3-030-33342-3_16

polymers, with significant variances in performance characteristics. In the following, the main classes of PCE products on the market are described and their general chemical composition is exhibited in Fig. 1.

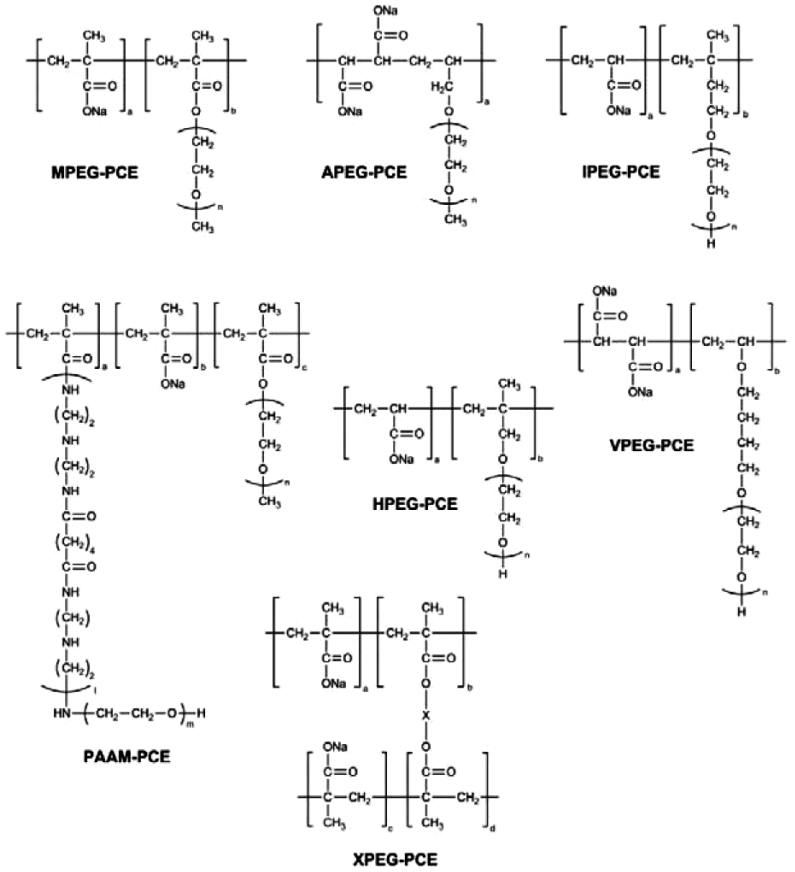

Fig. 1. Chemical structures of the different classes of PCE products currently produced by the industry.

MPEG-Type PCEs: They constitute the first type of PCE which was invented in Japan. MPEG-PCEs can be synthesized either via aqueous free radical copolymerization of methacrylic acid with an ω-methoxy poly(ethylene glycol) methacrylate ester macromonomer (this route is predominantly used by the industry) (Plank et al. 2008) or by esterification ("grafting") of short chain poly(meth)acrylic acid with ω-methoxy poly(ethylene glycol) (Guicquero et al. 1999). Note that both synthesis routes can lead to substantially different products, even when exactly the same molar ratios of monomers are used. Via esterification, a PCE polymer exhibiting a regular (statistical) repartition of side chains along the main chain is achieved while gradient polymers exhibiting a decreasing side chain density along the backbone are formed from the

copolymerization process as a result of the higher reactivity of the ester macromonomer versus methacrylic acid (Pourchet et al. 2012). Performance tests have revealed that in many cases gradient polymers perform better, because their blocks of polymethacrylic acid allow higher adsorption on cement. One major disadvantage of MPEG-PCEs is their limited stability (especially when acrylate instead of methacrylate ester macromonomers are used) which derives from hydrolysis of the ester linkage between the main and the side chain. Furthermore, the diol or diester content present in the raw materials must be kept below 1% to avoid undesirable crosslinking (Paas 2015).

APEG-Type PCEs: This kind is prepared via free radical copolymerization from α-allyl-ω-methoxy or ω-hydroxy poly(ethylene glycol) ether and maleic anhydride or acrylic acid as key monomers, either in bulk or in aqueous solution (Akimoto 1992). APEG-PCEs always possess a strictly alternating monomer sequence (ABAB), because the allyl ether macromonomer does not homopolymerize as a consequence of mesomeric stabilization of the allyl radical. This stabilization causes allyl ethers to react rather slowly and can lead to low conversion rates for the macromonomer. Polymerization in bulk works well for side chain lengths of up to 34 EO units while polymerization in water typically yields copolymers possessing very short trunk chains ("star polymers") made of ∼10 repeating units only which however were found to exhibit superior dispersing performance. The disadvantages of aqueous copolymerization are longer reaction times, lower conversion rates and lower concentration of the finished PCE solution.

Initially, APEG-PCEs suffered from a reputation of causing delayed plastification (i.e. the slump of concrete first increased over ∼30 min to reach a maximum, and then dropped). Meanwhile, this problem has been solved, for example by incorporation of specific comonomers as spacer molecules such as styrene or allyl maleate which can modulate the conformational flexibility of the trunk chain (Plank and Lange 2012). This method provides PCE molecules with pronounced stiffness which can adsorb faster and thus avoid the effect of delayed plastification.

***VPEG-Type PCEs*:** Such PCEs are obtained by aqueous free radical copolymerization of e.g. 4-hydroxy butyl poly(ethylene glycol) vinyl ether and maleic anhydride or acrylic acid (Albrecht 1996). Their polymerization must be conducted at temperatures <30 °C to avoid vinyl ether monomer degradation. As a result, a specific low temperature initiator such as Vazo 50 (2,2'-Azobis (2-methyl propionamidine) dihydrochloride) is required. The advantage of the vinyl over the allyl ether technology is the much higher reactivity of vinyl ethers.

HPEG-Type PCEs: Here, α-methallyl-ω-methoxy or ω-hydroxy poly(ethylene glycol) are used as macromonomers in copolymerization with e.g. acrylic acid (Hamada et al. 2001). This kind of PCE which is easy to manufacture in large industrial scale emerged a few years ago, especially in China. There, even a process has been developed where copolymerization is performed at room temperature and is applied in many factories (Wang et al. 2013). Most HPEG-PCEs can outperform the MPEG- or APEG-PCEs with respect to their dispersing ability.

IPEG-Type PCEs: This type of PCE (sometimes also referred to as TPEG-PCE) is synthesized from isoprenyl oxy poly(ethylene glycol) ether as macromonomer by copolymerization with e.g. acrylic acid (Yamamoto 2004). In recent years, this PCE

has become quite popular, especially in Japan and China, because of its excellent performance which often exceeds that of any other type of PCE, and its simple preparation utilizing free radical copolymerization. A disadvantage of IPEG-PCEs is their potential to decompose into isoprene, water and glycol (Nagare 2006). To prevent this undesired process, the IPEG macromonomer and the IPEG-PCE should not be handled in bulk, but always kept in aqueous solution.

XPEG-Type PCEs: It has been established before that the ability of an individual PCE molecule to cover as much surface area on cement as possible directly correlates to its dosage (Ohta 1997). Hence, polymers which stretch out further on the surface are believed to present more effective PCEs. Following this concept, slightly crosslinked PCE molecules utilizing diesters (e.g. synthesized from PEG and methacrylic acid or maleic anhydride) were shown to provide enhanced dispersion (Tahara 1995).

PAAM-Type PCEs: These zwitterionic PCEs possess mixed side chains composed of polyamidoamine (PAAM) and PEO segments. This structural motif distinguishes them fundamentally from all other PCEs which exclusively contain PEO/PPO side chains. The PAAM-type PCE is said to fluidify cement at w/c ratios as low as 0.12 (Amaya 2000). Its disadvantage is the high cost of the PAAM side chain.

1.2 New PCE Products

Industrial and academic researchers continue to develop and introduce new and improved polymers, despite of the great diversity of already existing PCE products. Those include:

Organo-Silane (OSi) Modified PCEs: They can be prepared by incorporating either 3-trimethoxysilyl propyl methacrylate (MAPTMS) or N-maleic γ-amidopropyl triethoxy silane (MAPS) as a new comonomer into a conventional PCE, e.g. the MPEG-type (Fig. 2) (Fan et al. 2012, Witt 2012). The consideration behind this concept was to achieve a chemical bond between C-S-H and the superplasticizer, made possible through condensation of silanol (-Si-OH) groups present in both compounds. If formed, such a bond would anchor the PCE molecule irreversibly on the surface of hydrating cement and prevent its desorption e.g. by sulfate ions or anionic retarders resulting from competitive adsorption.

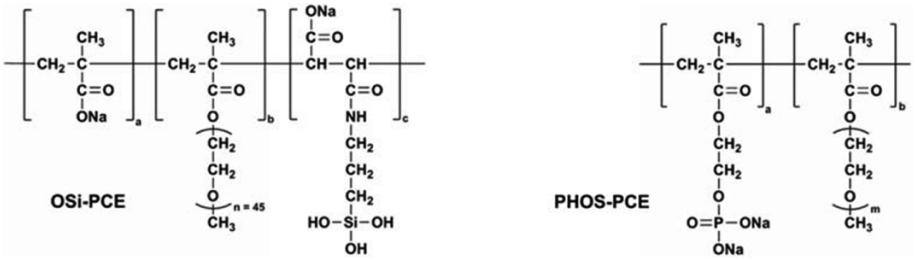

Fig. 2. Examples of organo-silane modified (OSi-PCEs) and phosphated PCEs (PHOS-PCEs).

Phosphated (PHOS) PCEs: Superplasticizers generally achieve their dispersing power through adsorption on the surface of cement, especially on ettringite (Yoshioka et al. 2002). Such adsorption is facilitated through anionic anchoring groups which typically include carboxylate or dicarboxylate groups. Some years ago it has been shown that phosphonate presents a more powerful anchoring group than carboxylate (Mosquet et al. 1997). Very recently, novel superplasticizers have been presented which incorporate phosphate as an anchoring group (Kraus 2011, Dalas et al. 2015). Phosphatation can be accomplished by esterification of e.g. hydroxyethyl methacrylate with phosphoric acid, leading to the PCE copolymer shown in Fig. 2. The phosphated PCEs are said to adsorb on cement almost instantaneously which presents a major advantage in specific concrete and dry-mix mortar applications. Furthermore, they appear to be more sulfate-tolerant, compared to conventional PCE superplasticizers, and often require lower dosages (Stecher and Plank 2019).

1.3 Tailoring PCEs to Specific Applications

Recently, substantial progress has been made in the optimization of current PCE products for difficult applications. Those include concretes of particularly low w/c ratios (<0.30) and the compatibility of PCEs with clay contaminants occurring in aggregates.

Stickiness of Concrete at Low w/c Ratio: The problem of stickiness and slow flow of concrete prepared at low w/c ratio is well-known and was solved as follows: It was found that the hydrophilic-lipophilic balance (HLB) value of a PCE molecule determines whether the concrete admixed with this polymer exhibits slow or fast flow (Lange et al. 2014). According to this study, PCE molecules should be as hydrophilic as possible and their HLB value should be >18.5. Such PCEs (preferably of IPEG- and APEG-type) produce cement pastes with particularly low plastic viscosity and exhibit fast flow without any stickiness. Such rheologically optimized concrete is easier to pump, spread and compact and presents a huge step forward in improving the workability of high-strength concretes of low w/c ratios.

Enhanced Clay Tolerance: Over the last years, applicators have observed that PCE superplasticizers – unlike polycondensates – exhibit a pronounced sensitivity to clay and silt contaminants (Jeknavorian et al. 2003, Atarashi et al. 2004). As a result, their performances are greatly reduced or the PCEs become entirely ineffective. Montmorillonite, a 2:1 smectite clay, has been found to be more harmful than other clay minerals such as kaolinites or muscovites (Lei and Plank 2014). Generally, the capacity of clays to sorb water, hydrate and swell leads to more viscous cement pastes. This effect results in a loss of workability or a higher water demand, independent of whether a superplasticizer is present or not.

Previous research has established that in cement pore solution, the surfaces of bentonite clay particles become positively charged as a result of Ca^{2+} adsorption onto the negative alumosilicate layers. Onto these surfaces, polyanionic superplasticizers such as polycondensates or polycarboxylates adsorb, thus resulting in a partial depletion of superplasticizer from the pore solution. This way, clay competes with cement for superplasticizer molecules. Moreover, PCE polymers can intercalate

chemically into the interlayer space between the individual alumosilicate layers of specific clay minerals, especially montmorillonite (bentonite), resulting in an organo-mineral phase whereby their poly(ethylene glycol) side chains occupy the interlayer space, as is shown in Fig. 3. This reaction with clay is specific for PCEs and is a consequence of their PEO side chains, as was evidenced by XRD measurements (Ng 2012a). Consequently, PCEs can be used up by clay by both surface adsorption and chemical sorption whereas polycondensates such as BNS are consumed only by surface interaction (Jardine 2002, Ng and Plank 2012b). This explains why PCEs are significantly more affected by clay than polycondensates.

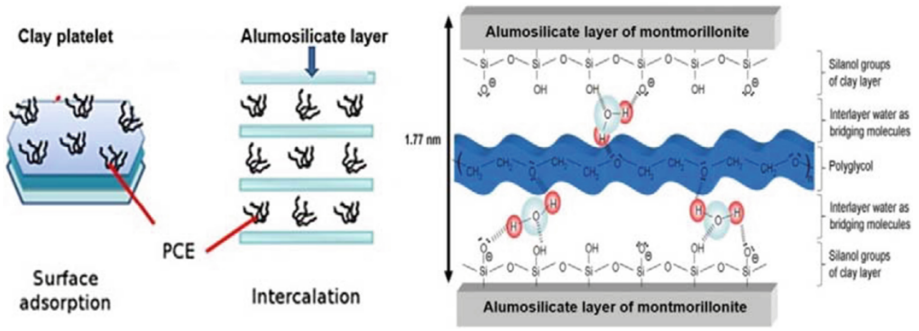

Fig. 3. Fundamental types of interaction between PCE and montmorillonite clay (left) and chemical sorption (intercalation) of a poly(ethylene glycol) side chain in between alumosilicate layers (right).

The industry has developed several strategies to mitigate the negative effects of clay on PCEs. The first concept includes the use of sacrificial agents.

Analysis of sorbed amounts of individual PCE constituents (backbone, represented by poly(methacrylic acid) and side chain, represented by poly(ethylene glycol)) revealed that the side chain sorbs in large amounts on clay (~400 mg MPEG/g clay) while the polymer trunk is consumed much less (~30 mg PMA/g clay) (Ng 2012a). This not only signifies that the PEO side chain present in PCE provides the main interaction with clay; it also offers a remedy for the problem whereby pure PEG or MPEG are utilized as sacrificial agents to occupy the interlayer spaces while the PCE molecule which exhibits a lower tendency to intercalate as a result of its anionic charge is preserved and can thus interact with the cement to achieve dispersion (Ng and Plank 2012b). As another remedy, addition of cationic polymers which inhibit the swelling of clay entirely has been proposed (Jacquet 2006). This method offers the advantages of zero water consumption because the clay will not hydrate at all. Additionally, the interlayer spacing will not be accessible for the PCEs.

Obviously, the best solution to the incompatibility problem of PCE and clay would be a novel PCE structure which does not contain PEO side chains. Recently, such polymers have been synthesized using either hydroxy alkyl esters of methacrylic acid or vinyl ethers as side chain bearing macromonomers (Lei and Plank 2012).

Utilizing XRD analysis, it was found that indeed these novel polycarboxylates do not undergo side chain intercalation with clay and adsorb in small quantities only (~25 mg polymer/g clay). Consequently, they exhibit robust performance even in the presence of clay contaminants. This behavior perfectly confirms the concept of non-PEO side chains as a remedy for the intercalation problem of conventional PCEs into clay structures.

2 Early Strength Enhancing Admixtures

A recent invention includes the application of C-S-H-PCE nanocomposites as seed crystals for the hydration of the silicate phases C_3S and C_2S (Nicoleau et al. 2011, 2013). The nanocomposites can be prepared by combining aqueous solutions of e.g. sodium silicate and calcium nitrate with a PCE solution. The resulting precipitate contains nanofoils of C-S-H with surface adsorbed and possibly intercalated PCE (Fig. 4).

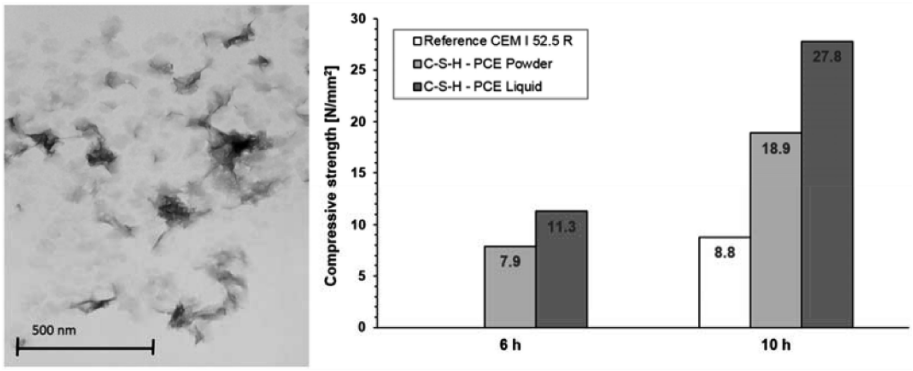

Fig. 4. TEM image of C-S-H-PCE nanocomposite foils (left) and their effectiveness as strength enhancing seeding material for a mortar prepared from CEM I 52.5R (right).

The nanofoils greatly accelerate the silicate hydration by reducing the free activation energy ΔG of the crystallization to zero. In cement hydration this barrier needs to be overcome to initiate C-S-H nucleation. The result is a much enhanced early strength development, especially after 6–12 h of hydration, without sacrificing the final strength as is the case for most common accelerators such as e.g. calcium nitrate, sodium silicate, sodium aluminate or aluminum dihydroxy formate (Fig. 4). Recently, it has been found that C-S-H-PCE nanocomposites also enhance the early strength of blended cements containing e.g. fly ash or calcined clays by accelerating the pozzolanic reaction (Kanchanason and Plank 2018).

3 Stabilizers

For highly dispersed concretes such as e.g. self-compacting concrete (SCC), polymeric stabilizers (also referred to as viscosity modifying agents, VMAs) are frequently applied to prevent disintegration and bleeding. Common stabilizers include welan gum, curdlan, hydroxypropyl cellulose, polyethylene glycol (Hibino 2000), and ATBS-based copolymers. Among the latter, two types have become quite popular in SCC mixes. The first one constitutes a terpolymer prepared via aqueous free radical copolymerization from 2-acrylamido-2-methylpropane sulfonic acid (ATBS), N-vinyl acetamide (NVA), acrylonitrile (ACN) and acrylamide (AA) while the second one comprises ATBS, N,N-dimethyl acrylamide (NNDMA) and, in some versions, tristyrylphenol poly(ethylene glycol) methacrylate ester as a third monomer. The ATBS-NNDMA copolymers can be prepared either via aqueous free radical copolymerization or through gel polymerization utilizing the Norrish-Trommsdorf effect (Futami 2003, Schinabeck 2005). The chemical structures of the ATBS-based stabilizers are displayed in Fig. 5. Both ATBS copolymers constitute linear molecules exhibiting high stiffness, owed to hydrogen bridging between ATBS and the neighboring NVA or NNDMA monomer.

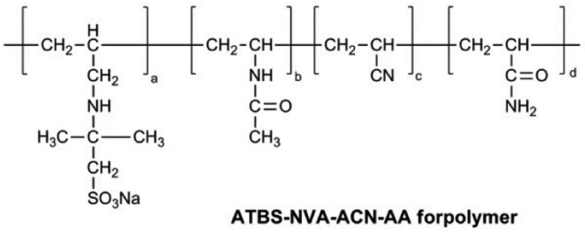

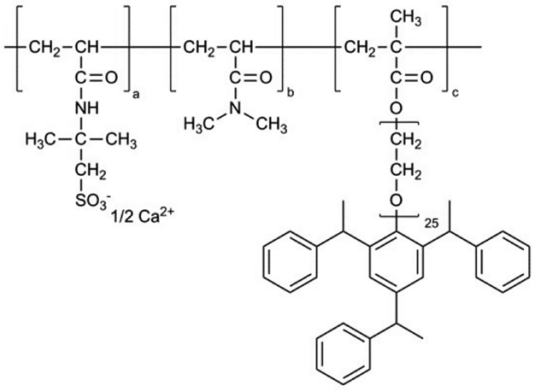

Fig. 5. Chemical structures of the ATBS-NVA-ACN-AA and ATBS-NNDMA-SEM copolymers commonly used as stabilizers in SCC.

Applicators of VMAs are well aware that these products not only can provide the desired effect, but also significantly impact on the rheology of concrete in a way that the fluidizing effect from PCE can be lost. Hence, a counterproductive (antagonistic) effect can occur which renders application of those stabilizing polymers tricky. To improve this situation, the interaction of PCE superplasticizers with ATBS/NNDMA and welan gum VMAs has been studied thoroughly.

Surprisingly, for the ATBS/NNDMA stabilizer it was found that at low dosages (0–0.1 wt%) it acts as a viscosifier in concrete while at higher additions it provides a strong dispersing effect (Fig. 6).

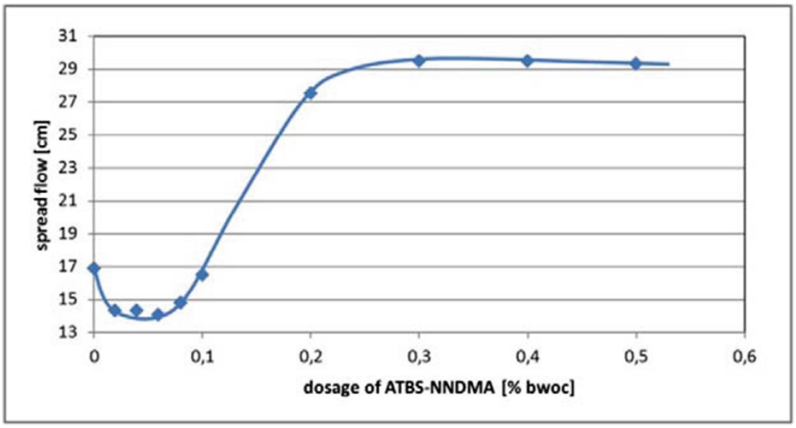

Fig. 6. Cement paste flow as a function of ATBS-NNDMA stabilizer addition (no PCE present).

Furthermore, when combined with PCE it is the stabilizing polymer which determines the flow regime, and not the PCE (Plank 2015). The reason behind this effect is that the ATBS copolymer preferably adsorbs on cement and thus prevents the PCE from adsorbing and becoming effective. The results suggest that when PCEs are combined with this ATBS copolymer, then a stabilizer dosage of >0.1% bwoc should be applied to avoid its thickening effect.

For welan gum VMA, a different scenario was found. According to these results, the stabilizing effect of welan gum biopolymer solely relies on its strong viscosifying effect on the cement pore solution which originates from its high adsorption on cement. Thus, with increased concentrations welan gum starts to destroy the fluidity generated by PCEs (Üzer and Plank 2016). Consequently, opposite to the ATBS/NNDMA stabilizer which requires a minimum dosage to avoid thickening, additions of welan gum to the PCE concrete should be kept as low as possible to avoid its negative effect on concrete rheology.

The investigations presented here suggest that admixture combinations are by no means trivial, and that understanding their mechanism of interaction with cement can help to optimize their performance.

4 Shrinkage-Reducing Admixtures

During its hydration and hardening, mortar and concrete undergo autogenous (= chemical) and dry (= physical) shrinkage (Lura et al. 2003, Tazawa et al. 1995). The latter is the consequence of water evaporation at the surface which causes a contractive force in the capillary pores and thus results in compaction. Previous studies have revealed that occurrence of physical shrinkage is dependent on the presence of pores exhibiting specific diameters, namely from ~10–50 nm (Wittmann 1982). Effective shrinkage-reducing agents (SRAs) are those which reduce the surface tension of the pore solution and which can modulate the pore size distribution in the cementitious matrix in such way that the shrinkage causing pore diameters are avoided. Diols, glycols, glycol ethers and amino terminated poly(ethylene-propylene) glycols have been identified as suitable SRAs (Fig. 7).

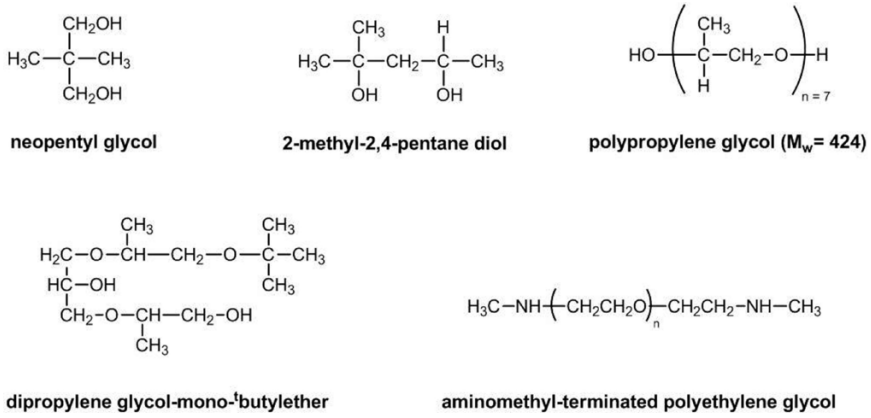

Fig. 7. Chemical structures of effective shrinkage-reducing agents (SRAs).

It is, however, well established that diols of quite similar structure and surface activity than those displayed in Fig. 7 do not provide any shrinkage-reducing effect at all, whereby the reason is still unknown. Furthermore, effective SRAs require extremely high dosages of 2–4% bwoc which are far beyond those for common functional admixtures used in concrete. Also, the reduction in shrinkage achieved from these admixtures is limited. Hence, it becomes obvious that a considerable gap with respect to the potency of SRAs and a thorough understanding of their working mechanism exists.

In recent years, two contributions on this subject were published. The first work presented that the pore-size modulating effect of SRAs is linked to their ability to form micelles of specific, large enough diameters which are the templates for pores which do not induce shrinkage (Kayello 2014). These micelles form at a stage in cement hydration when a significant amount of water has already been consumed and the SRAs are present in the pore solution at concentrations of 6–10%. Compounds which form micelles too early or too late in cement hydration cannot provide any shrinkage-reducing effect.

The second contribution utilized molecular modeling to identify potentially effective SRAs and then tested them in mortar to confirm the concept (Shlonimskaya et al. 2014). Based on a computer-aided molecular design (CAMD) approach that used the signature molecular descriptor, 2-propoxyethanol and 3-ethoxypropylamine were found to provide exceptional reduction in the surface tension of water. Their high shrinkage-reducing potential was confirmed in actual mortar tests.

Inspite of all this it obvious that our current technology of SRAs is quite limited and – compared to that existing in the field of e.g. superplasticizers or retarders – is far behind. More intense research is required to fill this gap in the future and to bring its technology to a level which allows a more effective control of physical shrinkage compared to the state of the art.

5 New Admixture Technologies – What Can We Expect in the Future?

5.1 Improved Curing Agents

Until now, a significant gap in current curing technology exists. The current situation on construction sites where large concrete slabs or decks are poured is that significant efforts have to be undertaken to reduce dry shrinkage and cracking on the surfaces. The most common practices include the spraying of water onto the concrete surface or coverage with a plastic foil to reduce water evaporation. Both methods are often not very effective, and on top they require a substantial amount of labor. Hence, the industry is challenged with developing admixtures which e.g. can be mixed into the fresh concrete and then prevent its surface desiccation, thus eliminating the need for post-curing of concrete. In light of this, superabsorbent polymers (SAPs) seem to be a promising candidate for the internal curing of concrete (Mignon et al. 2017). These cross-linked polymers which are typically synthesized from acrylic acid and/or acrylamide start to swell upon the contact with the pore solution. Consequently, a hydrogel is formed which gradually releases the absorbed water during the self-dessication of the concrete, thus mitigating the autogeneous shrinkage during hardening (Snoeck et al. 2017). Another type of curing agents are water evaporation retardants (e.g. poly lauryl methacrylate emulsions) which are applied on the surface of the plastic concrete to prevent the formation of plastic shrinkage cracks (Liu et al. 2010).

5.2 Admixtures Improving the Ductility of Concrete

Concrete presents a unique building material because of its easy preparation from abundantly available raw materials, its low cost and its enormous strength. Those excellent features have propelled the global volume of concrete poured to more than 30 billion tons per year. Inspite of these extraordinary properties, concrete suffers from one major deficiency which greatly limits its application: low ductility (= tensile or bending strength) and low fracture toughness (Fig. 8).

Compared to human bone for example, the fracture toughness of concrete is about 100 times lower. For a conventional concrete (w/c ratio $\sim$0.5), the tensile strength

reaches only ~10% of its compressive strength, thus rendering concrete a very brittle material. The problem becomes even worse when the w/c ratio is low. For example, in ultra-high strength concrete (UHPC, w/c = 0.25) the tensile strength develops to only 5% of the compressive strength. Consequently, such concrete is prone to crack formation through vibrational impact (on bridges e.g. from traffic, on buildings from wind forces, etc.).

In the future, the industry will be challenged with developing concepts which can reduce in-situ the brittleness of concrete. Potential solutions involve the addition of textile fibers or the generation of organo-mineral phases which are more flexible than conventional cement hydrates (e.g. meso crystals similar to those described for $CaCO_3$-PCE precipitates (Keller and Plank 2013), or Ca_2Al-polymer-LDH composites (Plank and Ng 2012)). In this respect, an interesting concept would be the in-situ formation of C-S-H-polymer nanocomposites similar to those described in Sect. 2 for C-S-H-PCE which potentially can improve the bending strength of concrete. Considering the magnitude of the task it might be useful to study concepts from nature such as they occur in mollusk shells which consist of calcite tablets with interstitial chitin (Mann 1993). Such biomimetic approaches will hopefully inspire researchers to propose solutions for this problem.

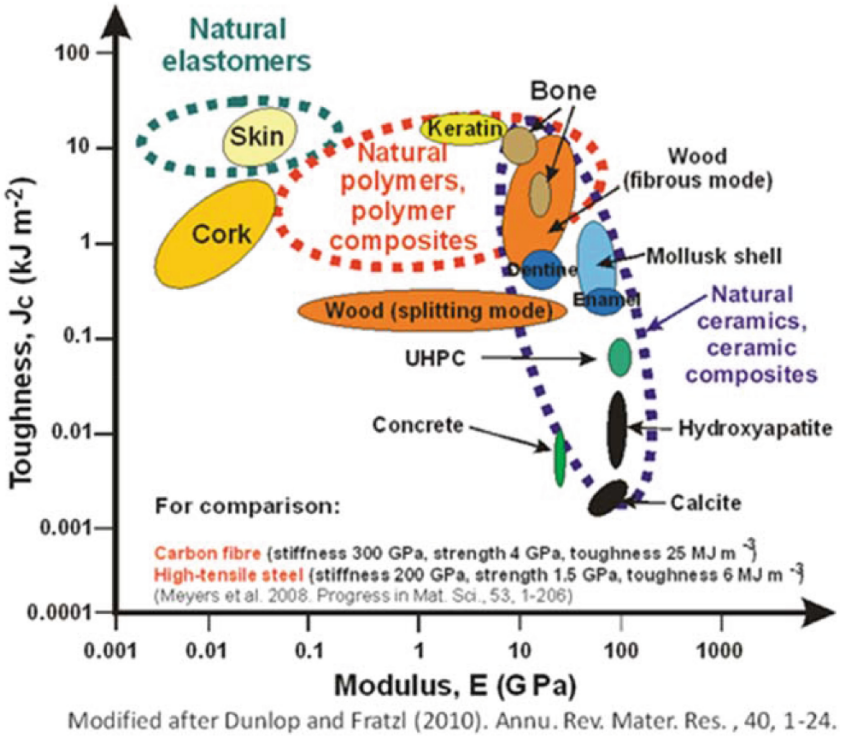

Fig. 8. Comparison of the fracture toughness of different natural or man-made materials including human bone and concrete.

6 Conclusion

Chemical admixtures have truly revolutionized modern concrete technology. They present a major driver for innovation in concrete and will continue to do so for many years to come. In the future, it would be extremely attractive to have admixtures which allow the safe application of self-compacting concrete delivered as ready-mixed concrete to the job site. Even more, to be able to control concrete consistency (fluidity) during delivery through the energy uptake of the rotating container of the concrete truck and energy-dependent PCE dosage would be most intriguing. Undoubtedly, the current admixture products will be refined further to become even more effective, and they will be tailored more specifically to distinct applications.

References

Akimoto, S., Honda, S., Yasukohchi, T.: Additives for Cement, EP 0,291,073 (1992)

Albrecht, G., Weichmann, J., Penkner, J., Kern, A.: Copolymers based on Oxyalkylene Glycol Alkenyl Ethers and Derivatives of Unsaturated Dicarboxylic Acids, EP 0,736,553 (1996)

Amaya, T., Ikeda, A., Imamura, J., Kobayashi, A., Saito, K., Danzinger, W., Tomoyose, T.: Cement Dispersant and Concrete Composition containing the Dispersant, WO 0,039,045 (2000)

Atarashi, D., Sakai, E., Obinata, R., Daimon, M.: Interactions between superplasticizers and clay minerals, Cement Sci. Concr. Technol. **58**, 387–392 (2004)

Dalas, F., Nonat, A., Pourchet, S., Mosquet, M., Rinaldi, D., Sabio, S.: Tailoring the anionic function and the side chains of comb-like superplasticizers to improve their adsorption. Cem. Concr. Res. **67**, 21–30 (2015)

Fan, W., Stoffelbach, F., Rieger, J., Regnaud, L., Vichot, A., Bresson, B., Lequeux, N.: A new class of organosilane-modified polycarboxylate superplasticizers with low sulfate sensitivity. Cem. Concr. Res. **42**, 166–172 (2012)

Futami, T., Yamaguchi, T., Tagoshi, H.: Use of a Polymer as a High-Flow Concrete Additive and Concrete Material Containing the Additive, EP 0,757,998 (2003)

Guicquero, J.P., Maitrasse, P., Mosquet, M.A., Sers, A.: A Water Soluble or Water Dispersible Dispersing Agent, FR 2,776,285 (1999)

Hamada, D., Yamato, F., Mizunuma, T., Ichikawa, H.: DE 10,048,139 A1 (2001)

Hibino, M.: Effect of viscosity enhancing agent on self-compactibility of fresh concrete. In: Sixth International Conference on Superplasticizers and other Chemical Admixtures in Concrete (CANMET/ACI), Nice, SP-195, pp. 305-320 (2000)

Hirata, T.: Cement dispersants, JP 842,022 (S59-018338) (1981)

Jacquet, A., Villard, E., Watt, O.: Method for inserting impurities, WO 2006,032,785 (2006)

Jardine, L., Koyata, H., Folliard, K., Ou, C.C., Jachimowicz, F., Chun, B., Jeknavorian, A.A., Hill, C.L.: Admixture and method for optimizing addition of EO/PO superplasticizer to concrete containing smectite clay-containing aggregates, U.S. 6,352,952 (2002)

Jeknavorian, A.A., Jardine, L., Ou, C.C., Koyata, H., Folliard, K.J. (2003) Interaction of superplasticizers with clay-bearing aggregates, In: Malhotra, V.M. (ed.) 7th CANMET/ ACI International Conference on Superplasticizers and Other Chemical Admixtures in Concrete, Berlin/Germany, ACI, SP-217, pp. 1293–1316

Kanchanason, V., Plank, J.: Effectiveness of a calcium silicate hydrate – polycarboxylate ether (C-S-H-PCE) nanocomposite on early strength development of fly ash cement. Constr. Build. Mater. **169**, 20–27 (2018)

Kayello, H.M., Naresh, K.R., Tadisina, R., Shlonimskaya, N., Biernacki, J.J., Visco, D.P.: An application of computer-aided molecular design (CAMD) using the signature molecular descriptor – Part 1. identification of surface tension reducing agents and the search for shrinkage reducing admixtures. J. Am. Ceram. Soc. **97**(2), 365–377 (2014)

Keller, H., Plank, J.: Mineralisation of $CaCO_3$ in the presence of polycarboxylate comb polymers. Cem. Concr. Res. **54**, 1–11 (2013)

Kraus, A., Dierschke, F., Becker, F., Schuhbeck, T., Grassl, H., Groess, K.: Method for producing phosphate polycondensation products and the use thereof, US patent 2011/0281975 A1 (2011)

Lange, A., Hirata, T., Plank, J.: Influence of the HLB value of polycarboxylate superplasticizers on the flow behavior of mortar and concrete. Cem. Concr. Res. **60**, 45–50 (2014)

Lei, L., Plank, J.: A concept for a polycarboxylate superplasticizer possessing enhanced clay tolerance. Cem. Concr. Res. **42**, 1299–1306 (2012)

Lei, L., Plank, J.: A study on the impact of different clay minerals on the dispersing force of conventional and modified vinyl ether based polycarboxylate superplasticizers. Cem. Concr. Res. **60**, 1–10 (2014)

Liu, J.P., Li, L., Miao, C.W., Tian, Q., Ran, Q.P., Wang, Y.J.: Characterization of the monolayers prepared from emulsions and its effect on retardation of water evaporation on the plastic concrete surface. Colloids Surf. A: Pysicochem. Eng. ASP. **366**(1–3), 208–212 (2010)

Lura, P., Jensen, O.M., van Breugel, K.: Autogenous shrinkage in high-performance cement paste: an evaluation. Cem. Concr. Res. **33**, 223–232 (2003)

Mann, S.: Molecular tectonics in biomineralization and biomimetic materials chemistry. Nature **365**, 499–505 (1993)

Mignon, A., Snoeck, D., Dubruel, P., Van Vlierberghe, S., De Belie, N.: Crack mitigation in concrete: superabsorbent polymers as key to success? Materials **10**(3), 237 (2017)

Mosquet, M., Chevalier, Y., Brunel, S., Guicquero, J.-P.: Polyethylene di-phosphonates as efficient dispersing polymers for aqueous suspensions. J. Appl. Pol. Sci. **65**, 2545–2555 (1997)

Nagare, K.: Storage and/or Transportation Method of Polyalkylene Glycol Monomers, US 7,030,282 B2 (2006)

Ng, S., Plank, J.: Study on the interaction of Na-montmorillonite clays with polycarboxylate based superplasticizers. In: Malhotra, V.M. (ed.) 10th CANMET/ACI Conference on Superplasticizers and Other Chemical Admixtures in Concrete (Proceeding Papers), ACI, Prague, pp. 407–421 (2012a)

Ng, S., Plank, J.: Interaction mechanisms between Na montmorillonite clay and MPEG-based polycarboxylate superplasticizers. Cem. Concr. Res. **42**, 847–854 (2012b)

Nicoleau, L., Albrecht, G., Lorenz, K., Jetzlsperger, E., Fridrich, D., Wohlhaupter, T., Dorfner, R., Leitner, H., Vierle, M., Schmitt, D., Braeu, M., Hesse, C., Montero, Pancera, S., Zuern, S., Kutschera, M.: Plasticizer-Containing Hardening Accelerator Composition, US 2011,0269,875 A1 (2011)

Nicoleau, L., Gädt, T., Chitu, L., Maier, G., Paris, O.: Oriented aggregation of calcium silicate hydrate platelets by the use of comb-like copolymers. Soft Matter **9**, 4864–4874 (2013)

Ohta, A., Sugiyama, T., Tanaka, Y.: Fluidizing mechanism and application of polycarboxylate-based superplasticizers, In: Malhotra, V.M. (ed.) 5th CANMET/ACI Conference on Superplasticizers and Other Chemical Admixtures in Concrete (Proceedings volume), Rome, ACI, SP-173, pp. 359–378 (1997)

Paas, J., Müller, M.W., Plank, J.: Influence of diester content in macromonomers on performance of MPEG-Based PCEs. In: Malhotra, V.M., Gupta, P.R., Holland, T.C. (eds.) 11th CANMET/ACI Conference on Superplasticizers and Other Chemical Admixtures in Concrete (Proceedings), ACI SP-302, Ottawa (Canada), pp. 199–210 (2015)

Plank, J., Pöllmann, K., Zouaoui, N., Andres, P.R., Schaefer, C.: Synthesis and performance of methacrylic ester based polycarboxylate superplasticizers possessing hydroxy terminated poly (ethylene glycol) side chains. Cem. Concr. Res. **38**, 1210–1216 (2008)

Plank, J., Lange, A.: Concrete Admixtures, EP 12,002,354.4 (2012)

Plank, J., Ng, S., Foraita, S.: Intercalation of Microbial Biopolymers Welan gum and EPS I into Double Layered Hydroxides, Zeitschrift für Naturforschung B 67b, 479-487 (2012)

Plank, J., Meyer, L.: New insights into physicochemical interactions occurring between polycarboxylate superplasticizers and a stabilizer in self-compacting concrete. J. Sustain. Cem.-Based Mat. **4**, 164–175 (2015)

Pourchet, S., Liautaud, S., Rinaldi, D., Pochard, I.: Effect of the repartition of the PEG side chains on the adsorption and dispersion behaviors of PCP in presence of sulfate. Cem. Concr. Res. **42**, 431–439 (2012)

Schinabeck, M., Friedrich, S., Holland, U., Pfeuffer, T., Eberwein, M., Schuhbeck, T.: Water-soluble copolymers containing sulfo groups, method for the production and use thereof, EP 1,763,546 (2005)

Shlonimskaya, N., Biernacki, J.J., Kayello, H.M., Visco, D.P.: An application of computer- aided molecular design (camd) using the signature molecular descriptor – part 2: evaluating newly identified surface tension-reducing substances for potential use as shrinkage-reducing admixtures. J. Am. Ceram. Soc. **97**(2), 378–385 (2014)

Snoeck, D., Pel, L., De Belie, N.: The water kinetics of superabsorbent polymers during cement hydration and internal curing visualized and studied by NMR. Sci. Rep. **7**, 9514 (2017)

Stecher, J., Plank, J.: Novel concrete superplasticizers based on phosphate esters. Cem. Concr. Res. **119**, 36–43 (2019)

Tahara, H., Ito, H., Mori, Y., Mizushima, M.: Cement Additive, Method for Producing the same, and Cement Composition, US 5,476,885 (1995)

Tazawa, E., Miyazawa, S., Kasai, T.: Chemical shrinkage and autogenous shrinkage of hydrating cement paste. Cem. Concr. Res. **25**, 288–292 (1995)

Üzer, E., Plank, J.: Impact of welan gum stabilizer on the dispersing performance of polycarboxylate superplasticizers. Cem. Concr. Res. **82**, 100–106 (2016)

Wang, Z.M., Xu, Y., Wu, H., Liu, X., Zheng, F.Y., Li, H.Q., Cui, S.P., Lan, M.Z., Wang, Y.L.: A Room Temperature Synthesis Method for Polycarboxylate Superplasticizer, CN 101974135 B (2013)

Witt, J., Plank, J.: A novel type of PCE possessing Silyl functionalities. In: Malhotra, V.M. (ed.) 10th CANMET/ACI Conference on Superplasticizers and Other Chemical Admixtures in Concrete (Proceedings), ACI, Prague, SP-288.04, pp. 57–70 (2012)

Wittmann, F.H.: Creep and Shrinkage in Concrete Structures, pp. 129–161. John Wiley & Sons Ltd, Hoboken (1982)

Yamamoto, M., Uno, T., Onda, Y., Tanaka, H., Yamashita, A., Hirata, T., Hirano, N.: Copolymer for Cement Admixtures and its Production Process and Use, US 6,727,315 (2004)

Yoshioka, K., Tazawa, E., Kawai, K., Enohata, T.: Adsorption characteristics of superplasticizers on cement component minerals. Cem. Concr. Res. **32**, 1507–1513 (2002)

9.2.5. Publikation #17: Flow-enhancing PCE-based superplasticizers for concretes of low W/C ratio such as UHPC

Publikation #17

Flow-enhancing PCE-based superplasticizers for concretes of low W/C ratio such as UHPC

Manuel Ilg, Johann Plank

In: B. Middendorf, E. Fehling, A. Wetzel (Eds.),
5th International Symposium on Ultra-High Performance Concrete and High Performance Construction Materials (HiPerMat)
Kassel (Germany), 2020
Proceedings, 65 – 66

Flow-enhancing PCE-based superplasticizers for concretes of low W/C ratio such as UHPC

Manuel Ilg, Johann Plank
Chair for Construction Chemistry, Department of Chemistry, Technische Universität München, Germany

1 Introduction

Applicators often report about a sticky and cohesive consistency of concretes prepared at low water to cement ratios ≤ 0.30. Even though those concretes can be highly fluidized with polycarboxylate superplasticizers (PCEs), they often exhibit a creeping flow behavior which impedes a fast placement on the job site. Such a rheology is highly disadvantageous for the processing (pumping, placing etc.) as it often leads to an incomplete filling of the formwork and hence to defects of the hardened concrete structure. Mechanistic studies revealed that the low flow speed of those concretes particularly originates from a high plastic viscosity of the lime phase [1, 2]. Unfortunately, the plastic viscosity cannot be substantially reduced by conventional PCEs, which is why new approaches have to be found, how the rheological properties can be improved. This paper aims to present recent advances and strategies that are currently discussed for lowering the sticky consistency of concretes at low w/c ratios.

2 Phosphate-group modified superplasticizers

One promising concept to improve the flow speed of concrete is to introduce highly negative phosphate groups into the PCE polymers. The chemical structures of such novel superplasticizers are illustrated in *Figure 1*. Recently, phosphated phenolethoxlyates *(a)* were brought on the market, which are synthesized by polycondensation from phenolethoxylate, a phenol ethoxy phosphate ester, phenol and formaldehyde. Thus, a polymer is obtained with a polyaromatic backbone holding polyethylene glycol side chains and phosphate ester groups. An alternative product is a polymer prepared by aqueous free radical copolymerization of hydroxyethylmethacrylate phosphate ester (HEMAP), methacylic acid and a polyethylene glycol methacrylate ester *(b)* [3]. It was found that such phosphated polymers exhibit a high dispersing capability and an excellent robustness in the presence of sulfates and other chemical additives. However, the most striking feature is their ability to enhance the flow speed of concrete and to reduce the stickiness at low w/c ratios. This can be attributed to their high adsorption affinity and the high hydrophilic character of the trunk chain resulting from the phosphate groups which effectuate a low plastic viscosity. Contrary to common PCEs, the phosphated polymers affect the yield stress as well as the plastic viscosity of the lime phase.

(a) phosphated phenolethoxylate **(b) phosphated MPEG-PCE**

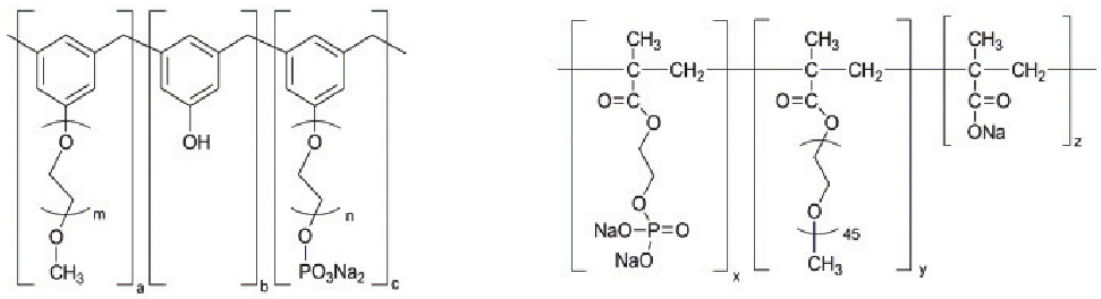

Figure 1: Chemical structures of phosphate-group bearing superplasticizers: (a) phosphated phenolethoxylate (polyarylether-based polymer) and (b) methacrylate-ester PCE exhibiting phosphate anchor groups.

3 Non-ionic small molecules as flow enhancers

Even simple blends of non-ionic small molecules like diethylene glycol with conventional PCEs can be used to improve the rheological properties. As can be seen from *Figure 2*, the effect of such auxiliary dispersants is particularly strong at very low w/c ratios (e.g. 0.22) where the cement particles are densely packed and the pore space becomes quite limited. However, the non-ionic co-dispersants not only increase the spread flow, but also enhance the flow speed as was confirmed by much faster V-funnel empty times of mortars exhibiting the same spread flow value [4]. Interestingly, the non-ionic molecules do not produce any fluidity when individually admixed to the cement and only work in combination with a PCE superplasticizer.

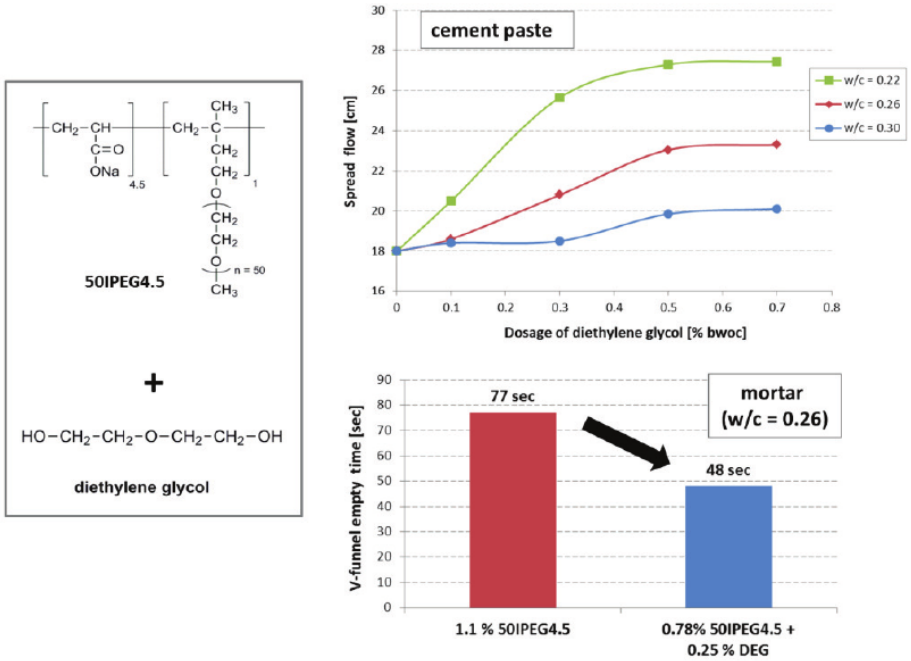

Figure 2: Effect of diethylene glycol as auxiliary dispersant on the spread flow of cement pastes and the V-funnel empty time of mortars at low w/c ratios.

The fluidizing effect of the co-dispersants can be explained by an osmotic spacer effect. Adsorption measurements have shown that the non-ionic molecules remain freely dissolved in the interstitial pore solution where they induce repulsive depletion forces, thus hindering the cement grains from flocculation. Otherwise, some parts of the pore solution would be depleted from the non-ionic molecules, which is energetically unfavourable and therefore avoided. Furthermore, it is assumed that such non-ionic co-dispersants create a lubricating layer around the particles and hence reduce the friction during flow.

References

[1] Banfill, P. F. G.: Additivity effects in the rheology of fresh concrete containing water-reducing admixtures. *Construction and Building Materials* 25, pp. 2955-2960, 2011.

[2] Liu, J.; Wang, K.; Zhang, Q.; Han, F.; Sha, J.; Liu, J.: Influence of superplasticizer dosage on the viscosity of cement paste with low water-binder ratio. *Construction and Building Materials* 149, pp. 359-366, 2017.

[3] Stecher, J.; Plank, J.: Novel concrete superplasticizers based on phosphate esters. *Cement and Concrete Research* 119, pp. 36-43, 2019.

[4] Ilg, M.; Plank, J.: Novel admixtures to reduce the stickiness of low w/c concretes. Proc. 12th International Conference on Superplasticizers and Other Chemical Admixtures in Concrete, Beijing 2018, pp. 77-88.